

**An investigation into dysfunctional feed-forward inhibition
within the cortico-thalamocortical network on absence seizure
generation using DREADD technology.**

UNIVERSITY
of
OTAGO



Te Whare Wānanga o Otāgo

NEW ZEALAND

Sandesh Panthi

A thesis submitted for the degree of
Doctor of Philosophy
at the University of Otago
Dunedin, New Zealand.

October 2020

Abstract

Childhood absence epilepsy (CAE) is one of the most prevalent paediatric epilepsies, accounting for between 10-17% of all diagnosed cases of epilepsies seen in school-aged children. Absence seizures are characterized by behavioural arrest/loss of awareness and electrographic signature of spike-wave discharges (SWDs) measuring 2.5-4 Hz on an electroencephalogram (EEG). These brief episodes of impaired consciousness can occur hundreds of times a day and might increase the chance of physical injury when undertaking activities like swimming and cycling. Current treatment options are not sufficient and up to 30% of patients are pharmaco-resistant. ~60% of children with CAE have severe neuropsychiatric comorbid conditions including attention deficits, mood disorders, impairments in memory and cognition. Ethosuximide (ETX), an anti-absence epileptic drug which was first introduced almost six decades ago remains the first choice for initial monotherapy for the treatment of CAE. Large-scale clinical trials suggested that efficacy of ethosuximide is considerably lower than previous findings. Thus, safe, effective and patient specific treatment approach is imperative. For this, it is crucial first to understand the precise cellular and molecular mechanisms of absence seizures which may enable the development of novel therapeutic targets and discovery of new anti-epileptic drugs (AEDs).

EEG and functional imaging evidence suggest that absence seizures are likely due to aberrant activity within the cortico-thalamocortical (CTC) network. Studies involving the genetic rodent models have shown that the cortex is the driving source for the origin of SWDs but is not capable of maintaining discharges on its own, nor is the thalamus. General consensus is that, within the CTC network, a cortical focus initiates rhythmic epileptic discharges, however, once the rhythmic oscillations are established, both the cortex and thalamus form an integrated network. Rhythmic absence-SWDs are sustained via the cortex and thalamus driving each other. Within the CTC network, feed-forward inhibition (FFI) is essential to prevent runaway excitation. FFI is mediated by fast spiking parvalbumin expressing (PV+) inhibitory interneurons in the somatosensory cortex (SScortex) and the reticular thalamic nucleus (RTN). Studies conducted in well-established stargazer mouse model of absence epilepsy with a genetic deficit in stargazin i.e. TARP [a transmembrane α -amino-3-hydroxy-5-methyl-4-isoxazolepropionic acid (AMPA) receptor regulatory protein] have shown reduced expression of GluA4-AMPA receptors at excitatory synapses in feed-forward inhibitory (PV+) interneurons in the SScortex and RTN thalamus of the CTC

network. However, the extent of this deficit in AMPARs expression impacting FFI and possibly contributing towards generation of absence-SWDs is not established via functional studies.

Hence, this thesis was aimed at investigating the impact of dysfunctional feed-forward inhibitory PV+ interneurons within CTC network on absence seizure generation and behaviour. For this purpose, inhibitory and excitatory Designer Receptors Exclusively Activated by Designer Drug (DREADD) approach was utilized to silence/excite feed-forward inhibitory PV+ interneurons within the CTC network. DREADD mediated regional silencing of PV+ interneurons within the CTC network generated ETX-sensitive absence-like SWDs. Activating PV+ interneurons either prevented or suppressed pentylenetetrazole (PTZ)-induced absence-SWDs. Finally, impact of impaired FFI in γ -aminobutyric acid (GABA) levels by affecting its synthesizing enzymes (GADs) and transporter proteins (GATs) in stargazer animal model of absence epilepsy and CNO treated inhibitory Gi-DREADD animals was determined. Results indicate that upregulation of GAD65 in the SS cortex of epileptic stargazers may be a consequence of absence seizures or this may have contribution in absence seizure generation.

The work presented in this thesis provide an electrophysiological insight into the possible mechanism underlying the absence seizure generation. This work provides convincing evidence that dysfunctional feed-forward inhibitory PV+ interneurons within the CTC network is likely to be involved in altered excitation/inhibition balance resulting SWDs as activating these interneurons dramatically protected animals from PTZ induced absence seizures. The clinical relevance of this study is that it potentially uncovers the possibility of focally targeting PV+ interneurons within the CTC network to control absence seizures in human patients.

**This thesis is dedicated to my sister Sheelu.
Her smile is always my biggest source of inspiration.**

Sheelu - this is for you!

Acknowledgements

Although words are not sufficient to express my gratitude to the people who were always available and helpful to me during this journey, I would like to acknowledge their support.

First and foremost, I would like to express my sincere gratitude to my supervisor A/P Beulah Leitch for providing me the opportunity to undertake this PhD project as well as for her encouragement and guidance during my time in the lab. It would not have been possible to finish without her continuous support, patience and care.

I also wish to acknowledge the suggestions of the members of my PhD advisory committee, Prof. Greg Anderson, Prof. Ping Liu and A/P Yusuf Cakmak.

I would like to thank University of Otago for the financial support during my PhD studies through a University of Otago Doctoral Scholarship. I am also grateful to Brain Health Research Centre (BHRC) for providing me the Roche Hännis Moller Doctoral Scholarship during the final stage of my PhD. I would also like to thank the Department of Anatomy, Division of Health Science and BHRC for providing the fund for conference travel.

I would also like to thank to all the wonderful staffs of various departments of the university who assisted me from the beginning. I would like to acknowledge all the technical support from IT (Tim, Tony and Robbie), OCCM (Andrew), BPU (Julia), and HTRU staffs.

Special thanks to Nadia Adotevi. I will never forget her help and company. Many thanks to Jack and Steve for your assistance and help.

I am also very grateful to all the present and past members of Dunedin Nepalese Society.

Most importantly, I would like to thank my family members for believing in me. My father for his life-long positivity, tireless understanding and unconditional support. My mother for her love, support and care. My brother Sanjeeb for always being there for me. To my nephew Oscar, thank you for being a part of my life. Sambriddhi, thanks for coming into my life. You have changed my world. Thanks for being so cool and for your continuous love, support, care.

You all have been my source of strength.

Thank You.

Publications/conferences arising from this thesis:

Journal publications:

Panthi, S. and Leitch, B., 2019. The impact of silencing feed-forward parvalbumin-expressing inhibitory interneurons in the cortico-thalamocortical network on seizure generation and behaviour. *Neurobiology of Disease*, 104610.

Oral presentations:

Panthi, S., & Leitch, B., 2019. Using DREADD technology to interrogate dysfunctional feed-forward inhibition within cortico-thalamo-cortical microcircuits to investigate absence seizure generation and altered behaviour. *39th Annual Meeting of the Australasian Neuroscience Society (ANS), Adelaide, Australia.*

Panthi, S., & Leitch, B., 2020. An investigation into dysfunctional feed-forward inhibition within the cortico-thalamocortical network on absence seizure generation using DREADD technology. *255th Otago Medical School Research Society (OMSRS) PhD student speaker awards, Dunedin, New Zealand.*

Panthi, S., & Leitch, B., 2021. An investigation into dysfunctional feed-forward inhibition within the cortico-thalamocortical network on absence seizure generation using DREADD technology. Invited speaker at Roche Pharmaceuticals, Auckland, New Zealand.

Poster presentations:

Panthi, S., & Leitch, B., 2018. Investigating mechanisms underlying absence epilepsy using DREADD technology to silence microcircuits within the cortico-thalamic-cortical network. *48th Annual Meeting of the Society for Neuroscience (SFN) conference, San Diego, CA, USA.*

Panthi, S., & Leitch, B., 2019. Investigating mechanisms underlying absence epilepsy using DREADD technology to silence microcircuits within the cortico-thalamic-cortical network. *13th Annual Brain Health Research Centre Annual Conference, at Dunedin, New Zealand.*

Awards:

2019: Poster prize at the 13th Annual Brain Health Research Centre conference.

2020: Roche Hanns Möhler Doctoral Scholarship

Table of Contents

Abstract	ii
Dedication	iv
Acknowledgements	v
Publications/conferences arising from this thesis	vi
Table of contents	vii
List of figures	xiv
List of tables	xvii
Abbreviations	xix
CHAPTER 1. Introduction	1
1.1 Epilepsy	1
1.1.1 Definition of epilepsy	2
1.1.2 Prevalence, incidence and mortality of epilepsy	2
1.1.3 Classification of epilepsy	5
1.2 Childhood absence epilepsy: the focus of this thesis	7
1.2.1 Absence epilepsy: overview	9
1.2.2 EEG features of absence seizures	9
1.2.3 Aetiology of absence epilepsy	11
1.2.4 Age of onset, prevalence and mortality of absence epilepsy	13
1.2.5 Prognosis and treatment of absence epilepsy	13
1.2.6 Pathogenesis of absence epilepsy in human patients and animal models	14
1.2.6.1 Animal models	15
1.2.6.2 Human patients	19
1.3 The Cortico-thalamocortical Network	21
1.3.1 The cerebral cortex	21
1.3.2 The thalamus	22
1.4 Microcircuit motifs of the CTC network	28
1.5 Parvalbumin-expressing (PV+) inhibitory interneurons	30
1.5.1 PV+ interneurons in CTC network	31

1.6	Functional roles of PV+ interneurons in CTC network	32
1.6.1	Feed-forward inhibition (FFI) in cortex	32
1.6.2	Feed-forward inhibition (FFI) in thalamus	32
1.7	PV+ interneurons and neurological disorders	32
1.8	PV+ interneurons and epilepsy	34
1.9	Manipulation of neuronal subpopulation	36
1.10	G Protein Coupled Receptors (GPCRs)	36
1.10.1	Complexity of GPCR signaling	39
1.10.2	Engineered GPCRs	39
1.10.2.1	Receptors Activated Solely by Synthetic Ligands (RASSLs)	39
1.10.2.2	Designer Receptors Exclusively Activated by Designer Drugs (DREADDs)	40
1.10.2.3	Designer drug CNO and recent developments	43
1.11	DREADD and Optogenetics	44
1.12	Use of DREADD technology to study various CNS disorders and animal behaviours	47
1.13	DREADD technology in epileptic-seizure related studies	49
1.14	Manipulating PV+ neurons with DREADDs	50
1.15	Rationale and aims of the thesis	54
1.16	Outline of thesis chapters	55
CHAPTER 2. Materials and Methods		56
2.1	Animals	56
2.1.1	Breeding paradigm for PV-Cre x hM4Di-flox and PV-Cre x hM3Dq-flox mice	56
2.1.2	Breeding paradigm for stargazer mice	57
2.2	Genotyping	58
2.2.1	DNA extraction from the ear-notches	58
2.2.2	Polymerase chain reaction (PCR)	59
2.2.3	Agarose Gel Electrophoresis	61
2.3	Immunofluorescence Confocal Microscopy	62
2.3.1	Animal perfusion and fixation	62
2.3.2	Tissue processing and immunolabelling	63

2.3.3	Confocal imaging and analysis	64
2.4	Electroencephalography (EEG) recordings	64
2.4.1	Surgical implantation of prefabricated headmounts and microcannulas	64
2.4.2	Post-operative care	65
2.4.3	EEG recording procedure	66
2.4.4	Analysis of EEG traces	66
2.4.5	Use of ethosuximide (ETX) to confirm absence-like nature of discharges	66
2.5	Drug/chemical preparation and delivery	67
2.5.1	Clozapine-N-oxide (CNO)	67
2.5.2	Ethosuximide (ETX)	67
2.5.3	Pentylentetrazole (PTZ)	67
2.6	Behavioural tests	69
2.6.1	Open-field test	69
2.6.2	Rotarod test	69
2.7	Western blotting	69
2.7.1	Tissue collection and processing	69
2.7.2	Protein quantification	70
2.7.3	Gel electrophoresis and blot transfer	71
2.7.4	Immunoblotting and analysis	72
2.8	Data analysis	73

CHAPTER 3. Impact of Silencing Feed-forward Inhibitory PV+ Interneurons on Absence Seizure Generation and Behaviour

3.1	Introduction	74
3.2	Methods	76
3.2.1	Immunofluorescence confocal microscopy, image acquisition and analysis	76
3.2.2	Surgical implantation of prefabricated headmounts and microcannulas for EEG recordings	76
3.2.3	Preparation and delivery of clozapine-N-oxide (CNO) and ethosuximide (ETX)	77
3.2.4	Behavioural tests	78
3.3	Results	79

3.3.1	Inhibitory (Gi) DREADD receptors are expressed in feed-forward inhibitory PV+ interneurons	79
3.3.2	Silencing feed-forward inhibitory PV+ interneurons via intraperitoneal (i.p.) and focal CNO injections generated absence-like seizures	81
3.3.3	Route of administration of CNO affected onset of bursts of oscillatory activity	86
3.3.4	ETX suppressed absence-like seizures generated by focal CNO injections	88
3.3.5	Silencing feed-forward inhibitory PV+ interneurons via intraperitoneal (i.p.) and focal CNO injections increased immobility	90
3.3.6	Silencing feed-forward inhibitory PV+ interneurons via intraperitoneal (i.p.) CNO injection impaired motor function, decreased locomotion and increased anxiety	92
3.3.7	Silencing feed-forward inhibitory PV+ interneurons via focal CNO injection decreased locomotion but did not impair motor function	94
3.4	Discussion	100
3.4.1	HA-tagged DREADD receptors are highly expressed in feed-forward inhibitory PV+ interneurons	101
3.4.2	Global and focal silencing of PV+ interneurons generated absence-like SWDs associated with behavioural arrest	102
3.4.3	Global and focal silencing of feed-forward inhibitory PV+ interneurons affected locomotory behaviours and mobility	104
3.5	Conclusion	107

CHAPTER 4. Effect of Activating Feed-forward Inhibitory PV+ Interneurons During Absence Seizures **108**

4.1	Introduction	108
4.2	Methods	109
4.2.1	Immunofluorescence confocal microscopy, image acquisition and analysis	109
4.2.2	Surgical implantation of prefabricated headmounts and microcannulas for EEG recordings	109
4.2.3	Preparation and delivery of CNO and PTZ	110
4.2.4	EEG recording and analysis of EEG traces	111

4.2.5	Data analysis	111
4.3	Results	111
4.3.1	Excitatory (Gq) DREADD receptors are expressed in feed-forward inhibitory PV+ interneurons	111
4.3.2	20mg/kg IP PTZ is required to induce absence-SWDs	112
4.3.3	Activating feed-forward inhibitory PV+ interneurons via focal CNO injection suppressed PTZ-induced absence seizures	115
4.3.3.1	Activating PV+ interneurons either prevented or delayed the onset of seizures in DREADD mice	118
4.3.3.2	Activating PV+ interneurons reduced the mean duration spent in seizures	124
4.3.3.3	Activating PV+ interneurons reduced total number of discharges and mean length of epileptic bursts	126
4.4	Discussion	130
4.4.1	Excitatory (Gq) DREADD receptors are highly expressed in feed-forward inhibitory PV+ interneurons	130
4.4.2	Activation of feed-forward inhibitory PV+ interneurons suppressed PTZ induced absence seizures	131
4.4.3	PV+ interneurons- a potential target for antiepileptic therapy?	133
4.5	Conclusion	135

Chapter 5. Impact of Dysfunctional FFI on GAD Isoforms and GABA Transporters

Evidence —from Epileptic Stargazers and CNO Treated

DREADD Animals 136

5.1	Introduction	137
5.2	Methods	138
5.2.1	Immunofluorescence Confocal Microscopy and analysis	138
5.2.2	Western blotting	141
5.2.3	Data analysis	142
5.3	Results	142

5.3.1	Expression pattern of GADs and GATs in the SS cortex and the thalamus of stargazers and non-epileptic controls	142
5.3.2	Quantification of staining intensity of GADs, GATs and PV labelling in the SS cortex and the thalamus of stargazers and non-epileptic controls	148
5.3.3	Relative expression of GADs and GATs in the tissue lysates of the SS cortex and the VP thalamus of stargazers	153
5.3.4	Expression of GADs and GATs was unchanged in DREADD animals	155
5.4	Discussion	157
5.4.1	Histochemical localization profile and staining intensity of GADs and GATs in the stargazer SS cortex and thalamus	157
5.4.1.1	GADs (65 and 67)	157
5.4.1.2	GATs (1 and 3)	159
5.4.2	Increased expression of GAD65 in the stargazer somatosensory cortex	161
5.5	Conclusion	162
Chapter 6. General Discussion		163
6.1	Overview of findings	163
6.2	Discussion of KEY Findings	164
6.2.1	Use of Cre-dependent DREADD to manipulate PV+ interneurons	164
6.2.2	Functionally silencing feed-forward PV+ interneurons generated absence-like SWDs, whereas activation prevented/suppressed PTZ-induced seizures	166
6.2.3	Functional silencing of feed-forward PV+ interneurons altered animal behavior	169
6.2.4	Impact of dysfunctional FFI on GABA synthesizing enzymes (GADs) and transport proteins (GATs)	171
6.3	Clinical Implications	172
6.4	Evaluation of Methods	173
6.4.1	DREADD approach	173
6.4.2	Immunofluorescence Confocal Microscopy	174
6.4.3	Surgical manipulation and EEG recording	175
6.4.4	Behavioral tests	175
6.4.5	Antibodies	176

6.4.6	Western blotting	176
6.5	Future experimental directions	178
6.6	Conclusion	181
References		182
Appendices		234

List of figures

Fig. 1.1	Worldwide estimated deaths due to epilepsy per million persons in 2012	4
Fig. 1.2	Framework for multilevel classification of the epilepsies as per 2017 ILAE scheme	6
Fig. 1.3	Framework for operational classification of seizure types as per 2017 ILAE scheme	6
Fig. 1.4	EEG recordings of absence seizures in a child with CAE and rodent genetic models of absence epilepsy	10
Fig. 1.5	Photograph and EEG profile of Constance and Kathryn, monozygous twins who suffered from childhood absence epilepsy	11
Fig. 1.6	An overview of models of epilepsy or epileptic seizures	15
Fig. 1.7	A simplified illustration of the CTC network showing reciprocal connections between cortex and thalamus	22
Fig. 1.8	Schematic representation of the 5 theories on the origin of generalized absence epilepsy	27
Fig. 1.9	Different microcircuit motifs involved in epilepsy	29
Fig. 1.10	Distribution and relative expression of different types of inhibitory interneurons in cortical layers and RTN thalamus	32
Fig. 1.11	General core structure and functioning of GPCRs	38
Fig. 1.12	Signalling pathways of common available DREADDs	42
Fig. 1.13	Schematic diagram of <i>in vivo</i> manipulation of neuronal population with DREADD technology using transgenic mice approach	51
Fig. 1.14	Schematic diagram of <i>in vivo</i> manipulation of neuronal population with DREADD technology using viral approach	52
Fig. 1.15	Manipulating PV+ neurons with inhibitory or excitatory DREADD using Cre-dependent transgenic mouse approach	53
Fig. 2.1	Breeding paradigm for DREADD animals	57
Fig. 2.2	Breeding paradigm for stargazer mice	58
Fig. 2.3	Representative image of genotype bands on agarose gel	62
Fig. 2.4	Image showing the headmounts, position of EEG electrodes and cannula placement, and preamplifier used in this study	65
Fig. 2.5	Microdissection of tissue from the brain	70
Fig. 3.1	Expression of Gi-DREADD receptors in PV+ interneurons	80

Fig. 3.2	Representative EEG traces of PV ^{Cre} /Gi-DREADD (DREADD) animals and non-DREADD WT controls after i.p. injection of CNO/vehicle	82
Fig. 3.3	Tonic-clonic convulsive seizures with very high amplitude in EEG were evident in one PV ^{Cre} /Gi-DREADD animal after intraperitoneal 5 mg/kg CNO injection	82
Fig. 3.4	Representative EEG traces of PV ^{Cre} /Gi-DREADD animals and non-DREADD WT controls after focal injection of CNO/vehicle into the SS cortex	84
Fig. 3.5	Tonic-clonic convulsive seizure in EEG was evident in one PV ^{Cre} /Gi-DREADD animal with 5 mg/kg CNO injected into the SS cortex	84
Fig. 3.6	Representative EEG traces of PV ^{Cre} /Gi-DREADD animals and non-DREADD WT controls after focal injection of CNO/vehicle into the RTN thalamus	85
Fig. 3.7	Overall comparison of various EEG parameters after i.p. and focal (SS cortex and RTN thalamus) injection of CNO during 1 hour of EEG recording	87
Fig. 3.8	ETX test conducted in PV ^{Cre} /Gi-DREADD animals	89
Fig. 3.9	Immobility in animals after CNO injection during 1 hour of EEG recording	91
Fig. 3.10	Parameters of open-field test after injection of different i.p. doses of CNO	93
Fig. 3.11	Latency of fall in rotarod test in animals after different doses of i.p. CNO injection	95
Fig. 3.12	Total distance travelled in open-field arena by animals after focal CNO/vehicle injection	97
Fig. 3.13	Latency of fall in rotarod test in animals after injection of different focal doses of CNO	99
Fig. 4.1	Schematic of the protocol for EEG recordings before and after focal CNO and intraperitoneal PTZ injections	110
Fig. 4.2	Expression of Gq-DREADD receptors in PV ⁺ interneurons	113
Fig. 4.3	Protocol of the pilot PTZ study and representative EEG traces	114
Fig. 4.4	First and last incident of seizure in animals after PTZ treatment on day 1	116
Fig. 4.5	Comparison of the % of time spent in seizures by animals on day 1 and day 2	117
Fig. 4.6	Graphs showing the latency to first seizure in animals	119
Fig. 4.7	Graphical display showing the latency to first absence seizure in animals	121
Fig. 4.8	Graphical display showing the latency to first tonic-clonic seizure in animals	122
Fig. 4.9	Graphs showing the latency to first myoclonic seizure in animals	123
Fig. 4.10	Mean duration spent in seizure by animals during 1 hour of EEG recording	125

Fig. 4.11	Total epileptic bursts and length of bursts during 1 hour of EEG recording	127
Fig. 4.12	Representative EEG traces from a PV ^{Cre} /Gq-DREADD animal after i.p. PTZ injection on day 1 and focal (SScortex) CNO and i.p. PTZ injection on day 2	128
Fig. 4.13	Representative EEG traces from a PV ^{Cre} /Gq-DREADD animal after i.p. PTZ injection on day 1 and focal (RTN) CNO and i.p. PTZ injection on day 2	129
Fig. 5.1	Schematic of the tissue sections chosen for confocal analyses	139
Fig. 5.2	Method of visual identification of cortical layers and analyses of confocal images	140
Fig. 5.3	Expression of GAD65 and GAD67 in cortical PV+ interneurons	144
Fig. 5.4	Expression of GAT-1 and GAT-3 in cortical PV+ interneurons	145
Fig. 5.5	Expression of GAD65 and GAD67 in thalamic PV+ interneurons	146
Fig. 5.6	Expression of GAT-1 and GAT-3 in thalamic PV+ interneurons	147
Fig. 5.7	Omission controls were employed to test the specificities of the antibodies used	148
Fig. 5.8	Confocal fluorescence intensity of PV labelling	149
Fig. 5.9	Confocal fluorescence intensity of GAD65 and GAD67 labelling	151
Fig. 5.10	Confocal fluorescence intensity of GAT-1 and GAT-3 labelling	152
Fig. 5.11	Western blot analysis of GAD65, GAD67 and GAT-3 in the SScortex	153
Fig. 5.12	Western blot analysis of GAD65, GAD67 and GAT-3 in the VP thalamus	154
Fig. 5.13	Western blot analysis of GAD65, GAD67 and GAT-3 in the SScortex of CNO (single dose) treated DREADD animals and their control counterparts	155
Fig. 5.14	Western blot analysis of GAD65, GAD67 and GAT-3 in the SScortex of CNO (three doses) treated DREADD animals and their control counterparts	156
Supp. Fig. 1	Image showing the localization and diffusion of methylene blue dye	237
Supp. Fig. 2	Schematic showing the mode of action of CNO and PTZ	238
Supp. Fig. 3	Image showing the localization and diffusion of methylene blue dye	239
Supp. Fig. 4	Non-cropped full western blots for antibodies used in this study	240
Supp. Fig. 5	Total distance spent in the peripheral zone (PZ) of open-field arena by animals	241
Supp. Fig. 6	Individual data points corresponding to the figure 3.9	242
Supp. Fig. 7	Individual data points corresponding to the figure 3.10	243

List of tables

Table 1.1	Behavioral features of various types of generalized onset seizures based on ILAE classification	8
Table 1.2	Epileptic features of genetic models of absence epilepsy in mice and rats	18
Table 2.1	Primers used for genotyping of PV ^{Cre} /Gi-DREADD & PV ^{Cre} /Gq-DREADD mice	59
Table 2.2	Primers used for genotyping of stargazer mice	59
Table 2.3	PCR mastermix preparation for animals of PV ^{Cre} /Gi-DREADD colony	60
Table 2.4	PCR mastermix preparation for animals of PV ^{Cre} /Gq-DREADD colony	60
Table 2.5	PCR mastermix preparation for animals of stargazer colony	60
Table 2.6	PCR cycle steps	61
Table 2.7	Primary antibodies used in this project for immunofluorescence confocal microscopy	63
Table 2.8	Secondary antibodies used in this project for immunofluorescence confocal microscopy	64
Table 2.9	List of published studies on mice defining the morphology and characteristics of absence-like SWDs	68
Table 2.10	Preparation of BSA standards	71
Table 2.11	Primary antibodies used in this project for western blotting	72
Table 2.12	Secondary antibodies used in this project for western blotting	73
Table 3.1	Number of animals used in EEG recordings for i.p. injection group	77
Table 3.2	Number of animals used in EEG recordings for focal injection group	77
Table 3.3	Number of animals used in behavioural tests for i.p. injection group	78
Table 3.4	Number of animals used in behavioural tests for focal injection group	79
Table 3.5	Comparison of various EEG parameters after focal CNO injection into the SS cortex or the RTN thalamus of PV ^{Cre} /Gi-DREADD animals during 1 hour of EEG recording	86
Table 3.6	Comparison of mean latency of fall of PV ^{Cre} /Gi-DREADD and non-DREADD animals after CNO/vehicle injection into SS cortex and RTN thalamus on rotarod test	100

Table 3.7 Comparison of the percentage of infection efficiency and specificity of labelling across the various regions of brain in studies utilizing PV-Cre mice and viral (AAV) method of DREADD delivery

102

Abbreviations

AAV	adeno-associated virus
AD	Alzheimer's disease
AED	anti-epileptic drug
AMPA	α -amino-3-hydroxy-5-methyl-4-isoxazolepropionic acid
ASD	autism spectrum disorder
BOLD	blood-oxygenation-level dependent
BSA	bovine serum albumin
CAE	childhood absence epilepsy
cAMP	Cyclic-Adenosine Monophosphate
CCK	cholecystokinin
CNO	clozapine-N-oxide
CT	corticothalamic
CTC	cortico-thalamocortical
CZ	central zone
DAG	diacylglycerol
DALY	disability-adjusted life year
DMSO	dimethyl sulfoxide
DREADDs	designer receptors exclusively activated by designer drugs
DTI	diffusion tensor imaging
EDTA	ethylenediaminetetraacetic acid
EEG	electroencephalogram

ERK1/2	extracellular signal-regulated kinases 1/2
ETX	ethosuximide
FBE	feed-back excitation
FBI	feed-back inhibition
FFE	feed-forward excitation
FFI	feed-forward inhibition
fMRI	functional magnetic resonance imaging
GABA	γ -aminobutyric acid
GAD	glutamic acid decarboxylase
GAERS	Genetic Absence Epilepsy Rat from Strasbourg
GFAP	glial fibrillary acidic protein
GAT	γ -aminobutyric acid transporter
GDP	guanosine diphosphate
GHB	γ -hydroxybutyric acid
GIRK	G protein-coupled inwardly rectifying potassium channel
GPCRs	G Protein Coupled Receptors
GTP	guanosine triphosphate
HA-tag	hemagglutinin-tag
Het	heterozygous
Homo	homozygous
ILAE	International League Against Epilepsy
i.p.	intraperitoneal
IP ₃	inositol 1,4,5-triphosphate

IOS	intrinsic optical signal
JAE	juvenile myoclonic epilepsy
KA	kainic acid
KCNQ	voltage-gated potassium channel
KO	knockout
KORD	κ -opioid-derived DREADD
LFP	local field potential
LORETA	low-resolution electromagnetic tomography
LV	lentivirus
MQH ₂ O	MilliQ water
MRI	magnetic resonance imaging
NE	non-epileptic
NIRS	near-infrared spectroscopy
NMDA	N-methyl-D-aspartate
NPY	neuropeptide Y
OCT	optical coherence tomography
PA	photoacoustic imaging
PB	phosphate buffer
PBS	phosphate-buffered saline
PCR	polymerase chain reaction
PD	Parkinson's disease
PET	positron emission tomography
PFA	paraformaldehyde

PIP ₂	phosphatidylinositol 4,5-biphosphate
PKC	protein kinase C
PLC	phospholipase C
PMRS	proton magnetic resonance spectroscopy
PMSF	phenylmethylsulfonyl fluoride
PN	postnatal day
PTZ	pentylene-tetrazole
PV+	parvalbumin expressing
PZ	peripheral zone
RASSLs	Receptors Activated Solely by Synthetic Ligands
ROI	region of interest
RT	room temperature
RTN	reticular thalamic nucleus
SDS-PAGE	sodium dodecyl sulphate–polyacrylamide gel electrophoresis
SEM	standard error of mean
SOM+	somatostatin expressing
SOUL	step-function opsin with ultra-high light sensitivity
SPECT	single photon emission spectroscopy
SScortex	somatosensory cortex
STG	stargazer
SWD	spike-wave discharge
TARP	transmembrane AMPA receptor regulatory proteins
TBE	Tris-buffered saline

TBS	Tris-buffered saline
TBST	TBS containing TritonX-100
TC	thalamocortical
TE	Tris-EDTA
TEMED	tetramethylethylenediamine
tTA	tetracycline-controlled transactivator protein
UV	ultraviolet light
VIP+	vasoactive intestinal polypeptide
VP	ventral posterior nucleus
VPL	ventral posterolateral nucleus
VPM	ventral posteromedial nucleus
VSD	voltage-sensitive dye imaging
WAG/Rij	Wistar Albino Glaxo rats from Rijswijk
WB	western blotting
WHO	World Health Organization
WT	wild type
4-AP	4-Aminopyridine
6-OHDA	6-hydroxydopamine

Chapter 1. Introduction

1.1 Epilepsy

The term ‘epilepsy’ is derived from the Greek word επιλαμβάνειν which means ‘to take hold of’ or ‘to seize’ (Engel and Pedley, 1997). The oldest detailed account of epilepsy to be found is the Babylonian textbook of medicine available in the British Museum which dates back to 2000 BC. This book accurately details information of many of the seizures we recognize today. It highlights a supernatural nature of this disorder, with each seizure type linked with the name of a spirit or god - usually evil. Therefore, epilepsy was often thought as a spiritual disorder. Hippocrates was the first to believe that epilepsy is a disorder of the brain and not a spiritual illness. In ‘The Sacred Disease’ (400 BC) Hippocrates wrote: *I am about to discuss the disease called “sacred”. It is not, in my opinion, any more divine or more sacred than any other diseases, but has a natural cause ... Its origin, like that of other diseases, lies in heredity ... the fact is that the cause of this affection ... is the brain ...*, (Jones and Withington, 1952). These statements were considered a revolutionary hypothesis at that time. During the 1750s, in Sweden, people with epilepsy were forbidden to marry by law and in the USA 17 states had similar legislation until 1956 (Brodie, 2003). Such supernatural views about epilepsy continued during 19th century and are still an issue in non-first world societies.

In 1849, physician Robert Bentley Todd gave a talk titled “On the Pathology and Treatment of Convulsive Diseases” in the Lumleian annual lectures series organized by Royal College of Physicians of London. He stated that ... *“epilepsy denotes a state of abnormal nutrition of the brain...the periodic evolution of the nervous force which gives rise to the epileptic paroxysm may be compared to the electric phenomenon described by Faraday under the name of disruptive discharge”* ... (Reynolds, 2005). In the 1890 edition of Lumleian lectures, a neurologist, John Hughlings Jackson, hypothesized that epileptic discharges are due to sudden brief electro-chemical discharges of energy in the brain (York and Steinberg, 2011). In 1912, Pavlev Yurevich Kaufman, a student in Russian physiologist Ivan Pavlov’s lab, first described experimentally induced seizures in dogs (Kaufman, 1912). Two years later, Polish scientists, Napoleon Cybulsky and Jelenska-Macieszyna officially published abnormal cortical discharges in the form of photographs (Cybulski and Jelenska-Macieszyna; 1914). German psychiatrist Hans Berger developed the first human electroencephalograph in 1929. The first effective antiepileptic drug, Bromide was introduced in 1857. Phenobarbitone and phenytoin were later introduced in 1912 and 1938, respectively. EEG helped to locate the origin of epileptic discharges and neurosurgical treatment was available during 1950s in Montreal, Paris

and London. In the last few decades, development of neuroimaging techniques, neurosurgical therapies and research facilities have allowed us to understand more about seizures. Additionally, the use of human EEG recordings and animal models have helped investigate the disease mechanisms and treatment options. Despite the development of cutting-edge experimental techniques and identification of various therapeutic targets, drug efficacy on human patients is disappointing and their development is very slow. Currently available anti-AEDs are ineffective or induce intolerable side effects in about a third of all patients. Similarly, although a considerable amount of effort has been put into enhancing the quality of life of epileptic patients, they still experience discrimination in society and are subjected to social stigma. Thus, identification of novel therapeutic targets for better understanding the mechanisms of seizures are needed for patient specific treatment.

1.1.1 Definition of epilepsy

Epilepsy is a neurological disorder characterized by recurring seizures. A seizure is a transient episode of abnormal electrical activity in the brain. Such episodes interrupt normal neuronal function and can be diagnosed by characterizing electrophysiological features in the EEG and expression of clinical behaviour (World Health Organization Fact Sheet, 2019). The International League Against Epilepsy (ILAE) is a major official scientific organization involved in epilepsy research, education and training since 1909. In 2005, ILAE defined epilepsy *“as a disorder of the brain characterized by an enduring predisposition to generate epileptic seizures and by the neurobiologic, cognitive, psychological, and social consequences of this condition. The definition of epilepsy requires the occurrence of at least one epileptic seizure. And, an epileptic seizure is a transient occurrence of signs and/or symptoms due to abnormal excessive or synchronous neuronal activity in the brain”* (Fisher et al., 2005). In 2014, ILAE released a more practical definition, which defines epilepsy as *“a disease of the brain defined by any of the following conditions 1. At least two unprovoked (or reflex) seizures occurring >24 h apart 2. One unprovoked (or reflex) seizure and a probability of further seizures similar to the general recurrence risk (at least 60%) after two unprovoked seizures, occurring over the next 10 years 3. Diagnosis of an epilepsy syndrome”* (Fisher et al., 2014).

1.1.2 Prevalence, incidence and mortality of epilepsy

Epilepsy has many possible causes, but for the majority of cases a cause is unknown or presumed to be genetic factors. Other causes of epilepsy include brain tumours, stroke, traumatic brain injury, infection, developmental brain abnormalities etc. Epilepsy is a disorder

with a high prevalence rate. The prevalence of epilepsy is defined as the total number of alive cases over a period of time. Recent studies have shown that prevalence of epilepsy ranges from 2.2-22.2/1000 in low income countries and 2.7-7.1/1000 in high income or developed economies. Lifetime prevalence of this disease ranges from 3.6-15.4/1000 in low income countries and 2.3-15.9/1000 in high income economies (Banerjee et al., 2009).

Incidence of epilepsy is defined as the total number of newly diagnosed cases of epilepsy over a period of time. It is generally calculated as cases per 100,000 populations/year. The worldwide annual incidence of epilepsy is 67.7 per 100,000. This figure varies with geography, age, ethnicity and socioeconomic difference (Sander et al., 2003; Fiest et al., 2017). Age-specific studies have shown that incidence of epilepsy to be higher between the first year of life to early childhood, lowest in the adult stage and subsequently increases in the elderly age group (Banerjee et al., 2009). WHO states that five million people are diagnosed with epilepsy each year (World Health Organization Fact Sheet, 2019).

Epilepsy is a very common disease in the elderly compared to other age groups, but studies have shown that the cumulative mortality rate at the age of 45 includes 25% of patients who develop epilepsy in childhood (Banerjee et al., 2009; Bell et al., 2014; Beghi and Giussani et al., 2018). Studies have also revealed that people with epilepsy are always at higher risk (3-4 times) of premature death compared to the normal population. The highest rate of premature mortality was found in countries with low and middle-income economies (Ding et al., 2006; Hitiris et al., 2007; Trinka et al., 2013; Keezer et al., 2016). Figure 1.1 shows worldwide deaths attributed to epilepsy per million. A report based on disability-adjusted life year (DALYs), which measures overall disease burden and life expectancy, showed that 3% of global DALYs were from neurological disorders of which epilepsy accounted for a quarter (Murray et al., 2013). Studies have also reported that up to 2% of paediatric population aged 0-17 have at least one active form of epilepsy (Forsgren, 2004; Russ et al., 2012; Zack and Kobau; 2017). Up to 10% of people worldwide experience seizure at least once in their lifetime.

Currently, 50 million people worldwide is believed to have epilepsy and 80% of them are from low-and middle-income countries (World Health Organization Fact Sheet, 2019). One in fifty New Zealanders are living with epilepsy (epilepsyfoundation.org.nz).

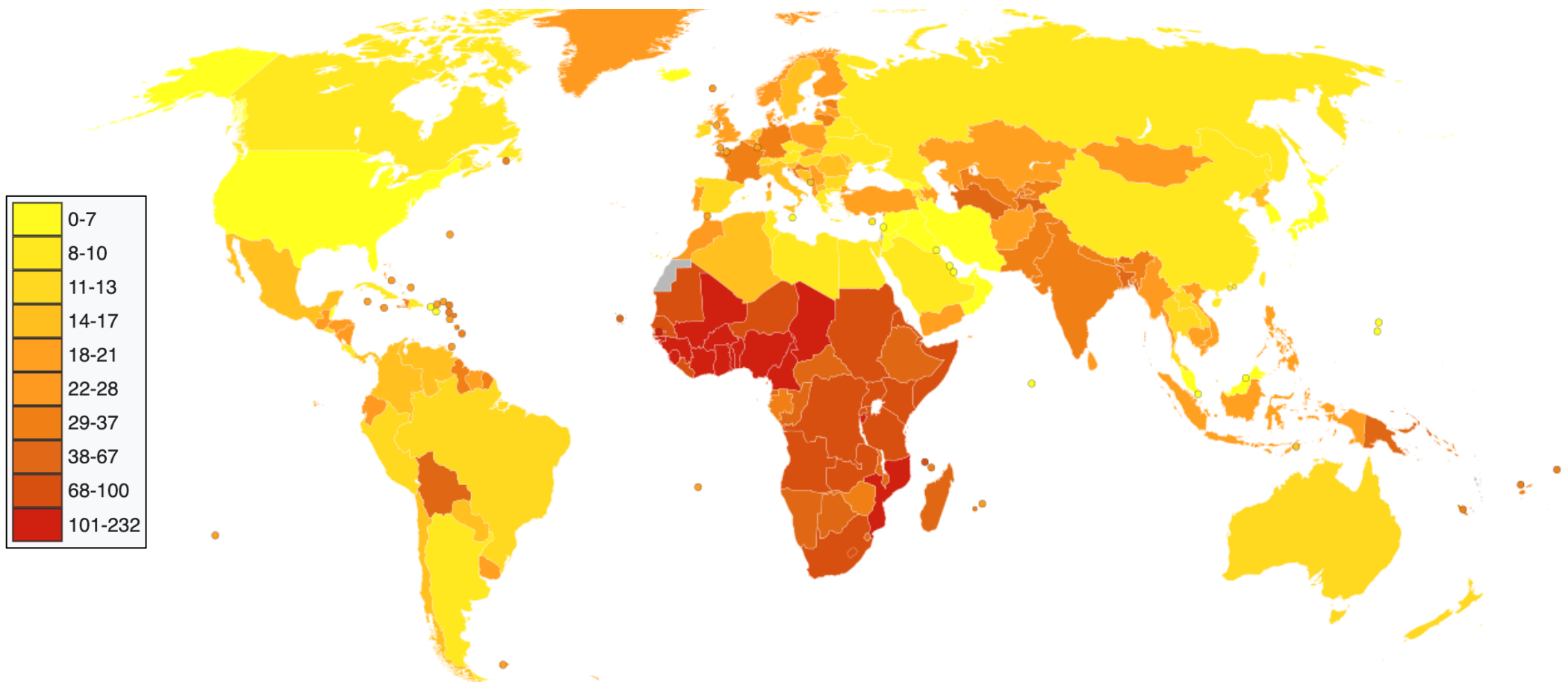


Fig. 1.1 Worldwide estimated deaths due to epilepsy per million persons in 2012. (Data from WHO, grouped by deciles)

1.1.3 Classification of epilepsy

Classification of epilepsy began in the 1960s (Marsan, 1965; Gastaut, 1970). The first official classification released by ILAE in 1981 was named the International Classification of Epileptic Seizures (ICES) (Angeles, 1981). According to this scheme, epileptic seizures were dichotomized into partial and generalized groups. Advancements in the scientific techniques and achieved research outcomes improved the understanding of epilepsy and various revisions of classification were made over the time. In 1985, the classification was revised again, and a dual dichotomy scheme was proposed. This classification was based on semiology (focus vs generalized seizures) and etiology (idiopathic vs symptomatic) (Dreifuss et al., 1985). In 2010, ILAE issued a report on revised terminologies and concepts for the organization of seizures and epilepsies (Berg et al., 2010). This scheme also introduced the concept of a 'neuronal network'. Seizures were classified on the basis of their point of origin. For example: focal seizure was defined as a seizure originating within a neuronal network affecting one hemisphere only. A generalized seizure was defined as a seizure which involves multiple points within neuronal networks distributed in both hemispheres. This scheme provoked controversy and scientists criticized the scheme for being too complicated for daily practice and lacking accurate scientific understanding (Ferrie, 2010; Guerrini, 2010; Wolf, 2010; Beghi, 2011; Duncan, 2011). In 2017, ILAE released a new classification for both seizures and epilepsies which reflect current scientific knowledge (Fisher et al., 2017a; 2017b, Scheffer et al., 2017) (Fig. 1.2 and 1.3). According to this proposal, epilepsy was classified on three levels i.e. seizure type, epilepsy type and epileptic syndrome (Fig. 1.2). The epilepsy classification divided epilepsies into four subtypes i.e. focal, generalized, combined generalized and focal, and unknown (Fig. 1.2). Diagnosis of epileptic syndromes was the third level of classification. This is important because diagnosis plays a crucial role in prognosis and treatment of epilepsy. In addition, etiological classification has been added which was previously advocated in the 2010 scheme. Structural, genetic, infectious, metabolic, immune, and unknown were the six etiological subgroups (Fig. 1.2). This scheme advised clinicians to categorize an epileptic disorder into one of the above etiological subgroups during every stage of diagnosis. According to this scheme, seizures were classified on clinical terms rather than pathogenic mechanisms i.e. focal, generalized, and unknown onset (Fig. 1.3).

Focal onset was subdivided on the basis of awareness or level of consciousness of the patient. Both focal and generalized seizures were subcategorized into motor and non-motor onset based

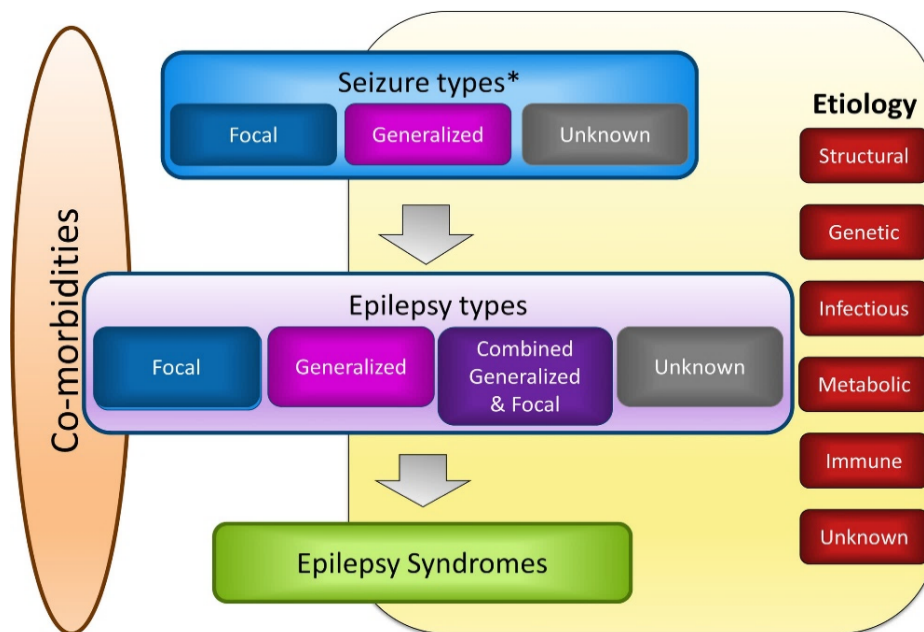


Fig. 1.2 Framework for multilevel classification of the epilepsies as per 2017 ILAE scheme. The asterisk (*) denotes onset of seizure. (Taken from Scheffer et al., 2017.)

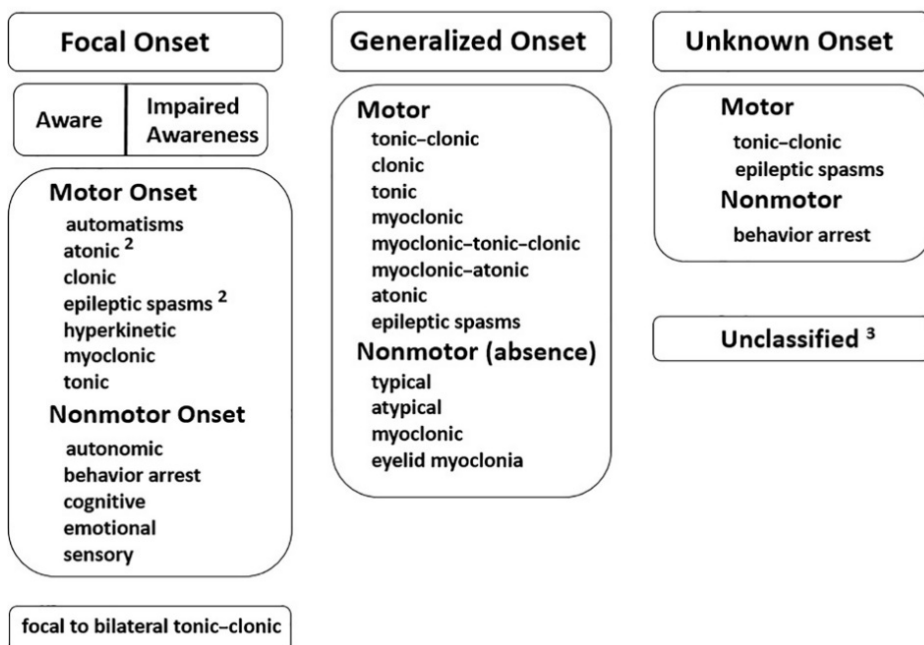


Fig. 1.3 Framework for operational classification of seizure types as per 2017 ILAE scheme. ²Degree of awareness usually is not specified. ³Due to inadequate information or inability to place in other categories. (Taken from Fisher et al., 2017a)

on the first signs or symptoms seen during the seizure. ‘Focal to bilateral tonic-clonic’ seizures were categorized as those focal seizures which later became generalized. Both subtypes of focal and generalized onset seizures were distinguished on the basis of clinical and video-EEG profiles. Unknown onset seizures were those seizures which did not conform to the requirement of focal or generalized onset or have not been sufficiently described to meet the criteria. This current ILAE classification system has more practical, descriptive and realistic approach to seizures from infant to adult patients compared to older versions. This version has provided a common language and updated view of seizures and epilepsies for clinical practice, research sector and teaching. However, recently, experts have outlined the shortcomings of this new scheme. Lüders and colleagues criticized this new classification for relying heavily on semiological parameters to classify seizures and mixing the semiological terms with epileptogenic zone terminologies. They also criticized the replacement of simple and widely accepted terminologies with complicated and less informative terms in this new version. They suggested that evolution of symptomatology is an important characteristic of epileptic seizures and the new version has limited this aspect by including very few repertoires for seizure evolutions. These experts also criticized the four-diagnostic level of ILAE 2017 classification by saying ‘redundant, overlapping and confusing’. They proposed a four-dimensional system of the classification of epilepsy i.e. seizure type, location of epileptogenic zone, etiology, and comorbidities (Lüders et al., 2019).

1.2 Childhood absence epilepsy: the focus of this thesis

ILAE 2017 basically classified seizures by onset: 1. focal onset seizures- which originate within one neuronal network and are restricted to one hemisphere of the brain, 2. generalized onset seizures- which originate at some point within the brain and involve neuronal networks of both hemispheres of the brain, 3. seizures with unclear onset or known onset but if clinician is less than 80% confident, they were recognized as the seizure of unknown onset. Focal seizures were again classified on the basis of the level of awareness and first motor or non-motor traits/features seen in the patient. As awareness is impaired, generalized onset seizures were not categorized on the basis of level of awareness. Generalized seizures were categorized on the basis of motor or non-motor manifestations where motor seizures are basically classified into two categories i.e. tonic-clonic and other motor seizures. Non-motor generalized seizures mainly refer to absence seizures (Fisher, 2017; Falco-Walter et al., 2018; Pack, 2019). Behavioral features of various types of generalized onset seizures as per ILAE classification are listed in Table 1.1.

Table 1.1 Behavioral features of various types of generalized onset seizures based on ILAE classification. (Adapted from Fisher, 2017; Falco-Walter et al., 2018; Pack, 2019)

Types of generalized onset seizures		Behavioral features
Motor	Tonic-clonic	Loss of awareness, rhythmic stiffening (tonic phase) and jerking (clonic phase) of limbs and face
	Clonic	Rhythmical jerking of limbs and/or face without stiffening phase
	Tonic	Stiffening of limbs without clonic jerking phase
	Myoclonic	Unsustained irregular bilateral jerking of eyes, face and limbs
	Myoclonic-tonic-clonic	Similar to tonic-clonic seizure but few myoclonic jerks on both sides of body
	Myoclonic-atonic	Few myoclonic jerks with a limp drop (especially children with Doose syndrome)
	Atonic	Sudden loss of muscle tone and strength (very brief)
	Epileptic spasms	Flexion of trunk and flexion/extension of limbs
Non-motor (absence)	Typical	Sudden loss of ongoing activity with sometimes eyes fluttering and head nodding (spike and wave discharges in EEG)
	Atypical	Similar to typical absence seizure but slow onset and recovery, and change in tone is seen
	Myoclonic	First few jerks and then an absence seizure
	Eyelid myoclonia	Jerk of the eyelids and deviation of the eyes (sometimes associated with absence seizures)

Non-motor or absence seizures are common in various forms of adult and pediatric epilepsies. However, CAE and juvenile absence epilepsy (JAE) are two epilepsy syndromes where absence seizures are the basic features. These two epilepsies have closely matching characteristics and they overlap in the age of onset. Children with CAE have more severe impairment of consciousness and more frequent absence seizures compared to JAE (Tenney and Glauser, 2013). CAE is the most common form (10-17%) of all pediatric epilepsies, which is the main focus of this thesis.

1.2.1 Absence epilepsy: an overview

Absence epilepsy is a genetic, generalized and non-convulsive form of epilepsy. This form of epilepsy is common in children 2-12 years of age and peaks between 5 and 7 years. This disorder is more prevalent in girls than in boys (Camfield et al., 1996; Matricardi et al., 2014). Absence seizures (previously termed as petit mal seizures) are characterized by a sudden and brief loss of consciousness that interrupt ongoing activity (Crunelli and Leresche, 2002a). The episode of 'absence' happens so fast that it is easy to miss or confuse with daydreaming or not paying attention. During these episodes, the child suddenly loses their sense of awareness followed by staring blankly into space and not responding to the surroundings. Absence seizures are also associated with eyelid flickering and purposeless movement of the fingers, hands and/or mouth. As soon as the seizure stops, the patient resumes their normal activities. Although the seizure of this kind only lasts for few seconds, it can occur hundreds of times a day (Panayiotopoulos, 1999) and may be associated with difficulties in learning, problems in visual attention, behavioural disorder, poor academic achievement and cognitive dysfunction (Vanasse et al., 2005; Caplan et al., 2008; Killory et al., 2011; Vega et al., 2011; Tenney and Glauser, 2013). This disorder is also believed to cause disruptions in the structural network of the developing brain and these alterations may cause the impairments to grow worse over time (Qiu et al., 2017). Similar to other forms of epilepsy, children with absence epilepsy may also undergo some form of social isolation and discrimination.

1.2.2 EEG features of absence seizures

The primary diagnostic test for absence seizures is EEG. The EEG signature of absence seizures is a bilateral synchronous SWDs measuring 2.5-4 Hz. SWDs consists of a high amplitude spike, positive transient and a slow wave as shown in figure 1.4A. These SWDs appear in clusters and can last for about 4-20 seconds (Panayiotopoulos, 2001). Studies conducted on human patients and animal model of absence epilepsy have shown that absence seizures are initiated from certain cortical regions (Meeren et al., 2002; Holmes et al., 2004; Gotman et al., 2005; Polack et al., 2007; Bai et al., 2010; Berman et al., 2010). During absence seizure, SWDs are also present in the thalamus (Williams, 1953; Velasco et al., 1989; Iannetti et al., 2001). This has led to a widespread consensus that SWDs seen in absence seizures are generated due to the dysfunctional behavior in the brain network involving cortex and thalamus (Kostopoulos, 2001; Blumenfeld; 2002; Crunelli and Leresche, 2002b). EEG traces from rodent genetic models of absence epilepsy showing the characteristic spike and wave pattern are also shown (Fig. 1.4B-D).

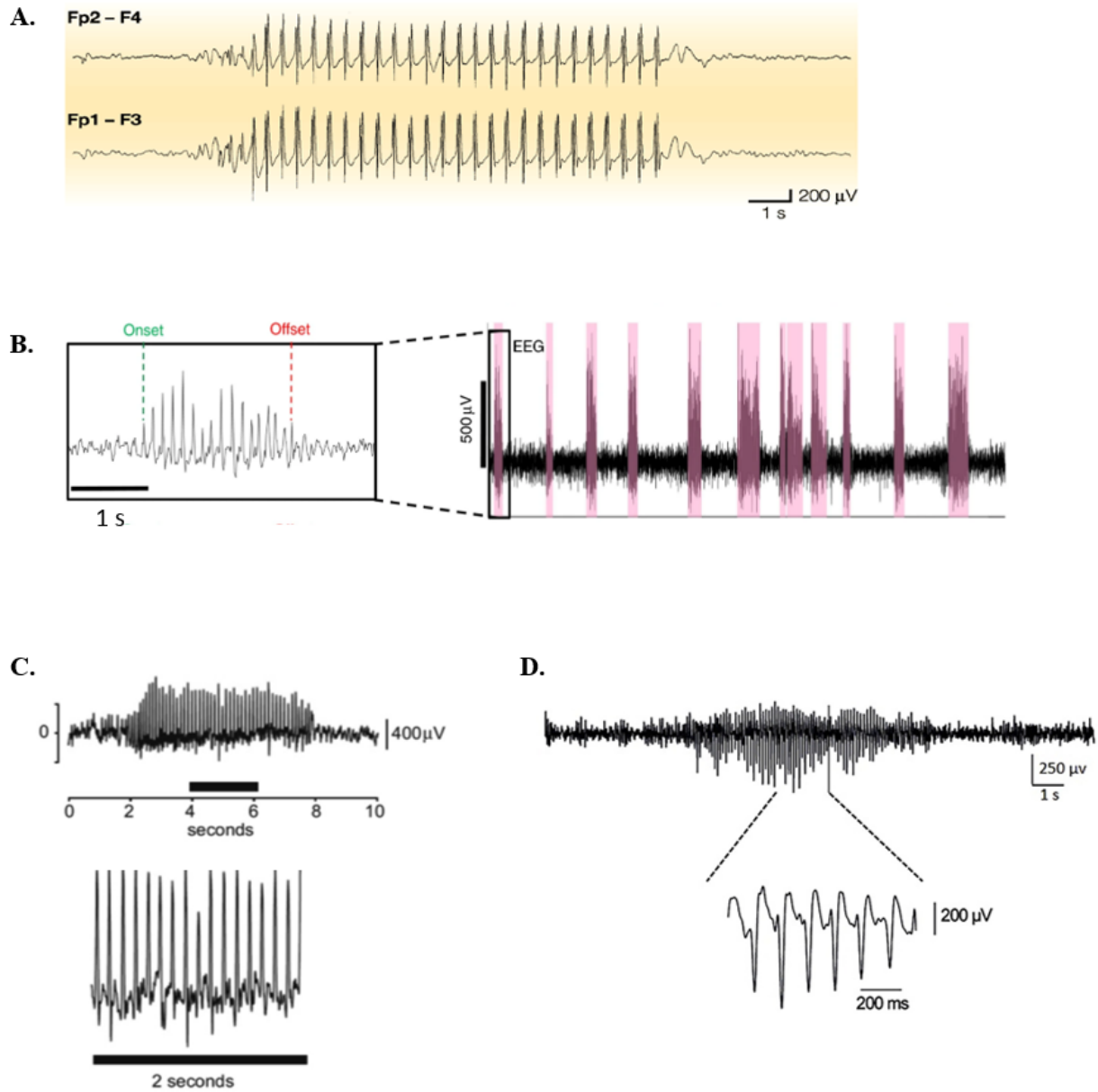


Fig. 1.4 EEG recordings of absence seizure in a child with CAE and rodent genetic models of absence epilepsy. (A) EEG recordings from a child with frequent absence seizures showing 3-Hz SWDs (Crunelli and Leresche, 2002a) and from rodent genetic models of absence epilepsy (B) stargazer mouse (Meyer et al., 2018) (C) Wistar Albino Glaxo from Rijswijk (WAG/Rij) rat (D'Amore et al., 2016) (D) Genetic Absence Epilepsy Rat from Strasbourg (GAERS) (Depaulis and Charpier, 2018).

1.2.3 Aetiology of absence epilepsy

Aetiology of absence epilepsy is considered to be genetic with complex and multiple gene defects (Steinlein, 2004). Studies have shown that if any individual's first-degree relative (a family member who shares about 50 percent of their genes) have positive history of this disorder, there is 16-45% chance that the individual will acquire absence epilepsy. Genetically identical monozygotic twins carry this risk from 70 to 85% (Fig. 1.5) (Bianchi, 1995; Loiseau et al., 1995; Berkovic, 1997; 1998; Scheffer and Berkovic, 2003). Even though the mode of inheritance is not yet completely understood, absence epilepsy is considered as a familial disease with complex genotype compared to other inherited epilepsies. In few cases, familial genetic defects have been linked with abnormal changes in membrane receptors and channels (Crunelli and Leresche, 2002a).

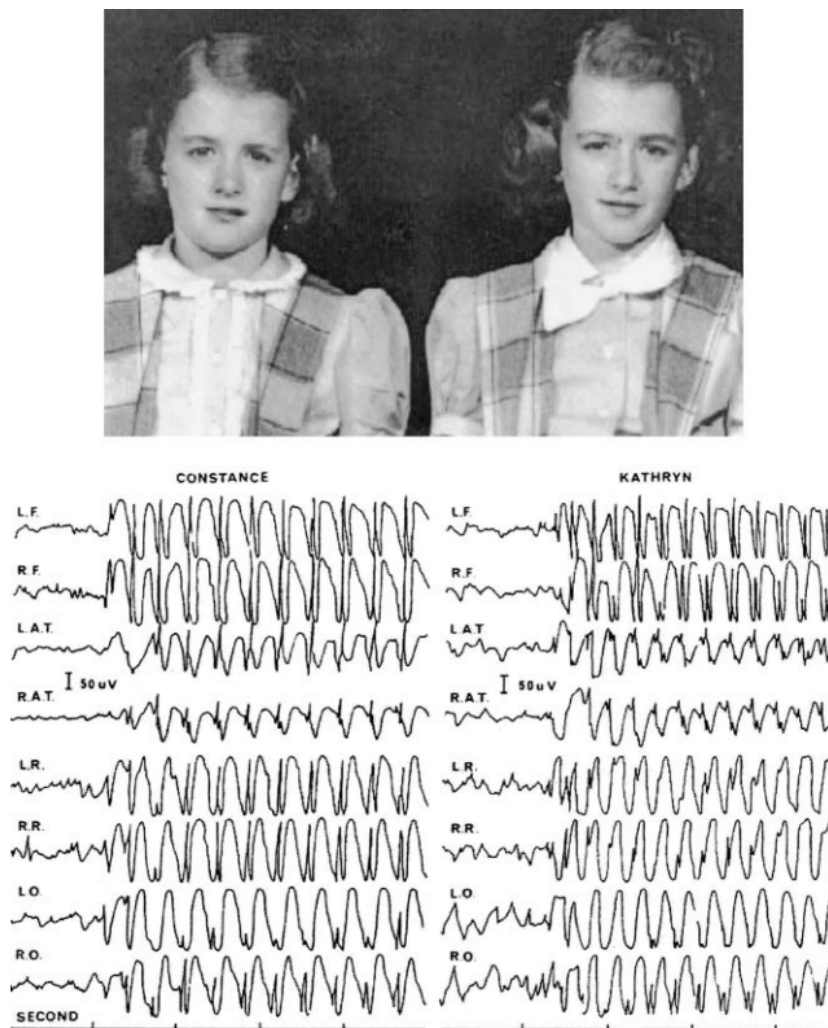


Fig 1.5 Photograph and EEG profile of Constance and Kathryn, monozygotic twins who suffered from childhood absence epilepsy. This case was reported by American neurologist William Gordon Lennox in 1949. (Adapted from Vadlamudi et al., 2004)

Genes associated with absence epilepsy are mostly found to be involved either with GABAergic neurotransmission or T-type calcium channel. Mutation in $\alpha 1$ subunit of GABA_A receptor was reported in patients with absence epilepsy (Feucht et al., 1999; Maljevic et al., 2006). Studies conducted in a Mexican population with history of absence epilepsy were reported to have multiple mutations in GABRB3 gene (which encodes for the $\beta 3$ subunit of GABA_A receptor) (Tanaka et al., 2008). Some possible association of this mutation and absence epilepsy were seen in studies conducted in Austria (Feucht et al., 1999; Urak et al., 2006) but such link was not observed in a study in Germany (Hempelmann et al., 2007). Mutation in GABRG2 gene which codes for the $\gamma 2$ subunit of this receptor was found to be associated with absence epilepsy (Wallace et al., 2001; Kananura et al., 2002; Kang and Macdonald, 2016). However, this mutation was not evident as a major genetic cause of absence epilepsy in two separate studies conducted on Chinese and Japanese subjects (Lu et al., 2002; Ito et al., 2005). A few cases of absence epilepsy were also linked to mutation in SLC2A1 gene [deficiency of Glucose transporter type 1 (GLUT1)] (Suls et al., 2009; Arsov et al., 2012; Muhle et al., 2013) and LGI4 gene (leucine-rich, glioma inactivated 4) (Gu et al., 2004).

CACNA1G, CACNA1H and CACNA1I are three different genes which encode three variants of the $\alpha 1$ subunits of T-type Ca²⁺ channel [i.e. $\alpha 1G$ (Ca_v3.1, chromosome 17q22), $\alpha 1H$ (Ca_v3.2, chromosome 16p13.3), and $\alpha 1I$ (Ca_v3.3, chromosome 22q13.1)]. Studies have revealed that CACNA1G and CACNA1H genes are not directly linked but have close association and may play a crucial role in the development of epileptic phenotype (Heron et al., 2004; Singh et al., 2007). CACNA1H was found to be a susceptible gene causing absence epilepsy in the Chinese Han population (Chen et al., 2003; Liang et al., 2006; 2007) and one rat model of absence epilepsy (GAERS) (Proft et al., 2017) but not in Caucasians (Heron et al., 2007). The CACNA1I gene has been reported to have no significant relationship with absence epilepsy in the Chinese Han population (Wang et al., 2006). Mutations of CACNG3 (which encodes $\gamma 3$ subunit of Ca²⁺ channel) (Everett et al., 2007a) and CLCN2 (which encodes chloride channel protein 2) (Everett et al., 2007b; Saint-Martin et al., 2009) genes have been linked to absence epilepsy. Mutations in CACNA1A gene which encodes for the $\alpha 1A$ subunit of P/Q-type high voltage gated Ca²⁺ channels have been reported in patients with absence seizure and episodic ataxia (Jouveneau et al., 2001; Imbrici et al., 2004). This mutation was also found in a few mouse models of absence epilepsy and ataxia (Fletcher et al., 1996; Doyle et al., 1997; Fletcher and Frankel, 1999; Wakamori et al., 1998). In summary, population-wide association analysis

and investigation of genetic variants in specific probands showed that no single gene is ubiquitously linked to absence epilepsy. It thus appears that this disorder is associated with multiple genetic defects. The search for a therapeutic target by utilizing animal models may provide useful information.

1.2.4 Age of onset, prevalence and mortality of absence epilepsy

Childhood absence epilepsy mostly occurs in children and may continue into adulthood. The age of onset of this disorder is 2-12 years with peak manifestations at 5-7 years of age. In terms of gender, boys and girls are equally affected but girls are believed to be more susceptible to develop absence epilepsy (Crunelli and Leresche, 2002a). One study has shown that 59-73% of cases of absence epilepsy occur in females (Durá and Yoldi, 2006). Prevalence of this disorder has been estimated from 0.4 to 0.7 per 1000 individuals (Jallon and Latour, 2005); and, the incidence of this disorder is 36 per 100,000 individuals (Aaberg et al., 2017). Absence epilepsy does not cause deaths directly but there is always a risk of physical injury to the children when individuals face episodes of absence seizures while swimming, cycling, etc. These injuries may lead to death.

1.2.5 Prognosis and treatment of absence epilepsy

Several epidemiologic cohort studies have reported wide range of remission rates of CAE. It should be noted that these remission rates depend on the different selection criteria adopted in those studies, diverse follow-up periods, age at last assessment, therapy, inclusion of absence epilepsies other than CAE etc. It has been reported that remission rate of absence epilepsy is up to 74% (Tenney and Glaucer, 2013). Five-year remission rate ranges from 56-65% (Wirrell et al., 1996; Trinkka et al., 2004). In one third of patients, seizures remain either as absence seizures (10-15%) or absences with either myoclonic or generalized tonic-clonic seizures (5-15%) or develop into juvenile myoclonic epilepsy (5-15%) (Camfield et al., 2014). One study showed that absences persisted beyond the age of 20 years in only 10% of patients (Loiseau et al., 1995). One recent study reported that if absence epilepsy persists beyond adolescence, long-term seizure and psychosocial outcome do not differ between childhood and juvenile onset of absence epilepsy (Holtkamp et al., 2017). JAE presents in late childhood or adolescence, where 80% of subjects suffer from generalized tonic-clonic seizures, infrequent typical absences and myoclonic jerks and often achieve seizure control. Patients with JAE usually require lifelong treatment (Wirrell et al., 2003). Studies have also shown that the tendency to develop generalized tonic-clonic seizure is high when absence epilepsy develops

later in childhood (past 8 years of age). Such risk is as high as 50% (Bouma et al., 1996). It is important to note that even after complete remission, individuals require special educational help. They face linguistic difficulties and are less likely to graduate from high school or attend college/university as their academic performance is below average. They also experience long term psychosocial impairment (Wirrell et al., 1997; Pavone et al., 2001; Camfield et al., 2014). Altogether, it seems that higher the patient's age, chance of terminal seizure remission increases and it's still unclear if CAE needs to be treated beyond adolescence.

AEDs are used for the treatment of CAE to reduce the frequency of seizures. ETX and valproic acid are the first choice AEDs used for the treatment of absence epilepsy which act on T-type calcium channel and sodium-channels. ETX reduces the amplitude of the low-threshold (T-type) calcium current in the neurons of the ventrobasal complex and the reticular nucleus of the thalamus; however, valproic acid is believed to increase the level of γ -aminobutyric acid (GABA) in the brain and affect sodium and calcium channels (Matricardi et al., 2014). Success rate of ETX and valproic acid lies between 70-80% (Richens, 1995; Schachter, 1997; Hwang et al., 2012), but a systemic review of clinical studies published in 2010 concluded that there is insufficient evidence to recommend any drugs for clinical practice against absence epilepsy. This review criticized the poor methodological quality and insufficient number of participants used in clinical trials (Posner et al., 2005). Large-scale clinical trials conducted after this publication suggest that efficacy of ETX and valproate were considerably lower i.e. 45-53% (ETX) and 44-58% (valproate) (Glauser et al., 2010; 2013) than previous findings. Patients unresponsive to monotherapy of either ETX or valproic acid and lamotrigine were found to have responded to a combination of two of the three drugs (Schachter, 1997; Glauser et al., 2010). Various other drugs such as clonazepam, benzodiazepine, and acetazolamide are also prescribed in small doses for the treatment of this disorder (Hughes, 2009; Panayiotopoulos, 1999). Medications that are used to treat convulsive seizures (such as phenytoin, carbamazepine, vigabatrin, tiagabine) have been found to worsen absence seizures (Schachter et al., 1997; Parker et al., 1998; Perucca et al., 1998) and to induce seizure in some cases (Schapel and Chadwick, 1996; Ettinger et al., 1999). Several studies have reported that AEDs can have adverse side effects in patients which include ataxia, sedation, dizziness and cognitive dysfunction. Seizure aggravation, poor efficiency, unpredictability of effect, loss of effect during prolonged treatment and drug resistance are other major problems associated with AEDs (Bauer, 1996; Abou-Khalil, 2012; van Luijtelaar and Sitnikova, 2006). The tolerability profile of each drug is different and drug interaction is another major issue in the clinical use of AEDs (Patsalos and Perucca, 2003a; 2003b; French and Pedley, 2008).

Hence, more targeted approaches are required for the treatment of absence epilepsy which are safe, effective, and patient specific. This requires a deep understanding of cellular and molecular mechanisms of absence seizures to develop novel therapeutic targets and discovery of new AEDs.

1.2.6 Pathogenesis of absence epilepsy in human patients and animal models

CAE is considered as a disorder with a multifactorial genetic etiology. No significant and conclusive findings were obtained from genetic analysis. Remission rates and effectiveness of treatment and are encouraging but not promising. Pathophysiological mechanisms are still unclear and mostly unknown. The use of animal models, however, has allowed us to conduct various types of experiments and interrogate the mechanisms underlying this disorder which are impossible to perform on human patients. Findings gathered from animal and human studies regarding the pathogenesis of this disease are described below.

1.2.6.1 Animal models

Animal models are powerful tools to examine and understand the basic principles and mechanisms of diseases and disorders. To date, various animal models of epilepsy or epileptic seizures are established and characterized. They mirror the genetic make-up and/or the phenotype of human epileptic patients. Some models of epilepsy or epileptic seizures are illustrated in the figure below (Fig. 1.6)

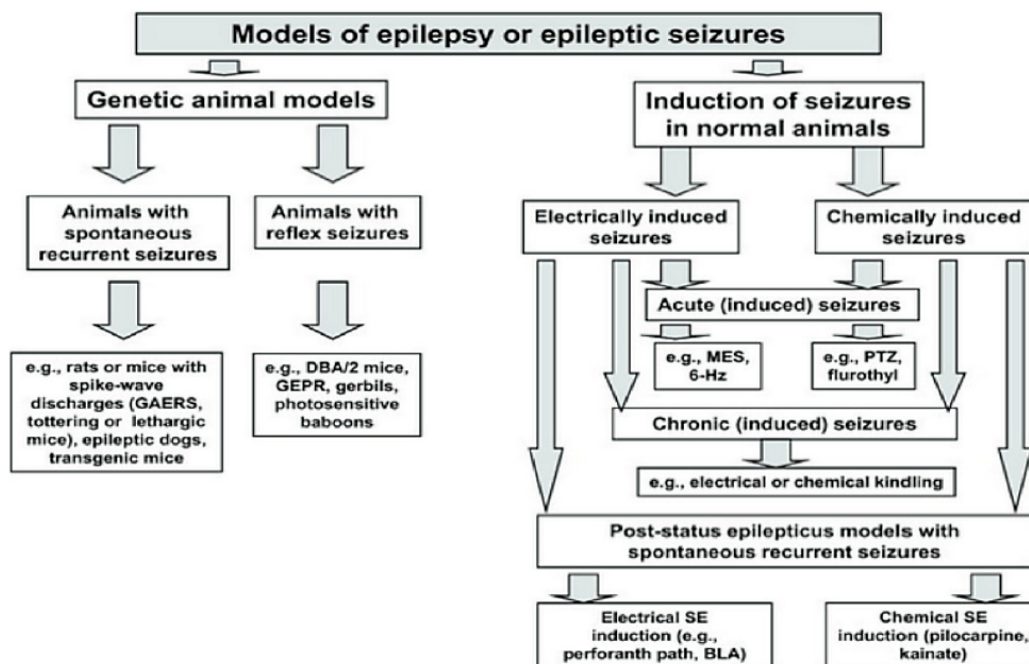


Fig. 1.6 An overview of models of epilepsy or epileptic seizures (Taken from D'Amore, 2016)

The focus of this thesis is absence epilepsy. So, the existing absence epilepsy models or absence seizure models will be briefly described.

Animal models related to absence epilepsy

The utility of any model depends on a number of parameters such as similarity to human condition and symptoms, predictive validity and tractability to investigation. The animal models related to absence epilepsy that has been developed and characterized can be broadly classified into two groups i.e. pharmacological models in which seizures are induced by the administration of drugs or chemical substances and genetic models which involve strains that are genetically predisposed to absence seizures. Pharmacological models are widely popular where chemicals such as PTZ, γ -Hydroxy-butyrate, penicillin, bicuculline, picrotoxin etc. are acutely or chronically administered to induce absence seizures. These models are normally used to elucidate the mechanisms of ictogenesis but not epileptogenesis (Avanzini, 1995; Kostopoulos, 2017). These chemicals are efficiently used to screen antiepileptic drugs in epileptic studies (Krall et al., 1978; Snead, 1992; Löscher, 2011; Velišková et al., 2017). On the other hand, genetic rodent models of absence epilepsy show spontaneous seizures and closely reflect the pathophysiology of human absence seizures. Genetic models are widely used to interrogate and understand the pathogenesis of absence epilepsy. Stargazer mouse, GAERS and WAG/Rij are currently the most widely used animal models of absence epilepsy which are briefly described below.

Stargazer mice

The stargazer mouse model is one of over 20 monogenic mouse mutants showing the same phenotype i.e. frequent SWDs associated with behavioral arrest that are sensitive towards anti-absence epileptic drug ethosuximide (Maheshwari and Noebels, 2014). In the 1980s, abnormal behavioural features such as unsteady gait and repeated head elevations were seen in A/J mouse inbred strain at The Jackson Laboratory (JAX#001756) (Noebels et al., 1990). Later, breeding studies revealed the genetic cause. Electro-clinical feature (6-7Hz SWDs with behavioural arrest) of this animal model was also characterized and was found to be similar to absence seizure in humans (Noebels et al., 1990). It was also revealed that SWDs first appear around postnatal days 17-18 in stargazers (Qiao and Noebels, 1993).

Stargazers are the result of defect in the calcium channel γ 2-subunit gene CACNG2 which reduces the expression of stargazin protein (Noebels et al., 1990; Letts et al., 1997; 1998). Stargazin is a transmembrane AMPAR regulatory protein (TARP) critical for synaptic

targeting and membrane trafficking of AMPARs at excitatory glutamatergic synapses (Chen et al., 2000). AMPA receptors are glutamate-gated ion channels, which primarily mediates the fast-excitatory synaptic transmission in CNS. Release of glutamate at the excitatory synapse leads to the rapid opening of AMPA receptors and membrane depolarization. Defects of the stargazin protein causes the loss of AMPARs which impairs excitation at glutamatergic synapses. This might lead to the loss of function of inhibitory neuron synapse and alter CTC network oscillations. Studies have shown that there is significant reduction of GluA4 containing subunits of AMPARs in cortical PV+ inhibitory neurons in stargazer mice. These studies concluded that loss of excitatory drive onto inhibitory PV+ interneurons may be involved in the generation of seizures (Adotevi and Leitch, 2016; 2017; 2019). Other studies have also shown that impaired AMPA receptor regulation in the SS cortex (Maheshwari et al., 2013) and thalamus (Menuz and Nicoll, 2008; Barad et al., 2012) may contribute in generation of absence seizures. In addition, GABA level (Hassan et al., 2018) and GABAR expression (Seo and Leitch, 2014; 2015) were found to be upregulated in the CTC network of stargazers. This is also believed to contribute to absence seizures in stargazer mice.

Rat absence epilepsy models

GAERS and WAG/Rij are the two most frequently used rat polygenic models of absence epilepsy (Marescaux and Vergnes, 1995; Coenen et al., 1992). GAERS were developed by selective breeding of the 30% of Wistar rats displaying short and irregular spontaneous SWDs. WAG/Rij strain is an inbred strain of albino rats. These rat models feature 7–11 Hz SWDs which starts in the cortex and spread bilaterally to both cortical and thalamic regions (Meeren et al., 2002; Polack et al., 2007; Rudolf et al., 2004). SWDs first appear at around 2 months and postnatal day 30 in WAG/Rij and GAERS, respectively (Coenen and Van Luijtelaar, 2003; Marescaux and Vergnes, 1995). In both models, number, duration and frequency of SWDs increases with age. Even though, the frequency of the oscillations seen in these rat models are higher than in human patients, the waveform of the SWDs in EEG is remarkably similar to the ictal waveforms seen in human patients with absence epilepsy (Sitnikova and van Luijtelaar, 2007).

In human absence seizure, SWDs typically recur at a slow frequency of about 3 Hz (2.5-4 Hz), whereas in rodent models they occur faster i.e. epileptic stargazers (6-7 Hz) and GAERS and WAG/Rij rats (7–11 Hz). Features of SWDs exhibit the same general trend and belong to the

Species	Strains	Age of onset	Duration of SWDs (sec)	Rhythmicity (Hz)	Reported mutations	Phenotypes
Mouse	Stargazer	PN17-18	6	6-7	CACNG2	Absence, ataxia, headtossing
	Tottering	~4 weeks	0.3-10	6-7	CACNA1A	Absence, ataxia, focal motor seizure
	Lethargic	After PN15	0.6-5	5-7	CACNB4	Absence, ataxia, focal motor seizure, lethargic, dyskinesia
	Ducky	-	0.6-5	5-7	CACNA2D2	Absence, ataxia, dyskinesia
	C3H/HeJ	~PN26	3.4	7-8	Natural IAP retrotransposon insertion in Gria4	Absence
	Rocker	-	1-1.7	6-7	CACNA1A (chemical mutagenesis)	Absence, ataxia, dyskinesia, tremor
Rat	GAERS	Oscillations: PN15-25	2-3	5-6	CACNA1H	Absence
		Mixed SWDs: PN26-40	5-9	5-6		
		SWD: >PN60	12-22	7-9		
	WAG/Rij	~2 months	1-45	7-11	-	Absence
	GRY	6-8 weeks	8-10	7-8	CACNA1A	Absence, ataxia
	SER	7-8 weeks	1-17	5-7	tm and zi	Absence, tonic, tonic-clonic

Table 1.2 Epileptic features of genetic models of absence epilepsy in mice and rats. The main characteristic is the presence of SWDs which varies in terms of duration and rhythmicity. The age of onset of SWDs also varies with strain and species. Reported mutations mainly concern calcium channels. PN: postnatal day (Adapted from Jarre et al., 2017).

same electrophysiological phenomena in all rodent models, some parameters of SWDs show slight to significant differences between rodent models (Onat et al., 2007, Akman et al., 2008, Chahboune et al., 2009). Akman and colleagues have reported that the number, cumulative total duration and mean duration of SWDs are significantly higher in GAERS compared to another rat model (WAG/Rij), while the discharge frequency is higher in the WAG/Rij.

In relation to the nature of the SWDs waveforms, spike (upward deflections) and late positive transient (downward deflections) are larger in the GAERS group implying a single cycle of the SWD contains more energy in faster components (spike and late positive transient) in the GAERS (Fig. 1.4). On the other hand, mean SWD frequency for WAG/Rij is significantly higher in the beginning of each SWD and decreased strongly than that in GAERS (Akman et al., 2010). Such differences in the SWD phenotype may be due to the changes in specific components of the basic mechanism that is probably common for both strains (Akman et al., 2010). Genetic studies on GAERS (Rudolf et al., 2004) and WAG/Rij (Gauguier et al., 2004) rats showed polygenic control of SWDs and also the differential effect of gene variants (at the loci) on the average duration and number of SWDs. One example of such difference was reported by Powell and colleagues in 2009. They found a T-type Ca²⁺ channel mutation plays significant role in the absence epilepsy phenotype in GAERS in terms of number and cumulative duration of seizures. Interestingly, WAG/Rij rats did not carry any copy of this mutation (Powell et al., 2009). Thus, differences in features of SWDs might be important variables in defining phenotypes of the absence epilepsy and distinctly different spike-wave cycle seen in GAERS compared to other models might be an additional phenotypic feature of absence epilepsy. The epileptic features of animals described above and other few other rodent models of absence epilepsy (such as tottering, ducky, rocker and C3H/Hej, GRY, SER etc.) are shown in the Table (Table 1.2).

1.2.6.2 Human patients

New imaging techniques have been particularly successful in detecting changes in the epileptic brain of human patients. These methods include magnetic resonance imaging (MRI), proton magnetic resonance spectroscopy (PMRS), low-resolution electromagnetic tomography (LORETA), positron emission tomography (PET), diffusion tensor imaging (DTI), functional MRI (fMRI), single photon emission spectroscopy (SPECT), intrinsic optical signal (IOS) imaging, and

near-infrared spectroscopy (NIRS) (Lenkov et al., 2013). Outcomes from the use of these techniques in patients with other forms of epilepsy have been very promising (Chahboune et al., 2009; Mishra et al., 2011), but these techniques are not heavily used and researched in patients with absence epilepsy. Most of the imaging techniques described below are based on the same basic principle that increased neuronal activity increases the metabolism which changes the cerebral blood flow and the amount of oxygen consumed.

Studies have shown that PET was the first imaging technique utilized in patients with absence epilepsy. Result from these studies indicated that there is an increase of neocortical and thalamic glucose metabolism in children with absence epilepsy (Engel et al., 1985;1996; Ochs et al., 1987; Iannetti et al., 2001). Similarly, 4-8% of the increase in thalamic blood flow was seen in patients during absence seizures (Prevett et al., 1995) and few contrasting results were observed. A SPECT study found an increased blood flow, but another technique, Doppler ultrasound, revealed reduction of blood flow in the middle cerebral artery during episodes of absence seizures (Bode, 1992; Yeni et al., 2000; Nehlig et al., 2004). NIRS reported increased cerebral blood volume in patients with convulsive seizures but in patients with absence epilepsy there was a mild reduction in cerebral blood volume (Haginoya et al., 2002).

A combination of LORETA and 256 channel EEG scalp recording with equivalent dipole (BESA) have shown that SWDs are distributed onto distal cortical areas during absence seizures (Holmes et al., 2004; Tucker et al., 2007; Clemens et al., 2011). The use of fMRI also demonstrated the participation of thalamic and cortical networks during absence seizures (Salek-Haddadi et al., 2003). Recently, combination EEG-fMRI has revealed changes in blood-oxygenation-level dependent (BOLD) effect in the basal ganglia–thalamocortical network during interictal and ictal events of absence seizures (Li et al., 2009). In agreement with the results from Li and colleagues, other studies have reported the involvement of cortical-subcortical network during absence seizures (Salek-Haddadi et al., 2003; Berman et al., 2010; Moeller et al., 2010). In addition to the methods explained above, other techniques such as optical imaging of intrinsic signal (IOS), voltage-sensitive dye imaging (VSD), photoacoustic imaging (PA) and optical coherence tomography (OCT) are also emerging as techniques offering maximum potential but have not been used extensively in absence seizure research (Lenkov et al., 2013).

Imaging studies on human patients have also indicated the involvement of cortical and thalamic regions of the brain during the episodes of absence seizures. These studies suggest that the

dysfunctional CTC network is one of the reasons underlying absence seizure generation. However, precise cellular and molecular mechanisms underlying absence seizure generation are not fully understood. Therefore, a deep understanding of anatomical framework and neuronal elements of CTC network, and their normal functioning is required which is described in the next section.

1.3 The Cortico-thalamocortical Network

The CTC network is the complex network of reciprocal connections between two crucial brain structures i.e. cortex and thalamus. Communication between these two regions are mediated by thalamocortical (TC) and corticothalamic (CT) pathways (Jones, 2002; Pinault and O'Brien, 2005). Anatomical function and structure of the CTC network can be divided into cortical and thalamic components.

1.3.1 The cerebral cortex

The cortical part is entirely composed of neocortex which makes up around 76% of the entire brain and 90% of the cerebral cortex. Cellular organization of the neocortex is a vertical six-layered arrangement into functional units called cortical layers (Noback et al., 2005). The cortex is made up of both excitatory and inhibitory neurons. 80% of all cortical neurons are excitatory pyramidal neurons while the remaining 20% are inhibitory interneurons (Markram et al., 2004). The most superficial layer I which is also known as the molecular or plexiform layer, contains very few neurons and mostly axons, dendrites and axon terminals of neurons whose cell bodies are located in deeper cortical layers. Layers II and IV contain densely packed granule cells and are known as the external granular layer and internal granular layer, respectively. Layers III and V contain mainly pyramidal cells which are referred to as the external pyramidal layer and internal pyramidal layer respectively. Layer VI is known as the multiform layer and contains several different neuronal types including some fusiform cells, granule cells and pyramidal cells. Cortical layers I-III primarily form intracortical connections whereas V-VI layers serve as the output layers connecting the cortex to other subcortical regions (Akgül and McBain, 2016). The internal granular layer (layer IV) and multiform layer (layer VI) are the integral part of the CTC network as layer IV receives TC projections from thalamic nuclei and layer VI sends reciprocal excitatory CT projections back to the thalamus (Markram et al., 2004). The cortex generally relies on potent

GABAergic inhibition to regulate neural cortical excitability and excitatory TC input (Jones, 2009).

1.3.2 The thalamus

The thalamus is situated between the cerebral cortex and midbrain, superior to the brain stem. It provides the largest source of afferent fibers to the cerebral cortex. It is functionally composed of different nuclei that are involved in the relay of motor and sensory signals to the cerebral cortex (Sherman and Guillery, 1996; 2002). Thalamic nuclei are reciprocally connected with the cortex which controls the flow of information to a specific cortical region (Siegel and Sapru, 2011).

Reticular thalamic nucleus (RTN)

During development, RTN migrates dorsally and ends up as a thin capsule of GABAergic neurons wrapping around the dorsal thalamus laterally, anteriorly, and partially posteriorly and ventrally. The RTN is also innervated by the basal forebrain and brain stem. The RTN allows the passage of

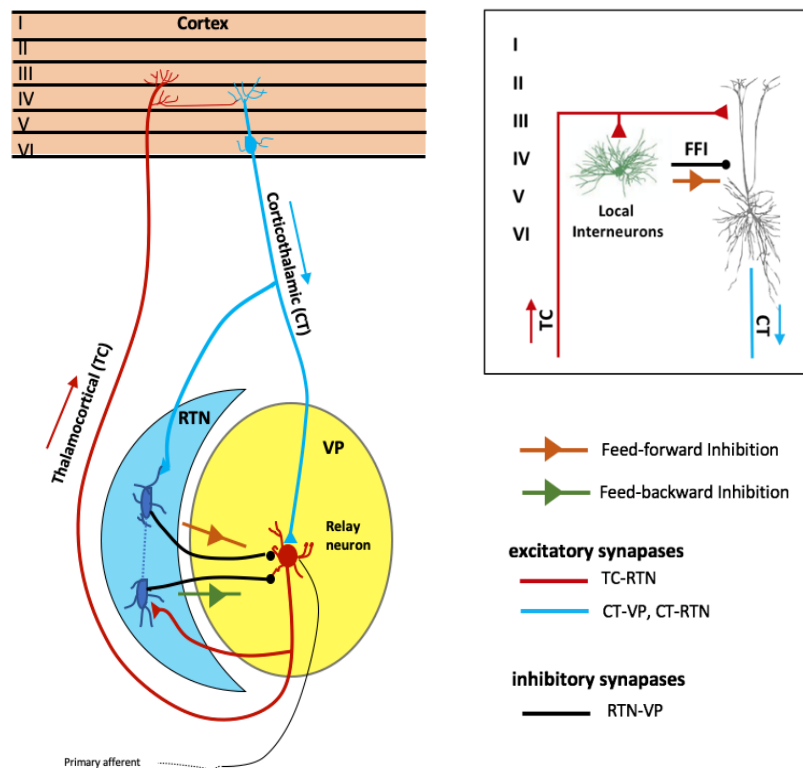


Fig. 1.7 A simplified illustration of the CTC network showing reciprocal connections between cortex and thalamus. (Adapted and modified from Sherman and Guillery, 1996; Khosravani and Zamponi, 2006)

the corticothalamic (CT) projection forming the CT-RTN connection. It also receives excitatory input from the thalamocortical (TC) relay neurons (Liu and Jones, 1999). TC and CT projections to the RTN are reciprocally connected which allows the RTN to evaluate information transmitted to-and-from the cortex (Steriade et al., 1987; Fuentealba et al., 2005a; 2005b) as shown in figure 1.7. CT inputs to the RTN are more numerous than TC inputs which forms about 70% of synapses onto the RTN neurons.

Ventral Posterior (VP) nucleus

The ventral posterior (VP) nucleus is composed of two nuclei i.e. ventral posterolateral nucleus (VPL) and ventral posteromedial nucleus (VPM). The relay neurons of the VP are excitatory, and these neurons receive excitatory input from the peripheral afferent fibers and cortical CT projections (Sherman and Guillery, 1996). The main source of inhibition in VP comes from the RTN (Fuentealba and Steriade, 2005a; 2005b). VP relay neurons also send excitatory TC projections to the cortical principal cells and collateral fibers to the RTN.

The fundamental anatomy of the various projections of the CTC network are listed below (McCafferty, 2014):

- 1) Thalamocortical (TC): thalamic nuclei to layer IV (primarily) of associated cortical region.
- 2) Intracortical connections: inter-layer (IV to II/III, IV to V/VI) and inter-region (II/III to II/III, II/III to V/VI).
- 3) Corticothalamic (CT): layers V and VI to specific and non-specific thalamic nuclei, the majority being precise reciprocals of TC projections.
- 4) Intrathalamic connections: extent unknown.
- 5) Thalamoreticular and corticoreticular: collaterals from TC and CT projections innervating RTN en route to associated cortical & thalamic region respectively.
- 6) Reticulothalamic: sole projections of RTN, inhibiting TC cells in the thalamic nucleus.
- 7) Intrareticular: inhibitory communications between neurons of the RTN.

Thalamic relay neurons of the VP region and the cortical pyramidal neurons form mutual excitatory connections that are regulated through the activation of inhibitory interneurons within the thalamus and the cortex (McCormick and Contreras, 2001). The organization of the CTC

circuitry allows the inhibitory neurons of the RTN to be excited by collateral inputs coming from both the cortex and the TC relay cells, thus shifting between oscillatory and burst firing modes in order to regulate external stimuli. These modes are dependent on the state of voltage-dependent T-type Ca^{2+} channels (Williams and Stuart, 2000), which are highly expressed in the cortex and thalamus and are positioned to regulate synchronized oscillations within the CTC circuitry. As illustrated in the figure 1.7, the thalamic relay neurons receive sensory afferents from the periphery and project excitatory glutamatergic TC fibers to the excitatory pyramidal neurons and fast spiking interneurons within layer IV of the cortex. In turn the cortical neurons project reciprocal CT fibers from layer VI to the thalamic relay neurons. TC and CT projections also send excitatory collaterals to RTN. RTN neurons via FFI generate GABA mediated inhibitory postsynaptic potentials (IPSPs) to VP relay neurons which hyperpolarizes thalamic relay neurons. The IPSP deactivate T-type calcium currents and produces action potential bursts of the relay neurons. This post inhibitory burst firing of the TC relay neurons then excites both cortex and RTN to begin a cycle of rhythmic oscillatory activity.

Neuronal firing in the CTC network is dependent on the physiological state of the animal. Sleep spindles are characterized by low amplitude/high frequency activity whereas wakefulness is characterized by high amplitude/low frequency activity. Normal activity of the components of CTC network results in rhythmic spindle-like oscillation (also known as synchronized neuronal firing) which are required for normal brain functioning.

Rhythmic spindle-like oscillations changes into pathological SWDs due to the dysfunctional behavior within the CTC network (Kostopoulos, 2001; Blumenfeld; 2002; Crunelli and Leresche, 2002a). However, there is a long-standing debate about the role of CTC components on the pathophysiology of absence seizures. The existing theories in the pathophysiology of absence seizures, various concepts postulated in the past regarding the involvement of cortex and thalamus in absence seizure generation and recent developments are briefly described below and illustrated in the figure 1.8.

Centrencephalic theory

This theory was based on the findings from the studies conducted in human patients and cats (Jasper and Kershman, 1941; Morison and Dempsey, 1942; Jasper et al., 1947). According to this theory, epileptic discharges originate from the ‘centrencephalic integrating system’ which is thought to be located in the brainstem and diencephalon (Penfield and Jasper, 1954).

Cortical theory

Studies conducted by Gibbs and Gibbs in 1952 and Bennett in 1953 raised concerns over the validity of the centrencephalic theory (Gibbs and Gibbs, 1952; Bennett, 1953). The cortical theory purposed the leading role of the cortex in the generation of generalized absence seizures which was later supported by the work from other research groups (Bancaud, 1969; Niedermeyer, 1972; Lüders, 1984). Altogether, these studies postulated that generalized absence seizures are primarily due to cortical abnormalities and thalamus only has a secondary role in carrying out the thalamocortical interactions.

Corticoreticular theory

In 1968, Gloor purposed the essential roles of both the cortex and reticular system (thalamus and brain stem) in the generation of absence seizures (Gloor, 1968). This proposal was later refined by a study in the cat model of feline penicillin generalized epilepsy (Prince and Farrell, 1969). This theory is still widely accepted although the specific roles of cortex and thalamus and the exact mechanisms are still debated.

Thalamic clock theory

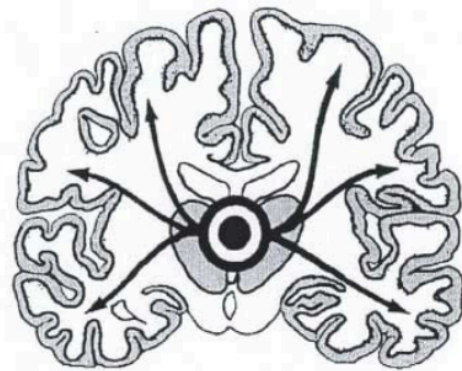
In 1991, Buzsàki proposed the thalamic clock theory. In his experiments, thalamic lesions (specifically RTN cells) stopped cortical high voltage spindles but ablation of cortex didn't abolish thalamic high voltage spindles in Fischer 344 rats. Buzsàki hypothesized that RTN contain the pacemaker cells for thalamus and phasic bursting in RTN induces bursting in TC relay cells which in turn excite more RTN cells. He further stated that these episodes recruit more cells until the entire thalamic network is involved in rhythmic discharges. These events finally force the rhythm onto the cortex (Buzsàki, 1991). This hypothesis was also supported by studies conducted in two other rat strains (GAERS and WAG/Rij) (Avanzini et al., 1992; Inoue et al., 1993; Seidenbecher et al., 1998). Altogether, these studies concluded that RTN serve as the pacemaker and TC relay cells drive cortical cells. This hypothesis established the thalamus as the generator of the cortical discharges.

Cortical focus theory and recent developments

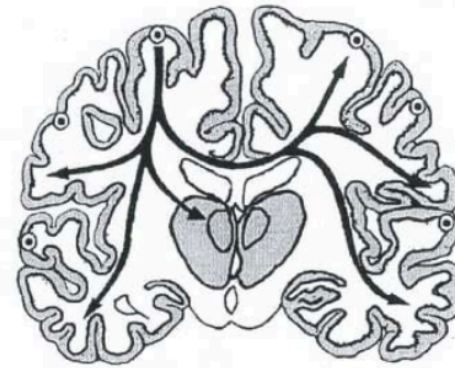
The cortical focus theory was proposed by Meeren and colleagues after performing nonlinear association analysis of the multi-site local field potentials measurements in the cortico-thalamic regions in WAG/Rij rats. They found that absence seizures initiate from the peri-oral region of primary SScortex. SWDs recorded in the other regions lagged behind this focal site. In their experiments, they consistently found cortical focus always leading the thalamic counterpart during the first few seconds (~500ms) of seizures. Afterwards, cortex and thalamus regions lag and lead the discharges in an unpredictable way (Meeren et al., 2002).

Results from other studies also supported the ‘cortical focus theory’. In GAERS, SWDs were found to be originated from SScortex (barrel field region) (Polack et al., 2007; Studer et al., 2019) and in pharmacological animal model (gamma-hydroxybutyric acid) absence seizures originated from prefrontal cortex (Snead et al., 1992; Venzi et al., 2015). This was confirmed when regional blocking of the firing of the neurons by infusing sodium channel blocker tetrodotoxin in SScortex (but not in motor cortex) of GAERS prevented absence seizures (Polack et al., 2009). These animal models were more sensitive to ethosuximide applied in the primary SScortex than ventrobasal thalamus or motor cortex (Marescaux et al., 1984; Richards et al., 2003; Manning et al., 2004). Notably, a recent study found that spontaneous SWDs seen in PLC β 4 knock-out mice originates from SScortex (Lee et al., 2019).

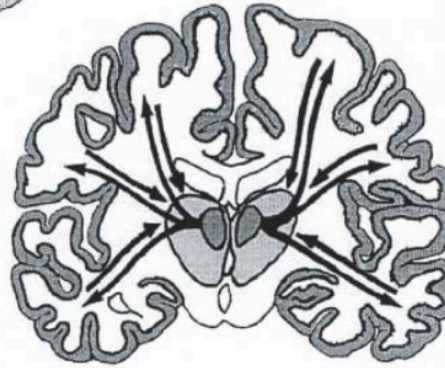
In relation to the initiation of absence seizure in human patients, EEG, MEG and fMRI studies conducted in young to adult populations, have shown neuronal activity changes in different regions of the cortex such as posterior cingulate cortex, precuneus, lateral parietal cortex and/or frontal cortex before the involvement of other regions of the brain (Holmes et al., 2004; Westmijse et al., 2009; Carney et al., 2010; Bai et al., 2011; Gupta et al., 2011; Benuzzi et al., 2012; Tenney et al., 2013; Wu et al., 2017). The first study on a cohort of patients with CAE have shown pre-ictal increase in blood oxygenation level-dependent signal amplitude in cortical area(s) (Bai et al., 2010, 2011; Moeller et al., 2010). Recently, a study investigated the dynamic behavior of large-scale brain networks by utilizing the phase synchrony data of the BOLD signal between different brain regions in people with generalized SWD and concluded that at least a minute before absence seizure there is a reduction of synchrony in occipital cortex and around 10 seconds prior to SWDs



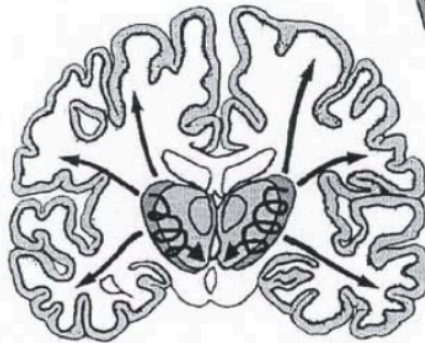
Centrecephalic Theory



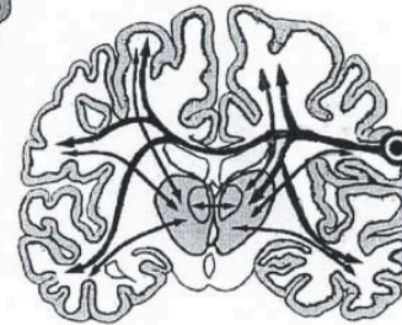
Cortical Theory



Corticoreticular Theory



Thalamic Clock Theory



Cortical Focus Theory

Fig. 1.8 Schematic representation of the 5 theories on the origin of generalized absence epilepsy. Thalamic theories are shown in the left side: the centrecephalic theory of Penfield and Jasper, and the thalamic clock theory of Buzsáki. Cortical theories are shown in the right side: the cortical theory of Bancaud, Lüders and Niedermeyer, and the cortical focus theory of Meeren and colleagues. Corticoreticular theory of Gloor is shown in the middle. (Taken from Lüders et al, 1984 and Meeren et al., 2005)

various cortical regions show linear and significant increase in synchrony. Such high level of synchrony was evident in the cortical regions even 20 seconds after the end of electrographic activity (Tangwiriyasakul et al., 2018). Rodent models of absence seizures, however, do not show widespread cortical changes in cerebral blood flow/volume and fMRI as seen in human patients. These variabilities might be due to the differences in cortical functions between human and animal models or mechanistic limitations of rodent models or anesthetics procedure used during animal imaging (reviewed in Crunelli et al., 2020). In summary, these data from animal and human studies indicate that altered cortical network is the originator of absence seizures.

However, experimental evidence suggests that thalamic regions are also responsible in generating absence-SWDs in animals (Avoli, 2012; Taylor and Crunelli, 2014; Luttjohann and Van Luijtelaar, 2015; Sorokin et al., 2017). Pharmacological manipulations such as infusion of GABA agonists into thalamus of GAERS promoted SWDs but infusion of GABA or glutamate antagonists prevented SWDs (Marescaux et al., 1992; Danober et al., 1998; Paz et al., 2007, Cope et al., 2009). Studies have shown that unilateral lesioning of the rostral region of RTN caused the complete suppression of SWDs but lesion on the caudal RTN (keeping rostral RTN intact) increased bilateral SWDs (Avanzini et al., 1993; van Luijtelaar & Weltink, 2001; Berdiev et al., 2007; Meeren et al., 2009). And, blocking GABA_A receptors of RTN (using antagonists) increased the duration and number of SWDs (Aker et al., 2002; 2006). Counterintuitively, cortical infusion of ethosuximide, lidocaine or tetrodotoxin significantly suppressed SWDs in epileptic animals (Polack et al., 2009, Manning et al., 2004, Sitnikova and van Luijtelaar, 2004) whereas thalamic delivery was not sufficient to cease SWDs (Richards et al., 2003, Polack et al., 2009). Altogether, these studies indicate that even though absence seizures are initiated in the cortex, thalamic components themselves can recruit cortical network for absence seizure generation.

The CTC oscillations are primarily dependent on GABAergic and glutamatergic neurotransmissions and normal CTC functioning is due to the reciprocity of the excitatory and inhibitory mechanisms which are described in terms of ‘microcircuits’ (Paz and Huguenard, 2015). Disruption or disturbance of any of these microcircuits may lead to the generation of seizure.

1.4 Microcircuit motifs of the CTC network

Feed-forward excitation (FFE), FFI, feed-back/recurrent excitation (FBE), feed-back/recurrent inhibition (FBI), convergence/divergence and counter inhibition are the common microcircuit motifs of brain. However, FFI, FBI, FBE and counter inhibition are the motifs of the CTC

networks whose dysfunctions have been identified in epilepsy (Fig. 1.9) (Paz and Huguenard, 2015). In the last few years, the importance of FFI in epilepsy research is gaining attention.

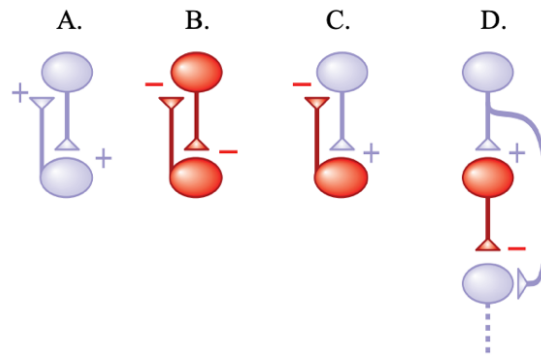


Fig. 1.9 Different microcircuit motifs involved in epilepsy. (A) Feedback/recurrent excitation (FBE): Presynaptic neuron excites a postsynaptic neuron and that postsynaptic neuron excites the presynaptic neuron. (B) Counter inhibition: Inhibitory interneurons form a network for inhibitory output. (C) Feed-back Inhibition (FBI): Activation of inhibitory neurons controls the local excitatory activity (D) Feed-forward Inhibition (FFI): An inhibitory interneuron is excited by a presynaptic cell which then inhibits the next follower cell. Purple and red represent excitatory glutamatergic and inhibitory GABAergic neurons, respectively. (Taken from Paz and Huguenard, 2015)

A. Feedback/recurrent excitation (FBE)

This is the major form of connectivity in the cortex and the hippocampus. Cortex mostly receives excitatory input from the cortical excitatory neurons (Braitenberg and Schutz, 1991) and few from the thalamic relay nuclei (Gil and Amitai, 1996; Porter et al., 2001). Recurrent excitation activates both excitatory pyramidal neurons and local inhibitory interneurons. The latter is believed to control the amplitude and spread of the recurrent excitation resulting in proportionality or balance (Douglas et al., 1999).

B. Counter inhibition

Counter inhibition occurs due to the suppression of the firing of inhibitory interneuron by another inhibitory interneuron. In a similar manner the suppressive effect on target excitatory cells via FFI and FBI, the counter inhibition forms a network for inhibitory output in some interneurons. Counter inhibition promotes excitatory activity by disinhibiting downstream excitatory cells. Such disinhibition between inhibitory interneurons (PV⁺ cells) promoting oscillatory output have been implicated in ictogenesis in limbic epilepsy (Grasse et al., 2013). The concept of intra-RTN inhibition (inside RTN) is thought to be an example of counter inhibition but this remains controversial because it is unclear that inhibition in RTN is either intra-RTN inhibition (via counter inhibition) or via external GABAergic inputs. An *in vivo* study conducted by deleting RTN specific GABAA receptor $\beta 3$ subunits caused the specific

loss of intra RTN inhibition and enhanced the generation of epileptic seizures (Huntsman et al., 1999). In support of this, it has been revealed that clonazepam reduces the output of RTN neurons to TC cells by uplifting (enhancing) intra RTN counter inhibition (Huguenard and Prince, 1994). Recently, using optogenetics, researchers have found that intra-RTN inhibition only occurs in mice up to two-weeks post birth (not in adult mice) and that the majority of GABAergic inputs come from other brain regions (Hou et al., 2016). This was also supported by another recent study which found that GABAergic neurons of the lateral hypothalamus innervate the RTN and induce excitation (Herrera et al., 2016). This is controversial since 1990s when some researchers found axonal collaterals between RTN neurons (Cox et al., 1996), whereas others did not find such projections (Pinault et al., 1997;1998).

C. Feedback inhibition (FBI)

Feedback inhibition mostly occurs within the local networks. It can be classified into recurrent and lateral feedback inhibition. In recurrent feedback inhibition, neurons are activated by local excitatory neurons and in turn inhibit the neurons that excited them. However, in lateral feedback inhibition neurons not only inhibit specific excitatory cells from which it received excitatory input but also targets others within the network (Tremblay et al., 2016).

D. Feed-forward inhibition (FFI)

FFI is the major inhibitory mechanism which regulates the excitation of excitatory neurons and synapses. In FFI, a presynaptic cell excites inhibitory neuron and inhibitory neuron then inhibit the next following cell. Changes in FFI in different circuits can cause abnormal circuit dynamics and can start epileptic seizures. FFI is primarily mediated by fast spiking parvalbumin-containing (PV+) inhibitory interneurons (Cammara et al., 2013; Paz and Huguenard, 2015; Jiang et al., 2016). PV+ interneurons upon receiving the excitatory input from the adjacent excitatory pyramidal neuron, fire and release GABA onto the other excitatory pyramidal neurons. PV+ interneurons make a synaptic contact with pyramidal cells in the cell bodies, axonal initial segment and proximal dendrites which enables powerful inhibition, and this limits excitation.

1.5 Parvalbumin-expressing (PV+) inhibitory interneurons

PV+ interneurons are the major class of GABAergic interneurons and are named after the characteristic protein they carry i.e. parvalbumin (a regulatory calcium-binding protein). They are found in cortical layer II-VI, RTN thalamus, cerebellum, hippocampal regions, and pars

reticulata of the substantia nigra (Celio, 1986; Cowan et al., 1990; Schwaller et al., 2002; Klausberger et al., 2005).

PV+ interneurons, typically have fast-spiking, low input resistance, and high-amplitude rapid after-hyperpolarization characteristics (Kawaguchi et al., 1987; Kawaguchi and Kubota, 1997), which enables them to fire a rapid train of action potentials unlike any other neuron in the cortex. They are therefore likely to have a profound impact on the spiking output of their targets (for review see Ferguson and Gao, 2018). In the SS cortex, PV+ interneurons synapse on to soma/proximal dendrites/axon initial segment of excitatory pyramidal cells (Inan and Anderson, 2014; Tremblay et al., 2016). PV+ interneurons are densely connected to pyramidal cells across cortical layers and areas influencing their excitability (Packer and Yuste, 2011; Hu et al., 2014). A single PV interneuron contacts nearly every local pyramidal neuron (Ferguson and Gao, 2018). Packer and Yuste (2011) estimated that a typical PV+ interneuron in the cortex makes contact with hundreds to thousands of post-synaptic targets (both pyramidal cells and other PV+ interneurons) and each excitatory pyramidal cell is contacted by ~50-200 inhibitory PV+ interneurons. Studies have shown that these interneurons have a major contribution in mediating FFI within the CTC network (Paz and Huguenard, 2015) and other brain networks involving the cortex and the thalamus (Delevich et al., 2015; Nassar et al., 2018). These interneurons mediate neuronal inhibition via feed-forward and/or feed-back mechanisms in other brain regions such as hippocampus (Kullman, 2011; Hu et al., 2014), striatum (Szydlowski et al., 2013) and amygdala (Lucas et al., 2016). These features and properties of PV+ interneurons enable them to prevent runaway excitation within the CTC network.

1.5.1 PV+ interneurons in CTC network

Inhibitory interneurons of the CTC network are classified on the basis of their morphological, anatomical, biophysical and synaptic properties. PV+ interneurons, somatostatin-expressing (SOM+) inhibitory interneurons and vasoactive intestinal polypeptide-expressing (VIP+) interneurons are the most common inhibitory interneurons in the CTC network (Tremblay et al., 2016). Based on the morphological features, PV+ interneurons are classified into basket and chandelier cells. Basket cells have curved axon terminals and target the soma and proximal dendrites of pyramidal neurons. Chandelier cells target axon initial segment of pyramidal cells and are named ‘chandelier’ because they resemble a ‘candelabrum’ (Inan and Anderson, 2014; Tremblay et al., 2016). Basket cells are the most common type of PV+ interneurons of the CTC network. PV+ interneurons (both basket and chandelier cells) represent 40% of total cortical GABAergic inhibitory interneurons. These interneurons occupy all cortical layers except for

layer 1 (Tremblay et al., 2016). Distribution and relative expression of different types of inhibitory interneurons within the CTC network cortical layers and RTN in mouse brain is shown below (Fig. 1.10).

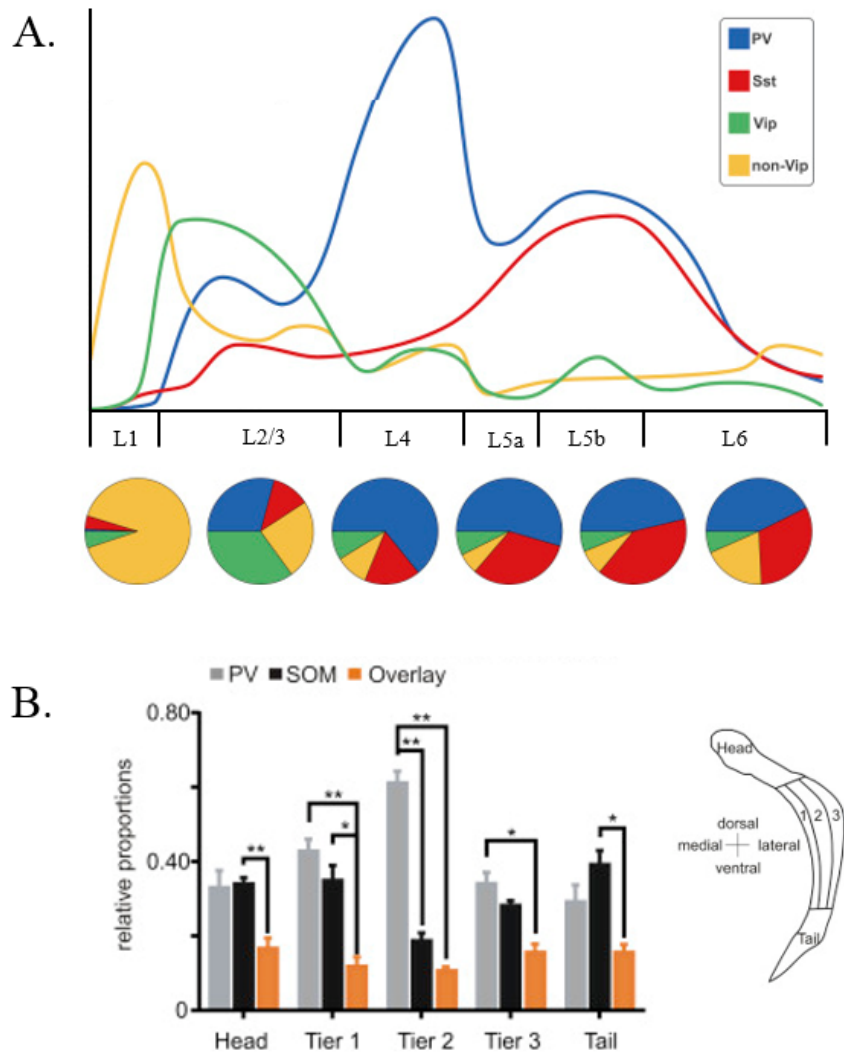


Fig. 1.10 Distribution and relative expression of different types of inhibitory interneurons in cortical layers and RTN thalamus. (A) Distribution of PV, SST, and VIP expressing interneurons in cortical layer 1-6 (Adapted from Tremblay et al., 2016) (B) Relative proportion of PV and SST expressing interneurons in the anterior-posterior, medial-lateral, and dorsal-ventral axes of RTN (Taken from Clemente-Pere et al., 2017).

1.6 Functional roles of PV+ interneurons in the CTC network

1.6.1 Feed-forward inhibition (FFI) in cortex

Sensory signals from relay neurons of VP region travel to layer IV of cortex. Intracortical circuits are connected and composed of a large number of excitatory neurons. These neurons boost the excitatory signals to deeper cortical layers. The incoming-excitatory sensory signals excite PV+ interneurons in the cortex, which causes the release of inhibitory neurotransmitter

GABA onto the excitatory neurons of the cortex. This causes a powerful inhibition which prevents runaway excitation in the neocortex.

1.6.2 Feed-forward inhibition (FFI) in thalamus

The thalamus is regarded as a sensory relay station which shapes sensory information by means of two inhibitory pathways i.e. feed-forward inhibition and feed-back inhibition. It receives excitatory input from afferent fibers in the periphery and CT projection from the cortex (Sherman and Guillery, 1996). CT neurons from cortical layer VI send reciprocal excitatory projections to the VP relay neurons and a collateral branch onto the PV+ inhibitory neurons of the RTN, which then provide FFI to VP relay neurons. Intra-RTN inhibition also occur at the same time which is believed to participate in an individual burst. The VP relay neurons also have excitatory collaterals to the RTN that generate feed-back inhibition on to VP relay neurons. It is believed that most of the inhibition in VP regions comes from the RTN via FFI which is regulated by PV+ interneurons (Fuentelba et al., 2005a; 2005b).

1.7 PV+ interneurons and neurological disorders

PV+ interneurons maintain a balance between excitation and inhibition within the CTC network. These interneurons are also involved in maintaining different brain functions and behaviours. It is thus possible that epilepsy and various neurological disorders arise as a result of disruption in the excitation/inhibition balance, dysfunction and impairment of PV+ interneurons (Marin et al., 2012; Hu et al., 2014). Dysfunction of these interneurons is regarded as one of the reasons for abnormal oscillatory rhythm and memory loss in amyloid precursor protein transgenic mice which mimic crucial aspects of Alzheimer's disease (AD) (Verret et al., 2012). Similar abnormalities of PV functioning were seen in other animal models of AD (Caccavano et al., 2020; Lu et al., 2020). Studies have shown a strong link between reduced expression of PV+ interneurons and GABA hypofunction in adult patients with schizophrenia (Akbarian et al., 1995; Hashimoto et al., 2003). Similar abnormalities were also seen in various animal models of schizophrenia (Lewis et al., 2012). Reduction in GABAergic transmission due to dysfunctional PV interneurons is believed to impair gamma oscillations leading to cognitive impairment in schizophrenia (Sohal et al., 2009; Cohen et al., 2015; Parker et al., 2020). Significant reduction in the number of these interneurons was observed in human patients suffering from Huntington disease (Kim et al., 2014). Studies conducted in animal models and human patients suffering from autism spectrum disorder have altered functioning of PV+ interneurons caused by either decrease in the number of PV+ cells or downregulation

of parvalbumin (Filice et al., 2016; Lauber et al., 2016; 2018; Hashemi et al., 2017). Studies have also outlined the important role of these interneurons in Parkinson's disorder (Salin et al., 2009; Gritton et al., 2019), neuropathic pain (Petitjean et al., 2015) and Tourette syndrome (Kalanithi et al., 2005; Kataoka et al., 2010).

1.8 PV+ interneurons and epilepsy

PV+ interneurons were first characterized and labelled as 'fast firing neurons' in the early 1980 (Celio et al., 1981; Celio, 1984; 1986) and the possibility of a relationship between these interneurons and epilepsy was reported a few years later (Sloviter, 1989; 1991a; 1991b). In 1996, abnormal patterns of immunostaining and altered cytoarchitecture of PV and GAD were reported in multiple regions of the neocortex in human patients with temporal lobe epilepsy (Marco et al., 1996). One year later, Scotti and colleagues reported the loss of hippocampal PV in seizing gerbils. They found a significant reduction in the density of PV stained neurons in repeatedly seizing gerbils compared to non-seizing controls (Scotti et al., 1997). PV deficient (PV^{-/-}) mice were more susceptible to PTZ-induced seizures (Schwaller et al., 2004) but such phenomena was not observed in kainate-induced seizures in PV^{-/-} mice (Bouilleret et al., 2000a). However, conflicting results have been obtained since then, which showed either substantial loss (Bouilleret et al., 2000b; Marx et al., 2013), transient (Sloviter, 1991b; Scotti et al., 1997; Wittner et al., 2001) or marginal (Wyeth et al., 2010) reduction of hippocampal PV expression in animal models and human subjects of epilepsy. Roles of dysfunctional hippocampal PV+ interneurons in epilepsy has also been extensively studied (see review Liu et al., 2014). It is widely established that PV+ interneurons regulate the network excitability and gamma oscillations in the cortex. Studies have shown that various subunits of voltage-gated sodium and potassium channels support the functioning of PV+ interneurons and impairment of parvalbumin functioning is also linked to defects or mutation of the genes encoding those ion channels which regulate the membrane excitability of cortex.

Mutations in the SCN1A gene which encodes for the voltage-gated sodium channel Nav1.1 represents a common genetic cause of generalized epilepsies and Dravet syndrome. Recent studies have shown that the inactivation of one SCN1A allele in PV interneurons results in spontaneous seizures in animals (Ogiwara et al., 2007; Dutton et al., 2013). Specific deletion of SCN1A in GABAergic inhibitory interneurons in the forebrain resulted in generalized seizures and premature death (Cheah et al., 2012).

Epilepsy phenotype seen in $KCNA1^{-/-}$ mice lacking the voltage-gated potassium channel Kv1.1 is attributed to the impaired excitability of cortical PV⁺ interneurons (Goldberg et al., 2008; Gautier et al., 2015). Kv3.1, Kv3.2 and Kv3.3, subunits of the Kv3 voltage-gated potassium ion channels are strongly expressed in cortical PV⁺ interneurons. A *de novo* mutation in KCNC1 gene (which encodes for Kv3.1) have been linked to progressive myoclonic childhood epilepsy (Muona et al., 2015). Studies have shown that knocking out Kv3.1 and Kv3.2 subunits in animals results in the impairment of thalamocortical oscillations (Espinosa et al., 2008), decreased cortical inhibition and increased susceptibility towards seizures (Lau et al., 2000). Mutations in the gene KCNA2, KCNB1, KCND3, KCNQ2, KCNQ3 which encodes for Kv1.2, Kv2.1, Kv4.3, Kv7.2 and Kv7.3 potassium channels respectively, have been linked with epilepsy in human patients (Soh et al., 2014; Saitsu et al., 2015; Smets et al., 2015; Syrbe et al., 2015) but the impact of the mutation on PV⁺ interneurons has not yet been established.

CaV2.1 (P/Q-type) calcium channels help to sustain GABA release from PV⁺ interneurons (Zaitsev et al., 2007). A recent study has shown that removal of the CACNA1A gene [which encodes the $\alpha 1$ subunit of CaV2.1 (P/Q-type) voltage-gated Ca²⁺ channel] from cortical PV⁺ interneurons generates generalized seizures in mice (Rossignol et al., 2013). The stargazer mouse model of absence epilepsy is another example. The stargazer mutation underlying the epileptic phenotype is a defect in the calcium channel $\gamma 2$ -subunit gene CACNG2, which reduces the expression of stargazin protein. This protein is a transmembrane AMPAR regulatory protein (TARP) which is crucial for synaptic targeting of AMPARs. Studies have shown that there is a significant loss of GluA4-containing AMPARs at excitatory synapses in PV⁺ interneurons of the cortex and RTN thalamus (Adotevi and Leitch, 2016; 2017; 2019; Barad et al., 2012; 2017) which is believed to impair FFI and might contribute to absence seizure generation. Other studies have also shown impaired expression and regulation of AMPA receptors in the PV⁺ interneurons in the SS cortex (Maheshwari et al., 2013) and the thalamus (Menuz and Nicoll, 2008) of stargazers.

Thus, multiple evidence has shown the functional importance of PV⁺ interneurons in regulating excitability of the neuronal network. Impaired function of these interneurons has also been associated with various neurological disorders including epilepsy. Some examples were described above. However, there is always a limitation of employing genetic models for the characterization of a specific neuronal subtype; for example, functional characterization of PV⁺ interneurons to pinpoint their specific roles by selective (neuron-specific) manipulation

in a given neuronal network would be more beneficial. Neuron-specific manipulation will allow us to test various hypothesis which are not possible in genetic model.

1.9 Manipulation of neuronal subpopulation

Selective control of a defined neuronal population is always a challenge. But for the better understanding of the neurons that may contribute to the functioning of the brain, behavior or phenotype, manipulation of selective neuronal population is crucial. Various strategies and techniques have been implemented in the past to selectively modulate neurons *in vivo* i.e. the use of electrical manipulation (such as microstimulation, electrolytic lesions), physical manipulation (such as ablation, thermal cooling), pharmacological manipulation (such as the use of agonists, antagonists, drug delivery) and genetic manipulation (such as overexpressing or knocking out of genes) (Carter and Shieh, 2015). However, these techniques were not precise and lacked temporal resolution. They also generated an off-target effect to surrounding cells. To overcome these problems and challenges, new tools have been developed and continuously optimized over the past few years.

Pharmacogenetics or chemogenetics is one of the emerging tools of modern neuroscience which is used to modulate, examine, and understand the targeted neuronal population of different regions of the brain. In simple terms, this technique refers to genetically encoded membrane receptors that are designed to be activated by specific chemical compounds. To date, the most technically successful chemogenetic tools are DREADDs. This novel technology involves insertion of engineered receptors (designer receptors) into specific neurons that are only activated by synthetic ligands (designer drugs) As explained above, FFI is essential to prevent runaway excitation within the CTC network which is regulated by PV+ interneurons. Thus, it is possible to alter/restore the actions of inhibitory feed-forward PV+ interneurons with DREADD technology. The use of DREADD technology to manipulate PV+ interneurons may be beneficial for understanding the mechanisms of absence seizures. As DREADDs are engineered G-protein coupled receptors (GPCRs), the next few sections will briefly explain about GPCRs and DREADD technology.

1.10 G Protein Coupled Receptors (GPCRs)

GPCRs are the largest known class of membrane receptors in eukaryotes. They are also known as seven-transmembrane domain receptors or serpentine receptors because of their seven transmembrane spanning alpha-helices (Bear et al., 2007). Humans have nearly 1000 known different types of GPCRs. These receptors are the targets of 30-50% of all modern medicinal

drugs (Overington et al., 2006). They can recognise a variety of ligands including peptides, hormones, lipids, neurotransmitters, photons and odorants. All GPCRs share a similar core structure consisting of an extracellular N-terminus, an intracellular C-terminus, three extracellular and three intracellular interhelical loops. The extracellular loops serve as binding sites for structurally distinct ligands whereas the intracellular loops provide multiple interaction sites for different subtypes of G-proteins (Thiel et al., 2013) (Fig. 1.11). G-proteins associated with GPCRs are heterotrimeric in structure i.e. they have α , β , and γ subunits. In the inactive state, GPCR remains as a heterotrimeric G protein complex (Bear et al., 2007) (Fig. 1.10). When any signalling molecule binds with GPCR, then it undergoes a conformational change. The exact mechanism of conformational change is not exactly understood, but it is believed that a receptor molecule always exists in conformational equilibrium between active and inactive biophysical states, with the binding of any signalling molecule shifting the equilibrium to the active state (Rubenstein and Lanzara, 1998). Because of this conformational change, α -subunit of G-protein exchanges guanosine diphosphate (GDP) for guanosine triphosphate (GTP). This causes the α -subunit to dissociate and move away from β - γ dimer. G_α and $G_{\beta\gamma}$ subunits are now available to activate effector protein. Effector protein may be different, based on the type of G protein-mediated signalling pathway. As long as the ligand or signalling molecule binds to GPCRs, this whole chain of event will happen repeatedly. G subunit is itself an enzyme which can hydrolyse GTP back to GDP and all subunits again can combine to form an inactive heterotrimer. This is the overall basic mechanism of the GPCR signalling pathway. G protein exerts its effect by activating certain enzymes. Stimulation of those enzymes triggers a series of biochemical reactions and lead to the activation of downstream enzymes which are called the second messenger cascade. The α -subunit of G protein mediates signal transduction in a variety of signalling pathways. There are four families of α -subunits ($G_{i/o}$, G_q , G_s , and $G_{12/13}$) (Digby et al., 2006; Wettschureck and Offermanns, 2005). There are two main signal transduction pathways that involve GPCRs which are briefly described below.

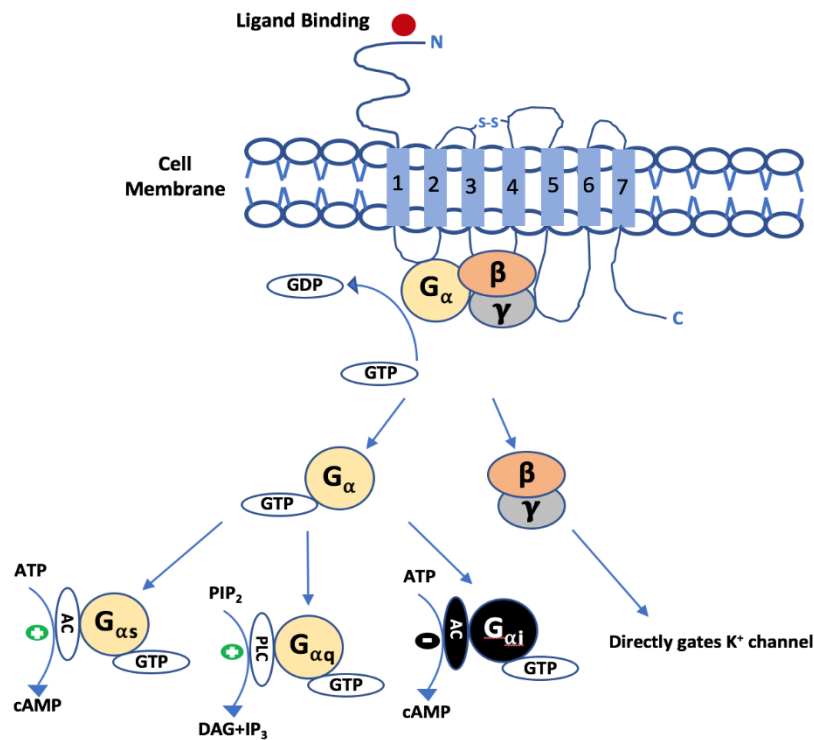


Fig. 1.11 General core structure and functioning of GPCRs. (Adapted from Thiel et al., 2013)

Phosphatidylinositol signalling pathway

The effector of this pathway is phospholipase C (PLC). The α -subunit of activated G protein binds and stimulates PLC. As PLC is a lipase enzyme, it catalyses the cleavage of phosphatidylinositol 4,5-biphosphate (PIP_2) into two-second messengers, diacylglycerol (DAG) and inositol 1,4,5-triphosphate (IP_3) (Fig. 1.11). Due to insoluble lipid properties of DAG, it remains within the plasma membrane and stimulates the downstream enzyme protein kinase C (PKC). PKC then regulates transcription, immune response, cell growth, and various biological processes through PKC-mediated phosphorylation of other proteins. IP_3 diffuses away in the cytosol and binds with IP_3 gated calcium channels found in the membrane of endoplasmic reticulum which elicit the release of calcium ions from the endoplasmic reticulum to the cytosol. Elevation of cytosolic Ca^{++} changes the membrane potential which triggers widespread long-lasting effects and stimulates various downstream enzymes.

Cyclic-Adenosine Monophosphate (cAMP) signalling pathway

This pathway is based on the two types of G-proteins, i.e. stimulatory G protein (G_s) and inhibitory G protein (G_i). However, the effector of both pathways is adenylyl cyclase (AC). In the G_s mediated pathway, after the α -subunit of G_s dissociates from β - γ dimer, it activates the effector protein adenylyl cyclase (AC). AC catalyses the conversion of adenosine triphosphate

(ATP) to cAMP which is the second messenger of this pathway. cAMP activates the downstream enzyme protein kinase A (PKA). In doing so, cAMP binds to the regulatory subunit of PKA and deactivate it by changing its structure which allows the catalytic subunit of PKA to become free. The kinase enzyme present in the catalytic subunit of PKA then phosphorylates its substrates and activates various transcription factors. However, G_i proteins inhibits the cAMP pathway by inhibiting AC, decreasing the production of cAMP from ATP which in turn results the reduced activity of cAMP-dependent kinase.

1.10.1 Complexity of GPCR signaling

Studies have shown that up to 50% of modern medicinal drugs target GPCRs and other membrane proteins (Hermans, 2003). Drugs targeting GPCRs are often nonspecific affecting the activity of more than one GPCR. The same GPCR is present in multiple tissues and a ligand can activate various GPCRs having different affinities towards the G protein. This might lead to the activation of various effector enzymes producing off-target effects. This might also confound *in vivo* studies. Various pharmacological approaches in the past have been developed to reduce the complexity of GPCR signalling by utilizing particular agonists and antagonists for specific GPCRs (Gurwitz et al., 1994; Wisler et al., 2007; Thomas et al., 2008; Digby et al., 2012). Most of these approaches were unsuccessful because they caused serious side effects, off-target effects and lacked selectivity (Conn et al., 2009; Agulhon et al., 2010). However, the idea of designing appropriate ligands with high specificity and selectivity to avoid undesirable GPCR-mediated adverse effects was never ruled out.

1.10.2 Engineered GPCRs

Over the last few decades various techniques have been developed and optimized for selective control of a defined cell population. Each approach has their own advantages and disadvantages. Sub-sections below will briefly describe the most recent and widely recognized chemogenetic tools based on G protein signalling, i.e. G-protein receptor-ligand system.

1.10.2.1 Receptors Activated Solely by Synthetic Ligands (RASSLs)

The first breakthrough in the development of designer GPCRs were called as Receptors Activated Solely by Synthetic Ligands (RASSLs). This technique was based on the use of artificial ligands to selectively activate designed GPCRs.

Strader and colleagues substituted a single amino acid residue to mutate the β -adrenergic receptors which were fully activated by catechol-containing esters and ketones, compounds which did not activate wild-type β -adrenergic receptors (Strader et al., 1987; 1991). Coward and colleagues applied the same rational approach to design GPCRs (Coward et al., 1998). After this study, there were series of investigations to develop designer GPCRs (Kristiansen et al., 2000; Pauwels and Colpaert, 2000; Srinivasan et al., 2003; 2007; Bruysters et al., 2005). The development of these modified receptors was very inspiring, and these novel tools were highly beneficial in various *in vivo* studies. However, several disadvantages were also noticed, since these designer receptors showed a significant degree of constitutive activity and resulted in serious side effects upon *in vivo* use. Few cases of off-target activity were also reported (Coward et al., 1998; Sweger et al., 2007; Rogan and Roth, 2011)

1.10.2.2 Designer Receptors Exclusively Activated by Designer Drugs (DREADDs)

To date, the most technically successful and widely used engineered GPCR is DREADD. DREADDs are mutationally modified muscarinic acetylcholine receptors. These receptors are only activated by clozapine-N-oxide (CNO) and do not respond to the muscarinic receptor agonist/endogenous ligand acetylcholine. Based upon the DREADDs we choose, different kind of signalling pathways (Gi, Gq, Gs) in the cell can be activated (Rogan and Roth, 2011). Muscarinic acetylcholine receptors consist of five subtypes (M1-M5). The coupling preference for M1, M3 and M5 receptors are towards Gq/11 proteins which leads to depolarization and neuronal firing whereas M2 and M4 receptors prefer Gi/o proteins that results neuronal silencing via hyperpolarization (Kruse et al., 2014).

The first set of experiments to modify and develop muscarinic acetylcholine receptor DREADD was performed by Armbruster et al., (2007). Initially, they used modified rat muscarinic (M3) receptor which had a deletion in its third intracellular loop (rM₃ Δ i3). This type of engineered receptor was previously used for ligand activation studies in mammals. They created ten independent clones of mutant rM₃ Δ i3, eight of these ten independent clones contained the Y148X^{3.33} mutation. They found that a majority of mutant receptors were unable to respond, however one clone was found to be mildly responsive to CNO. A subset of clones was selected and remutated to produce a second-generation library and to identify the mutants that exhibit high affinity for clozapine and CNO but not for acetylcholine. Those second generation rM₃ Δ i3 receptor mutants were finally screened with ~5nM CNO. Screening was based on the comparison of the pharmacological profile and responsiveness for CNO,

clozapine and acetylcholine. The two best clones were chosen and tested on a human cell line which resulted a new class of RASSLs and termed as DREADDs. The finally selected receptors had tyrosine in the 149th position of the third transmembrane replaced with cysteine and alanine present in the 239th position of the fifth transmembrane replaced with glycine which generated the hM3Dq DREADD. Similarly, two-point mutations (Y113C in the third transmembrane and A203G in the fifth transmembrane) resulted hM4Di DREADD. hM3Dq and hM4Di DREADD are the most common DREADD in use today (Armbruster et al., 2007). Brief description of commonly available DREADDs are stated below and respective signalling pathways are illustrated in the figure 1.12.

Gi-DREADDs (hM4Di and KORD)

Gi-DREADDs are designed to be used for neuronal silencing. Binding of CNO activates α -subunit which inhibits AC. This reduces the level of cAMP and the activity of PKA. The other subunit, i.e. $\beta\gamma$ interacts with G protein-coupled inwardly rectifying potassium channel (GIRKs) which causes the potassium ion to move outside. This causes the hyperpolarization and decreases the firing of presynaptic neurons (Armbruster et al., 2007; Rogan and Roth, 2011). Beside hM4Di, a k-opoid receptor-DREADD (KORD) has been recently developed. KORD is activated by a designer drug named Salvinorin B (Vardy et al., 2015).

Gq-DREADDs (hM3Dq)

Gq-DREADDs are used to induce neuronal firing and increase overall excitability. CNO binding activates PLC and that hydrolyses PIP₂ to DAG and IP₃. The hydrolysis of PIP₂ closes voltage-gated potassium channels causing depolarization and this induces neuronal firing (Guettier et al., 2009).

Gs-DREADD (rM3Ds)

This type of DREADD is based on the rat M3 muscarinic receptor. Upon CNO binding, Gs α -subunit activates AC, which helps the conversion of ATP to cAMP. This starts the PKA signaling pathway. Similarly, G_{olf} also signals through the same mechanism (Farrell et al., 2013).

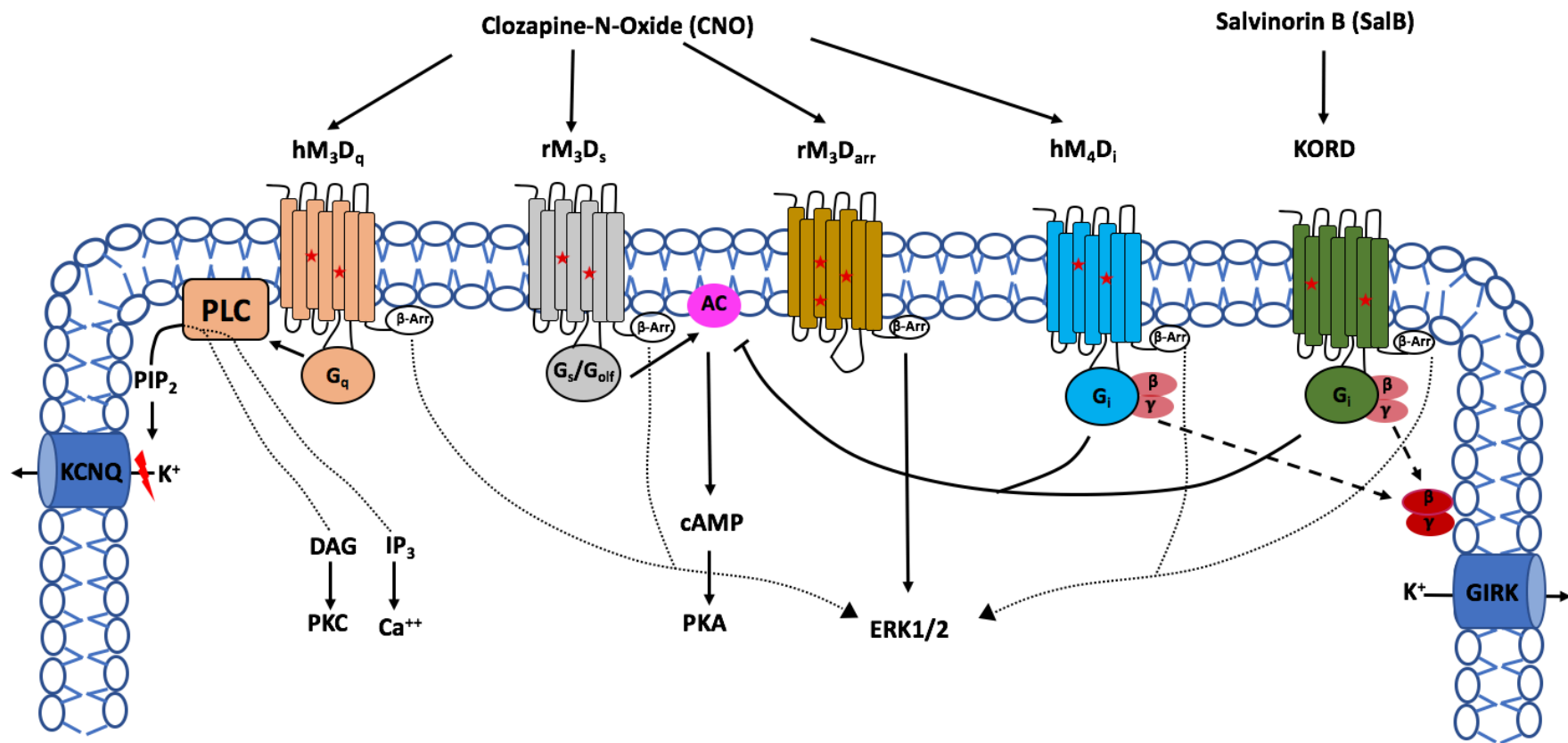


Fig 1.12 Signalling pathways of common available DREADDs. Red stars within the transmembrane signifies the location of point mutations performed in endogenous receptors to obtain various DREADDs. KCNQ, voltage-gated potassium channel; K⁺, potassium ion; PIP₂: phosphatidylinositol 4,5-bisphosphate, PLC, phospholipase C; DAG, diacyl glycerol; PKC, protein kinase C; IP₃, inositol-1,4,5-trisphosphate; β-Arr, β-arrestin; cAMP, cyclic adenosine monophosphate; PKA, protein kinase A; ERK1/2, extracellular signal-regulated kinases ½; GIRK, G protein-coupled inwardly rectifying potassium channel.

β-arrestin DREADD (rM₃D_{arr})

This β-arrestin-specific DREADD contains one point mutation in M₃ muscarinic DREADDs which only can activate M₃D-arr DREADD (Nakajima and Wess, 2012).

1.10.2.3 Designer drug CNO and recent developments

CNO is the designer drug for DREADD receptors. CNO was chosen as a designer drug mainly because of its inert nature towards endogenous targets and structural similarity to the antipsychotic drug Clozapine (parent compound of CNO). Structurally, CNO contains an N-oxide group whereas clozapine lacks this moiety. Negatively charged oxygen present in CNO creates electrostatic repulsion between the positively charged nitrogen molecule and the negatively charged side chain of the receptors. Thus, binding affinity of CNO with muscarinic receptors is lower compared to that of clozapine-receptor binding (Wess et al., 2013), and few mutations to muscarinic receptor family generated DREADD receptors that are sensitive towards CNO (Alexander et al., 2007). CNO is a highly potent, bioavailable, and pharmacologically inert drug. It has rapid biodistribution and CNS penetration. CNO mediated DREADD activation is also robust and prolonged (Rogan and Roth 2011; Roth et al., 2016). Reports have shown that systemic administration of CNO peaks in plasma between 15-30 min is effective up to 1 hour (Manvich et al., 2018; Jendryka et al., 2019), and almost undetectable after 2 h (Guettier et al., 2009); but behavioural and electrophysiological effects remain up to 9 h (Alexander et al., 2009).

However, recently the use of CNO as a designer drug for DREADDs was called into question. Studies showed that CNO is back-metabolizes to clozapine and N-desmethylclozapine (NDMC) after systemic administration into rodents (Manvich et al., 2018; Jendryka et al., 2019). Gomez and colleagues stated that back-metabolized clozapine may have contribution to DREADD activation but not CNO. They also concluded that accumulated clozapine may occupy other endogenous receptor targets in the brain (eg. dopamine, histamine, 5-HT), and produce unwanted off-target effects which may confound behavioural studies (Gomez et al., 2017). Whereas, another recent study demonstrated that the concentration of reverse-metabolized clozapine in plasma, cerebrospinal fluid and brain tissue is very low compared to CNO. The availability of both compounds in the brain varies with species (Jendryka et al., 2019). Thus, it's unlikely that DREADD activation is solely from back metabolized clozapine after CNO application. Similarly, numerous reports did not find any DREADD-independent behavioural effect of CNO (up to

10mg/kg) (Mahler et al., 2018). On the other hand, as suggested by Gomez et al., (2019) the use of low doses of clozapine as designer drug is also not an ideal approach (Goutaudier et al., 2019). It's not a surprise that CNO reverse-metabolizes to its parent compound upon peripheral injection, as it was previously demonstrated in mammalian species (Jann et al., 1994) and was recommended for use at lower doses (Roth et al., 2016). High affinity of clozapine for DREADDs was stated since its first development in 2007 (Alexander et al., 2009). Also, previous studies have also shown that clozapine increases anxiety in animals (Manzaneque et al., 2002) and is also linked to agranulocytosis and pro-epileptic effects (Ruffman et al., 2006). Other chemical approaches such as the use of olanzapine (Weston et al., 2019), compound 21, perlapine (Thompson et al., 2018; Jendryka et al., 2019), JHU37152 and JHU37160 (Bonaventura et al., 2019) to activate DREADD have been reported but these compounds are not yet fully characterized.

Altogether, these studies questioning the use of CNO as a designer drug, however, have highlighted important aspects of DREADD related experiments. It's now clear and widely established that depending upon the experimental approach, optimization of appropriate dose of CNO and the use of standard controls (non-DREADD expressing and saline treated DREADD animals) are highly recommended in DREADD based experiments. The use two different ligands to confirm DREADD mediated behavioural results are also recommended (Goutaudier et al., 2019).

1.11 DREADD and Optogenetics

In order to understand the scope and significance of DREADD technology, it is necessary to understand how this technique differs from other similar techniques such as optogenetics.

Optogenetics is another cutting-edge technique which uses the combination of optics and genetics to control, monitor, and modulate neuronal activity. It involves the use of light to control neurons which are genetically modified to express light sensitive channel (Deisseroth et al., 2006; Fenno et al., 2011). This technique allows the investigation of the neuronal manipulation in real time. In simple terms, light responsive proteins (opsins) are genetically introduced into the neuronal cell membrane and based on the intensity and wavelength of light, change of membrane potential is recorded. This provides direct control over neuronal activity as neurons communicate via changes of the cross-membrane voltage (Deisseroth, 2015; Zhang et al., 2007). Both chemogenetics and

optogenetics enable the pathway-specific silencing or activation of neurons and are targeted for cell-specific manipulation. Enhanced and selective control of neuronal population is the most common key advantage of chemogenetics and optogenetics (Tønnesen and Kokaia, 2017). While they serve similar purposes, both techniques offer different advantages and limitations. The few parameters in which chemogenetics (DREADD) and optogenetics differ are briefly described below.

Route of neuronal activation

DREADDs are easier to implement and more easily adapted for behavioural applications where CNO can be administered via various routes (systemic injections, focal injections, food, water) (Urban and Roth, 2015). But, optogenetics require the administration of light via expensive specialized instruments (Zhang et al., 2010). In DREADDs, administration of CNO via food or water seems very convenient and this approach is relatively less invasive. Repeated injection or regular handling of animals can be avoided, but the dose of CNO can be less precise (Urban and Roth, 2015).

Timing

One of the basic differences between both techniques is the onset of the effect. Optogenetics can reversibly manipulate neuronal activity in the range of milliseconds, the response is immediate. But in case of DREADDs, onset of receptor activation takes min. However, for lengthy behavioural experiments where prolonged neuronal modulation is required, DREADDs are ideal.

Frequency and concentration

One of the potential limitations of DREADD is that the amount and concentration of CNO required to control a given neuronal population is not fixed. DREADD would be more successful if this technique had the ability to determine the amount of CNO required for a neuronal response (Urban and Roth, 2015). With optogenetics, the experimenter has direct control over the light stimulation, so it's possible to maintain the frequency of neuronal activity. Optogenetics also allows the experimenter to record how the neurons respond to stimulation. This allows us to investigate various type of behaviour and activity based on the level of stimulation. However, one of the major

disadvantage associated with optogenetics is the difficulty in penetrating tissue by light (Pavlov and Schorge, 2014).

Possibility of multiplexing

Bidirectional control of neuronal activity is possible in both techniques. Currently, DREADD offers three options for neuronal silencing, i.e. hM4Di (CNO-mediated), KORD (Salvinorin B mediated), and GluCl (ivermectin mediated) (Armbruster et al., 2007; Frazier et al., 2013; Marchant et al., 2016; Vardy et al., 2015). Designer compounds for all three approaches are different and have a different pharmacology, thus multiplexing is possible. Multiplexing is also possible in optogenetics as actuators designed for this technique respond to blue, orange, yellow, green and red light. This selectivity gives us a theoretical possibility of multiplexing. However, various factors should be considered before multiplexing within the same experimental animal. Employment of DREADD and optogenetics in the same experimental animal provides another possibility for multiplexing (Forcelli, 2017).

Issues regarding CNO

CNO is the only agonist which is well characterized and widely used to activate DREADDs. So, the DREADD activity is fully dependent on the pharmacokinetic property of injected CNO (Forcelli, 2017). Studies have found that repeated CNO dosing in the same animal may create decreased responses due to the desensitization of DREADD receptors (Roth, 2016). Previously, it was established that back transformation of CNO to clozapine was only limited in human and guinea-pig but not in rats and mouse (Wess et al., 2013). Current reports suggest that back transformation of CNO to clozapine and N-desmethylozapine in mouse, rat and macaque subjects (MacLaren et al., 2016; Gomez et al., 2017; Raper et al., 2017; Jendryka et al., 2019). To resolve this issue, alternative chemical approaches for DREADD activation have been proposed but they are not yet fully characterized (Thompson et al., 2018; Weston et al., 2019; Bonaventura et al., 2019). On the other hand, optogenetics does not require any designer drug for neuronal silencing or activation but it requires surgical implantation of a device which might cause permanent damage to the brain affecting neuronal activity (Whissell et al., 2016). Optogenetics also requires expensive equipment such as optic fibres, light, waveform generators, and other specialized instruments to carry out the experiments. Recently, a new step-function opsin with

ultra-high light sensitivity (SOUL) has been engineered to minimize the invasive nature of optogenetics (Gong et al., 2020).

Scale and clinical aspect

One of the biggest advantages of DREADDs over optogenetics is scale. The human brain is around 1000-times larger than the rodent brain. The difference in the size of the brain and circuits make optogenetics more difficult to control neuronal activity using light. DREADD technology does not require implantation of hardware for long periods as in optogenetics. Even in the rodent brain, light distribution can be an issue. This difference in scale and size of distribution make the translation of findings from rodents to human challenging for optogenetics. The only advantage of specific distribution of light is that specific regions of brains can be targeted (Forcelli, 2017; Tønnesen and Kokaia, 2017). On the other hand, DREADD expression can be achieved by using double transgenic mice or by delivering virus into specific regions of brain and then systemic or focal administration of designer drug can activate DREADDs. Because of these advantages, research and studies are already started in non-human primates (Eldridge et al., 2016; Grayson et al., 2016; 2020; Upright et al., 2018; Bonaventura et al., 2019; Nagai et al., 2016; Deffains et al., 2020). As explained above, optogenetics is ahead of chemogenetics in real-time neuromodulation and temporal resolution. The popularity of optogenetics is trying to outstrip chemogenetics but, chemogenetics also offers several diverse features which cover various aspects of experiments.

1.12 Use of DREADD technology to study various CNS disorders and animal behaviours

DREADD technology has been extensively used in biomedical research particularly in neuroscience due to its ability to selectively activate or silence neuronal firing. This technology has been effectively used to understand the pathogenesis of various neurological disorders. Some recent findings are summarized below.

Alzheimer's disease (AD):

AD is a form of progressive dementia caused by depletion of neuronal cells. This disease is believed to be associated with the presence of intracellular neurofibrillary tangles and extracellular amyloid plaques [neurotoxic peptide amyloid beta ($A\beta$)]. These are considered as the neuropathologic hallmarks of AD. DREADD mediated inhibition in the cortex of AD-like mouse

markedly reduced the number of amyloid plaques and the levels of peptide amyloid beta in a dose dependent manner. This study targeted the cortical region as the cortex is prone to amyloid deposition (Yuan and Grutzendler, 2016). In another study, DREADD mediated activation of pyramidal neurons in the dorsal subiculum was able to reduce synaptic deficits with improved glutamatergic transmission between subiculum and nucleus accumbens. This enhanced hippocampal neuronal excitability in the Tg2576 mouse model of AD. The network involving the subiculum and nucleus accumbens is critical in formation of hippocampal-related spatial memory (Cordella et al., 2018). Other studies also used an excitatory DREADD approach to understand tau pathology in AD (Wu et al., 2016; Schultz et al., 2018).

Parkinson disease (PD):

PD is second most common neurodegenerative disorder after AD. Clinical signs of PD include bradykinesia, gait impairment, rigidity of muscles and tremor. Systemically, PD refers to the progressive loss of dopaminergic neurons in the substantia nigra leading to the reduced dopamine levels in the dorsal striatum that is believed to cause the abovementioned abnormalities. CNO mediated activation of DREADD expressing transplanted dopaminergic neurons in 6-hydroxydopamine (6-OHDA) lesioned mice had improved behavioural features (Dell'Anno et al., 2014; Aldrin-Kirk et al., 2016; Chen et al., 2016). Similar behavioural improvements were also seen in lactacystin rat model of PD after chemogenetic activation of cholinergic pedunculopontine neurons (Pienaar et al., 2015).

Down syndrome:

Down's syndrome is a common chromosomal disorder in which patients suffer from intellectual disability with clinical signs such as flat face and nasal bridge. This disorder affects most body systems and commonly leads to Alzheimer's dementia at a much earlier age. Fortress and colleagues found restored memory function and improved intellectual activity in an animal model of Down's syndrome using excitatory-DREADD approach (Fortress et al., 2015). Recently, using the inhibitory-DREADD approach it was revealed that loss of the pontine nucleus locus coeruleus-noradrenergic projections might be the underlying cause of dementia in individuals with this disorder (Hamlett et al., 2020).

Schizophrenia and autism spectrum disorders (ASD):

Cognitive inflexibility and attention deficits are common symptoms associated with schizophrenia. Selective inhibition of PV⁺ interneurons and GAD65 neurons of the ventral hippocampus using inhibitory DREADD approach induced behavioural features similar to schizophrenia. This linked the pathophysiology of schizophrenia to GABA dysfunction (Nguyen et al., 2014). Few other studies also utilized a DREADD approach to understand the pathophysiological mechanisms of cognitive impairment and other abnormalities seen in schizophrenia (Parnaudeau et al., 2013; Koike et al., 2016). Autism spectrum disorder (ASD) is another mental disorder which is characterized by impaired verbal, non-verbal communication and social behaviour. One study employed an excitatory-DREADD approach and revealed improved social behaviour in CNTNAP2 (gene identified as responsible for ASD) knockout mice by activating oxytocin expressing neurons in the hypothalamus (Peñagarikano et al., 2015).

Apart from neurological disorders, a DREADD based approach has been successfully employed to study animal behaviour such as learning (Maharjan et al., 2018), addiction (Ferguson and Neumaier, 2015; Dobrzanski and Kossut, 2017), memory (Tuscher et al., 2018), sleep (Varin and Bonnavion, 2018), feeding (Koch et al., 2015; Vardy et al., 2015; Luo et al., 2018), breathing (Brust et al., 2014; Sheikhabaei et al., 2018), anxiety (Zhang et al., 2017; Mazzone et al., 2018; Salvi et al., 2019), stress (Wei et al., 2018; Nawreen et al., 2019), decision making (Ferguson et al., 2013), fear (Arico et al., 2017; Gilman et al., 2018) etc.

1.13 DREADD technology in epileptic-seizure related studies

In 2015, Bryan Roth, the principal investigator of the research group which invented DREADD, mentioned seizures and Parkinson disease as the exceptional candidates for a DREADD based approach (English and Roth, 2015). Kätzel and colleagues were the first to report *in vivo* use of DREADDs in relation to epileptic seizures. In that work, CNO was able to stop chemically induced (pilocarpine or picrotoxin) focal seizures in rats (Kätzel et al., 2014). The first *in vitro* use of DREADD approach was reported in hippocampal slice cultures where Avaliani and colleagues expressed inhibitory DREADDs in hippocampal principal cells and administration of CNO was able to suppress epileptic activity (Avaliani et al., 2016). In another study, activation of PV interneurons via excitatory DREADD approach significantly reduced 4-aminopyridine (4-AP) induced seizure activity (Călin et al., 2018). Various studies have been published since then in

different rodent models where DREADDs have been used to understand more about seizures i.e. temporal lobe seizures (Fishell and Dimidschstein, 2018; Wang et al., 2018; Desloovere et al., 2019; Goossens et al., 2019), pilocarpine induced status epilepticus (Zhou et al., 2019) and amygdala kindled seizures (Wicker and Forcelli, 2016). However, to date, there are no published reports utilizing DREADD technology to investigate the functional roles of PV+ interneurons on absence seizure generation.

1.14 Manipulating PV+ interneurons with DREADDs *in vivo*

There are two main ways of manipulating neuronal population with DREADD technology *in vivo* i.e. viral approach and transgenic mouse approach. Both approaches can be further divided into two categories: Cre-dependent and Cre-independent. Schematic diagrams of manipulating neuronal subpopulation with DREADD technology are illustrated in figure 1.13 and 1.14.

The work included in this thesis is based on the Cre-dependent transgenic mouse approach (Zhu et al., 2016) where PV-Cre mice were crossed with DREADD (hM4Di or hM3Dq)-floxed mice so that the inhibitory or excitatory DREADD receptors are expressed into PV+ interneurons (Fig. 1.13). In the Tet-dependent transgenic mice approach, mice expressing tetracycline-sensitive DREADD are generated using Tet-off system (Fig. 1.13). Briefly, littermates from TRE (Tetracycline-responsive promoter element)-DREADD are crossed with mice having the tetracycline-controlled transactivator protein (tTA) driven by the promoter (such as CaMKII α , c-fos etc.). Normally, in the absence of tetracycline or its analog doxycycline, tTA binds to the TRE and activates transcription of the DREADD in the targeted brain regions. This is a reversible approach as administration of tetracycline or doxycycline eliminates DREADD expression. This approach is relatively less popular (Alexander et al., 2009; Garner et al., 2012; Zhu et al., 2014). Cre-dependent viral approach is popular and mostly used DREADD mediated approach. To establish the expression of DREADD receptors into specific neuronal population, virus particles containing DREADD construct are delivered into the appropriate regions of the brain (Fig.1.14). As mentioned previously, in this study, a Cre-dependent transgenic mouse approach was used to manipulate PV+ interneurons with DREADDs. PV-Cre mice were bred with either inhibitory DREADD (hM4Di-flox) mice or excitatory DREADD (hM3Dq-flox) mice to generate double transgenic mice expressing inhibitory or excitatory DREADD receptors in PV+ interneurons. hM4Di/hM3Dq-floxed mice have *loxP*-flanked STOP cassette designed to prevent transcription

Transgenic mouse

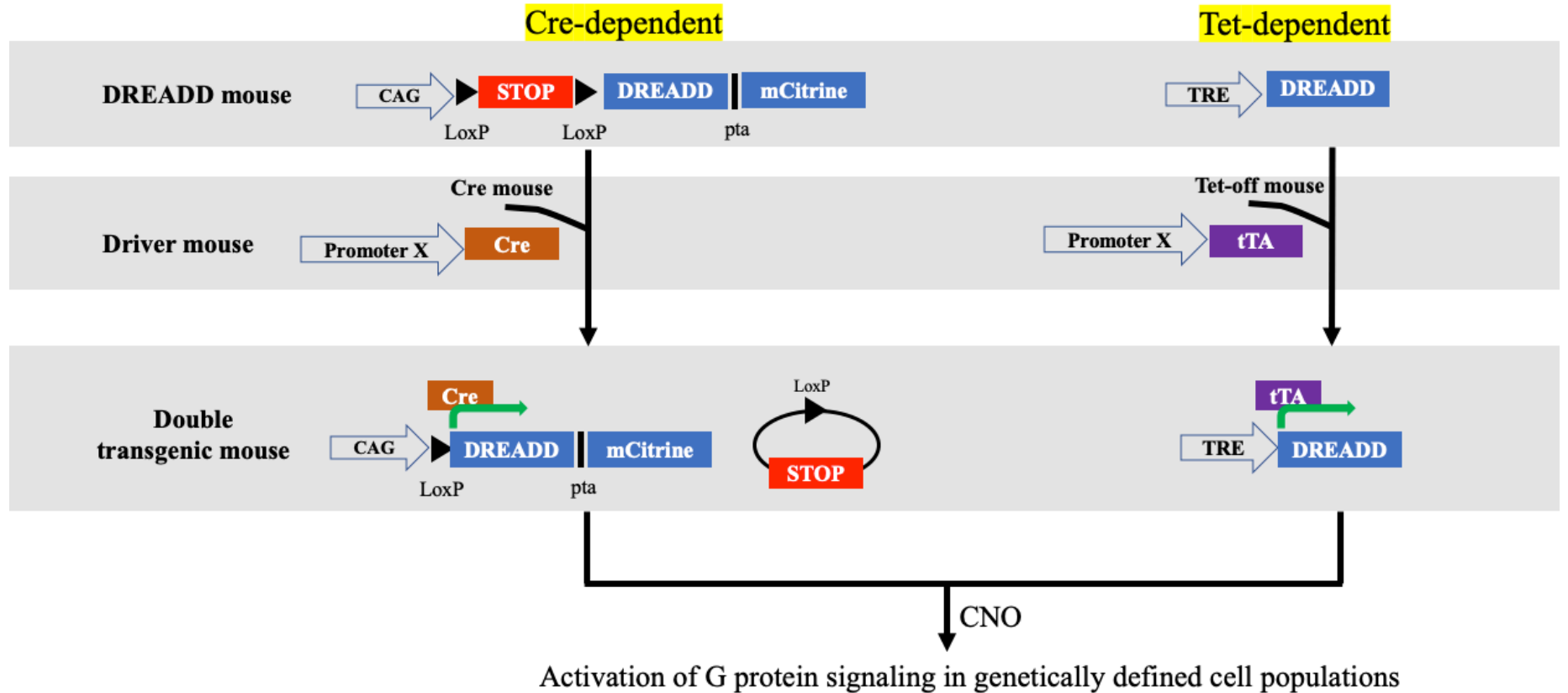


Fig. 1.13 Schematic diagram of *in vivo* manipulation of neuronal population with DREADD technology using transgenic mice approach. According to this approach, DREADD can be expressed genetically by crossing DREADD mice with Cre or Tet-off driver mouse lines and designer receptors are expressed only in the cell type specified by the driver used (Adapted from Zhu and Roth, 2015).

Viral approach

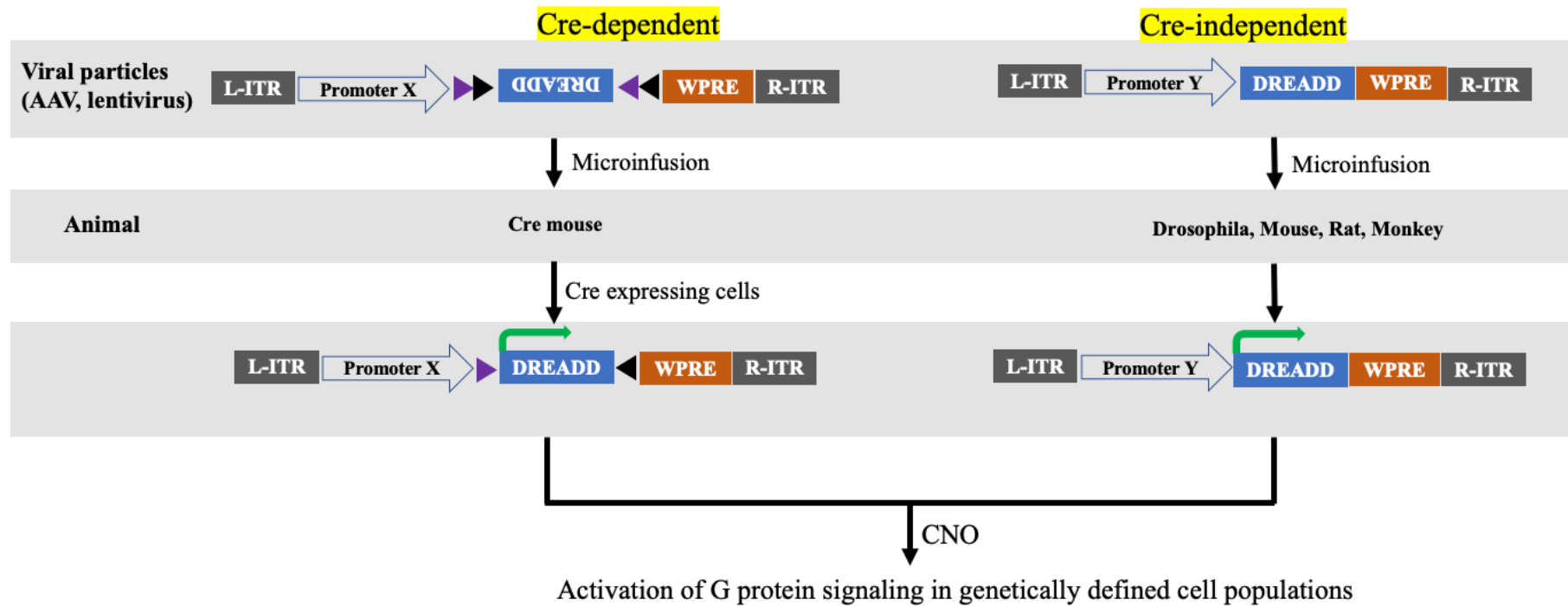
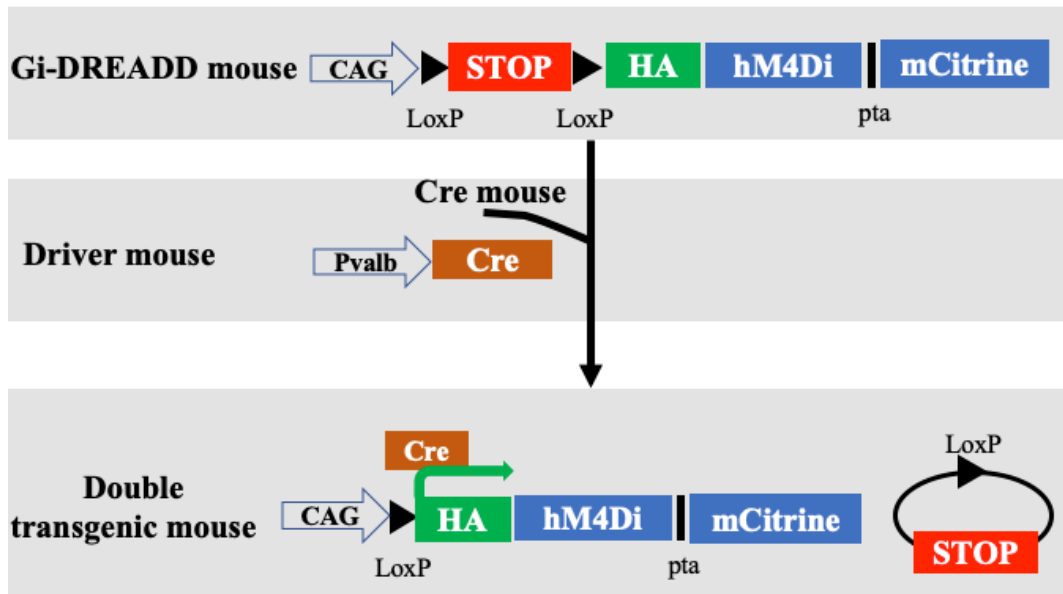


Fig. 1.14 Schematic diagram of *in vivo* manipulation of neuronal population with DREADD technology using viral approach. In viral approach, Cre-dependent and Cre-independent options are available. In the Cre-dependent approach, viral double-flanked inverted DREADD constructs are microinfused in brain regions of mice expressing cell-type specific Cre drivers (Adapted from Zhu and Roth, 2015)

Inhibitory DREADD mice (PV-Cre x hM4Di-flox)



Excitatory DREADD mice (PV-Cre x hM3Dq-flox)

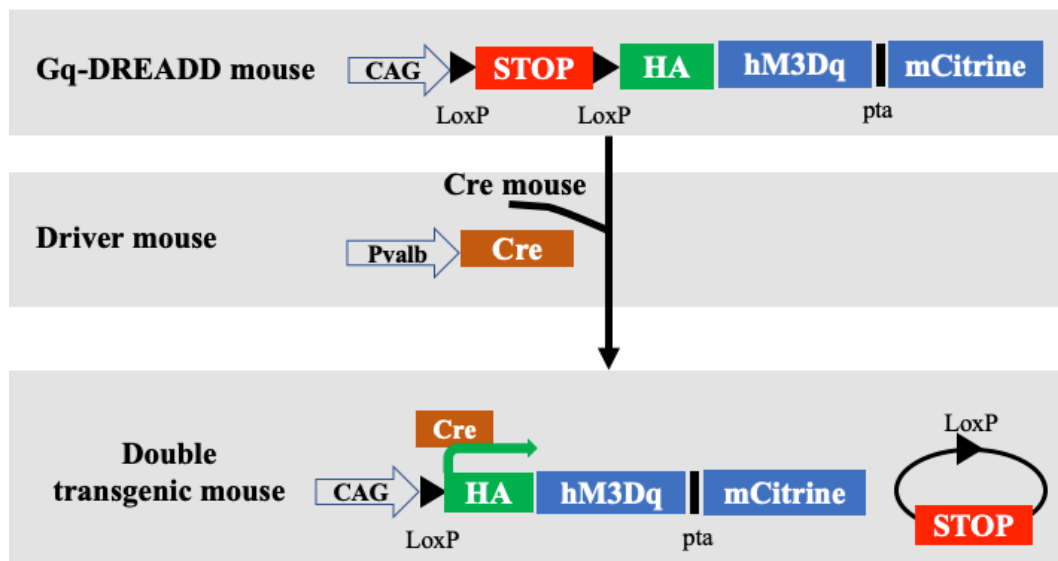


Fig. 1.15 Manipulating PV⁺ neurons with inhibitory or excitatory DREADD using Cre-dependent transgenic mouse approach.

of the downstream HA-hM4Di/hM3Dq-pta-mCitrine coding region (Fig. 1.15). Mating these strains removes the *loxP*-flanked STOP cassette only in the cell type specified by the Cre-recombinase system. This allows the strong expression of DREADD receptors only in PV+ interneurons.

1.15 Rationale and aims of the thesis

Although it is well established that absence seizures arise due to the disturbances within the CTC circuitry, the precise cellular and molecular mechanisms are still unclear. FFI is essential to prevent runaway excitation within the CTC network and is mediated by fast spiking PV+ inhibitory interneurons. Previously using stargazer mouse model of absence epilepsy, it has been demonstrated that loss of loss of excitatory drive (impaired AMPARs trafficking) to PV+ interneurons might be one of the reasons of impaired FFI within the CTC network and possibly contributing to absence seizure generation (Menuz and Nicoll, 2008; Barad et al., 2012; 2017; Maheshwari et al., 2013; Adotevi and Leitch, 2016; 2017; 2019). However, the extent to which the deficits in excitatory drive leads to dysfunctional FFI has not been established via functional studies. Hence, the aim of this project was to investigate the impact of dysfunctional FFI within the CTC network on absence seizure generation and behaviour. PV+ interneurons of the CTC network were functionally targeted by using DREADD technology. To target these interneurons, mice expressing Cre recombinase in PV+ interneurons (PV-Cre) were bred with inhibitory (hM4Di-flox) or excitatory (hM3Dq-flox) DREADD mice. Firstly, simultaneous video/EEG recordings and behavioural tests were used to investigate the impact of functionally silencing feed-forward inhibitory PV+ interneurons within the CTC network in terms of absence seizure generation and behavioural parameters. Secondly, the effect of functionally exciting these interneurons during chemically induced absence seizures was tested. Thirdly, the impact of dysfunctional FFI on the expression level of GABA synthesizing enzymes (GADs) and transport proteins (GATs) were examined in epileptic stargazers, as studies have shown that GABAergic system is heavily implicated in rodent absence seizure models (Cope et al., 2009; Seo and Leitch, 2014; 2015; Hassan et al., 2018). The findings from this project could provide an electrophysiological insight and advance our understanding of some mechanisms underlying absence seizures. This may help in developing future treatment strategies for patients who do not respond to treatment to the currently available AEDs.

The main objectives of this PhD project were to:

- 1) Assess the selective expression of inhibitory DREADD receptors in PV⁺ interneurons in PV^{Cre}/Gi-DREADD mice using immunohistochemistry.
- 2) Examine EEG signals before and after global and focal silencing of PV⁺ interneurons via CNO administration in PV^{Cre}/Gi-DREADD mice.
- 3) Investigate the behavioural changes in PV^{Cre}/Gi-DREADD mice after global and focal silencing of PV⁺ interneurons using open-field and rotarod tests.
- 4) Assess the selective expression of excitatory DREADD receptors in PV⁺ interneurons in PV^{Cre}/Gq-DREADD mice using immunohistochemistry.
- 5) Examine EEG signals during chemically induced absence seizures in PV^{Cre}/Gq-DREADD mice pre-treated with CNO to activate PV⁺ interneurons.
- 6) Investigate the expression pattern of GABA synthesizing enzymes (GADs – 65&67) and transport proteins (GATs –1&3) in the SS cortex and the thalamus of epileptic stargazers and non-epileptic controls via immunohistochemistry.
- 7) Demonstrate the relative expression of GADs and GATs in whole-tissue lysate of the SS cortex and the VP thalamus of epileptic stargazers and non-epileptic controls via western blotting.
- 8) Demonstrate the relative expression of GADs and GATs in whole-tissue lysate of the SS cortex of CNO treated PV^{Cre}/Gi-DREADD animals via western blotting.

1.16 Outline of thesis chapters

This thesis consists of 6 chapters. These include an introductory chapter, a methodology chapter, three experimental chapters and a general discussion chapter. Introductory chapter 1 provides in-depth, current and critical review of literatures and overall background to this PhD project. Chapter 2 provides a detailed account of materials and experimental methods employed to accomplish the research objectives. Chapter 3 represents the results of silencing feed-forward inhibitory PV⁺ interneurons in the CTC network on absence seizure generation and behavioural parameters outlined under objectives 1-3. The results from chapter 3 have been published (Panthi and Leitch, 2019). Chapter 4, based on objectives 4 and 5, discusses the impact of activating feed-forward inhibitory PV⁺ interneurons in the CTC network during chemically induced absence seizures. Chapter 5 demonstrates the expression profiles of GADs and GATs in epileptic stargazers and CNO treated inhibitory DREADD animals as outlined under objectives 6-8. Chapter 6 describes in-depth analysis of results obtained in this study including critiques of methodology employed and future directions.

Chapter 2. Materials and Methods

2.1 Animals

The animals used in this project were PV-Cre x hM4Di-flox mice, PV-Cre x hM3Dq-flox mice and stargazer mice. Mice were bred and housed at the University of Otago animal facility at controlled room temperature (22–24°C) with *ad libitum* access to food and water. All animal experiments were performed in accordance with the University of Otago Animal Ethics Committee under the AEC no. D94/16, AUP-19-98 and DET 32/17. DREADD related experiments were performed in both male and female mice whereas for stargazers based experiments only male mice used. All experiments were performed in adult animals (3 months of age). The weight of mice was between 23-43 g.

2.1.1 Breeding paradigm for PV-Cre x hM4Di-flox and PV-Cre x hM3Dq-flox mice

PV-Cre knockin, hM4Di-flox and hM3Dq-flox mice were obtained from Jackson Laboratories, USA. PV-Cre knockin mice express Cre recombinase in PV+ interneurons without disrupting endogenous parvalbumin expression. hM4Di-flox and hM3Dq-flox mice have a *loxP*-flanked STOP cassette designed to prevent transcription of the downstream HA-hM4Di-pta-mCitrine or HA-hM3Dq-pta-mCitrine coding region, respectively (Fig. 2.1). Mating these strains (PV-Cre and hM4Di-flox or hM3Dq-flox) removes the *loxP*-flanked STOP cassette only in the cell type specified by the Cre-recombinase system (Fig. 2.1). This allows the strong expression of hemagglutinin (HA)-tag only in PV+ interneurons. In this study, PV-Cre mice were crossed with either hM4Di-flox mice or hM3Dq-flox mice to generate double transgenic mice expressing inhibitory (Gi) or excitatory (Gq) DREADD receptors in PV+ interneurons, respectively. To establish and maintain PV-Cre x hM4Di-flox mice colony, homozygous female PV-Cre mice were crossed with either homozygous hM4Di-flox males to generate litters of homozygous PV-Cre x hM4Di-flox mice, or crossed with heterozygous hM4Di-flox males to generate litters with heterozygous PV-Cre x hM4Di-flox and non-DREADD expressing wild-type (WT) control littermates, as illustrated in Fig. 2.1. Similarly, in case of PV-Cre x hM3Dq-flox mice colony, homozygous female PV-Cre mice were crossed with heterozygous hM3Dq-flox males to generate litters with heterozygous PV-Cre x hM3Dq-flox and non-DREADD expressing wild-type (WT) control littermates, as illustrated in Fig. 2.1. Only female PV-Cre mice were crossed with either male hM4D or hM3Dq mice to avoid unwanted germline recombination.

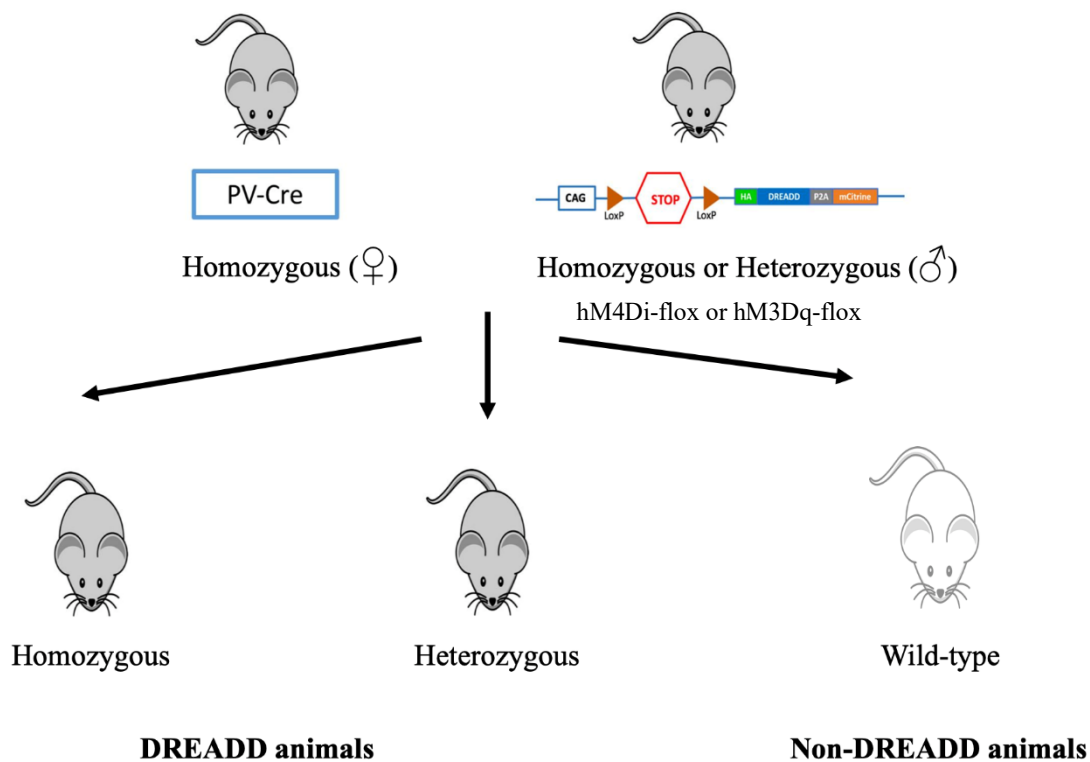


Fig. 2.1 Breeding paradigm for DREADD animals. Schematic showing breeding to generate PV-Cre x hM4Di-flox or PV-Cre x hM3Dq-flox offspring and non-DREADD wild type controls by crossing a female PV-Cre mouse with either a male hM3Dq-flox or male hM4Di-flox mouse.

2.1.2 Breeding paradigm for stargazer mice

Stargazer mice were obtained from Jackson Laboratories, USA. These mice have monogenic mutation of the stargazin allele on mouse chromosome 15. In case of stargazer animals, two colonies were kept and continuously maintained. Heterozygous males were mated with either heterozygous females or homozygous females as shown in figure 2.2. The offspring of Het x Het colony were wild type (+/+), heterozygous (+/stg), and homozygous mutant stargazer (stg/stg) mice, whereas offspring of the Het x Homo colony were +/stg and stg/stg mice (Fig. 2.2). Female homozygous stargazer mutant mice are fertile but male homozygous stargazer mutant mice are infertile. Mice used in this study were adult males aged 2-3 months. For comparative analysis in different experiments, homozygous stargazers (stg/stg) and non-epileptic control littermates (+/+ or +/stg) were used.

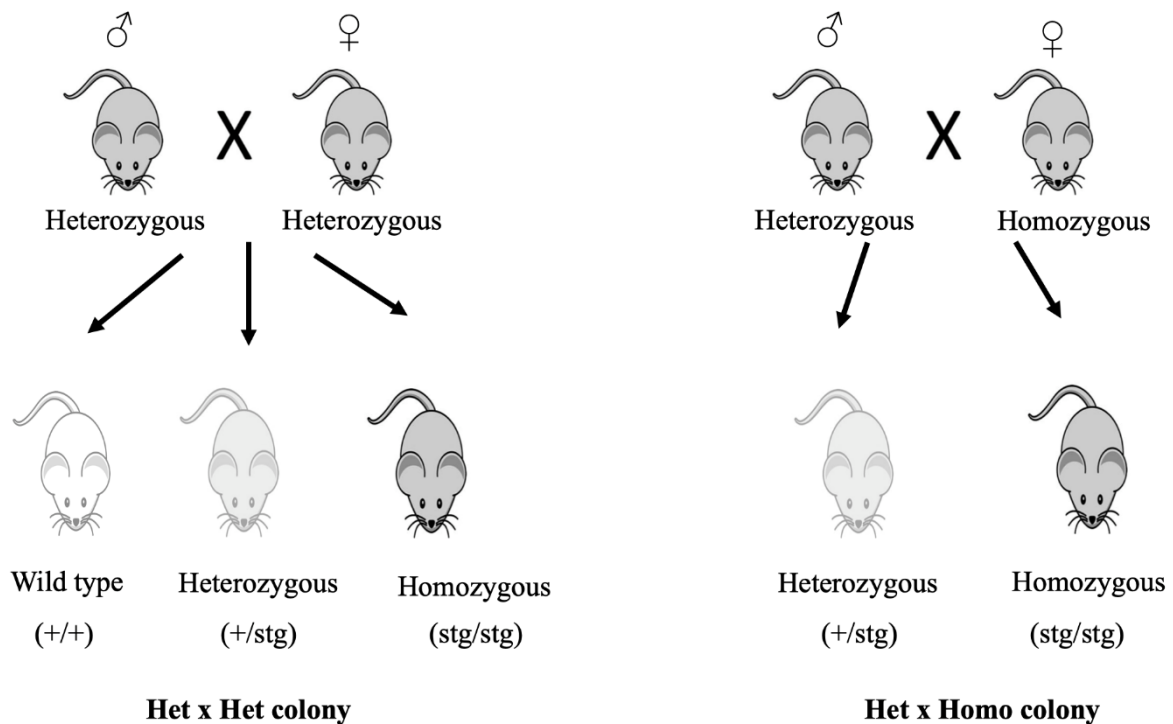


Fig. 2.2 Breeding paradigm for stargazer mice. Schematic showing breeding to generate stargazer mutant mice by crossing heterozygous males with either heterozygous females (Het x Het colony) or homozygous females (Het x Homo colony).

Animals used in this study are hereafter denoted as shown in the Table below:

Colony	Genotype	Hereafter denoted as
PV-Cre x hM4Di-flox (Inhibitory DREADD)	Homozygous or heterozygous	PV ^{Cre} /Gi-DREADD
	Wild type	Non-DREADD WT controls
PV-Cre x hM3Dq-flox (Excitatory DREADD)	Heterozygous	PV ^{Cre} /Gq-DREADD
	Wild type	Non-DREADD WT controls
Stargazer	Homozygous stargazers (stg/stg)	Epileptic stargazers (STG)
	Heterozygous (+/stg) and wild type (+/+)	Non-epileptic controls (NE)

2.2 Genotyping

2.2.1 DNA extraction from the ear-notches

Genotyping was performed to verify the mouse genotype. Ear notches were collected from the offspring of PV^{Cre}/Gi-DREADD mice, PV^{Cre}/Gq-DREADD mice and littermates from stargazer colony. Ear notches were mixed in 600µl of DNA lysis buffer (100mM Tris, 5mM EDTA, 0.2% SDS, 200mM NaCl, pH 8.5) and 5µl of proteinase K (Roche, Basel), and digested overnight at 55°C. Next day, microtubes were centrifuged at 13,000rpm for 10 min. Supernatant from microtubes were transferred into other microtubes containing 600µl of

isopropanol. Samples were again centrifuged at 13,000 rpm for 5 min. Supernatant from each tube was poured off carefully and remaining residual supernatant was pipetted out. The DNA pellet was then resuspended in 200µl of Tris-EDTA (TE) buffer (10mM Tris, 1mM EDTA, pH 8.0) and vortexed for few seconds before allowing it to dissolve for 1 hour at 55°C.

2.2.2 Polymerase chain reaction (PCR)

DNA obtained after the abovementioned procedure was processed for amplification using PCR. For animals from DREADD colonies (either from PV-Cre x hM4Di-flox or PV-Cre x hM3Dq-flox colony), PCR was performed separately to confirm Cre knockin and hM4Di-flox or hM3Dq-flox using primers listed in the Table below (Table 2.1). In case of littermates from stargazer colony common forward, wild type reverse and mutant reverse primers were used (Table 2.2). The information about the primers was obtained from The Jackson Laboratory website (Jax protocol-026219, 026220, 001756, 013148) and primers were purchased from Integrated DNA Technologies (IDT). According to the written instructions in the data sheets, primers were reconstituted in TE buffer (pH 8.0) and were stored at -20°C upon arrival.

Table 2.1 Primers used for genotyping of PV^{Cre}/Gi-DREADD and PV^{Cre}/Gq-DREADD mice.

Primer type	Sequence (5'→3')
hM4Di mutant forward	CGA AGT TAT TAG GTC CCT CGA C
hM4Di mutant reverse	TCA TAG CGA TTG TGG GAT GA
hM3Dq mutant forward	CGC CAC CAT GTA CCC ATA C
hM3Dq mutant reverse	GTG GTA CCG TCT GGA GAG GA
Wild type forward	AAG GGA GCT GCA GTG GAG TA
Wild type reverse	CCG AAA ATC TGT GGG AAG TC
Cre forward	CCT GGA AAA TGC TTC TGT CCG
Cre reverse	CAG GGT GTT ATA AGC AAT CCC

Table 2.2 Primers used for genotyping of stargazer mice.

Primer type	Sequence (5'→3')
Common forward	TAC TTC ATC CGC CAT CCT TC
Wild type reverse	TGG CTT TCA CTG TCT GTT GC
Mutant reverse	GAG CAA GCA GGT TTC AGG C

PCR mastermix was prepared as illustrated in table 2.3, 2.4, and 2.5.

Table 2.3 PCR mastermix preparation for animals of PV^{Cre}/Gi-DREADD colony.

For PV-Cre knockin		For hM4Di-flox	
PCR master mix components	Volume (µl) (each animal)	PCR master mix components	Volume (µl) (each animal)
Platinum PCR Supermix (Invitrogen, CA, USA)	12.5	Platinum PCR Supermix (Invitrogen, CA, USA)	12.5
Nuclease Free Water (Invitrogen, CA, USA)	8.5	Nuclease Free Water (Invitrogen, CA, USA)	8.5
Cre forward primer	0.5	hM4Di mutant forward primer	0.5
Cre reverse primer	0.5	hM4Di mutant reverse primer	0.5
Wild type forward primer	0.5	Wild type forward primer	0.5
Wild type reverse primer	0.5	Wild type reverse primer	0.5

Table 2.4 PCR mastermix preparation for animals of PV^{Cre}/Gq-DREADD colony.

For PV-Cre knockin		For hM3Dq-flox	
PCR master mix components	Volume (µl) (each animal)	PCR master mix components	Volume (µl) (each animal)
Platinum PCR Supermix (Invitrogen, CA, USA)	12.5	Platinum PCR Supermix (Invitrogen, CA, USA)	12.5
Nuclease Free Water (Invitrogen, CA, USA)	8.5	Nuclease Free Water (Invitrogen, CA, USA)	8.5
Cre forward primer	0.5	hM3Dq mutant forward primer	0.5
Cre reverse primer	0.5	hM3Dq mutant reverse primer	0.5
Wild type forward primer	0.5	Wild type forward primer	0.5
Wild type reverse primer	0.5	Wild type reverse primer	0.5

Table 2.5 PCR mastermix preparation for animals of stargazer colony.

PCR master mix components	Volume (µl) (each animal)
Platinum PCR Supermix (Invitrogen, CA, USA)	22.5
Common forward primer	0.25
Wild type reverse primer	0.3
Mutant reverse primer	0.2

For animals from PV-Cre x hM4Di-flox or PV-Cre x hM3Dq-flox colony, 2µl of genomic DNA was added to 23µl of PCR mastermix as shown in Table 2.3 and 2.4. In case of animals of

stargazer colony, 1.75µl of genomic DNA was mixed with 23.25µl of PCR mastermix as shown in Table 2.5. 25µl of the solution was homogenously mixed. The mixture was then processed for run in PCR machine (Supercycler SC-200, Kyratech, QLD, Australia) following the optimized PCR cycle steps (Table 2.6).

Table 2.6 PCR cycle steps

Step	Temperature (°C)	Time	Note
1	94	3 min	
2	94	30 seconds	Repeated 35 times
3	62	30 seconds	
4	72	30 seconds	
5	72	2 min	
6	10		Hold

2.2.3 Agarose Gel Electrophoresis

Agarose gel (2%) was prepared by mixing 1.6gm of agarose in 80ml of Tris-Borate-EDTA (TBE) buffer (90mM Tris, 90mM Boric acid, 3.18mM EDTA, pH 8.3). 10µl of the PCR product was loaded into each well of agarose gel. 5 µl of DNA ladder (TrackIt, Invitrogen, CA, USA) was added to one well as a reference ladder. The gel was allowed to run at 85V for 90 min and stained with SybrSafe (Life Technologies, CA, USA). The gel was then placed on a UV light source to view and photograph bands. Figure 2.3A, B and C are the representative images of genotype bands on an agarose gel for animals of PV-Cre x hM4Di-flox, PV-Cre x hM3Dq-flox and stargazer colonies, respectively.

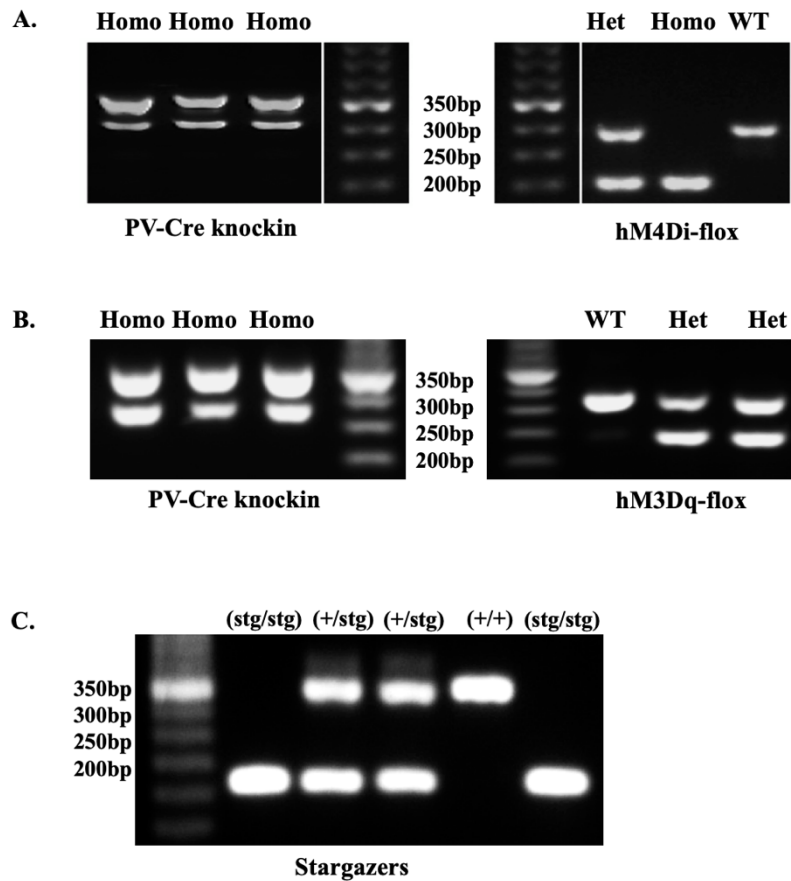


Fig. 2.3 Representative image of genotype bands on agarose gel. Images showing the (A) homozygous (Homo) PV-Cre knockin (350bp and 300bp) and the hM4Di-flox (B) homozygous (Homo) PV-Cre knockin (350bp and 300bp) and the hM3Dq-flox for three mice to verify PV-Cre knockin and hM4Di-flox or hM3Dq-flox. [for hM4Di-flox and hM3Dq-flox: heterozygous (het) 300 bp and 204 bp; homozygous (Homo) 204 bp; wild-type (WT) 300 bp] (C) Image showing the bands for wild-type (+/+) mice at 360 bp, heterozygous (+/stg) mice with two bands at 360 bp and 155 bp, and epileptic stargazers (stg/stg) with a band at 155 bp.

2.3 Immunofluorescence Confocal Microscopy

2.3.1 Animal perfusion and fixation

Adult mice from PV-Cre x hM4Di-flox, PV-Cre x hM3Dq-flox and stargazer colonies were deeply anesthetized with an intraperitoneal (i.p.) injection of 60mg/kg of sodium pentobarbital. Supplemental doses of pentobarbital were injected if required to achieve deep level of anaesthesia. Toe-pinch response method was used to determine the depth of anaesthesia using blunt forceps. Transcardial perfusion was performed with 5% heparin in 0.1M phosphate buffered saline (PBS) for first 30 seconds followed by 4% paraformaldehyde (PFA) in 0.1M Sorensen's phosphate buffer (PB) for next 10 min. Tremor was seen in the tail and toe of animals confirming the circulation of PFA (fixative) around the whole body. Heparin was used as an anticoagulant agent and PFA was used to preserve the histological integrity of the tissue. Brains were extracted and post-fixed in 4% PFA overnight at 4°C.

2.3.2 Tissue processing and immunolabelling

After post-fixation, brains were washed three times in 0.1M PB. This was followed by cryoprotection of the brains in increasing concentration of sucrose prepared in PBS i.e. 10% for 30 min, 20% for 30 min, and 30% at 4°C until the brains sunk to the bottom of the glass container. Sinking of the brains indicated the complete infiltration of sucrose into the brain. For sectioning, the cerebellum was dissected from the rest of the brain. Brains were sectioned into 30µm coronal sections. Cerebellum was also sectioned into 30µm thin sagittal sections. Sectioning was performed on a freezing cryostat (Leica CM1950, Wetzlar, Germany). Temperature inside the cryostat chamber was maintained to -20°C. Sections were collected into 12-well plates containing PBS.

Slices were then transferred into blocking buffer [4% Normal Goat Serum (NGS), 0.1% Bovine Serum Albumin (BSA), 0.1% Triton X-100 in PBS] for 2 h at room temperature. All sections were incubated in a mixture of primary antibodies for 48 h at 4°C. Primary antibody solution was prepared in PBS with 0.1% BSA and 0.3% Triton X-100. After incubation, tissue sections were washed in PBS for 45 min (15 min, 3 times each). Sections were then labelled with secondary antibodies for 12 h at 4°C. Secondary antibody solution was prepared in PBS. After labelling the tissues with secondary antibodies, they were washed in PBS for 30 min (10 min, 3 times each). Primary and secondary antibodies used for immunofluorescence confocal microscopy in this project are listed in Table 2.7 and Table 2.8, respectively. Sections were then mounted on polysine-coated glass slides and cover-slipped with mounting medium (1,4 diazabicyclo (2.2.2) octane DABCO-glycerol). Slides were left for air-drying in the dark at room temperature.

Table 2.7 Primary antibodies used in this project for immunofluorescence confocal microscopy

Target Protein	Type	Source/ Catalogue No.	Dilution
Parvalbumin	Mouse monoclonal	Swant/235	1:2000
Parvalbumin	Rabbit polyclonal	Swant/PV27	1:2000
HA-tag	Rabbit polyclonal	Cell Signalling/3724S	1:500
GAT-1	Rabbit polyclonal	Abcam/ab426	1:500
GAT-3	Rabbit polyclonal	Alomone Labs/AGT-003	1:200
GAD 65	Mouse monoclonal	Abcam/ab26113	1:500
GAD 67	Mouse monoclonal	Millipore/MAB5406	1:500

Table 2.8 Secondary antibodies used in this project for immunofluorescence confocal microscopy

Product	Secondary conjugate	Source/ Catalogue No.	Dilution
Goat anti-rabbit	Alexa Fluor 488	Life Technologies/11008	1:1000
Goat anti-mouse	Alexa Fluor 568	Life Technologies/11031	1:1000

2.3.3 Confocal imaging and analysis

Images were acquired using Nikon A1+ Inverted Confocal Laser Scanning Microscope with following channel configurations; green channel at 488nm laser excitation and red channel at 568nm laser excitation. During confocal imaging, detector offset for each channel were kept zero. Detector gain and laser power were optimized accordingly. Scan speed and image pixel size were also set accordingly. Confocal images were taken at 10X, 20X and 40X magnification. Cell counting and staining intensity analysis was performed with ImageJ software (version 1.51, NIH, USA) using the same settings for all animals and their respective control counterparts.

2.4 Electroencephalography (EEG) recordings

2.4.1 Surgical implantation of prefabricated headmounts and microcannulas

For survival surgeries performed in this project, twelve-weeks old PV^{Cre}/Gi-DREADD or PV^{Cre}/Gq-DREADD mice were ordered at least two days before scheduled surgery date. Animals were handled once daily for 2 days. During surgery, animals were fully anesthetized with a continuous flow of isoflurane and subcutaneously injected with 5mg/kg of Carprofen (for pain control) and 2mg/kg of Marcaine (for local anaesthesia). Animals were provided with supplemental heat during surgery by placing them on a small heat pad. Once animals were fully anesthetized, the head was fixed with a stereotaxic frame (David Kopf Instruments, Tujunga, CA, USA) and the scalp was shaved to expose the skin. A sagittal incision was made to expose the skull. Two pairs of holes were carefully drilled in the skull, each pair being 1.5 mm lateral on either side of the longitudinal fissure. The first pair was located 1 mm anterior to bregma and another pair was 3.5 mm anterior to bregma. Four stainless screws with lead wires attached

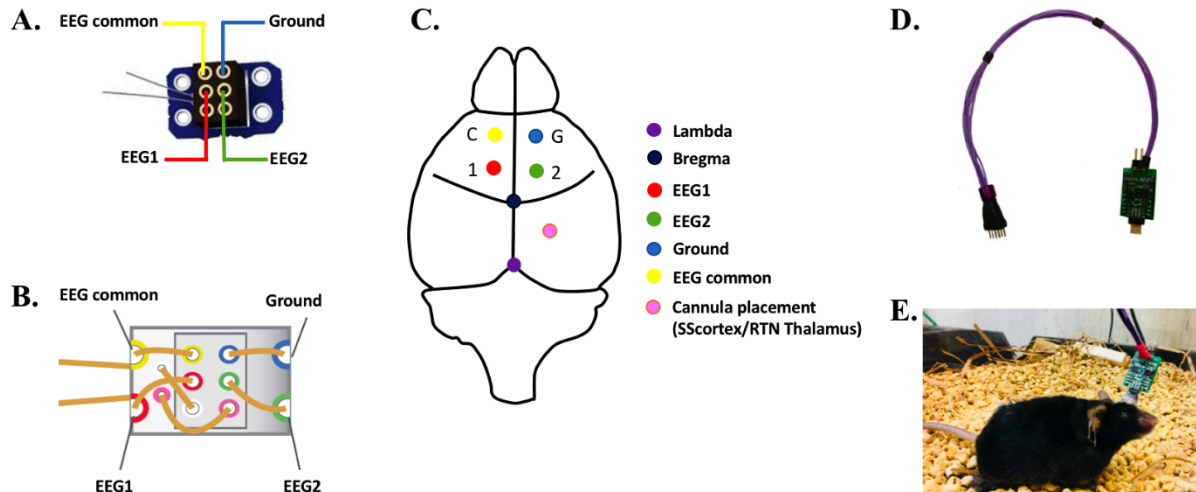


Fig. 2.4 Image showing the headmounts, position of EEG electrodes and cannula placement, and preamplifier used in this study. (A) Schematic showing the channels of prefabricated headmount used in this study. (B) Wiring and connection information of the prefabricated headmount. (C) Diagram showing the position of EEG electrodes and cannula placement. (D) Preamplifier used to amplify the EEG waveforms. (E) Photograph of an animal during EEG recording with preamplifier connected to the headmount.

(Pinnacle Technologies, Austin, TX, USA) were inserted through these burr holes. Prefabricated headmount (Pinnacle Technologies, Austin, TX, USA) was then placed over the head and lead wires were soldered to their respective channels of headmount (as illustrated in figure 2.4). The headmount with soldered regions was further secured using dental acrylic cement (Vertex Dental, Netherlands) and the loose skin around the incision site was then sutured (Sofsilks Sutures, Covidien, Ireland).

For focal CNO injections, one extra burr hole was drilled into the skull, based on the stereotaxic coordinates for either the SScortex (AP: -1.22 to -2.06 mm, ML: 2.8 mm, DV: -1.5 mm) or RTN thalamus (AP: -1.34 to -1.94 mm, ML: 2.1-2.3 mm, DV: -3.2 to -3.5 mm) (Mouse Brain Atlas, Paxinos and Franklin, 3rd Edition) for insertion of a guide cannula. A dummy cannula was inserted inside the guide cannula to prevent blood or any other fluid clogging it. Dummy and guide cannula for focal injections were obtained from Plastics One Inc., VA, USA. Dental acrylic cement was applied around the base of cannula to secure its position.

2.4.2 Post-operative care

Mice were placed inside individual cages as soon as they showed the signs of consciousness and activity after the surgical procedure. For four days post-surgery, animals were monitored twice daily. The food intake was monitored via body weight measurement and water intake

was measured by weighing the water bottle. Activity of animal during that period was also carefully monitored. Post-operative checks were restricted to once daily after fourth day, provided that animals showed sufficient recovery.

2.4.3 EEG recording procedure

After the full recovery of animals from surgical manipulation (at least seven days after surgery), EEG signals were recorded from the subdural space over the cerebral cortex using the Pinnacle mouse tethered system (Pinnacle Technologies, Austin, TX, USA) with simultaneous video recording. The prefabricated mouse headmount was attached to a preamplifier to amplify and filter the EEG waveforms. EEG signals were filtered at 0.5 Hz high pass and 50 Hz low pass. Before each recording, animals were acclimatized in testing environment and equipment for 1 hour. Sirenia® software was used for acquisition of EEG traces.

2.4.4 Analysis of EEG traces

Video/EEG analysis was performed offline manually by an investigator, blind to the genotype, scrolling through EEG traces using Seizure Pro® software. Bursts of paroxysmal oscillatory activity in EEG traces were defined as absence-like SWDs if they conformed to criteria published for the morphological characteristics of SWDs in mice and if they were associated with behavioural arrest (Table 2.9). Artefacts due to muscle activity (extremely fast spikes of 20–60ms of duration, not followed by slow waves, and mostly non-rhythmic), walking or scratching and grooming (rhythmic and high amplitude discharges) were readily recognised as such and on video were not associated with behavioural arrest hence they were not considered as epileptiform activity.

2.4.5 Use of ethosuximide (ETX) to confirm absence-like nature of discharges

In this study, to verify the absence-like nature of the epileptic discharges occurring in PV^{Cre}/Gi-DREADD animals, ETX was used. This drug is specific for absence seizures; therefore, it can be used to differentiate absence seizures from other EEG changes. Separate cohort of PV^{Cre}/Gi-DREADD animals were assigned to both the SS cortex and the RTN thalamus group. Animals were injected with 10mg/kg CNO focally on day 1 to confirm that CNO injection generates absence-like SWDs. After 24 h, on day 2, same animals were injected with ETX (200mg/kg, i.p.) and CNO (10 mg/kg, focal). Dose of ETX injection was based on previous published works on stargazer and tottering mouse models of absence epilepsy (Maheshwari et al., 2016; 2017).

2.5 Drug/chemical preparation and delivery

All drugs used in this study were prepared immediately before use. During experiments they were stored in refrigerator (4 degrees C).

2.5.1 Clozapine-N-oxide (CNO)

CNO or vehicle were injected intraperitoneally on the basis of the calculated dose for the body weight of the animal. For focal injection, 0.3 μ l of CNO was infused into the specific brain region at a rate of 0.1 μ l /min. During preparation, 1.5 mg of CNO (Advanced Molecular Technologies, Australia) was dissolved in 75 μ l of dimethyl sulfoxide (DMSO). The volume was then adjusted to 15 ml by addition of 0.9% sterile saline to prepare CNO of 0.1 mg/ml concentration (for 1 mg/kg dosage group). For 5 and 10 mg/kg dosage groups, CNO of 0.5 mg/ml and 1 mg/ml was prepared, respectively. Vehicle was prepared by mixing DMSO with 0.9% sterile saline. It was delivered via a Hamilton microinjection syringe attached to polythene tubing (Microtube Extrusions, Australia) and a 33-gauge internal cannula (Plastics One Inc., VA, USA) inserted into the previously implanted guide cannula. To verify the cannula tip localization and CNO diffusion to the specified focal regions, methylene blue dye was injected at the same volume and rate as CNO and histology was performed.

2.5.2 Ethosuximide (ETX)

ETX (Sigma Aldrich, USA) was first dissolved in 500 μ l DMSO. The volume was then adjusted to 10ml by addition of 0.9% sterile saline to prepare ETX of 20mg/ml concentration. ETX was injected intraperitoneally (200mg/kg) on the basis of calculated dose for the body weight of the animal.

2.5.3 Pentylenetetrazole (PTZ)

PTZ (Sigma Aldrich, USA) of 3mg/ml, 2mg/ml and 1mg/ml concentration was prepared in 0.9% sterile saline for 30mg/kg, 20 mg/kg and 10 mg/kg dosage groups, respectively. It was injected intraperitoneally on the basis of calculated dose for the body weight of the animal.

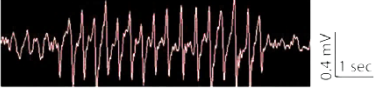


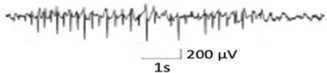


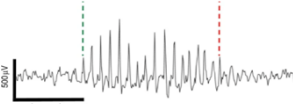

Published article (Animals used)	Criteria to fit as SWDs (quoted directly from the respective published articles)	Morphology of SWDs
Chung et al., 2009 (HCN2 knockout apathetic mice)	...repetitive rhythmic (2–8 Hz), high amplitude (>2 fold above background) sharp wave activity lasting longer than 1 second...	
Arain et al., 2012 (GABAA receptor $\alpha 1$ subunit knockout mice)	... SWDs were defined as trains (>1 sec) of rhythmic biphasic spikes, with a voltage at least twofold higher than baseline and that were associated with after going slow waves...	
Frankel et al., 2014 (C3H/He mice)	... at least 2 connected spike-wave complexes (typically spanning at least 0.5 seconds) with amplitudes at least two-fold higher than background...	
Kim et al., 2015 (Tottering-6j mice)	...A SWD lasting for >1 s was considered an absence-like seizure. When the time interval between two SWDs was <1 s, the discharges were regarded as a single seizure...	
Heuermann et al., 2016 (TRIP8b knockout mice)	...SWDs were scored for each animal only if the EEG demonstrated a distinct 3–8 Hz spike-wave morphology, with amplitudes at least 2 times higher than baseline...	
Maheshwari et al., 2016 (Stargazer and tottering mice)	...Seizure activity was defined by bilateral spike and wave discharges with amplitude $\geq 1.5 \times$ baseline voltage and concomitant video-recorded behavioural arrest...	
Meyer et al., 2018 (Stargazer mice)	...regular spike-wave burst structure, spike amplitude $1.5 \times$ baseline, spike frequency of 5–9 Hz, and a minimum duration of 0.5 second...	
This study	Bursts of oscillations were defined as SWD if they had a spike-wave structure (spike, positive transient, and slow wave pattern) with a frequency of 3–8 Hz, an amplitude at least two times higher than baseline and lasted for >1 second.	

Table 2.9 List of published studies on mice defining the morphology and characteristics of absence-like SWDs.

2.6 Behavioural tests

All animals were trained in moving rotarod for two consecutive days before the test day to make them accustomed in testing instrument and environment. On test day, mice were allowed to perform in open field and moving rotarod. Open field test was performed always before rotarod test. Both tests were conducted before and after CNO injection.

2.6.1 Open-field test

Animals were acclimatized to the testing room for 1 hour before starting the test. They were placed in opaque open field area (40x40x20cm). They were allowed to move freely in open field for 10 min and their movements were tracked with an overhead video camera linked with Top Scan software (Clever Sys Inc., USA).

2.6.2 Rotarod test

Rotarod test was conducted for 5 min in moving rotarod from 4-20 rpm (Rotamex 5.0, Columbus Instruments, USA). Three trials were performed for each mouse with 2 min gap between each trial. Latency of fall was recorded for each trial.

2.7 Western blotting

2.7.1 Tissue collection and processing

Animals were sacrificed by cervical dislocation. Brains were immediately extracted, snap-frozen on dry ice and stored at -80°C. The cerebellum was dissected from the rest of the brain. The forebrain was mounted in the cryostat chuck using embedding media (Leica Microsystems, USA). The temperature inside the cryostat chamber was always maintained at -10°C. 300 µm thick coronal sections were cut and thaw-mounted on glass slides. Slides were temporarily stored in polystyrene box containing dry ice to prevent the degradation of the tissues. The primary SS cortex and corresponding VP thalamus (Fig. 2.5) was punched out from the sections using 1.0 mm biopsy punches (Integra Miltex, 33-31AA) under dissecting microscope. Mouse brain atlas (Mouse Brain Atlas, Paxinos and Franklin, 3rd Edition) was used to identify primary SS cortex and VP thalamus in the coronal sections. Mircopunched tissues were collected into microtubes containing homogenization buffer (0.5M Tris, 100mM EDTA, 3% SDS, pH 6.8), 1% phenylmethylsulfonyl fluoride (PMSF) and 1% protease inhibitor (P8340, Sigma). Samples were sonicated for 5 min, heated for 2 min in hot bath at 100°C and then centrifuged at 13,000 rpm for 5 min at 4°C. Supernatant from each microtube was transferred into new microtube and stored at -80°C till use.

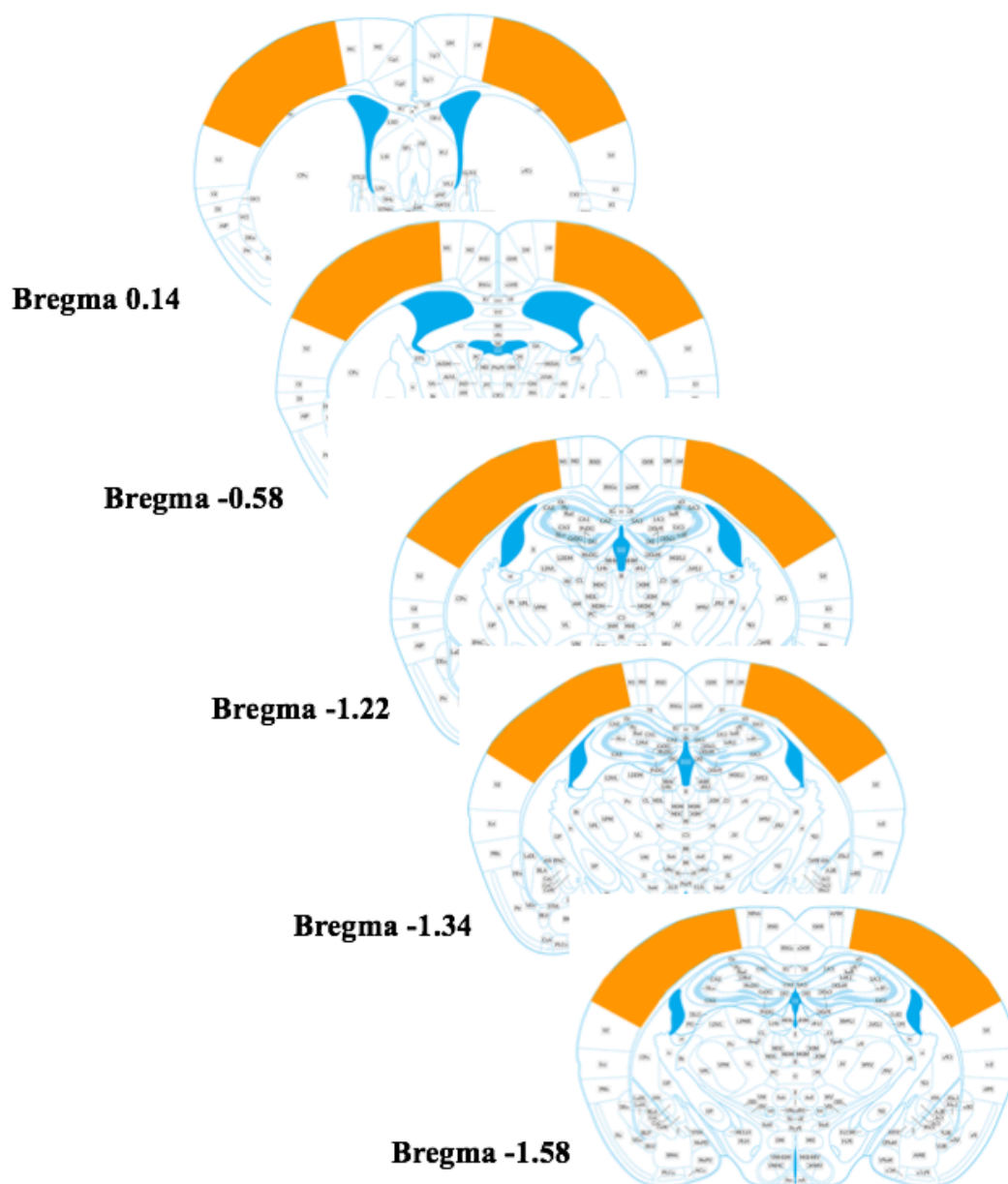


Fig. 2.5 Microdissection of tissue from the brain. Representative coronal sections of the mouse brain showing the SScortex (coloured portion). SScortex and corresponding VP thalamus regions were punched out from both hemispheres of coronal sections i.e. plates 25-46 in the mouse brain atlas (Franklin and Paxinos, 2008).

2.7.2 Protein quantification

Detergent compatible protein assay was used to determine the protein content in the brain samples. This assay was conducted according to the manufacturer's directions (DC protein assay, 500-0116, Bio-Rad). According to the protocol, BSA standards were first prepared (Table 2.10) in the same homogenization buffer as the brain samples. Same buffer was used to minimize the effect of buffer components. 5µl triplicates of each standard, brain sample and

blank (diluent only) were pipetted into a 96 well plate. 25µl of working reagent ‘A’ and 200µl of reagent ‘B’ was also added into each well. The plate was covered with aluminium foil and incubated at room temperature for 20 min. Absorbance was measured at 630 nm on plate reader. Protein concentration of brain samples was calculated after generating standard curve from BSA standards.

Table 2.10 Preparation of BSA standards

Standard concentration (µg/ml)	Diluent (µl)	1500 µg/ml standard	200 µg/ml standard
500	200	100	-
400	110	40	-
300	160	40	-
200	312	48	-
100	100	-	100
50	150	-	50
25	140	-	20

2.7.3 Gel electrophoresis and blot transfer

8.5% resolving gel and 4% stacking gel was prepared to run sodium dodecyl sulphate-polyacrylamide gel electrophoresis (SDS-PAGE) and to separate protein samples for immunodetection. Reagents for resolving gel were mixed in a falcon tube i.e. 6.81ml MQ H₂O (Milli-Q Integral, Millipore, Germany), 3.75ml Tris-HCl (1.5M, pH 8.8), 4.20ml of 30% acrylamide, 150µl of 10% SDS, 75µl of 10% APS and 7.5µl TEMED (for 2 gels). The mixture was poured into a plastic cassette and was left to set for 30 min. A layer of MQ H₂O was added on the top of resolving gel to prevent the gel from drying. Stacking gel was prepared in another falcon tube by mixing 3.01ml MQ H₂O, 1.25ml Tris HCl (0.5M, pH 6.8), 0.66ml of 30% acrylamide, 50µl of 10% SDS, 25µl of 10% APS and 5µl TEMED (for 2 gels). The layer of MQ H₂O added on the top of resolving gel was removed before pouring the stacking gel into the plastic cassette. An electrophoresis comb was inserted, and gel was allowed to set for half an hour. Brain samples containing 25µg protein were mixed with 4x loading buffer and MQ H₂O. The mixture was vortexed and heated for 10 min at 70°C. Samples were loaded into the gel after removing the comb. A reference protein ladder (Novex Sharp Pre-stained Protein Standard, LC 5800, CA, USA) was included in each gel to verify the molecular weight. SDS-PAGE was allowed to run in Mini-PROTEAN Tetra Vertical Electrophoresis Cell (Bio-Rad)

half-filled with running buffer (Tris-Glycine, 0.1% SDS) at 100V to 130V for about 90 min. Proteins were then transferred onto nitrocellulose membrane (RPN303D, GE Healthcare Life Sciences, Germany) in chilled transfer buffer (Tris-Glycine, 10% methanol, 0.025% SDS) at 100V for up to 80 min.

2.7.4 Immunoblotting and analysis

Following transfer of protein from gel onto nitrocellulose membrane, the membrane was washed in Tris buffered saline (TBS; 50mM Tris, 0.87% NaCl, pH 7.6) for 3-5 min. Membranes were blocked with Odyssey blocking buffer (Li-COR Biosciences) for 45 min at room temperature. Blocking was followed by 24 h incubation of membranes at 4°C with primary antibody solution. Primary antibody solution was prepared by mixing TBS-Tween (TBST i.e. TBS mixed with 0.1% Tween), blocking buffer and primary antibody. After incubation, the membranes were washed with TBS-Tween (3 times, 5 min each) and incubated with secondary antibodies diluted in TBS-Tween for 1 hour in the dark at room temperature. Primary and secondary antibodies used for western blotting experiments in this project are listed in Table 2.11 and Table 2.12, respectively. Membranes were washed with TBS-Tween (3 times, 5 min each) and TBS (2 times, 5 min each). After drying the membranes, they were scanned with the Odyssey Infrared Imaging System (Li-COR Biosciences). Protein bands were photographed and analyzed using Odyssey Image Studio Lite v3.1. The intensity of loading control (β -actin or α -tubulin) band was used to normalize other protein of interest.

Table 2.11 Primary antibodies used in this project for western blotting.

Target Protein	Type	Source/ Catalogue No.	Dilution
β -actin	Mouse monoclonal	Abcam/ab8226	1:1000
β -actin	Rabbit monoclonal	Cell Signalling/13E5	1:1000
α -tubulin	Rabbit polyclonal	Abcam/ab4074	1:5000
GAT-1	Rabbit polyclonal	Abcam/ab426	1:250-500
		Alomone Labs/AGT-001	1:200
GAT-3	Rabbit polyclonal	Alomone Labs/AGT-003	1:200
GAD65	Mouse monoclonal	Abcam/ab26113	1:750
GAD67	Mouse monoclonal	Millipore/MAB5406	1:2500

Table 2.12 Secondary antibodies used in this project for western blotting.

Product	Secondary conjugate	Source/ Catalogue No.	Dilution
Goat anti-rabbit	IRDye 680	Li-Cor Biosciences/926-32221	1:10000
Goat anti-rabbit	IRDye 800 CW	Li-Cor Biosciences /926-32211	1:10000
Goat anti-mouse	IRDye 800 CW	Li-Cor Biosciences /926-32210	1:10000

2.8 Data analysis

Statistical analyses of significant differences between mice groups i.e. DREADD animals and control animals (non-DREADD or vehicle treated DREADD) or epileptic stargazers and non-epileptic control littermates were calculated using appropriate statistical tests. The normality of the data was checked by using D'Agostino-Pearson normality test. In DREADD related experiments, comparison of values between before and after injection in same treatment group was performed using Wilcoxon matched-pairs signed-rank test. Tukey's post hoc multiple comparison test was performed to compare values from two independent treatment groups and Dunnett's post hoc multiple comparison test was used to compare treatment groups with single control. Statistical differences in staining intensity and expression levels of protein between epileptic stargazers and non-epileptic control littermates were tested using Mann-Whitney unpaired rank test. Data were presented as mean \pm standard error of the mean (SEM). All statistical analyses were performed in GraphPad Prism 8.0 with statistical significance set at $p < 0.05$.

CHAPTER 3. Impact of Silencing Feed-forward Inhibitory PV+ Interneurons on Absence Seizure Generation and Behaviour

3.1 Introduction

Absence epilepsy is due to the disruption of normal functioning of the CTC circuitry. Pathological SWDs seen in this form of epilepsy is believed to be mediated by multifactorial molecular and cellular mechanisms. Previous work conducted in Leitch laboratory in well-established stargazer mouse model of absence epilepsy has shown significant loss of AMPA receptors in PV+ interneurons potentially leading to the loss of FFI within the CTC network thus contributing to the generation of SWDs. However, it is not yet established whether the functional impairment of PV+ interneurons is directly involved in absence seizure generation. PV+ interneurons are the most common subset of GABAergic neurons within the brain (Kelsom and Lu, 2013; Hu et al., 2014; Tremblay et al., 2016). These interneurons regulate hyperexcitability of the entire brain and maintain a balance between excitation and inhibition (Paz and Huguenard, 2015; Jiang et al., 2016). They play critical roles in various brain functions such as behaviour (Ferguson and Gao, 2018), cognition (Bender et al., 2012; Murray et al., 2015), learning (Wolff et al., 2014; Lee et al., 2017), memory (Murray et al., 2011; Kim et al., 2016), generation of physiological oscillations (Sohal et al., 2009) etc. Impairment in the functioning of these interneurons contribute to different neurological and psychiatric disorders, including epilepsy (Jiang et al., 2016; Marafiga et al., 2020), Alzheimer's disease (Sanchez-Mejias et al., 2020), schizophrenia (Lewis et al., 2012; Nguyen et al., 2014) and autism (Wöhr et al., 2015).

PV+ interneurons are predominantly expressed in both components of the CTC network i.e. SScortex and RTN thalamus (Adams et al., 1997; Jones, 2002). In the CTC network, these interneurons provide strong FFI to the principal excitatory cortical neurons and to excitatory relay neurons in the VP thalamus. This inhibition prevents runaway excitation (Cammarota et al., 2013; Paz and Huguenard, 2015; Jinag et al., 2016). Moreover, these interneurons also mediate neuronal inhibition via feed-forward and/or feed-back mechanisms in other brain networks involving cortex and thalamus (Delevich et al., 2015; Nassar et al., 2018), and other brain regions such as hippocampus (Kullman et al., 2011; Hu et al., 2014), striatum (Szydlowski et al., 2013) and amygdala (Lucas et al., 2016).

In the stargazer mouse model of absence epilepsy, the mutation underlying the epileptic phenotype is a defect in the calcium voltage-gated channel auxiliary subunit gamma 2 i.e. CACNG2. This gene encodes the expression of a protein called stargazin (Noebels et al., 1990;

Letts et al., 1998). Stargazin is a transmembrane AMPAR regulatory protein (TARP) critical for synaptic targeting and membrane trafficking of AMPARs at excitatory glutamatergic synapses (Chen et al., 2000). Previous work from Leitch laboratory using this animal model reported that there is a loss of AMPA-type receptors at the excitatory synapses in feed-forward inhibitory PV⁺ interneurons of the CTC network. (Adotevi and Leitch, 2016; 2017; 2019; Barad et al., 2012; 2017). Other studies have also shown impaired AMPA receptor expression in these inhibitory interneurons in the SS cortex (Maheshwari et al., 2013) and the thalamus (Menuz and Nicoll, 2008) of the stargazers. Thus, loss of excitatory drive to these feed-forward inhibitory PV⁺ interneurons might potentially cause the loss of FFI and impaired FFI is likely to contribute to absence seizures in stargazer mice. GluA4 containing AMPA receptors are exclusively found at synapses on PV⁺ inhibitory interneurons (Kondo et al., 1997, Mineff and Weinberg, 2000) and knocking out GluA4 subunit of AMPA receptors (i.e. *Gria4*^{-/-} mouse) also resulted in absence seizures (Paz et al., 2011). Studies conducted in normal non-epileptic mice indicated that functionally silencing hippocampal PV⁺ interneurons generates epileptic seizures (such as temporal lobe seizures) (Drexel et al., 2017; 2019) and activation of these interneurons has anti-epileptic effects against PTZ-induced seizures (Clemente-Perez et al., 2017; Johnson et al., 2018), kainic acid (KA)-induced seizures (Wang et al., 2018), 4-aminopyridine (4-AP) induced seizures (Assaf and Schiller, 2016; Călin et al., 2018). However, the functional role of these interneurons within the CTC network on absence seizure has not yet been established.

Hence, the aim of this part of study was to investigate impact of functionally silencing feed-forward inhibitory PV⁺ interneurons of either the SS cortex or the RTN thalamus, in terms of absence seizure generation and behavioural parameters in non-epileptic (PV^{Cre}/Gi-DREADD) mice. DREADDs technology was used to silence PV⁺ interneurons in the SS cortex or the RTN thalamus. To selectively target these interneurons, mice expressing Cre recombinase in PV⁺ interneurons (PV-Cre) were bred with mice expressing inhibitory Gi-DREADD receptors i.e. hM4Di-flox mice. Expression of inhibitory Gi-DREADD receptors in PV⁺ interneurons was first confirmed via confocal fluorescence microscopy. Simultaneous video/EEG recordings were made after global (via i.p. CNO injection) and focal (via regional injection of CNO into either the SS cortex or the RTN thalamus) silencing of PV⁺ interneurons. Behavioural tests were also conducted to investigate the impact of silencing on motor function.

3.2 Methods

3.2.1 Immunofluorescence confocal microscopy, image acquisition and analysis

Immunofluorescence confocal microscopy was performed to confirm the expression of inhibitory Gi-DREADD receptors in PV⁺ interneurons. Antibodies against HA-tag (Cell Signaling, C29F4) and parvalbumin (Swant Inc., PV-235) were used to label DREADD receptors and PV⁺ interneurons, respectively. Immunolabelling was performed in brain sections from PV^{Cre}/Gi-DREADD mice ($n=13$) and non-DREADD WT control animals ($n=16$). Immunolabelling, confocal imaging, quantification of immunolabelled cells and analysis were performed as described previously in chapter 2 subsection 2.3. Images were taken in the brain regions with known PV⁺ interneurons distributions i.e. SS cortex, RTN thalamus and cerebellum. Immunolabelled cells in the SS cortex were counted using 10X magnified confocal images (total 2469 HA-tagged cells and 2423 PV cells counted). In the cerebellum 20X magnified confocal images were used (total 2258 HA-tagged cells and 2164 PV cells counted) whereas in the RTN thalamus cells were counted using 40X images (total 340 HA-tagged cells and 439 PV cells counted). Cell counting was based on 67 confocal images from PV^{Cre}/Gi-DREADD mice.

3.2.2 Surgical implantation of prefabricated headmounts and microcannulas for EEG recordings

To test the effect of global (i.p.) and focal (SS cortex or RTN thalamus) silencing of feed-forward inhibitory PV⁺ interneurons on absence seizure generation, EEG recordings were performed in PV^{Cre}/Gi-DREADD and non-DREADD WT control animals. Surgical manipulations for the implantation of prefabricated headmounts (Pinnacle Technologies, Austin, TX, USA) and microcannulas (Plastics One Inc., VA, USA) were performed as previously described in the chapter 2 subsection 2.4. Simultaneous video/EEG recordings were performed on animals 10 min before and for 1 hour after i.p. or focal injection of CNO/vehicle. Total number of animals used in these experiments are shown in the Tables below (Table 3.1 and Table 3.2).

Table 3.1 Number of animals used in EEG recordings for i.p. injection group.

CNO/vehicle	PV ^{Cre} /Gi-DREADD mice (DREADD)	Wild type control mice (Non-DREADD)
1 mg/kg	8	4
5 mg/kg	9	6
10 mg/kg	8	6
Vehicle	8	6

Table 3.2 Number of animals used in EEG recordings for focal (SScortex and RTN thalamus) injection group.

CNO/vehicle	SScortex group		RTN thalamus group	
	DREADD mice	Non-DREADD mice	DREADD mice	Non-DREADD mice
1 mg/kg	10	7	10	8
2.5 mg/kg	10	9	9	10
5 mg/kg	13	11	10	10
10 mg/kg	10	8	9	8
Vehicle	10	7	9	4

3.2.3 Preparation and delivery of clozapine-N-oxide (CNO) and ethosuximide (ETX)

CNO was freshly prepared before every scheduled experiment as previously described in chapter 2 subsection 2.5. CNO was injected intraperitoneally or focally (into the SScortex or the RTN thalamus) after 10 min of baseline EEG recordings. It was injected intraperitoneally on the basis of the calculated dose for the body weight of the animal. For focal injections, 0.3 μ l of CNO was infused into the specific brain region (either the SScortex or the RTN thalamus) at a rate of 0.1 μ l /min. It was delivered via a Hamilton microinjection syringe. At the end of focal EEG experiments, methylene blue dye was injected at the same volume and rate as CNO into the focal regions of the brain under investigation. Histology was performed to verify the localization of cannula tip and estimate the diffusion of CNO (see supplementary figure 1). The stereotaxic coordinates of the CNO and dye injections in the SScortex were 1.22 to 2.06 mm posterior to bregma, 2.8 mm lateral to the midline and 1.5 mm below the cortical surface. The coordinates for RTN thalamus injections were 1.34 to 1.94 mm posterior to bregma, 2.1-2.3 mm lateral to the midline and 3.2-3.5 mm ventral to the cortical surface (Mouse Brain Atlas, Paxinos and Franklin, 3rd edition). To characterize and verify the bursts of epileptic seizures

(spike and wave-like discharges) occurring after focal injection of CNO at doses 5-10mg/kg, impact of anti-absence epileptic drug ETX on seizure generation was tested. ETX was prepared as previously described in chapter 2. ETX was injected intraperitoneally (200mg/kg) on the basis of calculated dose for the body weight of the animal.

3.2.4 Behavioural tests

Two behavioural tests were employed to test the effect of global and focal silencing of PV+ interneurons in animal behaviour. Rotarod and open-field tests were used to examine the motor function of animals. Before the test day, animals were pretrained on a moving rotarod for two consecutive days to accustom them to the testing instrument and environment. On the test day, animals were acclimatized to the testing room for 1 hour before the experiment. Before CNO injection, mice were allowed to move freely in the open-field arena (40×40×20cm) for 10 min and their movements tracked with an overhead video camera linked to Top Scan software (Clever Sys Inc., USA). Open-field testing was followed by an interval of 3 min before three rotarod trials of 5 min each with 2 min gaps between successive trials. Rotarod testing was performed on a moving rotarod 4–20 RPM (Rotamex 5.0, Columbus Instruments, USA). Latency of fall was recorded for each trial. Both behavioural tests were performed after CNO injections according to the abovementioned protocol. Total number of animals used in these experiments are shown in Tables below (Table 3.3 and Table 3.4).

Table 3.3 Number of animals used in behavioural tests for i.p. injection group.

CNO/vehicle	PV ^{Cre} /Gi-DREADD mice (DREADD)	Wild type control mice (Non-DREADD)
1 mg/kg	20	10
5 mg/kg	20	9
10 mg/kg	20	10
Vehicle	20	8

Table 3.4 Number of animals used in behavioural tests for focal (SScortex and RTN thalamus) injection group.

CNO/vehicle	SScortex group		RTN thalamus group	
	DREADD mice	Non-DREADD mice	DREADD mice	Non-DREADD mice
1 mg/kg	9	7	10	8
2.5 mg/kg	9	10	11	10
5 mg/kg	10	9	13	8
10 mg/kg	11	7	10	8
Vehicle	11	7	10	8

3.3 Results

3.3.1 Inhibitory Gi-DREADD receptors are expressed in feed-forward inhibitory PV+ interneurons

Double-labelled immunohistochemistry with antibodies against HA-tag and PV was performed to confirm the expression of inhibitory DREADD receptors in PV+ interneurons of PV^{Cre}/Gi-DREADD mice (Fig.3.1). HA-tag for DREADD (identified by pseudocolour green) was only expressed in tissue sections from PV^{Cre}/Gi-DREADD mice but not in non-DREADD WT controls. PV+ interneurons were highly expressed throughout all SScortical layers (except layer 1), RTN thalamus and the cerebellar cortex of cerebellum in all genotypes. Co-localization of HA-tag in PV+ interneurons was found throughout the SScortex (Fig. 3.1A,B), the RTN thalamus (3.1C,D) and the cerebellar cortex of cerebellum (Fig. 3.1E,F). In the SScortex of PV^{Cre}/Gi-DREADD mice, almost all PV+ interneurons expressed HA-tag (Fig. 3.1A white arrows). The percentage of co-localization of HA-tag in PV+ interneurons in the SScortex was above 90% in PV^{Cre}/Gi-DREADD mice (Fig. 3.1B). Similarly, in the RTN thalamus, PV+ interneurons strongly expressed HA-tag (Fig. 3.1C white arrows). The percentage of co-localization of HA-tag in PV+ interneurons in the RTN thalamus was also above 90% in PV^{Cre}/Gi-DREADD mice (Fig. 3.1D). In both regions, very few cells appeared to be labelled for HA that were not also labelled for PV (red arrow). In the cerebellum, HA-tag was intensely expressed in PV+ Purkinje cell soma in PV^{Cre}/Gi-DREADD mice (Fig. 3.1E white arrows). The percentage of co-localization of HA-tag in PV+ inhibitory Purkinje cell soma was above 90%. (Fig. 3.1F). Co-labelling with HA-tag and PV antibody was seen throughout the molecular layer of cerebellar cortex of PV^{Cre}/Gi-DREADD mice, as dendritic projections from the Purkinje cells extend throughout the molecular layer. In contrast, there

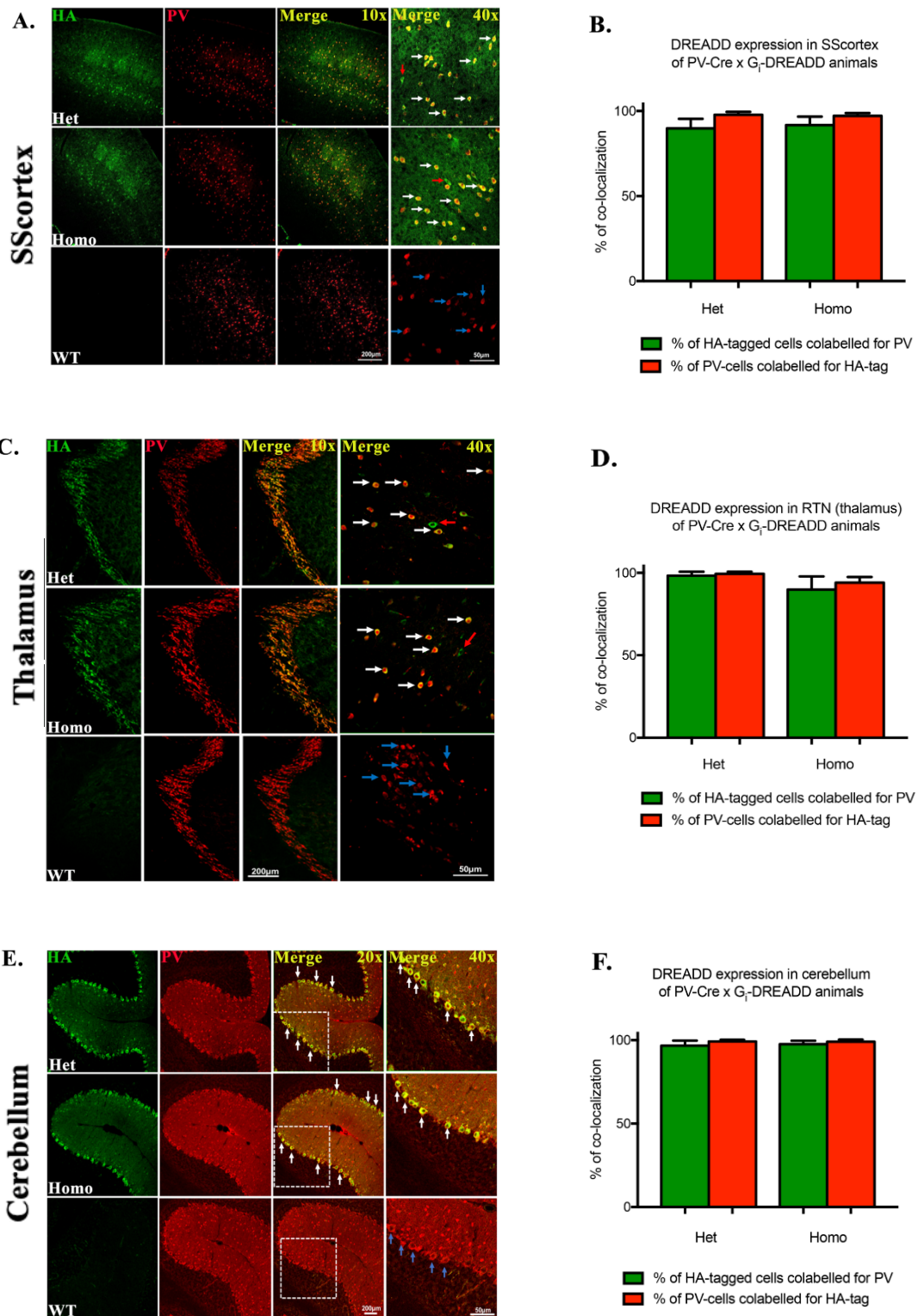


Fig. 3.1 Expression of Gi-DREADD receptors in PV+ interneurons. (A, C, E) Confocal images showing the expression of HA-tag in PV+ interneurons in the SScortex, the RTN thalamus and the cerebellar cortex of PV^{Cre}/Gi-DREADD animals, respectively. White arrows in merged images represent colocalized cells. Red arrows indicate the HA-positive neurons that are immunonegative for PV and blue arrows indicate PV+ neurons which are immunonegative for HA. (B, D, F) Percentage of co-localization of HA and PV in neurons in the SScortex, the RTN thalamus, and the cerebellum, respectively. Immunolabelled cells in the SScortex and the cerebellum were counted at 10X magnified confocal images whereas those in the RTN thalamus were counted using 40X images. (Het = PV^{Cre}/Gi-DREADD offspring from homozygous PV-Cre female and heterozygous hM4Di-flox male; Homo = PV^{Cre}/Gi-DREADD offspring from homozygous PV-Cre female and homozygous hM4Di-flox male; WT = Non-DREADD WT control animals). All values represent mean ± SEM.

was no HA-tag labelling in the non-DREADD WT controls (Fig. 3.1A,C,E, bottom panel).

3.3.2 Silencing feed-forward inhibitory PV+ interneurons via i.p. and focal CNO injections generated absence-like seizure

Firstly, as a proof of concept, the impact of globally silencing PV+ interneurons on seizure generation was tested via i.p. CNO injection. Simultaneous video/EEG recordings were performed on animals 10 min before and for 1 hour after i.p. CNO injection at doses of either 1 mg/kg (DREADD animals: $n = 8$; non-DREADD WT controls: $n = 4$), 5 mg/kg (DREADD animals: $n = 9$; non-DREADD WT controls: $n = 6$), 10 mg/kg (DREADD animals: $n = 8$; non-DREADD WT controls: $n = 6$), and vehicle-treated (DREADD animals: $n = 8$; non-DREADD WT controls: $n = 6$). Bursts of paroxysmal oscillatory activity (indicated by asterisks) was seen in both hemispheres of the brain which were associated with behavioural arrest (Fig. 3.2). Seizure activity was seen after 5 mg/kg and 10 mg/kg of i.p. CNO injection in PV^{Cre}/Gi-DREADD animals but not in the 1 mg/kg dose group, vehicle treated animals or non-DREADD WT control animals (Fig. 3.2). The bursts of paroxysmal oscillatory activity had a characteristic spike and wave-like morphological profile with a spike frequency between 3 and 7 Hz. In DREADD animals, the mean onset of seizure was 31.27 ± 5.46 min in the 5 mg/kg dose group ($n = 9$) and 28.91 ± 4.92 min in the 10 mg/kg group ($n = 8$). The mean number of bursts during 1 hour of EEG recording period was 4 ± 1.01 bursts in the 5 mg/kg dose group and 5.5 ± 1.37 in the 10 mg/kg group and was independent over increasing dose of CNO. Increasing dose of CNO also did not affect other EEG parameters such as mean spike frequency, mean duration of each burst and last incident of seizure during 1 hour of recording. The mean frequency of such discharges was 5.34 ± 0.76 spikes/sec and 5.18 ± 0.44 spikes/sec for 5 mg/kg and 10 mg/kg dose group of CNO, respectively. The mean duration of each burst was 3.16 ± 0.57 seconds and 4.01 ± 0.57 seconds for 5 mg/kg and 10 mg/kg dose group of CNO, respectively. During 1 hour of EEG recording, last incident of seizure was 43.54 ± 4.77 min and 34.17 ± 5.97 min after CNO injection for 5mg/kg and 10mg/kg dose group, respectively.

One PV^{Cre}/Gi-DREADD animal injected with 5mg/kg CNO displayed tonic-clonic convulsive type seizures after 22.58 min of CNO injection (Fig. 3.3). In this case the convulsive seizures were characterized by extremely high-amplitude spikes on the EEG and accompanied by severe jerking movements.

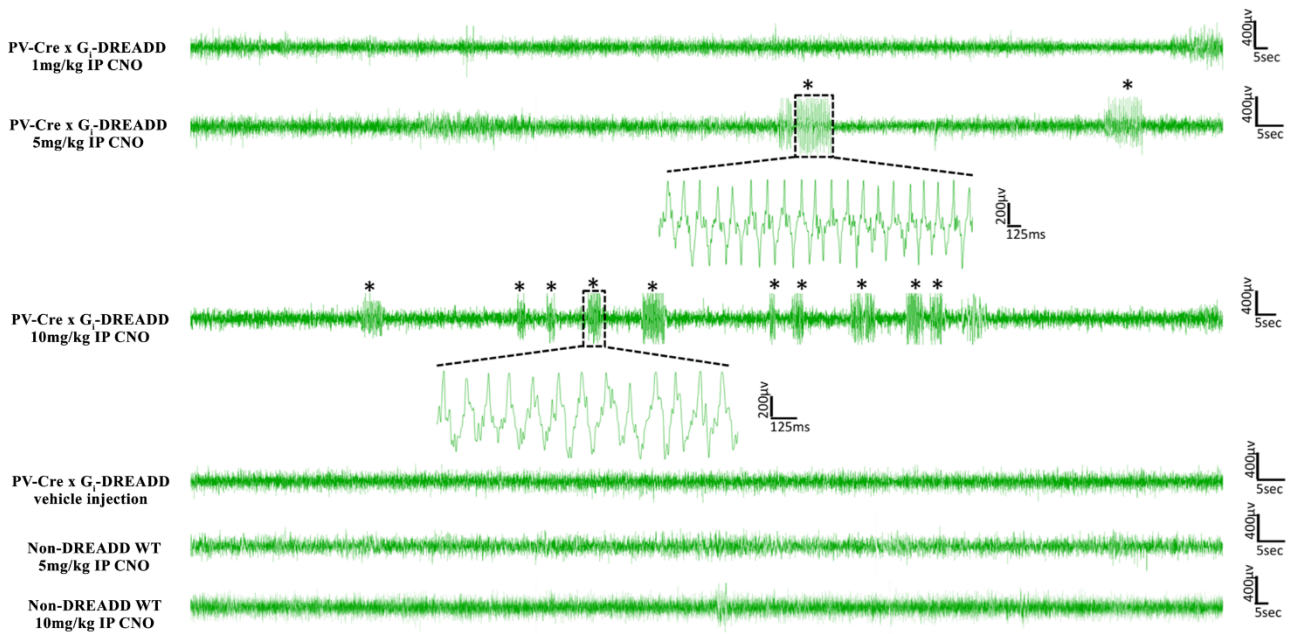


Fig. 3.2 Representative EEG traces of PV^{Cre}/Gi-DREADD (DREADD) animals and non-DREADD WT controls after i.p. injection of CNO/vehicle. Bursts of paroxysmal oscillatory activity (asterisks) with the characteristics of SWDs and associated behavioural arrest were seen only in DREADD animals injected with 5–10 mg/kg i.p. CNO. No SWDs were evident in 1 mg/kg or vehicle treated groups or non-DREADD WT control animals. All representative EEG traces were obtained from different animals. Each trace represents 3–6 min of EEG recording.

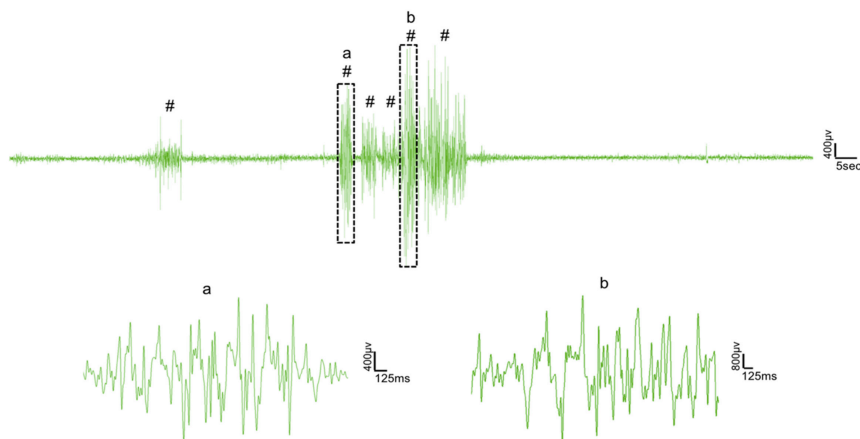


Fig. 3.3 Tonic-clonic convulsive seizures with very high amplitude in EEG were evident in one PV^{Cre}/Gi-DREADD animal after i.p. 5 mg/kg CNO injection. Hash signs (#) on the trace represent tonic-clonic seizures. Trace represents 3 min of EEG recording.

The characteristics and morphology of such discharges were very different to the rhythmic spike and wave oscillations seen in the other PV^{Cre}/Gi-DREADD animals in the 5 mg/kg and 10 mg/kg dose groups hence this animal was excluded from the analysis.

After confirming that global silencing of feed-forward inhibitory PV⁺ interneurons via i.p. CNO injection generates paroxysmal oscillatory discharges having similar morphological profiles of absence-like SWDs, CNO injections were targeted focally into either the SS cortex (Fig. 3.4) or the RTN thalamus (Fig. 3.6). Feed-forward inhibitory PV⁺ interneurons were directly silenced in either of these brain regions to test that loss of FFI within CTC network is one mechanism by which the normal physiological oscillations switch to pathological SWDs like oscillations as seen in absence seizures. Similar to the i.p. injection groups, EEG traces were recorded for 10 min before and for 1 hour after focal CNO/vehicle injection at doses of either 1, 2.5, 5 and 10 mg/kg. Different cohorts of animals were used in this experiment and each animal had only a cortical or thalamic canula inserted for injection of CNO. Injection of CNO into both focal regions (2.5, 5 and 10 mg/kg) in PV^{Cre}/Gi-DREADD animals generated bursts of paroxysmal oscillatory activity (indicated by asterisks on EEG traces) in both brain hemispheres and those bursts were associated with behavioural arrest (Fig 3.4 and 3.6). The morphology and character of such bursts were similar to absence-like SWDs. However, 1mg/kg CNO or vehicle treated DREADD animals and CNO treated non-DREADD animals showed no signs of seizures (Fig 3.4 and 3.6).

One PV^{Cre}/Gi-DREADD animal, when focally injected with 5 mg/kg CNO into the SS cortex showed a single tonic-clonic convulsive event with jerky body movements which lasted for just 3.61 seconds (Fig. 3.5). This animal was not included in the analyses of absence-like seizures.

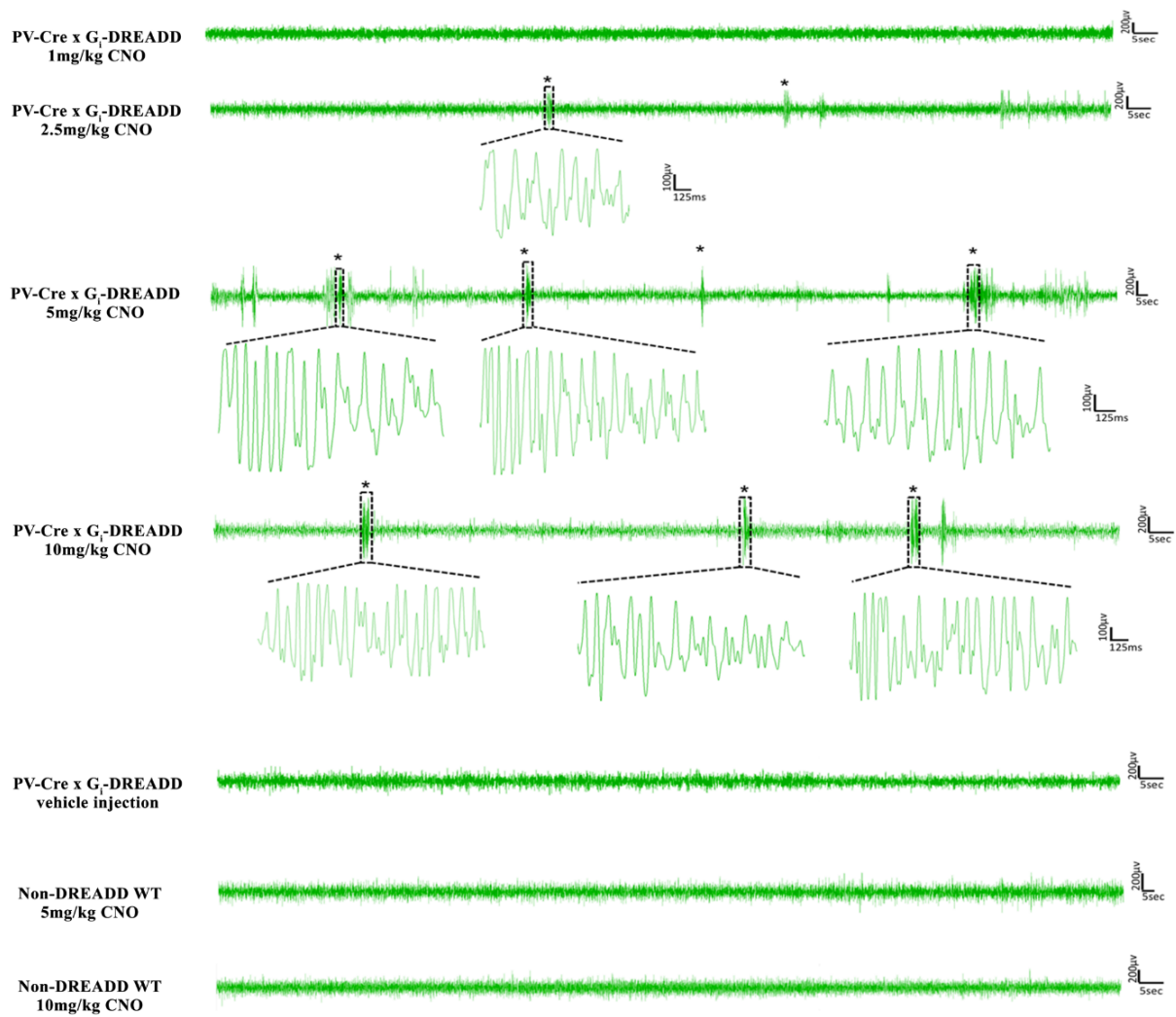


Fig. 3.4 Representative EEG traces of PV^{Cre}/Gi-DREADD (DREADD) animals and non-DREADD WT controls after focal injection of CNO/vehicle into the SS cortex. Bursts of paroxysmal oscillatory activity (asterisks) with the characteristics of SWDs and associated behavioural arrest were seen after CNO injection (2.5–10mg/kg) only in DREADD animals but not in 1mg/kg or vehicle treated groups or non-DREADD WT control animals. All representative EEG traces are from different animals. Each trace represents 3–6 min of EEG recording.

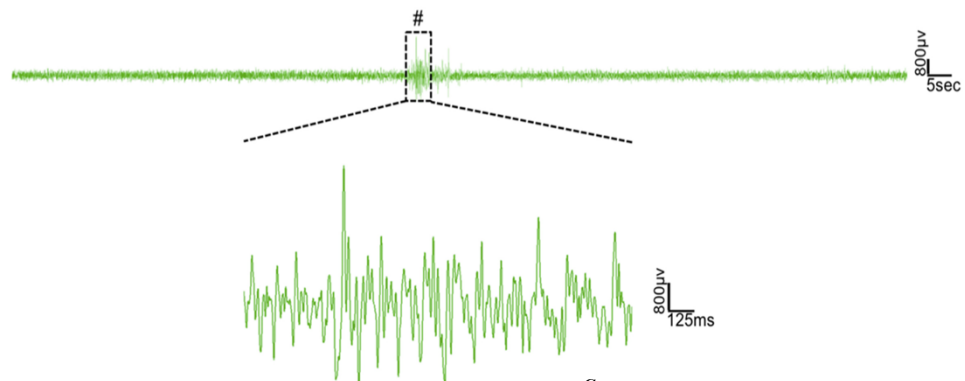


Fig. 3.5 Tonic-clonic convulsive seizure in EEG was evident in one PV^{Cre}/Gi-DREADD animal with 5 mg/kg CNO injected into the SS cortex. Hash sign (#) on the trace represents tonic-clonic seizure. Trace represents 3 min of EEG recording.

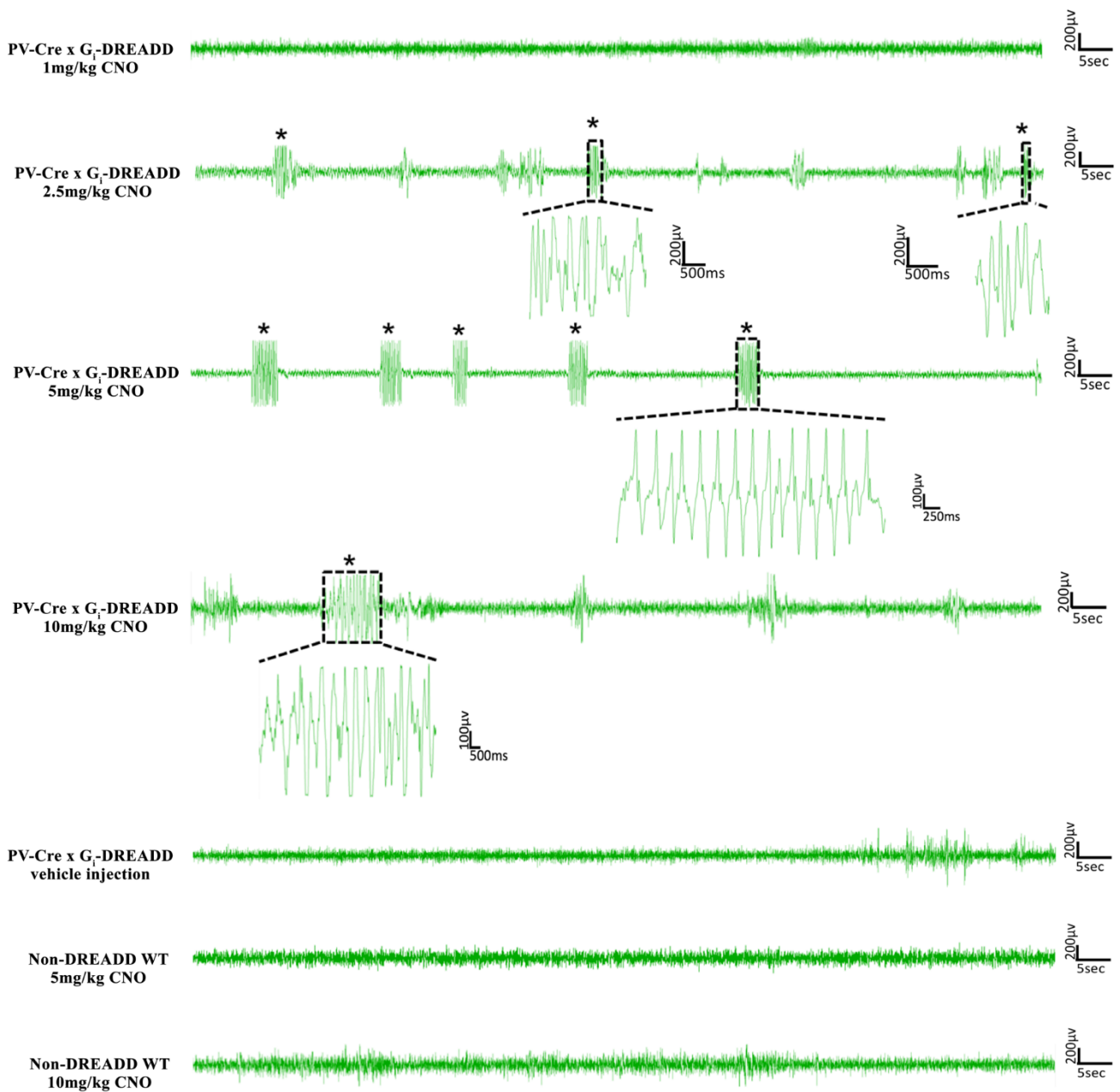


Fig. 3.6 Representative EEG traces of PV^{Cre}/Gi-DREADD (DREADD) animals and non-DREADD WT controls after focal injection of CNO/vehicle into the RTN thalamus. Bursts of paroxysmal oscillatory activity (asterisks) with the characteristics of SWDs and associated behavioural arrest were seen after CNO injection (2.5–10mg/kg) only in DREADD animals but not in 1mg/kg or vehicle treated groups or non-DREADD WT control animals. All representative EEG traces are from different animals. Each trace represents 2–3 min of EEG recording.

Analysis of the various EEG parameters in PV^{Cre}/Gi-DREADD mice injected with 2.5, 5 and 10 mg/kg CNO (both in the SS cortex and the RTN thalamus groups) showed that increasing dose of CNO has no significant difference in any parameters. Comparison is shown in the Table below (Table 3.5).

Table 3.5 Comparison of various EEG parameters after focal CNO injection into the SS cortex or the RTN thalamus of PV^{Cre}/Gi-DREADD animals during 1 hour of EEG recording.

EEG parameters	2.5 mg/kg CNO		5 mg/kg CNO		10 mg/kg CNO	
	SScortex (n=10)	RTN Thal. (n=9)	SScortex (n=13)	RTN Thal. (n=10)	SScortex (n=10)	RTN Thal. (n=9)
First incident of seizure (min)	14.69±2.26	12.5±2.02	13.89±2.93	15.25±3.96	14.76±2.75	10.14±1.83
Mean rate (discharges/hr)	6.9±1.01	4.44±0.98	6.46±1.54	5.8±1.95	6.7±1.58	5.55±1.26
Mean frequency (spikes/sec)	5.00±0.60	4.78±0.43	5.27±0.49	4.87±0.43	5.03±0.61	5.09±0.57
Mean duration of seizure (sec)	3.98±0.60	3.03±0.35	3.48±0.51	3.49±0.38	3.91±0.67	4.60±0.79
Last incident of seizure (min)	35.79±4.55	32.31±5.42	27.24±4.56	32.81±4.38	30.55±4.66	28.57±5.41

3.3.3 Route of administration of CNO affected onset of bursts of oscillatory activity

Impact of the route of CNO injection (i.p. or focal) on seizure generation was analysed which revealed that onset of seizures after focal injection was significantly faster than i.p. injection (Fig. 3.7A). The mean onset of seizures in the i.p. CNO injection group was at 31.27 ± 5.46 min ($n = 9$) for 5 mg/kg and 28.91 ± 4.92 min ($n = 8$) for the 10mg/kg dosage group. In the SS cortex group, mean onset of seizures was 13.89 ± 2.93 min ($n = 13$) after 5 mg/kg CNO, and 14.76 ± 2.75 min ($n = 10$) after 10 mg/kg CNO (Fig. 3.7A). In the thalamus group, mean seizure onset was 15.25 ± 3.96 min ($n = 10$) after 5 mg/kg CNO and 10.14 ± 1.83 min ($n = 9$) after 10 mg/kg CNO). Other parameters of EEG discharges such as burst rate, burst duration and spike frequency remained similar irrespective of the dose of CNO or the route of administration (Fig. 3.7B,C,D). No significant difference in mean rate of discharges/hour was seen after either i.p. [4 ± 1.01 and 5.50 ± 1.3 bursts/hour for 5 mg/kg ($n = 9$) and 10 mg/kg ($n = 8$) respectively] or focal administration of CNO: (SS cortex group: 6.46 ± 1.54 ($n = 13$) after 5 mg/kg CNO and 6.7 ± 1.58 ($n = 10$) after 10 mg/kg CNO; thalamus group: 5.8 ± 1.95 ($n = 10$) after 5 mg/kg CNO and 5.55 ± 1.26 ($n = 9$) after 10 mg/kg CNO) (Fig. 3.7B).

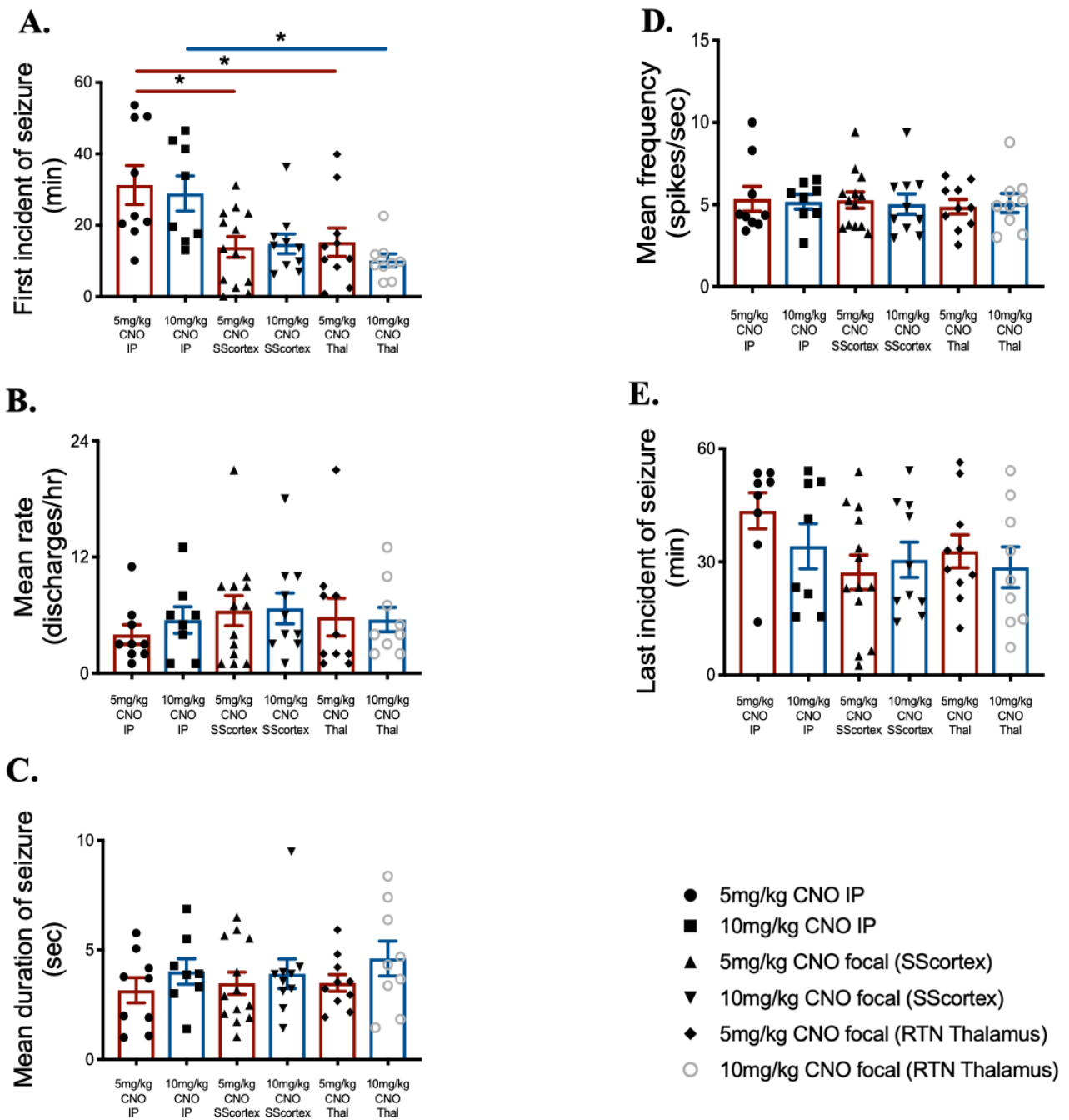


Fig. 3.7 Overall comparison of various EEG parameters after i.p. and focal (SScortex and RTN thalamus) injection of CNO during 1 hour of EEG recording. (A) First incident of seizure (B) Mean rate of discharges (C) Mean duration of seizure (D) Mean frequency of seizure (E) Last incident of seizure. All values represent mean \pm SEM. Comparisons between treatment groups were performed using Tukey's post hoc multiple comparison test.

Likewise, there was no significant difference in the mean duration of each seizure burst for any of the CNO levels tested via i.p. or focal routes i.e. i.p. group: 3.16 ± 0.57 seconds ($n = 9$) after 5 mg/kg CNO and 4.01 ± 0.57 seconds ($n = 8$) after 10 mg/kg CNO, SS cortex group: 3.48 ± 0.51 seconds ($n = 13$) after 5 mg/kg CNO and 3.91 ± 0.67 seconds ($n = 9$) after 10 mg/kg CNO, thalamus group: 3.49 ± 0.38 seconds ($n = 10$) after 5 mg/kg CNO and 4.60 ± 0.79 seconds ($n = 9$) after 10 mg/kg CNO (Fig. 3.7C). Similarly, no significant differences were seen in mean frequency of seizure (spikes/sec) i.e. i.p. group: 5.34 ± 0.76 ($n = 9$) after 5 mg/kg CNO and 5.18 ± 0.44 ($n = 8$) after 10 mg/kg CNO; SS cortex group: 5.27 ± 0.49 ($n = 13$) after 5 mg/kg CNO and 5.03 ± 0.61 ($n = 10$) after 10 mg/kg CNO; thalamus group: 4.87 ± 0.43 min ($n = 10$) after 5 mg/kg CNO and 5.09 ± 0.57 min ($n = 9$) after 10 mg/kg CNO (Fig. 3.7D). Likewise, no significant changes were seen also in the last incident of seizure across route of administration or dose level of CNO (Fig. 3.7E).

3.3.4 ETX suppressed absence-like seizures generated by focal CNO injections

Next, the impact of anti-absence epileptic drug ETX on seizure generation was investigated. ETX is widely used to prevent absence seizures in both human patients and genetic animal models of absence epilepsy. The rationale behind the use of ETX in this study was to confirm that the bursts of oscillatory absence-like SWDs occurring after focal injection of CNO at doses of 2.5–10 mg/kg are definite absence seizures and are not any other forms of EEG changes. CNO (10 mg/kg) was injected focally into a cohort of PV^{Cre}/Gi-DREADD mice (SScortex group: $n = 3$, (Fig. 3.8A); RTN thalamus group: $n = 4$, (Fig. 3.8B) and video/EEG recordings were made for 10 min before and for 1 hour post CNO injection. CNO induced bursts of oscillatory spikes and wave-like discharges in all mice tested. Next day, the same cohort of animals was treated with 200 mg/kg of ETX before 10 mg/kg CNO injection. EEG recordings were performed at least 1-hour post CNO injection. Administration of ETX completely prevented spikes and wave-like discharges in all tested PV^{Cre}/Gi-DREADD animals. This provided a strong evidence that the nature of epileptiform activity seen in EEG recordings after focal CNO injection was absence-like SWDs.

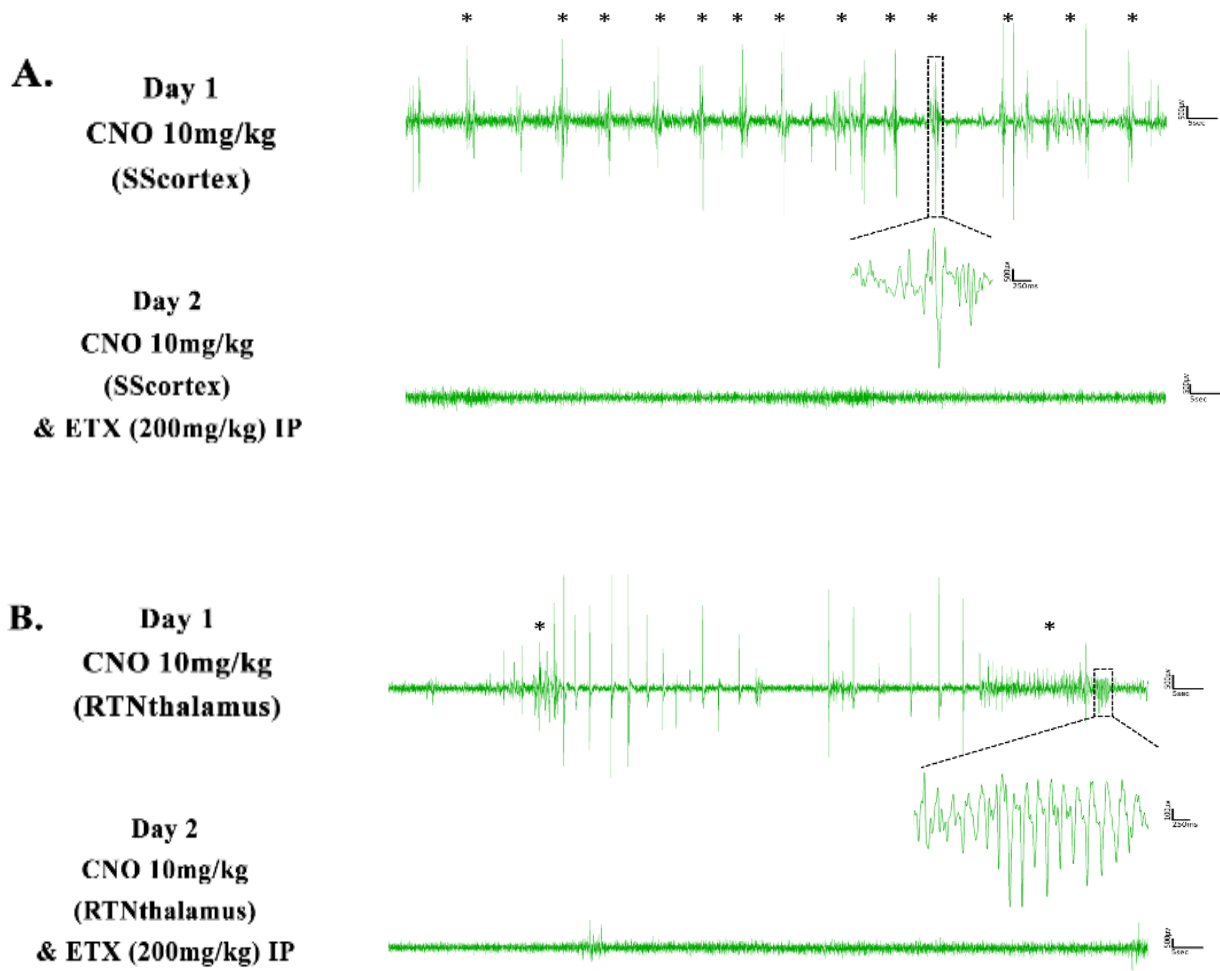


Fig. 3.8 ETX test conducted in $PV^{Cre}/Gi-DREADD$ animals. (A) Representative EEG traces from $PV^{Cre}/Gi-DREADD$ animal injected with 10mg/kg of CNO into the SScortex on day 1 showing bursts of discharges (asterisks). After 24 h, the same animal was treated with ETX (200mg/kg) prior to injection of 10mg/kg of CNO into the SScortex, which prevented SWDs. (B) Representative EEG traces from a $PV^{Cre}/Gi-DREADD$ animal injected with 10mg/kg of CNO into the RTN thalamus on day 1 showing bursts of discharges (asterisks). After 24 h, the same animal was injected focally with 10mg/kg of CNO into the RTN (thalamus) and ETX (200mg/kg) intraperitoneally which suppressed SWDs. Each trace represents 5-6 min of EEG recording.

3.3.5 Silencing feed-forward inhibitory PV⁺ interneurons via i.p. and focal CNO injections increased immobility

Silencing PV⁺ interneurons via i.p. and focal (SScortex or RTN thalamus) routes generated absence-like seizures which were evident during 1 hour of EEG recording. It was also revealed that silencing PV⁺ interneurons led to increased immobility in dose-dependent manner only in DREADD animals. Analysis of the data indicated that DREADD animals spent significantly more time immobile after i.p. CNO doses of 5 and 10mg/kg i.e. 45.89 ± 3.44 min ($n = 9$) and 52.61 ± 1.21 min ($n = 8$), respectively in comparison to vehicle-treated and 1mg/kg CNO injected animals, which were immobile for 29.27 ± 5.53 min ($n = 8$) and 34.20 ± 1.73 min ($n = 8$), respectively (Fig. 3.9A). Injection of CNO into non-DREADD WT control animals at doses 5 and 10mg/kg did not significantly change the mobility in animals i.e. 5mg/kg CNO group: 31.30 ± 1.55 min ($n = 6$), 10mg/kg CNO group: 34.11 ± 2.04 min ($n = 6$). Similarly, vehicle treated and 1 mg/kg CNO treated non-DREADD animals spent 26.63 ± 4.27 min ($n = 6$), 28.28 ± 4.59 min ($n = 4$) immobile, respectively (Fig. 3.9A).

In the SScortex group, DREADD mice injected with CNO doses of 2.5, 5 and 10 mg/kg spent significantly more time immobile after CNO treatment. The mean time spent immobile during the 1 hour recording period post CNO injection was: 39.09 ± 3.51 min ($n = 10$) after 2.5mg/kg; 49.76 ± 1.83 min ($n = 13$) after 5mg/kg and 45.64 ± 3.32 min ($n = 10$) after 10mg/kg compared to vehicle-treated 24.97 ± 3.74 min ($n = 10$) or 1mg/kg CNO injected 29.71 ± 4.05 min ($n = 10$) animals (Fig. 3.9B). Administration of CNO into non-DREADD WT control animals did not significantly change mobility compared to vehicle treated animals (2.5mg/kg CNO 33.54 ± 3.69 min ($n = 9$); 5mg/kg CNO 28.56 ± 2.12 min ($n = 11$); 10mg/kg CNO 34.20 ± 2.93 min ($n = 8$); vehicle 21.86 ± 2.69 min ($n = 7$); 1mg/kg CNO 30.72 ± 3.50 min ($n = 7$) (Fig. 3.9B).

Analysis of the data following focal injection of CNO into the RTN thalamus of DREADD mice also revealed animals spent more time immobile after higher 5-10 mg/kg doses, although this trend did not reach to significance (Fig. 3.9C). DREADD mice treated with vehicle, 1, 2.5, 5, and 10mg/kg CNO spent 37.43 ± 4.49 min ($n = 9$), 38.35 ± 4.0 min ($n = 10$), 34.10 ± 3.78 min ($n = 9$), 47.11 ± 2.54 min ($n = 10$), 46.82 ± 4.42 min ($n = 9$) immobile, respectively.

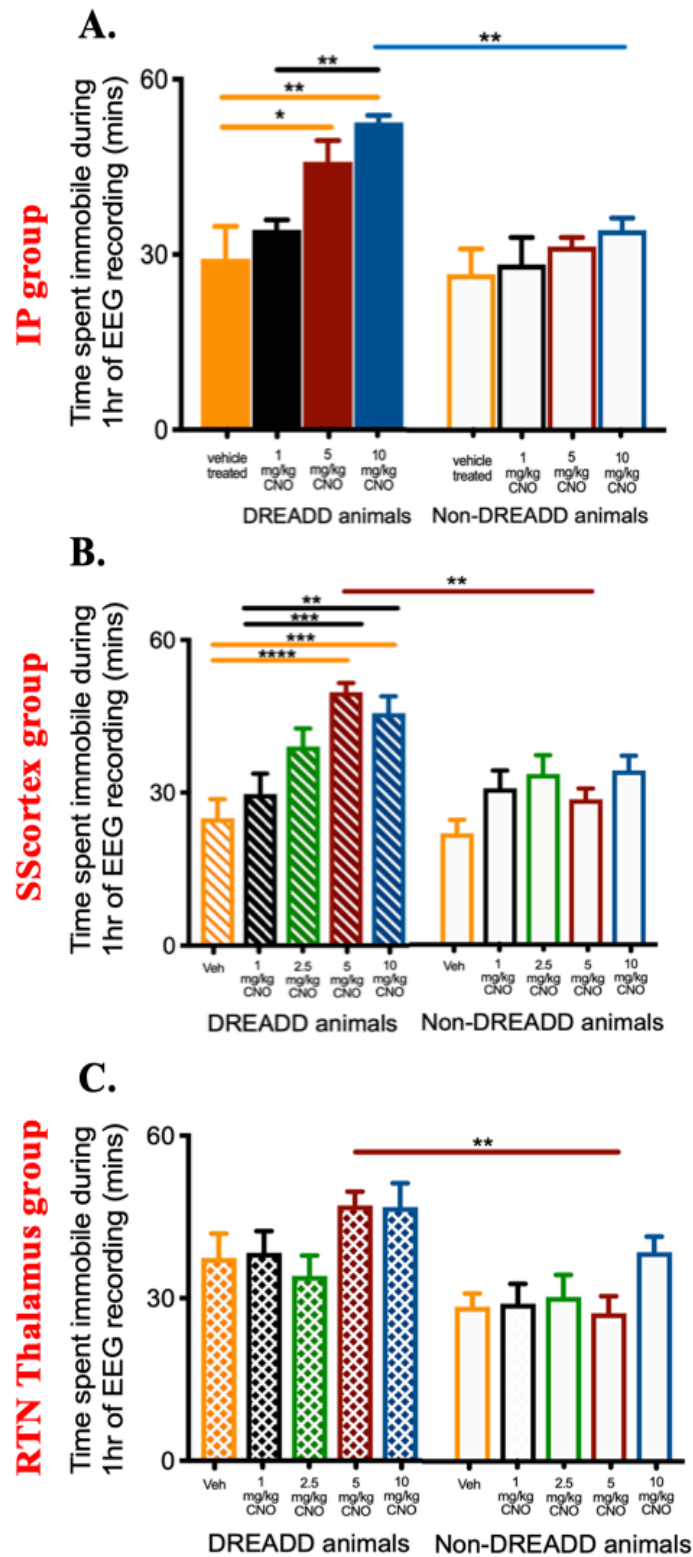


Fig. 3.9 Immobility in animals after CNO injection during 1 hour of EEG recording. Comparison of mean time spent immobile by PV^{Cre}/Gi-DREADD (DREADD) and non-DREADD animals during 1 hour of EEG recording after (A) I.P. CNO injection and focal CNO injection into the (B) SS cortex and (C) the RTN thalamus. All values represent mean \pm SEM. Comparison between treatment groups were performed using Tukey's post hoc multiple comparison test. (Individual data points are shown in appendix, page 242).

Injection of CNO into non-DREADD WT control animals of RTN thalamus group also did not significantly change mobility compared to vehicle treated animals and any of the dose levels tested (vehicle 28.53 ± 2.44 min ($n = 4$); 1mg/kg CNO 29.08 ± 3.69 min ($n = 8$); 2.5mg/kg CNO 30.30 ± 4.10 min ($n = 10$); 5mg/kg CNO 27.31 ± 3.15 min ($n = 10$); 10mg/kg CNO 38.63 ± 2.83 min ($n = 8$) (Fig. 3.9C).

3.3.6 Silencing feed-forward inhibitory PV+ interneurons via intraperitoneal (i.p.) CNO injection impaired motor function, decreased locomotion and increased anxiety

Impact of globally silencing PV+ interneurons on animal behaviour was tested by i.p. CNO injection in PV^{Cre}/Gi-DREADD mice and non-DREADD WT control mice. As rodent models of absence epilepsy exhibit absence seizures associated with behavioural arrest, impaired motor co-ordination and ataxia (Jarre et al., 2017), motor function in open-field and moving rotarod was tested in this study. Open-field test was conducted to examine the total distance travelled and the relative time spent in central and peripheral zones (CZ and PZ) in the open-field arena. Total ambulatory distance is correlated with the locomotory behaviour of the animal, whereas relative time spent in the CZ and PZ of the open field is an indicator of anxiety levels. Rotarod test was performed to evaluate motor coordination of animals.

Analysis of the open-field data revealed that there was a significant difference in all tested parameters in PV^{Cre}/Gi-DREADD mice treated with 5 mg/kg and 10 mg/kg of i.p. CNO compared to control non-DREADD WT littermates, or vehicle treated PV^{Cre}/Gi-DREADD mice. However, drug doses of 1 mg/kg i.p. CNO had no effect on PV^{Cre}/Gi-DREADD mice or controls. Movement track-paths recorded in the open-field arena revealed decreased locomotion and an increased tendency to stay in the PZ, after administration of higher (5-10 mg/kg) i.p. doses of CNO to DREADD mice (Fig. 3.10A). In the 5 mg/kg dose group, total ambulatory distance and total time spent in the PZ before CNO injection was 1562 ± 133.6 cm and 532.1 ± 7.62 seconds, respectively, which changed significantly after CNO injection to 553.3 ± 95.35 cm and 587.1 ± 3.88 seconds respectively ($n = 20$) (Fig.3.10B,C). Similarly, in 10 mg/kg dose group, total ambulatory distance and total time spent in the PZ changed significantly from 1769 ± 95.87 cm and 543.8 ± 6.38 seconds before CNO injection to 360.3 ± 88.62 cm and 591.9 ± 2.48 seconds respectively after CNO injection ($n = 20$) (Fig.3.8B,C). The percentage of time DREADD mice spent in CZ was significantly reduced

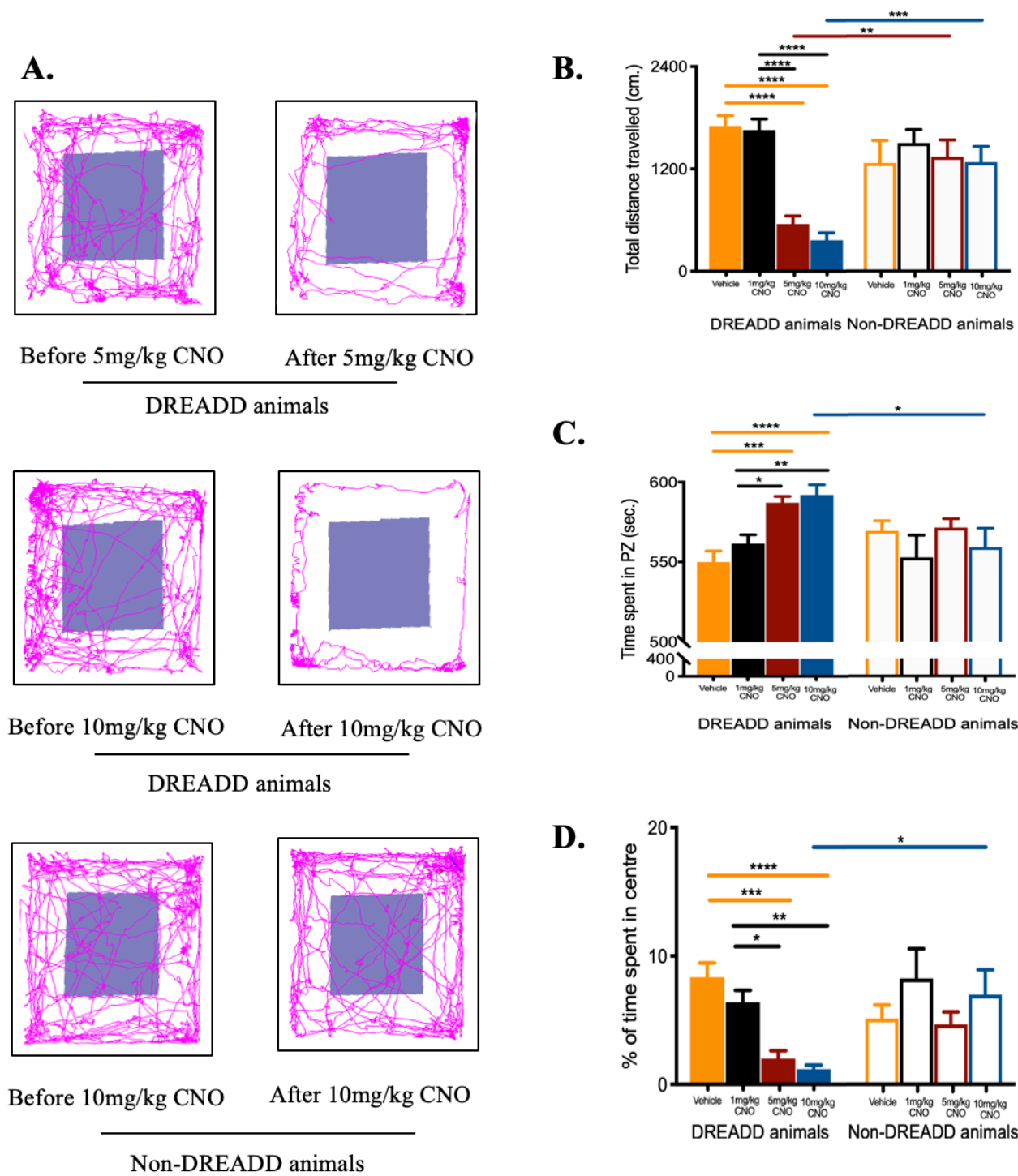


Fig. 3.10 Comparison of parameters of open-field test in animals after injection of different i.p. doses of CNO. (A) Representative images of movement track paths from open-field test for CNO treated PV^{Cre}/Gi-DREADD (DREADD) animals and non-DREADD WT control animals. Graph showing (B) total distance travelled (C) total time spent in PZ (D) % of time spent in CZ by DREADD and non-DREADD WT control mice after i.p. injection of CNO or vehicle. All values represent mean ± SEM. Comparisons between treatment groups were performed using Tukey's post hoc multiple comparison test. (Individual data points for B, C, D are shown in appendix, page 243).

after drug doses of 5-10 mg/kg (before 5 mg/kg CNO: $11.33 \pm 1.29\%$, after 5 mg/kg CNO: $2.01 \pm 0.62\%$; before 10 mg/kg CNO: $9.36 \pm 1.06\%$, after 10 mg/kg CNO: $1.18 \pm 0.31\%$; $n = 20$) (Fig. 3.10D). By contrast mice treated with 1 mg/kg CNO showed no significant changes in any of the parameters tested in open field. None of the control groups (vehicle treated or non-DREADD WT groups) also showed any changes in locomotion or relative time spent in the CZ or PZ (Fig. 3.10B,C,D). Thus, silencing feed-forward inhibitory PV⁺ interneurons via i.p. CNO injection at dose levels 5–10 mg/kg decreased locomotion and increased anxiety levels only in PV^{Cre}/Gi-DREADD animals.

To test the impact of silencing feed-forward inhibitory PV⁺ interneurons on motor coordination, the same cohort of animals was tested on a moving rotarod. Rotarod test is widely used to examine motor coordination in rodents. Rotarod data revealed that there was a significant difference in the mean latency of fall in PV^{Cre}/Gi-DREADD mice before and after i.p. CNO injection only in 5 mg/kg and 10 mg/kg dose group but not in 1 mg/kg dose group and vehicle treated group. In 5 mg/kg dose group, the mean latency of fall before CNO injection was 295.1 ± 1.23 seconds which decreased significantly after CNO injection i.e. 173.8 ± 6.21 seconds; $n = 20$ mice (Fig. 3.11A). Similarly, in 10 mg/kg dose group, the mean latency of fall reduced significantly from 294 ± 1.16 seconds before injection to 86.40 ± 4.30 seconds ($n = 20$) after CNO injection (Fig. 3.11A). However, mice treated with 1 mg/kg CNO showed no motor impairment on the rotarod (latency of fall before CNO injection = 296.30 ± 0.96 seconds; after CNO injection 286.7 ± 3.45 s; $n = 20$). Also, vehicle treated PV^{Cre}/Gi-DREADD mice showed no changes in motor co-ordination before and after CNO injection (latency of fall before CNO injection = 293.4 ± 2.45 seconds; after CNO injection 291.7 ± 2.17 s; $n = 20$). No significant differences were seen in vehicle and CNO treated non-DREADD WT control groups (Fig. 3.11B). Wilcoxon matched-pairs signed rank test was performed to compare mean latency between before and after injection in same treatment group (Fig. 3.9A,B) whereas Tukey's post hoc multiple comparison test was performed to compare treatment groups of DREADD and non-DREADD animals (Fig. 3.11C).

3.3.7 Silencing feed-forward inhibitory PV⁺ interneurons via focal CNO injection decreased locomotion but did not impair motor function

Impact of focally silencing feed-forward inhibitory PV⁺ interneurons on behavioural parameters was tested by CNO injection into either the SS cortex or the RTN thalamus of PV^{Cre}/Gi-DREADD mice and non-DREADD WT control mice. Separate cohort of animals

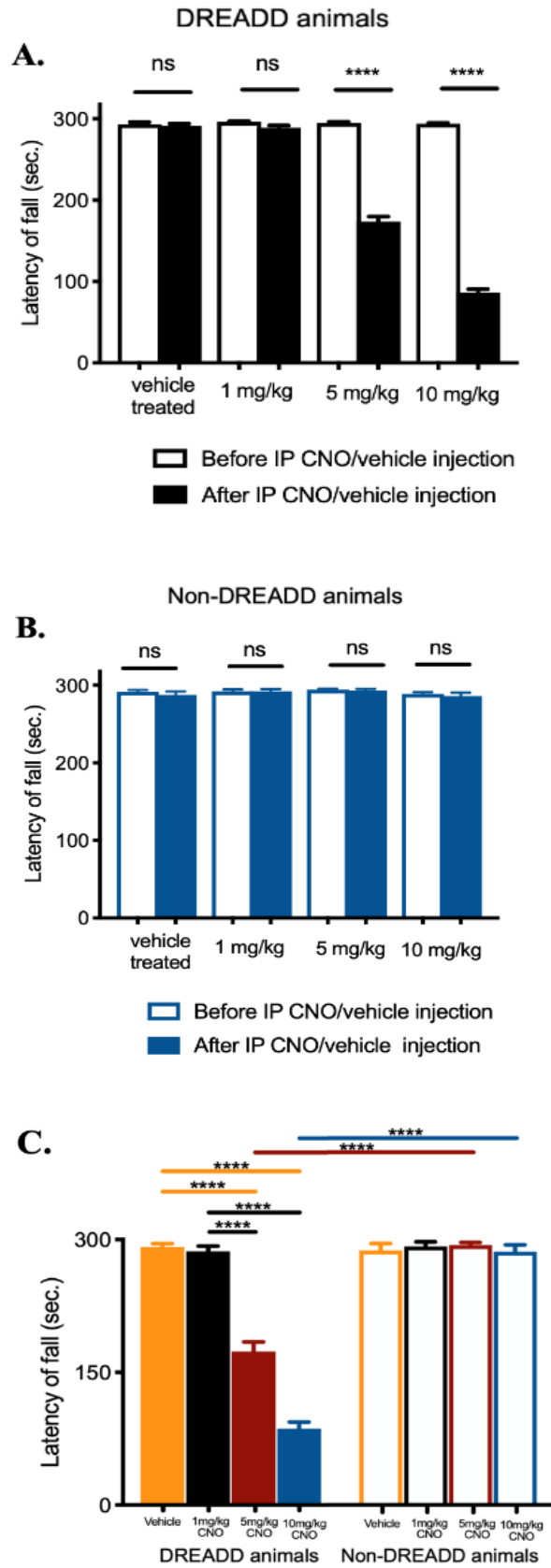


Fig. 3.11 Latency of fall in rotarod test in animals after different doses of i.p. CNO injection. (A) (B) Comparisons between before and after injection in same treatment group were performed using Wilcoxon matched-pairs signed-rank test. (C) Tukey's post hoc multiple comparison test to compare independent treatment groups of DREADD animals and non-DREADD animals. All values represent mean \pm SEM.

were assigned for both treatment groups. Locomotory behaviour in PV^{Cre}/Gi-DREADD mice was significantly changed in a dose dependent manner after focal injection of CNO.

CNO doses of 2.5–10 mg/kg injected into the SS cortex or the RTN thalamus significantly reduced the total ambulatory distance travelled by DREADD animals compared to before treatment, whereas CNO had no effect on non-DREADD WT controls. Dunnett's post hoc multiple comparison test showed statistically significant differences in the mean distance travelled after CNO doses of 2.5 mg/kg (820.9±202.1 cm; *n* = 9), 5 mg/kg (793.3±207.1 cm; *n* = 10), 10 mg/kg CNO (358.2±91.86 cm, *n* = 11) compared to before CNO/vehicle treatment (1950±109.6 cm, *n* = 9–11) in the SS cortex group (Fig. 3.12A). No significant changes were seen in non-DREADD WT control animals i.e. mean distance travelled after CNO doses of 2.5 mg/kg (1308±126.4 cm; *n* = 10), 5 mg/kg (1243±101.4 cm; *n* = 9), 10 mg/kg CNO (1233±132 cm, *n* = 7) compared to before CNO/vehicle treatment (1714±149.9 cm, *n* = 7–10) (Fig. 3.12C). Tukey's post hoc multiple comparison test also showed significant difference between DREADD and non-DREADD WT animals of 10mg/kg CNO treated group (Fig. 3.12E). Similarly, CNO injection into the RTN thalamus significantly reduced locomotion in DREADD animals of 2.5–10 mg/kg dose groups but not in non-DREADD WT controls. During the 10 min testing period before thalamic CNO injection, DREADD animals travelled 1786±124.32 cm (*n* = 10–13) in open-field arena; this decreased significantly after 2.5, 5 and 10 mg/kg of CNO injection to 265.1±88.69 cm (*n* = 11), 458.8±115.9 cm (*n* = 13), and 295.6±134.5 cm (*n* = 10), respectively via Dunnett's post hoc multiple comparison test (Fig. 3.12B). However, there was no change in the total ambulatory distance in non-DREADD WT controls i.e. mean distance travelled after CNO doses of 2.5 mg/kg (1063±189.5 cm; *n* = 10), 5 mg/kg (1184±213.5 cm; *n* = 8), 10 mg/kg (1236±147.6 cm, *n* = 8) compared to before CNO/vehicle treatment (1630±151.6 cm, *n* = 8–10) (Fig. 3.12D). Tukey's post hoc multiple comparison test also showed significant difference between DREADD and non-DREADD WT animals of 2.5 and 10mg/kg CNO treated group (Fig. 3.12F).

Impact of focally silencing PV⁺ interneurons on anxiety levels was also analysed. Higher doses of CNO injected into the SS cortex or the RTN thalamus significantly increased the time spent in the PZ by DREADD animals compared to before treatment, whereas CNO had no effect on non-DREADD WT controls. Dunnett's post hoc multiple comparison test showed statistically significant differences in the mean time spent in PZ after CNO doses of 2.5 mg/kg (587.2±4.49 sec; *n* = 9), 5 mg/kg (582.6±7.0 sec; *n* = 10), 10 mg/kg CNO

(593.9 ± 2.20 sec, $n = 11$) compared to before CNO/vehicle treatment (554.3 ± 6.125 sec, $n = 9-11$) in the SScortex group (supplementary figure 5, page 241). Similarly, in the RTN thalamus group, Dunnett's post hoc multiple comparison test showed statistically significant differences in the mean time spent in the PZ after CNO doses 5 mg/kg (583.8 ± 5.09 sec; $n = 13$), 10 mg/kg CNO (592.3 ± 3.75 sec, $n = 10$) compared to before CNO/vehicle treatment (551.1 ± 6.65 sec, $n = 10-13$) (supplementary figure 5, page 241). No significant changes were seen in non-DREADD WT control animals (supplementary figure 5, page 241).

Silencing feed-forward inhibitory PV⁺ interneurons via focal CNO injections into either the SScortex or the RTN thalamus did not cause impairment of motor control when tested on the moving rotarod. There was no significant difference in the mean latency of fall in PV^{Cre}/Gi-DREADD animals before and after focal CNO/vehicle injection at any dose. Likewise, there was no significant differences in the mean latency of fall in non-DREADD animals before and after focal CNO/vehicle injection at any dose. Comparison of the mean latency of fall between treatment groups and genotypes (DREADD and non-DREADD animals) before and after CNO/vehicle is shown in figure 3.13 and Table 3.6.

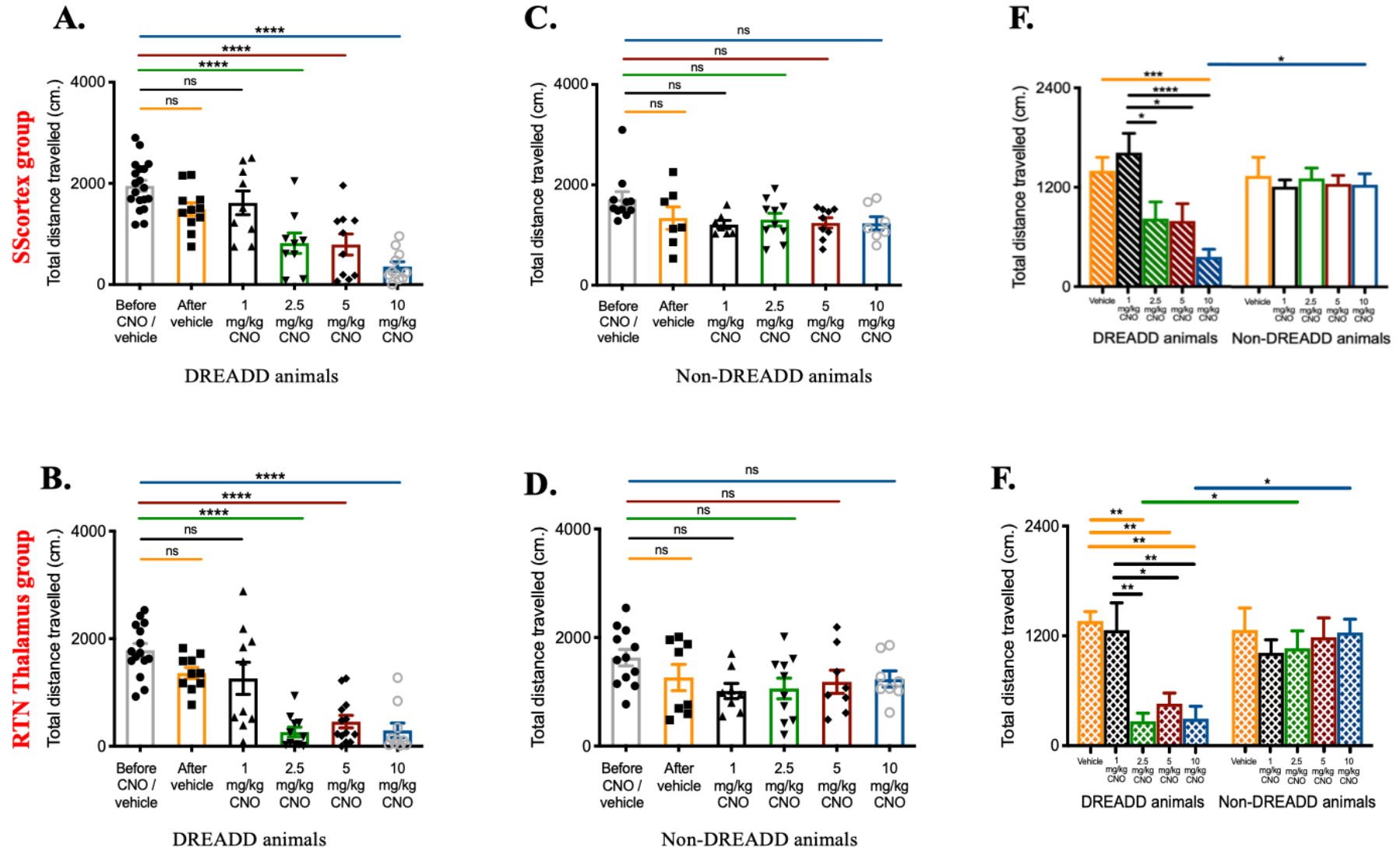


Fig. 3.12 Total distance travelled in open-field arena by animals after focal CNO/vehicle injection. Graphs (A) (C) (E) and (B) (D) (F) represent animals of the SScortex group and the RTN thalamus group, respectively. Comparisons between treatment groups in graphs A-D were performed using Dunnett's post hoc multiple comparison test keeping 'before CNO/vehicle treatment' as a single control. Tukey's post hoc multiple comparison test was performed to compare independent treatment groups of DREADD and non-DREADD WT animals in the (E) SScortex group and (F) RTN thalamus group. All values represent mean \pm SEM.

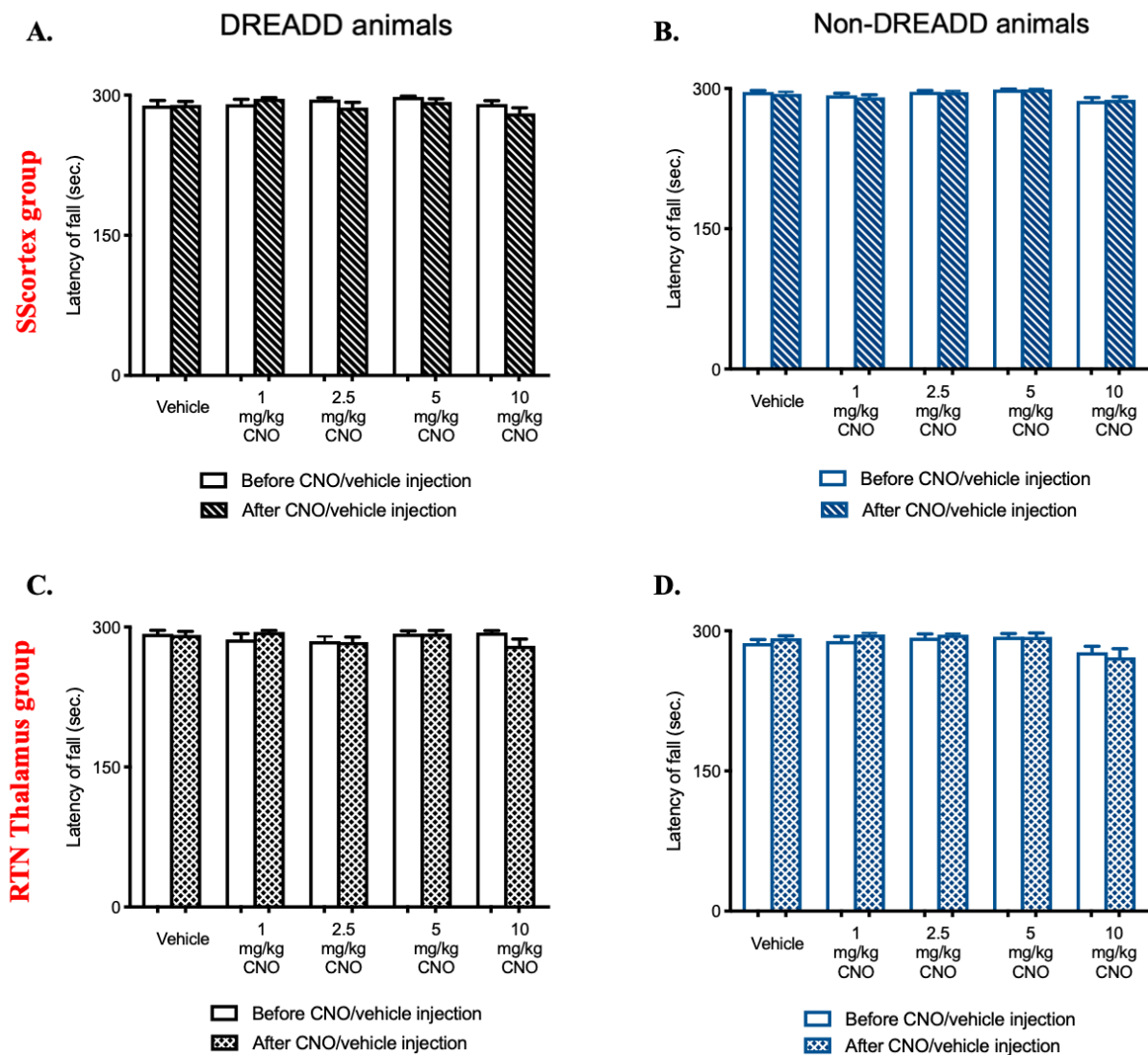


Fig. 3.13 Latency of fall in rotarod test in animals after injection of different focal doses of CNO. Graphs comparing mean latency of fall in rotarod test by PV^{Cre}/Gi-DREADD (DREADD) animals and non-DREADD WT controls after focal CNO/vehicle injection into the (A) (B) SS cortex and (C) (D) RTN thalamus. All values represent mean \pm SEM. Comparisons between before and after injection in same treatment group were performed using Wilcoxon matched-pairs signed-rank test. No significant differences were seen.

Table 3.6 Comparison of mean latency of fall of PV^{Cre}/Gi-DREADD and non-DREADD animals after CNO/vehicle injection into SS cortex and RTN thalamus on rotarod test.

Treatment Group		Mean latency of fall (seconds)					
		PV ^{Cre} /Gi-DREADD animals			Non-DREADD animals		
		Before injection	After injection	<i>n</i>	Before injection	After injection	<i>n</i>
SS cortex group	Vehicle	288.8±5.56	289.5±3.72	11	296.2±1.75	294.3±2.2	7
	1mg/kg CNO	290.4±5.03	296±1.38	9	292.7±2.17	290.4±2.83	7
	2.5mg/kg CNO	295.1±1.76	286.7±5.53	9	290.4±2.83	296.4±1.36	10
	5mg/kg CNO	298.1±0.93	292.8±3.41	10	298.9±0.59	299±0.57	9
	10mg/kg CNO	290.4±3.62	280.5±5.97	11	286.6±3.74	287.9±3.14	7
RTN thalamus group	Vehicle	292.7±3.90	291.6±3.73	10	286.9±3.90	292.2±2.47	8
	1mg/kg CNO	286.6±6.22	294.6±1.64	10	289±4.79	296.1±1.63	8
	2.5mg/kg CNO	284.9±5.03	284±5.22	11	292.7±3.86	295.9±1.14	10
	5mg/kg CNO	293±2.97	292.8±3.43	13	293.8±3.28	293.4±4.37	8
	10mg/kg CNO	294.1±2	280±7.10	10	277.1±6.34	271.8±9.04	8

3.4 Discussion

The work reported in this chapter demonstrated that global and focal silencing of PV+ interneurons within CTC network generates paroxysmal oscillatory activity similar to SWDs on EEG with associated behavioural arrest. Global silencing of PV+ interneurons impaired motor coordination, decreased locomotion, increased anxiety and immobility in PV^{Cre}/Gi-DREADD animals. Focal silencing also reduced locomotory behaviour and increased immobility, but motor function was not altered. In contrast, no significant changes were observed in non-DREADD WT controls or vehicle treated PV^{Cre}/Gi-DREADD mice. Administration of the anti-absence epileptic drug ethosuximide prevented the focally induced absence-like seizures in PV^{Cre}/Gi-DREADD mice. The data presented in this chapter have been published (Panthi and Leitch, 2019).

3.4.1 HA-tagged DREADD receptors are highly expressed in feed-forward inhibitory PV+ interneurons

Inhibitory Gi-DREADD receptors were highly expressed in PV+ interneurons of PV^{Cre}/Gi-DREADD mice. This was confirmed by the colocalization of DREADD HA-tag and PV in cells known to express the calcium binding protein PV. However, this co-labelling for HA-tag and PV was not seen in non-DREADD WT control animals. Analysis of the confocal images showed that PV+ interneurons were highly expressed in layers 2-6 of the SS cortex (except layer 1) in both PV^{Cre}/Gi-DREADD and non-DREADD WT control mice. This result is consistent to the labelling of PV cells in the SS cortex of epileptic stargazers and non-epileptic littermates in previously published study from our research group (Adotevi and Leitch, 2016) and other published rodent studies (Celio, 1986; Dávid et al., 2007; Tanahira et al., 2009; Xu et al., 2010). Labelling of PV+ interneurons in the RTN thalamus and Purkinje cells of the cerebellum was also in agreement with other published studies (De Talamoni et al., 1993; Arai et al., 1994; Schwaller et al., 2002; Csillik et al., 2005). Quantification data showed that colocalization of HA-tag in PV+ interneurons was above 90% in the SS cortex, the RTN thalamus, and the cerebellum whereas none of the PV+ interneurons in non-DREADD WT control mice showed labelling for HA-tag. These levels of co-expression in PV^{Cre}/Gi-DREADD mice are consistent with the Jackson Lab datasheet (008069) for PV-Cre mice which states that the recombination in PV-Cre knockin allele is around 90%.

There have been relatively few studies using DREADD technology to modulate PV+ interneurons. One recent report utilized transgenic mice approach i.e. PV-Cre x LSL-hM3Dq mice and reported exclusive colocalization of DREADD receptors in the PV expressing cells of the motor cortex and cerebellum. However, they did not quantify the colocalization (Johnson et al., 2018). Apart from that, most of the other studies have utilized DREADD-based recombinant lentiviral vector (LV) or adeno-associated viral vector (AAV) to express DREADD receptors into the specific regions of brain of PV-Cre transgenic mice. Some examples are shown in the Table below.

Table 3.7 Comparison of the percentage of infection efficiency and specificity of labelling across the various regions of brain in studies utilizing PV-Cre mice and viral (AAV) method of DREADD delivery.

Study	Region of the brain	Infection efficiency	Specificity
Yi et al., 2014	Hippocampus	~80%	~94%
Zou et al., 2016	Hippocampus	~71%	~96%
Xia et al., 2017	Medial prefrontal cortex	~85%	~93%
Chen et al., 2018	Barrel cortex	-	~95%
Hijazi et al., 2019	Hippocampus	83%	87%
Page et al., 2019	Prefrontal cortex	~92%	~96%
Bicks et al., 2020	Prefrontal cortex	-	~82%

Abovementioned studies have shown that the infection efficiency and specificity of labelling generally vary in viral mediated DREADD delivery, whereas in this current study percentage of DREADD receptors (HA-tagged cells) colabelled for PV and percentage of PV cells colabelled for DREADD receptors was above 90% in all tested regions (SScortex, RTN thalamus, and Purkinje cells of cerebellum).

3.4.2 Global and focal silencing of PV+ interneurons generated absence-like SWDs associated with behavioural arrest

DREADD receptors can be activated either via intraperitoneal (i.p.) or focal CNO injection into a specific brain region (Armbruster et al., 2007; Rogan and Roth, 2011). Studies have shown that CNO can be injected from 0.3-20mg/kg intraperitoneally to activate PV cells of the specific brain regions where viral DREADD construct have been injected to infect PV cells (Mahler et al., 2014; Zou et al., 2016; Chen et al., 2018; Ng et al., 2018; Page et al., 2019; Bicks et al., 2020). Studies have also shown that CNO can be injected focally for DREADD mediated activation of site-specific neurons (Mahler et al., 2014; Ge et al., 2017; Lichtenberg et al., 2017; McGlinchey and Aston-Jones, 2017). In this current study, firstly, as a proof of concept, PV^{Cre}/Gi-DREADD animals were intraperitoneally injected with CNO to investigate the impact of globally silencing feed-forward inhibitory PV+ interneurons on seizure generation. Secondly, PV+ interneurons of the CTC microcircuit (either the SScortex or the RTN thalamus) were targeted via focal CNO injection. Both global (i.p., 5mg/kg and 10mg/kg) and focal (2.5, 5 and 10mg/kg) silencing of PV+ interneurons generated paroxysmal oscillatory bursts. These bursts were identified as absence-like seizures based on their EEG signature similar to published criteria for SWDs i.e. trains (>1 second) of rhythmic spikes followed by

positive transient and slow wave with amplitude minimum two-times higher than baseline (see listed references in chapter 2, Table 2.9). Irrespective of the dose of CNO (2.5-10mg/kg) and route of administration (i.p. or focal), the mean duration and rhythmicity (spike frequency) of such bursts were 3-5 seconds and 3-7 Hz, respectively. Morphological profile, duration of seizure and frequency was consistent with the characteristics of SWDs seen in various rodent models of absence epilepsy (see review Jarre et al., 2017). However, mean onset of paroxysmal oscillatory bursts was significantly faster in focal group (~15 min) than i.p. group (~30 min). Peripheral administration of CNO requires additional time to cross the blood brain barrier first and into the brain. This finding was also similar to other published studies where they have shown that plasma level of CNO peaks within 30 min and sharply decline over next 2 h after systemic injection of CNO (MacLaren et al., 2016; Roth, 2016; Manvich et al., 2018; Jendryka et al., 2019). And, behavioural effects of CNO is seen up to 6 h of injection (Alexander et al., 2009). One recent study has shown that focal injection of CNO can robustly activate targeted neuronal population and time scale of this effect is from min to h (Stachniak et al., 2014) which is also similar to this study where mean onset of paroxysmal oscillatory bursts is ~15 min (SScortex and RTN thalamus group).

Studies have shown that permanent silencing of hippocampal PV+ interneurons generates clusters of epileptic discharges which progresses to spontaneous recurrent seizures (Drexel et al., 2017; 2019). These published results alongside the outcomes of this current study support the idea that functional silencing might restrict the GABA release from PV+ interneurons and disrupt the powerful inhibitory effect of these interneurons onto local excitatory neurons. This disruption can impair inhibition resulting the shift of excitation/inhibition balance more towards excitation causing the generation of epileptic discharges. Interestingly, voltage clamp recordings from principal excitatory cells after optogenetic suppression of the activity of PV+ (Moore et al., 2018) and SOM+ (Kato et al., 2017) interneurons in layer 4 of auditory cortex increased both excitation and inhibition to principal neurons. These studies concluded that the net effect of suppressing these interneurons results in a coordinated increase in both excitation and inhibition to principal neurons. Thus, it is important to note that altered activity of inhibitory interneurons in the inhibitory microcircuits affects not only inhibitory but also excitatory inputs to principal excitatory cells.

Recently published studies have raised questions over the use of CNO as the ‘designer drug’ for DREADD technology. Gomez and colleagues reported that CNO is reverse-metabolized to

clozapine after systemic CNO injection and reverse-metabolized clozapine may act as DREADD activator in brain tissue. They further stated that clozapine is an atypical antipsychotic having affinities towards various receptor targets which is capable of producing different behavioural and physiological effects. They reported decreased locomotion in non-DREADD WT controls after systemic injection of 1 mg/kg of CNO and 1 mg/kg of clozapine. Whereas, low subthreshold 0.1 mg/kg dose of clozapine significantly decreased locomotor activity in hM4Di expressing rats but not in controls. They suggested the use of low doses of clozapine (0.1 mg/kg) instead of CNO (Gomez et al., 2017) as a DREADD activator. However, the dose of clozapine recommended by Gomez and colleagues (0.1 mg/kg) has previously been found to increase anxiety in mice (Manzaneque et al., 2002). In addition to the psychiatric effects, clozapine was linked to agranulocytosis and found to have pro-epileptic effects (Ruffman et al., 2006). Other studies involving the use of CNO have failed to find DREADD-independent behavioural or off-target effects at doses up to 10 mg/kg, at least within a 30–150 min timeframe after i.p. injection (Mahler et al., 2014; Ge et al., 2017; Lichtenberg et al., 2017; McGlinchey and Aston-Jones, 2017). A recent study has demonstrated that, after the systemic administration of CNO, the concentration of reverse-metabolized clozapine in plasma, cerebrospinal fluid and brain tissue is very low compared to CNO and the brain availability of both compounds varies with species (Jendryka et al., 2019). It is now suggested and highly recommended to design experiments with non-DREADD expressing animals to control potential off-target effects of CNO/clozapine. In this current study, non-DREADD expressing WT controls were assigned for all doses of CNO (i.p. and focal). Vehicle-treated controls were also included in both treatment groups (i.p. and focal) and genotypes (DREADD and non-DREADD animals). Simultaneous video/EEG recording were conducted up to 1 hour of CNO injection. Importantly, non-DREADD wild-type controls and vehicle-treated controls showed no signs of epileptiform activity, at any of the CNO doses tested.

3.4.3 Global and focal silencing of feed-forward inhibitory PV+ interneurons affected locomotory behaviours and mobility

To understand the impact of silencing PV+ interneurons on behavioural terms, two behavioural tests were employed, as animal models of absence epilepsy show defective motor function including ataxia, head tossing, dyskinesia, and tremor as other behavioural features (Jarre et al., 2017).

In this study, global silencing of PV⁺ interneurons via i.p. CNO injection significantly impaired motor coordination on the rotarod test in a dose dependent manner. However, focal silencing of PV⁺ interneurons via CNO injection into the SS cortex and RTN thalamus did not change the motor performance in PV^{Cre}/Gi-DREADD mice. This is likely due to the fact that global silencing of PV⁺ interneurons via i.p. CNO injection silenced all PV⁺ interneurons including PV expressing Purkinje cells in the cerebellum. The cerebellum plays important role in motor control, precision, and accurate timing of the movement. However, focal silencing had no effect on motor performance as SS cortex and RTN thalamus are not the brain regions directly involved in motor co-ordination. Knockout mice (such as TARP γ -2 Purkinje cells knockout; γ -7 knock out) which lack excitatory input to Purkinje cells, show wide range of motor deficits including ataxic gait, severely reduced ambulation and rearing in the open-field, impaired performance in the wire hang test, and reduced forelimb and hindlimb grip strength on the rotarod (Yamazaki et al., 2015). One optogenetic study also found that activation of G_{i/o} pathway in Purkinje cells reduces motor coordination and control on the rotarod (Gutierrez et al., 2011). Other studies conducted on conditional Purkinje cell knockout animals also showed significantly impaired motor performance (Todorov et al., 2012; Tsai et al., 2012). Studies utilizing DREADD technology and viral methods to selectively silence or excite PV⁺ interneurons in brain regions, other than the cerebellum, have had no effect on motor performance in rotarod test. For example, DREADD mediated silencing of hippocampal PV neurons didn't change motor skills in PV-Cre mice (Hijazi et al., 2019). Chemogenetic excitation of PV⁺ interneurons in the dorsal horn in PV-Cre mice also had no significant effect in motor impairment (Petitjean et al., 2015). Likewise, Liu and colleagues also reported unaltered ability of motor coordination on rotarod tests after CNO mediated activation of PV⁺ interneurons in rostro-dorsal RTN in PV-Cre mice (Liu et al., 2017). Also, chemogenetic inactivation of hippocampal glutamatergic neurons in CaMKII α -hM4Di double transgenic mice had no effect on motor performance (Zhu et al., 2014). Thus, it can be concluded that decreased latency of fall or impaired motor skill in rotarod test of PV^{Cre}/Gi-DREADD animals in this study only after global silencing of PV⁺ interneurons are due to the silencing of feed-forward inhibitory PV⁺ interneurons of cerebellum.

In the open-field test, global silencing of PV⁺ interneurons significantly reduced locomotion in PV^{Cre}/Gi-DREADD animals after treatment with i.p. doses of CNO (i.e. 5 and 10mg/kg). These animals relatively spent more time in the peripheral zone and corners of the open-field arena and less time in the central zone in a dose dependent manner compared to that of vehicle-

treated PV^{Cre}/Gi-DREADD mice or CNO/vehicle treated non-DREADD WT control animals. Staying closely in proximity to the walls or decreased latency to enter the central part of the arena indicates anxiety-related behaviour in rodents (Prut and Belzung, 2003; Lipkind et al., 2004; Seibenhener and Wooten, 2015). In this particular experiment, the amount of time spent by non-DREADD animals in central zone before and after CNO treatment was around 5-8% which is in agreement with other published studies for WT control animals (Moy et al., 2007; Bailey and Crawley, 2009; de Oliveira et al., 2015) which also indicated that non-DREADD control and vehicle treated mice do not display anxiety-like behaviour. Thus, global silencing of PV⁺ interneurons was found to be linked with decreased locomotion and increased levels of anxiety.

In this study, focal silencing of PV⁺ interneurons of either the SS cortex or the RTN thalamus significantly reduced total ambulatory distance. Open-field test performed in PV knockout mice showed decreased locomotory behaviour and exploration (Farré-Castany et al., 2007). Similarly, in another study, PV knockout mice displayed less structured bouts of locomotion, less rearing activity (Wöhr et al., 2015) compared to that of WT animals. Other conditional PV knockout animals lacking TrKB (Lucas et al., 2014; Xenos et al., 2018) and KCC3 (Ding and Delpire, 2014) in PV⁺ interneurons also showed decreased locomotion. But variable results were found in studies utilizing chemogenetic manipulation of PV⁺ interneurons have shown variable outcome. Page and colleagues found that chronic activation of PV⁺ interneurons in the prefrontal cortex significantly increases anxiety (but unchanged locomotory behaviour) in female PV-Cre mice compared to the male counterparts. No significant differences in those parameters were observed after acute activation of PV cells (Page et al., 2019). Another study revealed increased anxiety without locomotory changes after acute injection of CNO in PV-Cre mice injected with excitatory (Gq) DREADD construct in the hippocampus (Zou et al., 2016). In contrast, chronic silencing of hippocampal PV⁺ interneurons (supplying CNO in drinking water for 27 days) in PV-Cre mice expressing inhibitory Gi-DREADD receptors, resulted no changes in locomotor activity and anxiety levels (Xia et al., 2017). Similarly, Perova and colleagues found no difference in locomotion between CNO treated and saline treated groups of PV-Cre animals virally injected with inhibitory Gi-DREADD receptors in the prefrontal cortex (Perova et al., 2015).

In this study it was also revealed that silencing PV⁺ interneurons via both global and focal route increases immobility during 1 hour of EEG recording. Immobility was seen only in higher

dose of CNO treated DREADD animal group but not in vehicle-treated group and non-DREADD WT control animals. Animal models of absence epilepsy show SWDs that are associated with behavioural arrest (Jarre et al., 2017). In this study, immobility/behavioural arrest was witnessed during seizure and between bursts of seizures. However, non-DREADD WT control animals showed no significant increment of immobility with the same doses of CNO. Thus, increased immobility after higher doses of CNO in this study might be linked to increased anxiety due to the silencing of PV+ interneurons (Tovote et al., 2015; Babaev et al., 2018). Moreover, PV knockout animals (Farré-Castany et al., 2007; Wöhr et al., 2015) and conditional PV knockout animals (Ding and Delpire, 2014; Lucas et al., 2014; Xenos et al., 2018) also displays decreased locomotion. It is important to note that increased immobility of DREADD animals after CNO injection in this study is not due to off-target activity of reverse metabolized clozapine because CNO treated non-DREADD animals and vehicle treated (DREADD and non-DREADD) animals had similar levels of immobility during 1-hour EEG recording.

3.5 Conclusion

In summary, the results from this chapter demonstrated that selectively silencing PV+ interneurons of feed-forward microcircuits in CTC network generates paroxysmal oscillatory bursts having similar morphology and characteristics of SWDs seen in various rodent models of absence epilepsy. Absence-like bursts seen in this study were also associated with behavioural arrest. This also provided us an understanding that functional loss of PV+ interneurons can disrupt FFI and this may be one of the mechanisms through which SWDs are generated. To further characterize the functional roles of PV+ interneurons on seizure generation, it is necessary to test the impact of activating PV+ interneurons during absence seizures. This forms the basis of the next chapter where impact of activating PV+ interneurons in the excitatory Gq-DREADD animals will be tested during chemically induced absence seizures.

Chapter 4. Effect of Activating Feed-forward Inhibitory PV+ Interneurons During Absence Seizures

4.1 Introduction

In the previous chapter, it was demonstrated that functionally silencing feed-forward inhibitory PV+ interneurons within the CTC network generates absence-like SWDs (Panthi and Leitch, 2019). Thus, the next important question in this study was whether activating feed-forward inhibitory PV+ interneurons in the CTC network during absence seizures would prevent or reduce seizure activity.

To do this, PTZ was used to induce seizures in excitatory Gq-DREADD (PV^{Cre}/Gq-DREADD) animals where the feed-forward inhibitory PV+ interneurons could be activated with CNO. PTZ is routinely used in epileptic studies to induce both absence and generalized tonic-clonic seizures (Snead, 1992; Velišková et al., 2017) and also has been used for the screening of antiepileptic drugs since 1970s (see reviews by Krall et al., 1978 and Löscher, 2011). PTZ impairs GABA mediated inhibition by antagonizing GABA_A receptors (Huang et al., 2001). The severity of PTZ induced seizure is dose dependent. Low dose PTZ (~20mg/kg) administration is an established experimental method to induce generalized absence seizures involving thalamocortical mechanisms whereas high doses (> 40mg/kg) induce spike trains with tonic-clonic seizures (Snead, 1992; Snead et al., 2000).

As previously stated, PV+ interneurons are responsible for preventing runaway excitation within CTC network and dysfunction of these interneurons leads to the generation of seizures (see reviews by Liu et al., 2014 and Jiang et al., 2016). In a recent study, optogenetic activation of PV+ interneurons of RTN thalamus during PTZ-induced seizures provided antiepileptic effects (Clemente-Perez et al., 2017). Furthermore, a DREADD based study has indicated that activating PV+ interneurons increases the latency and decreases the susceptibility of PTZ-induced tonic-clonic and myoclonic seizures (Johnson et al., 2018). Cortical activation of PV+ interneurons also terminated 4-AP induced spontaneous electrographic seizures (Assaf and Schiller, 2016). In other studies, activating hippocampal PV+ interneurons attenuated KA-induced temporal lobe seizures (Krook-Magnuson et al., 2013; Wang et al., 2018). Moreover, parvalbumin knockout (PV^{-/-}) mice have higher susceptibility to the chemically induced seizures and these animals experienced more severe seizures compared to WT controls (Schwaller et al., 2004). However, there have been no studies to date reporting the consequences of activating PV+ interneurons within CTC network during absence seizures.

Hence, the aim of this chapter was to investigate the impact of activating feed-forward inhibitory PV⁺ interneurons within the cortex and thalamus in excitatory Gq-DREADD (PV^{Cre}/Gq-DREADD) animals during PTZ-induced absence seizures. First, immunohistochemistry was performed to confirm the expression of excitatory Gq-DREADD receptors in the PV⁺ interneurons within the CTC network. Secondly, simultaneous video/EEG based PTZ experiments were performed in two steps. On day 1, PTZ was administered to test absence seizure generation in the cohort of experimental animals. This was then followed on day 2 by the activation of PV⁺ interneurons via focal CNO injection during PTZ-induced seizures.

4.2 Methods

4.2.1 Immunofluorescence confocal microscopy, image acquisition and analysis

To confirm the expression of excitatory Gq-DREADD receptors in feed-forward inhibitory PV⁺ interneurons of PV^{Cre}/Gq-DREADD mice, antibodies against HA-tag (Cell Signaling, C29F4) and parvalbumin (Swant Inc., PV-235) were used to label DREADD receptors and PV⁺ interneurons, respectively. Immunolabelling was performed on tissue sections from PV^{Cre}/Gq-DREADD mice and non-DREADD WT control animals. Immunolabelling, confocal imaging, quantification of immunolabelled cells and analysis were performed as described previously in chapter 2 subsection 2.3.

4.2.2 Surgical implantation of prefabricated headmounts and microcannulas for EEG recordings

To test the impact of activating feed-forward inhibitory PV⁺ interneurons during PTZ-induced absence seizures, EEG recordings were performed on PV^{Cre}/Gq-DREADD and non-DREADD WT control animals. Surgical manipulations for implantation of prefabricated headmounts (Pinnacle Technologies, Austin, TX, USA) and microcannulas (Plastics One Inc., VA, USA) were conducted according to procedures detailed in the chapter 2 subsection 2.4.

Before performing the main experiments, a pilot study was conducted to determine the dose of PTZ necessary to induce absence seizures. Briefly, a cohort of animals ($n=6$) were injected intraperitoneally with three different doses of PTZ (10, 20, 30 mg/kg). Based on simultaneous video/EEG data, a dose of 20mg/kg was selected.

For experimental tests, PV^{Cre}/Gq-DREADD ($n=14$) and non-DREADD WT control ($n=10$) animals were allocated to two different treatment groups: either SScortex implanted group (DREADD animals $n=7$; controls $n=5$) or RTN thalamus implanted group (DREADD animals

$n=7$; controls $n=5$). Experiments were performed on two consecutive days according to the schematic outlined in the figure 4.1 (see supplementary figure 2 for more details). On day 1, seizures were induced in all animals (PV^{Cre}/Gq-DREADD mice and non-DREADD WT control mice) by i.p. injection of 20mg/kg PTZ. After 24 h, on day 2, the same cohort of animals were treated with the same dose of PTZ (i.p.) and 5mg/kg CNO (into either the SS cortex or the RTN thalamus). The timing and dose of CNO was based on previous experiments in chapter 3 where 5mg/kg CNO was lowest yet effective dose that activated inhibitory Gi-DREADD receptors and generated absence-like seizures in PV^{Cre}/Gi-DREADD animals.

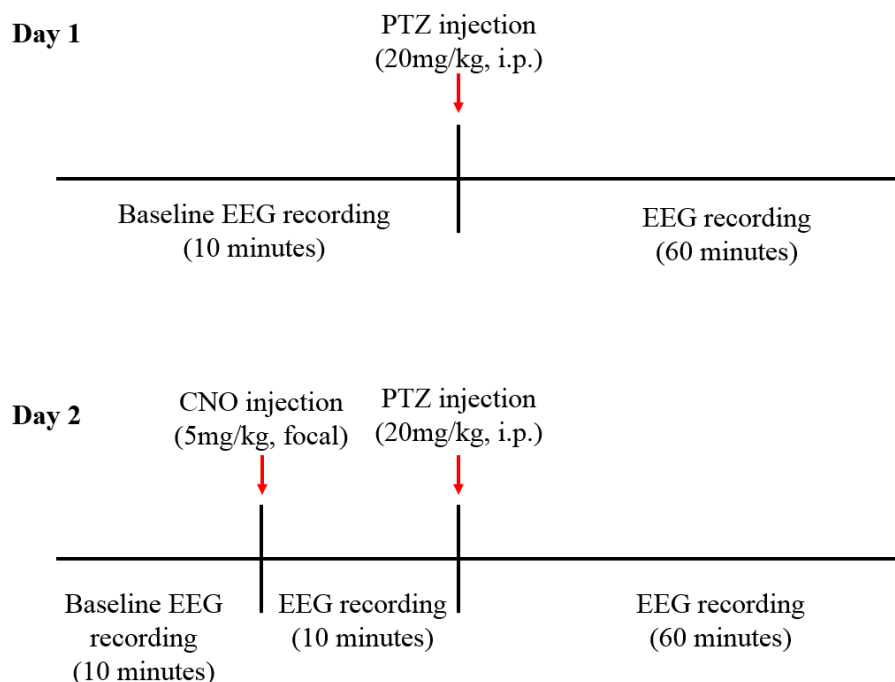


Fig. 4.1 Schematic of the protocol for EEG recordings before and after focal CNO and i.p. PTZ injections.

4.2.3 Preparation and delivery of CNO and PTZ

CNO and PTZ were freshly prepared before every scheduled experiment as previously described in chapter 2 subsection 2.5. On both days, PTZ was injected intraperitoneally (20mg/kg) based on the calculated dose for the body weight of the animal. On day 2, CNO (5mg/kg) was injected focally (either into SS cortex or RTN thalamus). After 10 min of baseline EEG recording, 0.3 μ l of CNO was infused into the regional areas at a rate of 0.1 μ l/min via Hamilton microinjection syringe. At the end of experiments, methylene blue dye was injected at the same volume and rate as CNO into the focal regions of the brain under investigation. Histology was performed to verify the localization of cannula tip and estimate the diffusion of CNO (see supplementary figure 2). The stereotaxic coordinates of the CNO and dye injections in the SS cortex were 1.22 to 2.06 mm posterior to bregma, 2.8 mm lateral to the midline and

1.5 mm below the cortical surface. The coordinates for RTN thalamus injections were 1.34 to 1.94 mm posterior to bregma, 2.1-2.3 mm lateral to the midline and 3.2-3.5 mm ventral to the cortical surface (Mouse Brain Atlas, Paxinos and Franklin, 3rd edition).

4.2.4 EEG recording and analysis of EEG traces

EEG recordings were performed according to procedures detailed in the chapter 2 subsection 2.4. Based on the video/EEG data, bursts of oscillations were counted as absence-like SWDs if they had a spike-wave structure (spike, positive transient, and slow wave pattern) with a frequency of 3–8 Hz, an amplitude at least two times higher than baseline and lasted for >1 second with behavioural arrest or motionless staring as behavioural features (based on the references listed in chapter 2, Table 2.9). Tonic-clonic seizures were characterized by high amplitude polyspikes. Behavioural expressions for tonic-clonic seizures ranged from clonic jerking with or without loss of balance (lying on belly or on cage walls) to wild jumping in some cases. Myoclonic seizures were characterized by brief (few seconds) jerks resulting sharp spikes in EEG (Lüttjohann et al., 2009; Van Erum et al., 2019). Bursts of absence-like seizures and myoclonic seizures spanning less than 1 second were also separately counted.

4.2.5 Data analysis

Statistical analysis of significant differences of the onset of seizures between PV^{Cre}/Gq-DREADD and non-DREADD WT control animals were calculated using Mantel-Cox log-rank test. Comparison within the same treatment group was performed using Wilcoxon matched-pairs signed-rank test. Comparison between treatment groups was performed using Mann Whitney unpaired rank test. Data were presented as mean ± standard error of the mean (SEM). All statistical analysis was performed in GraphPad Prism 8.0 with statistical significance set at $p < .05$.

4.3 Results

4.3.1 Excitatory Gq-DREADD receptors are expressed in feed-forward inhibitory PV+ interneurons

Double-labelled immunohistochemistry with antibodies against HA-tag and PV was performed to confirm the expression of excitatory Gq-DREADD receptors in PV+ interneurons of PV^{Cre}/Gq-DREADD mice (Fig. 4.2). HA-tag for DREADD (identified by pseudocolour green, panel 1) was only expressed in the brain sections from PV^{Cre}/Gq-DREADD mice but not in non-DREADD WT control animals. PV+ interneurons were highly expressed throughout all

SScortical layers (except layer I), within the RTN thalamus and the cerebellar cortex in all genotypes (identified by pseudocolour red, panel 2). Co-localization of HA-tag in PV+ interneurons was found throughout the SScortex (Fig. 4.2A,B), the RTN thalamus (Fig. 4.2C,D) and the cerebellar cortex (Fig. 4.2E,F). In the SScortex of PV^{Cre}/Gq-DREADD mice, PV+ interneurons highly expressed HA-tag (Fig. 4.2A white arrows); co-localization of HA-tag in PV+ interneurons was above 90% (Fig. 4.2B). Similarly, in the RTN thalamus, PV+ interneurons strongly expressed HA-tag (Fig. 4.2C white arrows); the percentage of co-localization of HA-tag in PV+ interneurons of RTN thalamus was also above 90% in PV^{Cre}/Gq-DREADD mice (Fig. 4.2D). In the cerebellum, HA-tag was highly expressed in PV+ Purkinje cell soma (Fig. 4.2E white arrows). The percentage of co-localization of HA-tag in PV+ inhibitory Purkinje cell soma was also above 90% (Fig. 4.2F). The pattern of staining and levels of colocalization between HA-tag and PV in all three brain regions of PV^{Cre}/Gq-DREADD animals were very similar to the results obtained in PV^{Cre}/Gi-DREADD animals as previously described in chapter 3 (figure 3.1).

4.3.2 20mg/kg IP PTZ is required to induce absence-SWDs

A pilot study was first conducted on a cohort of animals ($n=6$) to establish the dose of PTZ required to induce absence seizures (Fig. 4.3A). According to the literature, absence-SWDs can be induced in different mice and rat models using i.p. injections of PTZ at doses between 10 and 40 mg/kg (Marescaux et al., 1984; Snead et al., 2000; Girard et al., 2019; Van Erum et al., 2019). In this study, simultaneous video/EEG data showed that 10 mg/kg of PTZ did not induce seizures in any of the mice tested (Fig. 4.3B), whereas animals injected with 30mg/kg PTZ induced severe tonic-clonic seizures (Fig. 4.3D). In contrast, a dose of 20mg/kg consistently produced absence-SWDs. However, they were mixed with tonic-clonic and myoclonic seizures (Fig. 4.3C). This was the lowest dose that produced absence seizures.

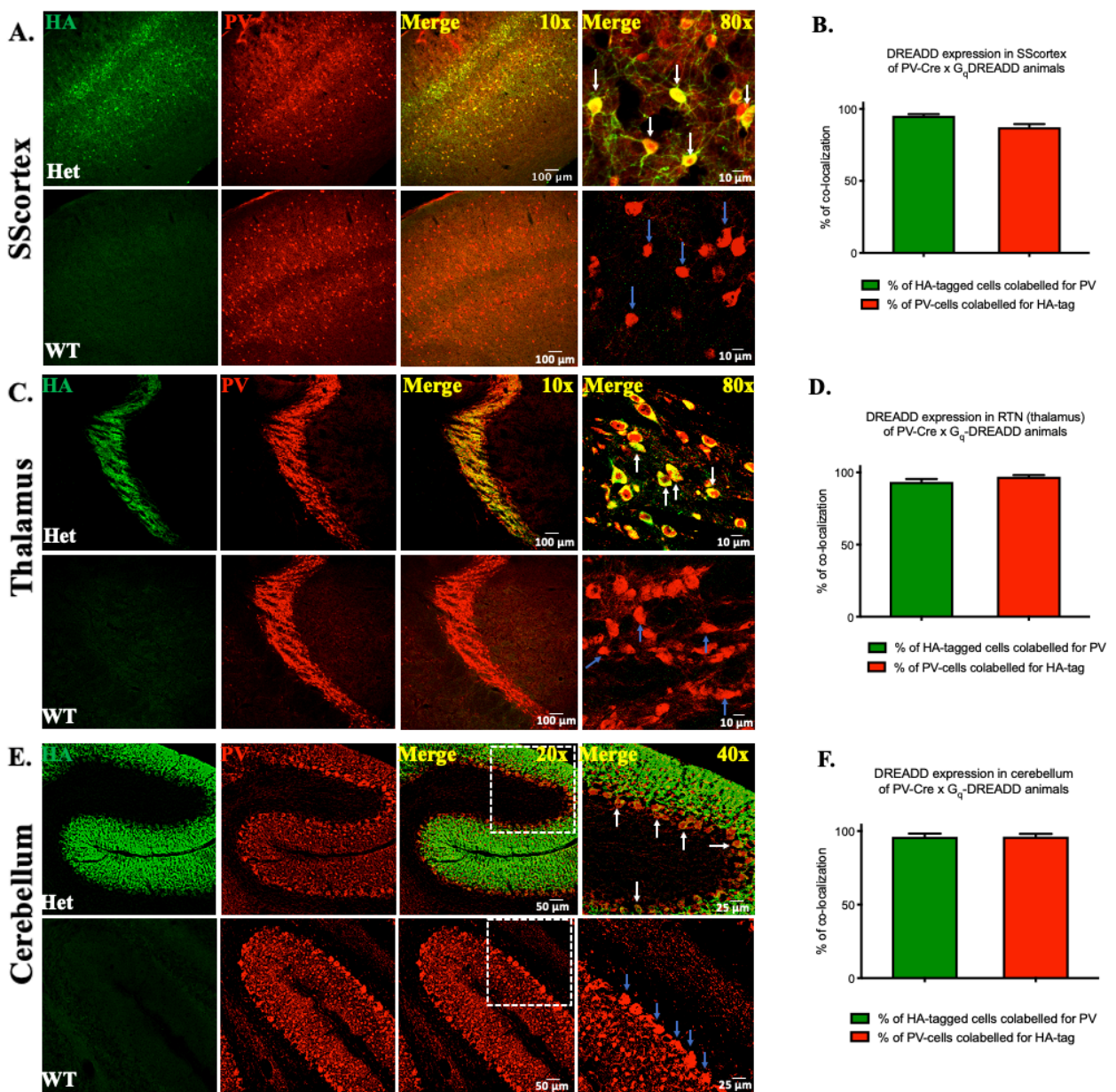


Fig. 4.2 Expression of Gq-DREADD receptors in PV+ interneurons. (A, C, E) Confocal images showing the expression of HA-tag in PV+ interneurons in the SS cortex, the RTN thalamus and the cerebellum of PV^{Cre}/Gq-DREADD animals, respectively. White arrows in merged images represent colocalized cells. Blue arrows indicate PV positive neurons which are immunonegative for HA. (B, D, F) Percentage of co-localization of HA-tag and PV in neurons in the SS cortex, the RTN thalamus, and the cerebellum, respectively. Immunolabelled cells in the SS cortex and the cerebellum were counted at 10x magnified confocal images whereas in the RTN thalamus cells were counted using 40x images. (Het = PV^{Cre}/Gq-DREADD offspring from homozygous PV-Cre female and heterozygous hM3Dq-flox male; WT = Non-DREADD wild type control animals). All values in graphs represent mean ± SEM.

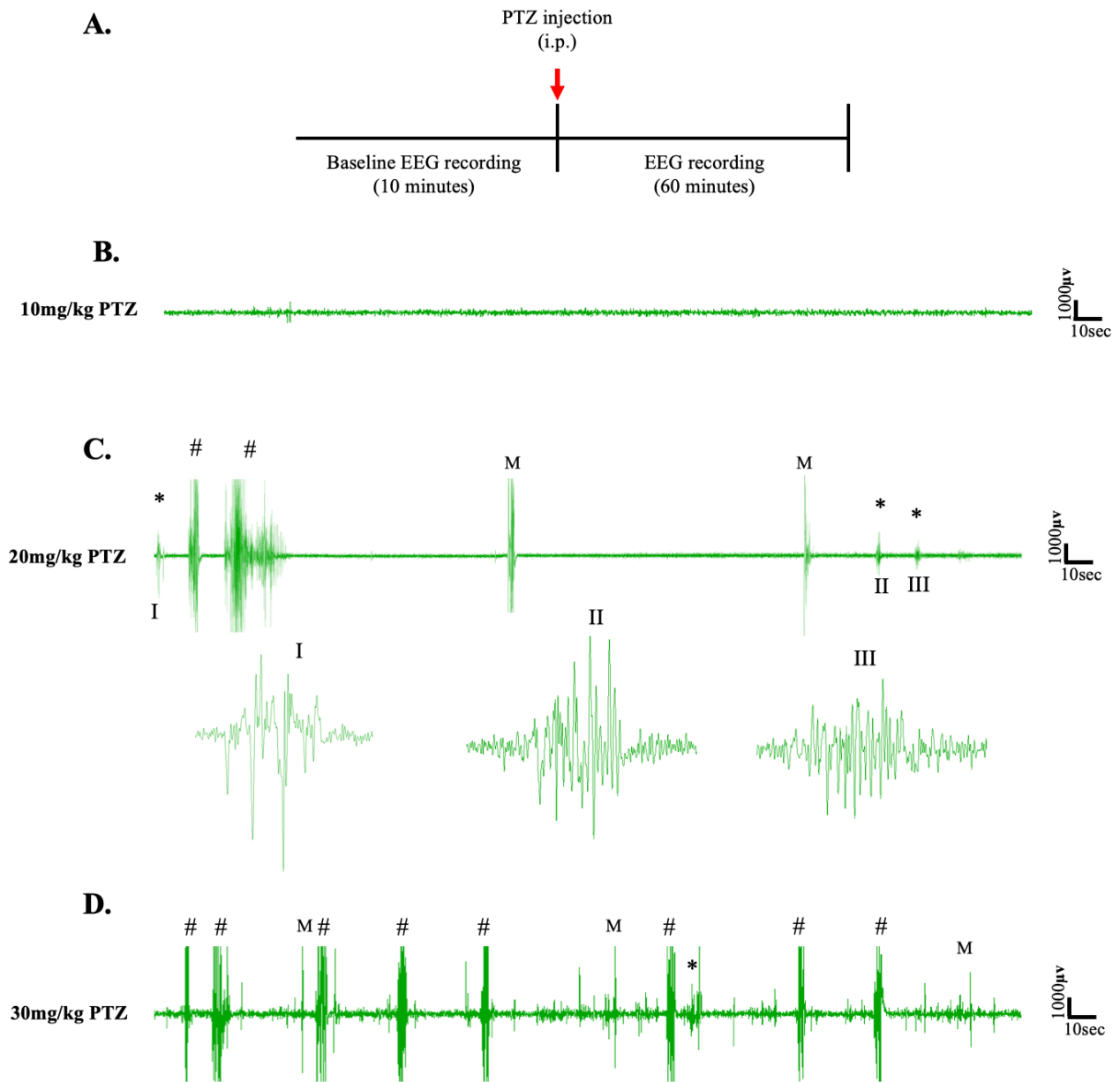


Fig. 4.3 Protocol of the pilot PTZ experiment and representative EEG traces. (A) Schematic protocol for EEG recordings before and after IP PTZ injection in the pilot study. Representative EEG traces from animals after (B) 10mg/kg (C) 20mg/kg (D) 30mg/kg of PTZ injection. Asterisks (*), hash signs (#) and M represent absence-like seizures, tonic-clonic seizures and myoclonic jerks, respectively. Each trace represents 5 min of EEG recording. All representative EEG traces were obtained from different animals.

Hence, 20mg/kg PTZ was selected as the dose required to elicit absence seizures in mice surgically implanted with either cortical or thalamic cannulae for subsequent experiments to test the impact of activating FFI during seizures.

4.3.3 Activating feed-forward inhibitory PV+ interneurons via focal CNO injection suppressed PTZ-induced absence seizures

Day 1: PTZ injection (20mg/kg, i.p.) only

On day 1, i.p. administration of PTZ (20mg/kg) induced seizures in all animals. However, various types of seizures were seen i.e. absence-like seizures, tonic-clonic seizures and myoclonic seizures. In the SS cortex treatment group, 20mg/kg PTZ administration induced absence seizures in 5 out of 7 PV^{Cre}/Gq-DREADD and 3 out of 5 non-DREADD WT controls. Six out of 7 PV^{Cre}/Gq-DREADD animals experienced tonic-clonic seizures whereas all non-DREADD WT controls had tonic-clonic seizures after systemic PTZ injection of 20mg/kg. Similarly, PTZ induced myoclonic seizures in only 3 animals of both PV^{Cre}/Gq-DREADD and non-DREADD WT control groups. In the RTN thalamus treatment group, absence seizures were observed in all DREADD mice ($n=7$) and in 3 out of the 5 non-DREADD WT controls. PTZ injection induced tonic-clonic seizures in only 3 out of 7 PV^{Cre}/Gq-DREADD animals whereas all non-DREADD WT animals of this treatment group experienced tonic-clonic seizures. Myoclonic seizures were seen in 5 out of 7 PV^{Cre}/Gq-DREADD and 3 out of 5 non-DREADD WT controls.

EEG data showed that the first incident of seizure (of any type) was very consistent. In the SS cortex group (Fig. 4.4A), mean onset of seizures was 3.65 ± 0.63 min in PV^{Cre}/Gq-DREADD ($n=7$) and 3.59 ± 0.62 min in the non-DREADD WT control animals ($n=5$), respectively. Similarly, in the RTN thalamus group (Fig. 4.4A), seizures were induced 3.82 ± 0.74 min and 3.87 ± 1.03 min after PTZ injection in PV^{Cre}/Gq-DREADD ($n=7$) and non-DREADD WT control animals ($n=5$), respectively. The last incident of seizure was also similar between the treatment groups. The last seizure burst was recorded 20.50 ± 7.87 min and 14.41 ± 6.03 min after PTZ injection in the PV^{Cre}/Gq-DREADD ($n=7$) and non-DREADD WT control animals ($n=5$) SS cortex groups, respectively (Fig. 4.4B). Similarly, in the RTN thalamus group, last epileptic burst was seen 13.07 ± 2.83 min and 14.27 ± 5.00 min after PTZ injection in PV^{Cre}/Gq-DREADD ($n=7$) and non-DREADD WT control animals ($n=5$), respectively (Fig. 4.4B).

So, in summary, there was no significant difference in the latency to first seizure and the last incident of seizure between treatment groups and genotypes (Fig. 4.4A,B) after a single injection of 20mg/kg i.p. PTZ on day 1.

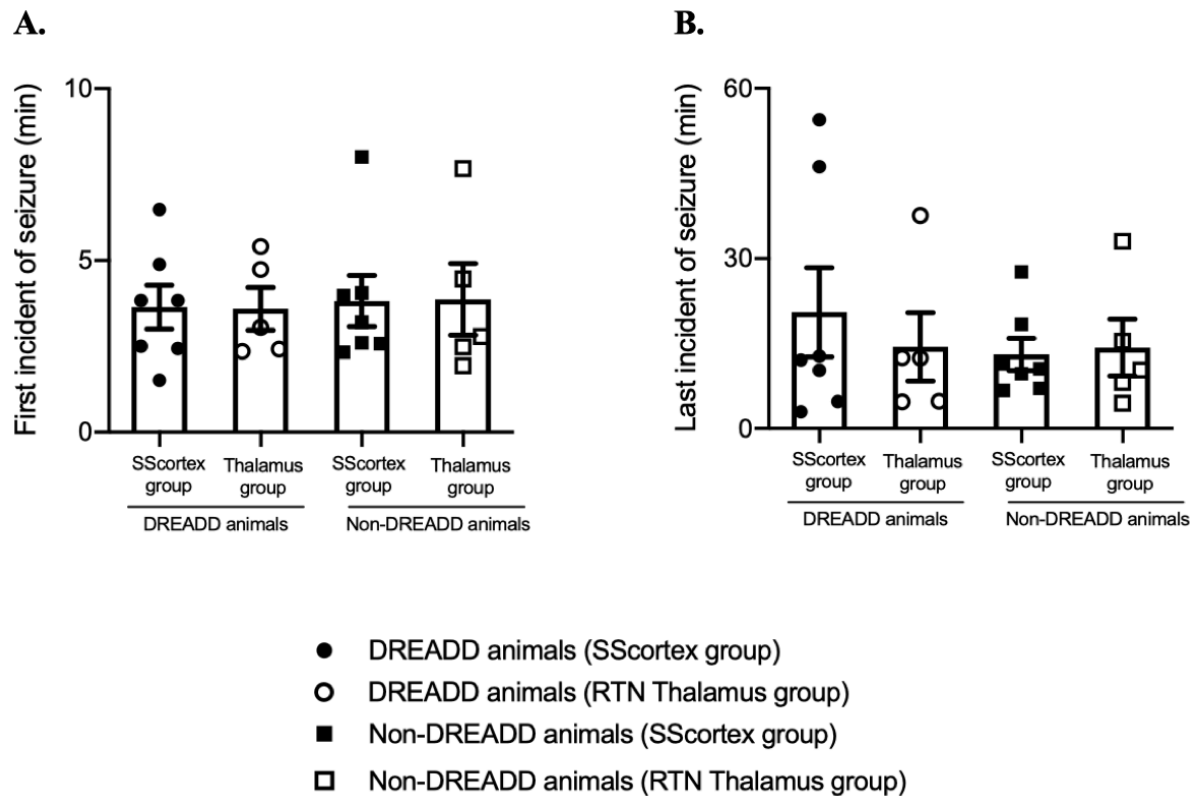


Fig. 4.4 First and last incident of seizure in animals after PTZ treatment on day 1. Comparison of (A) onset of seizure and (B) last incident of seizure during 1 hour of EEG recording in PV^{Cre}/Gq-DREADD (DREADD) (n=7) and non-DREADD (n=5) WT control animals of the SS cortex group and the RTN thalamus group after PTZ treatment on day 1. All values in graphs represent mean ± SEM. Comparison between treatment groups was performed using Mann Whitney unpaired rank test.

The percentage of time spent in each of the three different seizure types during 1 hour of EEG recording on day 1 after a single injection of PTZ is shown in figure 4.5A,C. PTZ treated PV^{Cre}/Gq-DREADD animals of the SS cortex group spent 36.13% of the total seizure period in absence-like seizures and 52.70% in tonic-clonic seizures (Fig. 4.5C). Likewise, non-DREADD WT control animals spent 48.10% of total seizure period in absence-like seizures and 42.71% of total seizure period in tonic-clonic seizure (Fig. 4.5C). In the RTN thalamus group, PV^{Cre}/Gq-DREADD animals spent 51.05% of total seizure period having absence-like seizures and 12.56% having tonic-clonic seizure (Fig. 4.5C). Non-DREADD WT animals of this group spent 30.92% of total seizure period in absence-like seizure and 49.23% of total seizure period in tonic-clonic seizure (Fig. 4.5C).

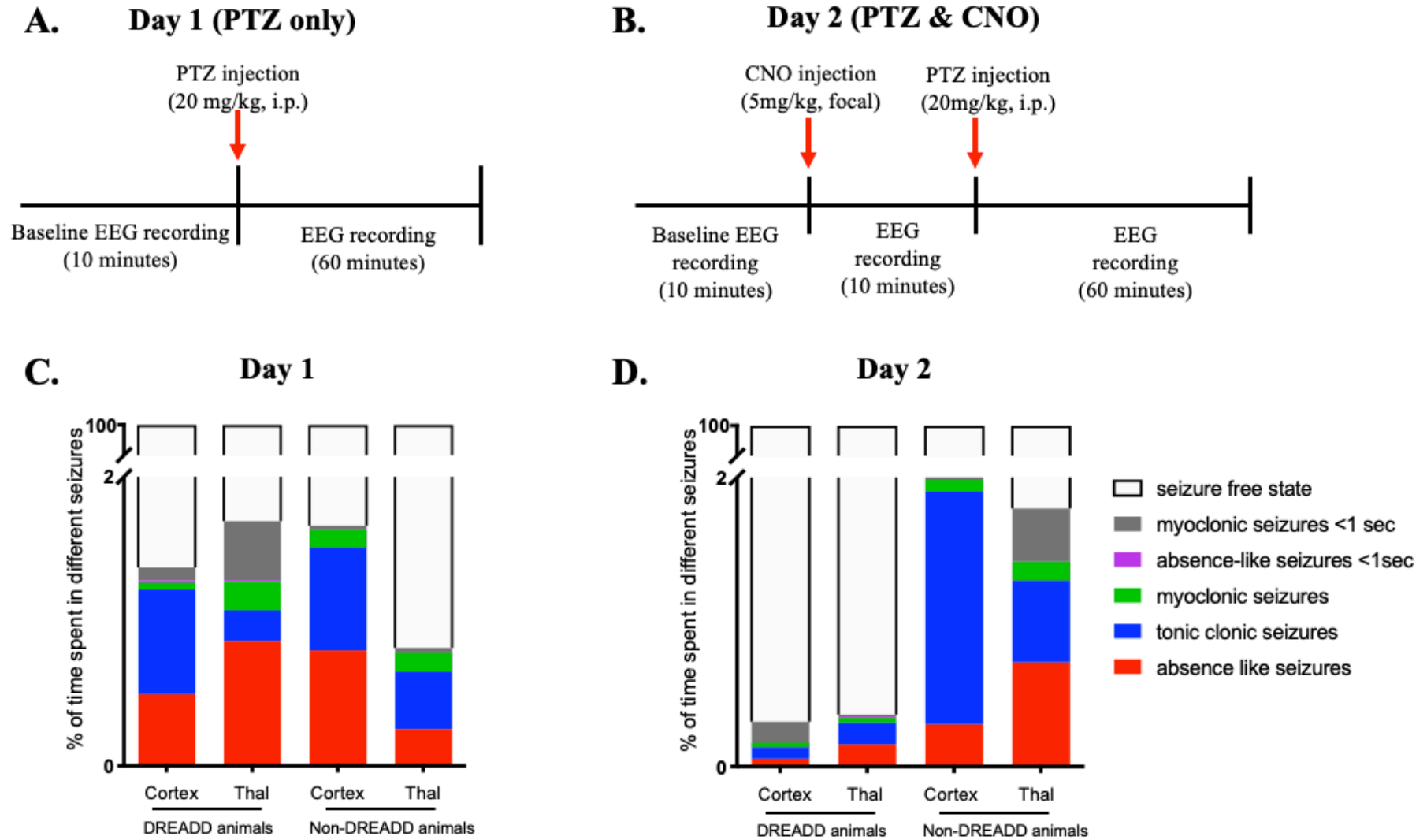


Fig. 4.5 Comparison of the % of time spent in seizures by animals on day 1 and day 2. Schematic of protocol for EEG recordings before and after (A) PTZ injection on day 1 and (B) PTZ and CNO injection on day 2. Comparison of the percentage of different types of seizures in PV^{Cre}/Gq-DREADD (DREADD) (n=7) and non-DREADD WT control (n=5) animals of the SS cortex and the RTN thalamus group after (C) PTZ injection on day 1 and (D) PTZ and CNO injection on day 2.

Day 2: CNO (5mg/kg, focal) and PTZ (20mg/kg, i.p.)

Having established that the seizure onset for PV^{Cre}/Gq-DREADD and non-DREADD WT animals is ~ 5 min post PTZ injection (on day 1), CNO (5mg/kg, focally; either into the SS cortex or the RTN thalamus) was injected 10 min prior PTZ (20mg/kg, i.p.) injection, on day 2 to test the impact of activating feed-forward inhibitory PV⁺ interneurons during PTZ-induced seizures. The timing and dose of CNO were chosen based on data from the previous experiments from chapter 3. 5mg/kg CNO was chosen because this is lowest yet effective dose that consistently generated absence-like seizures in PV^{Cre}/Gq-DREADD mice in experiments from chapter 3. Simultaneous video/EEG recordings were made according to the protocol outlined in schematic figure 4.5B. The percentage of time spent in each of the different seizure types during 1 hour of EEG recording on day 2 after CNO and PTZ administration is shown in figure 4.5D. On day 2, the relative time spent having seizures was substantially reduced in PV^{Cre}/Gq-DREADD animals of both treatment groups (cortical or thalamic) compared to day 1, whereas in non-DREADD WT controls there was no evidence of a reduction in seizures on day 2 (Fig. 4.5D).

4.3.3.1 Activating PV⁺ interneurons either prevented or increased the onset of seizures in DREADD mice

Activating PV⁺ interneurons prevented seizures in two out of 7 tested PV^{Cre}/Gq-DREADD animals of the SS cortex group i.e. 28% did not experience any types of seizure during 1 hour of EEG recording on day 2 (Fig 4.6). Likewise, in the RTN thalamus group, 3 out of 7 (42%) PV^{Cre}/Gq-DREADD animals were entirely seizure free on day 2 (Fig 4.6). Seizure activity on both days was further evaluated by analyzing the various parameters of EEG recording i.e. latency to first seizure, mean duration spent in seizures, total discharges/hr and mean length of bursts.

Activating PV⁺ interneurons increased the latency to first seizure (of any type)

A log-rank test was performed to compare the latency to the first seizure between treatment groups (Fig. 4.6). This test indicated that the latency to first seizure was significantly prolonged in PV^{Cre}/Gq-DREADD animals of both SS cortex and RTN thalamus groups on day 2 compared to that of day 1 (Fig 4.6).

On day 2, activating feed-forward inhibitory PV⁺ interneurons prevented PTZ-induced seizures in some mice as stated above. In the remaining PV^{Cre}/Gq-DREADD animals of both groups, the latency to first seizure was significantly prolonged.

SScortex group

RTN Thalamus group

Latency to first seizure (any of the three seizure type)

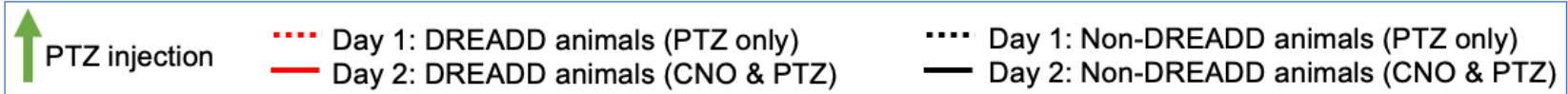
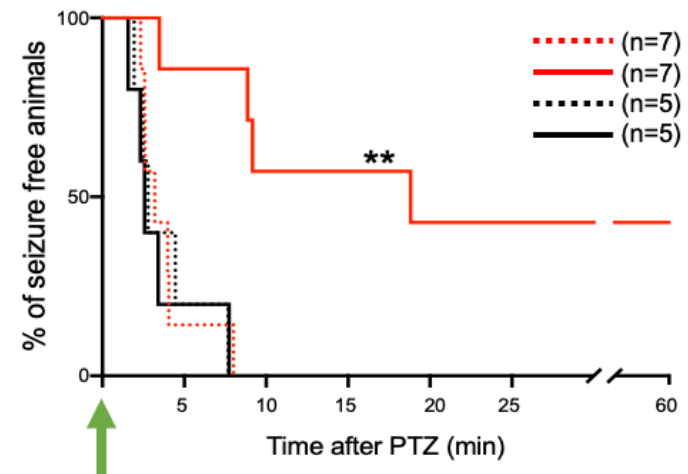
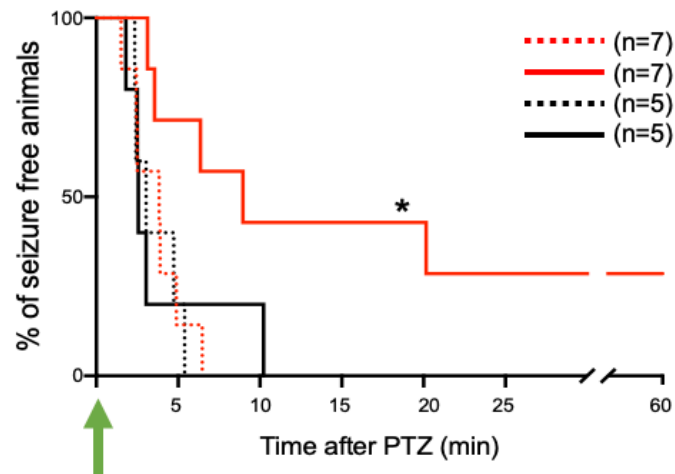


Fig. 4.6 Graphs showing the latency to first seizure in animals. Comparison of the latency to first seizure (any of the three seizure type) in DREADD and non-DREADD WT controls of the SScortex group and the RTN thalamus group between day 1 (PTZ only treated) and day 2 (CNO and PTZ treated). Comparisons between the treatment groups were made using log-rank test.

In the SScortex group, latency to first seizure was 4.32 ± 0.55 min ($n=5$) on day 1 which increased to 8.43 ± 31 min ($n=5$) on day 2. Likewise, in the RTN thalamus group, on day 1, mean onset of seizure was 3.24 ± 0.34 min ($n=4$), which increased to 10.08 ± 3.19 min ($n=4$) on day 2. In contrast, activation of PV⁺ interneurons did not prolong the latency to first seizure in non-DREADD WT control animals [SScortex group, day 1: 3.59 ± 0.62 min ($n=5$), day 2: 4.03 ± 1.56 min ($n=5$); RTN thalamus, day1; 3.87 ± 1.03 min ($n=5$), day 2: 3.51 ± 1.09 min ($n=5$)].

Activating PV⁺ interneurons also prolonged the latency to first absence, tonic-clonic and myoclonic seizure

Next, the individual seizure types were analyzed in relation to the latency to first seizure. Latency to first absence or tonic-clonic or myoclonic seizures in PTZ injected PV^{Cre}/Gq-DREADD animals pre-treated with CNO (in either of the brain regions of CTC network) on day 2 was delayed compared to that of day 1 (Fig. 4.7-4.9).

Absence seizures

In the SScortex group, on day 1, PTZ induced absence seizures in 5 PV^{Cre}/Gq-DREADD animals. All 5 animals were completely absence seizure free on day 2 when CNO and PTZ were co-administered (Fig. 4.7). In PV^{Cre}/Gq-DREADD animals of RTN thalamus group, 4 out of 7 (57%) animals did not experience absence seizure on day 2 (Fig. 4.7). In the remaining 3 animals, latency to first absence burst on day 2 was also prolonged compared to that of day 1 i.e. day 1: 3.71 ± 0.73 min; day 2: 13.55 ± 4.54 min.

Tonic-clonic seizures

PTZ treatment induced tonic-clonic seizures in 6 PV^{Cre}/Gq-DREADD animals of the SScortex group on day 1. On day 2, activation of feed-forward inhibitory PV⁺ interneurons 4 out of 6 (67%) PV^{Cre}/Gq-DREADD animals were completely free from tonic-clonic seizures (Fig. 4.8). The remaining animals showed increased onset of tonic clonic-seizures compared to that of day 1 i.e. day 1: 3.69 ± 1.19 min; day 2: 9.56 ± 5.64 min. Similarly, in the RTN thalamus group, PTZ treatment produced tonic clonic-seizures in 3 PV^{Cre}/Gq-DREADD animals on day 1. Upon co-administration of CNO and PTZ, on day 2, 67% animals did not experience any tonic-clonic seizures (Fig. 4.8).

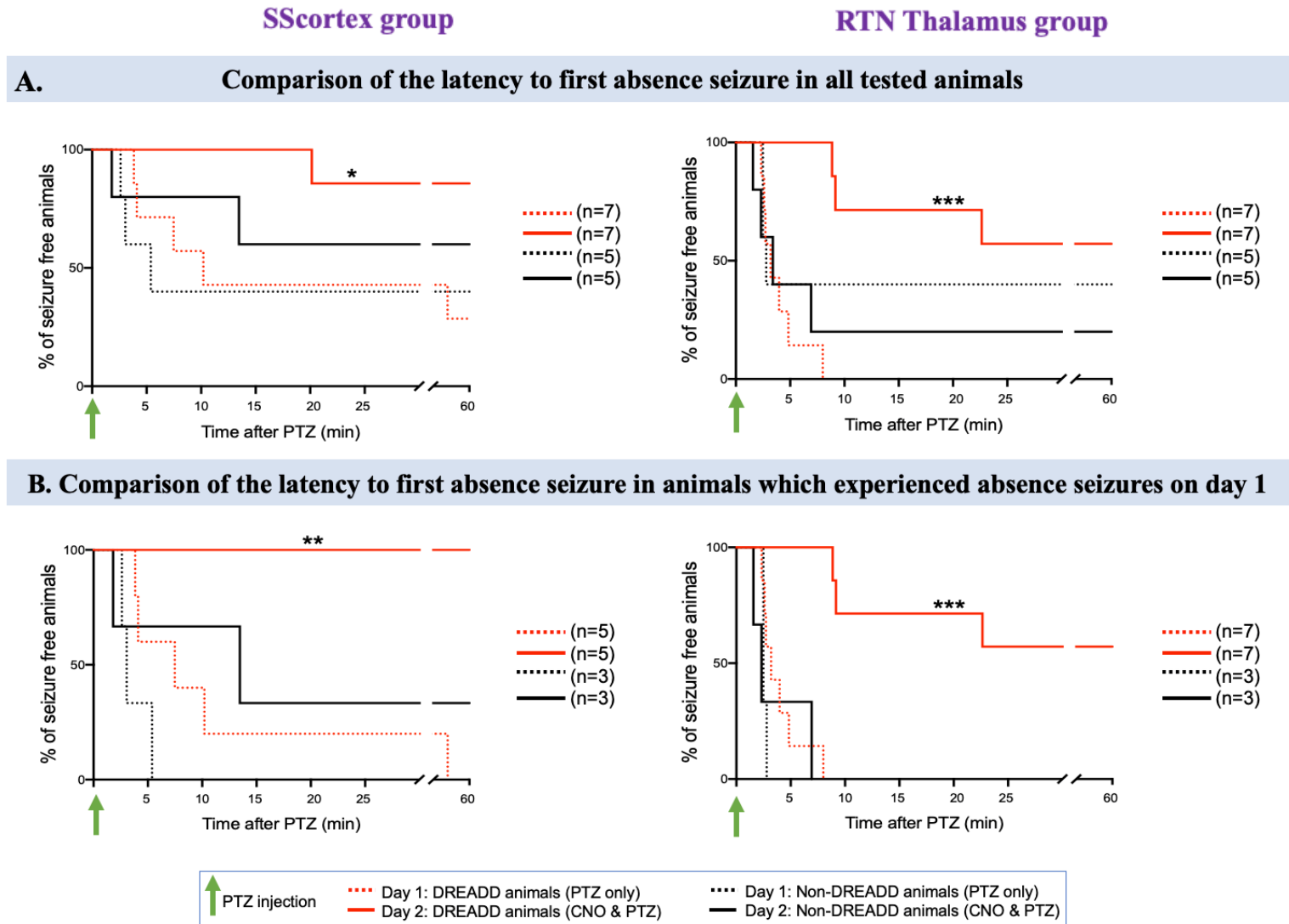


Fig. 4.7 Graphical display showing the latency to first absence seizure in animals. (A) Comparison of the latency to first absence seizure in all tested DREADD and non-DREADD WT controls of the SScortex group and the RTN thalamus group between day 1 (PTZ only treated) and day 2 (CNO and PTZ treated). (B) Comparison of the latency to first absence seizure in animals which experienced absence seizures on day 1 (PTZ only treated). Comparisons between the treatment groups were made using log-rank test.

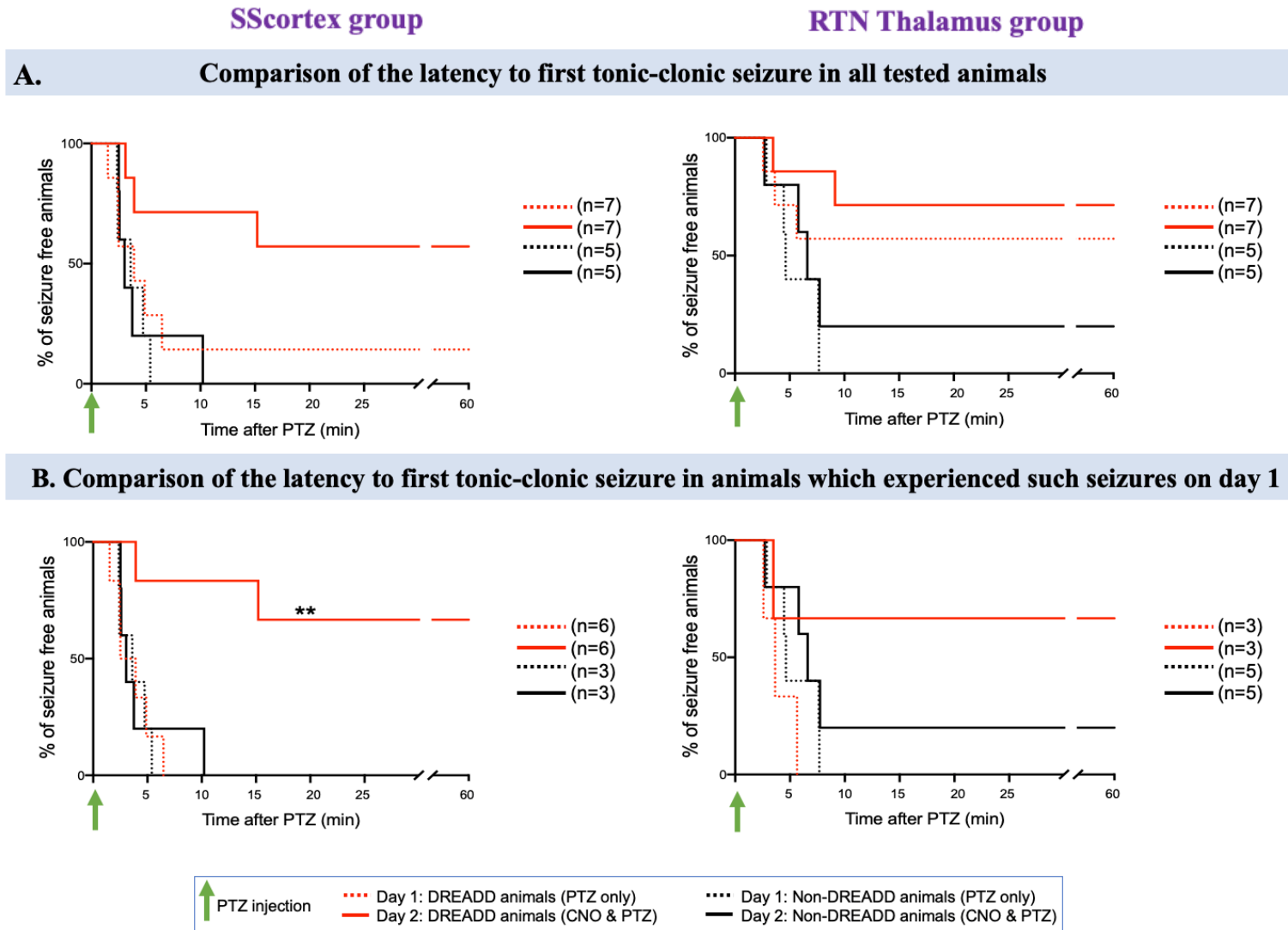


Fig. 4.8 Graphical display showing the latency to first tonic-clonic seizure in animals. (A) Comparison of the latency to first tonic-clonic seizure in all tested DREADD and non-DREADD WT controls of the SScortex group and the RTN thalamus group between day 1 (PTZ only treated) and day 2 (CNO and PTZ treated). (B) Comparison of the latency to first tonic-clonic seizure in animals which experienced tonic-clonic seizures on day 1 (PTZ only treated). Comparisons between the treatment groups were made using log-rank test.

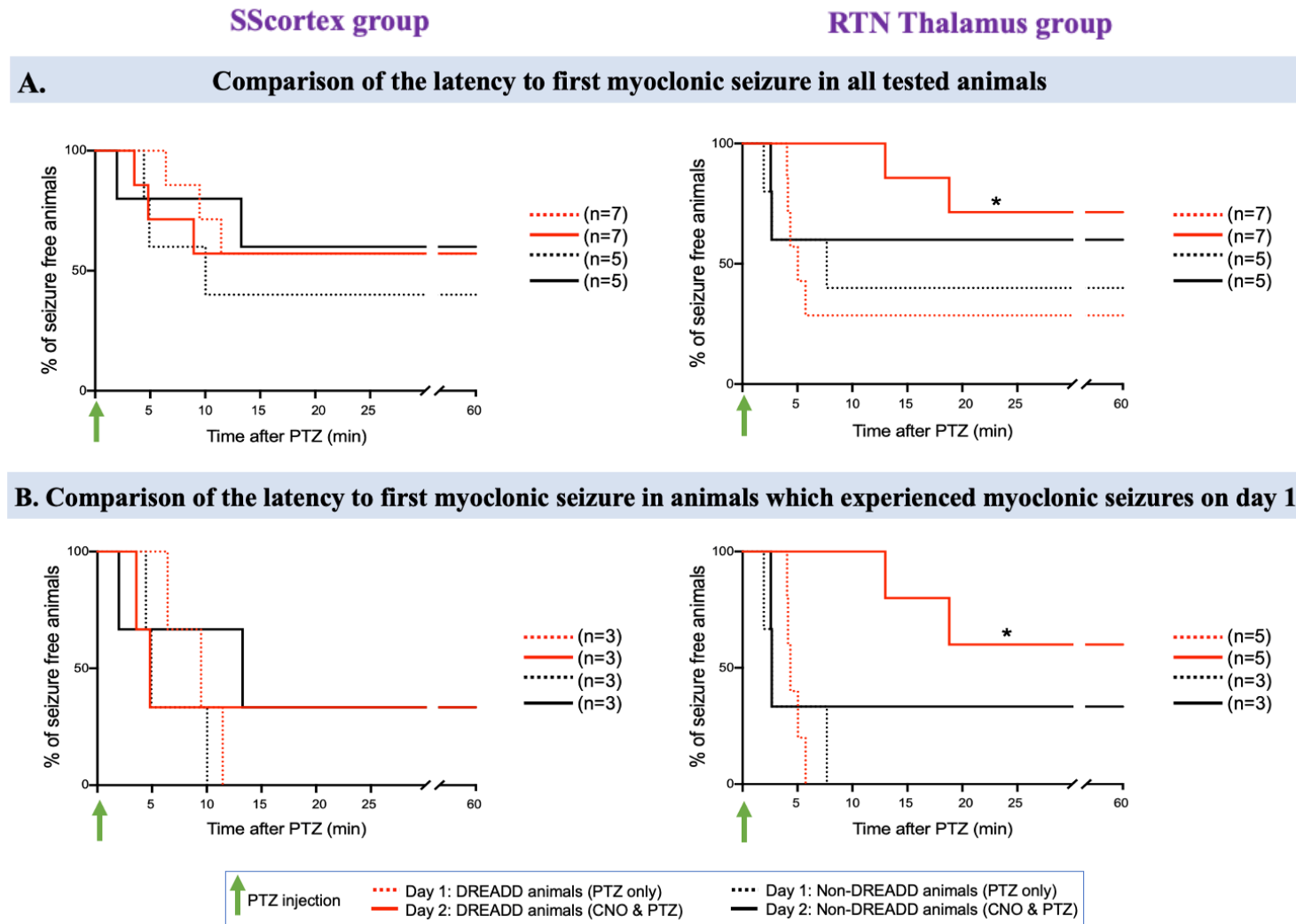


Fig. 4.9 Graphical display showing the latency to first myoclonic seizure in animals. (A) Comparison of the latency to first myoclonic seizure in all tested DREADD and non-DREADD WT controls of the SScortex group and the RTN thalamus group between day 1 (PTZ only treated) and day 2 (CNO and PTZ treated). (B) Comparison of the latency to first myoclonic seizure in animals which experienced myoclonic seizures on day 1 (PTZ only treated). Comparisons between the treatment groups were made using log-rank test.

Myo-clonic seizures

Similarly, 67% (2 out of 3) and 60% (3 out of 5) PV^{Cre}/Gq-DREADD animals of the SS cortex group and RTN thalamus group were completely free from myoclonic seizures on day 2 compared to day 1 (Fig. 4.9). Remaining animals of the RTN thalamus group also showed prolonged latency to first myoclonic seizures i.e. day 1: 4.24±0.10 min; day 2: 15.90±2.90 min. In comparison, on day 2, non-DREADD WT animals of either treatment group, did not show significant changes in the latency to first seizure compared to that of day 1 (Fig. 4.7-4.9).

4.3.3.2 Activating PV+ interneurons reduced the mean duration spent in seizures

On day 2, PV^{Cre}/Gq-DREADD animals in both the SS cortex and RTN thalamus groups, spent less time in PTZ-induced seizures compared to day 1. Mean duration spent in different type of seizures during 1 hour of EEG recording on both days is shown in figure 4.10. On day 1, PV^{Cre}/Gq-DREADD animals of the SS cortex group ($n=7$) spent 17.85±9.32 and 26.04±11.15 seconds in absence-like seizures and tonic-clonic seizures, respectively after PTZ administration which was reduced by 89.49% (to 1.876±1.87 seconds) and 88.91% (to 2.88±2.0 seconds) on day 2 after CNO and PTZ co-administration (Fig. 4.10). Similarly, PV^{Cre}/Gq-DREADD animals of the RTN thalamus group ($n=7$) also spent less time in absence like seizures on day 2 compared to that of day 1 (Fig. 4.10). During 1 hour of EEG recording, those animals spent 31.11±13.64 seconds in absence seizures on day 1 after PTZ administration which was reduced by 82.35% to 5.49±3.41 seconds on day 2 after co-administration of CNO and PTZ (Fig. 4.10). Interestingly, there was only 30% reduction in tonic-clonic seizures in this treatment group (day 1: 7.65±2.96 seconds, day 2: 5.37±3.53 seconds). In the SS cortex group, the duration spent in other types of seizures (myoclonic seizures, myoclonic jerks and absence-like seizures spanning <1 seconds) almost remained unchanged on both days, whereas duration spent in other types of seizures substantially decreased on day 2 in RTN thalamus group (Fig. 4.10). In contrast, non-DREADD WT animals did not experience a reduction in the time spent in seizures after CNO activation of FFI on day 2 compared to only PTZ treatment on day 1 (Fig 4.10).

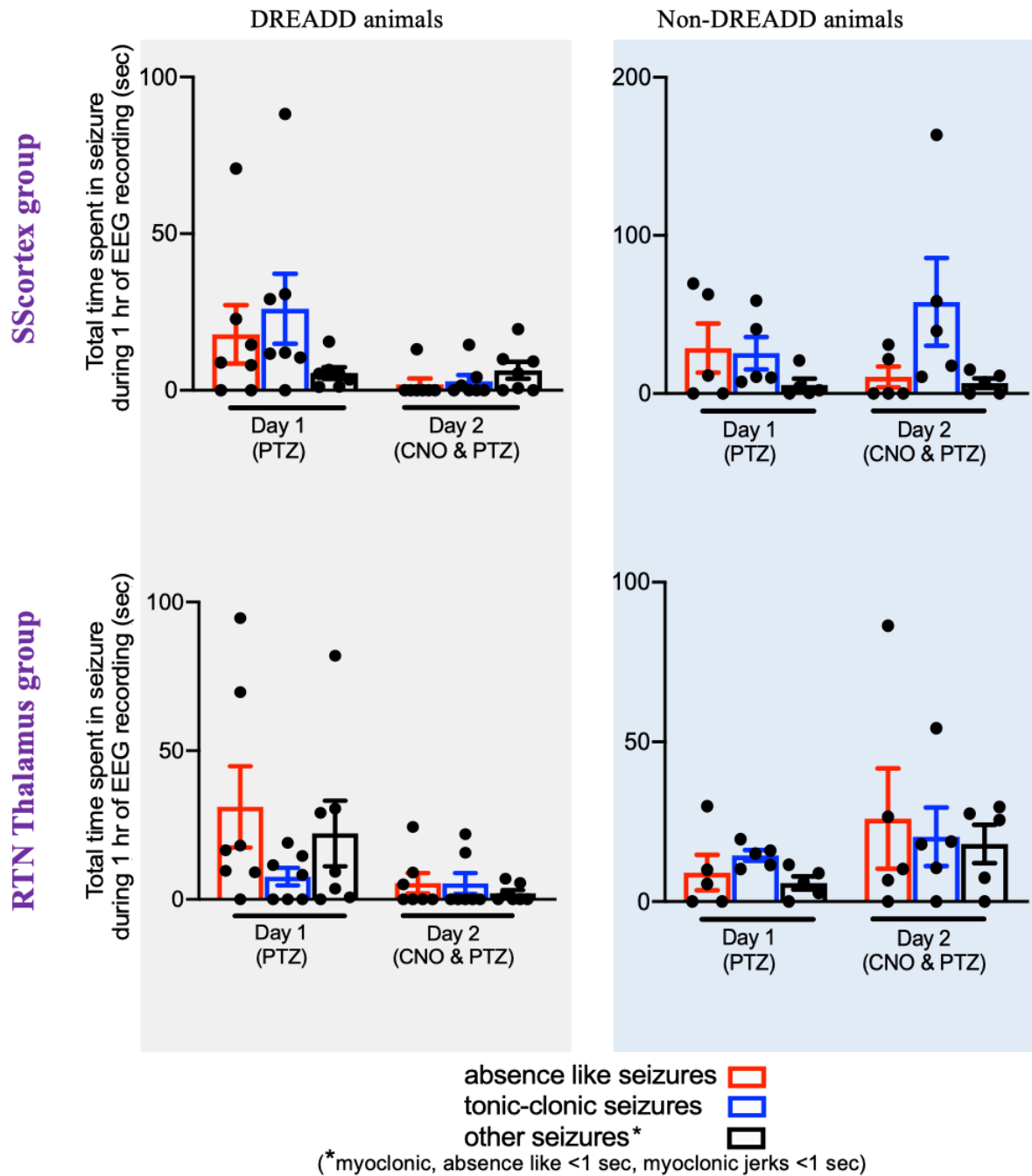


Fig. 4.10 Mean duration spent in seizure by animals during 1 hour of EEG recording. Graphs showing the total time spent in various types of seizures by PV^{Cre}/Gq -DREADD (DREADD) ($n=7$) and non-DREADD WT ($n=5$) animals of the SS cortex and the RTN thalamus group on day 1 and day 2. All values represent mean \pm SEM. Comparisons were performed using Wilcoxon matched-pairs signed-rank test.

4.3.3.3 Activating PV+ interneurons reduced total number of discharges and mean length of epileptic bursts

Analysis of the EEG data showed that total number of discharges (absence or tonic-clonic or myoclonic bursts) in PV^{Cre}/Gq-DREADD mice of both SS cortex group and the RTN thalamus group was reduced on day 2 compared to that of day 1 (Fig. 4.11). PV^{Cre}/Gq-DREADD animals of SS cortex group ($n=7$) treated with PTZ exhibited 4.57 ± 2.24 absence discharges which was reduced to 0.85 ± 0.85 discharges on day 2 (Fig. 4.11A). Similarly, these animals experienced 2.71 ± 1.28 tonic-clonic discharges and 2.14 ± 1.81 myoclonic jerks on day 1 which was reduced to 0.42 ± 0.205 tonic-clonic discharges and 0.71 ± 0.42 myoclonic jerks on day 2, respectively (Fig. 4.11A).

Similar effects were seen in RTN thalamus group. PV^{Cre}/Gq-DREADD animals of this group ($n=7$) treated with PTZ displayed 7.42 ± 2.58 absence-like discharges on day 1 which was reduced to 2.42 ± 1.41 discharges on day 2 (Fig. 4.11B). Those animals also displayed 0.57 ± 0.20 tonic-clonic discharges and 2.71 ± 1.26 myoclonic seizures on day 1 which were reduced to 0.28 ± 0.18 tonic-clonic discharges and 0.42 ± 0.29 myoclonic seizures on day 2 (Fig. 4.11B). Contrastingly, such type of reduction was not evident in non-DREADD WT animals (Fig. 4.11A,B).

Analysis of the EEG data also showed that, there was a reduction in mean duration of each epileptic burst in PV^{Cre}/Gq-DREADD animals on day 2 compared to that of day 1 (Fig. 4.11A,B). In the SS cortex group, the mean length of absence and tonic-clonic seizures was 3.21 ± 1.15 and 11.18 ± 3.40 seconds, respectively which decreased to 0.66 ± 0.43 and 3.60 ± 2.71 seconds on day 2 (Fig. 4.11A). Similar reductions were also seen in the PV^{Cre}/Gq-DREADD animals of RTN thalamus group. PV^{Cre}/Gq-DREADD animals of the RTN thalamus group on day 1 displayed absence and tonic-clonic seizures spanning 3.42 ± 0.86 and 7.65 ± 2.96 seconds, which was reduced to 0.90 ± 0.43 and 5.37 ± 3.53 seconds on day 2 (Fig. 4.11B). Overall, PV^{Cre}/Gq-DREADD animals of both treatment groups experienced a reduction in the number of epileptic discharges and mean length of such discharges on day 2, whereas non-DREADD WT control animals of both treatment groups did not show reductions in either number or duration of epileptic bursts (Fig. 4.11A,B). Representative EEG traces of 10 min after PTZ injection on day 1, and CNO & PTZ injection on day 2 in PV^{Cre}/Gq-DREADD animals are also presented for both SS cortex group (Fig. 4.12) and RTN thalamus group (Fig. 4.13).

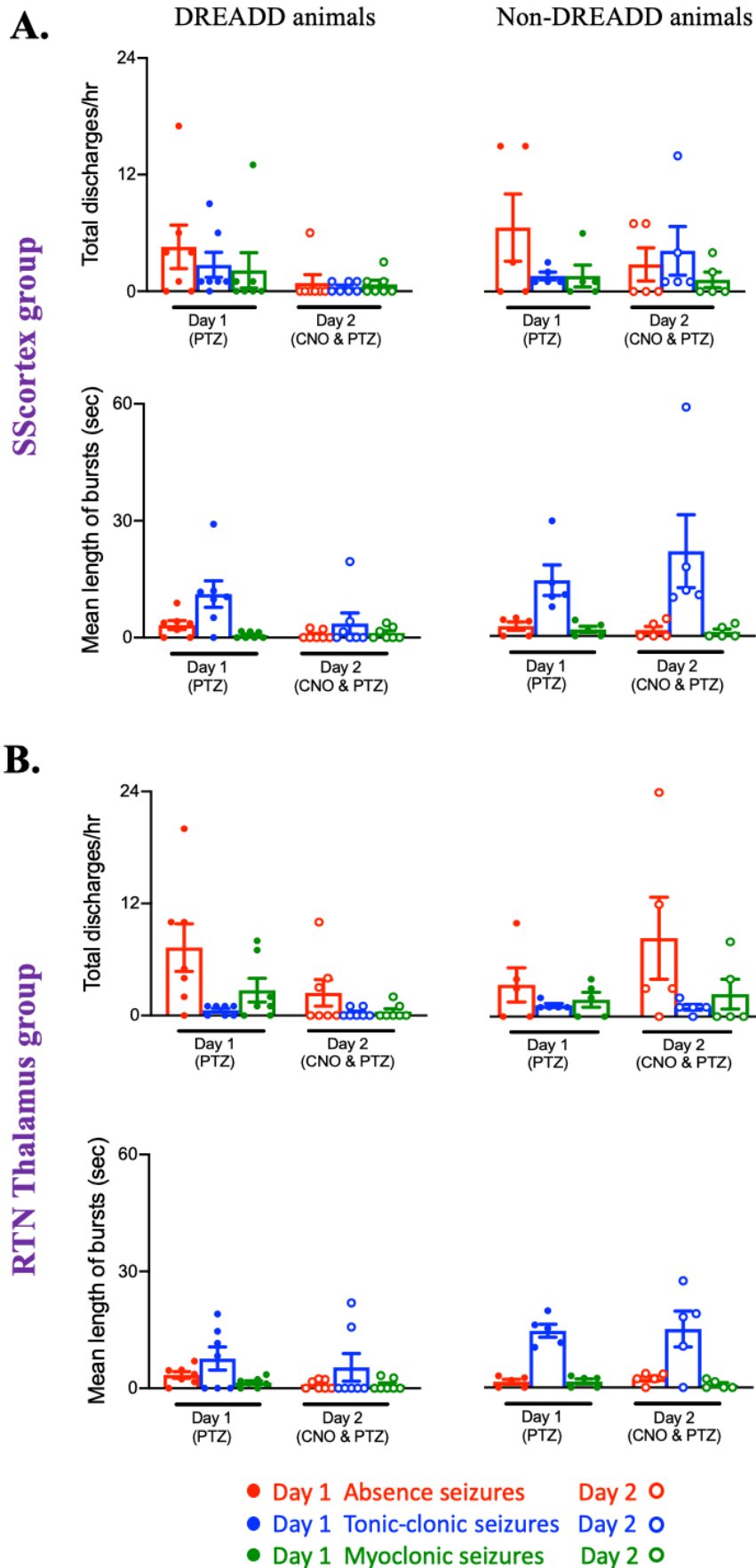
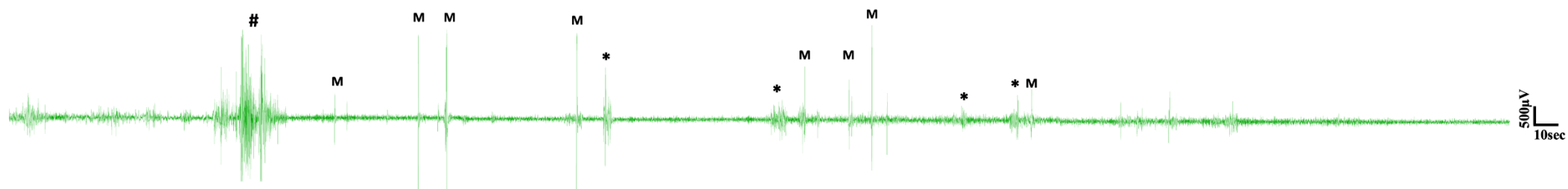


Fig. 4.11 Total epileptic bursts and length of bursts in animals during 1 hour of EEG recording. Comparison of mean number of epileptic bursts (discharges/hr) and mean length of bursts between PV^{Cre}/Gq-DREADD (DREADD) (n=7) and non-DREADD WT (n=5) animals of (A) the SScortex and (B) the RTN thalamus group after PTZ treatment on day 1 and CNO & PTZ treatment on day 2. All values represent mean \pm SEM. Comparisons were performed using Wilcoxon matched-pairs signed-rank test.

DAY 1: PTZ (i.p.) 20mg/kg



DAY 2: CNO (Focal: SScortex) 5mg/kg + PTZ (i.p.) 20mg/kg

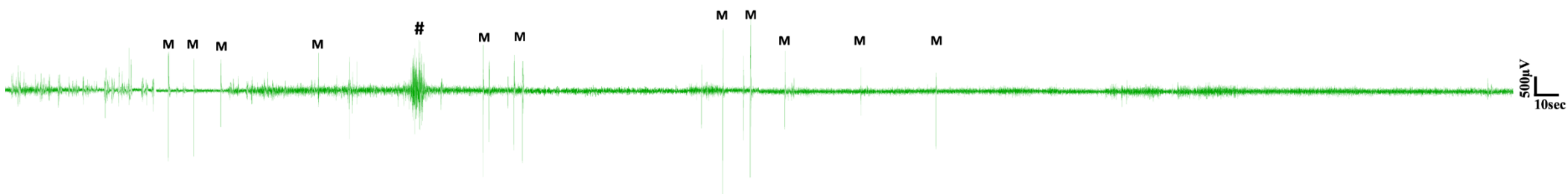
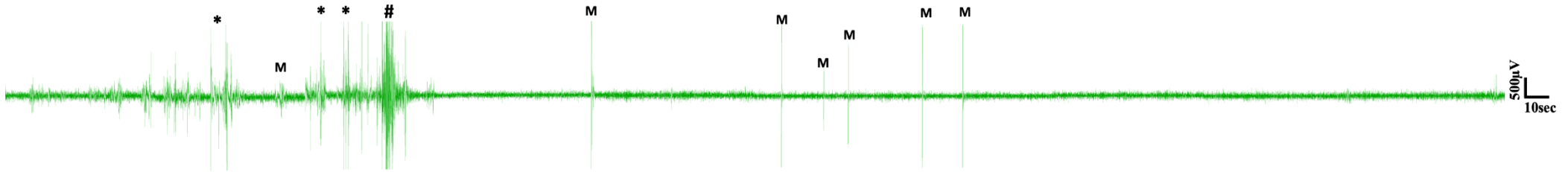


Fig. 4.12 Representative EEG traces from a $PV^{Cre}/Gq-DREADD$ animal after i.p. PTZ injection on day 1 and focal (SScortex) CNO and i.p. PTZ injection on day 2. Asterisks (*), hash signs (#) and M represent absence-like, tonic-clonic and myoclonic seizures, respectively. Each trace represents 10 min of EEG recording.

DAY 1: PTZ (i.p.) 20mg/kg



DAY 2: CNO (Focal: RTN thalamus) 5mg/kg + PTZ (i.p.) 20mg/kg

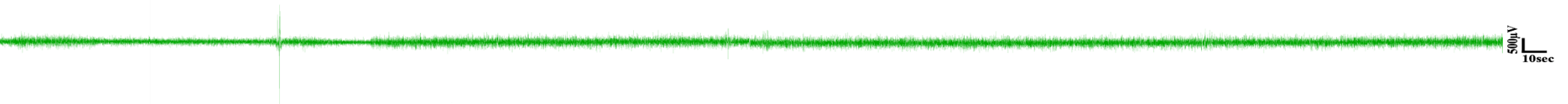


Fig. 4.13 Representative EEG traces from a $PV^{Cre}/Gq-DREADD$ animal after i.p. PTZ injection on day 1 and focal (RTN thalamus) CNO and i.p. PTZ injection on day 2. Asterisks (*), hash signs (#) and M represent absence-like, tonic-clonic and myoclonic seizures, respectively. Each trace represents 10 min of EEG recording.

4.4 Discussion

The study undertaken in this chapter demonstrated that activating feed-forward inhibitory PV+ interneurons in the CTC network possesses antiepileptic effects during chemically (PTZ) induced seizures. Analysis of the individual seizure types revealed that activation of PV+ interneurons was effective against PTZ-induced absence seizures including other forms of seizures induced by PTZ. Such activation either prevented or delayed the latency to first seizure, reduced the mean duration spent in seizures, decreased total discharges/hr and mean length of epileptic bursts. In contrast, such effects were not evident in non-DREADD WT control animals. These results demonstrate a potential for using PV+ interneurons as a therapeutic target to control absence seizures in some cases of absence epilepsy.

4.4.1 Excitatory Gq-DREADD receptors are highly expressed in feed-forward inhibitory PV+ interneurons

Confocal immunofluorescence microscopy confirmed the expression of excitatory (Gq) DREADD receptors in PV+ interneurons in PV^{Cre}/Gq-DREADD animals. DREADD HA-tag and PV were highly co-expressed in cells known to express calcium binding protein PV. None of the non-DREADD WT control animals showed colocalization between PV cells and HA-tag. The labelling of PV+ cells in this study was consistent with that of other published studies (del Río and DeFelipe, 1994; Tamamaki et al., 2003; Dávid et al., 2007; Fishell, 2007; Xu et al., 2010). PV^{Cre}/Gq-DREADD animals showed high colocalization (>90%) of PV cells and HA-tag in the SS cortex, the RTN thalamus and the Purkinje cells of cerebellum. This double transgenic approach of expressing DREADD receptors in feed-forward inhibitory PV+ interneurons was highly consistent compared to efficiency and specificity of viral mediated DREADD labelling in PV-Cre animals. Studies have shown that the infection efficiency and specificity of labelling vary between 70 and 95% in viral mediated delivery of DREADD constructs into brain regions (Zou et al., 2016; Xia et al., 2017; Hijazi et al., 2019; Bicks et al., 2020). In this current study, percentage of DREADD receptors (HA-tagged cells) colabelled for PV and percentage of PV cells colabelled for DREADD receptors (HA-tag) was always above 90% in all tested regions. This result is similar to the results obtained in chapter 3 (Panthi and Leitch, 2019) for inhibitory Gi-DREADD receptor expression.

4.4.2 Activation of feed-forward inhibitory PV+ interneurons suppressed PTZ induced absence seizures

PTZ is one of the chemicals that is widely used to induce generalized absence seizures in animals. Other chemicals such as γ -hydroxybutyrate (GHB), bicuculline, picrotoxin, penicillin are also routinely used to induce absence seizures (Snead et al., 1992; Kostopoulos et al., 2017), but PTZ has been preferentially used for testing new drugs against absence seizures for more than seventy years (Krall et al., 1978; Löscher, 2011). Moreover, use of low dose of PTZ is an established method to induce seizures within the thalamocortical circuit (Snead, 1992; Coulter and Lee, 1993).

In the pilot study, a single 20mg/kg (i.p.) dose of PTZ was sufficient to induce absence seizures in animals. However, a dose of 20mg/kg also induced absence seizures including tonic-clonic seizures and myoclonic seizures. Seizures were categorized on the basis of the morphology of EEG waveforms and behavioural features in the video. One recent study reported that administration of 20mg/kg (i.p.) dose of PTZ induced whisker trembling and SWDs with behavioural arrest in Tau58/4 transgenic mice (Van Erum et al., 2019). In another study Van Erum and colleagues also reported that the latency, severity and behavioural features of PTZ induced seizures vary with the concentration of PTZ, genotype and the age of the animal (Van Erum et al., 2020). These types of variability were also reported in rats (Klioueva et al., 2001; Lüttjohann et al., 2009). Importantly, in our current study, the proportion of absence and tonic-clonic seizures after PTZ treatment (on day1) in PV^{Cre}/Gq-DREADD and non-DREADD WT control animals was not significantly different. Thus, it can be concluded that various types of seizures seen even after injection of low dose (20mg/kg) of PTZ in this study might be due to strain related differences or transgene effect.

In the study reported in this thesis, the latency to first seizure after PTZ treatment (on day 1) was ~5 min which is consistent with other published studies in mice (Keskil et al., 2001; Medina et al., 2001; Ilhan et al., 2006; Erbayat-Altay et al., 2008; Nassiri-Asl et al., 2009; Koutroumanidou et al., 2013; Faghihi et al., 2017; de Freitas et al., 2018). These other studies have shown that irrespective of dose of PTZ (ranging from 20-80mg/kg, i.p.), the latency of seizure onset is around 5 min. One study, however, has reported that increasing the concentration of PTZ from 50-70mg/kg, decreases the time of onset of seizure from 300 seconds to 90 seconds (Schwaller et al., 2004). In another study conducted in mice, latency to seizure was decreased in animals injected with 60mg/kg compared to animals with 30-50

mg/kg dose of PTZ (Girard et al., 2019). Additionally, Van Erum and colleagues recently reported genotype and age-related differences in susceptibility and onset of PTZ-induced seizures (Van Erum et al., 2020). However, in the current study, regardless of genotype, first and last incident of seizure after PTZ administration on day 1, was very consistent in all animals of both treatment groups.

On day 2, PTZ (20mg/kg, i.p.) was tested after pre-treatment with CNO (5mg/kg, into either the SS cortex or the RTN thalamus). Such regional activation of PV⁺ interneurons significantly delayed the latency to first absence seizure (including other seizure types) compared to that of day 1 in PV^{Cre}/Gq-DREADD animals. Furthermore, there was a reduction in the total time spent in seizure, in the number of total discharges and mean duration of each bursts of discharges on day 2. However, non-DREADD WT control animals of both treatment groups (SS cortex and RTN thalamus) did not experience such protection or decreased seizure susceptibility on day 2.

Similar to these results, DREADD mediated activation of PV⁺ interneurons reduced the seizure susceptibility and severity of PTZ treated (50mg/kg) transgenic (PV-Cre x LSL-hM3Dq) animals (Johnson et al., 2018). In addition, Johnson and colleagues also performed complementary experiments where they injected AAV with excitatory DREADD (hM3Dq) constructs into the cortex of the PV-Cre mice. Similar antiepileptic effects were observed in animals when CNO and PTZ were co-administered using viral vector method (Johnson et al., 2018). Likewise, Clemente-Perez and colleagues used optogenetics to activate PV⁺ interneurons of the RTN thalamus which suppressed seizures induced by PTZ administration (35-60mg/kg) (Clemente-Perez et al., 2017). The protective role of these interneurons was also assessed in another study where authors found that the severity of PTZ induced seizure is significantly higher in parvalbumin-deficient mice (PV^{-/-}) compared to that of WT (PV^{+/+}) genotype (Schwaller et al., 2004).

Studies have shown that activation of PV⁺ interneurons of other regions of the brain also offers protective role against other chemically induced seizures. Chemogenetic activation of hippocampal PV⁺ interneurons suppressed 4-AP induced epileptiform activity in PV-Cre mice (Călin et al., 2018). Another study has also shown that stimulation of PV⁺ interneurons has similar protective effect against 4-AP induced spontaneous electrographic seizures (Assaf and Schiller, 2016). Activation of hippocampal PV⁺ interneurons also provided antiepileptic

effects against KA-induced temporal lobe seizures (Krook-Magnuson et al., 2013; Wang et al., 2018). Altogether, these findings indicate that PV⁺ interneurons might serve as a novel therapeutic target to control seizures.

4.4.3 PV⁺ interneurons- a potential target for antiepileptic therapy?

In the previous chapter, using inhibitory DREADD (PV^{Cre}/Gi-DREADD) animals, selective unilateral (one hemisphere) silencing of feed-forward inhibitory PV⁺ interneurons via regional injection of CNO either into the SS cortex or the RTN thalamus generated absence-like SWDs (Panthi and Leitch, 2019). Conversely, in this chapter, selectively activating these interneurons either prevented PTZ-induced absence seizures or suppressed the severity of absence seizures. Furthermore, PTZ induced tonic-clonic and myoclonic seizures were also reduced in severity by regional activation of feed-forward inhibitory PV⁺ interneurons.

As PV⁺ interneurons synapse on to soma/proximal dendrites/axon initial segment of excitatory pyramidal cells (Inan and Anderson, 2014; Tremblay et al., 2016) and axonal branches of a PV cell has contacts over thousands of pyramidal cells (Freund and Buzsaki, 1996; Packer and Yuste, 2011), activating them may have generated widespread post-synaptic inhibitory currents onto pyramidal neurons, thereby attenuating PTZ-induced seizures.

One study reported that targeting single type of interneuron may not always be sufficient to control seizures. Ledri and colleagues found that optogenetic activation of several subpopulation of interneurons of hippocampus [PV, SOM, Cholecystokinin (CCK), Neuropeptide Y (NPY)-expressing] more effectively inhibits 4-AP induced epileptiform activity in the brain slices compared to individual set of interneurons alone (Ledri et al., 2014). As several subclass of interneurons have different functional connectivity to the principal neurons, this approach might have powerfully inhibited various compartments of principal cells and efficiently suppressed epileptiform activity. Clearly, in this current study activating just PV⁺ interneurons had profound effect on suppressing seizures.

Similarly, other optogenetic studies revealed that activating hippocampal PV⁺ interneurons attenuate KA-induced temporal lobe seizures (Krook-Magnuson et al., 2013) and pilocarpine induced mesial temporal lobe seizures (Lévesque et al., 2019). Wang and colleagues used chemogenetics and reported the prominent role of hippocampal PV⁺ interneurons in blocking seizures in KA-induced temporal lobe epilepsy model (Wang et al., 2018). However, in some

studies activation of PV⁺ interneurons did not stop or shorten seizures as expected. Instead, such optogenetic activation triggered preictal and interictal spikes leading to seizure-like discharges in medial entorhinal slices perfused with the proconvulsive compound 4-AP (Yekhlief et al., 2015). In another optogenetic kindling epilepsy model, activation of these interneurons failed to attenuate seizures rather inhibition was effective in reducing the duration of seizures (Khoshkhoo et al., 2017), in direct contrast to previous optogenetic studies (Krook-Magnuson et al., 2013; Ledri et al., 2014). Thus, it is possible that impact of interneurons depends on their functional features based on their anatomical location and patterns of excitability of the regions under study.

Different outcomes in response after activating PV⁺ interneurons may also depend on the implemented experimental approach. Optogenetic activation of these interneurons in medial entorhinal cortex produced anti-epileptic effects when they were activated in the pre-ictal stage but ineffective when activated during an epileptic event (Yekhlief et al., 2015). Likewise, Assaf and Schiller revealed that optogenetic activation of cortical PV⁺ interneurons effectively suppresses 4-AP induced seizures when stimulated a few seconds before the onset of seizures, but it worsened the seizure control when activated between seizures i.e. interictal phase. In both studies, activation of PV⁺ interneurons did not block ongoing seizures. In this current study, to test the impact of activating feed-forward inhibitory PV⁺ interneurons during PTZ-induced absence seizure, animals were focally treated with CNO, 10 min prior i.p. PTZ injection. This was based on the result from the previous chapter where inhibitory Gi-DREADD receptor were activated ~15 min of focal CNO injection and result from the experiments conducted on day 1 in this chapter showed that PTZ induces seizures ~5 min post injection.

It is also important to mention that selective silencing of excitatory pyramidal neurons may have protective role against absence seizures. This approach is relatively unexplored. Few recent studies have shown that susceptibility of seizure activity reduces when excitatory neurons are targeted with chemogenetics (Kätzel et al., 2014; Avaliani et al., 2016; Chen et al., 2020) or optogenetics (Tønnesen et al., 2009; Krook-Magnuson et al., 2013). Studies have shown that chemogenetic silencing of CAMkinase expressing pyramidal cells in motor cortex (Katzel et al., 2014) and hippocampus (Chen et al., 2020) has antiepileptic effect against pilocarpine induced and kindling induced epileptic seizures, respectively. Optogenetics mediated silencing of excitatory neurons using halo rhodopsin (HR2) and exciting inhibitory

neurons using channel rhodopsin (Chr2) was effective against KA induced temporal lobe seizures.

4.5 Conclusion

Altogether, DREADD mediated activation of feed-forward inhibitory PV+ interneurons in either the SS cortex or the RTN thalamus of the CTC network yielded antiepileptic effects against absence seizures. Thus, these interneurons could serve as ‘choke points’ for anti-seizure therapy and the findings from this study could be highly significant in developing new targeted approach for the treatment of absence epilepsy. Data from this and the previous chapter have provided us an understanding that dysfunctional FFI is likely to be involved in the generation of absence seizures. It is possible that dysfunctional FFI may alter the synthesis and transport of inhibitory neurotransmitter (GABA) compromising GABAergic signalling. This forms the basis of next chapter where changes in the GABA levels in terms of GABA synthesizing enzymes and transport proteins will be tested.

Chapter 5. Impact of Dysfunctional FFI on GAD Isoforms and GABA Transporters— Evidence from Epileptic Stargazers and CNO Treated DREADD Animals

5.1 Introduction

In the previous two chapters, it was established that functionally silencing feed-forward inhibitory PV⁺ interneurons in the CTC network is sufficient to generate absence-like SWDs associated with behavioural arrest (Panthi and Leitch, 2019). Furthermore, activating FFI during PTZ-induced seizures abolishes absence seizures in the majority of animals and reduced the severity of seizures. In the stargazer mouse model of absence epilepsy, in which FFI is impaired, GABA levels are altered in CTC neurons. Hence, the aim of this chapter was to investigate whether impaired FFI impacts GABA expression by affecting its synthesizing enzymes (GAD65 and GAD67) or transporter proteins (GAT-1 and GAT-3).

Stargazer mice have a deficit in a protein called stargazin. Stargazin is a transmembrane AMPA receptor regulatory protein (TARP) which is responsible for trafficking AMPA receptors into the synapse and regulating their functions (Chen et al., 2000, Tomita et al., 2005). Our laboratory has previously reported that a deficit in stargazin in the stargazer model of absence epilepsy leads to the reduced expression of GluA4-AMPA receptors at excitatory synapses in feed-forward inhibitory (PV⁺) interneurons of the CTC network i.e. SS cortex (Adotevi and Leitch, 2016; 2017; 2019) and RTN thalamus (Barad et al., 2012; 2017). This impairment is likely to reduce FFI within the cortical and thalamic microcircuits of the CTC network. Additionally, it has been shown that both GABA receptors and GABA neurotransmitter are altered within the CTC network of epileptic stargazers. Phasic and tonic GABA_AR are specifically increased in the VP thalamus region (at synaptic and extrasynaptic sites on relay neurons) but not in the RTN thalamus (Seo and Leitch, 2014; 2015). Changes in GABA_AR expression in the stargazer VP thalamus only occur after seizure onset at PN16-18 (Seo and Leitch, 2017) suggesting a compensatory post-seizure effect that most likely contributes to seizure maintenance rather than generation. Likewise, GABA neurotransmitter levels have been found to be increased in the SS cortex (Hassan et al., 2018), but reduced in the VP thalamus of epileptic stargazers. No significant difference in the GABA levels expression were evident in the RTN thalamus of stargazers compared to non-epileptic controls (Leitch laboratory, pers. comm).

GABA levels are controlled by the enzymes responsible for their production (GAD65 and GAD67 which catalyze the synthesis of GABA from glutamate) and/or transporters that

mediate their reuptake (GAT-1 and GAT-3). GAD65 is mostly distributed in the axon terminals where it catalyzes GABA synthesis on demand, which is crucial for phasic inhibition (Tian et al., 1999). GAD67 is distributed throughout the neurons. It is responsible for synthesizing the majority of GABA and is important in mediating tonic inhibition (Asada et al., 1997; Schousboe and Waagepetersen, 2009). GAT-1 and GAT-3 are responsible for the recycling or removal of GABA from the synapse after its release from presynaptic terminals. GAT-1 is mainly expressed throughout neurons and in some astrocytic processes and is responsible for regulating GABA levels during sustained neuronal activity whereas GAT-3 is distributed primarily in astrocytes and regulates GABA levels in extrasynaptic areas (see reviews by Scimemi, 2014 and Melone et al., 2015).

Expression levels of GAD65 and GAD67 were reduced in human temporal lobe epilepsy patients (Wang et al., 2016). GAD65 knockout animals are highly vulnerable to seizures (Asada et al., 1996; Kash et al., 1997; Stork et al., 2000; Qi et al., 2018), whereas GAD67 knockout animals do not survive post-birth (Asada et al., 1997; Condie et al., 1997). It is important to mention that mice with a disrupted GAD67 allele, the GAD67 GFP knock-in mice (Gad67-GFP+/-), display abnormal locomotor behaviour or altered anxiety behaviour (Smith et al., 2018). Another study found that insertion of Cre into the VGAT gene (VGAT-Cre mice) disrupts expression at both mRNA and protein level and reduced GABAergic synaptic transmission (Straub et al., 2020).

In the GAERS, rat model of absence epilepsy, absence seizures are due to enhanced tonic inhibition within the VP thalamus as a result of failure in reuptake of extracellular GABA by GAT-1. Increased tonic GABAergic inhibition is evident in the VP thalamus of GAERS after postnatal day 17 and is sustained up to PN30 when SWDs first appear (Cope et al., 2009). These workers also reported increased tonic GABAergic inhibition in VP thalamus of stargazers; however, this was not evident until PN19-21, which is after seizures occur and thus unlikely to be causative of seizure generation in this model. In a recent study, GABA uptake assays were performed in primary cultures of astrocytes obtained from the thalamus and cortex of GAERS. Uptake activity of each transporter was determined by selectively blocking each transporter with specific drugs. GAT-1 and GAT-3 mediated uptake was decreased in thalamic astrocytes; and the GAT-3 mediated uptake was reduced in cortical astrocytes (Pina et al., 2019). These findings were also accompanied by increased levels of expression of GAT-1 and GAT-3 in cultured astrocytes obtained GAERS, with the exception of thalamic GAT-3 which

was decreased in astrocytes derived from epileptic animals (Pina et al., 2019). Moreover, GAT-1 knockout mouse shows spontaneous ETX-sensitive SWDs (Cope et al., 2009), physical and behavioural abnormalities (Jensen et al., 2003; Chiu et al., 2005). GAT-1 is functionally deficient in ventro basal astrocytes in GAERS (Pirttimaki et al., 2013).

Clearly, there are various mechanisms which can impair the normal GABAergic inhibition within the CTC network. Abnormalities in the expression of GADs and GATs may have a role in altered GABAergic inhibition leading to absence seizures within the CTC network. Expression level and localization profile of these protein targets are not yet studied using absence seizure model.

Hence, the aim of this chapter was to investigate whether altered GABA levels in the stargazer mouse model of absence epilepsy which has dysfunctional FFI are the result of altered expression of GADs and/or GATs. The first objective of this study was to examine the expression levels of GADs and GATs in the stargazer mouse model of absence epilepsy where seizure onset occurs early in postnatal development (PN17-18 days) (Qiao and Noebels, 1993), equivalent to age of onset in humans, and are chronic continuing throughout adulthood. This second objective was to examine whether acute functional silencing of FFI in DREADD mice is sufficient to alter the level of GADs and/or GATs and thus impacts GABA levels on presynaptic terminals.

5.2 Methods

Details of the confocal microscopy, western blotting procedures and analysis used in this study are fully described in chapter 2. Procedures that are specifically related to the experiments performed in this chapter are described below.

5.2.1 Immunofluorescence Confocal Microscopy and analysis

Immunofluorescence confocal microscopy was performed to investigate the expression pattern and staining intensity of GADs (65 and 67) and GATs (1 and 3) in the SS cortex and the thalamus (RTN and VP) of epileptic stargazers ($n=4$) and non-epileptic controls ($n=3$). Antibodies against GAD65, GAD67, GAT-1 and GAT-3 were used. Antibodies dilutions used in this experiment are listed in Table 2.7 and 2.8 (chapter 2). Confocal imaging was performed as described previously in chapter 2. Sections from the brain slices as shown on the schematic below were used (Fig. 5.1). Intensity of staining of GADs and GATs in PV⁺ interneurons in

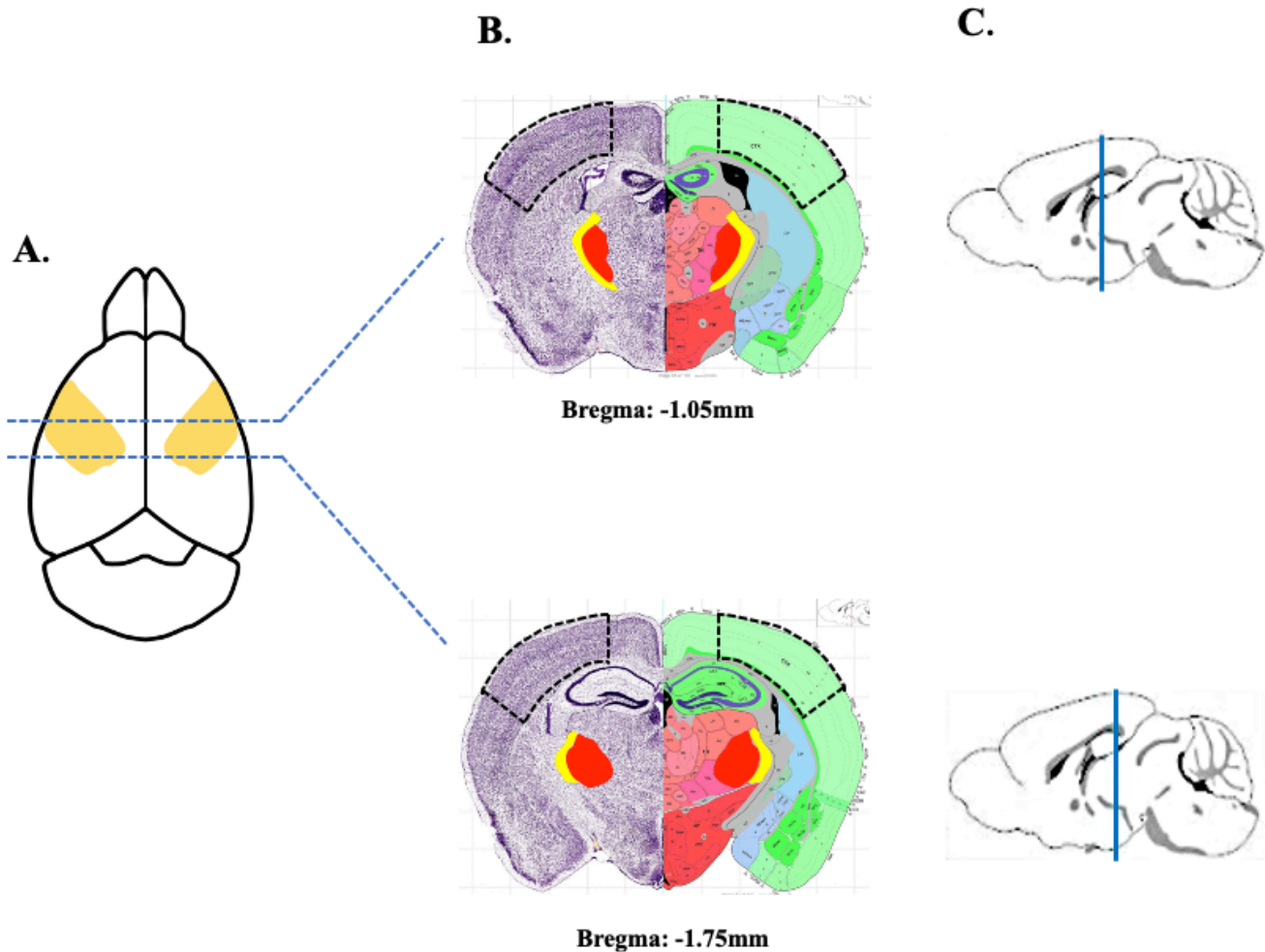


Fig. 5.1 Schematic of the tissue sections chosen for confocal analyses. (A) Scheme illustrating the mouse brain and approximate region of the primary SScortex (yellow shaded portion) (adapted from Greifzu et al., 2011) with (B) relative bregma readings and (C) the regions in the coronal plane from where tissue sections were chosen for confocal analyses. Black dotted boxes, yellow and red shaded regions in the figure B represent approximate SScortex, RTN and VP regions, respectively. (B and C were adapted from Allen Brain Atlas, online version, <https://mouse.brain-map.org/>).

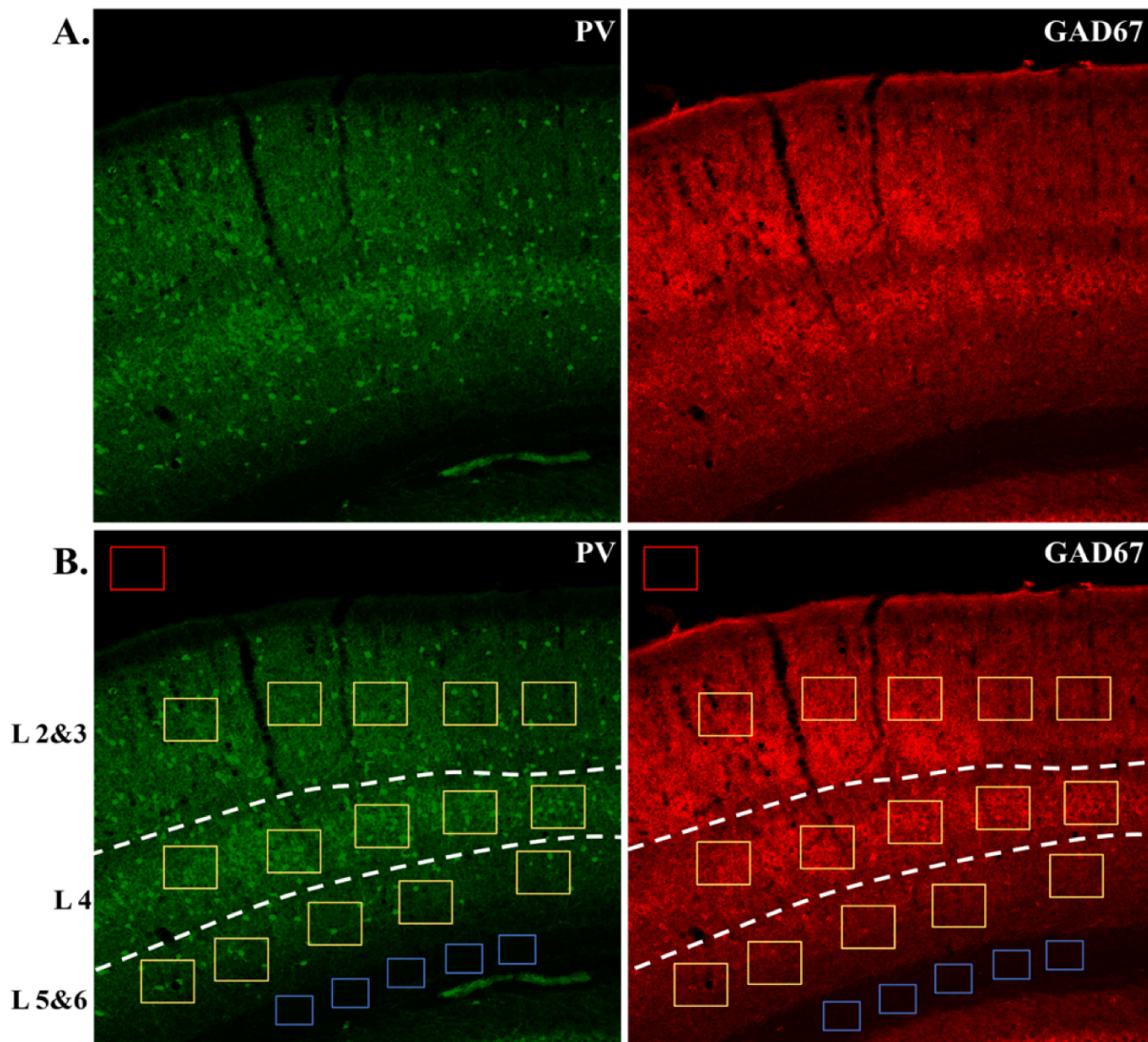


Fig. 5.2 Method of visual identification of cortical layers and analyses of confocal images. Representative confocal images showing the method of identification of cortical layers to measure the confocal fluorescence intensity for each layer and targeted proteins. (A) Layer 2&3 and 5&6 were separated from layer 4 by visual identification of the strong aggregation of PV+ cells in PV panel. (B) White dots were used to separate cortical layers in PV panel and same white dots were replicated in GADs or GATs panel. Rectangular region of interest (ROI) was randomly created for cortical layers (yellow box), external capsule (blue box) and the glass slide without tissue specimen (red box). Similar method was followed to measure staining intensity in the thalamus region.

the SS cortex and the thalamus was calculated using ImageJ software (NIH, USA). Layers of the SS cortex (2&3, 4 and 5&6) in the tissue sections were identified visually based on intensely labelled PV+ cells in layer 4 (Czeiger and White, 1997; Staiger et al., 1997; Dávid et al., 2007; Rudy et al., 2011; Xu et al., 2018) as shown in representative tissue section in the figure 5.2.

Mean intensity of staining of targeted proteins in each cortical layer i.e. 2&3, 4 and 5&6 was calculated by measuring the intensity within layer specific rectangular region of interest (ROI) (e.g. yellow ROI's) (Fig. 5.2). ROI's were randomly created and kept same for relevant confocal images. The background intensity for each image was the mean intensity of external capsule (blue ROI's) plus the intensity of regions of the glass slide without tissue specimen (red ROI) (Fig. 5.2). Layer specific staining intensity of each protein target (GADs, GATs and PV) was finally determined by calculating the ratio of mean intensity of staining to its background staining. Intensity calculation were based on 10-15 confocal images for each genotype and every abovementioned protein target.

5.2.2 Western blotting

To demonstrate the expression level of GADs and GATs, brain tissue from the SS cortex and the VP thalamus regions was extracted. 27 epileptic stargazers and 31 non-epileptic control animals from 20 different litters were included in the stargazer-based experiments.

In the DREADD-based experiments, brain tissue from the SS cortex of CNO treated PV^{Cre}/Gi-DREADD mice and control counterparts (vehicle treated PV^{Cre}/Gi-DREADD mice and CNO treated non-DREADD WT controls) was also extracted. 12 CNO treated DREADD animals, 8 vehicle treated DREADD animals and 8 CNO treated non-DREADD WT controls were used in the experiments. CNO/vehicle administered to different cohort of animals. In the first group, animals were intraperitoneally injected with single dose (10mg/kg) of CNO/vehicle and were sacrificed 30 min after injection. In second group, animals were treated with single but increasing dose of CNO/vehicle (i.e. 2.5, 5, 10mg/kg) focally into the SS cortex for 3 consecutive days. On the third day, 15 min after CNO/vehicle treatment, animals were sacrificed, and the brain was extracted. The timing of sacrifice was based on the result from the chapter 3 where silencing PV⁺ interneurons generated absence-like seizures ~30 and ~15 min after i.p. and focal CNO injection, respectively.

Tissue lysates were analysed with western blotting using appropriate antibodies to each protein targets (GADs and GATs). Primary and secondary antibodies used for this experiment are listed in Tables 2.11 and 2.12, respectively (chapter 2). Scanning and the analysis of the blots were performed as previously described in the chapter 2, subsection 2.7.

5.2.3 Data analysis

Comparison of intensity of staining between the cortical layers (2&3 vs 4 vs 5&6) and the thalamic regions (RTN vs VP) in both mice groups were performed using Wilcoxon matched-pairs signed-rank test and comparison of relevant layers/regions between mice groups were performed using Mann-Whitney unpaired rank test. Statistical differences in the expression levels of protein between epileptic stargazers and non-epileptic control littermates were tested using Mann-Whitney unpaired rank test. Data were presented as mean \pm standard error of the mean (SEM). All statistical analyses were performed in GraphPad Prism 8.0 with statistical significance set at $p < 0.05$.

5.3 Results

5.3.1 Expression pattern of GADs and GATs in the SScortex and the thalamus of stargazers and non-epileptic controls

The expression pattern of GADs and GATs in the PV+ interneurons in the SScortex (Fig. 5.3 and 5.4) and the thalamus (Fig. 5.5 and 5.6) was examined using confocal immunofluorescence microscopy. Tissue sections from epileptic stargazers and non-epileptic controls were double labelled with GADs or GATs and PV antibodies.

Expression pattern GADs in the SScortex

PV cells soma were brightly stained throughout all cortical layers (2-6) (Fig. 5.3 and 5.4). PV cells were most prominent in layer 4 of the SScortex which was visualized in the form of intense band in the SScortex (Fig. 5.3 and Fig. 5.4).

GAD65 expression was uniform throughout the cortical layers and the expression was restricted to the axon terminals. GAD65 staining did not colocalize to the cell bodies of PV+ interneurons (Fig. 5.3A). Magnified merged images (green boxes) showed the evidence of co-labelling of GAD65 positive puncta-like structures with PV+ interneurons (Fig. 5.3A).

GAD67 was strongly expressed in the cell bodies of the neurons. Cell bodies of PV+ interneurons were intensely colocalized with GAD67 (Fig. 5.3B). Colocalization was seen in both epileptic stargazers and non-epileptic littermates (Fig. 5.3B).

Overall, the staining pattern of GADs in the SScortex was similar for both epileptic stargazer and non-epileptic controls (Fig. 5.3A,B).

A. PV/GAD65 labelling

B. PV/GAD67 labelling

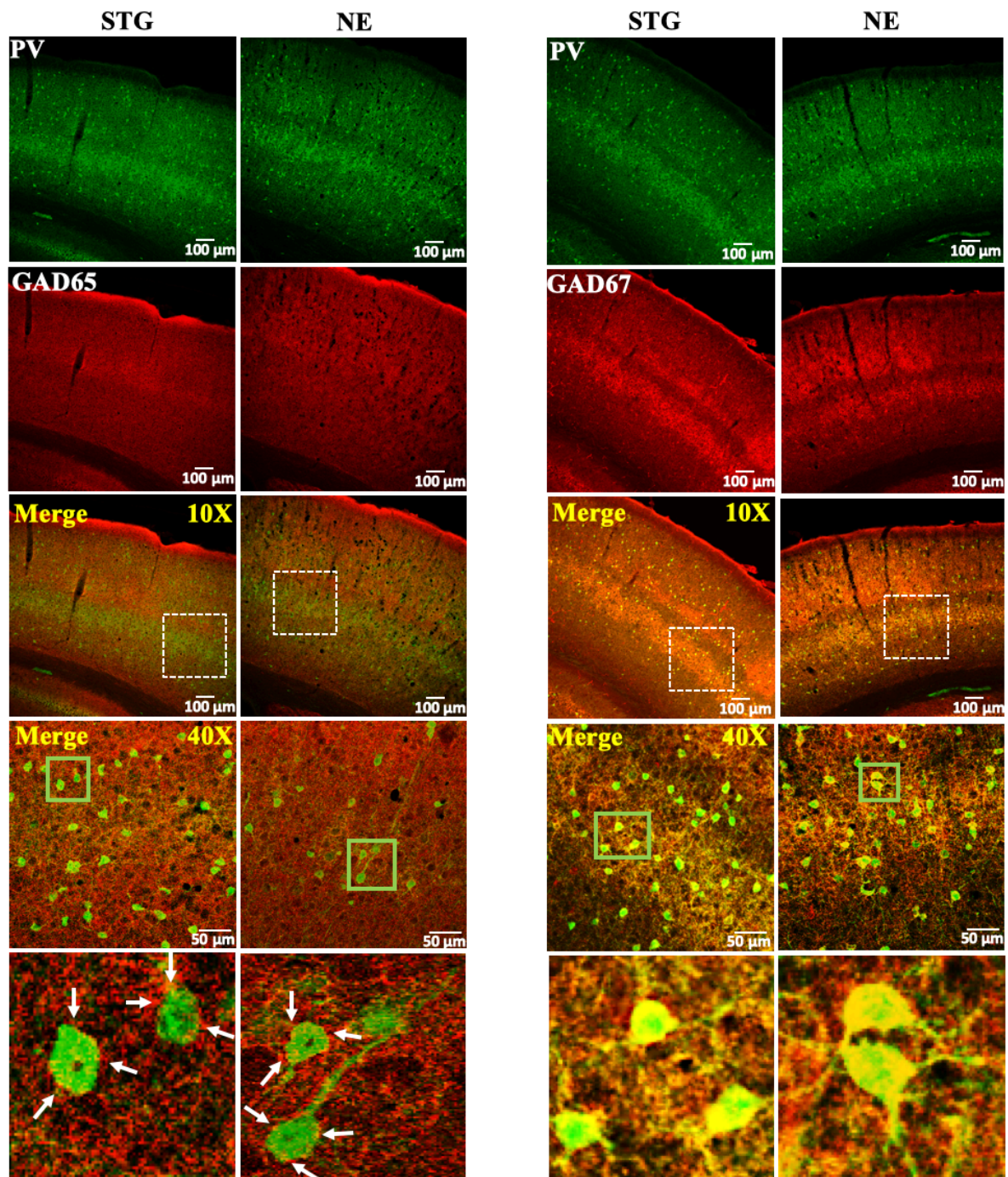
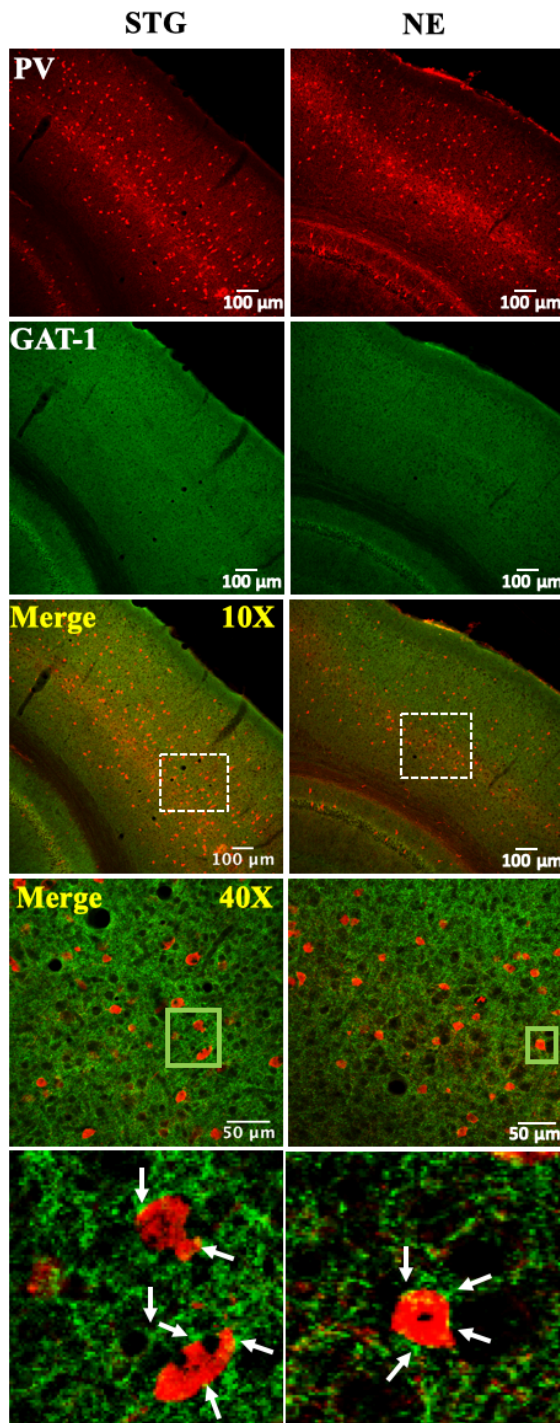


Fig. 5.3 Expression of GAD65 and GAD67 in cortical PV+ interneurons. Representative confocal images showing the expression of (A) GAD65 (B) GAD67 and PV+ interneurons in the SS cortex of epileptic stargazers (STG) and non-epileptic littermates (NE). Merged images at low magnification (10X) and medium magnification (40X) are shown. White dotted boxes indicate regions of magnified image in the SS cortex. Green boxes in the 40X merged images were magnified in the bottom panels of figures A and B to show puncta-like structures (white arrows) and co-localization, respectively.

A. PV/GAT-1 labelling



B. PV/GAT-3 labelling

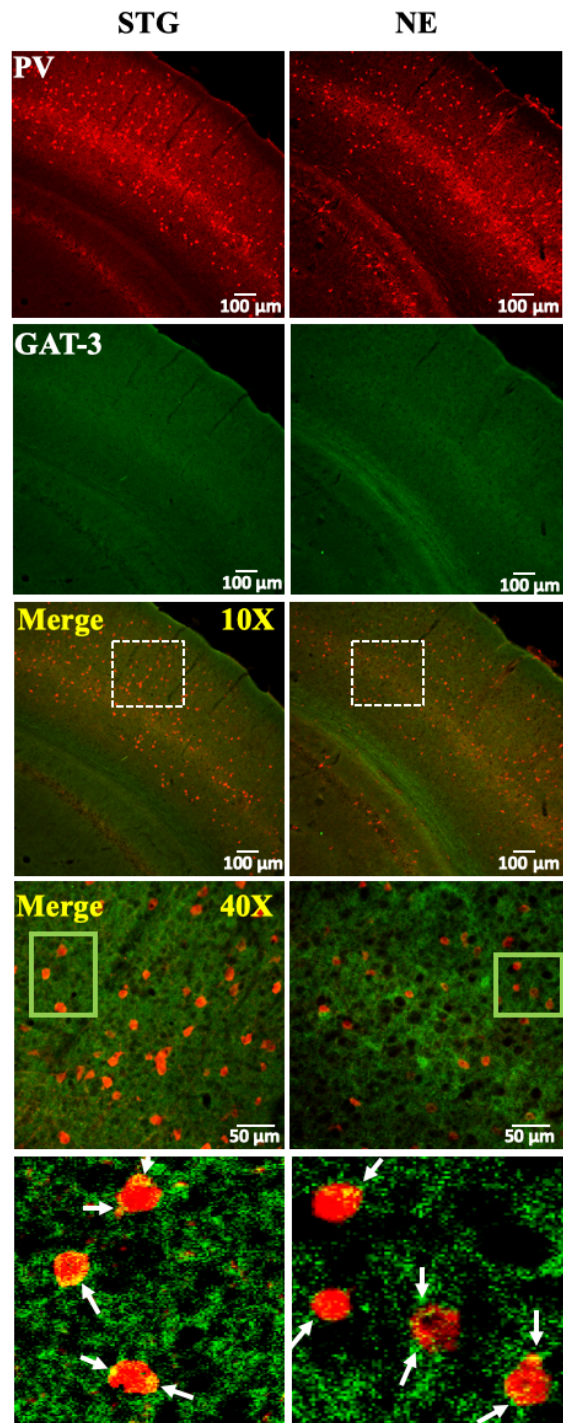


Fig. 5.4 Expression of GAT-1 and GAT-3 in cortical PV+ interneurons. Representative confocal images showing the expression of (A) GAT-1 (B) GAT-3 and PV+ interneurons in the SS cortex of epileptic stargazers (STG) and non-epileptic littermates (NE). Merged images at low magnification (10X) and medium magnification (40X) are shown. White dotted boxes indicate regions of magnified image in the SS cortex. Green boxes in the 40X merged images were magnified in the bottom panels of figures A and B to show puncta-like structures (white arrows).

Expression of GATs in the SScortex

Expression pattern of GAT-1 and GAT-3 across the SScortex was uniform (Fig. 5.4A,B). Colocalization between PV soma and GATs was not seen. However, both GATs were labelled in the punctuate-like structures around PV labelled cells in the SScortex (Fig. 5.4A,B; green box in 40X merged images). Visually, the staining pattern of GAT-1 and GAT-3 in the SScortex was not significantly different between epileptic stargazers and non-epileptic controls (Fig. 5.4A,B).

Expression of GADs in the thalamus

In the RTN thalamus, GAD65 expression was restricted to the axon terminals. GAD65 staining did not colocalize to the cell bodies of PV+ interneurons but magnified merged images (green boxes) showed GAD65 positive puncta-like structures surrounding PV cells (Fig. 5.5A). However, GAD67 was strongly expressed in the cell bodies of the neurons. Cell bodies of PV+ interneurons were intensely colocalized with GAD67 in the RTN thalamus (Fig. 5.5B). Colocalization was seen in both epileptic stargazers and non-epileptic littermates (Fig. 5.5B). Expression of both GADs in the VP thalamus was uniform (Fig. 5.5A,B) as VP contains the neuronal processes projecting from RTN. Overall, the staining pattern of GADs in thalamus (RTN and VP) was similar for both epileptic stargazer and non-epileptic controls (Fig. 5.5A,B).

Expression of GATs in the thalamus

Expression pattern of GAT-1 and GAT-3 was uniform in the RTN and VP thalamus (Fig. 5.6A,B). Colocalization between PV soma and GATs was not seen across the RTN thalamus. However, both GATs showed punctuate staining around PV labelled cells in the RTN thalamus (Fig. 5.6A,B, green box in 40X merged images). Overall, the staining pattern of GAT-1 and GAT-3 in the thalamus was not significantly different between epileptic stargazers and non-epileptic controls (Fig. 5.6A,B).

Altogether, it can be concluded that the visual expression pattern of GADs and GATs in the SScortex and the thalamus are not significantly different between epileptic stargazers and their and appear similar to published localization profile.

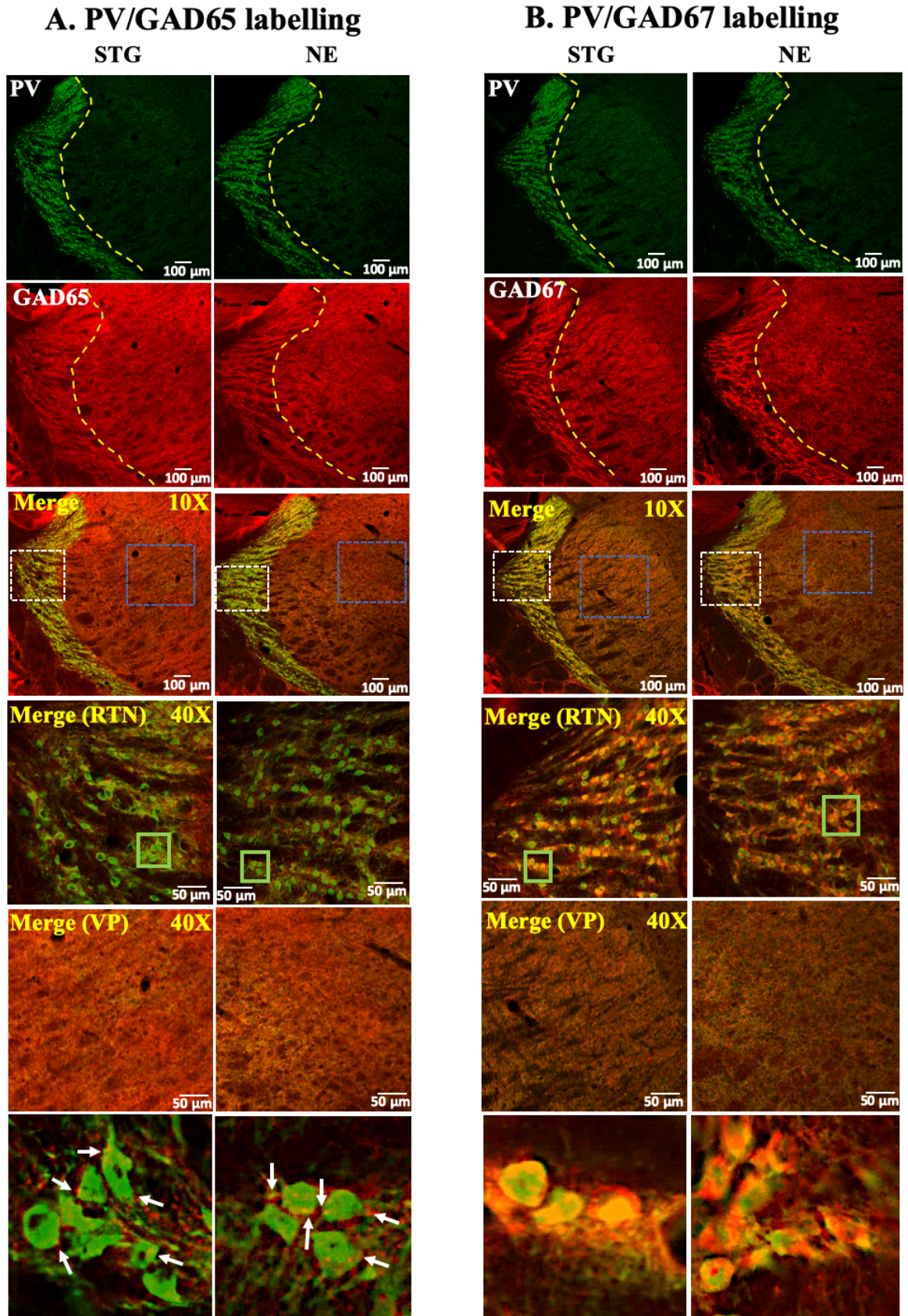


Fig. 5.5 Expression of GAD65 and GAD67 in thalamic PV+ interneurons. Representative confocal images showing the expression of (A) GAD65 (B) GAD67 and PV+ interneurons in the thalamus of epileptic stargazers (STG) and non-epileptic littermates (NE). Merged images at low magnification (10X) and medium magnification (40X) are shown. White and blue dotted boxes indicate regions of magnified image in the thalamus (fourth panel: RTN thalamus and fifth panel: VP thalamus). Green boxes in the 40X merged images of RTN thalamus were magnified in the bottom panels of figures A and B to show puncta-like structures (white arrows) and co-localization, respectively.

A. PV/GAT-1 labelling

B. PV/GAT-3 labelling

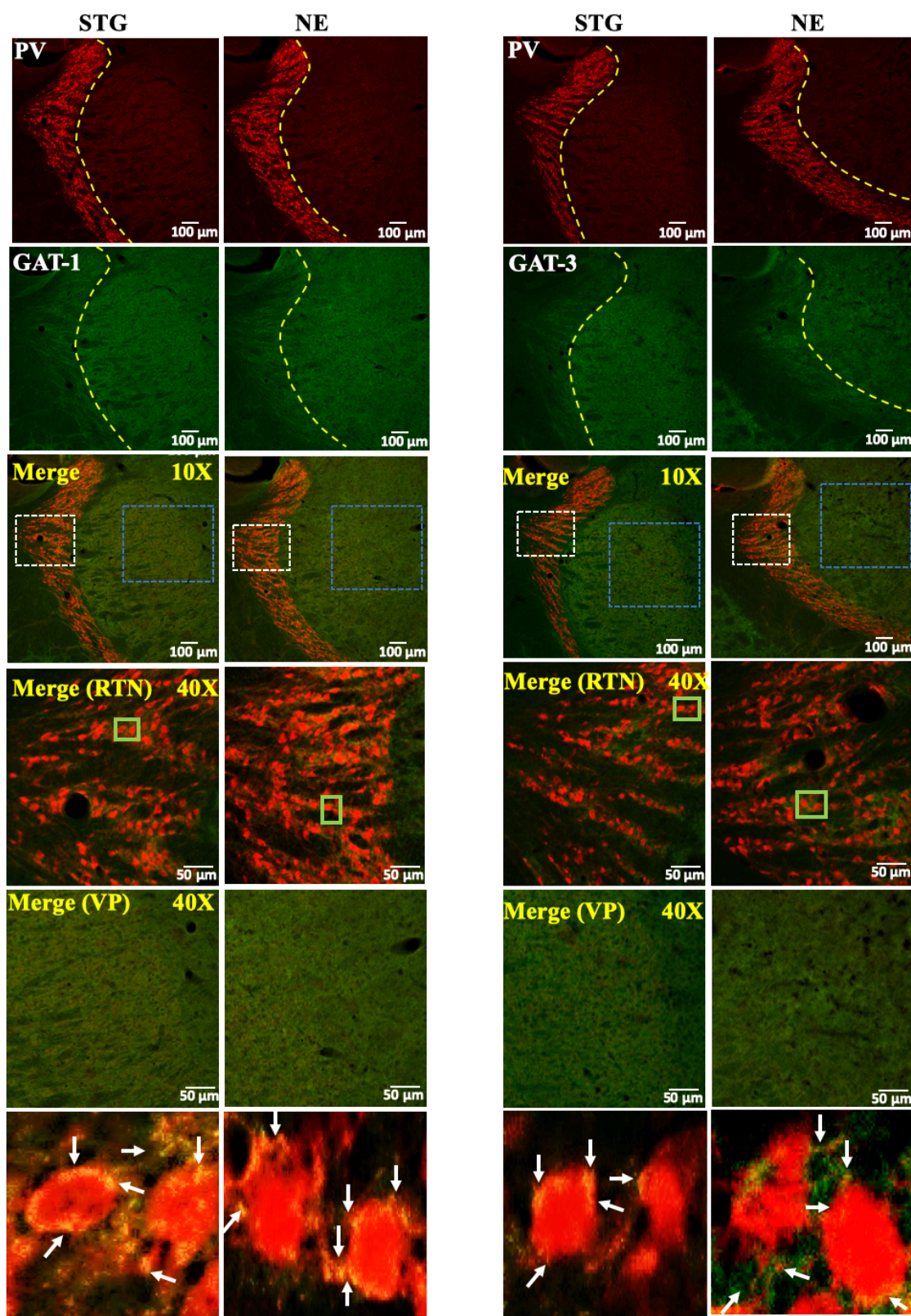
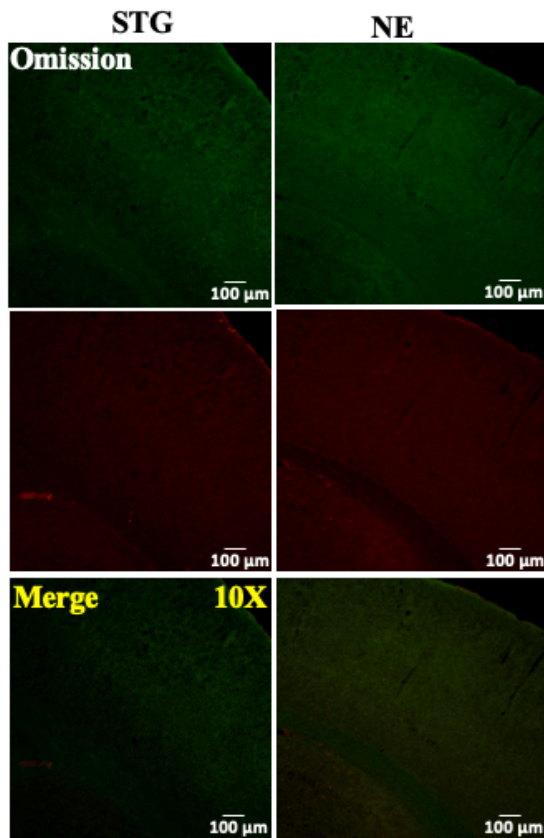


Fig. 5.6 Expression of GAT-1 and GAT-3 in thalamic PV+ interneurons. Representative confocal images showing the expression of (A) GAT-1 (B) GAT-3 and PV+ interneurons in the thalamus of epileptic stargazers (STG) and non-epileptic littermates (NE). Merged images at low magnification (10X) and medium magnification (40X) are shown. White and blue dotted boxes indicate regions of magnified image in the thalamus (fourth panel: RTN thalamus and fifth panel: VP thalamus). Green boxes in the 40X merged images of RTN thalamus were magnified in the bottom panels of figures A and B to show puncta-like structures (white arrows).

A. SScortex



B. Thalamus

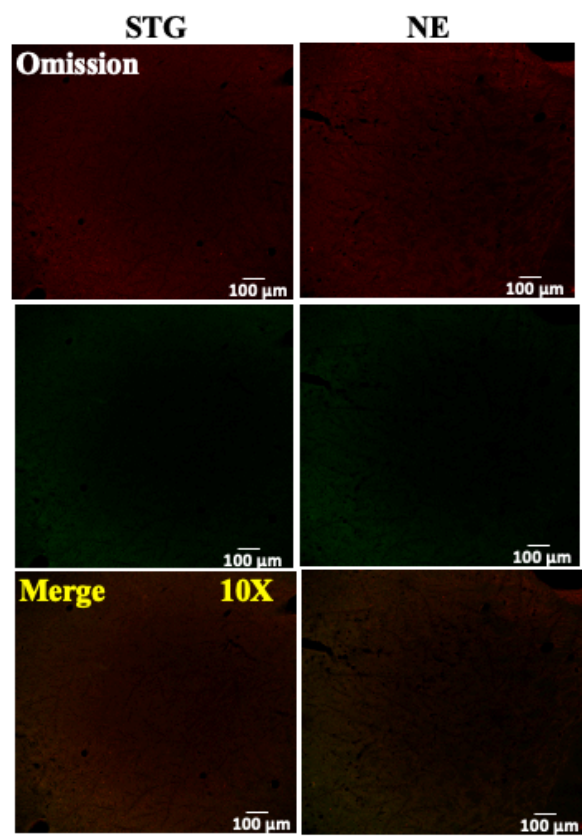


Fig. 5.7 Omission controls were employed to test the specificities of the antibodies used. Representative confocal images showing the specificity of secondary antibody binding after omission of primary antibodies in tissue sections from the (A) SScortex and (B) thalamus of epileptic stargazers (STG) and non-epileptic littermates (NE). Merged images at low magnification (10X) are also shown.

Omission of primary antibodies eliminated neuronal cell specific immunolabeling in tissue sections (Fig. 5.7A,B) which indicates the specificity of the antibodies used in this study.

5.3.2 Quantification of staining intensity of GADs, GATs and PV labelling in the SScortex and the thalamus of stargazers and non-epileptic controls

Confocal images were used to quantify staining pattern of GADs, GATs and PV in the SScortex, RTN and VP thalamus of epileptic stargazers and non-epileptic controls.

Data indicated that intensity of staining of PV significantly higher in layer 4 and 5&6 compared to layer 2&3 in both epileptic stargazers and non-epileptic controls (Fig. 5.8A). However, there was no significant difference in the staining intensity between the relevant cortical layers when compared between the genotypes (Fig. 5.8A). This finding is an agreement with the previous published work where authors quantified the number of PV+ interneurons across the cortical

Confocal fluorescence intensity of PV labelling

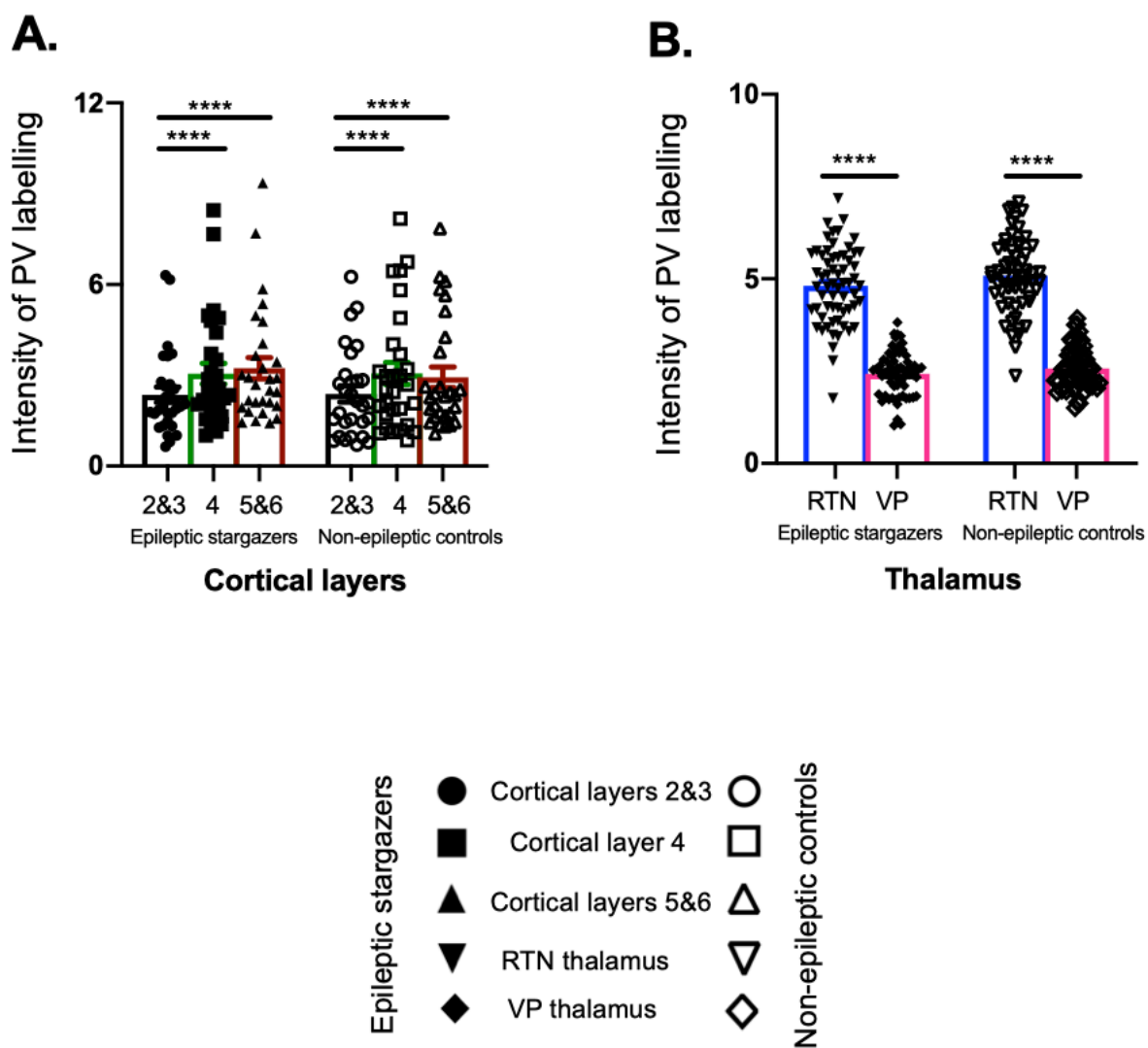


Fig. 5.8 Confocal fluorescence intensity of PV labelling. Graphs showing the comparison of confocal fluorescence intensity of PV labelling across (A) the cortical layers and (B) the thalamus in epileptic stargazers and non-epileptic littermates. All values represent mean \pm SEM. Comparisons between the cortical layers (2&3 vs 4 vs 5&6) and the thalamic regions (RTN vs VP) in both mice groups were performed using Wilcoxon matched-pairs signed-rank test and comparison of relevant layers/regions between mice groups were performed using Mann-Whitney unpaired rank test.

layers between epileptic stargazers and non-epileptic controls (Adotevi and Leitch, 2016). Intensity of PV labelling in the RTN was significantly higher compared to the VP, in both genotypes (Fig. 5.8B). However, no significant differences were seen in either the RTN or the VP region, when staining intensity of PV labelling was compared between mice groups (Fig. 5.8B).

Analysis of the confocal images showed that intensity of GAD65 (Fig. 5.9A) and GAD67 (Fig. 5.9C) labelling was significantly higher in layer 4 compared to other cortical layers in both epileptic stargazer and their non-epileptic littermates. The overall trend of cortical GADs staining in both genotypes was similar (Fig. 5.9A,C). There was no significant difference in the staining intensity between the relevant cortical layers of the genotypes (Fig. 5.9A,C). In the thalamus of both epileptic stargazers and non-epileptic controls, staining intensity of GAD65 was not significantly different between the RTN and the VP regions (Fig. 5.9B). However, intensity of GAD67 labelling in the RTN was significantly higher than the VP regions in both mice groups. However, between genotypes no significant differences in the staining intensity were seen in both thalamic regions (Fig. 5.9D).

The trend of GAT-1 labelling across the cortical layers of both epileptic stargazers and non-epileptic controls was similar (Fig. 5.10A). In both genotypes, staining intensity was higher in layer 2&3 and layer 4 compared to that of layer 5&6 (Fig. 5.10A). However, there was no significant difference in the staining intensity between the cortical layers when compared between the relevant cortical layers of mice groups (Fig. 5.10A). Intensity of GAT-3 labelling was higher in layer 4 and layer 5&6 compared to layer 2&3 in epileptic stargazers (Fig. 5.10C). Some variability in layer-wise expression in non-epileptic stargazer was seen (Fig. 5.10C). Thalamic staining intensity of GATs labelling was similar for both genotypes (Fig. 5.10B,D). Overall, there was no significant difference in the staining intensity between the relevant cortical layers (Fig. 5.10A,C) and thalamic regions (Fig. 5.10B,D) between mice groups.

Altogether, it can be concluded that staining intensities of GADs and GATs in the SS cortex and the thalamus are not significantly different between epileptic stargazers and their non-epileptic littermates and appear similar to published localization profile.

Confocal fluorescence intensity of GAD65 and GAD67 labelling

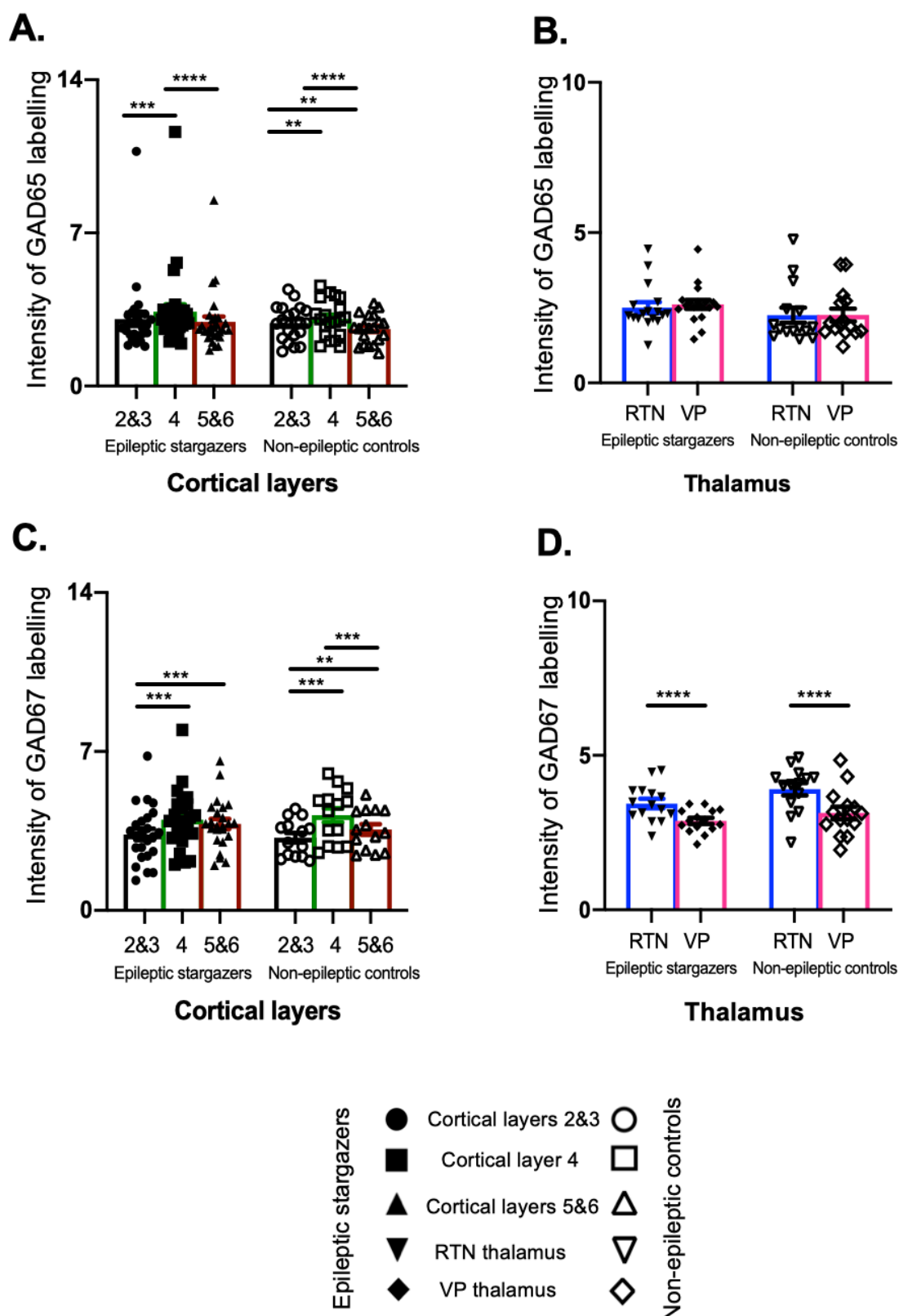


Fig. 5.9 Confocal fluorescence intensity of GAD65 and GAD67 labelling. Graphs showing the comparison of confocal fluorescence intensity of GAD65 and GAD67 labelling across (A,C) the cortical layers and (B,D) the thalamus in epileptic stargazers and non-epileptic littermates. All values represent mean \pm SEM. Comparisons between the cortical layers (2&3 vs 4 vs 5&6) and the thalamic regions (RTN vs VP) in both mice groups were performed using Wilcoxon matched-pairs signed-rank test and comparison of relevant layers/regions between mice groups were performed using Mann-Whitney unpaired rank test.

Confocal fluorescence intensity of GAT-1 and GAT-3 labelling

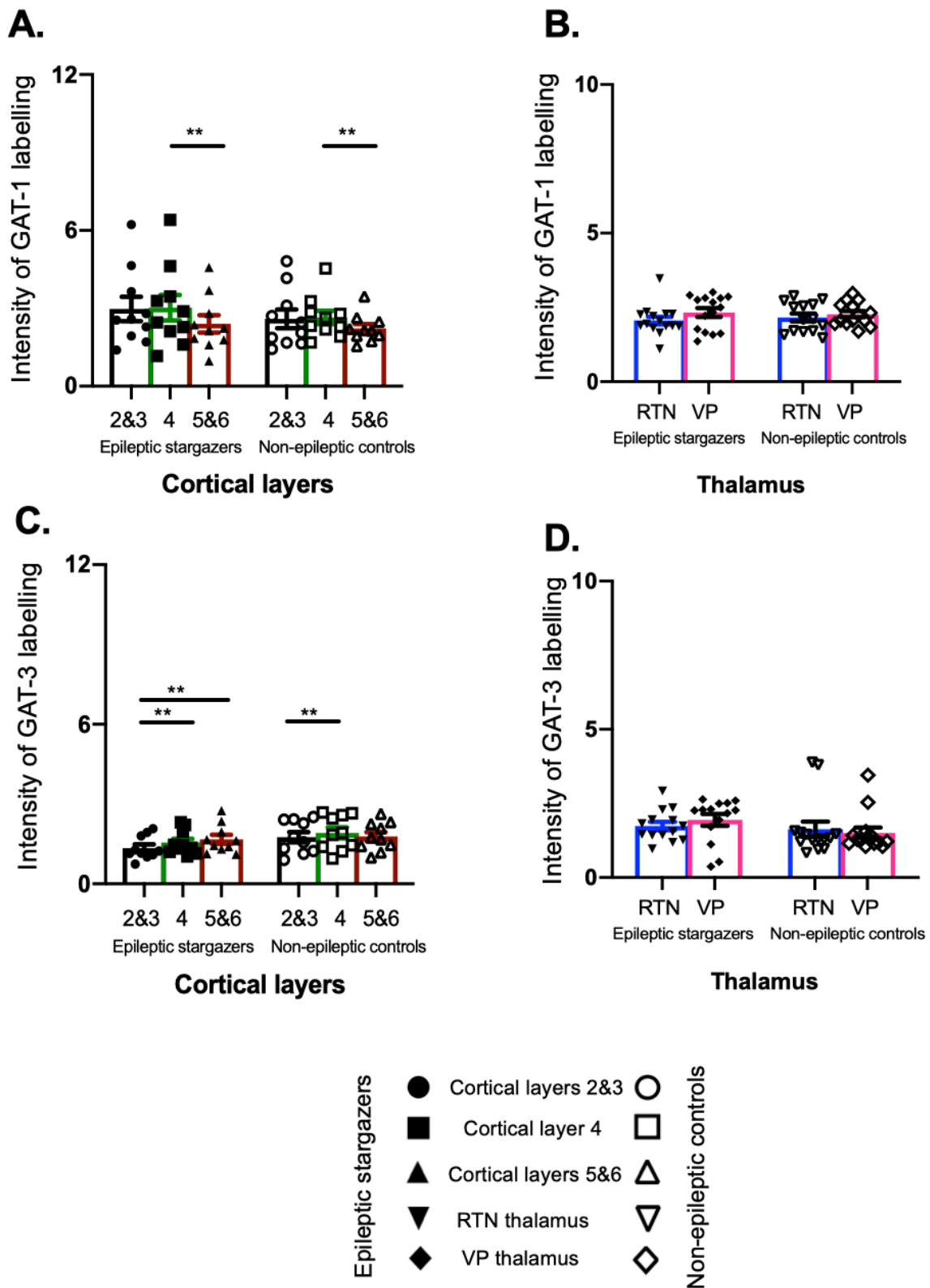


Fig. 5.10 Confocal fluorescence intensity of GAT-1 and GAT-3 labelling. Graphs showing the comparison of confocal fluorescence intensity of GAT-1 and GAT-3 labelling across (A,C) the cortical layers and (B,D) the thalamus in epileptic stargazers and non-epileptic littermates. All values represent mean \pm SEM. Comparisons between the cortical layers (2&3 vs 4 vs 5&6) and the thalamic regions (RTN vs VP) in both mice groups were performed using Wilcoxon matched-pairs signed-rank test and comparison of relevant layers/regions between mice groups were performed using Mann-Whitney unpaired rank test.

5.3.3 Relative expression of GADs and GATs in the tissue lysates of the SS cortex and the VP thalamus of stargazers via western blotting analysis

Next, western blotting analysis was performed to analyse the relative levels of GADs and GATs in the whole-tissue lysate of the SS cortex and the VP thalamus of epileptic stargazers and non-epileptic littermates. Data showed the protein level of GAD65 was significantly increased in SS cortex of epileptic stargazers above their non-epileptic littermates. In stargazers, there was a 24% increase in GAD65 expression (NE 1.00 ± 0.03 , $n=18$; STG 1.24 ± 0.11 , $n=15$; $p=0.024$, Fig. 5.11A,B). However, the expression of GAD67 and GAT-3 was not significantly different between genotypes (Fig. 5.13C-F). GAD67 expression trended towards higher levels in epileptic stargazers but didn't reach to significance i.e. NE 1.00 ± 0.07 , $n=16$; STG 1.217 ± 0.11 , $n=13$, Fig. 5.11C,D). There was no change in GAT-3 expression in epileptic stargazers (0.83 ± 0.07 , $n=12$) compared to non-epileptic littermates (1.00 ± 0.05 , $n=17$) (Fig. 5.11E,F).

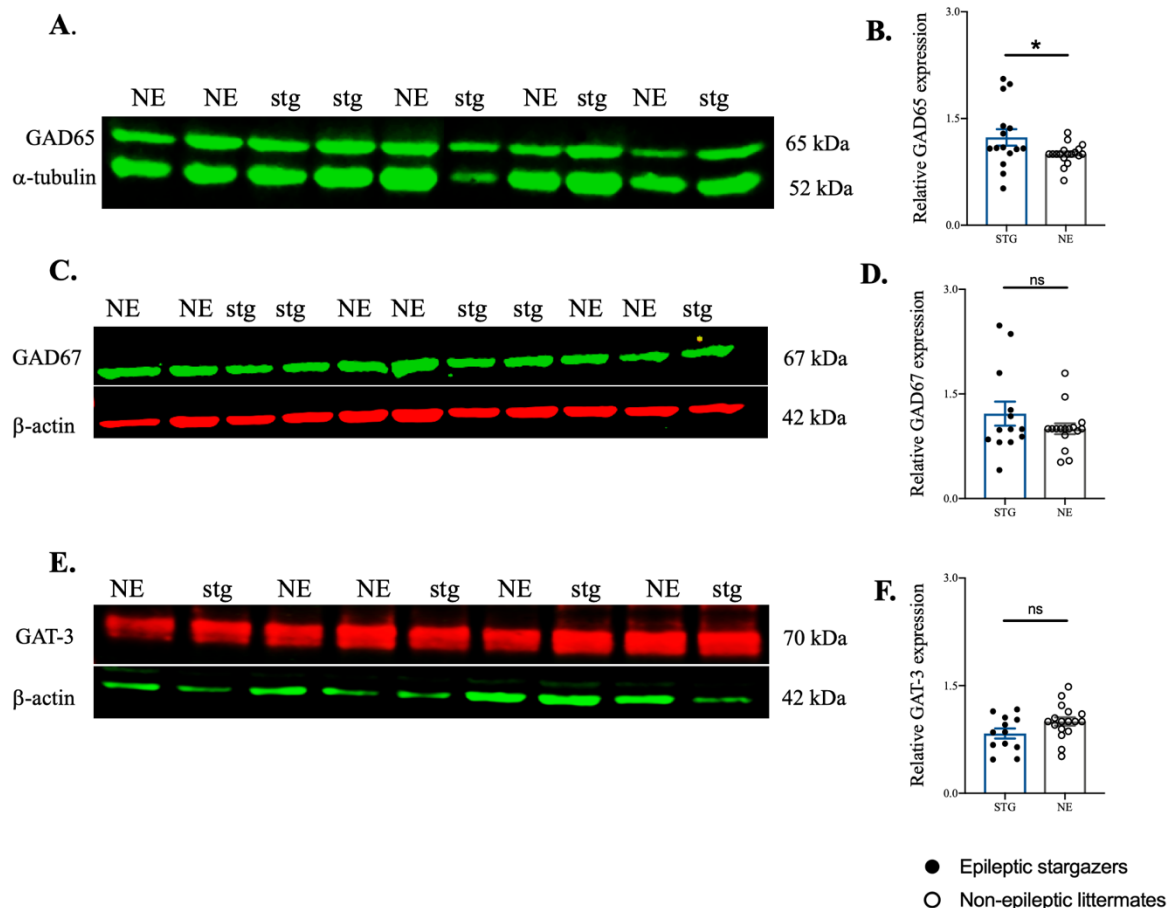


Fig. 5.11 Western blot analysis of GAD65, GAD67 and GAT-3 in the SS cortex of stargazers (stg) and non-epileptic littermates (NE). (A,C,E) Representative immunoblots showing expression of GAD65, GAD67 and GAT-3 with α -tubulin/ β -actin, respectively. (B,D,F) Relative expression of GAD65, GAD67 and GAT-3 in the SS cortex presented as bar graphs, respectively. All values represent mean \pm SEM. Comparisons were performed using Mann-Whitney unpaired rank test.

Data also showed that protein levels of GAD65, GAD67 and GAT-3 in the VP thalamus of epileptic stargazers and non-epileptic controls were unaltered. There were no statistically significant differences in the expression of GAD65, GAD67 and GAT-3 between the genotypes (Fig. 5.12A-F) i.e. GAD65 (NE 1.00 ± 0.03 , $n=9$; STG 1.38 ± 0.30 , $n=5$), GAD67 (NE 1.00 ± 0.07 , $n=9$; STG 0.94 ± 0.11 , $n=5$), GAT-3 (NE 1.00 ± 0.08 , $n=9$; STG 1.61 ± 0.30 , $n=5$).

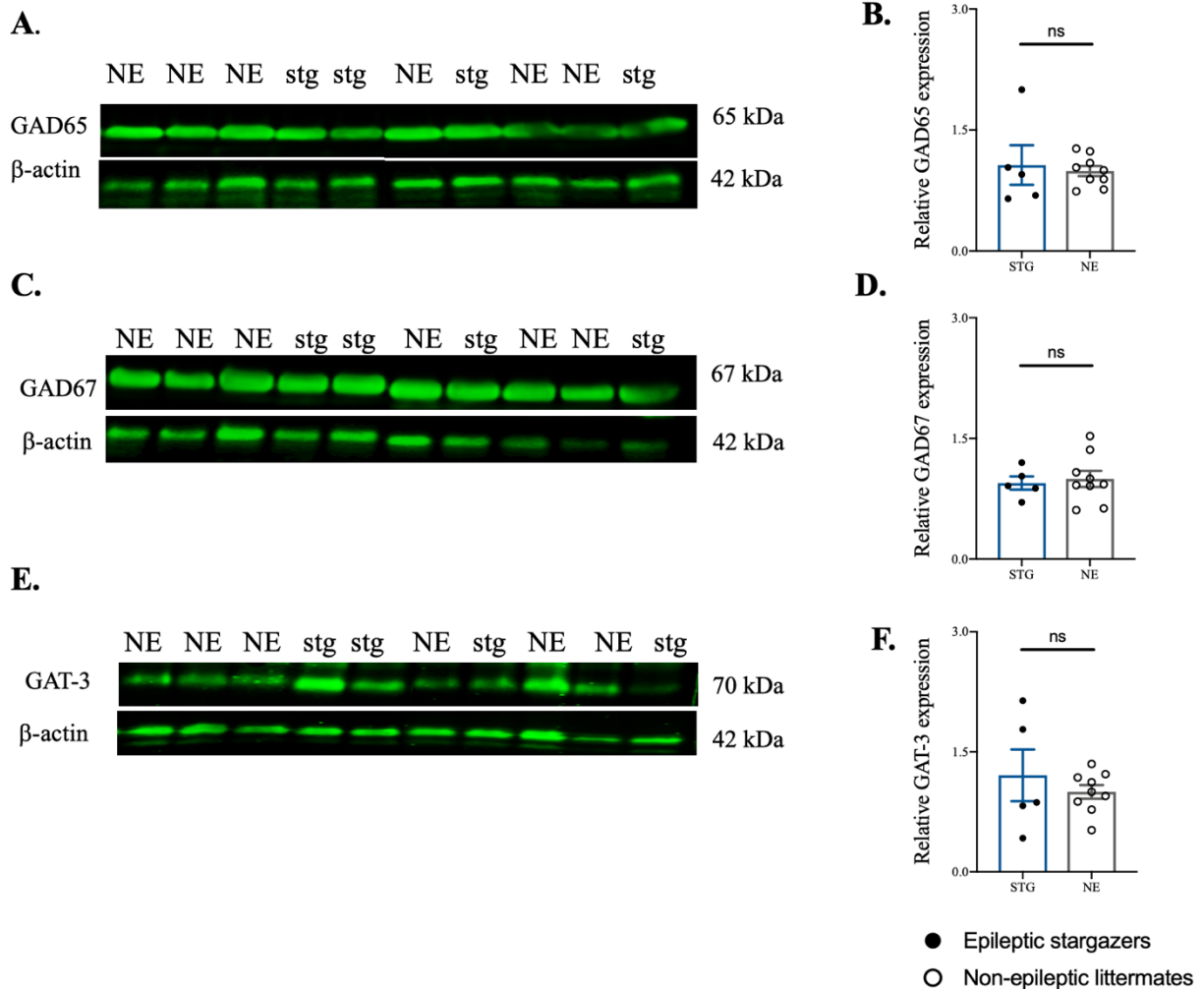


Fig. 5.12 Western blot analysis of GAD65, GAD67 and GAT-3 in the VP thalamus of stargazers (stg) and non-epileptic littermates (NE). (A,C,E) Representative immunoblots showing expression of GAD65, GAD67 and GAT-3 with β -actin, respectively. (B,D,F) Relative expression of GAD65, GAD67 and GAT-3 in the VP thalamus presented as bar graphs, respectively. All values represent mean \pm SEM. Comparisons were performed using Mann-Whitney unpaired rank test.

Overall, western blotting analysis has shown that GAD65 levels are significantly increased in the SS cortex of stargazer epileptic mice. A trend towards heightened levels of GAD67 in the SS cortex of epileptic animals and unaltered cortical levels of GAT3 have also been demonstrated. Neither of these protein targets showed significant difference in VP thalamus expression levels between mice groups.

5.3.4 Expression of GADs and GATs was unchanged in DREADD animals

To investigate whether acute functionally silencing FFI in DREADD animals is enough to cause alteration of GADs and GATs, western blotting was performed in whole-tissue lysate of the SS cortex of CNO treated DREADD animals and control counterparts (vehicle treated DREADD animals and CNO treated non-DREADD WT animals).

Expression level of GAD65, GAD67 and GAT-3 was not significantly different between CNO/vehicle treated (single i.p. dose of 10mg/kg) animal groups in the SS cortex (Fig. 5.13A-F) i.e. [GAD65: CNO treated DREADD animals (0.86 ± 0.03 , $n=6$); vehicle treated DREADD (0.82 ± 0.16 , $n=4$); CNO treated non-DREADD WT control animals (1.00 ± 0.1 , $n=4$); [GAD67:

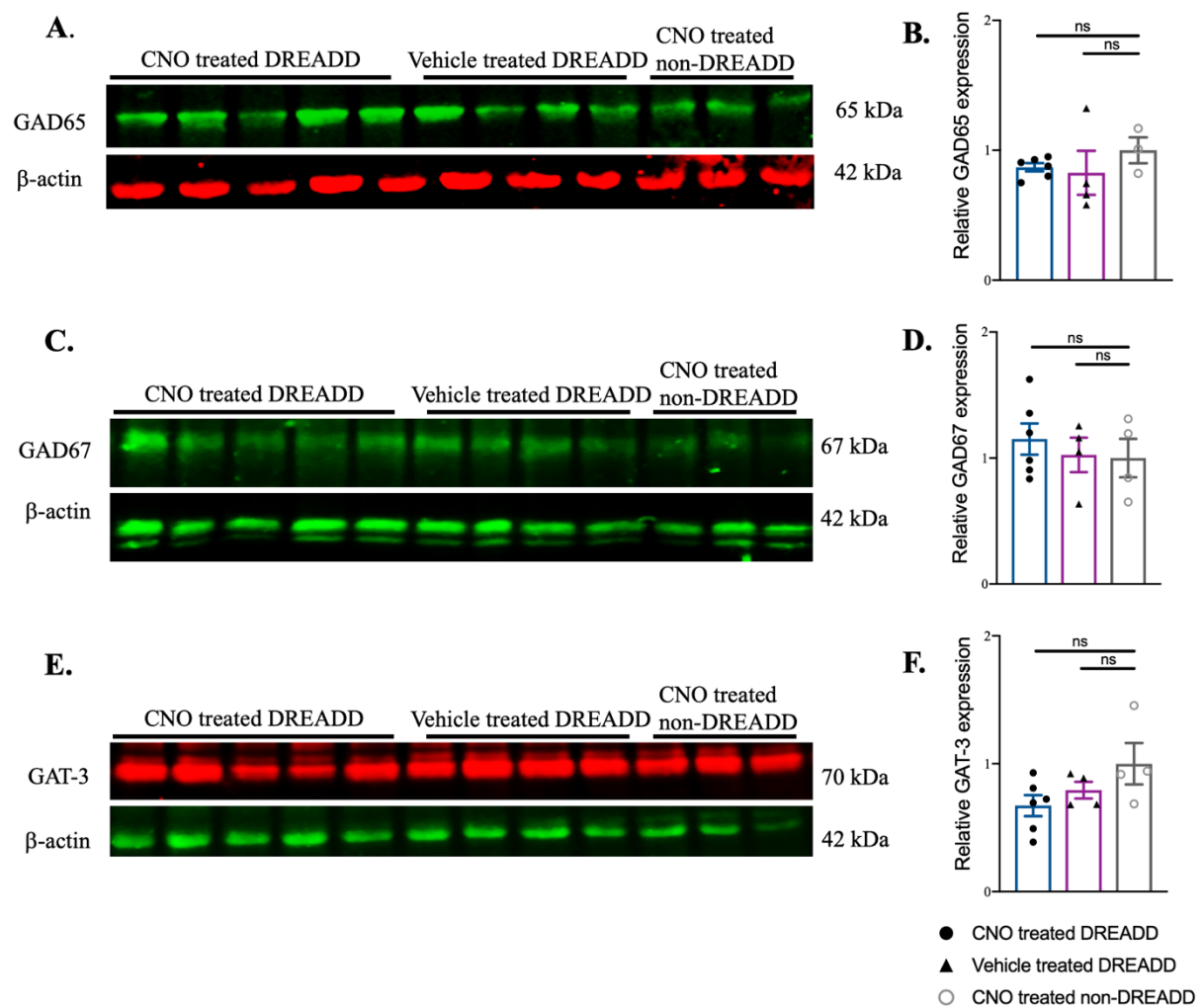


Fig. 5.13 Western blot analysis of GAD65, GAD67 and GAT-3 in the SS cortex of CNO treated (single dose) DREADD animals and their control counterparts. (A,C,E) Representative immunoblots showing expression of GAD65, GAD67 and GAT-3 with β -actin, respectively. (B,D,F) Relative expression of GAD65, GAD67 and GAT-3 in the SS cortex presented as bar graphs, respectively. All values represent mean \pm SEM. Comparisons were performed using Mann-Whitney unpaired rank test.

CNO treated DREADD animals (1.151 ± 0.12 , $n=6$); vehicle treated DREADD (1.025 ± 0.13 , $n=4$); CNO treated non-DREADD WT control animals (1.00 ± 0.15 , $n=4$); [GAT-3: CNO treated DREADD animals (0.62 ± 0.08 , $n=6$) and vehicle treated DREADD (0.79 ± 0.06 , $n=4$) compared to CNO treated non-DREADD WT control animals (1.00 ± 0.16 , $n=4$)].

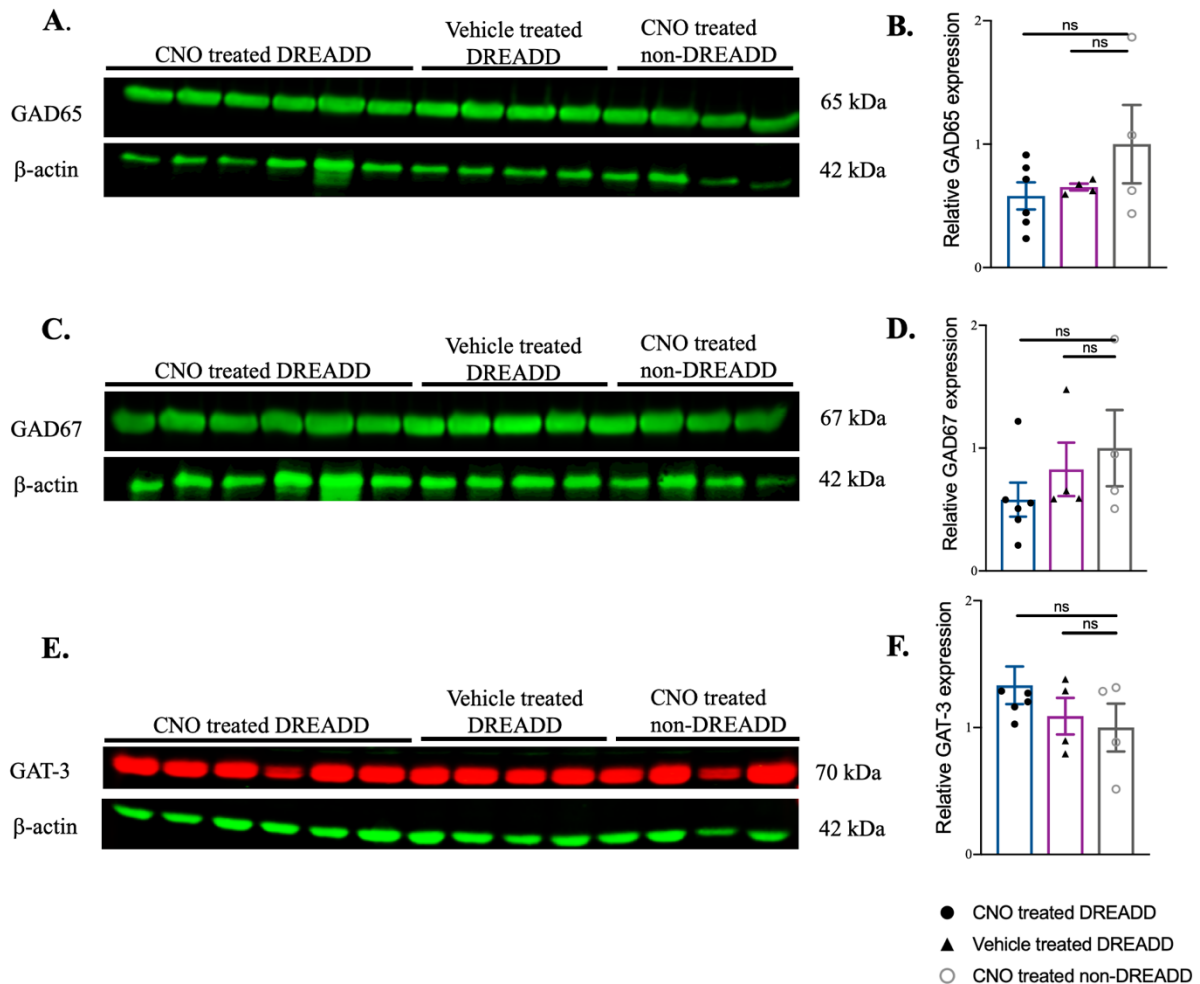


Fig. 5.14 Western blot analysis of GAD65, GAD67 and GAT-3 in the SS cortex of CNO treated (focal, three doses) DREADD animals and their control counterparts. (A,C,E) Representative immunoblots showing expression of GAD65, GAD67 and GAT-3 with β -actin, respectively. (B,D,F) Relative expression of GAD65, GAD67 and GAT-3 in the SS cortex presented as bar graphs, respectively. All values represent mean \pm SEM. Comparisons were performed using Mann-Whitney unpaired rank test.

Similarly, in the other group CNO/vehicle was injected focally where animals were treated with single but increasing dose of CNO/vehicle (i.e. 2.5, 5, 10mg/kg) focally into the SS cortex for 3 consecutive days. Relative expression of protein levels of GAD65, GAD67 and GAT-3 in the SS cortex was not significantly different (Fig. 5.14A-F) i.e. [(GAD65: CNO treated DREADD animals (0.58 ± 0.11 , $n=6$); vehicle treated DREADD (0.65 ± 0.02 , $n=4$); CNO treated non-DREADD WT control animals (1.00 ± 0.31 , $n=4$)] [(GAD67: CNO treated DREADD

animals (0.58 ± 0.13 , $n=6$); vehicle treated DREADD (0.82 ± 0.21 , $n=4$); CNO treated non-DREADD WT control animals (1.00 ± 0.31 , $n=4$); [(GAT-3: CNO treated DREADD animals (1.027 ± 0.14 , $n=6$); vehicle treated DREADD (0.79 ± 0.14 , $n=4$); CNO treated non-DREADD WT control animals (1.00 ± 0.18 , $n=4$)].

Unfortunately, GAT-1 was unable to be detected by antibodies from two different suppliers, despite using the highest recommended concentration.

5.4 Discussion

In this chapter the impact of loss of FFI on GABA synthesizing and transporting proteins were investigated. GAD65 levels were significantly increased in the SS cortex of epileptic stargazer mice compared to non-epileptic littermates, whereas levels of GAD67 and GAT-3 were unaltered. In contrast, none of these were altered in VP thalamus of epileptic stargazers. Acute administration of CNO into inhibitory Gi-DREADD animals, which is sufficient to generate absence-like seizure, did not change the expression level of these proteins.

5.4.1 Histochemical localization profile and staining intensity of GADs and GATs in the stargazer SS cortex and thalamus

5.4.1.1 GADs (65 and 67)

The PV staining pattern in all confocal images was similar to previous studies (Staiger et al., 1997; Dávid et al., 2007; Xu et al., 2009; Adotevi and Leitch, 2016). This pattern was visually indistinguishable, and the intensity of PV labelling was not statistically significant between epileptic stargazers and their non-epileptic control littermates. Omission control showed a very low level of background fluorescence.

GAD65 expression was uniform throughout the cortical layers and thalamus. GAD65 showed punctate staining due to its expression in axon terminals and no colocalization with PV+ soma occurred. This is in agreement with previous studies where GAD65 labelling was seen in the axon terminals scattered in the neuropil as well as the puncta outlining the cell bodies (Esclapez et al., 1993; Kiser et al., 1998; Tian et al., 1999). Some studies also found the expression pattern of GAD65 being age dependent (Kiser et al., 1998; Huang et al., 1999). GAD67 labelling was dense

and extensive not only in puncta and neuropil but also in the soma of PV labelled cells in the SS cortex which is in agreement with published rodent studies (Turner et al., 2010; Bean et al., 2014; Fujihara et al., 2015; Lazarus et al., 2015). GAD67 labelling was brighter in layer 4 compared to other cortical layers which is similar to previous published result (Cybulska-Klosowicz et al., 2013) (Fig. 5.3B). GAD67 staining was strong in the cell bodies of RTN thalamus similar to previous published reports (Esclapez et al., 1993; Delfs et al., 1996; Menuz and Nicoll, 2008; Seo and Leitch, 2014). Expression pattern GADs in the VP thalamus was uniform which may be due to the fact that VP contains the neuronal processes projecting from RTN.

Expression pattern of GADs in the SS cortex and thalamus was not visually different between epileptic stargazers and non-epileptic controls. Layer specific staining pattern of GADs in the SS cortex showed that even though there were differences in staining between layers in both epileptic and non-epileptic littermates but overall layer-specific staining intensity trend for each genotype was similar.

To date, there have been relatively few studies, focusing the expression and staining pattern of GADs in animal models of epilepsy. Few studies found that mRNA level of GADs decreases in the cerebral cortex and hippocampus in pilocarpine-treated rats, but such changes were not observed in the RTN thalamus (Esclapez and Houser, 1999; Kang et al., 2001). Another study has shown altered mRNA levels and density of GAD labelled neurons in piriform cortex after kainate and pilocarpine induced seizures (Freichel et al., 2006). Authors found loss of substantial number of GABAergic neurons followed by increased histochemical labelling of GAD isoforms in remaining neuronal population (Freichel et al., 2006). GAD expressing GABAergic neurons are bigger part of a network which are functionally connected to the excitatory neurons. One of the possible reasons of increased level of GADs in the abovementioned study could be the fact that GABAergic neurons may maintain high levels of activity by increasing GABA synthesis to control the increased excitability after pilocarpine or kainate injection. Such increase in GAD levels may help in regulating the inhibitory strength when the excitation is too high during seizures. Surprisingly, in this current study, expression pattern of GADs in epileptic stargazers which show spontaneous absence seizures was not changed in comparison to their non-epileptic counterparts. Importantly, GAD65 knockout animals were found to be more susceptible to seizures (Kash et al., 1997), whereas GAD 67 knockout animals did not survive after birth (Asada et al., 1997; Condie

et al., 1997). One study showed that GAD67 deficient mice has significantly reduced GAD65 puncta density in the cortex without ring-shaped structure (Chattopadhyaya et al., 2007). GAD65 knockout mice, however, did not show altered cortical morphology and expression level of GAD67 (Hensch et al., 1998). It is widely established that GAD65 and GAD67 synthesize GABA for different functional purpose and different developmental time period (Pinal and Tobin, 1998; Soghomonian and Martin, 1998). GABA synthesis from GAD65 is 'on demand' i.e. for vesicular release regulating phasic inhibition (Tian et al., 1999) whereas GAD67 is involved in the synthesis of majority of GABA for cytoplasmic store and regulation of tonic inhibition (Asada et al., 1997; Schousboe and Waagepetersen, 2009). Thus, it can be concluded that functional differences between GAD isoforms also reflect the difference of localization and expression pattern.

5.4.1.2 GATs (1 and 3)

GAT-1 and GAT-3 staining was uniform throughout the SS cortex and the thalamus and no differences in staining patterns were observed between epileptic stargazers and non-epileptic controls. Expression of GATs was primarily in the neuropil without co-labelling with soma of PV labelled cells. Puncta of both GATs were dispersed around the soma of PV cells. This is similar to a recent work in the rat cerebral cortex where authors found GAT-1 and GAT-3 immunopositive puncta and neuropil (Melone et al., 2015). In this study cortical intensity of GAT-1 staining was highest in the layer 2&3 and layer 4, regardless of genotype. This concurs with the previous work conducted in SD rats where authors found that GAT-1 mRNA hybridization signal is intense in layer 2-4 (Minelli et al., 1995). The same research group also revealed that the intensity of GAT-3 expression is mostly in the layer 4 (Minelli et al., 1996). Conversely, this current study found that GAT-3 immunoreactivity is in increasing order from cortical layer 2 to 6 in epileptic stargazers and some variations were observed in non-epileptic controls. This current study also found that immunoreactivity of GAT-3 across all cortical layers is relatively less intense compared to that of GAT-1 which again is in agreement to the studies published in rats (Minelli et al., 1995; 1996). Previous studies conducted in rat, monkey and humans revealed the expression of GAT-1 in neurons and astrocytes (see review Conti et al., 2004), whereas localization profile of GAT-3 was always been a matter of uncertainty as some studies showed the neuronal expression of GAT-3 (Clark et al., 1992; Durkin et al., 1995) and others highlighted exclusive astrocytic expression (Minelli et al., 1996). In a recent study, Melone and colleagues used electron microscopy and

revealed that GAT-1 immunoreactivity is 54% and 42% in neuronal and glial profiles whereas GAT-3 labelling was significantly higher in glial processes (72%) (Melone et al., 2015). Moreover, expression of GAT-1 in oligodendrocytes and microglia was also reported (Fattorini et al., 2017; 2020).

It is important to note that both GAT-1 and GAT-3 achieve adult-like pattern of expression by the second PN week in the thalamus and third PN week in the cortex (Vitellaro-Zuccarello et al., 2003) and this timing coincides with the developmental increase of tonic GABA_A current seen in GAERS (Cope et al., 2009). Cope and colleagues also found that blockade of thalamic GAT-1 induces ETX-sensitive SWDs in normal Wistar rats and GAT-1 knockout mice also show similar ETX-sensitive spontaneous SWDs (Cope et al., 2009). In another study, GAT-1 knockout mouse was found to have normal life span but had reduced body weight, tremor, gait abnormality and anxiety as physical and behavioural disorders (Jensen et al., 2003; Chiu et al., 2005). It is possible that these abnormalities seen in abovementioned rodent studies are due to compromised GABA uptake and dysfunctional GABA clearance from synaptic cleft due to dysfunctional GABA transporters (GATs).

In this study, proximal neurite processes of PV⁺ interneurons in layer 4 are from other neurons. Soma of PV⁺ interneurons labelled in the layer 4 have their axon terminals in other layers such as V and VI. This issue can be clarified by using cortical layer marker for layer V and VI i.e. Anti-BCL11B antibody (CTIP2). Another option would be using optical Z stacks images and 3D third party software to count puncta surrounding the soma and processes of PV⁺ cells. GAD65⁺-PV⁺ terminals that are less than 1 μm off the surface of pyramidal neurons of adjacent layers can also be counted and these may be the part of future study. As previously mentioned, GATs are expressed in astrocytes, with GAT-3 being exclusively astrocytic, use of suitable astrocytic markers such as N-Myc downstream-regulated gene 2 (NDRG2) or S100β or glial fibrillary acidic protein (GFAP) (Zhang et al., 2019) in histochemical studies may further enhance our understanding of absence seizures.

5.4.2 Increased expression of GAD65 in the stargazer somatosensory cortex

Western blotting result has shown that GAD65 levels are significantly increased in the SS cortex of epileptic stargazer mice. This result indicates that increased level of GABA seen in the SS cortex of epileptic stargazer (Hassan et al., 2018) is due to the increased level of its synthesis enzyme GAD65. However, it cannot be concluded that increased level of GAD65 which primarily involved in phasic inhibition in epileptic stargazer is a consequence of seizures or this has specific contribution in seizure generation. Thus, this upregulation alone might not necessarily trigger functional changes in epileptic stargazers. This also supports the evidence that dysfunction of GAT-1 leading to excess tonic inhibition might be a mechanism in stargazers which is previously reported in GAERS (Cope et al., 2009). However, due to issues in antibodies, this study was unable to quantify changes in GAT-1 levels via western blotting. As studies have shown the involvement of GAT-1 in absence seizures (Cope et al., 2009; Pirrtimaki et al., 2013), it would have been interesting to see the expression level of GAT-1 in the SS cortex and VP thalamus of stargazers in this study. No changes in the expression levels of GAT-3 in the SS cortex and the VP thalamus of stargazers were observed in this study which is consistent with published data of normal functional activity in the thalamus of GAERS (Pirrtimaki et al., 2013). Recent work in Leitch laboratory found that GABA levels in stargazers are reduced in VP thalamus (per. comm.). It is also important to mention that expression level of GADs was unaltered in RTN thalamus in GAERS and non-epileptic rats (Danober et al., 1998) and no significant difference was seen in the GABA levels in the RTN thalamus of stargazers and their non-epileptic controls (Leitch lab, pers. comm.).

On the other hand, no significant differences in the expression levels of GADs and GAT-3 were observed in the SS cortex of PV^{Cre}/Gi-DREADD animals and their control counterparts treated with CNO. One recent study also failed to detect any significant differences in the expression levels of GAD65/67 in the prefrontal cortex and hippocampus when PV was selectively knocked down in those regions (Perez et al., 2019). Alteration of GABAergic transmission via selective silencing of PV⁺ interneurons in this study generated absence-like seizures but changes were not seen in the GADs and GATs that are responsible in synthesis and reuptake of GABA. In other words, functional changes were not evident in protein level. It is possible that physiological factors that regulate the GABA level by adjusting GADs and GATs are not dependent over the subtle functional changes caused by silencing of PV⁺ interneurons in a specific microcircuitry. Thus, it can be concluded that ‘turning off’ the output of feed-forward inhibitory PV⁺ interneurons via

CNO injection might not have distinct role in changing or maintaining GABA level within the circuit even though same dose of CNO is sufficient to generate absence-like seizures. Additional experiments using electrophysiological or pharmacological tools are, however, necessary to revisit and validate these findings in the cellular level.

Of note, GAT inhibitors might also have therapeutic potential against absence seizures. It is believed that GAT inhibitors increase GABA levels in the synapse, facilitate inhibitory neurotransmission, inhibit neuronal excitability thereby mediate seizure protection (Madsen et al., 2010). GAT inhibitors such as tiagabine, EF1502 and SNAP-5114 has shown anti-convulsant activity against established model of epilepsy (Nielsen et al., 1991; Dalby, 2000; White et al., 2005). However, increasing the amount of extracellular GABA by using GAT inhibitors might not always alleviate all seizure types as tiagabine aggravate absence seizures in human patients and are contraindicated (Perucca et al., 1998; Ettinger et al., 1999; Panayiotopoulos, 1999). Nevertheless, inhibition of GABA uptake may be an interesting approach and also can be utilized in the proof-of-concept studies in various rodent models of absence epilepsy.

Altogether, it can be concluded that deregulation of GADs and GATs function may compromise GABAergic signalling and absence seizures. Additionally, astrocytes might be a crucial factor in the etiopathology of absence seizures. Importantly, study of these protein targets during developmental time points would specifically clarify their roles in absence seizure genesis.

5.5 Conclusion

Thus, it can be concluded that upregulation of GAD65 in the SS cortex of epileptic stargazers may be a consequence of absence seizures or this may have specific contribution in absence seizure generation. Experiments should be conducted over developmental time points (different juvenile ages and adulthood) which would clarify if seizure causes upregulation of GAD65, or if the dysfunctional FFI due to reduced PV+ interneuron activation even before seizure onset alters GAD65 levels. Additionally, optogenetic, chemogenetic or pharmacological manipulations should be performed to target GAD65 and to explore its role in absence seizure generation.

Chapter 6. General Discussion

This final chapter is a critical review of the findings of this PhD project. Firstly, a brief overview of the findings from the three experimental chapters is presented. This is followed by in-depth analysis of the data obtained from the experiments. This includes critical evaluation of the findings in relation to current published literature. Following this is a discussion of significance of findings and their feasibility in clinical terms and future therapeutic use. Experimental methods employed in this study are also critically assessed in this chapter. Also, direction for future experimental approach and studies are discussed.

6.1 Overview of findings

The experiments in chapter 3 were conducted to examine the impact of functionally silencing feed-forward inhibitory PV⁺ interneurons within the CTC network on seizure generation and behavior. Using confocal microscopy, the expression of the DREADD receptors in feed-forward inhibitory PV⁺ interneurons within the CTC network in PV^{Cre}/Gi-DREADD mice was first confirmed. Analysis of EEG traces revealed that focal silencing (regional injection of the designer drug CNO into the SS cortex or the RTN thalamus) of feed-forward inhibitory PV⁺ interneurons generates paroxysmal oscillatory activity similar to SWDs on EEG with associated behavioral arrest. Focal silencing also impaired locomotory behavior in PV^{Cre}/Gi-DREADD animals. Administration of the anti-absence drug (ETX) prevented the focally induced SWDs. Global silencing of all PV⁺ interneurons (via i.p. CNO injection) induced epileptiform activity with the characteristics of SWDs and decreased locomotion. Additionally, global silencing impaired motor control on the moving rotarod and increased anxiety in open-field test. In contrast, such effects were not evident in CNO treated non-DREADD WT controls or vehicle treated PV^{Cre}/Gi-DREADD animals.

Based on the findings from chapter 3 where silencing PV⁺ interneurons was linked to absence-like seizures, it was crucial to test the impact of activating these interneurons during absence seizures. Thus, in chapter 4, excitatory DREADD (PV^{Cre}/Gq-DREADD mice) approach was employed. Simultaneous video/EEG data revealed that selectively activating feed-forward inhibitory PV⁺ interneurons via focal CNO injection into either region of CTC network prevents PTZ-induced absence seizures or suppresses the severity of absence seizures. PTZ induced tonic-

clonic and myoclonic seizures were also reduced in severity by activation of feed-forward inhibitory PV⁺ interneurons. Activating these interneurons delayed the latency to first seizure, decreased mean duration spent in seizure, reduced total number of discharges and shortened the length of PTZ-induced seizures.

Chapter 5 aimed to investigate whether dysfunctional FFI impacts the inhibitory neurotransmitter GABA by altering expression of GADs and GATs. To do this, stargazer mouse model of absence epilepsy and CNO treated PV^{Cre}/Gq-DREADD animals were used. Analysis of the relative expression of GADs and GATs using western blotting showed that the protein level of GAD65 in whole SS cortex tissue was significantly increased in epileptic stargazers compared to their non-epileptic littermates. Levels of GAD67 and GAT-3 in the SS cortex of epileptic stargazers were unaltered. In the VP thalamus, the expression levels of these protein targets were unchanged in both mice groups. The expression levels of these proteins were also unchanged in PV^{Cre}/Gq-DREADD animals treated with CNO which is sufficient to generate absence-like seizures. Confocal microscopy revealed that there is no significant difference in the visual expression pattern and intensity of staining of GADs and GATs in the SS cortex and the thalamus between epileptic stargazers and their non-epileptic controls.

Overall, the results from this study using both inhibitory (Gi) and excitatory (Gq) DREADD approaches have enhanced our understanding that dysfunctional FFI in CTC microcircuits is likely to contribute in absence seizure generation and GAD65 upregulation may be a contributing or compensating mechanism for reduced FFI.

6.2 Discussion of KEY Findings

6.2.1 Use of Cre-dependent DREADD to manipulate PV⁺ interneurons

In this study, mice expressing inhibitory Gi-DREADDs (hM4Di-flox) or excitatory Gq-DREADDs (hM3Dq-flox) were bred with PV-Cre mice expressing Cre recombinase in PV⁺ interneurons. hM4Di-flox and hM3Dq-flox mice have a *loxP*-flanked STOP cassette designed to prevent transcription of the downstream HA-hM4Di-pta-mCitrine and HA-hM3Dq-pta-mCitrine coding region, respectively. Mating these strains via Cre-*loxP* recombination technology removes the *loxP*-flanked STOP cassette only in the cell type specified by the Cre-recombinase system and

generates littermates where HA-tagged DREADD receptors are specifically expressed in PV+ interneurons. The success of mating was first verified by testing the genetic make-up of animals via genotyping. Cellular expression and localization of HA-tagged DREADD receptors in PV+ cells were confirmed via confocal immunofluorescence microscopy.

In this study, labelling of PV was found in the SS cortex, RTN thalamus and the Purkinje cells of cerebellum of animals. This was consistent with other published studies describing distribution of PV+ neurons in the brain (del Río and DeFelipe, 1994; Tamamaki et al., 2003; Fishell, 2007; Xu et al., 2010). Expression pattern of PV in those brain regions was not visually distinguishable between genotypes (DREADD vs non-DREADD WT controls). The PV-Cre mouse used in this study was from Jackson laboratories (JAX stock #008069) which states when PV-Cre knockin allele is bred with a strain containing *loxP* site flanked sequence of interest, recombination occurs in more than 90% of neurons that express parvalbumin. In agreement to that statement, in this study, colocalization of HA-tagged DREADD receptor in PV+ interneurons were above 90% in the SS cortex, the RTN thalamus, and Purkinje cells of cerebellum, whereas none of the PV+ interneurons in non-DREADD WT control animals showed labelling for HA-tag.

The use of double transgenic mice approach used in this study is not the only way to establish the expression of DREADD receptors within PV cells. Cre-dependent/independent viral approach (Zhu and Roth, 2015) and Tet-dependent transgenic mice approach (Tet-off system) (Alexander et al., 2009; Zhu et al., 2014) are other ways of manipulating PV+ interneurons with DREADDs. Cre-dependent viral method is the most commonly used approach. According to this approach, virus (AAV or LV) particles containing DREADD construct are delivered into the targeted area in the brain of PV-Cre mice. This approach requires complicated stereotactic techniques and wait of 2-3 weeks time period for expression. Also, single injection can only deliver viral construct in one-specific region. Studies have shown that the infection efficiency and specificity of labelling vary between 70 and 90% (Yi et al., 2014; Zou et al., 2016; Chen et al., 2017; Xia et al., 2017; Hijazi et al., 2019; Page et al., 2019; Bicks et al., 2020). Another method is Tet-dependent transgenic mice approach where littermates from TRE (Tetracycline-responsive promoter element)-DREADD are crossed with mice having the tetracycline-controlled transactivator protein (tTA) driven by a promoter (such as CaMKII α , c-fos etc.). In the absence of tetracycline or its analog,

tTA binds to the TRE and activates transcription of the DREADD in the targeted brain regions. This is reversible approach as administration of tetracycline or doxycycline eliminates DREADD expression. This approach is relatively less popular and few published research articles are available (Alexander et al., 2009; Garner et al., 2012; Zhu et al., 2014).

One of the most important aspects of using double transgenic approach (PV^{Cre}/DREADD-floxed mice) utilized in this study is that DREADD receptors can be expressed in almost all PV+ interneurons (>90%) in different brain regions and PV+ interneurons can be activated via regional CNO injection into desired regions of the brain. Alternatively, DREADD expressing PV+ interneurons can be globally activated by systemic administration of CNO.

6.2.2 Functionally silencing feed-forward PV+ interneurons generated absence-like SWDs, whereas activation prevented/suppressed PTZ-induced seizures

This current study specifically targeted the most common type of GABAergic neurons (PV+ interneurons) of the CTC network. These interneurons primarily regulate the FFI within the network. As previously described, studies conducted in well-established stargazer model of absence epilepsy have shown abnormal expression of AMPA receptors particularly at input synapses of PV+ neurons can possibly impair FFI and contribute to the generation of absence-SWDs (Barad et al., 2012; Maheshwari et al., 2013; Adotevi and Leitch, 2016; 2017; 2019). However, the extent to which the deficits in AMPAR expression leads to dysfunctional FFI has not been examined through any functional studies. Functional recordings from PV+ interneurons of stargazer animals would be highly beneficial to determine the degree to which the impaired AMPA receptor might have been involved in the alteration of activity of PV+ interneurons. But, the distance between the stargazin locus to parvalbumin locus in chromosome 15 is very close and if stargazers are bred with promoter-driven animals, double crossover is very unlikely and identification of these cells during physiological study would be technically challenging (Maheshwari et al., 2013). To overcome these challenges, in this study, normal non-epileptic mice i.e. PV^{Cre}/Gi-DREADD and PV^{Cre}/Gq-DREADD were used. PV+ interneurons of the CTC network (SScortex and RTN thalamus) were functionally targeted (silenced or excited) by regional injection of CNO. Acute unilateral silencing of these interneurons in either regions of the CTC network generated absence-like discharges whereas activation efficiently prevented chemically

induced absence seizures. Thus, it is likely that PV+ interneurons within feed-forward inhibitory CTC microcircuit regulate the neuronal oscillations and prevent runaway excitation, and dysfunctional FFI within the microcircuit is likely to contribute in absence seizure generation.

PV+ interneurons in CTC network are connected to the cell bodies, proximal dendrites and axonal initial segments of excitatory neurons. Upon receiving excitatory input, it is possible that these interneurons fire and release inhibitory GABA onto the excitatory neurons which enables their powerful FFI and limit over excitation. Functional silencing of these interneurons via CNO application (into either the SScortex or the RTN thalamus) in this study might have prevented the role of PV+ interneurons in maintaining the FFI leading to the generation of absence-like SWDs. This is particularly interesting because functional activation of PV+ interneurons in both abovementioned regions suppressed chemically induced absence seizures. Additionally, functional activation also suppressed chemically induced tonic-clonic seizures and myoclonic jerks. These results support the idea that PV+ interneurons might serve as the ‘choke point’ for seizure control and this chemogenetic intervention of parvalbumin interneuron inhibitory reserve might capitalize as a personalized treatment approach in some cases of absence epilepsy.

Results from this thesis in light of recent developments and existing theories

There is a long-standing debate regarding the specific role of CTC components in the pathophysiology of absence seizures. Based on the results from animal models and human studies, various concepts and theories have been postulated since 1950s (see review Meeren et al., 2005). Cutting-edge techniques have been implemented to gain the mechanistic insights of this disease, but it is likely that we still have crucial gaps in the knowledge about the cellular, synaptic and network mechanisms involving the initiation and/or maintenance of absence seizures.

Studies conducted in animal models of absence epilepsy have provided evidence of the onset of seizure activity in the cortex specifically SScortex. Human studies also showed widespread cortical ictal and post-ictal changes in haemodynamic measurements (cerebral blood flow/volume and fMRI) before the involvement of other regions of the brain (see review Crunelli et al., 2020). On the other hand, since 1950s, many experimental studies have revealed that thalamic regions are also responsible in generating absence-SWDs. Recently, Sorokin and colleagues emphasized that thalamic components themselves can recruit epileptic cortical network for absence seizure generation (Sorokin et al., 2017). While altered cortical network is widely considered as the

originator of absence-SWDs, it is incapable of maintaining discharges on its own, nor is the thalamus. In this current study, it has been shown that selective inhibition of either cortical or thalamic PV⁺ interneurons elicits absence-like seizures in normal non-epileptic mice and activation of these interneurons terminates chemically induced absence seizures. Altogether, this study has shown that a subtle functional change in neuronal excitability even restricted to any of the components of CTC microcircuit can generate generalized absence-SWDs throughout the CTC network and activation significantly can prevent seizure activity. Similar localized changes by knocking out a single gene (*Cacna1a*, coding for P/Q-type Ca²⁺ channels) in layer 6 corticothalamic neurons generated absence seizures in non-epileptic mice (Bomben et al., 2016). Conditional knock out of Cav2.1 channel function from PV⁺ interneurons compromised GABA release from cortical PV⁺ neurons and generated various types of generalized seizures including absence seizures (Rossignol et al., 2013). One recent work has shown that, protein level of parvalbumin is lower in the SS cortex of WAG/Rij compared to wistar rats. Authors concluded that such reduction might be a contributing factor of SWDs in WAG/Rij rats (Arkan et al., 2019). Also, parvalbumin deficient mice has shown to have higher susceptibility and severity to chemically induced seizures (Schwaller et al., 2004).

Previously it was thought that a key aspect of absence network is a synchronized action potential firing of cortex, thalamus and SWDs seen in EEG. This was supported by *in vivo* studies conducted in feline model (reviewed in Gloor et al., 1990) and WAG/Rij model of absence epilepsy (Inoue et al., 1993), where action potential firing of cortical and thalamic neurons concurred with the spike component of the cortical SWDs. Previous *in vitro* studies suggested that seizure-related coordinated firing in the thalamocortical system is through bursts of action potential mediated by T-type calcium channel of thalamocortical relay neurons and reticular thalamic nuclei. It was thought that these neurons elicit burst of action potentials at each cycle of paroxysmal activity forming a rhythm. As thalamocortical cells are reciprocally connected with corresponding cortical regions, the cortical structure then thought to coordinate and/or fall into the rhythm generated by thalamic network (von Krosigk et al., 1993; McCormick and Contreras, 2001; also reviewed in Huguenard, 2019).

However, recent few studies have established that cortical, thalamocortical and RTN neurons are not 'hard wired' and these neurons are able to switch their firing pattern in successive paroxysmal

cycle and SWDs (McCafferty et al., 2018b; Meyer et al., 2018). These studies also showed that synchronized firing of these neurons during SWDs might be lower than previously thought. It is possible that widespread synchronous neural activity may not be a key feature of absence seizures and reductions in synchronized firing would not be a desired therapeutic goal. Altogether, use of modern techniques has provided new insights in understanding the ictogenesis of absence seizures. These studies have revealed the pre-ictal and ictal single cell temporal firing dynamics within the CTC network which was not established via previous *in vivo* and *in vitro* studies. However, it will always be a challenge to specifically isolate the exact roles of the cortical and thalamic components within CTC network in generation and/or maintenance of absence seizures.

Of note, the involvement of basal ganglia networks in absence seizures may also be important in understanding the pathophysiology of absence seizures. Ictal changes in fMRI-BOLD signals in the basal ganglia was seen in children with absence seizures. The ictogenic firing of cortico-striatal neurons and cortico-subthalamic neurons during SWDs in animal models also indicates the possibility of involvement of basal ganglia in absence seizure generation (see review Crunelli et al., 2020). Furthermore, striatal application of 1-naphthyl acetyl spermine (NASPM) which selectively blocks calcium-permeable AMPA receptors, and are highly expressed in striatal fast-spiking interneurons (PV+), induces absence seizures in wild-type mice and DREADD mediated activation of these interneurons remarkably reduces absence seizures in *Stxbp*^{+/-} mice (Miyamoto et al., 2019). There are few other technical aspects which should be taken into account such as brain slice studies vs intact brain, genetic epileptic animal model vs non-epileptic animals, invasive imaging vs non-invasive imaging and human data vs animal studies. Mechanistic limitation of brain functioning in animal models also should be considered.

6.2.3 Functional silencing of feed-forward PV+ interneurons altered animal behavior

Global and focal silencing of feed-forward inhibitory PV+ interneurons significantly reduced locomotory behavior in open-field test in inhibitory DREADD (PV^{Cre}/Gi-DREADD) animals. During 1-hour EEG recording, DREADD animals were also significantly immobile compared to their control counterparts. Interestingly, in previous studies, animals lacking parvalbumin (either PV knockout or conditional PV knockout) also showed decreased locomotory behavior (Farré-Castany et al., 2007; Ding and Delpire, 2014; Lucas et al., 2014; Wöhr et al., 2015; Xenos et al.,

2018). DREADD based studies utilizing PV-Cre animals have shown no changes in locomotion as those studies manipulated PV+ interneurons in other regions such as prefrontal cortex and hippocampus (Perova et al., 2015; Zou et al., 2016; Xia et al., 2017; Page et al., 2019). Global silencing also caused the animals to spend more time in the peripheral zone and corners of the open-field arena and less time in the central zone which indicated the increased anxiety in DREADD animals compared to their wild-type counterparts. Staying in the close proximity to the wall of the arena indicates anxiety-related behavior in rodents (Prut and Belzung, 2003; Lipkind et al., 2004; Seibenhener and Wooten, 2015). The anxiety level of non-DREADD WT control animals of open field was similar to other published studies for WT control animals (Moy et al., 2007; Bailey and Crawley, 2009; de Oliveira et al., 2015).

Global silencing of feed-forward inhibitory PV+ interneurons significantly impaired motor performance in moving rotarod test but focal silencing (into either the SS cortex or the RTN thalamus) did not alter the motor performance. This is likely due to the fact that global silencing of PV+ interneurons via i.p. CNO injection silenced all PV+ interneurons including PV expressing Purkinje cells in the cerebellum. Similar to the findings of this study, conditional Purkinje cell knockout animals also showed significantly impaired motor performance (Todorov et al., 2012; Tsai et al., 2012; Yamazaki et al., 2015). Moreover, DREADD based study using viral expression methods to selectively silence or excite PV+ interneurons in brain regions, other than the cerebellum, have had no effect on motor performance in rotarod test (Zhu et al., 2014; Petitjean et al., 2015; Liu et al., 2017; Hijazi et al., 2019). One optogenetic study found that activation of $G_{i/o}$ pathway in Purkinje cells significantly reduces motor coordination and control on the rotarod (Gutierrez et al., 2011).

Thus, it can be concluded that functional silencing of feed-forward inhibitory PV+ interneurons in the SS cortex or the RTN thalamus has impact on behavioral parameters such as locomotion, anxiety, motor performance. Studies have shown the involvement of these interneurons in cognition and learning (Verret et al., 2012; Donato et al., 2013; Cisneros-Franco et al., 2020; Lee et al., 2017; Parker, 2020). However, changes in locomotory behavior in relation to CTC feedforward microcircuits has not been directly established. Animals lacking *N*-methyl-D-aspartate (NMDA) transmission in PV+ interneurons (NMDAR knockout PV-Cre animals) of

SScortex is shown to have reduced (but statistically non-significant) locomotion (Carlen et al., 2012). Increased immobility and anxiety in CNO-treated DREADD animals might be due to the influence of the amygdala anxiety circuitry as basolateral amygdala receive inhibitory input from cortex and thalamus (Tovote et al., 2015; Babaev et al., 2018).

The PV⁺ interneurons provide powerful inhibitory effects to the huge network of glutamatergic excitatory neurons. The functional loss of PV⁺ interneurons in CTC feed-forward microcircuits via DREADD approach employed in this study, may have affected pyramidal neurons within the SScortex or the RTN thalamus and disrupted coordinated firing between the groups of pyramidal cells leading to the reduction in coordinated activity of other networks and circuits of the brain. This also might be one of the answers to the impaired animal behavior in this study.

6.2.4 Impact of dysfunctional FFI on GABA synthesizing enzymes (GADs) and transport proteins (GATs)

Expression level of GAD65 was upregulated in the SScortex of stargazers while other protein targets (GAD67 and GAT-3) were unaltered. Visual staining pattern and staining intensities of GADs and GATs in the SScortex and thalamic regions (RTN and VP) were similar and unaltered between epileptic stargazers and non-epileptic controls. Expression level of all protein targets (GADs and GAT-3) in the PV^{Cre}/Gi-DREADD animals treated with CNO was also unchanged.

Upregulation of GAD65 in the SScortex of stargazer was in agreement with the result of another study where GABA level was found to be increased in the SScortex of epileptic stargazers (Hassan et al., 2018). Stargazers show spontaneous seizures which may have long-term changes in the CTC circuit leading to the continuous increased activity of excitatory neurons. To overcome this situation, GABA synthesis should be increased at the synaptic sites to regulate such excitatory activity. Thus, upregulation of GAD65 might be a part of adaptive response or compensatory changes in epileptic stargazers.

In addition, this upregulation of GAD65 [which primarily acts in phasic inhibition (Erlander et al., 1991)], in epileptic stargazers (Hassan et al., 2018) supports the GAT-1 dysfunction seen in GAERS (Cope et al., 2009). Cope and colleagues found that excess extrasynaptic GABA_A receptor-dependent tonic inhibition might be a contributory factor in generating seizures in

GAERS and stargazers. In relation to human patients, SL6A1 mutation leading to GAT-1 loss of function (Mattison et al., 2018) is the most common epileptic phenotype in children (Dikow et al., 2014; Johannesen et al., 2018). One human study revealed higher GABA levels in the ipsilateral thalamus of a child with SWDs (Leal et al., 2016).

It is important to note that, crossbreeding GABA_AR δ subunit knockout mice with stargazer mice removes the absence seizure phenotype (McCafferty et al., 2018a). Thus, GAT-1 agonists and δ -containing GABA_A receptors may be new targets for the treatment of absence seizures. Studies have shown that GAT inhibitors such as tiagabine has anti-convulsant activity against established model of epilepsy (Nielsen et al., 1991; Dalby, 2000; White et al., 2005) but aggravates absence seizures in human patients and are contraindicated (Perucca et al., 1998; Ettinger et al., 1999; Panayiotopoulos, 1999). Expression level of the GAT-3 was unchanged in this study which is consistent with reports of normal functional activity in the thalamus of GAERS (Pirttimaki et al., 2013). A recent study conducted GABA uptake assays and examined the protein expression levels of GATs using primary culture of cortical and thalamic astrocytes from GAERS which suggested that dysfunction GAT transporters may contribute in absence seizures and astrocytes may be an important factor in understanding the pathophysiology of this disorder (Pina et al., 2019). Thus, this study alone cannot conclude that increased level of GAD65 in epileptic stargazer is either a consequence of seizures or this has specific contribution in seizure generation. Western blotting alongside with electrophysiological experiments should be performed during developmental time point which can clarify the specific roles of GADs and GATs.

6.3 Clinical Implications

Absence seizures associated with generalized synchronous 3-4 Hz SWDs are characterized by brief, frequent and sudden alteration of awareness during childhood, referred as childhood absence epilepsy. This disorder is also associated with cognitive weakness, impaired learning, psychosocial problems as well as physical safety. Anti-seizure medications such as ethosuximide, valproic acid, lamotrigine etc. are commonly used first-line agents to control the seizures but clinical trials have found that freedom from treatment failure of these medications is considerably lower and not promising (Glauser et al., 2010; 2013; Cnaan et al., 2017). The remission rate is only 58% (Kim et al., 2016). Compared to other focal seizures, there are very few monotherapy based long term

clinical trials conducted in absence epileptic patients, which directly affects in evidence-based decision-making during treatment. Clinical use of other broad-spectrum anti-seizure medications as anti-absence drug is also not encouraging (Nolan et al., 2019). The poor efficacy and serious side effects of these first-line prescribed medications may be due to their broad mechanism involving reduction of excitation. ‘One for all’ concept of prescribing first-line medications to every cases of CAE is also a major reason behind decreased efficacy of these drugs. As neurophysiology of the neuronal networks contributing in seizure generation might vary from patient to patient, there is always a need of patient-specific treatment approach. This requires a deep understanding of cellular and molecular mechanism of normal functioning of brain microcircuits and gene targets which might be responsible in the genesis of absence seizures.

The work conducted in this thesis highlighted the functional role of most prominent GABAergic interneurons (parvalbumin expressing) of the brain which regulates inhibition within the microcircuit involving cortex and thalamus i.e. CTC network. The results from this thesis indicated that impaired FFI due to dysfunctional PV+ interneurons within CTC network might be one of the potential mechanisms of absence seizure generation and altered behavioral pattern. These findings are based on both inhibitory and excitatory approach. Thus, novel therapeutic compounds should be employed to target these interneurons in the specific-brain regions for the treatment of some cases of childhood absence epilepsy.

6.4 Evaluation of Methods

6.4.1 DREADD approach

Techniques like chemogenetics and optogenetics have revolutionized neuroscience by providing new tools to selectively manipulate the activity of specific neuronal population. DREADDs technique employed in this thesis provides slow but extended modulation of system. Optogenetics allow fast neuronal modulation with high temporal resolution. However, for lengthy experiments DREADDs are always ahead and effective as thermal properties of light system in optogenetics have shown to produce nonspecific effects (Owen et al., 2019).

There are few limitations associated with DREADD (chemogenetics) technology. For example, CNO is the only designer drug for this technique so the neuronal activation depends over the

pharmacology of CNO. The mode of neuronal activation is acute and it does not permanently silence or activates neurons. In this study, CNO was used as the ‘designer drug’ to silence or activate feed-forward inhibitory PV⁺ interneurons. The use of CNO as the ‘designer drug’ has recently been called into question, especially DREADD specific actions of CNO delivered intraperitoneally was a subject to criticism (Gomez et al., 2017). Gomez and colleagues showed the possibility of off target/sedative effect in animals due to the reverse metabolization of CNO to clozapine after systemic injection. This work included in this thesis was particularly aware of this and behavioral experiments were planned to avoid or overcome the possibility of such consequences. To minimize such potential off-target effects, non-DREADD WT animals and vehicle-treated controls were included in all CNO doses of every behavioral and EEG experiments performed. Alternative chemical approach such as the use of olanzapine, compound 21, JHU37152 and JHU37160 to activate DREADD have recently been proposed but these compounds are not yet fully characterized (Thompson et al., 2018; Bonaventura et al., 2019; Jendryka et al., 2019; Weston et al., 2019). The use two different ligands to confirm DREADD mediated behavioural results is also recently suggested (Goutaudier et al., 2019) which can be implemented in the future studies.

6.4.2 Immunofluorescence Confocal Microscopy

Confocal microscopy was performed to confirm the selective expression of inhibitory (Gi) and excitatory (Gq) DREADD receptors in PV⁺ interneurons and to investigate the layer specific expression pattern of GADs and GATs. Confocal microscopy is an excellent technique to examine the cellular expression and co-localization of two or more molecules at the same physical position in a given biological sample. However, there is always a compromise between magnification, resolution and scan time during confocal imaging. The higher the magnification and resolution, the more time is required for the scan which frequently causes the photobleaching of the specimen. In this study, anti-fade DABCO-glycerol solution was used as mounting medium to minimize the photobleaching (Longin et al., 1993; Ono et al., 2001). Slides were foiled and stored in dark to preserve fluorescent dyes. Background signal was subtracted from the measurements to accurately measure the intensity of signal of interest (Waters, 2009). Confocal imaging, quantitative measurements and analysis of the data from the tissue sections of relevant genotypes were performed in parallel manner.

6.4.3 Surgical manipulation and EEG recording

In this study, surgical manipulations were performed on animals to implant electrodes, prefabricated headmounts and microcannulas for EEG recordings. In the beginning of this study, very few animals experienced excessive operative bleeding during surgical procedures. However, no major surgical complications in animals were seen during this entire study. Animals were injected with drugs for pain control and local anesthesia prior surgical procedures. Surgeries were performed in continuous flow of isoflurane gas (inhalation anesthetic) and supplemental heat (by using heat pad). Animals were rested at least seven days to allow full recovery from surgical manipulation. Animals were monitored and handled every day after their arrival to the animal facility and were also acclimatized to testing environment and equipment before every EEG recording.

In this study, EEG signals were recorded using the Pinnacle mouse tethered system (Pinnacle Technologies, Austin, TX, USA). Recently, Bluetooth wireless amplifier EEG system is introduced which is claimed to produce artifact-free data with simple implant procedure. It seems to be more portable and cost-effective (Ref: Pinnacle website). However, battery life of the bluetooth device might be an issue for lengthy experimental procedures. In this study, video/EEG analysis was performed offline by manually scrolling through EEG traces and absence-like SWDs were confirmed electro-clinically i.e. visual inspection of the morphology/characteristics of EEG profile and animal behavior in the video. However, software platforms such as MATLAB and Python offer various graphic user interfaces like EEGLab, Brainstorm, FieldTrip, PyEEG etc. for easy and precise quantification of EEG parameters, power spectral analysis, statistical analysis and for the removal of artifacts (Maheshwari et al., 2020). Multiple screws for the acquisition of electrocorticogram traces along with local field potential from the targeted sites (SScortex and RTN thalamus) can be very useful to correlate the EEG activity with site specific firing of PV+ neurons (Clemente-Perez et al., 2017). These approaches can be utilized in future experiments.

6.4.4 Behavioral tests

In this study, two motor function tests were employed to investigate the impact of silencing (global and focal) feed-forward inhibitory PV+ interneurons on animal behavior. Open-field and rotarod tests were included to determine behavioral parameters such as locomotion and motor coordination. These tests are established tools to measure such parameters in rodents. Use of these

tests have yielded significant conclusive findings. Additionally, other behavioral tests can be implemented in future studies to establish behavioral-EEG phenotyping and to quantify various other behavioral parameters.

6.4.5 Antibodies

The antibodies used in this study are commercially available, well characterized and widely used in many published studies. Dilution level of antibodies for use in the different experiments were optimized based on manufacturers protocol and guidelines. Appropriate loading controls (β -actin or α -tubulin) were used in western blotting experiments. Single band of loading control and protein target was confirmed by comparing them with reference protein ladder corresponding to the molecular weights specified by manufacturer. The incubation time in primary and secondary antibody solution for both western blotting and confocal IHC techniques was optimized.

6.4.6 Western blotting

Western blotting is extensively used analytical technique to separate and identify proteins. This technique is used to measure the amount of protein expressed in a sampled tissue. In this study, western blotting was employed to compare the changes in expression of protein targets (GADs and GATs) between epileptic stargazers and non-epileptic controls, and CNO-treated DREADD animals, CNO-treated non-DREADD animals and vehicle-treated DREADD animals. Sample preparation is a major step in western blotting. To avoid protease degradation of proteins, collected brain tissue from the animals was quickly snap-frozen and lysed. Buffers used during sample preparation and electrophoresis were always freshly prepared.

There are different ways of detecting protein of interest from the blot, namely colorimetric, chemiluminescent and infrared methods. In this study, infrared fluorescent detection method was employed. In this method, secondary antibody is conjugated to NIR (near-infrared) fluorescent dye. Blots were documented in NIR imaging system i.e. Odyssey Imaging system. This is a quantitative two-color detection method which has several advantages over conventional detection methods. This imaging system provides low background autofluorescence and high sensitivity. Fluorescent signal is directly proportional to the target protein content and unaffected by exposure time. Additionally, two protein targets of same molecular weight can be detected by using different

IR dye having different emission spectra. Normalization against loading control is also very easy and more accurate. In this study, inspite of using antibodies from two different suppliers and even after using highest recommended concentration, GAT-1 was not detected in the same tissue samples that were used to detect other protein targets. One of the reasons might be the miss-folding of proteins which can obstruct the binding of the epitope to the recognition site of antibody.

It is true that western blotting is used as a first pass test. The expectation is that antibodies that stain a single band corresponding the mass of the intended target are more likely to be specific in IHC analysis. The expression level of protein targets (GADs and GATs) (via WB) and their localization profile (via IHC) is not yet reported in stargazers mouse model of absence epilepsy. This is the first study to do so. Thus, in this study, WB and IHC were performed at the same time. In this study, GAD65 expression was significantly increased in stargazers compared to non-epileptic control in western blotting but this was not replicated in IHC and GAT-1 labelling was observed in IHC but was unable to be detected in western blotting. Epitope, a part of antigen which is recognized by the primary antibody may not be identically available in WB and IHC assays. Tissue samples are treated differently in WB and IHC and this influences the epitopes exposed on the target protein which might have profound consequences for the ability of a given antibody to bind specifically to its target.

6.4.7 Uses and limitations of absence seizure rodent models

Pharmacological models of absence epilepsy deal with the mechanisms of ictogenesis. In addition to absence seizures, all pharmacological animal models present dose, age, time dependent tonic-clonic and myoclonic generalized seizures and sedation and anesthesia (with GABAA receptor antagonists and GABA agonists) (Kostopoulos, 2017). To study epileptogenesis, the process by which normal brain develops epilepsy, genetic animal models are the best. However, these are also associated with limitations. In addition to SWDs, genetic models such as stargazers display ataxia and movement disorders, which are not features of CAE (Panayiotopoulos, 1999). In this respect, rat models (GAERS and WAG/Rij), have a certain advantage, only SWDs are observed with behavioural arrest and no other behavioural abnormalities (Jarre et al., 2017). One drawback of mouse model is that they offer monogenic mutations, whereas CAE in human patients is considered as complex with multiple genetic anomalies. That is why the polygenic rat model of

absence epilepsy are known to better simulate CAE. All animal models display 5-9 Hz SWDs instead of the 2.5-4 Hz frequency observed in patients with CAE. The most important limitation of genetic rodent models is the persistence of SWDs in adulthood. On the contrary, absence seizures progressively disappears at adulthood in human patients (Jarre et al., 2017). However, rodent models of absence epilepsy have greatly contributed on the genetics of absence epilepsy and strongly improved our understanding of the pathophysiology of this disease.

6.5 Future experimental directions

Chronic activation of PV cells in absence seizure models and functional tests in stargazers

In this study, acute activation of PV⁺ interneurons during chemically induced seizures was found to have anti-epileptic effect in non-epileptic mice. Thus, the next key challenge would be chronically activating PV⁺ neurons in rodent models of absence epilepsy to see if that can ‘reset’ epileptogenic circuits. GABA current in stargazer cortical and thalamic neurons could be measured using the optogenetics approach. Similarly, AMPA currents in PV⁺ interneurons could be measured to confirm whether reduction in AMPA receptor expression result in decreased AMPA excitatory post synaptic potential. Experiments can be conducted to restore stargazin mutation in stargazer CTC network using AAV vectors in order to establish the impact of loss of AMPAR expression in PV⁺ interneurons to the stargazer epileptic phenotype.

Identification and characterization of specific subtypes of PV cell responsible for the effect

In this study, PV⁺ interneurons as a group were manipulated using Cre-*loxP* recombination approach. While effective, it could not distinguish the differences among the subtypes of PV⁺ interneurons. Thus, this study was unable to specify the subtypes of PV⁺ interneurons responsible for the effects. In fact, until now, techniques which specifically target subtypes of PV⁺ interneurons are not established. However, given that basket cells are the most common type of PV⁺ interneurons within the CTC network, it is likely that outcomes from this study can be mostly attributed to basket cells. With the advancements in genetic manipulations, it can be predicted that we will be able to study the functions of specific subtypes of PV⁺ interneurons in the near future.

Local field potential (LFP) measurements alongside electrocorticography

This current study recorded EEG from cranial surface of animals. One unfortunate aspect of EEG is that local neuronal activity has to pass through brain, cerebrospinal fluid, meninges and skull before reaching to the electrodes. EEG signals also often get mixed up with disturbances from the other body activities in the form of artefacts. Seizure activity seen in the scalp EEG is from the coordination of firing of neural population and/or synaptic responses. Thus, EEG is not sufficient to measure specific changes in the local field activity arising from the shift in action potential of PV+ interneurons of either the SS cortex or the RTN thalamus. To isolate the specific roles of PV+ interneurons of specific brain regions on absence seizure genesis, maintenance or generalization, LFP measurement is imperative. In relation to this current study, LFP measurements will enable us to determine the latency of activation (silencing or excitation) of DREADD expressing PV+ interneurons after regional CNO injection. This will also allow us to correlate simultaneous LFP changes at the targeted site with changes in SWDs in EEG. This is important because firing of cortical, thalamocortical and RTN neurons in epileptic animals (GAERS) was found to be decreased 2-3 seconds before SWDs were detected in EEG (McCafferty et al. 2018b). LFP measurements will also allow us to investigate the impact of ipsilateral manipulation to the contralateral CTC circuit. Bilateral silencing and activation of these interneurons are other options for future studies. Ex vivo whole cell patch-clamp experiments in brain slices can also be included in future studies. Focal inhibition of PV+ interneurons of RTN would be expected to not only reduce FFI to the thalamocortical relay neurons but also intra RTN inhibition. Also, this could have an effect on the other RTN and its microcircuitry. Thus, the effect of RTN mediated FFI and intra-RTN inhibition could be part of a potential future study using LFP measurements. This is particularly important because different studies have shown conflicting functional consequences of altered inhibition within RTN.

Possibilities of multiplexing with chemo- and/or opto-genetics

Optogenetic and chemogenetics have their own pros and cons. Optogenetics is ahead of chemogenetics in real-time neuromodulation and increased temporal resolution. However, it should be noted that utilizing these two approaches have produced similar outcomes (Zhu et al., 2016). In relation to this current study, use of both approaches in a same animal to silence and/or activate the CTC feed-forward microcircuits of the SS cortex or the RTN thalamus would answer

many critical questions. This might be possible because optogenetics requires light to regulate the excitability and chemogenetics requires a designer drug. Thus, *in vivo* multiplexing using these two different approaches may be a part of future studies. Multiplexing within chemogenetics is also possible as Vardy and colleagues have successfully combined inhibitory KORD and excitatory hM3Dq (DREADD) in same animal to study behaviour (Vardy et al., 2015).

Use of alternative DREADD agonists

Recently, the use of designer drug CNO to activate DREADDs has become controversial (Gomez et al., 2017) and many reports published since then suggested alternative approaches, the need of optimization of CNO dose, and the use of standard controls in DREADD based experiments. Alternative DREADD activators such as compound 21, olanzapine, perlapine etc. can be used for future *in vivo* studies. Thus, the strength of genetics by paying attention to the shortcomings of pharmacology is required to maximize the potential of the chemogenetic approach.

Study of GADs and GATs over multiple developmental time points

This study concluded that the upregulation of GAD65 in the SS cortex of adult epileptic stargazers might be a compensatory or contributory mechanism for reduced FFI. However, future experiments should cover multiple developmental time points such as before after seizure onset. This is particularly important because formation and maturation of CTC network, expression of stargazin and AMPA receptors, and other phenotypic changes in stargazers are developmentally regulated i.e., at PN7–10: thalamocortical and corticothalamic connections are complete, feed-forward inhibition starts, at PN13-15: the first observable phenotypic features (ataxic gait) appear, at PN17–18: absence seizures are observed. Moreover, studies have shown that developing brain are more vulnerable to seizures (Ben-Ari, 2006; Jacobs et al., 2009). Seizure onset in stargazer mutant mouse is around PN17-18 (Qiao and Noebels, 1993) and childhood absence epilepsy also develops early on in childhood (Tenney and Glauser, 2013). Thus, study of the developmental changes of GADs and GATs in animal models of absence epilepsy could be a part of future studies. Additionally, optogenetic, chemogenetic or pharmacological manipulations should be performed to target GAD65 and to explore its role in absence seizure generation. For example: Stargazers first crossed with GAD65-Cre and the offspring from that colony crossed with hM4Di-flox or

hM3Dq-flox animals to manipulate (silence or activate) GAD expressing neurons within CTC network.

PV/DREADD approach feasible as a future treatment option?

Findings of the scientific observations always should direct towards their possibility of translation into clinical research i.e. the bench to bedside process. Many bench-side successes often get lost in translation. Several research groups have begun exploring the less invasive DREADD based methods. Some of them succeeded in extending this approach from rodents to non-human primates (Grayson et al., 2016; Upright et al., 2018; Bonaventura et al., 2019; Deffains et al., 2020). This should be considered as a milestone as it opens the doors towards human studies. In relation to PV/DREADD approach for anti-epileptic therapy, the safety and efficacy viral vector should be first considered before any clinical trials. However, interneuron-specific promoter small enough for virus (AAV)-based gene therapy is yet to be identified. Altogether, even if DREADD approach fails to deliver on the future therapeutic use, undoubtedly this technique will continue to help decipher the underlying mechanisms of seizure genesis helping us to understand the etiology of the disease and to develop more effective drugs.

6.6 Conclusion

Childhood absence epilepsy is most common form of pediatric epilepsy which is characterized by SWDs associated with impaired awareness. Imbalanced excitation/inhibition in the CTC network is regarded as the cause but precise mechanisms are still unclear and likely to be multifactorial. Pharmacological treatment methods are possible but are ineffective for one third of patients. Hence, patient specific treatment approaches are imperative to improve the quality of life of patients. However, designing novel and effective epilepsy treatments is always a challenge. This requires a deep understanding and identification of different cellular and molecular mechanisms underlying absence seizures. Analysis of patient-specific genetic mutations is also crucial to develop personalized treatments.

The work included in this thesis shed new light on the impact of functionally manipulating the most common GABAergic interneurons within the CTC network on absence seizure generation. This study also examined the expression level of enzyme synthesizing GABA (GADs) and proteins mediating its reuptake (GATs) which are also important in regulating inhibition. This study has

shown that functional disruption of FFI within the CTC microcircuit is one of the causative mechanisms for the generation absence seizures. Additionally, upregulation of one of the isoforms of GABA synthesizing enzyme i.e. GAD65 might be a compensatory or contributory mechanism for reduced FFI. These data could contribute towards an understanding of the underlying cellular and molecular mechanisms causing pathological CTC oscillations that could be targeted in the development of future treatment strategies for absence seizures.

References

- Aaberg, K.M., Surén, P., Søråas, C.L., Bakken, I.J., Lossius, M.I., Stoltenberg, C. and Chin, R., 2017. Seizures, syndromes, and etiologies in childhood epilepsy: the International League Against Epilepsy 1981, 1989, and 2017 classifications used in a population-based cohort. *Epilepsia*, 58(11), pp.1880-1891.
- Abou-Khalil, B., 2012. Antiepileptic drugs: advantages and disadvantages. In *Handbook of clinical neurology* (Vol. 108, pp. 723-739). Elsevier.
- Adams, N.C., Lozsádi, D.A. and Guillery, R.W., 1997. Complexities in the thalamocortical and corticothalamic pathways. *European journal of neuroscience*, 9(2), pp.204-209.
- Adotevi, N.K. and Leitch, B., 2016. Alterations in AMPA receptor subunit expression in cortical inhibitory interneurons in the epileptic stargazer mutant mouse. *Neuroscience*, 339, pp.124-138.
- Adotevi, N.K. and Leitch, B., 2017. Synaptic changes in AMPA receptor subunit expression in cortical parvalbumin interneurons in the stargazer model of absence epilepsy. *Frontiers in molecular neuroscience*, 10, pp.434.
- Adotevi, N.K. and Leitch, B., 2019. Cortical expression of AMPA receptors during postnatal development in a genetic model of absence epilepsy. *International journal of developmental neuroscience*, 73, pp.19-25.
- Agulhon, C., Fiacco, T.A. and McCarthy, K.D., 2010. Hippocampal short-and long-term plasticity are not modulated by astrocyte Ca²⁺ signalling. *Science*, 327(5970), pp.1250-1254.
- Agulhon, C., Boyt, K.M., Xie, A.X., Friocourt, F., Roth, B.L. and McCarthy, K.D., 2013. Modulation of the autonomic nervous system and behaviour by acute glial cell Gq protein-coupled receptor activation in vivo. *The Journal of physiology*, 591(22), pp.5599-5609.
- Akbarian, S., Kim, J.J., Potkin, S.G., Hagman, J.O., Tafazzoli, A., Bunney, W.E. and Jones, E.G., 1995. Gene expression for glutamic acid decarboxylase is reduced without loss of neurons in prefrontal cortex of schizophrenics. *Archives of general psychiatry*, 52(4), pp.258-266.

Aker, R.G., Özkara, Ç., Dervent, A. and Onat, F.Y., 2002. Enhancement of spike and wave discharges by microinjection of bicuculline into the reticular nucleus of rats with absence epilepsy. *Neuroscience letters*, 322(2), pp.71-74.

Aker, R.G., Özyurt, H.B., Yananli, H.R., Çakmak, Y.Ö., Özkaynakçı, A.E., Sehirli, Ü., Saka, E., Çavdar, S. and Onat, F.Y., 2006. GABAA receptor mediated transmission in the thalamic reticular nucleus of rats with genetic absence epilepsy shows regional differences: Functional implications. *Brain research*, 1111(1), pp.213-221.

Akgül, G. and McBain, C.J., 2016. Diverse roles for ionotropic glutamate receptors on inhibitory interneurons in developing and adult brain. *The Journal of physiology*, 594(19), pp.5471-5490.

Akman, O., Demiralp, T., Aker, R., Ateş, N. and Onat, F., 2008. A comparative study between two rat strains of absence epilepsy: morphology of spike-and-wave discharges. *Frontiers in Human Neuroscience*.

Akman, O., Demiralp, T., Ates, N. and Onat, F.Y., 2010. Electroencephalographic differences between WAG/Rij and GAERS rat models of absence epilepsy. *Epilepsy research*, 89(2-3), pp.185-193.

Aldrin-Kirk, P., Heuer, A., Wang, G., Mattsson, B., Lundblad, M., Parmar, M. and Björklund, T., 2016. DREADD modulation of transplanted DA neurons reveals a novel parkinsonian dyskinesia mechanism mediated by the serotonin 5-HT₆ receptor. *Neuron*, 90(5), pp.955-968.

Alexander, G.M., Rogan, S.C., Abbas, A.I., Armbruster, B.N., Pei, Y., Allen, J.A., Nonneman, R.J., Hartmann, J., Moy, S.S., Nicoletis, M.A. and McNamara, J.O., 2009. Remote control of neuronal activity in transgenic mice expressing evolved G protein-coupled receptors. *Neuron*, 63(1), pp.27-39.

Angeles, D.K., 1981. Proposal for revised clinical and electroencephalographic classification of epileptic seizures. *Epilepsia*, 22(4), pp.489-501.

Arai, R., Jacobowitz, D.M. and Deura, S., 1994. Distribution of calretinin, calbindin-D28k, and parvalbumin in the rat thalamus. *Brain research bulletin*, 33(5), pp.595-614.

Arain, F.M., Boyd, K.L. and Gallagher, M.J., 2012. Decreased viability and absence-like epilepsy in mice lacking or deficient in the GABAA receptor α 1 subunit. *Epilepsia*, 53(8), pp. e161-e165.

Arkan, S., Kasap, M., Akman, Ö., Akpınar, G., Ateş, N. and Karson, A., 2019. The lower expression of parvalbumin in the primary somatosensory cortex of WAG/Rij rats may facilitate the occurrence of absence seizures. *Neuroscience letters*, 709, p.134299.

Armbruster, B.N., Li, X., Pausch, M.H., Herlitze, S. and Roth, B.L., 2007. Evolving the lock to fit the key to create a family of G protein-coupled receptors potently activated by an inert ligand. *Proceedings of the national academy of sciences*, 104(12), pp.5163-5168.

- Arsov, T., Mullen, S.A., Rogers, S., Phillips, A.M., Lawrence, K.M., Damiano, J.A., Goldberg-Stern, H., Afawi, Z., Kivity, S., Trager, C. and Petrou, S., 2012. Glucose transporter 1 deficiency in the idiopathic generalized epilepsies. *Annals of neurology*, 72(5), pp.807-815.
- Arico, C., Bagley, E.E., Carrive, P., Assareh, N. and McNally, G.P., 2017. Effects of chemogenetic excitation or inhibition of the ventrolateral periaqueductal gray on the acquisition and extinction of Pavlovian fear conditioning. *Neurobiology of learning and memory*, 144, pp.186-197.
- Asada, H., Kawamura, Y., Maruyama, K., Kume, H., Ding, R.G., Ji, F.Y., Kanbara, N., Kuzume, H., Sanbo, M., Yagi, T. and Obata, K., 1996. Mice lacking the 65 kDa isoform of glutamic acid decarboxylase (GAD65) maintain normal levels of GAD67 and GABA in their brains but are susceptible to seizures. *Biochemical and biophysical research communications*, 229(3), pp.891-895.
- Asada, H., Kawamura, Y., Maruyama, K., Kume, H., Ding, R.G., Kanbara, N., Kuzume, H., Sanbo, M., Yagi, T. and Obata, K., 1997. Cleft palate and decreased brain γ -aminobutyric acid in mice lacking the 67-kDa isoform of glutamic acid decarboxylase. *Proceedings of the national academy of sciences*, 94(12), pp.6496-6499.
- Assaf, F. and Schiller, Y., 2016. The antiepileptic and ictogenic effects of optogenetic neurostimulation of PV-expressing interneurons. *Journal of neurophysiology*, 116(4), pp.1694-1704.
- Avanzini, G., De Curtis, M., Marescaux, C., Panzica, F., Spreafico, R. and Vergnes, M., 1992. Role of the thalamic reticular nucleus in the generation of rhythmic thalamo-cortical activities subserving spike and waves. In *Generalized Non-Convulsive Epilepsy: Focus on GABA-B Receptors* (pp. 85-95). Springer, Vienna.
- Avanzini, G., Vergnes, M., Spreafico, R. and Marescaux, C., 1993. Calcium-dependent regulation of genetically determined spike and waves by the reticular thalamic nucleus of rats. *Epilepsia*, 34(1), pp.1-7.
- Avaliani, N., Andersson, M., Runegaard, A.H., Woldbye, D. and Kokaia, M., 2016. DREADDs suppress seizure-like activity in a mouse model of pharmacoresistant epileptic brain tissue. *Gene therapy*, 23(10), pp.760-766.
- Avanzini, G., 1995. Animal models relevant to human epilepsies. *The italian journal of neurological sciences*, 16(1-2), pp.5-8.
- Avoli, M. and de Curtis, M., 2011. GABAergic synchronization in the limbic system and its role in the generation of epileptiform activity. *Progress in neurobiology*, 95(2), pp.104-132.
- Avoli, M., 2012. A brief history on the oscillating roles of thalamus and cortex in absence seizures. *Epilepsia*, 53(5), pp.779-789.

- Babaev, O., Chatain, C.P. and Krueger-Burg, D., 2018. Inhibition in the amygdala anxiety circuitry. *Experimental & molecular medicine*, 50(4), pp.1-16.
- Bai, X., Vestal, M., Berman, R., Negishi, M., Spann, M., Vega, C., Desalvo, M., Novotny, E.J., Constable, R.T. and Blumenfeld, H., 2010. Dynamic time course of typical childhood absence seizures: EEG, behaviour, and functional magnetic resonance imaging. *Journal of neuroscience*, 30(17), pp.5884-5893.
- Bai, X., Guo, J., Killory, B., Vestal, M., Berman, R., Negishi, M., Danielson, N., Novotny, E.J., Constable, R.T. and Blumenfeld, H., 2011. Resting functional connectivity between the hemispheres in childhood absence epilepsy. *Neurology*, 76(23), pp.1960-1967.
- Bailey, K.R., Crawley, J.N., 2009. Anxiety-related behaviors in mice. In *Methods of behavior analysis in neuroscience*, 2nd ed. (ed. Buccafusco JJ), CRC Press, Boca Raton, FL, USA.
- Bancaud, J., Physiopathogenesis of generalized epilepsies of organic nature (stereoencephalographic study). 1969. In: Gastaut H, Jasper HH, Bancaud J, Wasthregny A, eds. *The Physio pathogenesis of the Epilepsies*. Springfield, Ill: Charles C Thomas Publisher. 158-185
- Banerjee, P.N., Filippi, D. and Hauser, W.A., 2009. The descriptive epidemiology of epilepsy—a review. *Epilepsy research*, 85(1), pp.31-45.
- Barad, Z., Shevtsova, O., Arbuthnott, G.W. and Leitch, B., 2012. Selective loss of AMPA receptors at corticothalamic synapses in the epileptic stargazer mouse. *Neuroscience*, 217, pp.19-31.
- Barad, Z., Grattan, D.R. and Leitch, B., 2017. NMDA receptor expression in the thalamus of the stargazer model of absence epilepsy. *Scientific reports*, 7, pp. 42926.
- Bauer, J., 1996. Seizure-inducing effects of antiepileptic drugs: a review. *Acta neurologica scandinavica*, 94(6), pp.367-377.
- Bean, J.C., Lin, T.W., Sathyamurthy, A., Liu, F., Yin, D.M., Xiong, W.C. and Mei, L., 2014. Genetic labeling reveals novel cellular targets of schizophrenia susceptibility gene: distribution of GABA and non-GABA ErbB4-positive cells in adult mouse brain. *Journal of neuroscience*, 34(40), pp.13549-13566.
- Bear, M. F., Connors, B. W., and Paradiso, M. A. 2007. *Neuroscience*. Lippincott Williams & Wilkins.
- Beenhakker, M.P. and Huguenard, J.R., 2009. Neurons that fire together also conspire together: is normal sleep circuitry hijacked to generate epilepsy? *Neuron*, 62(5), pp.612-632.
- Beghi, E. and Giussani, G., 2018. Aging and the epidemiology of epilepsy. *Neuroepidemiology*, 51(3-4), pp.216-223.

- Bell, G.S., Neligan, A. and Sander, J.W., 2014. An unknown quantity—the worldwide prevalence of epilepsy. *Epilepsia*, 55(7), pp.958-962.
- Ben-Ari, Y., 2006. Basic developmental rules and their implications for epilepsy in the immature brain. *Epileptic disorders*, 8(2), pp.91-102.
- Bender, A.C., Morse, R.P., Scott, R.C., Holmes, G.L. and Lenck-Santini, P.P., 2012. SCN1A mutations in Dravet syndrome: impact of interneuron dysfunction on neural networks and cognitive outcome. *Epilepsy & behaviour*, 23(3), pp.177-186.
- Bennett, F.E., 1953. Intracarotid and intravertebral metrazol in petit mal epilepsy. *Neurology*, 3(9), pp.668-668.
- Benuzzi, F., Mirandola, L., Pugnaghi, M., Farinelli, V., Tassinari, C.A., Capovilla, G., Cantalupo, G., Beccaria, F., Nichelli, P. and Meletti, S., 2012. Increased cortical BOLD signal anticipates generalized spike and wave discharges in adolescents and adults with idiopathic generalized epilepsies. *Epilepsia*, 53(4), pp.622-630.
- Berdiev, R.K., Chepurinov, S.A., Veening, J.G., Chepurnova, N.E. and Van Luijtelaaar, G., 2007. The role of the nucleus basalis of Meynert and reticular thalamic nucleus in pathogenesis of genetically determined absence epilepsy in rats: a lesion study. *Brain research*, 1185, pp.266-274.
- Berg, A.T., Berkovic, S.F., Brodie, M.J., Buchhalter, J., Cross, J.H., van Emde Boas, W., Engel, J., French, J., Glauser, T.A., Mathern, G.W. and Moshé, S.L., 2010. Revised terminology and concepts for organization of seizures and epilepsies: report of the ILAE Commission on Classification and Terminology, 2005–2009. *Epilepsia*, 51(4), pp.676-685.
- Berkovic, S.F., 1997. Epilepsy genes and the genetics of epilepsy syndromes: the promise of new therapies based on genetic knowledge. *Epilepsia*, 38, pp.S32-S36.
- Berkovic, S.F., Howell, R.A., Hay, D.A. and Hopper, J.L., 1998. Epilepsies in twins: genetics of the major epilepsy syndromes. *Annals of neurology*, 43(4), pp.435-445.
- Berman, R., Negishi, M., Vestal, M., Spann, M., Chung, M.H., Bai, X., Purcaro, M., Motelow, J.E., Danielson, N., Dix-Cooper, L. and Enev, M., 2010. Simultaneous EEG, fMRI, and behaviour in typical childhood absence seizures. *Epilepsia*, 51(10), pp.2011-2022.
- Bernstein, E.M. and Quick, M.W., 1999. Regulation of γ -aminobutyric acid (GABA) transporters by extracellular GABA. *Journal of biological chemistry*, 274(2), pp.889-895.
- Bezaire, M.J. and Soltesz, I., 2013. Quantitative assessment of CA1 local circuits: knowledge base for interneuron-pyramidal cell connectivity. *Hippocampus*, 23(9), pp.751-785.
- Bianchi A., 1995. Study of concordance of symptoms in families with absence epilepsies. In: Typical Absences and Related Epileptic Syndromes (Duncan JS, Panayiotopoulos CP, eds), pp. 328–337. London: Churchill Livingstone.

- Bicks, L.K., Yamamuro, K., Flanigan, M.E., Kim, J.M., Kato, D., Lucas, E.K., Koike, H., Peng, M.S., Brady, D.M., Chandrasekaran, S. and Norman, K.J., 2020. Prefrontal parvalbumin interneurons require juvenile social experience to establish adult social behaviour. *Nature communications*, 11(1), pp.1-15.
- Blumenfeld, H., 2002. The thalamus and seizures. *Archives of neurology*, 59(1), pp.135-137.
- Bode, H., 1992. Intracranial blood flow velocities during seizures and generalized epileptic discharges. *European journal of paediatrics*, 151(9), pp.706-709.
- Bonaventura, J., Eldridge, M.A., Hu, F., Gomez, J.L., Sanchez-Soto, M., Abramyan, A.M., Lam, S., Boehm, M.A., Ruiz, C., Farrell, M.R. and Moreno, A., 2019. High-potency ligands for DREADD imaging and activation in rodents and monkeys. *Nature communications*, 10(1), pp.1-12.
- Bouilleret, V., Schwaller, B., Schurmans, S., Celio, M.R. and Fritschy, J.M., 2000a. Neurodegenerative and morphogenic changes in a mouse model of temporal lobe epilepsy do not depend on the expression of the calcium-binding proteins parvalbumin, calbindin, or calretinin. *Neuroscience*, 97(1), pp.47-58.
- Bouilleret, V., Loup, F., Kiener, T., Marescaux, C. and Fritschy, J.M., 2000b. Early loss of interneurons and delayed subunit-specific changes in GABAA-receptor expression in a mouse model of mesial temporal lobe epilepsy. *Hippocampus*, 10(3), pp.305-324.
- Bomben, V.C., Aiba, I., Qian, J., Mark, M.D., Herlitze, S. and Noebels, J.L., 2016. Isolated P/Q calcium channel deletion in layer VI corticothalamic neurons generates absence epilepsy. *Journal of neuroscience*, 36(2), pp.405-418.
- Bouma, P.A.D., Westendorp, R.G.J., Van Dijk, J.G., Peters, A.C.B. and Brouwer, O.F., 1996. The outcome of absence epilepsy: a meta-analysis. *Neurology*, 47(3), pp.802-808.
- Bragina, L., Marchionni, I., Omrani, A., Cozzi, A., Pellegrini-Giampietro, D.E., Cherubini, E. and Conti, F., 2008. GAT-1 regulates both tonic and phasic GABAA receptor-mediated inhibition in the cerebral cortex. *Journal of neurochemistry*, 105(5), pp.1781-1793.
- Braitenberg, V. and Schutz, A., 1991. Anatomy of the cortex: studies of brain function.
- Brodie, M.J., 2003. The history and stigma of epilepsy. *Epilepsia*, 44, pp.12-14.
- Brust, R.D., Corcoran, A.E., Richerson, G.B., Nattie, E. and Dymecki, S.M., 2014. Functional and developmental identification of a molecular subtype of brain serotonergic neuron specialized to regulate breathing dynamics. *Cell reports*, 9(6), pp.2152-2165.
- Bruysters, M., Jongejan, A., Akdemir, A., Bakker, R.A. and Leurs, R., 2005. A Gq/11-coupled mutant histamine H1 receptor F435A activated solely by synthetic ligands (RASSL). *Journal of biological chemistry*, 280(41), pp.34741-34746.

- Buzsáki, G., 1991. The thalamic clock: emergent network properties. *Neuroscience*, 41(2-3), pp.351-364.
- Caccavano, A., Bozzelli, P.L., Forcelli, P.A., Pak, D.T., Wu, J.Y., Conant, K. and Vicini, S., 2020. Inhibitory parvalbumin basket cell activity is selectively reduced during hippocampal sharp wave ripples in a mouse model of familial Alzheimer's disease. *Journal of neuroscience*.
- Călin, A., Stancu, M., Zagrean, A.M., Jefferys, J.G., Ilie, A.S. and Akerman, C.J., 2018. Chemogenetic recruitment of specific interneurons suppresses seizure activity. *Frontiers in cellular neuroscience*, 12, p.293.
- Camfield, C.S., Camfield, P.R., Gordon, K., Wirrell, E. and Dooley, J.M., 1996. Incidence of epilepsy in childhood and adolescence: a population-based study in Nova Scotia from 1977 to 1985. *Epilepsia*, 37(1), pp.19-23.
- Camfield, C.S., Berg, A., Stephani, U. and Wirrell, E.C., 2014. Transition issues for benign epilepsy with centrotemporal spikes, non-lesional focal epilepsy in otherwise normal children, childhood absence epilepsy, and juvenile myoclonic epilepsy. *Epilepsia*, 55, pp.16-20.
- Cammarota, M., Losi, G., Chiavegato, A., Zonta, M. and Carmignoto, G., 2013. Fast spiking interneuron control of seizure propagation in a cortical slice model of focal epilepsy. *The journal of physiology*, 591(4), pp.807-822.
- Caplan, R., Siddarth, P., Stahl, L., Lanphier, E., Vona, P., Gurbani, S., Koh, S., Sankar, R. and Shields, W.D., 2008. Childhood absence epilepsy: behavioural, cognitive, and linguistic comorbidities. *Epilepsia*, 49(11), pp.1838-1846.
- Carlen, M., Meletis, K., Siegle, J.H., Cardin, J.A., Futai, K., Vierling-Claassen, D., Ruehlmann, C., Jones, S.R., Deisseroth, K., Sheng, M.I.M.C. and Moore, C.I., 2012. A critical role for NMDA receptors in parvalbumin interneurons for gamma rhythm induction and behaviour. *Molecular psychiatry*, 17(5), pp.537-548.
- Carney, P.W., Masterton, R.A., Harvey, A.S., Scheffer, I.E., Berkovic, S.F. and Jackson, G.D., 2010. The core network in absence epilepsy: differences in cortical and thalamic BOLD response. *Neurology*, 75(10), pp.904-911.
- Carter, M. and Shieh, J.C., 2015. *Guide to research techniques in neuroscience*. Academic Press.
- Celio, M.R. and Heizmann, C.W., 1981. Calcium-binding protein parvalbumin as a neuronal marker. *Nature*, 293(5830), pp.300-302.
- Celio, M.R., 1984. Parvalbumin as a marker of fast firing neurons. *Neuroscience letters supplement*, 18, p.S332.
- Celio, M.R., 1986. Parvalbumin in most gamma-aminobutyric acid-containing neurons of the rat cerebral cortex. *Science*, 231(4741), pp.995-997.

- Chahboune, H., Mishra, A.M., DeSalvo, M.N., Staib, L.H., Purcaro, M., Scheinost, D., Papademetris, X., Fyson, S.J., Lorincz, M.L., Crunelli, V. and Hyder, F., 2009. DTI abnormalities in anterior corpus callosum of rats with spike-wave epilepsy. *Neuroimage*, 47(2), pp.459-466.
- Chattopadhyaya, B., Di Cristo, G., Wu, C.Z., Knott, G., Kuhlman, S., Fu, Y., Palmiter, R.D. and Huang, Z.J., 2007. GAD67-mediated GABA synthesis and signalling regulate inhibitory synaptic innervation in the visual cortex. *Neuron*, 54(6), pp.889-903.
- Cheah, C.S., Frank, H.Y., Westenbroek, R.E., Kalume, F.K., Oakley, J.C., Potter, G.B., Rubenstein, J.L. and Catterall, W.A., 2012. Specific deletion of NaV1.1 sodium channels in inhibitory interneurons causes seizures and premature death in a mouse model of Dravet syndrome. *Proceedings of the national academy of sciences*, 109(36), pp.14646-14651.
- Chen, L., Chetkovich, D.M., Petralia, R.S., Sweeney, N.T., Kawasaki, Y., Wenthold, R.J., Brecht, D.S. and Nicoll, R.A., 2000. Stargazin regulates synaptic targeting of AMPA receptors by two distinct mechanisms. *Nature*, 408(6815), pp.936-943.
- Chen, Y., Lu, J., Pan, H., Zhang, Y., Wu, H., Xu, K., Liu, X., Jiang, Y., Bao, X., Yao, Z. and Ding, K., 2003. Association between genetic variation of CACNA1H and childhood absence epilepsy. *Annals of neurology*, 54(2), pp.239-243.
- Chen, Y., Xiong, M., Dong, Y., Haberman, A., Cao, J., Liu, H., Zhou, W. and Zhang, S.C., 2016. Chemical control of grafted human PSC-derived neurons in a mouse model of Parkinson's disease. *Cell stem cell*, 18(6), pp.817-826.
- Chen, C.C., Lu, J., Yang, R., Ding, J.B. and Zuo, Y., 2018. Selective activation of parvalbumin interneurons prevents stress-induced synapse loss and perceptual defects. *Molecular psychiatry*, 23(7), pp.1614-1625.
- Chiu, C.S., Brickley, S., Jensen, K., Southwell, A., Mckinney, S., Cull-Candy, S., Mody, I. and Lester, H.A., 2005. GABA transporter deficiency causes tremor, ataxia, nervousness, and increased GABA-induced tonic conductance in cerebellum. *Journal of neuroscience*, 25(12), pp.3234-3245.
- Chung, W.K., Shin, M., Jaramillo, T.C., Leibel, R.L., LeDuc, C.A., Fischer, S.G., Tzilianos, E., Gheith, A.A., Lewis, A.S. and Chetkovich, D.M., 2009. Absence epilepsy in apathetic, a spontaneous mutant mouse lacking the h channel subunit, HCN2. *Neurobiology of disease*, 33(3), pp.499-508.
- Cisneros-Franco, J.M., Thomas, M.E., Regragui, I., Lane, C.P., Ouellet, L. and de Villers-Sidani, E., 2020. Regulation of perceptual learning by chronic chemogenetic manipulation of parvalbumin-positive interneurons. *bioRxiv*.
- Clark, J.A., Deutch, A.Y., Gallipoli, P.Z. and Amara, S.G., 1992. Functional expression and CNS distribution of a β -alanine-sensitive neuronal GABA transporter. *Neuron*, 9(2), pp.337-348.

- Clemens, B., Puskas, S., Bessenyey, M., Emri, M., Spisák, T., Koselák, M., Hollódy, K., Fogarasi, A., Kondákor, I., Füle, K. and Bense, K., 2011. EEG functional connectivity of the intrahemispheric cortico-cortical network of idiopathic generalized epilepsy. *Epilepsy research*, 96(1-2), pp.11-23.
- Clemente-Perez, A., Makinson, S.R., Higashikubo, B., Brovarney, S., Cho, F.S., Urry, A., Holden, S.S., Wimer, M., Dávid, C., Fenno, L.E. and Acsády, L., 2017. Distinct thalamic reticular cell types differentially modulate normal and pathological cortical rhythms. *Cell reports*, 19(10), pp.2130-2142.
- Cnaan, A., Shinnar, S., Arya, R., Adamson, P.C., Clark, P.O., Dlugos, D., Hirtz, D.G., Masur, D., Glauser, T.A. and Childhood Absence Epilepsy Study Group, 2017. Second monotherapy in childhood absence epilepsy. *Neurology*, 88(2), pp.182-190.
- Coenen, A.M.L., Drinkenburg, W.H.I.M., Inoue, M. and Van Luijtelaar, E.L.J.M., 1992. Genetic models of absence epilepsy, with emphasis on the WAG/Rij strain of rats. *Epilepsy research*, 12(2), pp.75-86.
- Coenen, A.M.L. and Van Luijtelaar, E.L.J.M., 2003. Genetic animal models for absence epilepsy: a review of the WAG/Rij strain of rats. *Behaviour genetics*, 33(6), pp.635-655.
- Cohen, S.M., Tsien, R.W., Goff, D.C. and Halassa, M.M., 2015. The impact of NMDA receptor hypofunction on GABAergic neurons in the pathophysiology of schizophrenia. *Schizophrenia research*, 167(1-3), pp.98-107.
- Conn, P.J., Jones, C.K. and Lindsley, C.W., 2009. Subtype-selective allosteric modulators of muscarinic receptors for the treatment of CNS disorders. *Trends in pharmacological sciences*, 30(3), pp.148-155.
- Condie, B.G., Bain, G., Gottlieb, D.I. and Capecchi, M.R., 1997. Cleft palate in mice with a targeted mutation in the γ -aminobutyric acid-producing enzyme glutamic acid decarboxylase 67. *Proceedings of the national academy of sciences*, 94(21), pp.11451-11455.
- Conti, F., Minelli, A. and Melone, M., 2004. GABA transporters in the mammalian cerebral cortex: localization, development and pathological implications. *Brain research reviews*, 45(3), pp.196-212.
- Cope, D.W., Di Giovanni, G., Fyson, S.J., Orbán, G., Errington, A.C., Lőrincz, M.L., Gould, T.M., Carter, D.A. and Crunelli, V., 2009. Enhanced tonic GABA A inhibition in typical absence epilepsy. *Nature medicine*, 15(12), p.1392.
- Cordella, A., Krashia, P., Nobili, A., Pignataro, A., La Barbera, L., Viscomi, M.T., Valzania, A., Keller, F., Ammassari-Teule, M., Mercuri, N.B. and Berretta, N., 2018. Dopamine loss alters the hippocampus-nucleus accumbens synaptic transmission in the Tg2576 mouse model of Alzheimer's disease. *Neurobiology of disease*, 116, pp.142-154.

- Coulter, D.A. and Lee, C.J., 1993. Thalamocortical rhythm generation in vitro: extra- and intracellular recordings in mouse thalamocortical slices perfused with low Mg²⁺ medium. *Brain research*, 631(1), pp.137-142.
- Cowan, R.L., Wilson, C.J., Emson, P.C. and Heizmann, C.W., 1990. Parvalbumin-containing GABAergic interneurons in the rat neostriatum. *Journal of comparative neurology*, 302(2), pp.197-205.
- Coward, P., Wada, H.G., Falk, M.S., Chan, S.D., Meng, F., Akil, H. and Conklin, B.R., 1998. Controlling signaling with a specifically designed Gi-coupled receptor. *Proceedings of the national academy of sciences*, 95(1), pp.352-357.
- Cox, C.L., Huguenard, J.R. and Prince, D.A., 1996. Heterogeneous axonal arborizations of rat thalamic reticular neurons in the ventrobasal nucleus. *Journal of comparative neurology*, 366(3), pp.416-430.
- Crunelli, V. and Leresche, N., 2002a. Childhood absence epilepsy: genes, channels, neurons and networks. *Nature reviews neuroscience*, 3(5), pp.371-382.
- Crunelli, V. and Leresche, L., 2002b. Block of thalamic T-type Ca²⁺ channels by ethosuximide is not the whole story. *Epilepsy currents*, 2(2), pp.53-56.
- Crunelli, V., Lőrincz, M.L., McCafferty, C., Lambert, R.C., Leresche, N., Di Giovanni, G. and David, F., 2020. Clinical and experimental insight into pathophysiology, comorbidity and therapy of absence seizures. *Brain*, 143(8), pp.2341-2368.
- Csillik, B., Mihály, A., Krisztin-Péva, B., Chadaide, Z., Samsam, M., Knyihár-Csillik, E. and Fenyó, R., 2005. GABAergic parvalbumin-immunoreactive large caliciform presynaptic complexes in the reticular nucleus of the rat thalamus. *Journal of chemical neuroanatomy*, 30(1), pp.17-26.
- Cybulska-Klosowicz, A., Posluszny, A., Nowak, K., Siucinska, E., Kossut, M. and Liguz-Leczna, M., 2013. Interneurons containing somatostatin are affected by learning-induced cortical plasticity. *Neuroscience*, 254, pp.18-25.
- Cybulski, N., and Jelenska-Macieszyna, 1914. Action currents of the cerebral cortex. *Bulletin International de l'Academie des Sciences de Cracovie B*, pp.776-81.
- Czeiger, D. and White, E.L., 1997. Comparison of the distribution of parvalbumin-immunoreactive and other synapses onto the somata of callosal projection neurons in mouse visual and somatosensory cortex. *Journal of comparative neurology*, 379(2), pp.198-210.
- Dalby, N.O., 2000. GABA-level increasing and anticonvulsant effects of three different GABA uptake inhibitors. *Neuropharmacology*, 39(12), pp.2399-2407.

- D'Amore, V., 2016. *The role of group I metabotropic glutamate receptors in absence epilepsy* (Doctoral dissertation).
- Danover, L., Deransart, C., Depaulis, A., Vergnes, M. and Marescaux, C., 1998. Pathophysiological mechanisms of genetic absence epilepsy in the rat. *Progress in neurobiology*, 55(1), pp.27-57.
- Dávid, C., Schleicher, A., Zuschratter, W. and Staiger, J.F., 2007. The innervation of parvalbumin-containing interneurons by VIP-immunopositive interneurons in the primary somatosensory cortex of the adult rat. *European journal of neuroscience*, 25(8), pp.2329-2340.
- De Curtis, M. and Gnatkovsky, V., 2009. Re-evaluating the mechanisms of focal ictogenesis: the role of low-voltage fast activity. *Epilepsia*, 50(12), pp.2514-2525.
- Deffains, M., Hai Nguyen, T., Orignac, H., Biendon, N., Dovero, S., Bezard, E. and Boraud, T., 2020. In vivo electrophysiological validation of DREADD-based modulation of pallidal neurons in the non-human primate. *European journal of neuroscience*.
- Deisseroth, K., Feng, G., Majewska, A.K., Miesenböck, G., Ting, A. and Schnitzer, M.J., 2006. Next-generation optical technologies for illuminating genetically targeted brain circuits. *Journal of neuroscience*, 26(41), pp.10380-10386.
- Delevich, K., Tucciarone, J., Huang, Z.J. and Li, B., 2015. The mediodorsal thalamus drives feedforward inhibition in the anterior cingulate cortex via parvalbumin interneurons. *Journal of neuroscience*, 35(14), pp.5743-5753.
- de Freitas, M.L., Mello, F.K., de Souza, T.L., Grauncke, A.C.B., Figuera, M.R., Royes, L.F.F., Furian, A.F. and Oliveira, M.S., 2018. Anticonvulsant-like effect of thromboxane receptor agonist U-46619 against pentylenetetrazol-induced seizures. *Epilepsy research*, 146, pp.137-143.
- Delfs, J.M., Ciaramitaro, V.M., Soghomonian, J.J. and Chesselet, M.F., 1996. Unilateral nigrostriatal lesions induce a bilateral increase in glutamate decarboxylase messenger RNA in the reticular thalamic nucleus. *Neuroscience*, 71(2), pp.383-395.
- del Río, M.R. and DeFelipe, J., 1994. A study of SMI 32-stained pyramidal cells, parvalbumin-immunoreactive chandelier cells, and presumptive thalamocortical axons in the human temporal neocortex. *Journal of comparative neurology*, 342(3), pp.389-408.
- Dell'Anno, M.T., Caiazzo, M., Leo, D., Dvoretzkova, E., Medrihan, L., Colasante, G., Giannelli, S., Theka, I., Russo, G., Mus, L. and Pezzoli, G., 2014. Remote control of induced dopaminergic neurons in parkinsonian rats. *The Journal of clinical investigation*, 124(7), pp.3215-3229.
- de Oliveira, C.V., Grigoletto, J., Funck, V.R., Ribeiro, L.R., Royes, L.F.F., Figuera, M.R., Furian, A.F. and Oliveira, M.S., 2015. Evaluation of potential gender-related differences in behavioral and cognitive alterations following pilocarpine-induced status epilepticus in C57BL/6 mice. *Physiology & behaviour*, 143, pp.142-150.

- Depaulis, A. and Charpier, S., 2018. Pathophysiology of absence epilepsy: Insights from genetic models. *Neuroscience letters*, 667, pp.53-65.
- Desloovere, J., Boon, P., Larsen, L.E., Merckx, C., Goossens, M.G., Van den Haute, C., Baekelandt, V., De Bundel, D., Carrette, E., Delbeke, J. and Meurs, A., 2019. Long-term chemogenetic suppression of spontaneous seizures in a mouse model for temporal lobe epilepsy. *Epilepsia*, 60(11), pp.2314-2324.
- De Talamoni, N., Smith, C.A., Wasserman, R.H., Beltramino, C., Fullmer, C.S. and Penniston, J.T., 1993. Immunocytochemical localization of the plasma membrane calcium pump, calbindin-D28k, and parvalbumin in Purkinje cells of avian and mammalian cerebellum. *Proceedings of the national academy of sciences*, 90(24), pp.11949-11953.
- Devienne, G., Picaud, S., Cohen, I., Piquet, J., Tricoire, L., Testa, D., Di Nardo, A., Rossier, J., Cauli, B. and Lambolez, B., 2019. Regulation of perineuronal nets in the adult cortex by the electrical activity of parvalbumin interneurons. *bioRxiv*, pp. 671719
- Digby, G.J., Lober, R.M., Sethi, P.R. and Lambert, N.A., 2006. Some G protein heterotrimers physically dissociate in living cells. *Proceedings of the national academy of sciences*, 103(47), pp.17789-17794.
- Digby, G.J., Noetzel, M.J., Bubser, M., Utley, T.J., Walker, A.G., Byun, N.E., Lebois, E.P., Xiang, Z., Sheffler, D.J., Cho, H.P. and Davis, A.A., 2012. Novel allosteric agonists of M1 muscarinic acetylcholine receptors induce brain region-specific responses that correspond with behavioral effects in animal models. *Journal of neuroscience*, 32(25), pp.8532-8544.
- Dikow, N., Maas, B., Karch, S., Granzow, M., Janssen, J.W., Jauch, A., Hinderhofer, K., Sutter, C., Schubert-Bast, S., Anderlid, B.M. and Dallapiccola, B., 2014. 3p25.3 microdeletion of GABA transporters SLC6A1 and SLC6A11 results in intellectual disability, epilepsy and stereotypic behaviour. *American journal of medical genetics Part A*, 164(12), pp.3061-3068.
- Ding, D., Wang, W., Wu, J., Ma, G., Dai, X., Yang, B., Wang, T., Yuan, C., Hong, Z., de Boer, H.M. and Prilipko, L., 2006. Premature mortality in people with epilepsy in rural China: a prospective study. *The lancet neurology*, 5(10), pp.823-827.
- Ding, J. and Delpire, E., 2014. Deletion of KCC3 in parvalbumin neurons leads to locomotor deficit in a conditional mouse model of peripheral neuropathy associated with agenesis of the corpus callosum. *Behavioural brain research*, 274, pp.128-136.
- Dobrzanski, G. and Kossut, M., 2017. Application of the DREADD technique in biomedical brain research. *Pharmacological reports*, 69(2), pp.213-221.
- Donato, F., Rompani, S.B. and Caroni, P., 2013. Parvalbumin-expressing basket-cell network plasticity induced by experience regulates adult learning. *Nature*, 504(7479), pp.272-276.

- Douglas, R., Koch, C., Mahowald, M. and Martin, K., 1999. The role of recurrent excitation in neocortical circuits. In *Models of cortical circuits*, pp. 251-282. Springer, Boston, MA.
- Doyle, J., Ren, X., Lennon, G. and Stubbs, L., 1997. Mutations in the Cacn11a4 calcium channel gene are associated with seizures, cerebellar degeneration, and ataxia in tottering and leaner mutant mice. *Mammalian genome*, 8(2), pp.113-120.
- Dreifuss, F.E., Martinez-Lage, M. and Johns, R.A., 1985. Proposal for classification of epilepsies and epileptic syndromes. *Epilepsia*, 26(3), pp.268-278.
- Drexel, M., Romanov, R.A., Wood, J., Weger, S., Heilbronn, R., Wulff, P., Tasan, R.O., Harkany, T. and Sperk, G., 2017. Selective silencing of hippocampal parvalbumin interneurons induces development of recurrent spontaneous limbic seizures in mice. *Journal of neuroscience*, 37(34), pp.8166-8179.
- Drexel, M., Bukovac, A., Tasan, R. O., Sperk, G., 2019. Permanent functional silencing of hippocampal parvalbumin- or somatostatin-interneurons induces epilepsy. In *Society for neuroscience, 2019*.
- Duncan, J.S., 2011. The evolving classification of seizures and epilepsies. *Epilepsia*, 52(6), pp.1204-1205.
- Durá, T.T. and Yoldi, M.P., 2006, Typical absence seizure: epidemiological and clinical characteristics and outcome. In *Anales de pediatria (Barcelona, Spain: 2003)* (Vol. 64, No. 1, pp. 28-33).
- Durkin, M.M., Smith, K.E., Borden, L.A., Weinshank, R.L., Branchek, T.A. and Gustafson, E.L., 1995. Localization of messenger RNAs encoding three GABA transporters in rat brain: an in situ hybridization study. *Molecular brain research*, 33(1), pp.7-21.
- Dutton, S.B., Makinson, C.D., Papale, L.A., Shankar, A., Balakrishnan, B., Nakazawa, K. and Escayg, A., 2013. Preferential inactivation of Scn1a in parvalbumin interneurons increases seizure susceptibility. *Neurobiology of disease*, 49, pp.211-220.
- Eldridge, M.A., Lerchner, W., Saunders, R.C., Kaneko, H., Krausz, K.W., Gonzalez, F.J., Ji, B., Higuchi, M., Minamimoto, T. and Richmond, B.J., 2016. Chemogenetic disconnection of monkey orbitofrontal and rhinal cortex reversibly disrupts reward value. *Nature neuroscience*, 19(1), pp.37-39.
- Engel Jr, J., Lubens, P., Kuhl, D.E. and Phelps, M.E., 1985. Local cerebral metabolic rate for glucose during petit mal absences. *Annals of Neurology*, 17(2), pp.121-128.
- Engel, J., 1996. Excitation and inhibition in epilepsy. *Canadian journal of neurological sciences*, 23(3), pp.167-174.

- Engel, J. and Pedley, T. A., 1997. *Epilepsy: a comprehensive textbook*. Philadelphia, Lippincott-Raven.
- English, J.G. and Roth, B.L., 2015. Chemogenetics—a transformational and translational platform. *JAMA neurology*, 72(11), pp.1361-1366.
- Erbayat-Altay, E., Yamada, K.A., Wong, M. and Thio, L.L., 2008. Increased severity of pentylentetrazol induced seizures in leptin deficient ob/ob mice. *Neuroscience letters*, 433(2), pp.82-86.
- Erlander, M. G., Tillakaratne, N. J. K., Feldblum, S., Patel, N. & Tobin, A. J., 1991. Two genes encode distinct glutamate decarboxylases. *Neuron* 7, pp. 91–100.
- Errington, A.C., Cope, D.W. and Crunelli, V., 2011. Augmentation of tonic GABAA inhibition in absence epilepsy: therapeutic value of inverse agonists at extrasynaptic GABAA receptors. *Advances in pharmacological sciences*, 2011.
- Esclapez, M., Tillakaratne, N.J., Tobin, A.J. and Houser, C.R., 1993. Comparative localization of mRNAs encoding two forms of glutamic acid decarboxylase with nonradioactive in situ hybridization methods. *Journal of comparative neurology*, 331(3), pp.339-362.
- Esclapez, M. and Houser, C.R., 1999. Up-regulation of GAD65 and GAD67 in remaining hippocampal GABA neurons in a model of temporal lobe epilepsy. *Journal of comparative neurology*, 412(3), pp.488-505.
- Espinosa, F., Torres-Vega, M.A., Marks, G.A. and Joho, R.H., 2008. Ablation of Kv3. 1 and Kv3. 3 potassium channels disrupt thalamocortical oscillations in vitro and in vivo. *Journal of neuroscience*, 28(21), pp.5570-5581.
- Ettinger, A.B., Bernal, O.G., Andriola, M.R., Bagchi, S., Flores, P., Just, C., Pitocco, C., Rooney, T., Tuominen, J. and Devinsky, O., 1999. Two cases of nonconvulsive status epilepticus in association with tiagabine therapy. *Epilepsia*, 40(8), pp.1159-1162.
- Everett, K.V., Chioza, B., Aicardi, J., Aschauer, H., Brouwer, O., Callenbach, P., Covanis, A., Dulac, O., Eeg-Olofsson, O., Feucht, M. and Friis, M., 2007a. Linkage and association analysis of CACNG3 in childhood absence epilepsy. *European journal of human genetics*, 15(4), pp.463-472.
- Everett, K., Chioza, B., Aicardi, J., Aschauer, H., Brouwer, O., Callenbach, P., Covanis, A., Dooley, J., Dulac, O., Durner, M. and Eeg-Olofsson, O., 2007b. Linkage and mutational analysis of CLCN2 in childhood absence epilepsy. *Epilepsy research*, 75(2-3), pp.145-153.
- Faghihi, N. and Mohammadi, M.T., 2017. Anticonvulsant and Antioxidant Effects of Pitavastatin Against Pentylentetrazol-Induced Kindling in Mice. *Advanced pharmaceutical bulletin*, 7(2), p.291.

- Falco-Walter, J.J., Scheffer, I.E. and Fisher, R.S., 2018. The new definition and classification of seizures and epilepsy. *Epilepsy research*, 139, pp.73-79.
- Farré-Castany, M.A., Schwaller, B., Gregory, P., Barski, J., Mariethoz, C., Eriksson, J.L., Tetko, I.V., Wolfer, D., Celio, M.R., Schmutz, I. and Albrecht, U., 2007. Differences in locomotor behavior revealed in mice deficient for the calcium-binding proteins parvalbumin, calbindin D-28k or both. *Behavioural brain research*, 178(2), pp.250-261.
- Farrell, M.S., Pei, Y., Wan, Y., Yadav, P.N., Daigle, T.L., Urban, D.J., Lee, H.M., Sciaky, N., Simmons, A., Nonneman, R.J. and Huang, X.P., 2013. AG α s DREADD Mouse for Selective Modulation of cAMP Production in Striato-pallidal Neurons. *Neuropsychopharmacology*, 38(5), pp.854-862.
- Fattorini, G., Melone, M., Sánchez-Gómez, M.V., Arellano, R.O., Bassi, S., Matute, C. and Conti, F., 2017. GAT-1 mediated GABA uptake in rat oligodendrocytes. *Glia*, 65(3), pp.514-522.
- Fattorini, G., Catalano, M., Melone, M., Serpe, C., Bassi, S., Limatola, C. and Conti, F., 2020. Microglial expression of GAT-1 in the cerebral cortex. *Glia*, 68(3), pp.646-655.
- Fenno, L., Yizhar, O. and Deisseroth, K., 2011. The development and application of optogenetics. *Annual review of neuroscience*, 34, pp.389-412.
- Ferguson, S.M., Phillips, P.E., Roth, B.L., Wess, J. and Neumaier, J.F., 2013. Direct-pathway striatal neurons regulate the retention of decision-making strategies. *Journal of Neuroscience*, 33(28), pp.11668-11676.
- Ferguson, S.M. and Neumaier, J.F., 2015. Using DREADDs to investigate addiction behaviors. *Current opinion in behavioural sciences*, 2, pp.69-72.
- Ferguson, B.R. and Gao, W.J., 2018. PV interneurons: critical regulators of E/I balance for prefrontal cortex-dependent behaviour and psychiatric disorders. *Frontiers in neural circuits*, 12, p.37.
- Ferrie, C.D., 2010. Terminology and organization of seizures and epilepsies: radical changes not justified by new evidence. *Epilepsia*, 51(4), pp.713-714.
- Feucht, M., Fuchs, K., Pichlbauer, E., Hornik, K., Scharfetter, J., Goessler, R., Füreder, T., Cvetkovic, N., Sieghart, W., Kasper, S. and Aschauer, H., 1999. Possible association between childhood absence epilepsy and the gene encoding GABRB3. *Biological psychiatry*, 46(7), pp.997-1002.
- Fiest, K.M., Sauro, K.M., Wiebe, S., Patten, S.B., Kwon, C.S., Dykeman, J., Pringsheim, T., Lorenzetti, D.L. and Jetté, N., 2017. Prevalence and incidence of epilepsy: a systematic review and meta-analysis of international studies. *Neurology*, 88(3), pp.296-303.

- Filice, F., Vörckel, K.J., Sungur, A.Ö., Wöhr, M. and Schwaller, B., 2016. Reduction in parvalbumin expression not loss of the parvalbumin-expressing GABA interneuron subpopulation in genetic parvalbumin and shank mouse models of autism. *Molecular brain*, 9(1), p.10.
- Fishell, G., 2007. Perspectives on the developmental origins of cortical interneuron diversity. In *Novartis Foundation symposium*, 288, pp. 21-35.
- Fishell, G. and Dimidschstein, J., New York University, 2018. Compositions and method for reducing seizures. *U.S. Patent Application* 15/561,547.
- Fisher, R.S., Boas, W.V.E., Blume, W., Elger, C., Genton, P., Lee, P. and Engel Jr, J., 2005. Epileptic seizures and epilepsy: definitions proposed by the International League Against Epilepsy (ILAE) and the International Bureau for Epilepsy (IBE). *Epilepsia*, 46(4), pp.470-472.
- Fisher, R.S., Acevedo, C., Arzimanoglou, A., Bogacz, A. and CrossH, E., 2014. A practical clinical definition of epilepsy. *Epilepsia*, 55(4), pp.475-82.
- Fisher, R.S., 2017. The new classification of seizures by the International League Against Epilepsy 2017. *Current neurology and neuroscience reports*, 17(6), p.48.
- Fisher, R.S., Cross, J.H., French, J.A., Higurashi, N., Hirsch, E., Jansen, F.E., Lagae, L., Moshé, S.L., Peltola, J., Roulet Perez, E. and Scheffer, I.E., 2017a. Operational classification of seizure types by the International League Against Epilepsy: Position Paper of the ILAE Commission for Classification and Terminology. *Epilepsia*, 58(4), pp.522-530.
- Fisher, R.S., Cross, J.H., D'souza, C., French, J.A., Haut, S.R., Higurashi, N., Hirsch, E., Jansen, F.E., Lagae, L., Moshé, S.L. and Peltola, J., 2017b. Instruction manual for the ILAE 2017 operational classification of seizure types. *Epilepsia*, 58(4), pp.531-542.
- Fletcher, C.F., Lutz, C.M., O'Sullivan, T.N., Shaughnessy Jr, J.D., Hawkes, R., Frankel, W.N., Copeland, N.G. and Jenkins, N.A., 1996. Absence epilepsy in tottering mutant mice is associated with calcium channel defects. *Cell*, 87(4), pp.607-617.
- Fletcher, C.F. and Frankel, W.N., 1999. Ataxic mouse mutants and molecular mechanisms of absence epilepsy. *Human molecular genetics*, 8(10), pp.1907-1912.
- Forcelli, P.A., 2017. Applications of optogenetic and chemogenetic methods to seizure circuits: Where to go next?. *Journal of neuroscience research*, 95(12), pp.2345-2356.
- Forsgren, L., 2004. Incidence and prevalence. In: *Epilepsy in children*, 2nd ed. London: Arnold, pp.21-25.
- Fortress, A.M., Hamlett, E.D., Vazey, E.M., Aston-Jones, G., Cass, W.A., Boger, H.A. and Granholm, A.C.E., 2015. Designer receptors enhance memory in a mouse model of Down syndrome. *Journal of neuroscience*, 35(4), pp.1343-1353.

- Frankel, W.N., Beyer, B., Maxwell, C.R., Pretel, S., Letts, V.A. and Siegel, S.J., 2005. Development of a new genetic model for absence epilepsy: spike-wave seizures in C3H/He and backcross mice. *Journal of neuroscience*, 25(13), pp.3452-3458.
- Franklin, K.B. and Paxinos, G., 2008. *The mouse brain in stereotaxic coordinates*. Academic Press, New York.
- Frazier, S.J., Cohen, B.N. and Lester, H.A., 2013. An engineered glutamate-gated chloride (GluCl) channel for sensitive, consistent neuronal silencing by ivermectin. *Journal of biological chemistry*, 288(29), pp.21029-21042.
- Freichel, C., Potschka, H., Ebert, U., Brandt, C. and Löscher, W., 2006. Acute changes in the neuronal expression of GABA and glutamate decarboxylase isoforms in the rat piriform cortex following status epilepticus. *Neuroscience*, 141(4), pp.2177-2194.
- French, J.A. and Pedley, T.A., 2008. Initial management of epilepsy. *New england journal of medicine*, 359(2), pp.166-176.
- Freund, T.F. and Buzsaki, G., 1996. Interneurons of the hippocampus. *Hippocampus*, 6(4), pp.347-470.
- Fuentealba, P. and Steriade, M., 2005a. The reticular nucleus revisited: intrinsic and network properties of a thalamic pacemaker. *Progress in neurobiology*, 75(2), pp.125-141.
- Fuentealba, P., Timofeev, I., Bazhenov, M., Sejnowski, T.J. and Steriade, M., 2005b. Membrane bistability in thalamic reticular neurons during spindle oscillations. *Journal of neurophysiology*, 93(1), pp.294-304.
- Fujihara, K., Miwa, H., Kakizaki, T., Kaneko, R., Mikuni, M., Tanahira, C., Tamamaki, N. and Yanagawa, Y., 2015. Glutamate decarboxylase 67 deficiency in a subset of GABAergic neurons induces schizophrenia-related phenotypes. *Neuropsychopharmacology*, 40(10), pp.2475-2486.
- Garner, A.R., Rowland, D.C., Hwang, S.Y., Baumgaertel, K., Roth, B.L., Kentros, C. and Mayford, M., 2012. Generation of a synthetic memory trace. *Science*, 335(6075), pp.1513-1516.
- Gastaut, H., 1970. Clinical and electroencephalographical classification of epileptic seizures. *Epilepsia*, 11(1), pp.102-112.
- Gautier, N.M. and Glasscock, E., 2015. Spontaneous seizures in Kcna1-null mice lacking voltage-gated Kv1. 1 channel activate fos expression in select limbic circuits. *Journal of neurochemistry*, 135(1), pp.157-164.
- Ge, F., Wang, N., Cui, C., Li, Y., Liu, Y., Ma, Y., Liu, S., Zhang, H. and Sun, X., 2017. Glutamatergic projections from the entorhinal cortex to dorsal dentate gyrus mediate context-induced reinstatement of heroin seeking. *Neuropsychopharmacology*, 42(9), pp.1860-1870.

- Gibbs, F.A. and Gibbs, E.L., 1952. *Atlas of Electroencephalography*. Cambridge, Mass: Addison-Wesley Publishers, 2.
- Gil, Z. and Amitai, Y., 1996. Properties of convergent thalamocortical and intracortical synaptic potentials in single neurons of neocortex. *Journal of neuroscience*, 16(20), pp.6567-6578.
- Gilman, T.L., Dutta, S., Adkins, J.M., Cecil, C.A. and Jasnow, A.M., 2018. Basolateral amygdala Thy1-expressing neurons facilitate the inhibition of contextual fear during consolidation, reconsolidation, and extinction. *Neurobiology of learning and memory*, 155, pp.498-507.
- Girard, B., Tuduri, P., Moreno, M.P., Sakkaki, S., Barboux, C., Bouschet, T., Varrault, A., Vitre, J., Mccort-Tranchepain, I., Dairou, J. and Acher, F., 2019. The mGlu7 receptor provides protective effects against epileptogenesis and epileptic seizures. *Neurobiology of disease*, 129, pp.13-28.
- Glauser, T.A., Cnaan, A., Shinnar, S., Hirtz, D.G., Dlugos, D., Masur, D., Clark, P.O., Capparelli, E.V. and Adamson, P.C., 2010. Ethosuximide, valproic acid, and lamotrigine in childhood absence epilepsy. *New England journal of medicine*, 362(9), pp.790-799.
- Glauser, T.A., Cnaan, A., Shinnar, S., Hirtz, D.G., Dlugos, D., Masur, D., Clark, P.O., Adamson, P.C. and Childhood Absence Epilepsy Study Team, 2013. Ethosuximide, valproic acid, and lamotrigine in childhood absence epilepsy: initial monotherapy outcomes at 12 months. *Epilepsia*, 54(1), pp.141-155.
- Gloor, P., 1968. Generalized Cortico-Reticular Epilepsies Some Considerations on the Pathophysiology of Generalized Bilaterally Synchronous Spike and Wave Discharge. *Epilepsia*, 9(3), pp.249-263.
- Goldberg, E.M., Clark, B.D., Zagha, E., Nahmani, M., Erisir, A. and Rudy, B., 2008. K⁺ channels at the axon initial segment dampen near-threshold excitability of neocortical fast-spiking GABAergic interneurons. *Neuron*, 58(3), pp.387-400.
- Gomez, J.L., Bonaventura, J., Lesniak, W., Mathews, W.B., Sysa-Shah, P., Rodriguez, L.A., Ellis, R.J., Richie, C.T., Harvey, B.K., Dannals, R.F. and Pomper, M.G., 2017. Chemogenetics revealed: DREADD occupancy and activation via converted clozapine. *Science*, 357(6350), pp.503-507.
- Gong, X., Mendoza-Halliday, D., Ting, J.T., Kaiser, T., Sun, X., Bastos, A.M., Wimmer, R.D., Guo, B., Chen, Q., Zhou, Y. and Pruner, M., 2020. An Ultra-Sensitive Step-Function Opsin for Minimally Invasive Optogenetic Stimulation in Mice and Macaques. *Neuron*, 398, pp.30239-30247
- Goossens, M.G., Boon, P., Christiaen, E., Vonck, K., Carrette, E., Desloovere, J., Van den Haute, C., Baekelandt, V., Wadman, W., Vanhove, C. and Raedt, R., 2019. Chemogenetic therapy strongly suppresses hippocampal excitability and spontaneous seizures in a rat model for temporal lobe epilepsy. In *5th Congress of the European Academy of Neurology*, 26(1), pp. 416.

- Gotman, J., Grova, C., Bagshaw, A., Kobayashi, E., Aghakhani, Y. and Dubeau, F., 2005. Generalized epileptic discharges show thalamocortical activation and suspension of the default state of the brain. *Proceedings of the national academy of sciences*, 102(42), pp.15236-15240.
- Goutaudier, R., Coizet, V., Carcenac, C. and Carnicella, S., 2019. DREADDs: The Power of the Lock, the Weakness of the Key. Favouring the Pursuit of Specific Conditions Rather than Specific Ligands. *eNeuro*, 6(5).
- Grasse, D.W., Karunakaran, S. and Moxon, K.A., 2013. Neuronal synchrony and the transition to spontaneous seizures. *Experimental neurology*, 248, pp.72-84.
- Grayson, D.S., Bliss-Moreau, E., Machado, C.J., Bennett, J., Shen, K., Grant, K.A., Fair, D.A. and Amaral, D.G., 2016. The rhesus monkey connectome predicts disrupted functional networks resulting from pharmacogenetic inactivation of the amygdala. *Neuron*, 91(2), pp.453-466.
- Greifzu, F., Schmidt, S., Schmidt, K.F., Kreikemeier, K., Witte, O.W. and Löwel, S., 2011. Global impairment and therapeutic restoration of visual plasticity mechanisms after a localized cortical stroke. *Proceedings of the National Academy of Sciences*, 108(37), pp.15450-15455.
- Gritton, H.J., Howe, W.M., Romano, M.F., DiFeliceantonio, A.G., Kramer, M.A., Saligrama, V., Bucklin, M.E., Zemel, D. and Han, X., 2019. Unique contributions of parvalbumin and cholinergic interneurons in organizing striatal networks during movement. *Nature neuroscience*, 22(4), pp.586-597.
- Gu, W., Sander, T., Becker, T. and Steinlein, O.K., 2004. Genotypic association of exonic LGI4 polymorphisms and childhood absence epilepsy. *Neurogenetics*, 5(1), pp.41-44.
- Guerrini, R., 2010. Classification concepts and terminology: Is clinical description assertive and laboratory testing objective? *Epilepsia*, 51(4), pp.718-720.
- Guettier, J.M., Gautam, D., Scarselli, M., de Azua, I.R., Li, J.H., Rosemond, E., Ma, X., Gonzalez, F.J., Armbruster, B.N., Lu, H. and Roth, B.L., 2009. A chemical-genetic approach to study G protein regulation of β cell function in vivo. *Proceedings of the national academy of sciences*, 106(45), pp.19197-19202.
- Gupta, D., Ossenblok, P. and van Luijtelaar, G., 2011. Space-time network connectivity and cortical activations preceding spike wave discharges in human absence epilepsy: a MEG study. *Medical & biological engineering & computing*, 49(5), pp.555-565.
- Gurwitz, D., Haring, R., Heldman, E., Fraser, C.M., Manor, D. and Fisher, A., 1994. Discrete activation of transduction pathways associated with acetylcholine m1 receptor by several muscarinic ligands. *European journal of pharmacology*, 267(1), pp.21-31.
- Gutierrez, D.V., Mark, M.D., Masseck, O., Maejima, T., Kuckelsberg, D., Hyde, R.A., Krause, M., Kruse, W. and Herlitze, S., 2011. Optogenetic control of motor coordination by Gi/o protein-

coupled vertebrate rhodopsin in cerebellar Purkinje cells. *Journal of biological chemistry*, 286(29), pp.25848-25858.

Haginoya, K., Munakata, M., Kato, R., Yokoyama, H., Ishizuka, M. and Iinuma, K., 2002. Ictal cerebral haemodynamic of childhood epilepsy measured with near-infrared spectrophotometry. *Brain*, 125(9), pp.1960-1971.

Hamlett, E.D., Ledreux, A., Gilmore, A., Vazey, E.M., Aston-Jones, G., Boger, H.A., Paredes, D. and Granholm, A.C.E., 2020. Inhibitory designer receptors aggravate memory loss in a mouse model of down syndrome. *Neurobiology of disease*, 134, p.104616.

Hashemi, E., Ariza, J., Rogers, H., Noctor, S.C. and Martínez-Cerdeño, V., 2017. The number of parvalbumin-expressing interneurons is decreased in the prefrontal cortex in autism. *Cerebral cortex*, 27(3), pp.1931-1943.

Hashimoto, T., Volk, D.W., Eggan, S.M., Mirnics, K., Pierri, J.N., Sun, Z., Sampson, A.R. and Lewis, D.A., 2003. Gene expression deficits in a subclass of GABA neurons in the prefrontal cortex of subjects with schizophrenia. *Journal of neuroscience*, 23(15), pp.6315-6326.

Hassan, M., Adotevi, N. K. & Leitch, B., 2018. GABAergic changes in the somatosensory cortex of the stargazer mouse model of absence epilepsy. In *Australasian neuroscience society, 38th annual scientific meeting 2018*.

Hempelmann, A., Cobilanschi, J., Heils, A., Muhle, H., Stephani, U., Weber, Y., Lerche, H. and Sander, T., 2007. Lack of evidence of an allelic association of a functional GABRB3 exon 1a promoter polymorphism with idiopathic generalized epilepsy. *Epilepsy research*, 74(1), pp.28-32.

Hensch, T.K., Fagiolini, M., Mataga, N., Stryker, M.P., Baekkeskov, S. and Kash, S.F., 1998. Local GABA circuit control of experience-dependent plasticity in developing visual cortex. *Science*, 282(5393), pp.1504-1508.

Hermans, E., 2003. Biochemical and pharmacological control of the multiplicity of coupling at G-protein-coupled receptors. *Pharmacology & therapeutics*, 99(1), pp.25-44.

Heron, S.E., Phillips, H.A., Mulley, J.C., Mazarib, A., Neufeld, M.Y., Berkovic, S.F. and Scheffer, I.E., 2004. Genetic variation of CACNA1H in idiopathic generalized epilepsy. *Annals of neurology*, 55(4), pp.595-596.

Heron, S.E., Scheffer, I.E., Berkovic, S.F., Dibbens, L.M. and Mulley, J.C., 2007. Channelopathies in idiopathic epilepsy. *Neurotherapeutics*, 4(2), pp.295-304.

Herrera, C.G., Cadavieco, M.C., Jego, S., Ponomarenko, A., Korotkova, T. and Adamantidis, A., 2016. Hypothalamic feedforward inhibition of thalamocortical network controls arousal and consciousness. *Nature neuroscience*, 19(2), pp.290-298.

- Heuermann, R.J., Jaramillo, T.C., Ying, S.W., Suter, B.A., Lyman, K.A., Han, Y., Lewis, A.S., Hampton, T.G., Shepherd, G.M., Goldstein, P.A. and Chetkovich, D.M., 2016. Reduction of thalamic and cortical Ih by deletion of TRIP8b produces a mouse model of human absence epilepsy. *Neurobiology of disease*, 85, pp.81-92.
- Hijazi, S., Heistek, T.S., Scheltens, P., Neumann, U., Shimshek, D.R., Mansvelder, H.D., Smit, A.B. and van Kesteren, R.E., 2019. Early restoration of parvalbumin interneuron activity prevents memory loss and network hyperexcitability in a mouse model of Alzheimer's disease. *Molecular psychiatry*, pp.1-19.
- Hitiris, N., Mohanraj, R., Norrie, J. and Brodie, M.J., 2007. Mortality in epilepsy. *Epilepsy & behavior*, 10(3), pp.363-376.
- Holmes, M.D., Brown, M. and Tucker, D.M., 2004. Are "generalized" seizures truly generalized? Evidence of localized mesial frontal and frontopolar discharges in absence. *Epilepsia*, 45(12), pp.1568-1579.
- Hou, G., Smith, A.G. and Zhang, Z.W., 2016. Lack of intrinsic GABAergic connections in the thalamic reticular nucleus of the mouse. *Journal of neuroscience*, 36(27), pp.7246-7252.
- Hu, H., Gan, J. and Jonas, P., 2014. Fast spiking, parvalbumin+ GABAergic interneurons: From cellular design to microcircuit function. *Science*, 345(6196), p.1255263.
- Huang, Z.J., Kirkwood, A., Pizzorusso, T., Porciatti, V., Morales, B., Bear, M.F., Maffei, L. and Tonegawa, S., 1999. BDNF regulates the maturation of inhibition and the critical period of plasticity in mouse visual cortex. *Cell*, 98(6), pp.739-755.
- Huang, R.Q., Bell-Horner, C.L., Dibas, M.I., Covey, D.F., Drewe, J.A. and Dillon, G.H., 2001. Pentylentetrazole-induced inhibition of recombinant γ -aminobutyric acid type A (GABAA) receptors: mechanism and site of action. *Journal of pharmacology and experimental therapeutics*, 298(3), pp.986-995.
- Hughes, J.R., 2009. Absence seizures: a review of recent reports with new concepts. *Epilepsy & behaviour*, 15(4), pp.404-412.
- Huguenard, J.R. and Prince, D.A., 1994. Clonazepam suppresses GABAB-mediated inhibition in thalamic relay neurons through effects in nucleus reticularis. *Journal of neurophysiology*, 71(6), pp.2576-2581.
- Huguenard, J., 2019. Current controversy: spikes, bursts, and synchrony in generalized absence epilepsy: unresolved questions regarding thalamocortical synchrony in absence epilepsy. *Epilepsy currents*, 19(2), pp.105-111.
- Huntsman, M.M., Porcello, D.M., Homanics, G.E., DeLorey, T.M. and Huguenard, J.R., 1999. Reciprocal inhibitory connections and network synchrony in the mammalian thalamus. *Science*, 283(5401), pp.541-543.

- Hwang, H., Kim, H., Kim, S.H., Kim, S.H., Lim, B.C., Chae, J.H., Choi, J.E., Kim, K.J. and Hwang, Y.S., 2012. Long-term effectiveness of ethosuximide, valproic acid, and lamotrigine in childhood absence epilepsy. *Brain and development*, 34(5), pp.344-348.
- Iannetti, P., Spalice, A., De Luca, F., Boemi, S., Festa, A. and Maini, C.L., 2001. Ictal single photon emission computed tomography in absence seizures: apparent implication of different neuronal mechanisms. *Journal of child neurology*, 16(5), pp.339-344.
- Ilhan, A., Iraz, M., Kamisli, S. and Yigitoglu, R., 2006. Pentylentetrazol-induced kindling seizure attenuated by Ginkgo biloba extract (EGb 761) in mice. *Progress in neuro-psychopharmacology and biological psychiatry*, 30(8), pp.1504-1510.
- Imbrici, P., Jaffe, S.L., Eunson, L.H., Davies, N.P., Herd, C., Robertson, R., Kullmann, D.M. and Hanna, M.G., 2004. Dysfunction of the brain calcium channel CaV2. 1 in absence epilepsy and episodic ataxia. *Brain*, 127(12), pp.2682-2692.
- Inan, M. and Anderson, S.A., 2014. The chandelier cell, form and function. *Current opinion in neurobiology*, 26, pp.142-148.
- Inoue, M., Duysens, J., Vossen, J.M. and Coenen, A.M., 1993. Thalamic multiple-unit activity underlying spike-wave discharges in anesthetized rats. *Brain research*, 612(1-2), pp.35-40.
- Ito, M., Ohmori, I., Nakahori, T., Ouchida, M. and Ohtsuka, Y., 2005. Mutation screen of GABRA1, GABRB2 and GABRG2 genes in Japanese patients with absence seizures. *Neuroscience letters*, 383(3), pp.220-224.
- Jacobs, M.P., Leblanc, G.G., Brooks-Kayal, A., Jensen, F.E., Lowenstein, D.H., Noebels, J.L., Spencer, D.D. and Swann, J.W., 2009. Curing epilepsy: progress and future directions. *Epilepsy & behaviour*, 14(3), pp.438-445.
- Jallon, P. and Latour, P., 2005. Epidemiology of idiopathic generalized epilepsies. *Epilepsia*, 46, pp.10-14.
- Jann, M.W., Lam, Y.W. and Chang, W.H., 1994. Rapid formation of clozapine in guinea-pigs and man following clozapine-N-oxide administration. *Archives internationales de pharmacodynamie et de therapie*, 328(2), pp.243-250.
- Jarre, G., Guillemain, I., Deransart, C. and Depaulis, A., 2017. Genetic models of absence epilepsy in rats and mice. In *Models of Seizures and Epilepsy*, pp. 455-471. Academic Press.
- Jasper, H. and Kershman, J., 1941. Electroencephalographic classification of the epilepsies. *Archives of neurology & psychiatry*, 45(6), pp.903-943.
- Jasper, H.H., 1974. Experimental studies on the functional anatomy of petit mal epilepsy. *Association for research in nervous and mental disease*, 26, pp. 272-298.

- Jendryka, M., Palchauthuri, M., Ursu, D., van der Veen, B., Liss, B., Kätzel, D., Nissen, W. and Pekcec, A., 2019. Pharmacokinetic and pharmacodynamic actions of clozapine-N-oxide, clozapine, and compound 21 in DREADD-based chemogenetics in mice. *Scientific reports*, 9(1), pp.1-14.
- Jensen, K., Chiu, C.S., Sokolova, I., Lester, H.A. and Mody, I., 2003. GABA transporter-1 (GAT1)-deficient mice: differential tonic activation of GABAA versus GABAB receptors in the hippocampus. *Journal of neurophysiology*, 90(4), pp.2690-2701.
- Jiang, X., Lachance, M. and Rossignol, E., 2016. Involvement of cortical fast-spiking parvalbumin-positive basket cells in epilepsy. *Progress in brain research*, 226, pp. 81-126.
- Johannesen, K.M., Gardella, E., Linnankivi, T., Courage, C., de Saint Martin, A., Lehesjoki, A.E., Mignot, C., Afenjar, A., Lesca, G., Abi-Warde, M.T. and Chelly, J., 2018. Defining the phenotypic spectrum of SLC6A1 mutations. *Epilepsia*, 59(2), pp.389-402.
- Johnson, E., Gurani, S., Dhamne S., Lee, H., Hensch, T. and Rotenberg, A., 2018. Attenuation of seizure susceptibility through chemo-genetic mobilization of parvalbumin interneuron inhibitory reserve. *72nd Annual Meeting of American Epilepsy Society (Abst. 3.049)*
- Jones, W.H.S., and Withington, E.T., 1952. Hippocrates with an English Translation. Harvard University Press.
- Jones, E.G., 2002. Thalamic circuitry and thalamocortical synchrony. *Philosophical transactions of the Royal society of London. series B: Biological Sciences*, 357(1428), pp.1659-1673.
- Jones, E.G., 2009. Synchrony in the interconnected circuitry of the thalamus and cerebral cortex. *Annals of the New York academy of sciences*, 1157(1), pp.10-23.
- Jouveneau, A., Eunson, L.H., Spauschus, A., Ramesh, V., Zuberi, S.M., Kullmann, D.M. and Hanna, M.G., 2001. Human epilepsy associated with dysfunction of the brain P/Q-type calcium channel. *The Lancet*, 358(9284), pp.801-807.
- Kananura, C., Haug, K., Sander, T., Runge, U., Gu, W., Hallmann, K., Rebstock, J., Heils, A. and Steinlein, O.K., 2002. A splice-site mutation in GABRG2 associated with childhood absence epilepsy and febrile convulsions. *Archives of neurology*, 59(7), pp.1137-1141.
- Kang, T.C., Kim, H.S., Seo, M.O., Choi, S.Y., Kwon, O.S., Baek, N.I., Lee, H.Y. and Won, M.H., 2001. The temporal alteration of GAD67/GAD65 ratio in the gerbil hippocampal complex following seizure. *Brain research*, 920(1-2), pp.159-169.
- Kang, J.Q. and Macdonald, R.L., 2016. Molecular pathogenic basis for GABRG2 mutations associated with a spectrum of epilepsy syndromes, from generalized absence epilepsy to Dravet syndrome. *JAMA neurology*, 73(8), pp.1009-1016.

- Kash, S.F., Johnson, R.S., Tecott, L.H., Noebels, J.L., Mayfield, R.D., Hanahan, D. and Baekkeskov, S., 1997. Epilepsy in mice deficient in the 65-kDa isoform of glutamic acid decarboxylase. *Proceedings of the national academy of sciences*, 94(25), pp.14060-14065.
- Kash, S.F., Tecott, L.H., Hodge, C. and Baekkeskov, S., 1999. Increased anxiety and altered responses to anxiolytics in mice deficient in the 65-kDa isoform of glutamic acid decarboxylase. *Proceedings of the national academy of sciences*, 96(4), pp.1698-1703.
- Kato, H.K., Asinof, S.K. and Isaacson, J.S., 2017. Network-level control of frequency tuning in auditory cortex. *Neuron*, 95(2), pp.412-423.
- Kalanithi, P.S., Zheng, W., Kataoka, Y., DiFiglia, M., Grantz, H., Saper, C.B., Schwartz, M.L., Leckman, J.F. and Vaccarino, F.M., 2005. Altered parvalbumin-positive neuron distribution in basal ganglia of individuals with Tourette syndrome. *Proceedings of the national academy of sciences*, 102(37), pp.13307-13312.
- Kataoka, Y., Kalanithi, P.S., Grantz, H., Schwartz, M.L., Saper, C., Leckman, J.F. and Vaccarino, F.M., 2010. Decreased number of parvalbumin and cholinergic interneurons in the striatum of individuals with Tourette syndrome. *Journal of comparative neurology*, 518(3), pp.277-291.
- Kätzel, D., Nicholson, E., Schorge, S., Walker, M.C. and Kullmann, D.M., 2014. Chemical-genetic attenuation of focal neocortical seizures. *Nature communications*, 5(1), pp.1-9.
- Kaufman, P.Y., 1912. Electrical phenomena in the cerebral cortex. *Obozrenie Psikiatrii, Nevrologii i Eksperimentalnoy Psikhologii (St. Petersburg)*, 7, pp.403-424.
- Keezer, M.R., Bell, G.S., Neligan, A., Novy, J. and Sander, J.W., 2016. Cause of death and predictors of mortality in a community-based cohort of people with epilepsy. *Neurology*, 86(8), pp.704-712.
- Kelsom, C. and Lu, W., 2013. Development and specification of GABAergic cortical interneurons. *Cell & bioscience*, 3(1), p.19.
- Keskil, I.S., Keskil, Z.A., Canseven, A.G. and Seyhan, N., 2001. No effect of 50 Hz magnetic field observed in a pilot study on pentylenetetrazol-induced seizures and mortality in mice. *Epilepsy research*, 44(1), pp.27-32.
- Khoshkhoo, S., Vogt, D. and Sohal, V.S., 2017. Dynamic, cell-type-specific roles for GABAergic interneurons in a mouse model of optogenetically inducible seizures. *Neuron*, 93(2), pp.291-298.
- Khosravani, H. and Zamponi, G.W., 2006. Voltage-gated calcium channels and idiopathic generalized epilepsies. *Physiological reviews*, 86(3), pp.941-966.
- Killory, B.D., Bai, X., Negishi, M., Vega, C., Spann, M.N., Vestal, M., Guo, J., Berman, R., Danielson, N., Trejo, J. and Shisler, D., 2011. Impaired attention and network connectivity in childhood absence epilepsy. *Neuroimage*, 56(4), pp.2209-2217.

- Klioueva, I.A., van Luijtelaar, E.L.J.M., Chepurnova, N.E. and Chepurnov, S.A., 2001. PTZ-induced seizures in rats: effects of age and strain. *Physiology & Behavior*, 72(3), pp.421-426.
- Kim, E.H., Thu, D.C., Tippett, L.J., Oorschot, D.E., Hogg, V.M., Roxburgh, R., Synek, B.J., Waldvogel, H.J. and Faull, R.L., 2014. Cortical interneuron loss and symptom heterogeneity in Huntington disease. *Annals of neurology*, 75(5), pp.717-727.
- Kim, T.Y., Maki, T., Zhou, Y., Sakai, K., Mizuno, Y., Ishikawa, A., Tanaka, R., Niimi, K., Li, W., Nagano, N. and Takahashi, E., 2015. Absence-like seizures and their pharmacological profile in tottering-6j mice. *Biochemical and biophysical research communications*, 463(1-2), pp.148-153.
- Kim, D., Jeong, H., Lee, J., Ghim, J.W., Her, E.S., Lee, S.H. and Jung, M.W., 2016. Distinct roles of parvalbumin-and somatostatin-expressing interneurons in working memory. *Neuron*, 92(4), pp.902-915.
- Kiser, P.J., Cooper, N.G. and Mower, G.D., 1998. Expression of two forms of glutamic acid decarboxylase (GAD67 and GAD65) during postnatal development of rat somatosensory barrel cortex. *Journal of comparative neurology*, 402(1), pp.62-74
- Klausberger, T., Marton, L.F., O'Neill, J., Huck, J.H., Dalezios, Y., Fuentealba, P., Suen, W.Y., Papp, E., Kaneko, T., Watanabe, M. and Csicsvari, J., 2005. Complementary roles of cholecystinin-and parvalbumin-expressing GABAergic neurons in hippocampal network oscillations. *Journal of neuroscience*, 25(42), pp.9782-9793.
- Klioueva, I.A., van Luijtelaar, E.L.J.M., Chepurnova, N.E. and Chepurnov, S.A., 2001. PTZ-induced seizures in rats: effects of age and strain. *Physiology & behaviour*, 72(3), pp.421-426.
- Koch, M., Varela, L., Kim, J.G., Kim, J.D., Hernández-Nuño, F., Simonds, S.E., Castorena, C.M., Vianna, C.R., Elmquist, J.K., Morozov, Y.M. and Rakic, P., 2015. Hypothalamic POMC neurons promote cannabinoid-induced feeding. *Nature*, 519(7541), pp.45-50.
- Koike, H., Demars, M.P., Short, J.A., Nabel, E.M., Akbarian, S., Baxter, M.G. and Morishita, H., 2016. Chemogenetic inactivation of dorsal anterior cingulate cortex neurons disrupts attentional behaviour in mouse. *Neuropsychopharmacology*, 41(4), pp.1014-1023.
- Kondo, M., Sumino, R. and Okado, H., 1997. Combinations of AMPA receptor subunit expression in individual cortical neurons correlate with expression of specific calcium-binding proteins. *Journal of neuroscience*, 17(5), pp.1570-1581.
- Kostopoulos, G.K., 2001. Involvement of the thalamocortical system in epileptic loss of consciousness. *Epilepsia*, 42, pp.13-19.
- Kostopoulos, G.K., 2017. Pharmacologically Induced Animal Models of Absence Seizures. In *Models of seizures and epilepsy* (pp. 553-567). Academic Press.

- Koutroumanidou, E., Kimbaris, A., Kortsaris, A., Bezirtzoglou, E., Polissiou, M., Charalabopoulos, K. and Pagonopoulou, O., 2013. Increased seizure latency and decreased severity of pentylenetetrazol-induced seizures in mice after essential oil administration. *Epilepsy research and treatment*, 2013.
- Krall, R.L., Penry, J.K., White, B.G., Kupferberg, H.J. and Swinyard, E.A., 1978. Antiepileptic drug development: II. Anticonvulsant drug screening. *Epilepsia*, 19(4), pp.409-428.
- Kristiansen, K., Kroeze, W.K., Willins, D.L., Gelber, E.I., Savage, J.E., Glennon, R.A. and Roth, B.L., 2000. A highly conserved aspartic acid (Asp-155) anchors the terminal amine moiety of tryptamines and is involved in membrane targeting of the 5-HT_{2A} serotonin receptor but does not participate in activation via a “salt-bridge disruption” mechanism. *Journal of Pharmacology and Experimental Therapeutics*, 293(3), pp.735-746.
- Krook-Magnuson, E., Armstrong, C., Oijala, M. and Soltesz, I., 2013. On-demand optogenetic control of spontaneous seizures in temporal lobe epilepsy. *Nature communications*, 4(1), pp.1-8.
- Kruse, A.C., Kobilka, B.K., Gautam, D., Sexton, P.M., Christopoulos, A. and Wess, J., 2014. Muscarinic acetylcholine receptors: novel opportunities for drug development. *Nature reviews Drug discovery*, 13(7), pp.549-560.
- Kullmann, D.M., 2011. Interneuron networks in the hippocampus. *Current opinion in neurobiology*, 21(5), pp.709-716.
- Lau, D., de Miera, E.V.S., Contreras, D., Ozaita, A., Harvey, M., Chow, A., Noebels, J.L., Paylor, R., Morgan, J.I., Leonard, C.S. and Rudy, B., 2000. Impaired fast spiking suppressed cortical inhibition, and increased susceptibility to seizures in mice lacking Kv3. 2 K⁺ channel proteins. *Journal of neuroscience*, 20(24), pp.9071-9085.
- Lauber, E., Filice, F. and Schwaller, B., 2016. Prenatal valproate exposure differentially affects parvalbumin-expressing neurons and related circuits in the cortex and striatum of mice. *Frontiers in molecular neuroscience*, 9, p.150.
- Lazarus, M.S., Krishnan, K. and Huang, Z.J., 2015. GAD67 deficiency in parvalbumin interneurons produces deficits in inhibitory transmission and network disinhibition in mouse prefrontal cortex. *Cerebral cortex*, 25(5), pp.1290-1296.
- Leal, A., Vieira, J.P., Lopes, R., Nunes, R.G., Gonçalves, S.I., da Silva, F.L. and Figueiredo, P., 2016. Dynamics of epileptic activity in a peculiar case of childhood absence epilepsy and correlation with thalamic levels of GABA. *Epilepsy & behaviour case reports*, 5, pp.57-65.
- Ledri, M., Madsen, M.G., Nikitidou, L., Kirik, D. and Kokaia, M., 2014. Global optogenetic activation of inhibitory interneurons during epileptiform activity. *Journal of neuroscience*, 34(9), pp.3364-3377.

- Lee, K., Holley, S.M., Shobe, J.L., Chong, N.C., Cepeda, C., Levine, M.S. and Masmanidis, S.C., 2017. Parvalbumin interneurons modulate striatal output and enhance performance during associative learning. *Neuron*, 93(6), pp.1451-1463.
- Lee, S., Hwang, E., Lee, M. and Choi, J.H., 2019. Distinct Topographical Patterns of Spike-Wave Discharge in Transgenic and Pharmacologically Induced Absence Seizure Models. *Experimental neurobiology*, 28(4), p.474.
- Lenkov, D.N., Volnova, A.B., Pope, A.R. and Tsytsarev, V., 2013. Advantages and limitations of brain imaging methods in the research of absence epilepsy in humans and animal models. *Journal of neuroscience methods*, 212(2), pp.195-202.
- Letts, V.A., Valenzuela, A., Kirley, J.P., Sweet, H.O., Davisson, M.T. and Frankel, W.N., 1997. Genetic and physical maps of the stargazer locus on mouse chromosome 15. *Genomics*, 43(1), pp.62-68.
- Letts, V.A., Felix, R., Biddlecome, G.H., Arikath, J., Mahaffey, C.L., Valenzuela, A., Bartlett, F.S., Mori, Y., Campbell, K.P. and Frankel, W.N., 1998. The mouse stargazer gene encodes a neuronal Ca²⁺-channel γ subunit. *Nature genetics*, 19(4), pp.340-347.
- Lévesque, M., Chen, L.Y., Etter, G., Shiri, Z., Wang, S., Williams, S. and Avoli, M., 2019. Paradoxical effects of optogenetic stimulation in mesial temporal lobe epilepsy. *Annals of neurology*, 86(5), pp.714-728.
- Lewis, D.A., Curley, A.A., Glausier, J.R. and Volk, D.W., 2012. Cortical parvalbumin interneurons and cognitive dysfunction in schizophrenia. *Trends in neurosciences*, 35(1), pp.57-67.
- Liang, J., Zhang, Y., Wang, J., Pan, H., Wu, H., Xu, K., Liu, X., Jiang, Y., Shen, Y. and Wu, X., 2006. New variants in the CACNA1H gene identified in childhood absence epilepsy. *Neuroscience letters*, 406(1-2), pp.27-32.
- Liang, J., Zhang, Y., Chen, Y., Wang, J., Pan, H., Wu, H., Xu, K., Liu, X., Jiang, Y., Shen, Y. and Wu, X., 2007. Common polymorphisms in the CACNA1H gene associated with childhood absence epilepsy in Chinese Han population. *Annals of human genetics*, 71(3), pp.325-335.
- Lichtenberg, N.T., Pennington, Z.T., Holley, S.M., Greenfield, V.Y., Cepeda, C., Levine, M.S. and Wassum, K.M., 2017. Basolateral amygdala to orbitofrontal cortex projections enable cue-triggered reward expectations. *Journal of neuroscience*, 37(35), pp.8374-8384.
- Lipkind, D., Sakov, A., Kafkafi, N., Elmer, G.I., Benjamini, Y. and Golani, I., 2004. New replicable anxiety-related measures of wall vs. center behavior of mice in the open field. *Journal of applied physiology*, 97(1), pp.347-359.

- Li, Q., Luo, C., Yang, T., Yao, Z., He, L., Liu, L., Xu, H., Gong, Q., Yao, D. and Zhou, D., 2009. EEG-fMRI study on the interictal and ictal generalized spike-wave discharges in patients with childhood absence epilepsy. *Epilepsy research*, 87(2-3), pp.160-168.
- Liu, X.B. and Jones, E.G., 1999. Predominance of corticothalamic synaptic inputs to thalamic reticular nucleus neurons in the rat. *Journal of comparative neurology*, 414(1), pp.67-79.
- Liu, G.X., Cai, G.Q., Cai, Y.Q., Sheng, Z.J., Jiang, J., Mei, Z., Wang, Z.G., Guo, L. and Fei, J., 2007. Reduced anxiety and depression-like behaviors in mice lacking GABA transporter subtype 1. *Neuropsychopharmacology*, 32(7), pp.1531-1539.
- Liu, G.X., Liu, S., Cai, G.Q., Sheng, Z.J., Cai, Y.Q., Jiang, J., Sun, X., Ma, S.K., Wang, L., Wang, Z.G. and Fei, J., 2007. Reduced aggression in mice lacking GABA transporter subtype 1. *Journal of neuroscience research*, 85(3), pp.649-655.
- Liu, Y.Q., Yu, F., Liu, W.H., He, X.H. and Peng, B.W., 2014. Dysfunction of hippocampal interneurons in epilepsy. *Neuroscience bulletin*, 30(6), pp.985-998.
- Liu, J., Zhang, M.Q., Wu, X., Lazarus, M., Cherasse, Y., Yuan, M.Y., Huang, Z.L. and Li, R.X., 2017. Activation of parvalbumin neurons in the rostro-dorsal sector of the thalamic reticular nucleus promotes sensitivity to pain in mice. *Neuroscience*, 366, pp.113-123.
- Loiseau, P., Duché, B. and Pédespan, J.M., 1995. Absence epilepsies. *Epilepsia*, 36(12), pp.1182-1186.
- Longin, A., Souchier, C., Ffrench, M. and Bryon, P.A., 1993. Comparison of anti-fading agents used in fluorescence microscopy: image analysis and laser confocal microscopy study. *Journal of histochemistry & cytochemistry*, 41(12), pp.1833-1840.
- Löscher, W., 2011. Critical review of current animal models of seizures and epilepsy used in the discovery and development of new antiepileptic drugs. *Seizure*, 20(5), pp.359-368.
- Lu, J., Chen, Y., Zhang, Y., Pan, H., Wu, H., Xu, K., Liu, X., Jiang, Y., Bao, X., Ding, K. and Shen, Y., 2002. Mutation screen of the GABAA receptor gamma 2 subunit gene in Chinese patients with childhood absence epilepsy. *Neuroscience letters*, 332(2), pp.75-78.
- Lu, M.H., Zhao, X.Y., Xu, D.E., Chen, J.B., Ji, W.L., Huang, Z.P., Pan, T.T., Xue, L.L., Wang, F., Li, Q.F. and Zhang, Y., 2020. Transplantation of GABAergic Interneuron Progenitor Attenuates Cognitive Deficits of Alzheimer's Disease Model Mice. *Journal of Alzheimer's disease*, (Preprint), pp.1-16.
- Lucas, E.K., Jegarl, A. and Clem, R.L., 2014. Mice lacking TrkB in parvalbumin-positive cells exhibit sexually dimorphic behavioral phenotypes. *Behavioural brain research*, 274, pp.219-225.
- Lucas, E.K., Jegarl, A.M., Morishita, H. and Clem, R.L., 2016. Multimodal and site-specific plasticity of amygdala parvalbumin interneurons after fear learning. *Neuron*, 91(3), pp.629-643.

- Lüders, H., Lesser, R.P., Dinner, D.S. and Morris, H.H., 1984. Generalized epilepsies: a review. *Cleveland clinic quarterly*, 51, pp.205-226.
- Lüders, H., Akamatsu, N., Amina, S., Baumgartner, C., Benbadis, S., Bermeo-Ovalle, A., Bleasel, A., Bozorgi, A., Carreño, M., Devereaux, M. and Fernandez-Baca Vaca, G., 2019. Critique of the 2017 epileptic seizure and epilepsy classifications. *Epilepsia*, 60(6), pp.1032-1039.
- Luo, S.X., Huang, J., Li, Q., Mohammad, H., Lee, C.Y., Krishna, K., Kok, A.M.Y., Tan, Y.L., Lim, J.Y., Li, H. and Yeow, L.Y., 2018. Regulation of feeding by somatostatin neurons in the tuberal nucleus. *Science*, 361(6397), pp.76-81.
- Luo, Z.Y., Huang, L., Lin, S., Yin, Y.N., Jie, W., Hu, N.Y., Hu, Y.Y., Guan, Y.F., Liu, J.H., You, Q.L. and Chen, Y.H., 2020. Erbin in amygdala parvalbumin-positive neurons modulates anxiety-like behaviours. *Biological psychiatry*, 87(10), pp.926-936.
- Lüttjohann, A., Fabene, P.F. and van Luijtelaaar, G., 2009. A revised Racine's scale for PTZ-induced seizures in rats. *Physiology & behaviour*, 98(5), pp.579-586.
- Lüttjohann, A., Schoffelen, J.M. and Van Luijtelaaar, G., 2013. Peri-ictal network dynamics of spike-wave discharges: phase and spectral characteristics. *Experimental neurology*, 239, pp.235-247.
- Lüttjohann, A. and van Luijtelaaar, G., 2015. Dynamics of networks during absence seizure's on- and offset in rodents and man. *Frontiers in physiology*, 6, p.16.
- MacLaren, D.A., Browne, R.W., Shaw, J.K., Radhakrishnan, S.K., Khare, P., España, R.A. and Clark, S.D., 2016. Clozapine N-oxide administration produces behavioral effects in Long-Evans rats: implications for designing DREADD experiments. *Eneuro*, 3(5).
- Madsen, K.K., White, H.S. and Schousboe, A., 2010. Neuronal and non-neuronal GABA transporters as targets for antiepileptic drugs. *Pharmacology & therapeutics*, 125(3), pp.394-401.
- Maharjan, D.M., Dai, Y.Y., Glantz, E.H. and Jadhav, S.P., 2018. Disruption of dorsal hippocampal–prefrontal interactions using chemogenetic inactivation impairs spatial learning. *Neurobiology of learning and memory*, 155, pp.351-360.
- Maheshwari, A., Nahm, W. and Noebels, J., 2013. Paradoxical proepileptic response to NMDA receptor blockade linked to cortical interneuron defect in stargazer mice. *Frontiers in cellular neuroscience*, 7, p.156.
- Maheshwari, A. and Noebels, J.L., 2014. Monogenic models of absence epilepsy: windows into the complex balance between inhibition and excitation in thalamocortical microcircuits. *Progress in brain research*, 213, pp. 223-252.

Maheshwari, A., Marks, R.L., Yu, K.M. and Noebels, J.L., 2016. Shift in interictal relative gamma power as a novel biomarker for drug response in two mouse models of absence epilepsy. *Epilepsia*, 57(1), pp.79-88.

Maheshwari, A., Akbar, A., Wang, M., Marks, R.L., Yu, K., Park, S., Foster, B.L. and Noebels, J.L., 2017. Persistent aberrant cortical phase–amplitude coupling following seizure treatment in absence epilepsy models. *The Journal of physiology*, 595(23), pp.7249-7260.

Maheshwari, A., 2020. Rodent EEG: Expanding the Spectrum of Analysis. *Epilepsy Currents*, 20(3), pp. 149-153.

Mahler, S.V., Vazey, E.M., Beckley, J.T., Keistler, C.R., McGlinchey, E.M., Kaufling, J., Wilson, S.P., Deisseroth, K., Woodward, J.J. and Aston-Jones, G., 2014. Designer receptors show role for ventral pallidum input to ventral tegmental area in cocaine seeking. *Nature neuroscience*, 17(4), p.577.

Mahler, S.V. and Aston-Jones, G., 2018. CNO Evil? Considerations for the use of DREADDs in behavioural neuroscience. *Neuropsychopharmacology*, 43(5), p.934.

Maljevic, S., Krampfl, K., Cobilanschi, J., Tilgen, N., Beyer, S., Weber, Y.G., Schlesinger, F., Ursu, D., Melzer, W., Cossette, P. and Bufler, J., 2006. A mutation in the GABAA receptor $\alpha 1$ -subunit is associated with absence epilepsy. *Annals of neurology*, 59(6), pp.983-987.

Manning, J.A., Richards, D.A., Leresche, N., Crunelli, V. and Bowery, N.G., 2004. Cortical-area specific block of genetically determined absence seizures by ethosuximide. *Neuroscience*, 123(1), pp.5-9.

Manvich, D.F., Webster, K.A., Foster, S.L., Farrell, M.S., Ritchie, J.C., Porter, J.H. and Weinshenker, D., 2018. The DREADD agonist clozapine N-oxide (CNO) is reverse-metabolized to clozapine and produces clozapine-like interoceptive stimulus effects in rats and mice. *Scientific reports*, 8(1), pp.1-10.

Manzaneque, J.M., Brain, P.F. and Navarro, J.F., 2002. Effect of low doses of clozapine on behaviour of isolated and group-housed male mice in the elevated plus-maze test. *Progress in neuro-psychopharmacology and biological psychiatry*, 26(2), pp.349-355.

Marafiga, J.R., Pasquetti, M.V. and Calcagnotto, M.E., 2020. GABAergic interneurons in epilepsy: More than a simple change in inhibition. *Epilepsy & Behaviour*, p.106935.

Marchant, N.J., Whitaker, L.R., Bossert, J.M., Harvey, B.K., Hope, B.T., Kaganovsky, K., Adhikary, S., Prisinzano, T.E., Vardy, E., Roth, B.L. and Shaham, Y., 2016. Behavioural and physiological effects of a novel kappa-opioid receptor-based DREADD in rats. *Neuropsychopharmacology*, 41(2), pp.402-409.

- Marco, P., Sola, R.G., Pulido, P., Alijarde, M.T., Sanchez, A., Cajal, S.R.Y. and DeFelipe, J., 1996. Inhibitory neurons in the human epileptogenic temporal neocortex: an immunocytochemical study. *Brain*, 119(4), pp.1327-1347.
- Marescaux, C., Micheletti, G., Vergnes, M., Depaulis, A., Rumbach, L. and Warter, J.M., 1984. A model of chronic spontaneous petit mal-like seizures in the rat: comparison with pentylenetetrazol-induced seizures. *Epilepsia*, 25(3), pp.326-331.
- Marescaux, C., Vergnes, M. and Depaulis, A., 1992. Genetic absence epilepsy in rats from Strasbourg—a review. In *Generalized Non-Convulsive Epilepsy: Focus on GABA-B Receptors*, pp.37-69.
- Marescaux, C. and Vergnes, M., 1995. Genetic absence epilepsy in rats from Strasbourg (GAERS). *The Italian journal of neurological sciences*, 16(1-2), pp.113-118.
- Marín, O., 2012. Interneuron dysfunction in psychiatric disorders. *Nature Reviews Neuroscience*, 13(2), pp.107-120.
- Markram, H., Toledo-Rodriguez, M., Wang, Y., Gupta, A., Silberberg, G. and Wu, C., 2004. Interneurons of the neocortical inhibitory system. *Nature reviews neuroscience*, 5(10), pp.793-807.
- Marsan, C.A., 1965. A newly proposed classification of epileptic seizures. Neurophysiological basis. *Epilepsia*, 6(4), pp.275-296.
- Marx, M., Haas, C.A. and Häussler, U., 2013. Differential vulnerability of interneurons in the epileptic hippocampus. *Frontiers in cellular neuroscience*, 7, p.167.
- Matricardi, S., Verrotti, A., Chiarelli, F., Cerminara, C. and Curatolo, P., 2014. Current advances in childhood absence epilepsy. *Paediatric neurology*, 50(3), pp.205-212.
- Mattison, K.A., Butler, K.M., Inglis, G.A.S., Dayan, O., Boussidan, H., Bhambhani, V., Philbrook, B., da Silva, C., Alexander, J.J., Kanner, B.I. and Escayg, A., 2018. SLC 6A1 variants identified in epilepsy patients reduce γ -aminobutyric acid transport. *Epilepsia*, 59(9), pp.e135-e141.
- Mazzone, C.M., Pati, D., Michaelides, M., DiBerto, J., Fox, J.H., Tipton, G., Anderson, C., Duffy, K., McKlveen, J.M., Hardaway, J.A. and Magness, S.T., 2018. Acute engagement of Gq-mediated signaling in the bed nucleus of the stria terminalis induces anxiety-like behavior. *Molecular psychiatry*, 23(1), pp.143-153.
- McCafferty, C.P., 2014. *Firing dynamics of thalamic neurones during genetically determined experimental absence seizures* (Doctoral dissertation, Cardiff University).
- McCafferty, C., Connelly, W.M., Celli, R., Ngomba, R.T., Nicoletti, F. and Crunelli, V., 2018a. Genetic rescue of absence seizures. *CNS neuroscience & therapeutics*, 24(8), p.745.

- McCafferty, C., David, F., Venzi, M., Lőrincz, M.L., Delicata, F., Atherton, Z., Recchia, G., Orban, G., Lambert, R.C., Di Giovanni, G. and Leresche, N., 2018b. Cortical drive and thalamic feed-forward inhibition control thalamic output synchrony during absence seizures. *Nature neuroscience*, 21(5), pp.744-756.
- McCormick, D.A. and Contreras, D., 2001. On the cellular and network bases of epileptic seizures. *Annual review of physiology*, 63(1), pp.815-846.
- McGlinchey, E.M. and Aston-Jones, G., 2018. Dorsal hippocampus drives context-induced cocaine seeking via inputs to lateral septum. *Neuropsychopharmacology*, 43(5), pp.987-1000.
- Medina, A.E., Manhães, A.C. and Schmidt, S.L., 2001. Sex differences in sensitivity to seizures elicited by pentylenetetrazol in mice. *Pharmacology biochemistry and behaviour*, 68(3), pp.591-596.
- Meeren, H.K., Pijn, J.P.M., van Luijtelaar, G., E.L., Coenen, A.M. and da Silva, F.H.L., 2002. Cortical focus drives widespread corticothalamic networks during spontaneous absence seizures in rats. *Journal of neuroscience*, 22(4), pp.1480-1495.
- Meeren, H. K., van Luijtelaar, G., da Silva, F.L. and Coenen, A.M., 2005. Evolving concepts on the pathophysiology of absence seizures: the cortical focus theory. *Archives of neurology*, 62(3), pp.371-376.
- Meeren, H.K., Veening, J.G., Mödersheim, T.A., Coenen, A.M. and Van Luijtelaar, G., 2009. Thalamic lesions in a genetic rat model of absence epilepsy: dissociation between spike-wave discharges and sleep spindles. *Experimental neurology*, 217(1), pp.25-37.
- Melone, M., Ciappelloni, S. and Conti, F., 2015. A quantitative analysis of cellular and synaptic localization of GAT-1 and GAT-3 in rat neocortex. *Brain structure and function*, 220(2), pp.885-897.
- Menuz, K. and Nicoll, R.A., 2008. Loss of inhibitory neuron AMPA receptors contributes to ataxia and epilepsy in stargazer mice. *Journal of neuroscience*, 28(42), pp.10599-10603.
- Meyer, J., Maheshwari, A., Noebels, J. and Smirnakis, S., 2018. Asynchronous suppression of visual cortex during absence seizures in stargazer mice. *Nature communications*, 9(1), pp.1-9.
- Miyamoto, H., Tatsukawa, T., Shimohata, A., Yamagata, T., Suzuki, T., Amano, K., Mazaki, E., Raveau, M., Ogiwara, I., Oba-Asaka, A. and Hensch, T.K., 2019. Impaired cortico-striatal excitatory transmission triggers epilepsy. *Nature communications*, 10(1), pp.1-13.
- Minelli, A., Brecha, N.C., Karschin, C., DeBiasi, S. and Conti, F., 1995. GAT-1, a high-affinity GABA plasma membrane transporter, is localized to neurons and astroglia in the cerebral cortex. *Journal of neuroscience*, 15(11), pp.7734-7746.

- Minelli, A., DeBiasi, S., Brecha, N.C., Zuccarello, L.V. and Conti, F., 1996. GAT-3, a high-affinity GABA plasma membrane transporter, is localized to astrocytic processes, and it is not confined to the vicinity of GABAergic synapses in the cerebral cortex. *Journal of neuroscience*, 16(19), pp.6255-6264.
- Mishra, A.M., Bai, H., Gribizis, A. and Blumenfeld, H., 2011. Neuroimaging biomarkers of epileptogenesis. *Neuroscience letters*, 497(3), pp.194-204.
- Mineff, E.M. and Weinberg, R.J., 2000. Differential synaptic distribution of AMPA receptor subunits in the ventral posterior and reticular thalamic nuclei of the rat. *Neuroscience*, 101(4), pp.969-982.
- Moeller, F., LeVan, P., Muhle, H., Stephani, U., Dubeau, F., Siniatchkin, M. and Gotman, J., 2010. Absence seizures: individual patterns revealed by EEG-fMRI. *Epilepsia*, 51(10), pp.2000-2010.
- Moeller, F., Muthuraman, M., Stephani, U., Deuschl, G., Raethjen, J. and Siniatchkin, M., 2013. Representation and propagation of epileptic activity in absences and generalized photoparoxysmal responses. *Human brain mapping*, 34(8), pp.1896-1909.
- Moore, A.K., Weible, A.P., Balmer, T.S., Trussell, L.O. and Wehr, M., 2018. Rapid rebalancing of excitation and inhibition by cortical circuitry. *Neuron*, 97(6), pp.1341-1355.
- Morison, R.S. and Dempsey, E.W., 1941. A study of thalamo-cortical relations. *American journal of physiology-legacy content*, 135(2), pp.281-292.
- Moy, S.S., Nadler, J.J., Young, N.B., Perez, A., Holloway, L.P., Barbaro, R.P., Barbaro, J.R., Wilson, L.M., Threadgill, D.W., Lauder, J.M. and Magnuson, T.R., 2007. Mouse behavioural tasks relevant to autism: phenotypes of 10 inbred strains. *Behavioural brain research*, 176(1), pp.4-20.
- Muhle, H., Helbig, I., Frøslev, T.G., Suls, A., von Spiczak, S., Klitten, L.L., Dahl, H.A., Brusgaard, K., Neubauer, B., De Jonghe, P. and Tommerup, N., 2013. The role of SLC2A1 in early onset and childhood absence epilepsies. *Epilepsy research*, 105(1-2), pp.229-233.
- Muona, M., Berkovic, S.F., Dibbens, L.M., Oliver, K.L., Maljevic, S., Bayly, M.A., Joensuu, T., Canafoglia, L., Franceschetti, S., Michelucci, R. and Markkinen, S., 2015. A recurrent de novo mutation in KCNC1 causes progressive myoclonus epilepsy. *Nature genetics*, 47(1), p.39.
- Murray, A.J., Sauer, J.F., Riedel, G., McClure, C., Ansel, L., Cheyne, L., Bartos, M., Wisden, W. and Wulff, P., 2011. Parvalbumin-positive CA1 interneurons are required for spatial working but not for reference memory. *Nature neuroscience*, 14(3), p.297.
- Murray, C.J., Vos, T., Lozano, R., Naghavi, M., Flaxman, A.D., Michaud, C., Ezzati, M., Shibuya, K., Salomon, J.A., Abdalla, S. and Aboyans, V., 2013. Disability-adjusted life years (DALYs) for 291 diseases and injuries in 21 regions, 1990–2010: a systematic analysis for the Global Burden of Disease Study 2010. *The Lancet*, 380(9859), pp.2197-2223.

- Murray, A.J., Woloszynowska-Fraser, M.U., Ansel-Bollepalli, L., Cole, K.L., Foggetti, A., Crouch, B., Riedel, G. and Wulff, P., 2015. Parvalbumin-positive interneurons of the prefrontal cortex support working memory and cognitive flexibility. *Scientific reports*, 5, p.16778.
- Nagai, Y., Kikuchi, E., Lerchner, W., Inoue, K.I., Ji, B., Eldridge, M.A., Kaneko, H., Kimura, Y., Oh-Nishi, A., Hori, Y. and Kato, Y., 2016. PET imaging-guided chemogenetic silencing reveals a critical role of primate rostro medial caudate in reward evaluation. *Nature communications*, 7(1), pp.1-8.
- Nagai, Y., Miyakawa, N., Takuwa, H., Hori, Y., Oyama, K., Ji, B., Takahashi, M., Huang, X.P., Slocum, S.T., DiBerto, J.F. and Xiong, Y., 2020. Deschloroclozapine, a potent and selective chemogenetic actuator enables rapid neuronal and behavioural modulations in mice and monkeys. *Nature neuroscience*, 23, pp.1157-1167.
- Nägga, K., Bogdanovic, N. and Marcusson, J., 1999. GABA transporters (GAT-1) in Alzheimer's disease. *Journal of neural transmission*, 106(11-12), pp.1141-1149.
- Nakajima, K.I. and Wess, J., 2012. Design and functional characterization of a novel, arrestin-biased designer G protein-coupled receptor. *Molecular pharmacology*, 82(4), pp.575-582.
- Nassar, M., Simonnet, J., Huang, L.W., Mathon, B., Cohen, I., Bendels, M.H., Beraneck, M., Miles, R. and Fricker, D., 2018. Anterior thalamic excitation and feedforward inhibition of presubicular neurons projecting to medial entorhinal cortex. *Journal of neuroscience*, 38(28), pp.6411-6425.
- Nassiri-Asl, M., Zamansoltani, F. and Torabinejad, B., 2009. Antiepileptic effects of quinine in the pentylenetetrazol model of seizure. *Seizure*, 18(2), pp.129-132.
- Nawreen, N., Morano, R., Mahbod, P., Cotella, E.M., Dalal, K., Fitzgerald, M., Martelle, S., Packard, B.A., Moloney, R.D. and Herman, J.P., 2019. Chemogenetic Inhibition of Infralimbic Prefrontal Cortex GABAergic Parvalbumin-positive Interneurons Attenuates Chronic Stress Adaptions in Male Mice. *bioRxiv*, p.792721.
- Nehlig, A., Valenti, M.P., Thiriaux, A., Hirsch, E., Marescaux, C. and Namer, I.J., 2004. Ictal and interictal perfusion variations measured by SISCOM analysis in typical childhood absence seizures. *Epileptic disorders*, 6(4), pp.247-253.
- Ng, L.H.L., Huang, Y., Han, L., Chang, R.C.C., Chan, Y.S. and Lai, C.S.W., 2018. Ketamine and selective activation of parvalbumin interneurons inhibit stress-induced dendritic spine elimination. *Translational psychiatry*, 8(1), pp.1-15.
- Nguyen, R., Morrissey, M.D., Mahadevan, V., Cajanding, J.D., Woodin, M.A., Yeomans, J.S., Takehara-Nishiuchi, K. and Kim, J.C., 2014. Parvalbumin and GAD65 interneuron inhibition in the ventral hippocampus induces distinct behavioural deficits relevant to schizophrenia. *Journal of neuroscience*, 34(45), pp.14948-14960.

- Niedermeyer, E., 1996. Primary (idiopathic) generalized epilepsy and underlying mechanisms. *Clinical electroencephalography*, 27(1), pp.1-21.
- Nielsen, E.B., Suzdak, P.D., Andersen, K.E., Knutsen, L.J., Sonnewald, U. and Braestrup, C., 1991. Characterization of tiagabine (NO-328), a new potent and selective GABA uptake inhibitor. *European journal of pharmacology*, 196(3), pp.257-266.
- Noback, C.R., Ruggiero, D.A., Demarest, R.J. and Strominger, N.L. eds., 2005. *The human nervous system: structure and function* (No. 744). Springer Science & Business Media.
- Noebels, J.L., Qiao, X., Bronson, R.T., Spencer, C. and Davisson, M.T., 1990. Stargazer: a new neurological mutant on chromosome 15 in the mouse with prolonged cortical seizures. *Epilepsy research*, 7(2), pp.129-135.
- Nolan, D., Lester, S.G., Rau, S.M. and Shellhaas, R.A., 2019. Clinical Use and Efficacy of Levetiracetam for Absence Epilepsies. *Journal of child neurology*, 34(2), pp.94-98.
- Ochs, R.F., Gloor, P., Tyler, J.L., Wolfson, T., Worsley, K., Andermann, F., Diksic, M., Meyer, E. and Evans, A., 1987. Effect of generalized spike-and-wave discharge on glucose metabolism measured by positron emission tomography. *Annals of Neurology*, 21(5), pp.458-464.
- Ogiwara, I., Miyamoto, H., Morita, N., Atapour, N., Mazaki, E., Inoue, I., Takeuchi, T., Itohara, S., Yanagawa, Y., Obata, K. and Furuichi, T., 2007. Nav1. 1 localizes to axons of parvalbumin-positive inhibitory interneurons: a circuit basis for epileptic seizures in mice carrying a Scn1a gene mutation. *Journal of neuroscience*, 27(22), pp.5903-5914.
- Onat, F.Y., Aker, R.G., Gurbanova, A.A., Ateş, N. and Van Luijtelaar, G., 2007. The effect of generalized absence seizures on the progression of kindling in the rat. *Epilepsia*, 48, pp.150-156.
- Ono, M., Murakami, T., Kudo, A., Isshiki, M., Sawada, H. and Segawa, A., 2001. Quantitative comparison of anti-fading mounting media for confocal laser scanning microscopy. *Journal of histochemistry & cytochemistry*, 49(3), pp.305-311.
- Opazo, P. and Choquet, D., 2011. A three-step model for the synaptic recruitment of AMPA receptors. *Molecular and cellular neuroscience*, 46(1), pp.1-8.
- Overington, J.P., Al-Lazikani, B. and Hopkins, A.L., 2006. How many drug targets are there? *Nature reviews drug discovery*, 5(12), pp.993-996.
- Owen, S.F., Liu, M.H. and Kreitzer, A.C., 2019. Thermal constraints on in vivo optogenetic manipulations. *Nature neuroscience*, 22(7), pp.1061-1065.
- Pack, A.M., 2019. Epilepsy Overview and Revised Classification of Seizures and Epilepsies. *CONTINUUM: Lifelong Learning in Neurology*, 25(2), pp.306-321.

- Packer, A.M. and Yuste, R., 2011. Dense, unspecific connectivity of neocortical parvalbumin-positive interneurons: a canonical microcircuit for inhibition? *Journal of neuroscience*, 31(37), pp.13260-13271.
- Page, C.E., Shepard, R., Heslin, K. and Coutellier, L., 2019. Prefrontal parvalbumin cells are sensitive to stress and mediate anxiety-related behaviours in female mice. *Scientific reports*, 9(1), pp.1-9.
- Panayiotopoulos, C.P., 1999. Typical absence seizures and their treatment. *Archives of disease in childhood*, 81(4), pp.351-355.
- Panayiotopoulos, C.P., 2001. Treatment of typical absence seizures and related epileptic syndromes. *Paediatric drugs*, 3(5), pp.379-403.
- Panthi, S. and Leitch, B., 2019. The impact of silencing feed-forward parvalbumin-expressing inhibitory interneurons in the cortico-thalamocortical network on seizure generation and behaviour. *Neurobiology of disease*, 132, p.104610.
- Parker, A.P.J., Agathonikou, A., Robinson, R.O. and Panayiotopoulos, C.P., 1998. Inappropriate use of carbamazepine and vigabatrin in typical absence seizures. *Developmental medicine & child neurology*, 40(8), pp.517-519.
- Parker, M.E., 2020. Optogenetics: illuminating the role of PV interneuron dysfunction in the cognitive symptoms of schizophrenia. *USURJ: University of Saskatchewan undergraduate research journal*, 6(2).
- Parnaudeau, S., O'Neill, P.K., Bolkan, S.S., Ward, R.D., Abbas, A.I., Roth, B.L., Balsam, P.D., Gordon, J.A. and Kellendonk, C., 2013. Inhibition of mediodorsal thalamus disrupts thalamo-frontal connectivity and cognition. *Neuron*, 77(6), pp.1151-1162.
- Patsalos, P.N. and Perucca, E., 2003. Clinically important drug interactions in epilepsy: general features and interactions between antiepileptic drugs. *The Lancet neurology*, 2(6), pp.347-356.
- Patsalos, P.N. and Perucca, E., 2003. Clinically important drug interactions in epilepsy: interactions between antiepileptic drugs and other drugs. *The Lancet neurology*, 2(8), pp.473-481.
- Pauwels, P.J. and Colpaert, F.C., 2000. Disparate ligand-mediated Ca²⁺ responses by wild-type, mutant Ser200Ala and Ser204Ala α 2A-adrenoceptor: Ga15 fusion proteins: evidence for multiple ligand-activation binding sites. *British journal of pharmacology*, 130(7), pp.1505-1512.
- Pavlov, I. and Schorge, S., 2014. From treatment to cure: stopping seizures, preventing seizures, and reducing brain propensity to seize. *International review of neurobiology*, 114, pp. 279-299.
- Pavone, P., Bianchini, R., Trifiletti, R.R., Incorpora, G., Pavone, A. and Parano, E., 2001. Neuropsychological assessment in children with absence epilepsy. *Neurology*, 56(8), pp.1047-1051.

Paz, J.T., Chavez, M., SAILLET, S., Deniau, J.M. and Charpier, S., 2007. Activity of ventral medial thalamic neurons during absence seizures and modulation of cortical paroxysms by the nigrothalamic pathway. *Journal of neuroscience*, 27(4), pp.929-941.

Paz, J.T., Bryant, A.S., Peng, K., Fenno, L., Yizhar, O., Frankel, W.N., Deisseroth, K. and Huguenard, J.R., 2011. A new mode of corticothalamic transmission revealed in the *Gria4*^{-/-} model of absence epilepsy. *Nature neuroscience*, 14(9), p.1167.

Paz, J.T. and Huguenard, J.R., 2015. Microcircuits and their interactions in epilepsy: is the focus out of focus? *Nature neuroscience*, 18(3), p.351.

Peñagarikano, O., Lázaro, M.T., Lu, X.H., Gordon, A., Dong, H., Lam, H.A., Peles, E., Maidment, N.T., Murphy, N.P., Yang, X.W. and Golshani, P., 2015. Exogenous and evoked oxytocin restores social behavior in the *Cntnap2* mouse model of autism. *Science translational medicine*, 7(271), p.271ra8.

Penfield, W.G., and Jasper, H. H., 1954. Epilepsy and the Functional Anatomy of the Human Brain. Little, Brown and Co., Boston, Mass.

Perez, S.M., Boley, A. and Lodge, D.J., 2019. Region specific knockdown of Parvalbumin or Somatostatin produces neuronal and behavioural deficits consistent with those observed in schizophrenia. *Translational psychiatry*, 9(1), pp.1-13.

Perova, Z., Delevich, K. and Li, B., 2015. Depression of excitatory synapses onto parvalbumin interneurons in the medial prefrontal cortex in susceptibility to stress. *Journal of neuroscience*, 35(7), pp.3201-3206.

Perucca, E., Gram, L., Avanzini, G. and Dulac, O., 1998. Antiepileptic drugs as a cause of worsening seizures. *Epilepsia*, 39(1), pp.5-17.

Petitjean, H., Pawlowski, S.A., Fraine, S.L., Sharif, B., Hamad, D., Fatima, T., Berg, J., Brown, C.M., Jan, L.Y., Ribeiro-da-Silva, A. and Braz, J.M., 2015. Dorsal horn parvalbumin neurons are gatekeepers of touch-evoked pain after nerve injury. *Cell reports*, 13(6), pp.1246-1257.

Pienaar, I.S., Gartside, S.E., Sharma, P., De Paola, V., Gretenkord, S., Withers, D., Elson, J.L. and Dexter, D.T., 2015. Pharmacogenetic stimulation of cholinergic pedunculopontine neurons reverses motor deficits in a rat model of Parkinson's disease. *Molecular neurodegeneration*, 10(1), p.47.

Pina, C., Morais, T.P., Sebastiao, A.M., Crunelli, V. and Vaz, S.H., 2019. Astrocytic GABA transporter dysfunction in childhood absence epilepsy. In *XIV European Meeting on Glial Cells in Health and Disease, Porto*.

Pinal, C.S. and Tobin, A.J., 1998. Uniqueness and redundancy in GABA production. *Perspectives on developmental neurobiology*, 5, pp.109-118.

- Pinault, D., Smith, Y. and Deschênes, M., 1997. Dendrodendritic and axoaxonic synapses in the thalamic reticular nucleus of the adult rat. *Journal of neuroscience*, 17(9), pp.3215-3233.
- Pinault, D., Leresche, N., Charpier, S., Deniau, J.M., Marescaux, C., Vergnes, M. and Crunelli, V., 1998. Intracellular recordings in thalamic neurones during spontaneous spike and wave discharges in rats with absence epilepsy. *The Journal of physiology*, 509(2), pp.449-456.
- Pinault, D., 2003. Cellular interactions in the rat somatosensory thalamocortical system during normal and epileptic 5–9 Hz oscillations. *The Journal of physiology*, 552(3), pp.881-905
- Pinault, D. and O'Brien, T.J., 2005. Cellular and network mechanisms of genetically determined absence seizures. *Thalamus & related systems*, 3(3), pp.181-203.
- Pirttimaki, T., Parri, H.R. and Crunelli, V., 2013. Astrocytic GABA transporter GAT-1 dysfunction in experimental absence seizures. *The Journal of physiology*, 591(4), pp.823-833.
- Polack, P.O., Guillemain, I., Hu, E., Deransart, C., Depaulis, A. and Charpier, S., 2007. Deep layer somatosensory cortical neurons initiate spike-and-wave discharges in a genetic model of absence seizures. *Journal of neuroscience*, 27(24), pp.6590-6599.
- Polack, P.O., Mahon, S., Chavez, M. and Charpier, S., 2009. Inactivation of the somatosensory cortex prevents paroxysmal oscillations in cortical and related thalamic neurons in a genetic model of absence epilepsy. *Cerebral Cortex*, 19(9), pp.2078-2091.
- Porter, J.T., Johnson, C.K. and Agmon, A., 2001. Diverse types of interneurons generate thalamus-evoked feedforward inhibition in the mouse barrel cortex. *Journal of neuroscience*, 21(8), pp.2699-2710.
- Posner, E.B., Mohamed, K.K. and Marson, A.G., 2005. Ethosuximide, sodium valproate or lamotrigine for absence seizures in children and adolescents. *Cochrane database of systematic reviews*, (4).
- Powell, K.L., Cain, S.M., Ng, C., Sirdesai, S., David, L.S., Kyi, M., Garcia, E., Tyson, J.R., Reid, C.A., Bahlo, M. and Foote, S.J., 2009. A Cav3.2 T-type calcium channel point mutation has splice-variant-specific effects on function and segregates with seizure expression in a polygenic rat model of absence epilepsy. *Journal of Neuroscience*, 29(2), pp.371-380.
- Prevett, M.C., Duncan, J.S., Jones, T., Fish, D.R. and Brooks, D.J., 1995. Demonstration of thalamic activation during typical absence seizures using H2 15O and PET. *Neurology*, 45(7), pp.1396-1402.
- Prince, D.A. and Farrell D., 1969. "Centrencephalic" spike and wave discharges following parenteral penicillin injection in the cat (abstract) *Neurology*, 19, pp.19309-19310.
- Proft, J., Rzhetsky, Y., Lazniewska, J., Zhang, F.X., Cain, S.M., Snutch, T.P., Zamponi, G.W. and Weiss, N., 2017. The Cacna1h mutation in the GAERS model of absence epilepsy enhances

T-type Ca²⁺ currents by altering calnexin-dependent trafficking of Ca_v3.2 channels. *Scientific reports*, 7(1), pp.1-13.

Prut, L. and Belzung, C., 2003. The open field as a paradigm to measure the effects of drugs on anxiety-like behaviours: a review. *European journal of pharmacology*, 463(1-3), pp.3-33.

Qi, J., Kim, M., Sanchez, R., Ziaee, S.M., Kohtz, J.D. and Koh, S., 2018. Enhanced susceptibility to stress and seizures in GAD65 deficient mice. *PloS one*, 13(1).

Qiao, X. and Noebels, J.L., 1993. Developmental analysis of hippocampal mossy fiber outgrowth in a mutant mouse with inherited spike-wave seizures. *Journal of neuroscience*, 13(11), pp.4622-4635.

Qiu, W., Yu, C., Gao, Y., Miao, A., Tang, L., Huang, S., Jiang, W., Sun, J., Xiang, J. and Wang, X., 2017. Disrupted topological organization of structural brain networks in childhood absence epilepsy. *Scientific reports*, 7(1), pp.1-10.

Raper, J., Morrison, R.D., Daniels, J.S., Howell, L., Bachevalier, J., Wichmann, T. and Galvan, A., 2017. Metabolism and distribution of clozapine-N-oxide: implications for nonhuman primate chemogenetics. *ACS chemical neuroscience*, 8(7), pp.1570-1576.

Reynolds, E.H., 2005. Robert Bentley Todd's electrical theory of epilepsy. *Epilepsia*, 46(7), pp.991-994.

Richards, D.A., Manning, J.P.A., Barnes, D., Rombola, L., Bowery, N.G., Caccia, S., Leresche, N. and Crunelli, V., 2003. Targeting thalamic nuclei is not sufficient for the full anti-absence action of ethosuximide in a rat model of absence epilepsy. *Epilepsy research*, 54(2-3), pp.97-107.

Richens A., 1995. Ethosuximide and valproate. In: *Typical Absences and Related Epileptic Syndromes* (Duncan JS, Panayiotopoulos CP, eds). London: Churchill Livingstone.

Rogan, S.C. and Roth, B.L., 2011. Remote control of neuronal signalling. *Pharmacological reviews*, 63(2), pp.291-315.

Rossignol, E., Kruglikov, I., Van Den Maagdenberg, A.M., Rudy, B. and Fishell, G., 2013. Ca_v2.1 ablation in cortical interneurons selectively impairs fast-spiking basket cells and causes generalized seizures. *Annals of neurology*, 74(2), pp.209-222.

Roth, B.L., 2016. DREADDs for neuroscientists. *Neuron*, 89(4), pp.683-694.

Rubenstein, L.A. and Lanzara, R.G., 1998. Activation of G protein-coupled receptors entails cysteine modulation of agonist binding. *Journal of molecular structure*, 430, pp.57-71.

Rudolf, G., Thérèse Bihoreau, M., F. Godfrey, R., P. Wilder, S., D. Cox, R., Lathrop, M., Marescaux, C. and Gauguier, D., 2004. Polygenic control of idiopathic generalized epilepsy phenotypes in the genetic absence rats from Strasbourg (GAERS). *Epilepsia*, 45(4), pp.301-308.

- Rudy, B., Fishell, G., Lee, S. and Hjerling-Leffler, J., 2011. Three groups of interneurons account for nearly 100% of neocortical GABAergic neurons. *Developmental neurobiology*, 71(1), pp.45-61.
- Ruffmann, C., Bogliun, G. and Beghi, E., 2006. Epileptogenic drugs: a systematic review. *Expert review of neurotherapeutics*, 6(4), pp.575-589.
- Russ, S.A., Larson, K. and Halfon, N., 2012. A national profile of childhood epilepsy and seizure disorder. *Pediatrics*, 129(2), pp.256-264.
- Sabers, A., Møller, A., Scheel-Krüger, J. and Dam, A.M., 1996. No loss in total neuron number in the thalamic reticular nucleus and neocortex in the genetic absence epilepsy rats from Strasbourg. *Epilepsy research*, 26(1), pp.45-48.
- Saint-Martin, C., Gauvain, G., Teodorescu, G., Gourfinkel-An, I., Fedirko, E., Weber, Y.G., Maljevic, S., Ernst, J.P., Garcia-Olivares, J., Fahlke, C. and Nabbout, R., 2009. Two novel CLCN2 mutations accelerating chloride channel deactivation are associated with idiopathic generalized epilepsy. *Human mutation*, 30(3), pp.397-405.
- Saitou, H., Akita, T., Tohyama, J., Goldberg-Stern, H., Kobayashi, Y., Cohen, R., Kato, M., Ohba, C., Miyatake, S., Tsurusaki, Y. and Nakashima, M., 2015. De novo KCNB1 mutations in infantile epilepsy inhibit repetitive neuronal firing. *Scientific reports*, 5(1), pp.1-14.
- Salek-Haddadi, A., Lemieux, L., Merschhemke, M., Friston, K.J., Duncan, J.S. and Fish, D.R., 2003. Functional magnetic resonance imaging of human absence seizures. *Annals of Neurology*, 53(5), pp.663-667.
- Salin, P., López, I.P., Kachidian, P., Barroso-Chinea, P., Rico, A.J., Gómez-Bautista, V., Coulon, P., Kerkerian-Le Goff, L. and Lanciego, J.L., 2009. Changes to interneuron-driven striatal microcircuits in a rat model of Parkinson's disease. *Neurobiology of disease*, 34(3), pp.545-552.
- Salvi, S.S., Pati, S., Chaudhari, P.R., Tiwari, P., Banerjee, T. and Vaidya, V.A., 2019. Acute chemogenetic activation of CamKII α -positive forebrain excitatory neurons regulates anxiety-like behaviour in mice. *Frontiers in behavioural neuroscience*, 13, p.249.
- Sanchez-Mejias, E., Nuñez-Díaz, C., Sanchez-Varo, R., Gomez-Arboledas, A., Garcia-Leon, J.A., Fernandez-Valenzuela, J.J., Mejias-Ortega, M., Trujillo-Estrada, L., Baglietto-Vargas, D., Moreno-Gonzalez, I. and Davila, J.C., 2020. Distinct disease-sensitive GABAergic neurons in the perirhinal cortex of Alzheimer's mice and patients. *Brain pathology*, 30(2), pp.345-363.
- Sander, J.W., 2003. The epidemiology of epilepsy revisited. *Current opinion in neurology*, 16(2), pp.165-170.
- Schachter, S., 1997. Treatment of Seizures. In: *The Comprehensive Evaluation and Treatment of Epilepsy* (Schachter S, Schomer D, eds). Academic Press.

- Schapel, G. and Chadwick, D., 1996. Tiagabine and non-convulsive status epilepticus. *Seizure*, 5(2), pp.153-156.
- Scheffer, I.E. and Berkovic, S.F., 2003. The genetics of human epilepsy. *Trends in pharmacological sciences*, 24(8), pp.428-433.
- Scheffer, I.E., Berkovic, S., Capovilla, G., Connolly, M.B., French, J., Guilhoto, L., Hirsch, E., Jain, S., Mathern, G.W., Moshé, S.L. and Nordli, D.R., 2017. ILAE classification of the epilepsies: position paper of the ILAE Commission for Classification and Terminology. *Epilepsia*, 58(4), pp.512-521.
- Schousboe, A. and Waagepetersen, H.S., 2007. GABA: homeostatic and pharmacological aspects. *Progress in brain research*, 160, pp.9-19.
- Schousboe, A. and Waagepetersen, H.S., 2009. Gamma-aminobutyric acid (GABA). In *Encyclopedia of Neuroscience*, pp. 511-515. Academic Press.
- Schultz Jr, M.K., Gentzel, R., Usenovic, M., Gretzula, C., Ware, C., Parmentier-Batteur, S., Schachter, J.B. and Zariwala, H.A., 2018. Pharmacogenetic neuronal stimulation increases human tau pathology and trans-synaptic spread of tau to distal brain regions in mice. *Neurobiology of disease*, 118, pp.161-176.
- Schwaller, B., Meyer, M. and Schiffmann, S., 2002. 'New' functions for 'old' proteins: the role of the calcium-binding proteins calbindin D-28k, calretinin and parvalbumin, in cerebellar physiology. Studies with knockout mice. *The Cerebellum*, 1(4), pp.241-258.
- Schwaller, B., Tetko, I.V., Tandon, P., Silveira, D.C., Vreugdenhil, M., Henzi, T., Potier, M.C., Celio, M.R. and Villa, A.E.P., 2004. Parvalbumin deficiency affects network properties resulting in increased susceptibility to epileptic seizures. *Molecular and cellular neuroscience*, 25(4), pp.650-663.
- Scimemi, A., 2014. Structure, function, and plasticity of GABA transporters. *Frontiers in cellular neuroscience*, 8, p.161.
- Sciolino, N.R., Plummer, N.W., Chen, Y.W., Alexander, G.M., Robertson, S.D., Dudek, S.M., McElligott, Z.A. and Jensen, P., 2016. Recombinase-dependent mouse lines for chemogenetic activation of genetically defined cell types. *Cell reports*, 15(11), pp.2563-2573.
- Scotti, A.L., Bollag, O., Kalt, G. and Nitsch, C., 1997. Loss of perikaryal parvalbumin immunoreactivity from surviving GABAergic neurons in the CA1 field of epileptic gerbils. *Hippocampus*, 7(5), pp.524-535.
- Seibenhener, M.L. and Wooten, M.C., 2015. Use of the open field maze to measure locomotor and anxiety-like behavior in mice. *Journal of visualized experiments*, 96, p.e52434.

- Seidenbecher, T., Staak, R. and Pape, H.C., 1998. Relations between cortical and thalamic cellular activities during absence seizures in rats. *European journal of neuroscience*, 10(3), pp.1103-1112.
- Seo, S. and Leitch, B., 2014. Altered thalamic GABAA-receptor subunit expression in the stargazer mouse model of absence epilepsy. *Epilepsia*, 55(2), pp.224-232.
- Seo, S. and Leitch, B., 2015. Synaptic changes in GABAA receptor expression in the thalamus of the stargazer mouse model of absence epilepsy. *Neuroscience*, 306, pp.28-38.
- Seo, S. and Leitch, B., 2017. Postnatal expression of thalamic GABAA receptor subunits in the stargazer mouse model of absence epilepsy. *NeuroReport*, 28(18), pp.1255-1260.
- Sheikhabaehi, S., Turovsky, E.A., Hosford, P.S., Hadjihambi, A., Theparambil, S.M., Liu, B., Marina, N., Teschemacher, A.G., Kasparov, S., Smith, J.C. and Gourine, A.V., 2018. Astrocytes modulate brainstem respiratory rhythm-generating circuits and determine exercise capacity. *Nature communications*, 9(1), pp.1-10.
- Sherman, S.M. and Guillery, R.W., 1996. Functional organization of thalamocortical relays. *Journal of neurophysiology*, 76(3), pp.1367-1395.
- Sherman, S.M. and Guillery, R.W., 2002. The role of the thalamus in the flow of information to the cortex. *Philosophical transactions of the royal society of London. Series B: biological sciences*, 357(1428), pp.1695-1708.
- Siegel, A. and Sapru, H.N., 2011. The upper motor neurons. Essential neuroscience Philadelphia.
- Singh, B., Monteil, A., Bidaud, I., Sugimoto, Y., Suzuki, T., Hamano, S.I., Oguni, H., Osawa, M., Alonso, M.E., Delgado-Escueta, A.V. and Inoue, Y., 2007. Mutational analysis of CACNA1G in idiopathic generalized epilepsy. *Human mutation*, 28(5), pp.524-525.
- Sitnikova, E. and van Luijtelaar, G., 2004. Cortical control of generalized absence seizures: effect of lidocaine applied to the somatosensory cortex in WAG/Rij rats. *Brain research*, 1012(1-2), pp.127-137.
- Sitnikova, E. and Van Luijtelaar, G., 2007. Electroencephalographic characterization of spike-wave discharges in cortex and thalamus in WAG/Rij rats. *Epilepsia*, 48(12), pp.2296-2311.
- Sitnikova, E., Kulikova, S., Birioukova, L. and Raevsky, V.V., 2011. Cellular neuropathology of absence epilepsy in the neocortex: a population of glial cells rather than neurons is impaired in genetic rat model. *Acta neurobiologiae experimentalis*, 71(2), pp.263-268.
- Sloviter, R.S., 1989. Calcium-binding protein (calbindin-D28k) and parvalbumin immunocytochemistry: localization in the rat hippocampus with specific reference to the selective vulnerability of hippocampal neurons to seizure activity. *Journal of comparative neurology*, 280(2), pp.183-196.

Sloviter, R.S., 1991a. Permanently altered hippocampal structure, excitability, and inhibition after experimental status epilepticus in the rat: the “dormant basket cell” hypothesis and its possible relevance to temporal lobe epilepsy. *Hippocampus*, 1(1), pp.41-66.

Sloviter, R.S., Sollas, A.L., Barbaro, N.M. and Laxer, K.D., 1991b. Calcium-binding protein (calbindin-D28K) and parvalbumin immunocytochemistry in the normal and epileptic human hippocampus. *Journal of comparative neurology*, 308(3), pp.381-396.

Smith, K.M., 2018. Hyperactivity in mice lacking one allele of the glutamic acid decarboxylase 67 gene. *ADHD Attention Deficit and Hyperactivity Disorders*, 10(4), pp.267-271

Smets, K., Duarri, A., Deconinck, T., Ceulemans, B., van de Warrenburg, B.P., Züchner, S., Gonzalez, M.A., Schüle, R., Synofzik, M., Van der Aa, N. and De Jonghe, P., 2015. First de novo KCND3 mutation causes severe Kv4. 3 channel dysfunctions leading to early onset cerebellar ataxia, intellectual disability, oral apraxia and epilepsy. *BMC medical genetics*, 16(1), p.51.

Snead, O.C., 1992. Pharmacological models of generalized absence seizures in rodents. In *Generalized Non-Convulsive Epilepsy: Focus on GABA-B Receptors*, pp.7-19, Springer, Vienna.

Snead, O.C., Banerjee, P.K., Burnham, M. and Hampson, D., 2000. Modulation of absence seizures by the GABAA receptor: a critical role for metabotropic glutamate receptor 4 (mGluR4). *Journal of neuroscience*, 20(16), pp.6218-6224.

Soghomonian, J.J. and Martin, D.L., 1998. Two isoforms of glutamate decarboxylase: why? *Trends in pharmacological sciences*, 19(12), pp.500-505.

Soh, H., Pant, R., LoTurco, J.J. and Tzingounis, A.V., 2014. Conditional deletions of epilepsy associated KCNQ2 and KCNQ3 channels from cerebral cortex cause differential effects on neuronal excitability. *Journal of neuroscience*, 34(15), pp.5311-5321.

Sohal, V.S., Zhang, F., Yizhar, O. and Deisseroth, K., 2009. Parvalbumin neurons and gamma rhythms enhance cortical circuit performance. *Nature*, 459(7247), pp.698-702.

Sohal, V.S. and Huguenard, J.R., 2003. Inhibitory interconnections control burst pattern and emergent network synchrony in reticular thalamus. *Journal of neuroscience*, 23(26), pp.8978-8988.

Sorokin, J.M., Davidson, T.J., Frechette, E., Abramian, A.M., Deisseroth, K., Huguenard, J.R. and Paz, J.T., 2017. Bidirectional control of generalized epilepsy networks via rapid real-time switching of firing mode. *Neuron*, 93(1), pp.194-210.

Srinivasan, S., Vaisse, C. and Conklin, B.R., 2003. Engineering the Melanocortin-4 Receptor to Control Gs Signalling in Vivo. *Annals of the New York academy of sciences*, 994(1), pp.225-232.

- Srinivasan, S., Santiago, P., Lubrano, C., Vaisse, C. and Conklin, B.R., 2007. Engineering the melanocortin-4 receptor to control constitutive and ligand-mediated GS signalling in vivo. *PLoS One*, 2(8).
- Stachniak, T.J., Ghosh, A. and Sternson, S.M., 2014. Chemogenetic synaptic silencing of neural circuits localizes a hypothalamus-midbrain pathway for feeding behaviour. *Neuron*, 82(4), pp.797-808.
- Staiger, J.F., Freund, T.F. and Zilles, K., 1997. Interneurons immunoreactive for vasoactive intestinal polypeptide (VIP) are extensively innervated by parvalbumin-containing boutons in rat primary somatosensory cortex. *European journal of neuroscience*, 9(11), pp.2259-2268.
- Steinlein, O.K., 2004. Genes and mutations in human idiopathic epilepsy. *Brain and Development*, 26(4), pp.213-218.
- Strader, C.D., Sigal, I.S., Register, R.B., Candelore, M.R., Rands, E. and Dixon, R.A., 1987. Identification of residues required for ligand binding to the beta-adrenergic receptor. *Proceedings of the national academy of sciences*, 84(13), pp.4384-4388.
- Strader, C.D., Gaffney, T., Sugg, E.E., Candelore, M.R., Keys, R., Patchett, A.A. and Dixon, R.A., 1991. Allele-specific activation of genetically engineered receptors. *Journal of Biological Chemistry*, 266(1), pp.5-8.
- Steriade, M., Domich, L., Oakson, G. and Deschenes, M., 1987. The deafferented reticular thalamic nucleus generates spindle rhythmicity. *Journal of neurophysiology*, 57(1), pp.260-273.
- Straub, J., Gawda, A., Ravichandran, P., McGrew, B., Nylund, E., Kang, J., Burke, C., Vitko, I., Scott, M., Williamson, J. and Joshi, S., 2020. Characterization of kindled VGAT-Cre mice as a new animal model of temporal lobe epilepsy. *Epilepsia*, 61(10), pp.2277-2288.
- Stork, O., Ji, F.Y., Kaneko, K., Stork, S., Yoshinobu, Y., Moriya, T., Shibata, S. and Obata, K., 2000. Postnatal development of a GABA deficit and disturbance of neural functions in mice lacking GAD65. *Brain research*, 865(1), pp.45-58.
- Studer, F., Laghouati, E., Jarre, G., David, O., Pouyatos, B. and Depaulis, A., 2019. Sensory coding is impaired in rat absence epilepsy. *The Journal of physiology*, 597(3), pp.951-966.
- Suls, A., Mullen, S.A., Weber, Y.G., Verhaert, K., Ceulemans, B., Guerrini, R., Wuttke, T.V., Salvo-Vargas, A., Deprez, L., Claes, L.R. and Jordanova, A., 2009. Early-onset absence epilepsy caused by mutations in the glucose transporter GLUT1. *Annals of Neurology*, 66(3), pp.415-419.
- Sweger, E.J., Casper, K.B., Scarce-Levie, K., Conklin, B.R. and McCarthy, K.D., 2007. Development of hydrocephalus in mice expressing the Gi-coupled GPCR Ro1 RASSL receptor in astrocytes. *Journal of neuroscience*, 27(9), pp.2309-2317.

- Syrbe, S., Hedrich, U.B., Riesch, E., Djémié, T., Müller, S., Möller, R.S., Maher, B., Hernandez-Hernandez, L., Synofzik, M., Caglayan, H.S. and Arslan, M., 2015. De novo loss-of-function mutations in KCNA2 cause epileptic encephalopathy. *Nature genetics*, 47(4), pp.393-399.
- Szydlowski, S.N., Dorocic, I.P., Planert, H., Carlén, M., Meletis, K. and Silberberg, G., 2013. Target selectivity of feedforward inhibition by striatal fast-spiking interneurons. *Journal of neuroscience*, 33(4), pp.1678-1683.
- Tanahira, C., Higo, S., Watanabe, K., Tomioka, R., Ebihara, S., Kaneko, T. and Tamamaki, N., 2009. Parvalbumin neurons in the forebrain as revealed by parvalbumin-Cre transgenic mice. *Neuroscience research*, 63(3), pp.213-223.
- Tanaka, M., Olsen, R.W., Medina, M.T., Schwartz, E., Alonso, M.E., Duron, R.M., Castro-Ortega, R., Martinez-Juarez, I.E., Pascual-Castroviejo, I., Machado-Salas, J. and Silva, R., 2008. Hyperglycosylation and reduced GABA currents of mutated GABRB3 polypeptide in remitting childhood absence epilepsy. *The American journal of human genetics*, 82(6), pp.1249-1261.
- Tangwiriyasakul, C., Perani, S., Centeno, M., Yaakub, S.N., Abela, E., Carmichael, D.W. and Richardson, M.P., 2018. Dynamic brain network states in human generalized spike-wave discharges. *Brain*, 141(10), pp.2981-2994.
- Tamamaki, N., Yanagawa, Y., Tomioka, R., Miyazaki, J.I., Obata, K. and Kaneko, T., 2003. Green fluorescent protein expression and colocalization with calretinin, parvalbumin, and somatostatin in the GAD67-GFP knock-in mouse. *Journal of comparative neurology*, 467(1), pp.60-79.
- Taylor H, Crunelli V., 2014. Optogenetic drive of thalamocortical neurons can block and induce experimental absence seizures in freely moving animals. *Society for neuroscience meeting*, Washington (DC). Abstract 314.07.
- Tenney, J.R. and Glauser, T.A., 2013. The Current State of Absence Epilepsy: Can We Have Your Attention? The Current State of Absence Epilepsy. *Epilepsy currents*, 13(3), pp.135-140.
- Thiel, G., Kaufmann, A. and Rössler, O.G., 2013. G-protein-coupled designer receptors—new chemical-genetic tools for signal transduction research. *Biological chemistry*, 394(12), pp.1615-1622.
- Thomas, R.L., Mistry, R., Langmead, C.J., Wood, M.D. and Challiss, R.J., 2008. G protein coupling and signaling pathway activation by m1 muscarinic acetylcholine receptor orthosteric and allosteric agonists. *Journal of pharmacology and experimental therapeutics*, 327(2), pp.365-374.
- Thompson, K.J., Khajehali, E., Bradley, S.J., Navarrete, J.S., Huang, X.P., Slocum, S., Jin, J., Liu, J., Xiong, Y., Olsen, R.H. and Diberto, J.F., 2018. DREADD agonist 21 is an effective agonist for muscarinic-based DREADDs in vitro and in vivo. *ACS pharmacology & translational science*, 1(1), pp.61-72.

- Tian, N., Petersen, C., Kash, S., Baekkeskov, S., Copenhagen, D. and Nicoll, R., 1999. The role of the synthetic enzyme GAD65 in the control of neuronal γ -aminobutyric acid release. *Proceedings of the national academy of sciences*, 96(22), pp.12911-12916.
- Todorov, B., Kros, L., Shyti, R., Plak, P., Haasdijk, E.D., Raike, R.S., Frants, R.R., Hess, E.J., Hoebeek, F.E., De Zeeuw, C.I. and van den Maagdenberg, A.M., 2012. Purkinje cell-specific ablation of Ca_v2.1 channels is sufficient to cause cerebellar ataxia in mice. *The Cerebellum*, 11(1), pp.246-258.
- Tomita, S., Adesnik, H., Sekiguchi, M., Zhang, W., Wada, K., Howe, J.R., Nicoll, R.A. and Brecht, D.S., 2005. Stargazin modulates AMPA receptor gating and trafficking by distinct domains. *Nature*, 435(7045), pp.1052-1058.
- Tønnesen, J., Sørensen, A.T., Deisseroth, K., Lundberg, C. and Kokaia, M., 2009. Optogenetic control of epileptiform activity. *Proceedings of the National Academy of Sciences*, 106(29), pp.12162-12167.
- Tønnesen, J. and Kokaia, M., 2017. Epilepsy and optogenetics: can seizures be controlled by light? *Clinical science*, 131(14), pp.1605-1616.
- Tovote, P., Fadok, J.P. and Lüthi, A., 2015. Neuronal circuits for fear and anxiety. *Nature reviews neuroscience*, 16(6), pp.317-331.
- Tremblay, R., Lee, S. and Rudy, B., 2016. GABAergic interneurons in the neocortex: from cellular properties to circuits. *Neuron*, 91(2), pp.260-292.
- Trinka, E., Baumgartner, S., Unterberger, I., Unterrainer, J., Luef, G., Haberlandt, E. and Bauer, G., 2004. Long-term prognosis for childhood and juvenile absence epilepsy. *Journal of neurology*, 251(10), pp.1235-1241.
- Trinka, E., Bauer, G., Oberaigner, W., Ndayisaba, J.P., Seppi, K. and Granbichler, C.A., 2013. Cause-specific mortality among patients with epilepsy: results from a 30-year cohort study. *Epilepsia*, 54(3), pp.495-501.
- Tsai, P.T., Hull, C., Chu, Y., Greene-Colozzi, E., Sadowski, A.R., Leech, J.M., Steinberg, J., Crawley, J.N., Regehr, W.G. and Sahin, M., 2012. Autistic-like behaviour and cerebellar dysfunction in Purkinje cell Tsc1 mutant mice. *Nature*, 488(7413), pp.647-651.
- Tucker, D.M., Brown, M., Luu, P. and Holmes, M.D., 2007. Discharges in ventromedial frontal cortex during absence spells. *Epilepsy & behaviour*, 11(4), pp.546-557.
- Turner, C.P., DeBenedetto, D., Ware, E., Stowe, R., Lee, A., Swanson, J., Walburg, C., Lambert, A., Lyle, M., Desai, P. and Liu, C., 2010. Postnatal exposure to MK801 induces selective changes in GAD67 or parvalbumin. *Experimental brain research*, 201(3), pp.479-488.

- Tuscher, J.J., Taxier, L.R., Fortress, A.M. and Frick, K.M., 2018. Chemogenetic inactivation of the dorsal hippocampus and medial prefrontal cortex, individually and concurrently, impairs object recognition and spatial memory consolidation in female mice. *Neurobiology of learning and memory*, 156, pp.103-116.
- Upright, N.A., Brookshire, S.W., Schnebelen, W., Damatac, C.G., Hof, P.R., Browning, P.G., Croxson, P.L., Rudebeck, P.H. and Baxter, M.G., 2018. Behavioral effect of chemogenetic inhibition is directly related to receptor transduction levels in rhesus monkeys. *Journal of Neuroscience*, 38(37), pp.7969-7975.
- Urak, L., Feucht, M., Fathi, N., Hornik, K. and Fuchs, K., 2006. A GABRB3 promoter haplotype associated with childhood absence epilepsy impairs transcriptional activity. *Human molecular genetics*, 15(16), pp.2533-2541.
- Urban, D.J. and Roth, B.L., 2015. DREADDs (designer receptors exclusively activated by designer drugs): chemogenetic tools with therapeutic utility. *Annual review of pharmacology and toxicology*, 55, pp.399-417.
- Vadlamudi, L., Andermann, E., Lombroso, C.T., Schachter, S.C., Milne, R.L., Hopper, J.L., Andermann, F. and Berkovic, S.F., 2004. Epilepsy in twins: insights from unique historical data of William Lennox. *Neurology*, 62(7), pp.1127-1133
- Vanasse, C.M., Beland, R., Carmant, L. and Lassonde, M., 2005. Impact of childhood epilepsy on reading and phonological processing abilities. *Epilepsy & behaviour*, 7(2), pp.288-296.
- Van Erum, J., Van Dam, D. and De Deyn, P.P., 2019. PTZ-induced seizures in mice require a revised Racine scale. *Epilepsy & behaviour*, 95, pp.51-55.
- Van Erum, J., Valkenburg, F., Van Dam, D. and De Deyn, P.P., 2020. Pentylentetrazole-induced Seizure Susceptibility in the Tau58/4 Transgenic Mouse Model of Tauopathy. *Neuroscience*, 425, pp.112-122.
- van Luijtelaar, E.L., Weltink, J., 2001. Sleep spindles and spike-wave discharges in rats. In: Alex L. van Bommel, et al. (eds.), *Sleep-wake research in the Netherlands*, Van Zuiden, Alphen: Het Zuiden, 12, pp.81–86.
- van Luijtelaar, G. and Sitnikova, E., 2006. Global and focal aspects of absence epilepsy: the contribution of genetic models. *Neuroscience & biobehavioural reviews*, 30(7), pp.983-1003.
- Vardy, E., Robinson, J.E., Li, C., Olsen, R.H., DiBerto, J.F., Giguere, P.M., Sassano, F.M., Huang, X.P., Zhu, H., Urban, D.J. and White, K.L., 2015. A new DREADD facilitates the multiplexed chemogenetic interrogation of behaviour. *Neuron*, 86(4), pp.936-946.
- Varin, C. and Bonnavion, P., 2018. Pharmacosynthetic deconstruction of sleep-wake circuits in the brain. In *Sleep-Wake neurobiology and pharmacology*, pp.153-206. Springer, Cham.

- Vega, C., Guo, J., Killory, B., Danielson, N., Vestal, M., Berman, R., Martin, L., Gonzalez, J.L., Blumenfeld, H. and Spann, M.N., 2011. Symptoms of anxiety and depression in childhood absence epilepsy. *Epilepsia*, 52(8), pp.e70-e74.
- Velasco, M., Velasco, F., Velasco, A.L., Luján, M. and del Mercado, J.V., 1989. Epileptiform EEG activities of the Centro median thalamic nuclei in patients with intractable partial motor, complex partial, and generalized seizures. *Epilepsia*, 30(3), pp.295-306.
- Velišková, J., Shakarjian, M.P. and Velišek, L., 2017. Systemic chemoconvulsants producing acute seizures in adult rodents. In *Models of seizures and epilepsy*, pp.491-512. Academic Press.
- Venzi, M., Di Giovanni, G. and Crunelli, V., 2015. A critical evaluation of the gamma-hydroxybutyrate (GHB) model of absence seizures. *CNS neuroscience & therapeutics*, 21(2), pp.123-140.
- Verret, L., Mann, E.O., Hang, G.B., Barth, A.M., Cobos, I., Ho, K., Devidze, N., Masliah, E., Kreitzer, A.C., Mody, I. and Mucke, L., 2012. Inhibitory interneuron deficit links altered network activity and cognitive dysfunction in Alzheimer model. *Cell*, 149(3), pp.708-721.
- von Krosigk, M., Bal, T. and McCormick, D.A., 1993. Cellular mechanisms of a synchronized oscillation in the thalamus. *Science*, 261(5119), pp.361-364.
- Vitellaro-Zuccarello, L., Calvaresi, N. and De Biasi, S., 2003. Expression of GABA transporters, GAT-1 and GAT-3, in the cerebral cortex and thalamus of the rat during postnatal development. *Cell and tissue research*, 313(3), pp.245-257.
- Wakamori, M., Yamazaki, K., Matsunodaira, H., Teramoto, T., Tanaka, I., Niidome, T., Sawada, K., Nishizawa, Y., Sekiguchi, N., Mori, E. and Mori, Y., 1998. Single tottering mutations responsible for the neuropathic phenotype of the P-type calcium channel. *Journal of biological chemistry*, 273(52), pp.34857-34867.
- Wallace, R.H., Marini, C., Petrou, S., Harkin, L.A., Bowser, D.N., Panchal, R.G., Williams, D.A., Sutherland, G.R., Mulley, J.C., Scheffer, I.E. and Berkovic, S.F., 2001. Mutant GABA A receptor γ 2-subunit in childhood absence epilepsy and febrile seizures. *Nature genetics*, 28(1), pp.49-52.
- Wang, J., Zhang, Y., Liang, J., Pan, H., Wu, H., Xu, K., Liu, X., Jiang, Y., Shen, Y. and Wu, X., 2006. CACNA1I is not associated with childhood absence epilepsy in the Chinese Han population. *Pediatric neurology*, 35(3), pp.187-190.
- Wang, J.G., Cai, Q., Zheng, J., Dong, Y.S., Li, J.J., Li, J.C., Hao, G.Z., Wang, C. and Wang, J.L., 2016. Epigenetic suppression of GADs expression is involved in temporal lobe epilepsy and pilocarpine-induced mice epilepsy. *Neurochemical research*, 41(7), pp.1751-1760.
- Wang, Y., Liang, J., Chen, L., Shen, Y., Zhao, J., Xu, C., Wu, X., Cheng, H., Ying, X., Guo, Y. and Wang, S., 2018. Pharmacogenetic therapeutics targeting parvalbumin neurons attenuate temporal lobe epilepsy. *Neurobiology of disease*, 117, pp.149-160.

- Warren, R., Tremblay, N. and Dykes, R.W., 1989. Quantitative study of glutamic acid decarboxylase-immunoreactive neurons and cytochrome oxidase activity in normal and partially deafferented rat hindlimb somatosensory cortex. *Journal of comparative neurology*, 288(4), pp.583-592
- Waters, J.C., 2009. Accuracy and precision in quantitative fluorescence microscopy. *Journal of cell biology*, 185, pp.1135-1148.
- Wei, J., Zhong, P., Qin, L., Tan, T. and Yan, Z., 2018. Chemicogenetic restoration of the prefrontal cortex to amygdala pathway ameliorates stress-induced deficits. *Cerebral cortex*, 28(6), pp.1980-1990.
- Wettschureck, N. and Offermanns, S., 2005. Mammalian G proteins and their cell type specific functions. *Physiological reviews*, 85(4), pp.1159-1204.
- Wess, J., Nakajima, K. and Jain, S., 2013. Novel designer receptors to probe GPCR signalling and physiology. *Trends in pharmacological sciences*, 34(7), pp.385-392.
- Westmijse, I., Ossenblok, P., Gunning, B. and Van Luijtelaar, G., 2009. Onset and propagation of spike and slow wave discharges in human absence epilepsy: a MEG study. *Epilepsia*, 50(12), pp.2538-2548.
- Weston, M., Kaserer, T., Wu, A., Mouravlev, A., Carpenter, J.C., Snowball, A., Knauss, S., von Schimmelmann, M., Düring, M.J., Lignani, G. and Schorge, S., 2019. Olanzapine: A potent agonist at the hM4D (Gi) DREADD amenable to clinical translation of chemogenetics. *Science advances*, 5(4), p. eaaw1567.
- Wettschureck, N. and Offermanns, S., 2005. Mammalian G proteins and their cell type specific functions. *Physiological reviews*, 85(4), pp.1159-1204.
- Whissell, P.D., Tohyama, S. and Martin, L.J., 2016. The use of DREADDs to deconstruct behaviour. *Frontiers in genetics*, 7, p.70.
- White, H.S., Watson, W.P., Hansen, S.L., Slough, S., Perregaard, J., Sarup, A., Bolvig, T., Petersen, G., Larsson, O.M., Clausen, R.P. and Frølund, B., 2005. First demonstration of a functional role for central nervous system betaine/ γ -aminobutyric acid transporter (mGAT2) based on synergistic anticonvulsant action among inhibitors of mGAT1 and mGAT2. *Journal of Pharmacology and Experimental Therapeutics*, 312(2), pp.866-874.
- WHO Factsheet 2019. <https://www.who.int/en/news-room/fact-sheets/detail/epilepsy>
- Wicker, E. and Forcelli, P.A., 2016. Chemogenetic silencing of the midline and intralaminar thalamus blocks amygdala-kindled seizures. *Experimental neurology*, 283, pp.404-412.
- Williams, S.R. and Stuart, G.J., 2000. Site independence of EPSP time course is mediated by dendritic I_h in neocortical pyramidal neurons. *Journal of neurophysiology*, 83(5), pp.3177-3182.

- Williams, D., 1953. A study of thalamic and cortical rhythms in petit mal. *Brain*, 76(1), pp.50-69.
- Wirrell, E.C., Camfield, C.S., Camfield, P.R., Gordon, K.E. and Dooley, J.M., 1996. Long-term prognosis of typical childhood absence epilepsy: remission or progression to juvenile myoclonic epilepsy. *Neurology*, 47(4), pp.912-918.
- Wirrell, E.C., Camfield, C.S., Camfield, P.R., Dooley, J.M., Gordon, K.E. and Smith, B., 1997. Long-term psychosocial outcome in typical absence epilepsy: sometimes a wolf in sheep's clothing. *Archives of pediatrics & adolescent medicine*, 151(2), pp.152-158.
- Wisler, J.W., DeWire, S.M., Whalen, E.J., Violin, J.D., Drake, M.T., Ahn, S., Shenoy, S.K. and Lefkowitz, R.J., 2007. A unique mechanism of β -blocker action: carvedilol stimulates β -arrestin signaling. *Proceedings of the national academy of sciences*, 104(42), pp.16657-16662.
- Wittner, L., Maglóczky, Z., Borhegyi, Z., Halasz, P., Tóth, S., Eröss, L., Szabo, Z. and Freund, T.F., 2001. Preservation of perisomatic inhibitory input of granule cells in the epileptic human dentate gyrus. *Neuroscience*, 108(4), pp.587-600.
- Wolf, P., 2010. Much ado about nothing? *Epilepsia*, 51(4), pp.717-718.
- Wolff, S.B., Gründemann, J., Tovote, P., Krabbe, S., Jacobson, G.A., Müller, C., Herry, C., Ehrlich, I., Friedrich, R.W., Letzkus, J.J. and Lüthi, A., 2014. Amygdala interneuron subtypes control fear learning through disinhibition. *Nature*, 509(7501), pp.453-458.
- Wöhr, M., Orduz, D., Gregory, P., Moreno, H., Khan, U., Vörckel, K.J., Wolfer, D.P., Welzl, H., Gall, D., Schiffmann, S.N. and Schwaller, B., 2015. Lack of parvalbumin in mice leads to behavioral deficits relevant to all human autism core symptoms and related neural morphofunctional abnormalities. *Translational psychiatry*, 5(3), pp. e525-e525.
- Wu, J.W., Hussaini, S.A., Bastille, I.M., Rodriguez, G.A., Mrejeru, A., Rilett, K., Sanders, D.W., Cook, C., Fu, H., Boonen, R.A. and Herman, M., 2016. Neuronal activity enhances tau propagation and tau pathology in vivo. *Nature neuroscience*, 19(8), p.1085.
- Wu, C., Xiang, J., Sun, J., Huang, S., Tang, L., Miao, A., Zhou, Y., Chen, Q., Hu, Z. and Wang, X., 2017. Quantify neuromagnetic network changes from pre-ictal to ictal activities in absence seizures. *Neuroscience*, 357, pp.134-144.
- Wyeth, M.S., Zhang, N., Mody, I. and Houser, C.R., 2010. Selective reduction of cholecystokinin-positive basket cell innervation in a model of temporal lobe epilepsy. *Journal of Neuroscience*, 30(26), pp.8993-9006.
- Xenos, D., Kamceva, M., Tomasi, S., Cardin, J.A., Schwartz, M.L. and Vaccarino, F.M., 2018. Loss of TrkB signalling in parvalbumin-expressing basket cells results in network activity disruption and abnormal behaviour. *Cerebral Cortex*, 28(10), pp.3399-3413.

- Xia, F., Richards, B.A., Tran, M.M., Josselyn, S.A., Takehara-Nishiuchi, K. and Frankland, P.W., 2017. Parvalbumin-positive interneurons mediate neocortical-hippocampal interactions that are necessary for memory consolidation. *Elife*, 6, p.e27868.
- Xu, X., Roby, K.D. and Callaway, E.M., 2010. Immunochemical characterization of inhibitory mouse cortical neurons: three chemically distinct classes of inhibitory cells. *Journal of Comparative Neurology*, 518(3), pp.389-404.
- Xu, D., Cui, J., Wang, J., Zhang, Z., She, C. and Bai, W., 2018. Improving the Application of High Molecular Weight Biotinylated Dextran Amine for Thalamocortical Projection Tracing in the Rat. *Journal of visualized experiments*, (134), p.e55938.
- Yamazaki, M., Le Pichon, C.E., Jackson, A.C., Cerpas, M., Sakimura, K., Scearce-Levie, K. and Nicoll, R.A., 2015. Relative contribution of TARPs γ -2 and γ -7 to cerebellar excitatory synaptic transmission and motor behaviour. *Proceedings of the national academy of sciences*, 112(4), pp. E371-E379.
- Yekhleif, L., Breschi, G.L., Lagostena, L., Russo, G. and Taverna, S., 2015. Selective activation of parvalbumin-or somatostatin-expressing interneurons triggers epileptic seizure like activity in mouse medial entorhinal cortex. *Journal of neurophysiology*, 113(5), pp.1616-1630.
- Yeni, S.N., Kabasakal, L., Yalçinkaya, C., Nisli, C. and Dervent, A., 2000. Ictal and interictal SPECT findings in childhood absence epilepsy. *Seizure*, 9(4), pp.265-269.
- Yi, F., Ball, J., Stoll, K.E., Satpute, V.C., Mitchell, S.M., Pauli, J.L., Holloway, B.B., Johnston, A.D., Nathanson, N.M., Deisseroth, K. and Gerber, D.J., 2014. Direct excitation of parvalbumin-positive interneurons by M1 muscarinic acetylcholine receptors: roles in cellular excitability, inhibitory transmission and cognition. *The Journal of physiology*, 592(16), pp.3463-3494.
- Yuan, P. and Grutzendler, J., 2016. Attenuation of β -amyloid deposition and neurotoxicity by chemogenetic modulation of neural activity. *Journal of neuroscience*, 36(2), pp.632-641.
- York III, G.K. and Steinberg, D.A., 2011. Hughlings Jackson's neurological ideas. *Brain*, 134(10), pp.3106-3113.
- Zack, M.M. and Kobau, R., 2017. National and state estimates of the numbers of adults and children with active epilepsy—United States, 2015. *Morbidity and mortality weekly report*, 66(31), p.821.
- Zaitsev, A.V., Povysheva, N.V., Lewis, D.A. and Krimer, L.S., 2007. P/Q-type, but not N-type, calcium channels mediate GABA release from fast-spiking interneurons to pyramidal cells in rat prefrontal cortex. *Journal of neurophysiology*, 97(5), pp.3567-3573.
- Zhang, F., Wang, L.P., Brauner, M., Liewald, J.F., Kay, K., Watzke, N., Wood, P.G., Bamberg, E., Nagel, G., Gottschalk, A. and Deisseroth, K., 2007. Multimodal fast optical interrogation of neural circuitry. *Nature*, 446(7136), pp.633-639.

Zhang, F., Gradinaru, V., Adamantidis, A.R., Durand, R., Airan, R.D., De Lecea, L. and Deisseroth, K., 2010. Optogenetic interrogation of neural circuits: technology for probing mammalian brain structures. *Nature protocols*, 5(3), p.439.

Zhang, Y., Jiang, Y.Y., Shao, S., Zhang, C., Liu, F.Y., Wan, Y. and Yi, M., 2017. Inhibiting medial septal cholinergic neurons with DREADD alleviated anxiety-like behaviours in mice. *Neuroscience letters*, 638, pp.139-144.

Zhang, Z., Ma, Z., Zou, W., Guo, H., Liu, M., Ma, Y. and Zhang, L., 2019. The Appropriate Marker for Astrocytes: Comparing the Distribution and Expression of Three Astrocytic Markers in Different Mouse Cerebral Regions. *BioMed research international*, 2019.

Zhou, Q.G., Nemes, A.D., Lee, D., Ro, E.J., Zhang, J., Nowacki, A.S., Dymecki, S.M., Najm, I.M. and Suh, H., 2019. Chemogenetic silencing of hippocampal neurons suppresses epileptic neural circuits. *The Journal of clinical investigation*, 129(1), pp.310-323.

Zhu, H., Pleil, K.E., Urban, D.J., Moy, S.S., Kash, T.L. and Roth, B.L., 2014. Chemogenetic inactivation of ventral hippocampal glutamatergic neurons disrupts consolidation of contextual fear memory. *Neuropsychopharmacology*, 39(8), pp.1880-1892.

Zhu, H. and Roth, B.L., 2015. DREADD: a chemogenetic GPCR signalling platform. *International Journal of Neuropsychopharmacology*, 18(1).

Zhu, H., Aryal, D.K., Olsen, R.H., Urban, D.J., Swearingen, A., Forbes, S., Roth, B.L. and Hochgeschwender, U., 2016. Cre-dependent DREADD (designer receptors exclusively activated by designer drugs) mice. *Genesis*, 54(8), pp.439-446.

Zhu, Y., Wienecke, C.F., Nachtrab, G. and Chen, X., 2016. A thalamic input to the nucleus accumbens mediates opiate dependence. *Nature*, 530(7589), pp.219-222.

Zou, D., Chen, L., Deng, D., Jiang, D., Dong, F., McSweeney, C., Zhou, Y., Liu, L., Chen, G., Wu, Y. and Mao, Y., 2016. DREADD in parvalbumin interneurons of the dentate gyrus modulates anxiety, social interaction and memory extinction. *Current molecular medicine*, 16(1), pp.91-102.

Appendix

Preparation of reagents and solutions

0.1M Sorensen's phosphate buffer (PB)

- Solution A: 28.39 gm of Na_2HPO_4 in 1L MQ H_2O
- Solution B: 27.59 gm $\text{NaH}_2\text{PO}_4 \times \text{H}_2\text{O}$ in 1L MQ H_2O
- 4 parts of solution A and 1 part of solution B was mixed.

10x PBS

- 5.675 gm Na_2HPO_4
- 1.361 gm KH_2PO_4
- 43.8 gm NaCl
- 0.5 L MQ H_2O

8% PFA (always made fresh on the day of perfusion)

- 20 gm PFA mixed with 200 ml MQ H_2O
- Solution was heated up to 60 °C with continuous stirring
- Few drops of 0.1 M NaOH was added
- Solution was filtered
- Volume was adjusted to 250 ml with MQ H_2O

4% PFA

- 250 ml of 8% PFA mixed with 250 ml of 0.2 M PB

5% Heparin

- 5 ml of Heparin mixed with 10 ml of 10X PBS and 85 ml of MQ H_2O

Sucrose solution (cryoprotectant)

- 30% sucrose: 30 gm sucrose in 100 ml PBS
- 20% sucrose: 20 ml of 30% sucrose solution mixed with 10 ml PBS
- 10% sucrose: 10 ml of 30% sucrose solution mixed with 10 ml PBS

IHC Blocking buffer

- 4% Normal Goat Serum (NGS)
- 0.1% Bovine Serum Albumin (BSA)
- 0.1% Triton X-100 in PBS

IHC Primary antibody solution

- 0.1% BSA
- 0.3% Triton X-100 in PBS

IHC Secondary antibody solution

- 0.3% Triton X-100 in PBS
-

DABCO-glycerol

- 15 ml Glycerol-gelatin
- 37.5 mg DABCO

WB Homogenization buffer

- 0.5 M Tris (pH6.8)
- 100 mM EDTA
- 3% SDS, pH 6.8

10x Tris-Glycine buffer

- 144 gm Glycine
- 30.3 gm Tris-base
- 1 L MQ H₂O

WB Running buffer

- 100 ml 10x Tris-Glycine buffer
- 10 ml 10% SDS
- 1 L MQ H₂O

WB Transfer buffer

- 100 ml 10x Tris-Glycine buffer
- 100 ml methanol
- 2.5 ml 10% SDS
- 1 L MQ H₂O

5x Tris buffered saline (TBS)

- 30 gm Tris
- 43.5 gm NaCl
- 1 L MQ H₂O

TBS-Tween

- 200 ml 5x TBS
- 1 ml Tween-20
- 1 L MQ H₂O

DNA lysis buffer (pH 8.5)

- 12.11 gm Tris-base
- 1.80 gm EDTA
- gm SDS
- 11.68 gm NaCl
- 1 L MQ H₂O

TE buffer (pH 8.0)

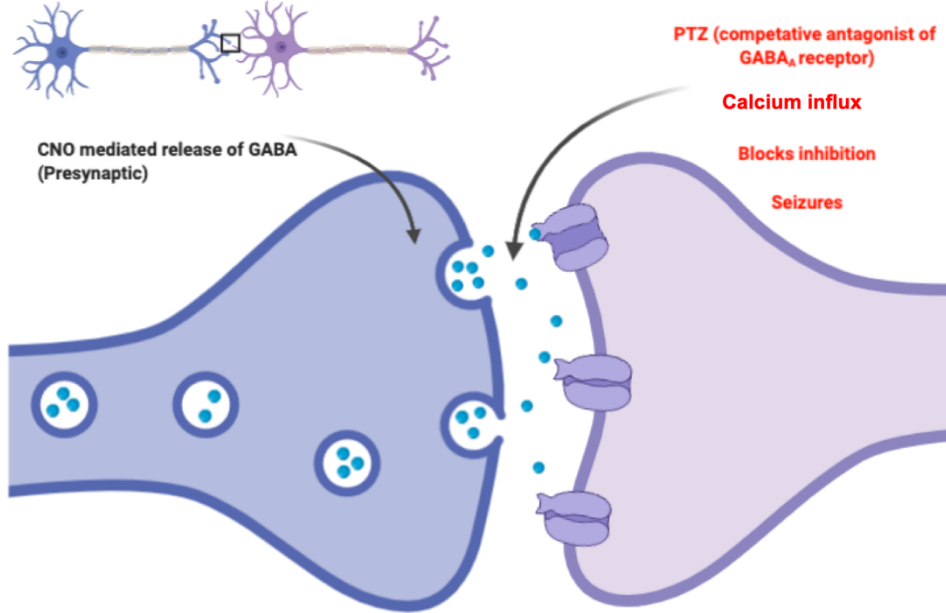
- 1.211 gm Tris base
- 0.372 gm EDTA
- 1 L MQ H₂O

10x TBE buffer

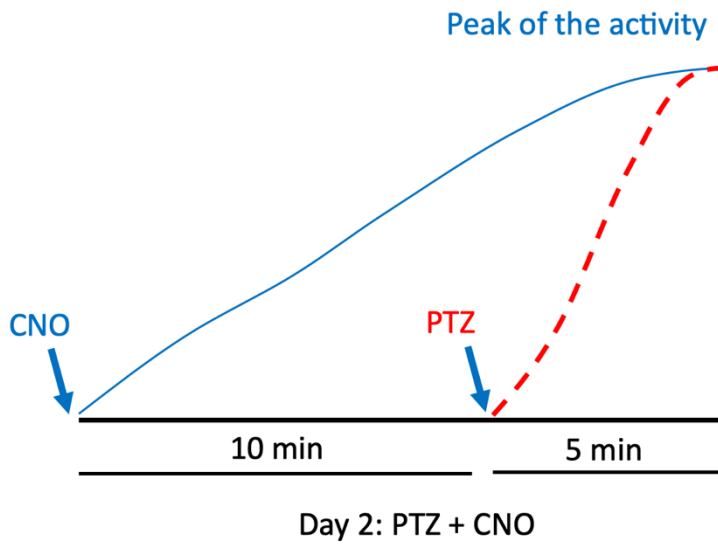
- 108 gm Tris base, 55 gm Boric acid
- 9.3 gm EDTA with 1 L MQ H₂O

Supplementary Fig. 2 (A) CNO acts presynaptically facilitating GABA release and PTZ acts on GABA_A receptors of postsynaptic neurons to induce seizures. (B) CNO was injected 10 min before PTZ injection on day 2. This was based on the results from chapter 3 where CNO activated PV+ neurons within 15 min and in chapter 4 (day 1) PTZ induced seizures in animals around 5 min.

A.

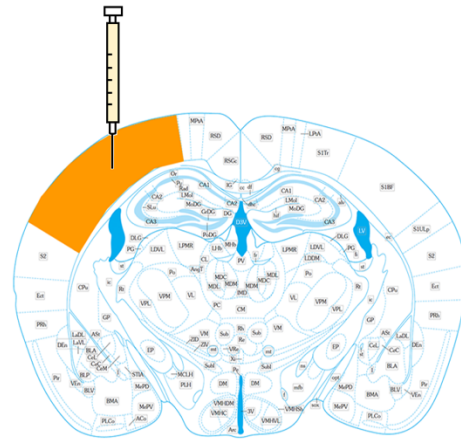
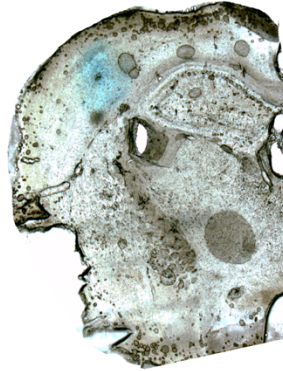


B.



Supplementary Fig. 3 Image showing the localization and diffusion of methylene blue dye in PV^{Cre}/Gq-DREADD animal. Representative coronal slices of mouse brain showing histological localization of methylene blue dye injected via a cannula located in either (A) SS cortex and (B) thalamus, verifying CNO site of diffusion within those regions. Coronal slice drawings were adapted from Mouse Brain Atlas Paxinos and Franklin, 3rd edition.

A.



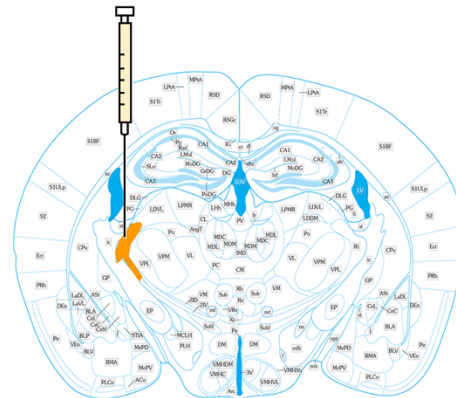
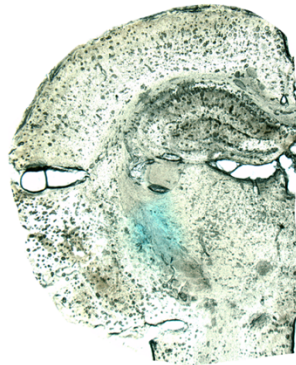
Bregma -1.58

AP -1.22mm to -2.06mm

ML: 2.8mm

DV: -1.5mm

B.



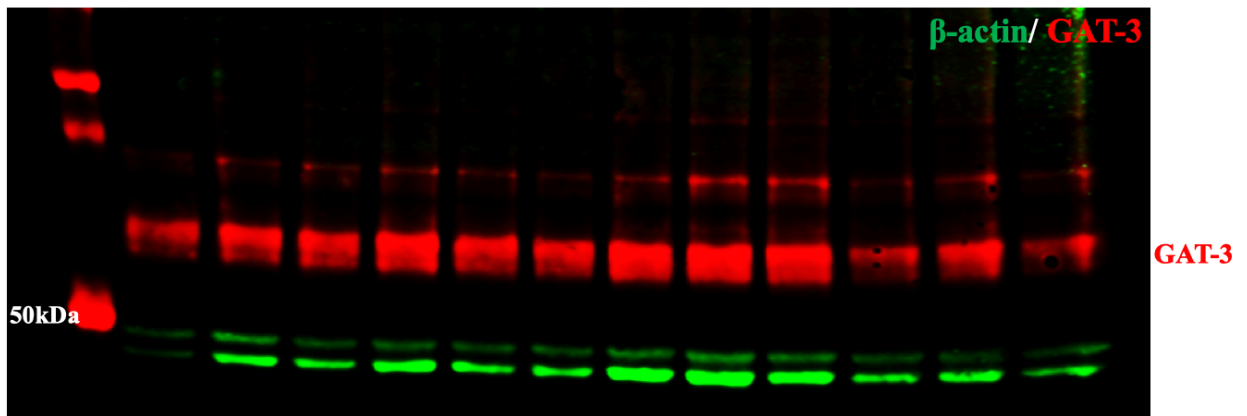
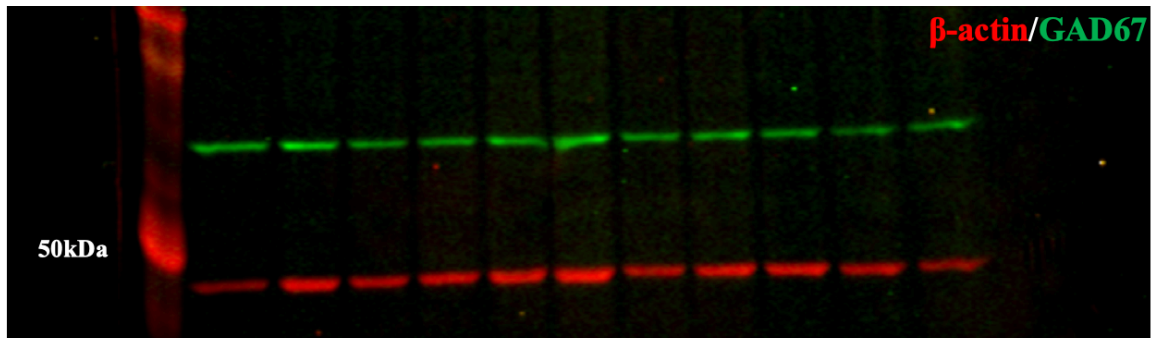
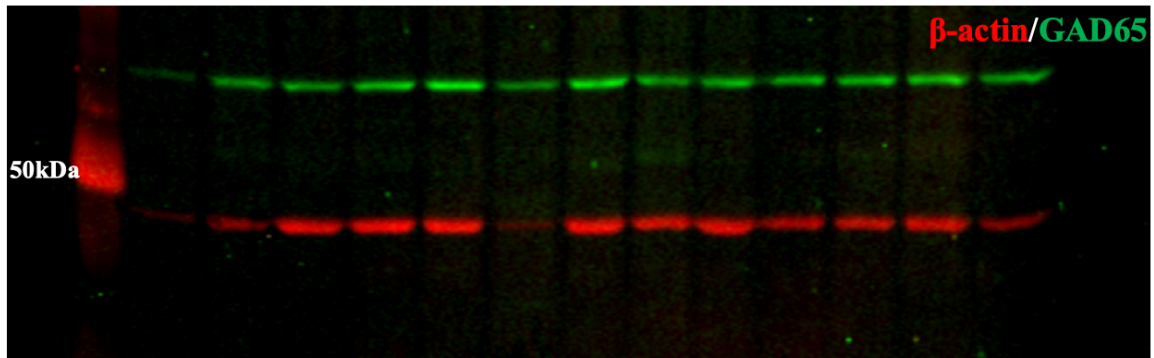
Bregma -1.58

AP -1.34mm to -1.94mm

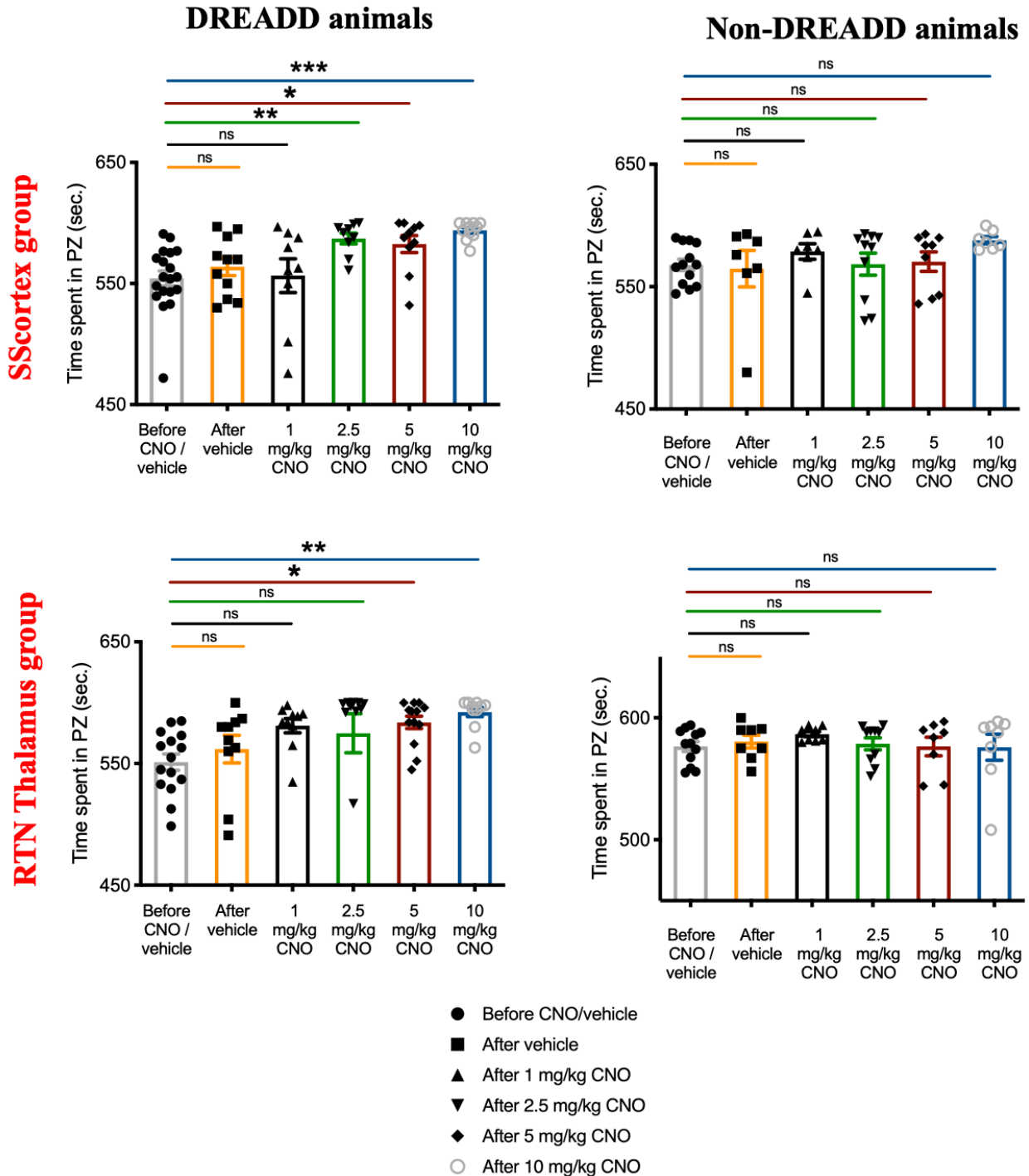
ML : 2.1-2.3mm

DV: -3.2 to -3.5mm

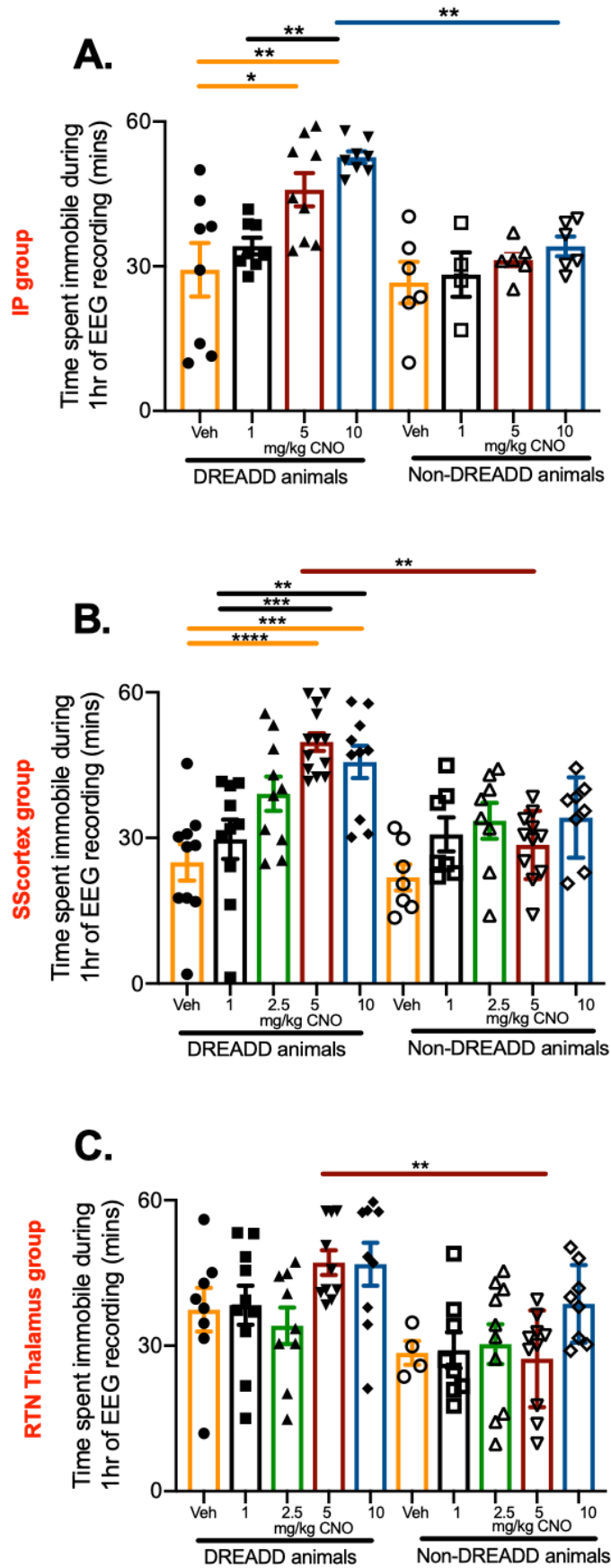
Supplementary Fig. 4 Non-cropped full western blots for antibodies used in this study.
(β -actin: ~42kDa, GAD65: ~65kDa, GAD67: ~67kDa, GAT-3: ~65-70kDa)



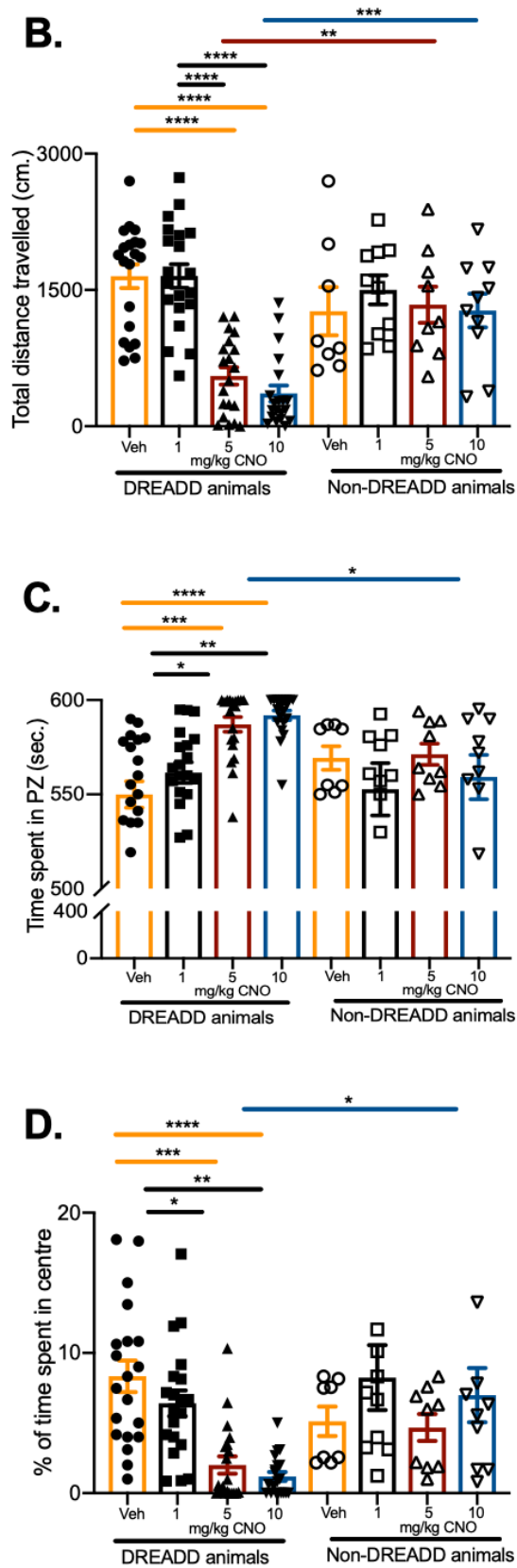
Supplementary Fig. 5 Total time spent in the peripheral zone (PZ) of open-field arena by animals after focal CNO/vehicle injection. Graphs represent animals of the SS cortex group and the RTN thalamus group. Comparisons between treatment groups were performed using Dunnett's post hoc multiple comparison test keeping 'before CNO/vehicle treatment' as a single control. All values represent mean \pm SEM.



Supplementary Fig. 6 Individual data points corresponding to the figure 3.9.
 (Immobility in animals after CNO injection during 1 hour of EEG recording.)



Supplementary Fig. 6 Individual data points corresponding to the figure 3.10.
 (Comparison of parameters of open-field test in animals after injection of different i.p. doses of CNO.)





The impact of silencing feed-forward parvalbumin-expressing inhibitory interneurons in the cortico-thalamocortical network on seizure generation and behaviour



Sandesh Panthi, Beulah Leitch*

Department of Anatomy, School of Biomedical Sciences, and Brain Health Research Centre, University of Otago, Dunedin, New Zealand

ARTICLE INFO

Keywords:

Feedforward inhibition
Cortico-thalamocortical
Somatosensory cortex
Parvalbumin
GABAergic interneurons
DREADDs
Absence seizures
Motor dysfunction

ABSTRACT

Feed-forward inhibition (FFI) is an essential mechanism within the brain, to regulate neuronal firing and prevent runaway excitation. In the cortico-thalamocortical (CTC) network, fast spiking parvalbumin-expressing (PV+) inhibitory interneurons regulate the firing of pyramidal cells in the cortex and relay neurons in the thalamus. PV+ interneuron dysfunction has been implicated in several neurological disorders, including epilepsy. Previously, we demonstrated that loss of excitatory AMPA-receptors, specifically at synapses on PV+ interneurons in CTC feedforward microcircuits, occurs in the stargazer mouse model of absence epilepsy. These mice present with absence seizures characterized by spike and wave discharges (SWDs) on electroencephalogram (EEG) and concomitant behavioural arrest, similar to childhood absence epilepsy. The aim of the current study was to investigate the impact of loss of FFI within the CTC on absence seizure generation and behaviour using new Designer Receptor Exclusively Activated by Designer Drug (DREADD) technology. We crossed PV-Cre mice with Cre-dependent hM4Di DREADD strains of mice, which allowed Cre-recombinase-mediated restricted expression of inhibitory G_i-DREADDs in PV+ interneurons. We then tested the impact of global and focal (within the CTC network) silencing of PV+ interneurons. CNO mediated silencing of all PV+ interneurons by intraperitoneal injection caused the impairment of motor control, decreased locomotion and increased anxiety in a dose-dependent manner. Such silencing generated pathological oscillations similar to absence-like seizures. Focal silencing of PV+ interneurons within cortical or thalamic feedforward microcircuits, induced SWD-like oscillations and associated behavioural arrest. Epileptiform activity on EEG appeared significantly sooner after focal injection compared to peripheral injection of CNO. However, the mean duration of each oscillatory burst and spike frequency was similar, irrespective of mode of CNO delivery. No significant changes were observed in vehicle-treated or non-DREADD wild-type control animals. These data suggest that dysfunctional feed-forward inhibition in CTC microcircuits may be an important target for future therapy strategies for some patients with absence seizures. Additionally, silencing of PV+ interneurons in other brain regions may contribute to anxiety related neurological and psychiatric disorders.

1. Introduction

Parvalbumin-expressing (PV+) inhibitory interneurons are the most common type of GABAergic neurons within the brain (Kelsom and Lu, 2013; Hu et al., 2014; Pelkey et al., 2017). They mediate fast feed-

forward inhibition (FFI) and prevent runaway excitation (Cammarota et al., 2013; Paz and Huguenard, 2015; Jiang et al., 2016) in neural networks. They also contribute to feed-back inhibition and are critically involved in the generation of physiological oscillations within brain networks (Sohal et al., 2009; Armstrong and Soltesz, 2012).

Abbreviations: AAV, adeno-associated vector; AMPA, α -amino-3-hydroxy-5-methyl-4-isoxazolepropionic acid; CNO, clozapine-N-oxide; CT, corticothalamic; CTC, cortico-thalamocortical; CZ, central zone; DREADDs, designer receptor exclusively activated by designer drugs; EEG, electroencephalogram; ETX, ethosuximide; FFI, feed-forward inhibition; GABA, γ -aminobutyric acid; GAERS, genetic absence epilepsy rat from Strasbourg; GPCR, G-protein coupled receptor; IP, intraperitoneal; LV, lentiviral vector; NGS, normal goat serum; PBS, phosphate buffered saline; PFA, paraformaldehyde; PV+, parvalbumin expressing; PZ, peripheral zone; RTN, reticular thalamic nuclei; SS cortex, somatosensory cortex; SWDs, spike-wave discharges; TC, thalamocortical; VP, ventral posterior; WT, wild-type

* Corresponding author at: Department of Anatomy, School of Biomedical Sciences, Brain Health Research Centre, University of Otago, PO Box 913, Dunedin, New Zealand.

E-mail address: beulah.leitch@otago.ac.nz (B. Leitch).

<https://doi.org/10.1016/j.nbd.2019.104610>

Received 16 April 2019; Received in revised form 10 August 2019; Accepted 4 September 2019

Available online 05 September 2019

0969-9961/ © 2019 Elsevier Inc. All rights reserved.

Additionally, they play roles in brain plasticity, cognition and learning (Milenkovic et al., 2013). PV+ interneuron dysfunction has been implicated in several neurological and psychiatric disorders, including epilepsy, autism, depression, schizophrenia and Alzheimer's disease (Lewis et al., 2012; Marín, 2012; Holland et al., 2014; Nguyen et al., 2014; Dodell-Feder et al., 2015; Evans et al., 2015).

In the cortico-thalamocortical (CTC) network PV+ interneurons are strategically positioned to provide strong feed-forward inhibition to the principal excitatory cortical neurons (pyramidal cells) and also to excitatory relay (thalamocortical TC) neurons in the ventroposterior (VP) thalamus. Sensory information is relayed through the thalamus to the somatosensory (SS) cortex via thalamocortical (TC) projections from the VP relay neurons to cortical layer IV; the cortex is reciprocally connected back to the thalamus via corticothalamic (CT) projections from pyramidal cells to the thalamic VP neurons. Surrounding the VP thalamus is the reticular thalamic nucleus (RTN) comprising a shell of PV+ inhibitory interneurons. The RTN inhibitory interneurons receive strong excitation via collaterals from CT projections and provide FFI to the VP relay neurons. Oscillations within the CTC network are directly related to the stronger synaptic excitation in the CT-RTN pathway than the CT-VP route, favouring activation of the RTN PV+ inhibitory interneurons (Warren et al., 1994; Paz et al., 2011). CTC network oscillations are initiated when FFI is followed by T-current dependent post-inhibitory rebound bursts of action potentials in VP relay neurons. The VP relay neurons in turn re-excite PV+ inhibitory interneurons in RTN via TC projection collaterals thereby activating feedback inhibition and oscillatory neural activity within the CTC network (Williams and Stuart, 2000; Beenhakker and Huguenard, 2009; Avoli, 2012). CTC oscillations, thus involve the finely tuned synchronous firing of thalamic and cortical neurons at specific frequencies. Disruption in the balance between excitation and inhibition within these CTC microcircuits can swing the network into hyperexcitability and hypersynchronous, pathological oscillations (McCormick and Diego, 2001; Crunelli and Nathalie, 2002), which are manifest as absence seizures and spike-wave discharges (SWDs) on electroencephalogram (EEG) (Panayiotopoulos, 2001).

We previously reported that absence seizures in the stargazer mouse model of absence epilepsy are associated with a loss of glutamatergic α -amino-3-hydroxy-5-methyl-4-isoxazolepropionic acid receptors (AMPA-type receptors), specifically at excitatory synapses in PV+ interneurons in the RTN thalamus and SS cortex (Barad et al., 2012; Adotevi and Leitch, 2016, 2017, 2019) due to a deficit in the transmembrane AMPA receptor regulatory protein (TARPs gamma-2) also called stargazin. Loss of excitatory drive to PV+ inhibitory interneurons would potentially lead to impaired FFI and disinhibition within these CTC microcircuits. The PV+ interneurons in the RTN thalamus and SS cortex express predominantly GluA4-AMPA receptors and knockout of this type of AMPA receptor subunit in the *Gria4*^{-/-} mouse also results in absence seizures (Paz et al., 2011). Further evidence that activation of PV+ interneurons and FFI are important in seizure prevention, comes from *in vivo* optogenetic activation of these interneurons, which has been shown to interrupt spontaneous ongoing seizures (e.g. in temporal lobe epilepsy Krook-Magnuson et al., 2013; and stroke-induced thalamocortical epilepsy Paz et al., 2013). However, other *in vitro* studies on brain slices suggest that optogenetic activation of GABAergic interneurons can enhance epileptiform activity (Yekhlef et al., 2014; Shiri et al., 2015). In the Genetic Absence Epilepsy Rat from Strasbourg (GAERS) enhancement of tonic inhibition in the VP thalamus is associated with absence seizures (Cope et al., 2009; Crunelli et al., 2012). So, while there is evidence that activation of PV+ expressing interneurons and FFI prevents seizure spread in both experimental models (Trevelyan et al., 2007; Cammarota et al., 2013) and patients (Schevon et al., 2012) there is also conflicting evidence from *in vitro* studies that increased GABAergic inhibition may, under certain conditions and dependent upon the brain region tested, initiate seizures (Sessolo et al., 2015).

To investigate whether loss of excitation to PV+ interneurons and FFI within the CTC network can lead to the generation of pathological SWDs and absence seizures *in vivo*, we used Designer Receptors Exclusively Activated by Designer Drugs (DREADDs) technology to selectively silence PV+ interneurons in the cortex and thalamus. DREADDs are mutationally modified muscarinic receptors (Armbruster et al., 2007; Rogan and Roth, 2011). Based on the G-protein coupled receptor (GPCR) signalling cascade modified, DREADDs can be of various types (Armbruster et al., 2007). However, G_i-DREADD (hM4Di for neuronal silencing) and G_q-DREADD (hM3Dq for neuronal firing) are the most common available DREADDs. These engineered GPCRs are only activated by the designer drug clozapine-N-Oxide (CNO). DREADDs can be expressed in specific cell types using viral delivery methods (Agulhon et al., 2013; Fortress et al., 2015; Pina et al., 2015; Falkner et al., 2016; Lopez et al., 2016; Fernandez et al., 2017) or double-transgenic mice approaches (Sciolino et al., 2016; Zhu et al., 2016).

To date, there have been only a few studies using DREADD technology to modulate PV+ interneurons; these have used PV-Cre mice injected with DREADD-based recombinant lentiviral vector (LV) or adeno-associated viral (AAV) vector for region and cell specific DREADD receptor expression (Kaplan et al., 2016; Zou et al., 2016; Drexel et al., 2017; Xia et al., 2017). In our study, we use recently developed Cre-dependent DREADD mice (Zhu et al., 2016) crossed with PV-Cre mice to express G_i-DREADDs in PV+ interneurons in the brain. We report the physiological and behavioural impact of silencing these interneurons both globally and focally in the CTC network, in terms of seizure generation and motor function using simultaneous EEG/video recording and behavioural tests.

2. Materials & methods

2.1. Animals and breeding paradigm

Experiments were performed on adult male and female transgenic mice expressing inhibitory DREADD receptors in PV+ interneurons. PV-Cre mice and Cre-recombinase conditional DREADD lines (Zhu et al., 2016) were obtained from Jackson Laboratories, USA. To avoid unwanted germline recombination, only female PV-Cre were crossed with male hM4Di-floxed mice (JAX stock #008069). Homozygous female PV-Cre mice were crossed with homozygous hM4Di-floxed males to generate litters of PV-Cre/G_i-DREADD mice, or crossed with heterozygous hM4Di-floxed males to generate litters with PV-Cre/G_i-DREADD and non-DREADD expressing wild-type (WT) control littermates, as illustrated in Fig. 1A. Mating these strains (PV-Cre and hM4Di-floxed) removes the loxP site-flanked STOP signal only in the cell type specified by the Cre driver used. A hemagglutinin (HA)-tag is present alongside the DREADD sequence in the targeting vector used to generate the DREADD transgenic mice. Antibodies directed against the HA-tag can be used to detect the location of the DREADD receptor in the cell after Cre-mediated removal of the STOP cassette under the strong control of the CAG promoter (Zhu et al., 2016). Mice were bred and housed at the University of Otago Animal Facility. All mice were housed at controlled room temperature (22–24 °C). Mice had *ad libitum* access to food and water. All animal procedures were approved by the University of Otago Animal Welfare Office and Ethics Committee (D94/16).

2.2. Genotyping

Genotyping was performed on ear-punches from offspring of PV-Cre/G_i-DREADD crossed mice. Briefly, ear-punches were digested in lysis buffer and proteinase K at 55 °C overnight. Next day, after several centrifugation procedures, DNA was obtained and processed for PCR. Genotyping was done to confirm PV-Cre and hM₄Di expression separately using the following Cre, hM₄Di mutant and wild-type primers

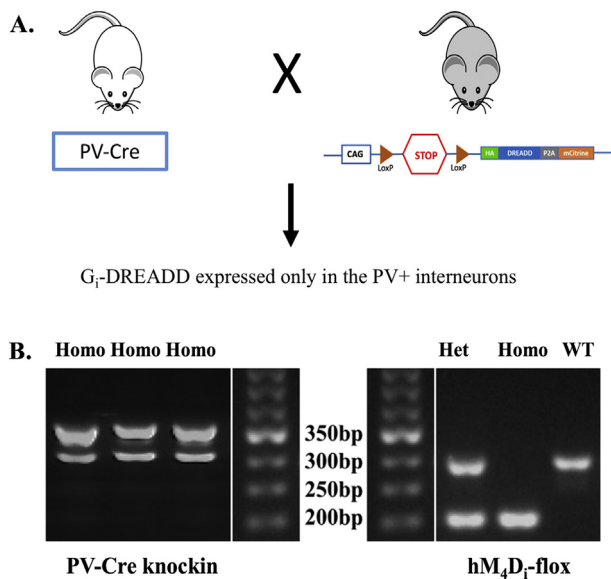


Fig. 1. (A) Schematic showing breeding to generate PV-Cre/ G_I -DREADD offspring and WT (non-DREADD) control mice by crossing a female homozygous PV-Cre mouse with either a homozygous or heterozygous G_I -DREADD male mouse. (B) Representative gel electrophoresis blot showing the homozygous (Homo) PV-Cre knockin (350 bp and 300 bp) and the hM4Di-flox [heterozygous (Het) 300 bp and 204 bp; homozygous (Homo) 204 bp; wild-type (WT) 300 bp] for three mice to verify PV-Cre knockin and hM4Di-flox. Genotyping was performed separately for PV-Cre knockin and hM4Di-flox in the same mouse.

(Integrated DNA Technologies, USA): CCT GGA AAA TGC TTC TGT CCG Cre-forward; CAG GGT GTT ATA AGC AAT CCC reverse for Cre allele; CGA AGT TAT TAG GTC CCT CGA C hM4Di-flox forward; TCA TAG CGA TTG TGG GAT GA reverse for hM4Di-flox allele; AAG GGG CTG CAG TGG AGT A wild-type forward; CCG AAA ATC TGT GGG AAG TC reverse for wild-type allele. Agarose gel (2%) electrophoresis was performed and the PCR product allowed to run at 70–80 V for ~2 h. Finally, the gel was placed on a UV light source to view and photograph bands. Fig. 1B is a representative image for the PV-Cre knockin and hM4Di-flox for three separate mice. Bands at 350 bp and 300 bp indicate the PV-Cre knockin. For hM4Di-flox, bands at 300 bp and 204 bp indicate the heterozygous hM4Di-flox, a band at 204 bp represents the homozygous hM4Di-flox, and a band at 300 bp confirmed wild-type mice.

2.3. Immunofluorescence confocal microscopy and image acquisition

Pentobarbital (60 mg/kg) was injected intraperitoneally to deeply anesthetize the mice. Transcardial perfusion was performed with 5% heparin in phosphate buffered saline (PBS) and 4% paraformaldehyde (PFA) in 0.1 M Sorensen's phosphate buffer. Brains were extracted and post-fixed in 4% PFA overnight at 4 °C. Post-fixation was followed by cryoprotection in increasing concentrations of sucrose in PBS (10%, 20%, and 30%). The cerebellum was dissected from the rest of the brain and sliced into 30- μ m sagittal sections on a cryostat (Leica CM1950, Wetzlar, Germany) and collected in PBS, the rest of the brain was sectioned into 30- μ m coronal sections. Slices were then transferred into blocking buffer (4% Normal Goat Serum (NGS), 0.1% Bovine Serum Albumin (BSA), 0.1% Triton X-100) for 2 h at room temperature. All sections were incubated in a cocktail of primary antibodies, rabbit anti-HA-tag, Cell Signalling (1:500) and mouse anti-parvalbumin (PV), Swant Inc. (1:2000), for 48 h at 4 °C. After incubation, tissue sections were washed in PBS for 45 min (15 min, 3 times each). Sections were then labelled with secondary antibodies, rabbit IgG, Alexa Fluor 488, Life Tech/A-11008 (1:1000); mouse IgG, Alexa Fluor 568, Life Tech/A-11031 (1:1000) for 12 h at 4 °C followed by PBS washing. Sections were

then mounted on polysine-coated glass slides and cover-slipped with mounting medium (1,4 diazabicyclo (2.2.2) octane DABCO-glycerol). Images were acquired using Nikon A1+ Inverted Confocal Laser Scanning Microscope with channel configuration; HA-tag (green channel, 488 nm laser excitation) and PV (red channel, 568 nm laser excitation). All immunolabelled cells in the SS cortex and cerebellum sections were counted at 10 \times in confocal images whereas those in RTN thalamus were counted using 40 \times confocal images. Cell counting was performed with ImageJ software (NIH, USA).

2.4. Surgical implantation of prefabricated headmounts and micro cannulas

Twelve-week old animals were single caged and handled for 2 days before surgery. Prefabricated mouse headmounts (Pinnacle Technologies, Austin, TX, USA) were surgically implanted at least one week before scheduled EEG test recording. Briefly, animals were anesthetized with a continuous flow of isoflurane and subcutaneously injected with 5 mg/kg of Carprofen and 2 mg/kg of Marcaine. Once the animal was fully anesthetized, the head was fixed with a stereotaxic frame (David Kopf Instruments, Tujunga, CA, USA) and the scalp shaved to expose the skin. A sagittal incision was made to expose the skull. Two pairs of holes were carefully drilled in the skull, each pair being 1.5 mm lateral on either side of the longitudinal fissure. The first pair were located 1 mm anterior to bregma and other two 3.5 mm anterior to bregma. Four stainless screws with lead wires attached (Pinnacle Technologies, Austin, TX, USA) were inserted through these burr holes. Screws were soldered to their respective channels of headmount. The headmount with soldered regions was further secured using dental acrylic cement (Vertex Dental, Netherlands); the loose skin around the incision site was then sutured.

For focal CNO injections, one extra burr hole was drilled into the skull, based on the stereotaxic coordinates for either the SS cortex or thalamus (Mouse Brain Atlas, Paxinos and Franklin, 3rd Edition) for insertion of a guide cannula (the location of the cannula tip was validated by histology post-mortem in all mice, see Supplementary Fig. 1). A dummy cannula was inserted inside the guide cannula to prevent blood or any other fluid clogging it. Dental acrylic cement was applied around the base of cannula to secure its position. Mice were allowed to recover for at least one week and monitored carefully for 24 h immediately after surgery, then twice daily. Carprofen (5 mg/kg, SC), was administered if any signs of discomfort were seen. After full recovery, EEG recordings and behavioural testing were performed according to the protocols outlined below. The experimenter was blind to the genotype.

2.5. Drug preparation and delivery

CNO was freshly prepared at the required dose concentration, prior to each experiment. Briefly, 1.5 mg of CNO (Advanced Molecular Technologies, Australia) was dissolved in 75 μ l of dimethyl sulfoxide (DMSO). The volume was then adjusted to 15 ml by addition of 0.9% sterile saline to prepare CNO of 0.1 mg/ml concentration (for 1 mg/kg dosage group). For 5 and 10 mg/kg dosage groups, CNO of 0.5 mg/ml and 1 mg/ml was prepared. Vehicle was prepared by mixing DMSO with 0.9% sterile saline. CNO or vehicle were injected intraperitoneally on the basis of the calculated dose for the body weight of the animal. For focal injection, 0.3 μ l of CNO was infused into the specific brain region at a rate of 0.1 μ l /min. It was delivered via a Hamilton micro-injection syringe attached to polythene tubing (Microtube Extrusions, Australia) and a 33-gauge internal cannula (Plastics One Inc., VA, USA) inserted into the previously implanted guide cannula. At termination of CNO focal experiments, methylene blue dye was injected at the same volume and rate as CNO into the focal region of the brain under investigation (either SS cortex and RTN thalamus) and histology performed to verify correct cannula tip localization and estimate drug diffusion from the injection site (see Supplementary Fig. 1).

The impact of the absence seizure specific anti-epileptic drug ethosuximide (ETX) (Sigma-Aldrich, USA) was tested at 200 mg/kg body weight. ETX was first dissolved in 500 μ l DMSO; the volume was then adjusted to 10 ml by addition of 0.9% sterile saline to prepare ETX of 20 mg/ml concentration. ETX was injected intraperitoneally (200 mg/kg) on the basis of calculated dose for the body weight of the animal.

2.6. Behavioural tests

For behavioural testing of motor function, all animals were first pre-trained on a moving rotarod for two consecutive days before the test day, adopting the same protocol as the test regime, to accustom them to the testing instrument and environment. On the test day, animals were acclimatized to the testing room for 1 h prior to CNO injection and testing in an opaque open-field area (40 \times 40 \times 20 cm). Mice were allowed to move freely in the open-field for 10 min, and their movements tracked with an overhead video camera linked to Top Scan software (Clever Sys Inc., USA). Open-field testing was followed by an interval of 3 min before three rotarod trials of 5 min each with 2 min gaps between successive trials. Rotarod testing was performed on a moving rotarod 4–20 RPM (Rotamex 5.0, Columbus Instruments, USA). Latency of fall was recorded for each trial.

The same protocol was followed for behavioural testing before and after CNO injection at drug doses ranging from 1 to 10 mg/kg and also before and after vehicle treatment. CNO was injected intraperitoneally (IP) at doses of 1 mg/kg (DREADD animals: $n = 19$, non-DREADD controls: $n = 9$), 5 mg/kg (DREADD animals: $n = 18$, non-DREADD controls: $n = 8$), 10 mg/kg (DREADD animals: $n = 18$, non-DREADD controls: $n = 9$), or vehicle (DREADD animals: $n = 15$, non-DREADD controls: $n = 8$). CNO was injected focally at 1, 2.5, 5, 10 mg/kg into either the SS cortex [(1 mg/kg DREADD animals: $n = 5$, non-DREADD controls: $n = 4$); (2.5 mg/kg DREADD animals: $n = 6$, non-DREADD controls: $n = 7$); (5 mg/kg DREADD animals: $n = 7$, non-DREADD controls: $n = 6$); (10 mg/kg DREADD animals: $n = 9$, non-DREADD controls: $n = 4$); (vehicle-treated DREADD animals: $n = 6$, non-DREADD controls: $n = 4$)] or RTN thalamus [(1 mg/kg DREADD animals: $n = 7$, non-DREADD controls: $n = 4$); (2.5 mg/kg DREADD animals: $n = 7$, non-DREADD controls: $n = 6$); (5 mg/kg DREADD animals: $n = 10$, non-DREADD controls: $n = 4$); (10 mg/kg DREADD animals: $n = 7$, non-DREADD controls: $n = 4$); (vehicle-treated DREADD animals: $n = 6$, non-DREADD controls: $n = 4$)].

2.7. EEG recording and analysis of EEG traces

EEG signals were recorded from the subdural space over the cerebral cortex in freely moving mice using the Pinnacle mouse tethered system (Pinnacle Technologies, Austin, TX, USA) with simultaneous video recording. The prefabricated mouse headmount was attached to a preamplifier to amplify and filter the EEG waveforms. EEG signals were filtered at 0.5 Hz high pass and 50 Hz low pass. Sirenia[®] software was used for acquisition of EEG traces. EEG/video analysis was performed offline manually by an investigator, blind to the genotype, scrolling through EEG traces using Seizure Pro[®] software. Bursts of paroxysmal oscillatory activity in EEG traces were defined as absence-like SWD seizures if they conformed to criteria published for the morphological characteristics of SWDs in mice and if they were associated with behavioural arrest. Briefly, bursts of oscillations were counted as SWD if they had a spike-wave structure (spike, positive transient, and slow wave pattern) with a frequency of 3–8 Hz, an amplitude at least two-times higher than baseline, and lasted for > 1 s (Chung et al., 2009; Arain et al., 2012; Frankel et al., 2014; Kim et al., 2015; Heuermann et al., 2016; Maheshwari et al., 2016; Meyer et al., 2018). Artefacts due to muscle activity (extremely fast spikes of 20–60 ms of duration, not followed by slow waves, and mostly non-rhythmic), walking or scratching and grooming (rhythmic and high amplitude discharges)

were readily recognised as such and on video were not associated with behavioural arrest hence they were not considered as epileptiform activity.

2.8. Data analysis

Statistical analyses of significant differences between DREADD animals and non-DREADD WT controls or vehicle-treated animals were calculated using two-way ANOVA for testing between groups (DREADD animals versus non-DREADD animals) and CNO/vehicle as factors. Comparison between two independent treatment groups was performed using Tukey's post hoc multiple comparison test. Dunnett's post hoc multiple comparison test was used to compare treatment groups with a single control. Comparison between before and after injection in same treatment group was performed using Wilcoxon matched-pairs signed-rank test. Data were presented as mean \pm standard error of the mean (SEM). All statistical analysis was performed in GraphPad Prism 8.0 with statistical significance set at $p < .05$.

3. Results

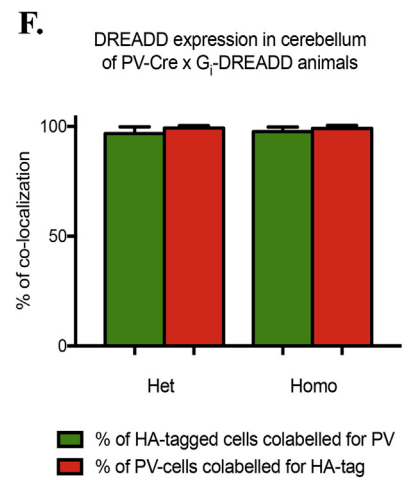
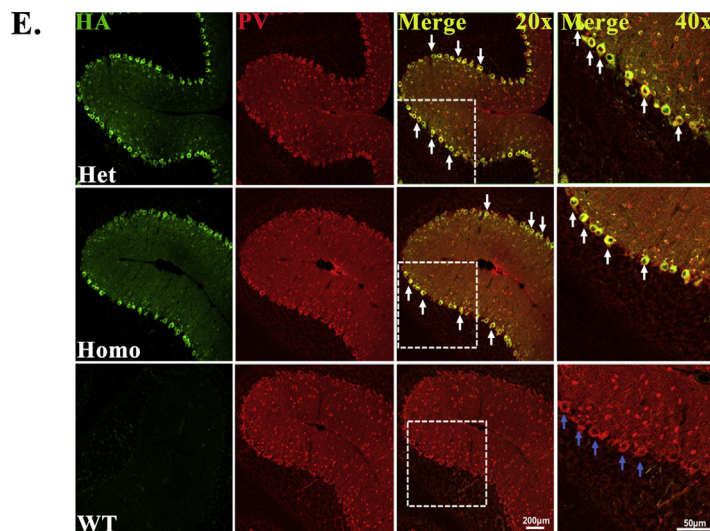
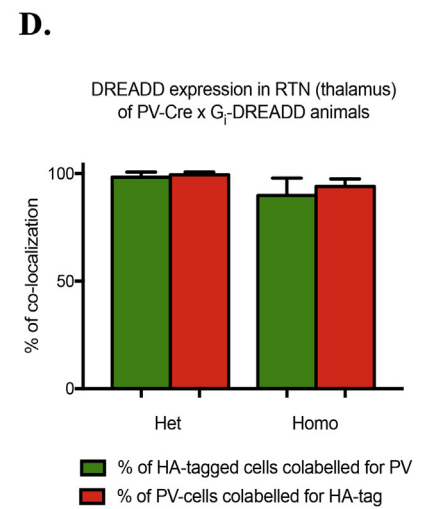
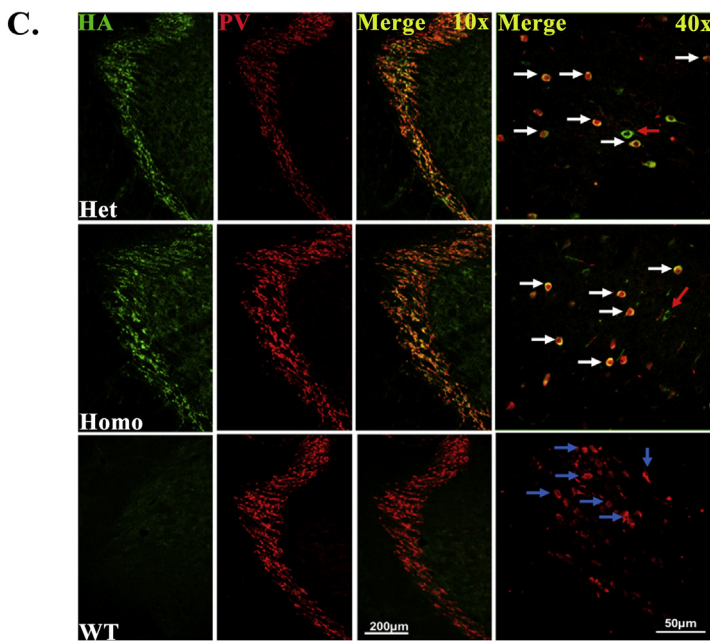
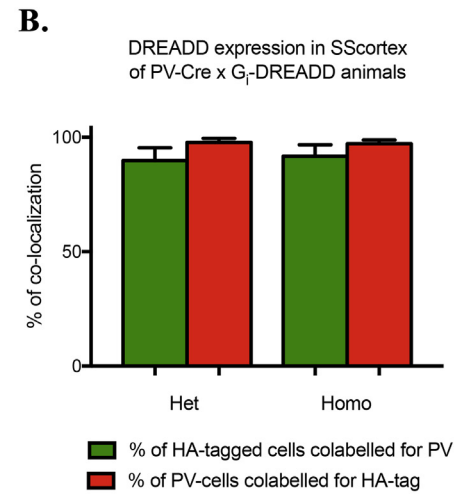
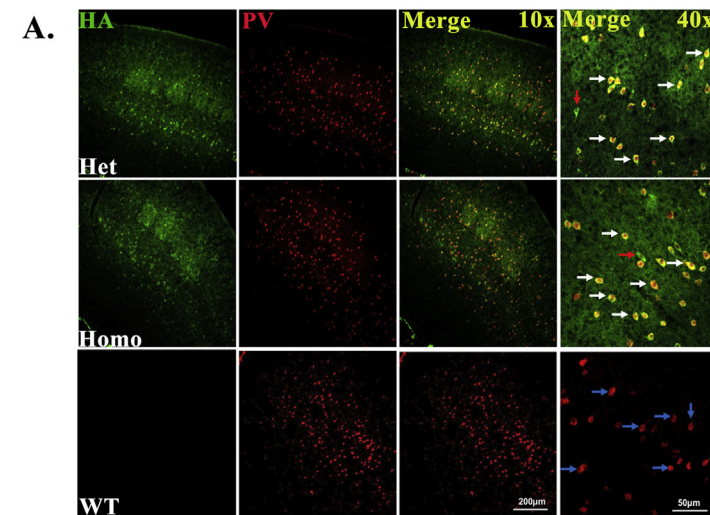
3.1. DREADD receptors are expressed in PV+ interneurons

To confirm that DREADD receptors were selectively expressed in PV+ interneurons, we first performed double-labelled immunohistochemistry with antibodies against HA-tag and PV, on brain sections with known PV+ GABAergic interneurons distributions (Fig. 2). Co-localization of HA-tag in PV+ interneurons was found throughout the SS cortex (Fig. 2A,B), RTN thalamus (Fig. 2C,D), and the cerebellar cortex of cerebellum (Fig. 2E,F). HA-tag for G_i-DREADD (identified by pseudocolour green) was only expressed in brain sections from PV-Cre/G_i-DREADD mice but not in non-DREADD WT controls.

PV+ interneurons were highly expressed throughout all SS cortical layers except layer I in all genotypes (PV-Cre/G_i-DREADD and non-DREADD WT controls) in agreement with published descriptions for PV immunoreactivity in cortical layers in rodents (del Río and DeFelipe, 1994; Tamamaki et al., 2003; Fishell, 2007; Xu et al., 2010). Most PV-expressing neurons in the SS cortex are basket cells (Meyer et al., 2002) and chandelier cells (Inda et al., 2009). In the SS cortex of PV-Cre/G_i-DREADD mice, almost all PV+ interneurons expressed HA-tag (Fig. 2A white arrows). The percentage of co-localization of HA-tag in PV+ interneurons in the SS cortex was above 90% in PV-Cre/G_i-DREADD mice (Fig. 2B). Similarly, the RTN thalamus, which comprises predominantly GABAergic, PV+ interneurons strongly expressed HA-tag (Fig. 2C white arrows). The RTN represents a shell of inhibitory feed-forward interneurons which project onto the relay neurons of the ventroposterior (VP) region of the thalamus. The percentage of co-localization of HA-tag in PV+ interneurons of RTN thalamus was also above 90% in PV-Cre/G_i-DREADD mice (Fig. 2D). In the CTC network, very few cells appeared to be labelled for HA that were not also labelled for PV (red arrow). In the cerebellum, HA-tag was intensely expressed in PV+ Purkinje cell soma in PV-Cre/G_i-DREADD mice (Fig. 2E white arrows). The percentage of co-localization of HA-tag in PV+ inhibitory Purkinje cell (PC) soma was above 90%. (Fig. 2F). Co-labelling with HA-tag and PV antibody was seen throughout the molecular layer of cerebellar cortex of PV-Cre/G_i-DREADD mice, as dendritic projections from the Purkinje cells extend throughout the molecular layer. In contrast, there was no HA-tag in the non-DREADD WT controls (Fig. 2A, C, E, bottom panel).

3.2. Silencing PV+ interneurons via intraperitoneal (IP) CNO injection impaired motor function and increased anxiety

Next we tested the behavioural impact of globally silencing PV+ interneurons expressing G_i-DREADD receptors, by IP injection of CNO (Fig. 3). In particular we focussed on motor function in open-field



(caption on next page)

Fig. 2. (A, C, E) Confocal images showing the expression of HA-tag in PV-interneurons in SS cortex, RTN thalamus, and cerebellum respectively (HA panel 1, PV panel 2, merged images panel 3, enlarged $40\times$ merged images panel 4). Neurons with co-localized markers are identified by pseudo-colour yellow in $40\times$ merged images (white arrows). Red arrows indicate the HA-positive neurons that are immunonegative for PV and blue arrows indicate PV positive neurons which are immunonegative for HA. (B, D, F) Percentage of co-localization of HA and PV in neurons in the SS cortex, RTN thalamus, and cerebellum, respectively. All immunolabelled cells in SS cortex and cerebellum sections were counted at $10\times$ in confocal images whereas those in RTN thalamus were counted using $40\times$ images. (Het = PV-Cre/Gi-DREADD offspring from homozygous PV-Cre female and heterozygous Cre-dependent hM4Di male; Homo = PV-Cre/Gi-DREADD offspring from homozygous PV-Cre female and homozygous Cre-dependent hM4Di male; WT = Non-DREADD WT control animals). (For interpretation of the references to colour in this figure legend, the reader is referred to the web version of this article.)

(Fig. 3B–D, Supplementary Fig. 2) and rotarod tests (Fig. 3E), as rodent models of absence epilepsy exhibit absence seizures associated with behavioural arrest, loss of motor co-ordination, and ataxia (Jarre et al., 2017). Open-field testing was performed according to the protocol outlined in schematic Fig. 3A, to determine the total distance travelled in the open-field and the relative time spent in central and peripheral zones (CZ and PZ). Total ambulatory distance is correlated with the locomotory behaviour of the animal, whereas relative time spent in the CZ and PZ of the open-field is an indicator of anxiety levels. There was a significant difference in all tested parameters in PV-Cre/Gi-DREADD mice treated with 5 mg/kg and 10 mg/kg of IP CNO compared to control non-DREADD WT littermates, or vehicle treated PV-Cre/Gi-DREADD mice. However, drug doses of 1 mg/kg IP CNO had no effect on PV-Cre/Gi-DREADD mice or controls.

Movement track-paths recorded in the open-field arena revealed decreased locomotion and an increased tendency to stay in the PZ, after administration of higher (5–10 mg/kg) IP doses of CNO to DREADD mice (Fig. 3B). In the 5 mg/kg dose group, total ambulatory distance and total time spent in the PZ before CNO injection was 1513.07 ± 143.54 cm and 534.57 ± 7.24 s, respectively, which changed significantly after CNO injection to 487.40 ± 93.32 cm and 589.20 ± 4.0 s respectively ($n = 18$) (Supplementary Fig. 2A,E). Similarly, in 10 mg/kg dose group, total ambulatory distance and total time spent in the PZ changed significantly from 1709.58 ± 96.5 cm and 550.21 ± 4.74 s before CNO injection to 303.38 ± 84.90 cm and 594.75 ± 1.44 s respectively after CNO injection ($n = 18$) (Supplementary Fig. 2A,E). The percentage of time DREADD mice spent in CZ (Fig. 3D; Supplementary Fig. 2C) was significantly reduced after drug doses of 5–10 mg/kg (before 5 mg/kg CNO: 10.90 ± 1.21 , after 5 mg/kg CNO: 1.80 ± 0.67 ; before 10 mg/kg CNO: 8.30 ± 0.79 , after 10 mg/kg CNO: 0.87 ± 0.24 ; $n = 18$). In contrast mice treated with 1 mg/kg CNO showed no significant changes in any of the parameters tested in open field. None of the control groups (vehicle treated or non-DREADD WT groups) showed any changes in locomotion or relative time spent in the CZ or PZ (Fig. 3C,D; Supplementary Fig. 2B,D,F). The non-DREADD WT mice spent a similar amount of time in the CZ as the vehicle group before and after CNO administration (6–8%) which was consistent with published data for WT control mice in other studies investigating anxiety-related behaviours in mice (Bailey and Crawley, 2009) indicating that non-DREADD control and vehicle treated mice do not display anxiety-like behaviour. Thus, silencing PV+ interneurons via IP CNO injection at dose levels 5–10 mg/kg decreased locomotion and increased anxiety levels only in PV-Cre/Gi-DREADD animals.

To test the impact of silencing feed-forward PV+ interneurons on motor co-ordination, the same cohort of animals was tested on a moving rotarod, which is widely used to evaluate motor coordination in rodents, and is especially sensitive in detecting cerebellar dysfunction. Each mouse was tested on the moving rotarod for three successive trials of 5 mins before and after IP CNO injection at doses of either 1, 5, and 10 mg/kg (Fig. 3A, E & Supplementary Fig. 3A,B). There was a significant difference in the mean latency of fall in PV-Cre/Gi-DREADD mice before and after peripheral (IP) CNO injection of 5 mg/kg and 10 mg/kg but not after 1 mg/kg (Fig. 3E & Supplementary Fig. 3A). In 5 mg/kg dose group, the mean latency of fall before CNO injection was 294.57 ± 1.35 s which decreased significantly after CNO injection (175.39 ± 6.64 s; $n = 18$ mice). Similarly, in 10 mg/kg dose group, the

mean latency of fall reduced significantly from 293.39 ± 1.27 s before injection to 89.09 ± 4.38 s ($n = 18$) after CNO injection. However, mice treated with 1 mg/kg CNO showed no motor impairment on the rotarod (latency of fall before CNO injection = 296.10 ± 1.01 s; after CNO injection 288 ± 3.33 s; $n = 19$) (Fig. 3E & Supplementary Fig. 3A). Control vehicle treated PV-Cre/Gi-DREADD mice showed no changes in motor co-ordination before and after CNO injection (latency of fall before CNO injection = 294.58 ± 1.96 s; after CNO injection 289.55 ± 2.57 s; $n = 15$). Likewise, Tukey's post hoc multiple comparison test and Wilcoxon matched-pairs signed-rank test showed no significant difference between vehicle and CNO treated non-DREADD WT control groups (Fig. 3E; Supplementary Fig. 3B).

3.3. Silencing PV+ interneurons via intraperitoneal (IP) CNO injection increased immobility and generated absence-like seizures

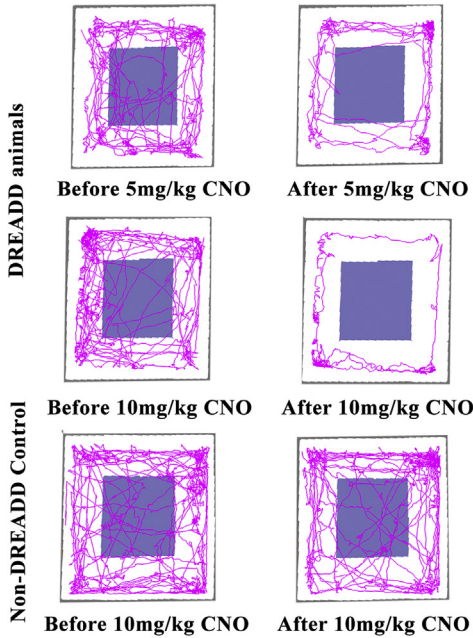
To test the effect of silencing feed-forward PV+ interneurons on seizure generation, EEG recordings were first performed on a cohort of PV-Cre/Gi-DREADD and non-DREADD WT control animals surgically implanted with surface EEG electrodes and injected with IP CNO. The EEG testing protocol and electrode placement are illustrated in Fig. 4A & B, respectively. Simultaneous EEG/video recording was performed on animals 10 min before and for 1 h after IP CNO injection at doses of either 1 mg/kg (DREADD animals: $n = 8$; non-DREADD WT controls: $n = 4$), 5 mg/kg (DREADD animals: $n = 9$; non-DREADD WT controls: $n = 6$), 10 mg/kg (DREADD animals: $n = 5$; non-DREADD WT controls: $n = 6$), and vehicle-treated (DREADD animals: $n = 8$; non-DREADD WT controls: $n = 6$). Bursts of paroxysmal oscillatory activity (indicated by asterisks) associated with behavioural arrest were seen after IP CNO injection of 5 mg/kg and 10 mg/kg in PV-Cre/Gi-DREADD animals but not in the 1 mg/kg dose group, vehicle treated animals or non-DREADD WT control animals (Fig. 4D). IP CNO injection also led to increased immobility in PV-Cre/Gi-DREADD animals in a dose-dependent manner. Analysis of the mean time spent immobile during EEG recording indicated that animals spent significantly more time immobile after CNO doses of 5 and 10 mg/kg of IP CNO 47.28 ± 3.23 min ($n = 9$) and 50.83 ± 2.74 min ($n = 5$) respectively, compared to vehicle-treated and 1 mg/kg CNO injected animals, which were immobile for 29.70 ± 5.70 min ($n = 8$) and 34.19 ± 1.73 min ($n = 8$) respectively. Injection of CNO into non-DREADD WT control animals at doses 5 and 10 mg/kg did not significantly change mobility compared to vehicle treated animals (5 mg/kg CNO 34.01 ± 2.93 min ($n = 6$), 10 mg/kg CNO 35.28 ± 2.86 min ($n = 6$) or vehicle 31.62 ± 3.17 min ($n = 6$), (Fig. 4C).

Analysis of the bursts of paroxysmal oscillatory activity (with associated behavioural arrest) in PV-Cre/Gi-DREADD mice injected with 5 and 10 mg/kg IP CNO, indicated mean seizure onset at 31.26 ± 5.46 min in the 5 mg/kg dose group ($n = 9$) and 36.21 ± 5.58 in 10 mg/kg group ($n = 5$) (Fig. 4E). However, the first seizure detected in an IP cohort mouse was 10.14 min. The mean number of bursts during the 1 h EEG recording period, was 4 ± 1.01 bursts in the 5 mg/kg dose group and 5.8 ± 2.27 in the 10 mg/kg group (Fig. 4E). EEG trace parameters such as mean spike frequency, mean duration of each burst, and time of last seizure were not significantly different. The bursts of paroxysmal oscillatory activity had a characteristic spike and wave-like morphological profile with a spike

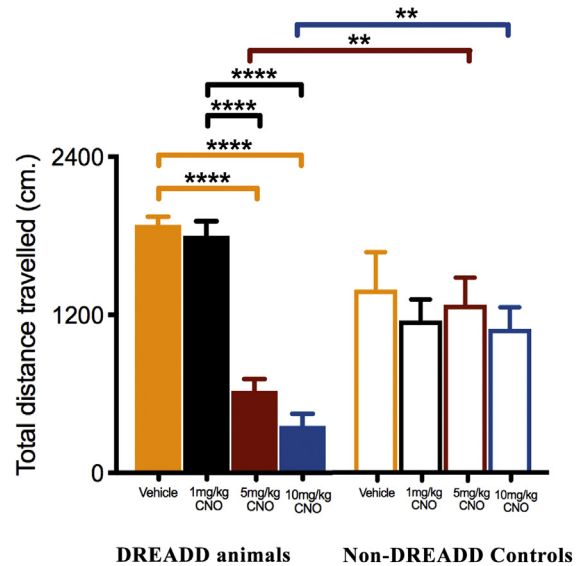
IP CNO/Vehicle Injection

Acclimatization	Open field test	Gap	Rotarod test Trial 1	Gap	Rotarod test Trial 2	Gap	Rotarod test Trial 3	↓	Open field test	Gap	Rotarod test Trial 1	Gap	Rotarod test Trial 2	Gap	Rotarod test Trial 3
60 min	10 min	3 min	5 min	2 min	5 min	2 min	5 min		10 min	3 min	5 min	2 min	5 min	2 min	5 min

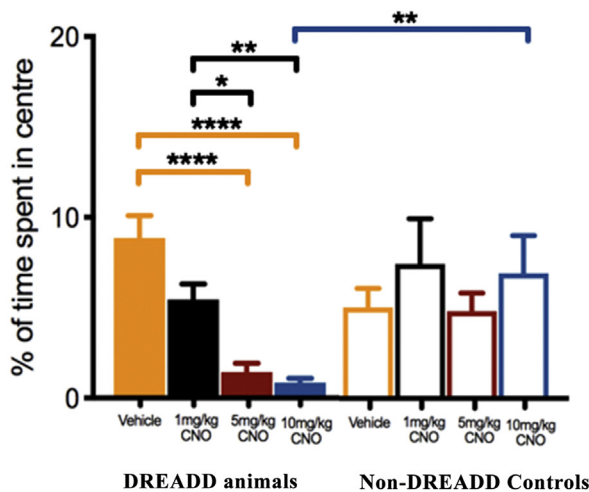
B. Open-Field Test Movement Track Path



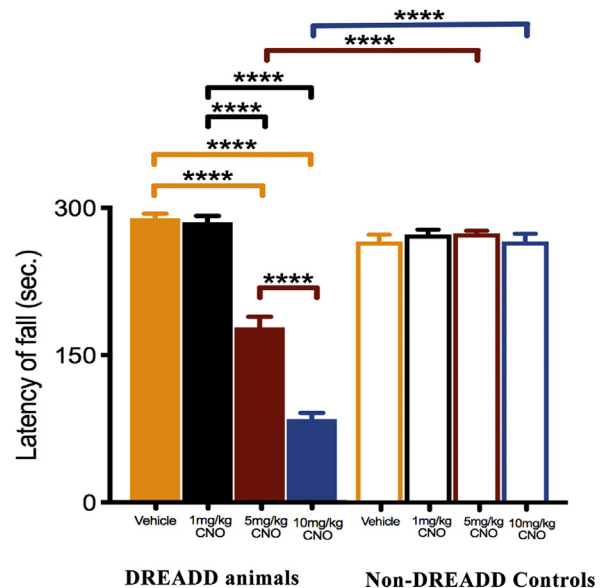
C. Open-Field Test Total Distance Travelled



D. Open-Field Test Time Spent in Central Zone



E. Rotarod Test



(caption on next page)

frequency between 3 and 6 Hz. The frequency (spikes/s), was calculated based on number of spikes with an amplitude minimum two-times higher than baseline, followed by positive transient, and slow wave pattern. The mean frequency of such discharges was 5.35 ± 0.76 spikes/s and 4.76 ± 0.64 spikes/s for 5 mg/kg and 10 mg/kg dose

group of CNO, respectively (Fig. 4E). The mean duration of each burst was 3.16 ± 0.58 s and 4.77 ± 0.63 s for 5 mg/kg and 10 mg/kg dose group of CNO, respectively (Fig. 4E). In all cases, behavioural arrest was associated with these bursts of oscillatory activity. Only one PV-Cre/G_i-DREADD animal, injected with 5 mg/kg IP CNO, displayed

Fig. 3. (A) Schematic of protocol for behavioural testing before and after IP CNO/vehicle injection. (B) Open-field test: representative images of movement track paths showing decreased locomotion and increased tendency to stay in peripheral zone (PZ) by CNO treated DREADD animals but not non-DREADD WT control animals. (C) Open-field test: graph of total distance travelled by DREADD and non-DREADD WT control mice after IP injection of CNO or vehicle. Total ambulatory distance was significantly reduced in open-field testing of DREADD animals after CNO doses of 5 mg/kg ($n = 18$) and 10 mg/kg ($n = 18$) but not 1 mg/kg ($n = 19$) or vehicle ($n = 15$). There were no changes in non-DREADD WT control animals [1 mg/kg ($n = 9$), 5 mg/kg ($n = 8$), 10 mg/kg ($n = 9$), vehicle treated ($n = 8$)]. (D) Open-field test: graph showing % of time spent in central zone by DREADD and non-DREADD WT control animals after IP CNO or vehicle injection. DREADD mice treated with 5–10 mg/kg CNO ($n = 18$ for both doses) spent significantly less time in the central zone compared to 1 mg/kg ($n = 19$) or vehicle ($n = 15$) treated animals or non-DREADD WT controls. There were no significant differences between non-DREADD WT controls or vehicle treated mice [1 mg/kg dosage group ($n = 9$), 5 mg/kg dosage group ($n = 8$), 10 mg/kg dosage group ($n = 9$), vehicle treated ($n = 8$)]. (E) Rotarod test: graph showing the comparison of latency of fall between DREADD and non-DREADD control animals after different doses of IP CNO injection. Motor co-ordination was significantly reduced in DREADD animals after 5 mg/kg ($n = 18$) and 10 mg/kg ($n = 18$) doses but not 1 mg/kg ($n = 19$) or in the vehicle treated ($n = 15$) group. There was no change in the latency of fall in non-DREADD control animals [1 mg/kg ($n = 9$), 5 mg/kg ($n = 8$), 10 mg/kg ($n = 9$), vehicle treated ($n = 8$)]. All values represent mean \pm SEM. Comparisons between treatment groups were performed using Tukey's post hoc multiple comparison test.

tonic-clonic convulsive type seizures after 22.58 min of CNO injection (see Supplementary Fig. 4A). In this case the convulsive seizures were characterized by extremely high-amplitude (up to 3990 μ v) spikes on the EEG and accompanied by severe jerking movements. The characteristics and morphology of such discharges were very different to the rhythmic spike and wave oscillations seen in the other PV-Cre/G_i-DREADD animals in the 5 mg/kg and 10 mg/kg dose groups hence this animal was excluded from the analysis.

3.4. Silencing PV+ interneurons via focal CNO injection into the SS cortex or RTN (thalamus) generated absence-like seizures associated with behavioural arrest

Having confirmed that global silencing of PV+ interneurons via IP CNO injection causes bursts of paroxysmal oscillatory discharges comprising spikes and wave-like discharges, we next performed targeted CNO injections focally into either the SS cortex (Fig. 5) or the RTN thalamus (Fig. 6). The aim was to directly silence PV+ feed-forward interneurons in either of these brain regions to test our hypothesis that loss of feed-forward inhibition specifically within CTC network microcircuits, is one mechanism by which the CTC can switch into hyperexcitable pathological oscillations evident as SWDs in absence seizures. Evidence in the literature suggests that the cortex is the site of seizure initiation while the thalamus is primarily involved in seizure maintenance (Meeren et al., 2002; Polack et al., 2007).

Simultaneous EEG/video recordings were made of PV-Cre/G_i-DREADD and non-DREADD WT control animals based on the experimental procedure illustrated in Figs. 5A and 6A. EEG traces were recorded for 10 min before and 1 h after either vehicle or focal CNO injection at doses of either 1, 2.5, 5 and 10 mg/kg. Different cohorts of animals were used for testing the impact of silencing PV+ interneurons in the SS cortex (Fig. 5) and RTN thalamus (Fig. 6) i.e. each animal had only a cortical or thalamic canula inserted surgically, not both. Analysis of EEG traces following focal injection of CNO revealed bursts of paroxysmal oscillatory activity (indicated by asterisks on EEG traces) in both brain hemispheres and concomitant behavioural arrest after focal CNO injection of 2.5, 5 and 10 mg/kg in PV-Cre/G_i-DREADD animals into either cortical or thalamic regions (Fig. 5E, 6E; Supplementary Figs. 5–7) but not 1 mg/kg.

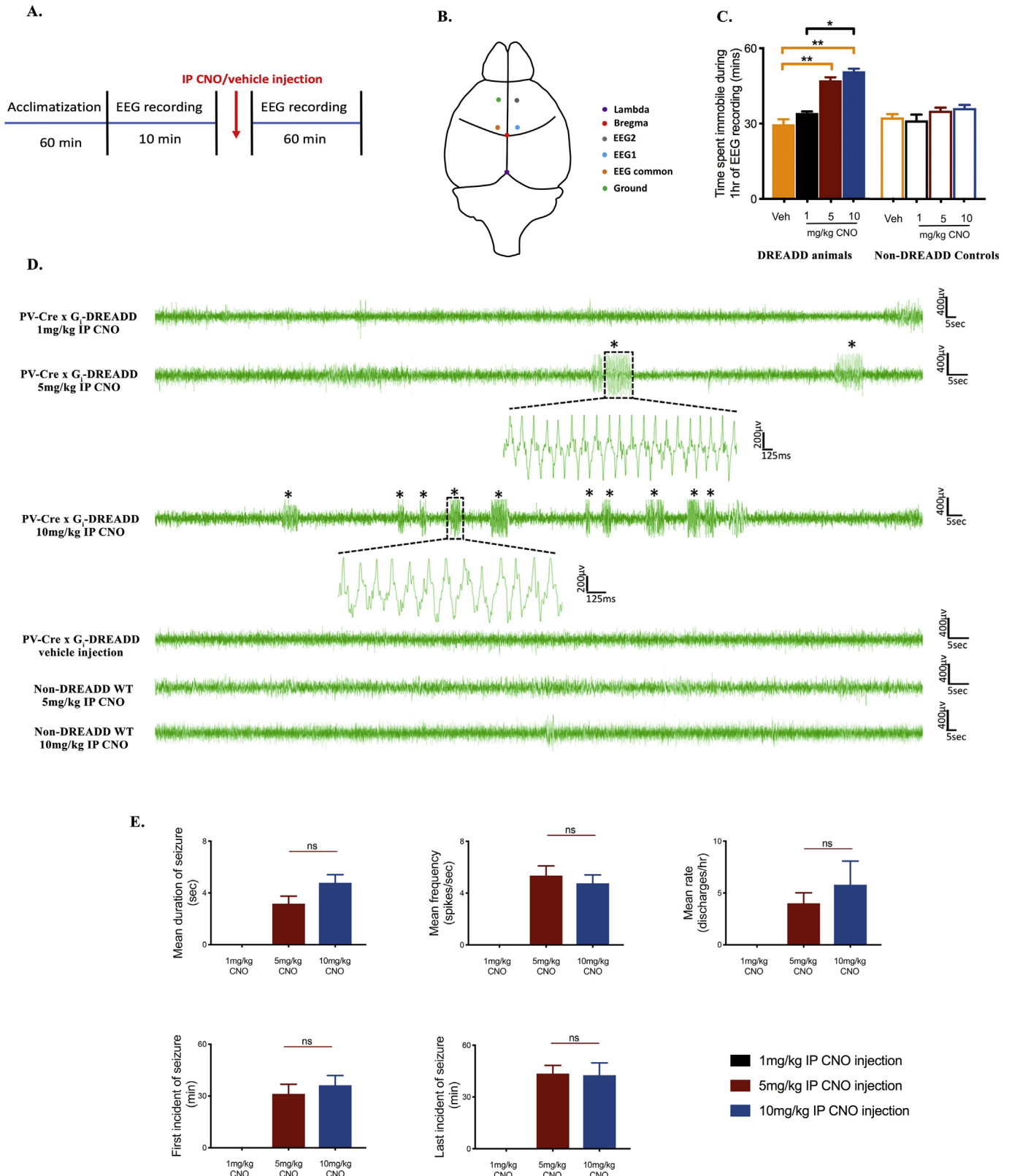
The bursts of oscillatory activity recorded after CNO focal injections into the SS cortex (Fig. 5E) were characterized as bilateral SWDs based on spike amplitude (minimum two-times higher than baseline), positive transient, and slow wave pattern. There was no significant difference in mean duration of seizure (s), mean frequency (spikes/s), and mean rate (discharges/h) across all 3 doses of CNO (Fig. 5F). The mean frequency/rhythmicity (Hz) of epileptiform activity was consistent with the characteristics of SWDs associated with absence seizures in other mouse models of absence epilepsy (Jarre et al., 2017). All PV-Cre/G_i-DREADD animals tested with CNO drug doses of 2.5, 5 and 10 mg/kg focally injected into the SS cortex displayed these characteristic SWDs ($n = 26$) with the exception of one animal. This PV-Cre/G_i-DREADD animal, when focally injected with 5 mg/kg CNO (SS cortex) showed a single

tonic-clonic convulsive event with jerky body movements which lasted for just 3.61 s (see Supplementary Fig. 4B). This animal was not included in the analyses of absence-like seizures. None of the non-DREADD WT control animals exhibited signs of paroxysmal oscillatory activity at any of the drug doses tested (Fig. 5E). No bursts of oscillatory activity were seen in any of the 1 mg/kg dose groups or in vehicle treated PV-Cre/G_i-DREADD animals. The DREADD mice injected with CNO doses of 2.5, 5 and 10 mg/kg spent significantly more time immobile after treatment. The mean time spent immobile during the 1 h recording period post CNO injection was: 39.91 \pm 3.41 min ($n = 6$) after 2.5 mg/kg; 47.80 \pm 2.20 min ($n = 11$) after 5 mg/kg; and 47.32 \pm 3.65 min ($n = 9$) after 10 mg/kg compared to vehicle-treated 19.64 \pm 6.56 min ($n = 4$) or 1 mg/kg CNO injected 25.30 \pm 6.05 min ($n = 7$) animals. Injection of CNO into non-DREADD WT control animals did not significantly change mobility compared to vehicle treated animals (2.5 mg/kg CNO 36.20 \pm 3.21 min ($n = 6$); 5 mg/kg CNO 32 \pm 0.923 min ($n = 8$); 10 mg/kg CNO 30.44 \pm 3.48 min ($n = 4$); vehicle 25.97 \pm 1.97 min ($n = 4$); (Fig. 5D).

Analysis of video/EEG data following focal injection of CNO into the RTN thalamus of PV-Cre/G_i-DREADD mice also revealed animals spent more time immobile after higher 5–10 mg/kg doses, although this trend did not reach significance (Fig. 6D). Injection of CNO into non-DREADD WT control animals did not significantly change mobility compared to vehicle treated animals (Fig. 6D) at any of the dose levels tested. The oscillatory discharges recorded after CNO injection into the RTN thalamus demonstrated a complex spike-wave structure. These discharges, when analysed on an expanded time scale, comprised repetitive spikes, positive transients with multiple waves (Fig. 6E) similar to the absence-like seizures seen in GABA_A receptor alpha-1 subunit KO mice (Arain et al., 2012). However, like the SS cortex group, there was no significant difference in mean spike frequency (spikes/s), mean duration of each oscillatory burst, or burst rate (number of oscillatory bursts/h) across all 3 doses of CNO (Fig. 6F). They were clearly not polyspike-and-wave discharges (PSD) associated with myoclonic seizures, which consist of very brief (< 0.5 s), high frequency (approximately 50 ms interspike interval) complexes (García-Cabrero et al., 2012; Arain et al., 2015). SWDs can be differentiated from PSDs based on two morphological features: SWDs have a lower spike frequency (interspike interval 125–166 ms), and a higher rhythmicity than the PSDs. In our study, the mean interspike interval for all three (IP, SS cortex, thalamus) modes of CNO injection was 209.02 \pm 24.74 ms (total 263 epileptiform discharges counted). The complex SWD-like oscillations evident after focal CNO injections, were also associated with behavioural arrest. None of the non-DREADD WT control animals exhibited any signs of paroxysmal oscillatory activity at any of the CNO drug doses tested by focal injection into the thalamus (Fig. 6E).

3.5. Treatment with ETX suppressed absence-like seizures generated by focal CNO injections

To further characterise the bursts of oscillatory spikes and wave-like discharges occurring after focal injection of CNO at doses of 5–10 mg/



(caption on next page)

kg, we investigated the impact of the anti-epileptic drug ethosuximide (ETX) on seizure generation (Supplementary Fig. 8). ETX is specific for absence seizures; therefore it can be used to differentiate absence seizures from other EEG changes. CNO (10 mg/kg) was injected focally into a cohort of PV-Cre/Gi-DREADD mice (SS cortex group: $n = 3$,

Supplementary Fig. 8A; RTN thalamus group: $n = 4$, Supplementary Fig. 8B) and video/EEG recordings made for 10 min before and 60 min post CNO injection. CNO induced bursts of oscillatory spikes and wave-like discharges in all mice tested. To test if the anti-absence drug ETX was able to block seizure activity, the same cohort of animals was

Fig. 4. (A) Schematic of protocol for EEG recordings before and after IP CNO/vehicle injection. (B) Diagram showing the position of EEG electrodes; recordings were made from EEG1 and EEG2 channels. (C) Graph showing time spent immobile by DREADD and non-DREADD animals during 1 h of EEG recording period after IP CNO injection. Immobility in DREADD animals was dose dependent and statistically significant at 5–10 mg/kg compared to vehicle treated mice (DREADD animals: vehicle treated $n = 8$; CNO treated 1 mg/kg $n = 8$; 5 mg/kg $n = 9$; 10 mg/kg; $n = 5$). CNO did not affect mobility in non-DREADD WT control mice compared to vehicle treated mice (non-DREADD control animals: vehicle treated $n = 6$; CNO 1 mg/kg $n = 4$; 5 mg/kg $n = 6$; 10 mg/kg $n = 6$). (D) Representative EEG traces of DREADD animals and non-DREADD controls after IP injection of CNO or vehicle. Bursts of paroxysmal oscillatory activity (asterisks) with the characteristics of SWDs and associated behavioural arrest were seen only in DREADD animals injected with 5–10 mg/kg IP CNO. SWDs were characterized by spike, positive transient and slow-wave pattern with spike amplitude $2 \times$ baseline, spike frequency of > 2 Hz and a minimum duration of 1 s. No SWDs were evident in 1 mg/kg or vehicle treated groups or non-DREADD WT control animals. All representative EEG traces were obtained from different animals. Each trace represents 3–6 min of EEG recording. (E) Comparison of different parameters of EEG recording after IP CNO injection in DREADD animals. No significant changes were seen in any of the parameters. All values represent mean \pm SEM. Comparisons between treatment groups were performed using Tukey's post hoc multiple comparison test.

subsequently injected with 200 mg/kg of ETX prior to injection of 10 mg/kg CNO and recorded continuously for at least 1 h post CNO injection. Administration of ETX prevented spikes and wave-like discharges in all tested PV-Cre/Gi-DREADD animals, which provides strong supporting evidence for the absence-like nature of these discharges.

3.6. Route of administration affects onset of bursts of oscillatory activity

Analysis of the impact of the route of CNO injection (IP or focal) on seizure generation revealed an earlier onset of seizures after focal injection than IP injection (Fig. 7A). The mean onset of seizures in the IP CNO injection group was at 31.27 ± 5.46 min ($n = 9$) for 5 mg/kg and 36.22 ± 5.58 min ($n = 5$) for the 10 mg/kg dosage group. In the SS cortex group, mean onset of seizures was 14.94 ± 3.35 min ($n = 11$) after 5 mg/kg CNO, and 14.71 ± 3.08 min ($n = 9$) after 10 mg/kg CNO (Fig. 7A). In the thalamus group, mean seizure onset was 18.58 ± 6.14 min ($n = 6$) after 5 mg/kg CNO, and 9.60 ± 3.42 min ($n = 5$) after 10 mg/kg CNO. However, irrespective of route of administration, seizures were first evident in some animals within each dosage group by 15 mins post CNO injection (first seizure detected in an IP cohort mouse was 10.14 min, in focal SS cortex cohort mouse was 6.09 min and in focal thalamus cohort mouse was 6.79 min); seizures had terminated in all animals by 60 min post CNO injection (Fig. 7B).

Other morphological features of the discharges (spike frequency, burst duration and burst rate) remained consistent irrespective of CNO drug dose level or route of administration. No significant differences were seen in the mean duration of each seizure burst for any of the drug levels tested via IP or focal routes i.e. IP group: 3.16 ± 0.58 s ($n = 9$) after 5 mg/kg CNO, and 4.78 ± 0.63 s ($n = 5$) after 10 mg/kg CNO, SS cortex group: 3.02 ± 0.48 s ($n = 11$) after 5 mg/kg CNO, and 3.29 ± 0.30 s ($n = 9$) after 10 mg/kg CNO, thalamus group: 3.14 ± 0.33 s ($n = 6$) after 5 mg/kg CNO, and 3.54 ± 0.91 s ($n = 5$) after 10 mg/kg CNO (Fig. 7C). Similarly, no significant differences were seen in mean frequency of seizure (spikes/s) i.e. IP group: 5.35 ± 0.76 min ($n = 9$) after 5 mg/kg CNO, and 4.76 ± 0.64 min ($n = 5$) after 10 mg/kg CNO; SS cortex group: 5.57 ± 0.53 min ($n = 11$) after 5 mg/kg CNO, and 5.26 ± 0.64 min ($n = 9$) after 10 mg/kg CNO; thalamus group: 5.14 ± 0.65 min ($n = 6$) after 5 mg/kg CNO, and 5.56 ± 0.94 min ($n = 5$) after 10 mg/kg CNO (Fig. 7D). Likewise, there was no significant difference in mean rate of discharges/h after either IP (4 ± 1.01 and 5.80 ± 2.27 bursts/h for 5 mg/kg and 10 mg/kg respectively) or focal administration of CNO (SS cortex group: 4.91 ± 1.07 ($n = 11$) after 5 mg/kg CNO, and 7.11 ± 1.71 ($n = 9$) after 10 mg/kg CNO; thalamus group: 3.67 ± 1.38 ($n = 6$) after 5 mg/kg CNO, and 5.20 ± 1.46 ($n = 5$) after 10 mg/kg CNO) (Fig. 7E).

3.7. Focal silencing of PV+ interneurons in CTC network had no effect on motor co-ordination on the rotarod but significantly altered locomotory behaviour in the open-field

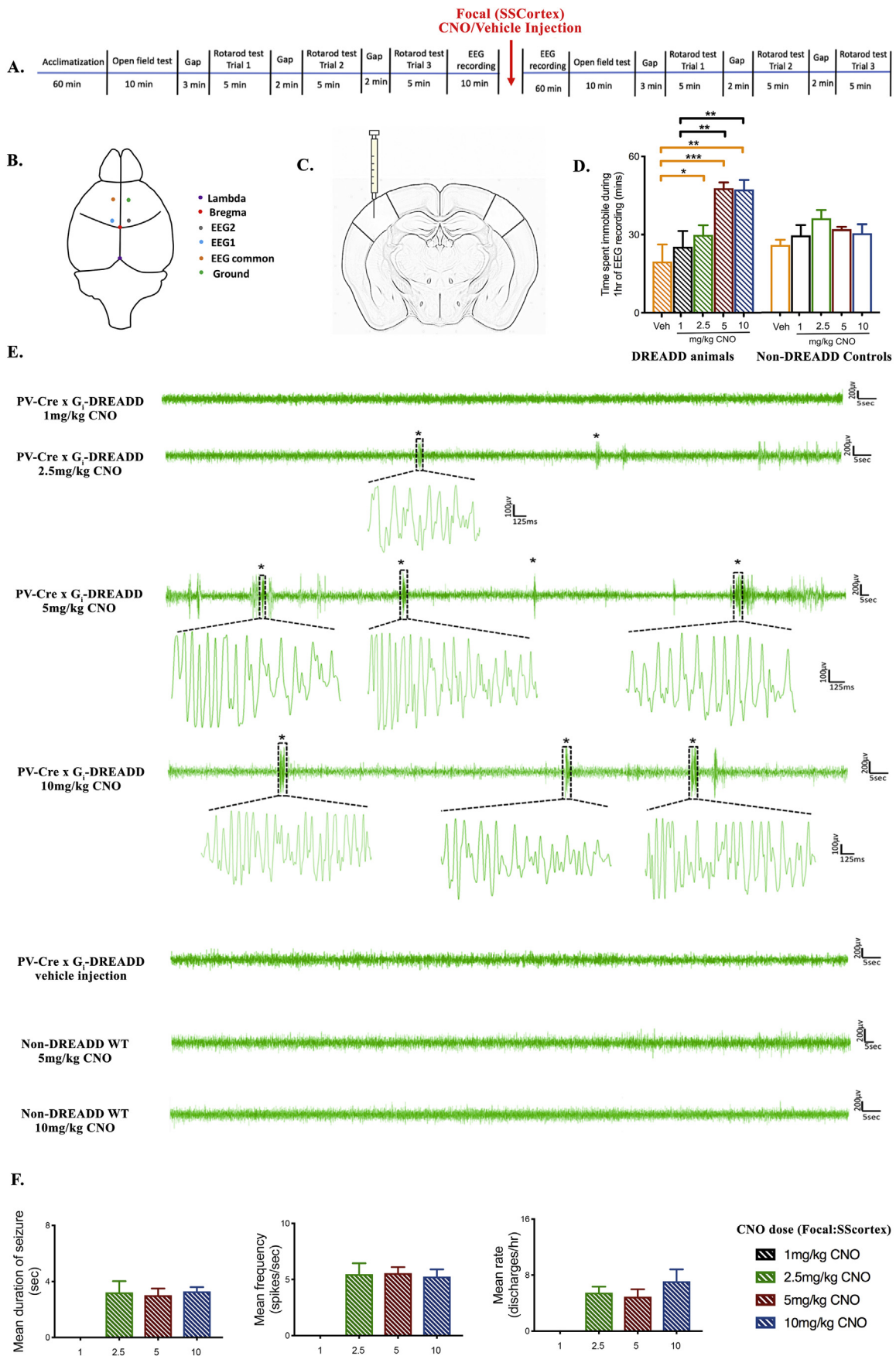
Silencing PV+ interneurons via focal CNO injection into either the cortex or thalamus did not cause impairment of motor control tested on

the rotarod. There were no significant differences in the latency of fall in PV-Cre/Gi-DREADD animals at any dose of CNO tested compared to non-DREADD WT controls and vehicle treated groups (Supplementary Fig. 3 C–F).

However, when tested in the open-field, locomotory behaviour in PV-Cre/Gi-DREADD was altered after focal injection of CNO in a dose dependent manner (Fig. 8; Supplementary Fig. 9). CNO doses 2.5–10 mg/kg of CNO injected into the SS cortex (Supplementary Fig. 9A,B) or thalamus (Supplementary Fig. 9C,D) significantly reduced the total ambulatory distance travelled by DREADD animals compared to before treatment, whereas CNO had no effect on non-DREADD WT controls. Dunnett's post hoc multiple comparison test showed statistically significant differences in the mean distance travelled after CNO doses of 2.5 mg/kg (1097.97 ± 214.38 cm; $n = 6$), 5 mg/kg (692.99 ± 213.07 cm; $n = 7$), 10 mg/kg CNO (451.43 ± 120.19 cm, $n = 9$) compared to before CNO/vehicle treatment (1857.95 ± 139.31 cm, $n = 6–9$) in the SS cortex group (Fig. 8A). No significant changes were seen in non-DREADD WT control animals ($n = 4–7$ per treatment group) (Fig. 8B, Supplementary Fig. 9B). Similarly, CNO injection into the thalamus significantly reduced locomotion in the DREADD 2.5–10 mg/kg dose groups but not non-DREADD controls (Supplementary Fig. 9 C,D). During the 10 min testing period prior to CNO thalamic injection, DREADD animals travelled 1747.48 ± 164.42 cm ($n = 7–10$) in open-field arena; this decreased significantly after 2.5, 5 and 10 mg/kg of CNO injection to 338.14 ± 123.72 cm ($n = 7$), 463.85 ± 144.72 cm ($n = 10$), and 244.14 ± 110.33 cm ($n = 7$) respectively (Fig. 8C). Again, there was no change in the total ambulatory distance in non-DREADD WT controls ($n = 4–6$ per treatment group) (Fig. 8D, Supplementary Fig. 9D) after CNO injection into the thalamus compared to before CNO/vehicle injections.

4. Discussion

The current study has shown that silencing PV+ interneurons in the CTC network, by focal injection of CNO into either the SS Cortex or RTN thalamus, of mice expressing Gi-DREADD receptors in PV+ inhibitory neurons leads to the generation of bursts of paroxysmal oscillatory activity with characteristic SWD-like morphology on EEG, similar to absence seizures in genetic mouse models of absence epilepsy. Seizures were associated with behavioural arrest but the periods of immobility were not restricted to just the duration of the oscillatory burst. The arrested behaviour continued for extended periods throughout a series of oscillatory bursts and was associated with reduced locomotion in open-field testing. Global silencing of all PV+ interneurons with a single dose of CNO, in addition to causing epileptiform oscillations on EEG and impaired locomotor function in open-field testing, resulted in increased time spent in peripheral zones (indicative of increased anxiety) and loss of motor co-ordination on rotarod tests. The latter behavioural effect may reflect silencing of PV+ interneurons in brain regions other than the CTC network, as this effect was not evident on focal silencing of CTC PV+ interneurons.



(caption on next page)

Fig. 5. (A) Schematic of protocol for EEG recordings/behavioural testing before and after focal CNO/vehicle injection into SS cortex. (B) Diagram showing the position of EEG electrodes; recordings were made from EEG1 and EEG2 channels. The headmount was rotated by 90° from the previous setup (as explained in Fig. 4B). Changes were made to record EEG traces from both hemispheres of the brain. (C) Schematic representation of CNO delivery in SS cortex (modified from Allen Mouse Brain Atlas) (D) Graph showing time spent immobile by DREADD and non-DREADD animals after focal CNO injection into the SS cortex. Immobility in DREADD animals was dose dependent and statistically significant at 2.5–10 mg/kg compared to vehicle treated mice (DREADD animals: vehicle treated $n = 4$; CNO treated 1 mg/kg $n = 7$; 2.5 mg/kg $n = 6$; 5 mg/kg $n = 11$; 10 mg/kg $n = 9$). CNO did not affect mobility in non-DREADD WT control mice compared to vehicle treated mice (non-DREADD control animals: vehicle treated $n = 4$; CNO 1 mg/kg $n = 4$; 2.5 mg/kg $n = 6$; 5 mg/kg $n = 8$; 10 mg/kg $n = 4$). (E) Representative EEG traces of DREADD animals and non-DREADD controls after focal injection of CNO/vehicle into SS cortex. Bursts of paroxysmal oscillatory activity (indicated by asterisks) associated with behavioural arrest were seen after CNO injection (2.5–10 mg/kg) only in DREADD animals but not in 1 mg/kg or vehicle treated groups or non-DREADD WT control animals. SWDs were characterized as explained in Fig. 4D. All representative EEG traces are from different animals. Each traces represent 3–6 min of EEG recording. (F) Comparison of different parameters of EEG recording after focal CNO injection into the SS cortex of DREADD animals. All values represent mean \pm SEM. Comparisons between treatment groups were performed using Tukey's post hoc multiple comparison test.

4.1. HA-tagged DREADD receptor is highly expressed in PV+ interneurons

Validation of the selective expression of inhibitory hM4Di-DREADD receptor in PV+ interneurons in PV-Cre/G_i-DREADD mice was provided by the high co-expression of labelling for the DREADD HA-tag and PV in cells known to express the calcium-binding protein PV (e.g. thalamic RTN soma and cerebellar Purkinje cells) but absence of staining for HA-tag in PV+ interneurons in non-DREADD WT littermate controls. The labelling of PV+ cells in our study was consistent with that of other published studies describing distribution of PV+ neurons in the brain (del Río and DeFelipe, 1994; Tamamaki et al., 2003; Fishell, 2007; Xu et al., 2010). PV+ interneurons were highly expressed in SS cortical layers II–VI but not in layer I, in all PV-Cre/G_i-DREADD mice and non-DREADD WT controls, which is similar to our previously published studies on PV-immunoreactivity in the cortex of stargazer model of absence epilepsy and non-epileptic littermates (Adotevi and Leitch, 2016) and other rodent studies (Celio, 1986; Tanahira et al., 2009; Xu et al., 2010). PV-Cre/G_i-DREADD mice showed extremely high co-localization (> 90%) of HA-tag in PV+ interneurons in SS cortex, RTN thalamus and Purkinje cells of cerebellum, whereas none of the PV+ interneurons in non-DREADD WT control animals showed labelling for HA-tag. These levels of co-expression in PV-Cre/G_i-DREADD mice are consistent with the Jackson Lab datasheet (008069) for PV-Cre mice which states that the recombination in PV-Cre knockin allele is around 90%.

To date, there have been relatively few studies, which have used DREADD technology to modulate PV+ interneurons. Reports in the literature on the expression levels of DREADD receptor in PV+ interneurons, are limited to those that have used viral vectors to deliver the DREADD receptor into PV-Cre transgenic mice; either DREADD-based recombinant lentiviral vector (LV) or adeno-associated viral vector (AAV). Specific PV+ cells have been targeted by viral vector injections into different regions of the brain including the hippocampus (Yi et al., 2014; Zou et al., 2016; Drexel et al., 2017; Xia et al., 2017; Calin et al., 2018); medial prefrontal cortex (mPFC) (Perova et al., 2015); primary visual cortex (Kaplan et al., 2016); and frontal cortex (Ng et al., 2018). These studies reported percentage co-localization of DREADD receptor with PV+ interneurons between 70 and 85% in the targeted brain regions. Hence, viral infection efficiency using LV and AAV mediated DREADD expression, is below the 90% achieved in our study.

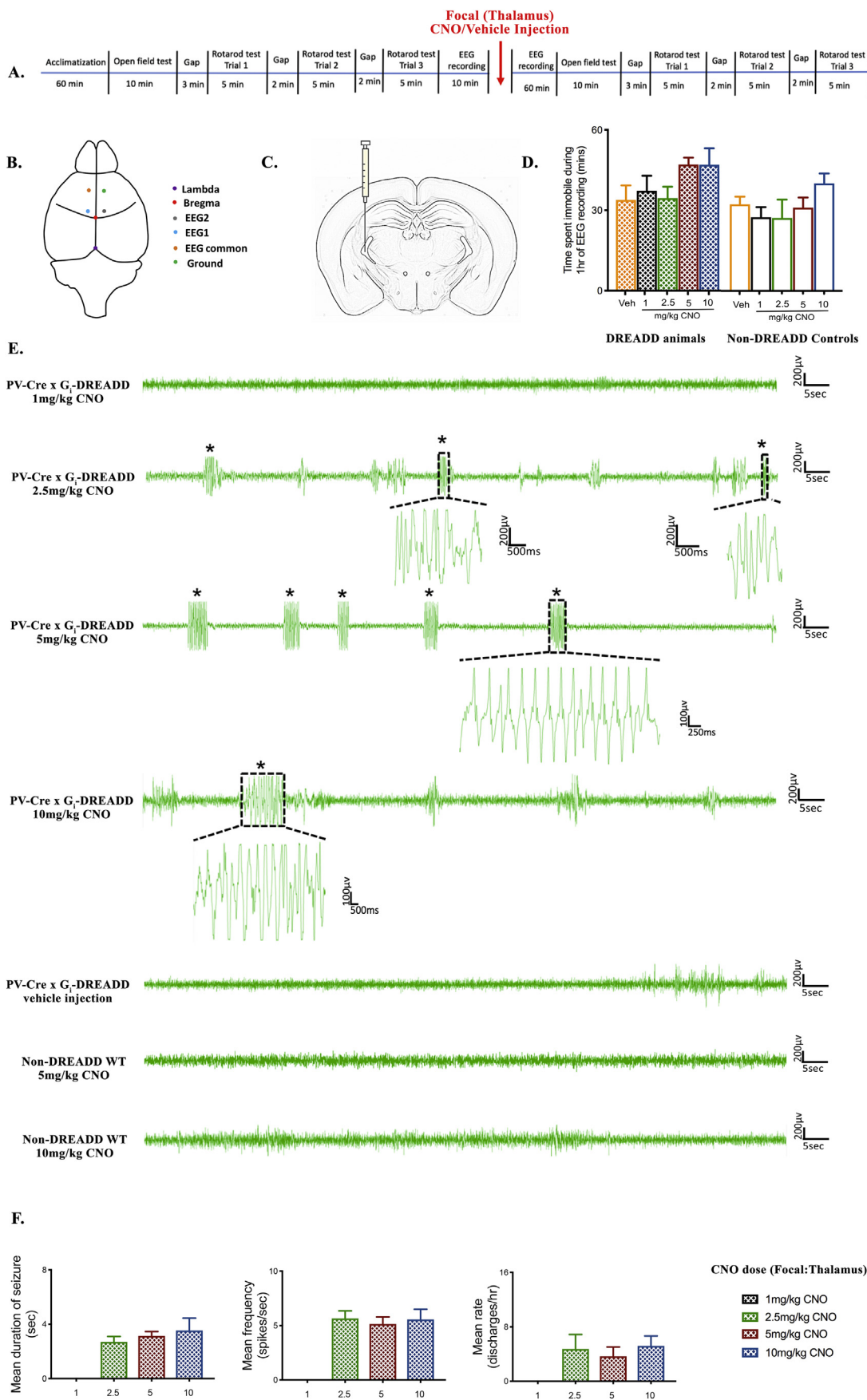
4.2. Global silencing of PV+ interneurons affects motor function and anxiety levels

We employed two motor function tests to investigate the impact of globally silencing PV+ inhibitory interneurons on locomotor behaviour, as rodent models of absence epilepsy display altered motor function including ataxia and impairment of motor co-ordination (Jarre et al., 2017). The stargazer model of absence epilepsy, which has reduced excitatory input to PV+ inhibitory interneurons in the CTC network, and in the cerebellum (due to reduced synaptic AMPA receptors), presents with several phenotypic features including absence seizures, head tossing and cerebellar ataxia (Noebels et al., 1990; Letts,

2005; Menuz and Nicoll, 2008; Yamazaki et al., 2015).

In the present study, motor performance on the rotarod test was significantly impaired in a dose dependent manner only after global silencing of PV+ interneurons via IP CNO injection, but not after focal injection of CNO into the SS cortex or RTN thalamus in PV-Cre/G_i-DREADD mice. This is likely due to the silencing of PV+ Purkinje cells in the cerebellar cortex, as knockout mice (TARP γ -2 PC KO; γ -7 KO), which lack excitatory input to Purkinje cells, display wide-ranging motor deficits including ataxic gait, severely reduced ambulation and rearing in the open-field, impaired performance in the wire hang test, and reduced forelimb and hindlimb grip strength on the rotarod (Yamazaki et al., 2015). The cerebellum plays a vital role in the motor control, precision and accurate timing of movement. IP injection of CNO into PV-Cre/G_i-DREADD mice would cause the global silencing of PV+ interneurons including the cerebellar Purkinje cells. In contrast, focal CNO injection into the SS cortex and thalamus had no effect on rotarod performance. The SS cortex and RTN thalamus are not the brain regions directly involved in regulation of motor co-ordination hence silencing of PV+ interneurons in CTC network would not be expected to be associated with loss of motor co-ordination on the rotarod. Similarly, other studies using DREADD technology and viral expression methods to selective silence or excite PV+ interneurons in specific brain regions, other than the cerebellum, have had no effect on motor coordination in rotarod tests. For example, Liu et al. (2017) reported no motor impairment on rotarod tests following CNO activation of PV+ interneurons in the rostro-dorsal RTN, using viral-mediated focal expression of hM3Dq-DREADD in PV-Cre mice. Likewise, specifically exciting PV+ interneurons in the dorsal horn produced no significant motor impairment via rotarod testing (Petitjean et al., 2015). Chemo-genetic inactivation of the target neurons of PV+ interneurons e.g. hippocampal glutamatergic neurons in CaMKII α -hM4Di mice, also has no effect on motor control (Zhu et al., 2014). From these collective studies and given that the rotarod test is especially sensitive in detecting cerebellar dysfunction, we conclude that impairment in rotarod performance in our PV-Cre/G_i-DREADD transgenic mice only after global silencing of PV+ interneurons, is a consequence of silencing cerebellar PV+ neurons.

Assessment of locomotor activity in open-field tests following global silencing of PV+ interneurons also revealed a significant reduction in the total ambulatory distance travelled in PV-Cre/G_i-DREADD before and after treatment with IP CNO doses of 5–10 mg/kg. Furthermore, we found that this group of mice spent relatively more time in the peripheral zones and corners of the maze and less time in the central zone compared to the other treatment groups (vehicle treated G_i-DREADD or CNO/vehicle treated non-DREADD WT controls). Staying in close proximity to the walls of the maze, is indicative of an anxiety-related behaviour (Seibenhener and Michael, 2015). Increased anxiety is also associated with reduced locomotion (Ennaceur, 2014). Hence, global silencing of PV+ inhibitory interneurons appears to be associated with increased levels of anxiety, coupled with reduced locomotion. Interestingly, PV knock-out mice also display decreased locomotion (Farré-Castany et al., 2007), less structured bouts of locomotion, less rearing activity, but not increased anxiety (Wöhr et al., 2015) compared to that



(caption on next page)

Fig. 6. (A) Schematic of protocol for EEG recordings/behavioural tests before and after focal CNO/vehicle injection into RTN (thalamus). (B) Diagram showing the position of EEG electrodes; recordings were made from EEG1 and EEG2 channels from both hemispheres of the brain (as explained in Fig. 5B). (C) Schematic representation of CNO delivery in RTN (modified from Allen Mouse Brain Atlas) (D) Graph showing time spent immobile by DREADD and non-DREADD animals after focal CNO injection into the RTN thalamus. Immobility increased in DREADD animals as CNO dose was increased but did not reach statistical significance (DREADD animals: vehicle treated $n = 5$; CNO 1 mg/kg $n = 5$; 2.5 mg/kg $n = 6$; 5 mg/kg $n = 6$; 10 mg/kg $n = 5$). No differences were seen in non-DREADD control animals (non-DREADD control animals: vehicle treated $n = 4$; CNO 1 mg/kg $n = 4$; 2.5 mg/kg $n = 6$; 5 mg/kg $n = 6$; 10 mg/kg $n = 4$). (E) Representative EEG traces of DREADD animals and non-DREADD controls after focal injection of CNO/vehicle into RTN. Bursts of paroxysmal oscillatory activity (indicated by asterisks) associated with behavioural arrest were seen after CNO injection (2.5–10 mg/kg) only in DREADD animals but not in 1 mg/kg or vehicle treated groups or non-DREADD WT control animals. SWDs were characterized as explained in Fig. 4D. All representative EEG traces are from different animals. Each traces represent 2–3 min of EEG recording. (F) Comparison of different parameters of EEG recording after focal CNO injection in RTN (thalamus) of PV-Cre/ G_i -DREADD animals. All values represent mean \pm SEM. Comparisons between treatment groups were performed using Tukey's post hoc multiple comparison test.

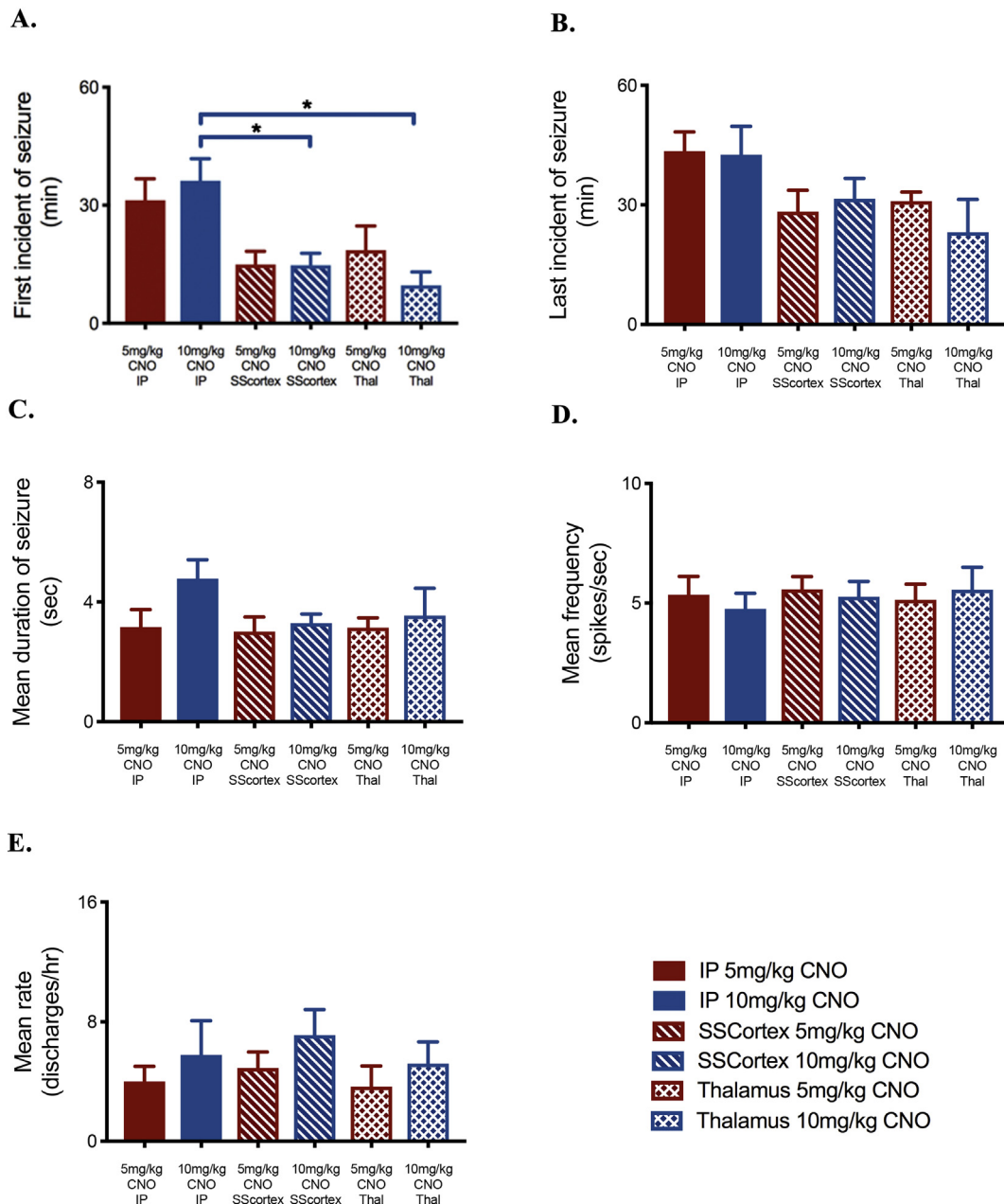


Fig. 7. Overall comparison of various EEG parameters after IP and focal (SScortex and RTN thalamus) injection during 1 h of EEG recording. (A) First incident of seizure (B) Last incident of seizure (C) Mean duration of seizure (D) Mean frequency of seizure (E) Mean rate of discharges (IP: 5 mg/kg $n = 9$; 10 mg/kg $n = 5$; SS cortex: 5 mg/kg $n = 11$; 10 mg/kg $n = 9$; RTN thalamus: 5 mg/kg $n = 6$; 10 mg/kg, $n = 5$). All values represent mean \pm SEM. Comparisons between treatment groups were performed using Tukey's post hoc multiple comparison test.

Open-field Test

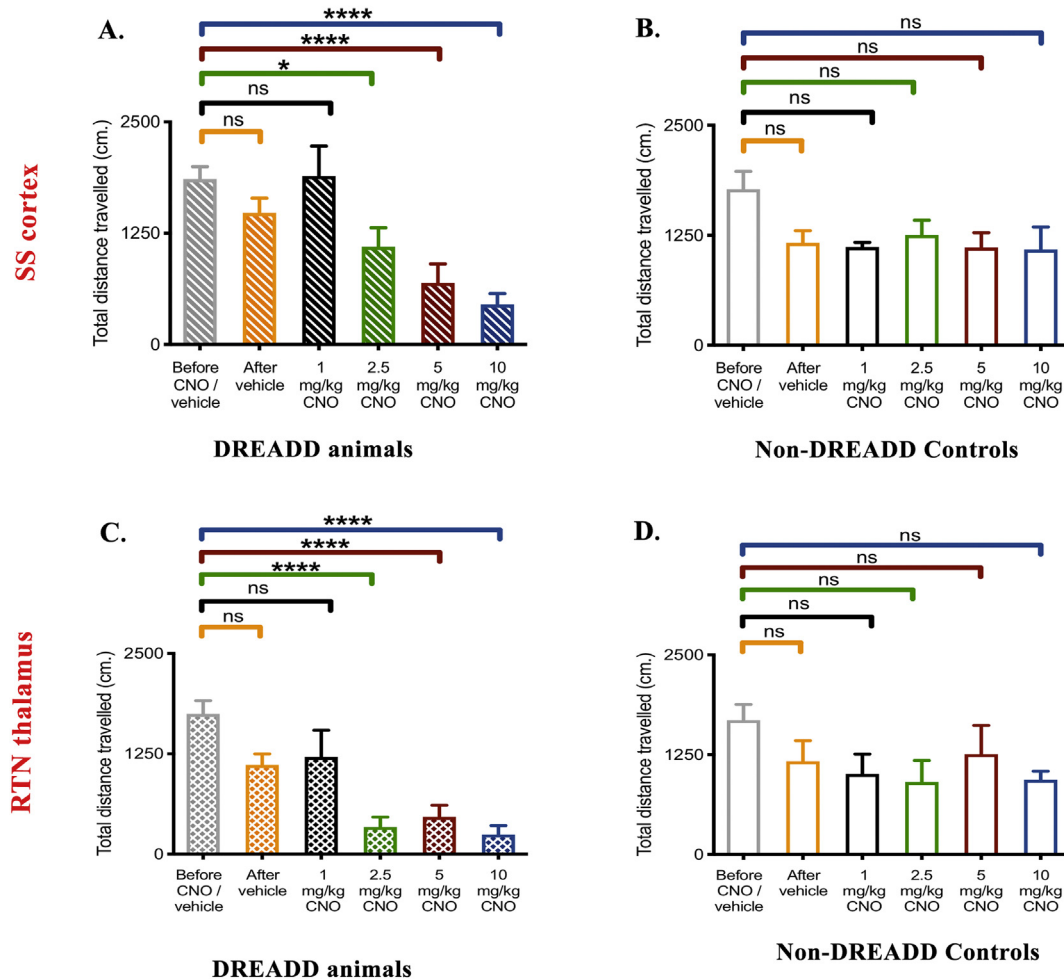


Fig. 8. Graphs comparing total distance travelled in open-field by DREADD mice and non-DREADD controls after focal CNO injection (A) CNO injection into SS cortex significantly reduced total ambulatory distance at higher doses (2.5–10 mg/kg) in DREADD mice but not vehicle treated or 1 mg/kg CNO treated animals (vehicle treated $n = 6$; CNO 1 mg/kg $n = 5$; 2.5 mg/kg $n = 6$; 5 mg/kg $n = 7$; 10 mg/kg $n = 9$). (B) No significant differences in ambulatory distance were seen in CNO or vehicle treated non-DREADD controls (vehicle treated group, $n = 4$; CNO 1 mg/kg $n = 4$; 2.5 mg/kg $n = 7$; 5 mg/kg $n = 6$; 10 mg/kg $n = 4$). (C) CNO injection into RTN thalamus also significantly reduced total ambulatory distance at higher dose (2.5–10 mg/kg) in DREADD mice but not vehicle treated or 1 mg/kg CNO treated animals (vehicle treated group, $n = 6$; CNO 1 mg/kg $n = 7$; 2.5 mg/kg $n = 7$; 5 mg/kg $n = 10$; 10 mg/kg $n = 7$). (D) No significant differences in ambulatory distance were seen in CNO or vehicle treated non-DREADD controls (vehicle treated group, $n = 4$; CNO 1 mg/kg $n = 4$; 2.5 mg/kg $n = 6$; 5 mg/kg $n = 4$; 10 mg/kg $n = 4$). All values represent mean \pm SEM. Comparisons between treatment groups were performed using Dunnett's post hoc multiple comparison test keeping 'before CNO/vehicle treatment' as a single control.

of WT animals. Other conditional PV knock-out animals (lacking TrkB and KCC3 in PV+ interneurons, respectively) also displayed decreased locomotion compared to their WT counterparts (Ding and Delpire, 2014; Lucas et al., 2014). Studies on PV $^{-/-}$ mice indicate that absence of PV results in an activity-dependent increase in inhibition thus shifting the E/I balance towards increased inhibition not a loss of feed-forward inhibition. Decreased PV expression, which occurs in the PV knock-out mouse (Wöhr et al., 2015) would likely result in enhanced inhibition due to increased presynaptic GABA release and postsynaptic GABA-mediated currents (Vreugdenhil et al., 2003). Conversely, loss of PV interneurons would reduce inhibitory input to principal excitatory neurons (Marín, 2012). In our PV-Cre/Gi-DREADD mice, the PV interneurons are silenced leading to reduced feed-forward inhibition, not loss of PV protein.

Other studies have shown differential effects of acute and chronic activation or silencing of PV+ interneurons. Zou et al. (2016) demonstrated that selective activation of PV+ interneurons in the hippocampal dentate gyrus (using a single CNO injection in PV-Cre

transgenic mice with virally expressed excitatory G_q-DREADD), induced an anxiolytic effect without affecting locomotor activity or depression-related behaviour. In contrast, chronic silencing of hippocampal PV+ interneurons, by supplying CNO in drinking water for 27 days to PV-Cre transgenic mice expressing G_i-DREADD receptors in this brain region, resulted in no changes in locomotor activity and anxiety levels (Xia et al., 2017). Similarly, Perova et al. (2015) found no difference in locomotion between CNO treated and saline treated groups of PV-Cre animals virally injected with G_i-DREADDs in the prefrontal cortex.

4.3. Silencing PV+ interneurons via focal CNO injection into the SS cortex or RTN (thalamus) generated absence-like seizures associated with behavioural arrest

To investigate the impact of silencing PV+ interneurons within the CTC network on seizure generation, and test our hypothesis that loss of feed-forward inhibition can underlie pathological SWDs in some genetic models of absence epilepsy, we first checked global silencing of PV+

interneurons via IP CNO injection as proof of concept. The DREADD receptor can be specifically activated via either peripheral (IP) or focal injection of CNO into a specific brain region (Armbruster et al., 2007; Dong et al., 2010; Rogan and Roth, 2011). Both global and focal silencing of PV+ interneurons within CTC microcircuits, resulted in arrested behaviour and bursts of paroxysmal oscillations with a spike frequency of 3–7 Hz. These oscillatory bursts were identified as SWD-like based on their EEG signature conforming to previous published criteria for SWD, i.e. trains (> 1 s) of rhythmic biphasic spikes with spike amplitude minimum two-times higher than baseline, positive transient, and slow- afterwave pattern (Arain et al., 2012, 2015). Their mean frequency/rhythmicity (Hz) was consistent with the characteristics of SWDs associated with absence seizures in various rodent models of absence epilepsy (Jarre et al., 2017). Each burst of oscillatory activity, had a conserved morphological profile with respect to burst duration and spike frequency, irrespective of drug dose (2.5–10 mg/kg) or route of administration. The mean duration of each burst was 3–5 s and mean spike frequency was between 3 and 7 Hz after both IP and focal (cortical or thalamic) CNO injections. However, mean onset of epileptiform oscillatory activity was faster (~15 min) after focal administration of CNO directly into the brain than IP peripheral injection (~30 min), as would be expected since CNO delivered peripherally requires additional time to be transported from site of injection across the blood brain barrier and into the brain. Following peripheral administration of CNO, plasma levels of the drug peak within 30 min and then sharply decline over the subsequent 2 h period (Guettier et al., 2009; MacLaren et al., 2016; Roth, 2016; Manvich et al., 2018; Jendryka et al., 2019). Although plasma levels of CNO decline quickly, behavioural effects of the drug may be evident for up to 6 h (Alexander et al., 2009).

Recently published studies have questioned the DREADD specific actions of CNO delivered peripherally. It has been shown that CNO is reverse-metabolized to clozapine after intraperitoneal CNO injection via cytochrome P450 enzymes within 1 h in liver (Gomez et al., 2017; Manvich et al., 2018; Jendryka et al., 2019), leading to the possibility that behavioural changes witnessed in animals after IP CNO injection might be off-target/sedative effects of clozapine (reverse-metabolized CNO) at endogenous sites rather than specifically DREADD-dependent effects of CNO (MacLaren et al., 2016; Ilg et al., 2018). As cytochrome P450 enzymes are also present at low levels in the brain (Mahler and Aston-Jones, 2018), it is also possible that CNO may be directly metabolized to clozapine in the brain upon focal injections. Converted clozapine reaches maximal cerebrospinal fluid concentrations at 2 to 3 h after IP CNO injection in non-human primates (Raper et al., 2017). In support of this, Gomez et al. (2017) reported decreased locomotion at this time point in non-DREADD WT controls after systemic injection of 1 mg/kg of CNO and 1 mg/kg of clozapine. Whereas, low subthreshold 0.1 mg/kg dose of clozapine significantly decreased locomotor activity in hM4Di expressing rats but not in controls, suggesting that systemic subthreshold clozapine injections induce preferential DREADD-mediated behaviours. However, other studies have failed to find DREADD-independent behavioural sedative or off-target effects (Mahler and Aston-Jones, 2018). Mahler and Aston-Jones reported no significant effects on various motivated behaviours in non-DREADD-expressing animals, injected with CNO at doses up to 10 mg/kg, at least within a 30–150 min timeframe after IP injection (Mahler and Aston-Jones, 2018). This underscores the fact that if converted clozapine levels remain within the range of specificity for DREADDs during a given time period, but below that for altering signalling at endogenous receptors during the allotted testing period, CNO can be a suitable agonist for use in such experiments. These authors concluded that the major claim in the Gomez et al., (2017) study that CNO should be abandoned as a DREADD agonist is premature and that the researchers should use the relatively well-characterized CNO until a more selective agonist is fully characterized. Moreover, an even more recent study by Jendryka et al. (2019) demonstrated that the concentration of reverse-metabolized

clozapine in plasma, cerebrospinal fluid and brain tissue is very low compared to CNO and that the brain availability of both compounds varies with species. It is now accepted that most potential off-target effects of CNO/clozapine are well controlled by administration of CNO to non-DREADD-expressing animals. In our study we tested all CNO doses (administered IP and focally directly into the brain), in both G_i-DREADD mice and their non-DREADD WT control littermates. We also conducted vehicle controls. All EEG/video recording was conducted in the first 60 min post CNO injection; all EEG/behavioural testing was completed within 100 min post CNO injection. None of the non-DREADD WT control littermates showed any bursts of epileptiform activity or SWDs, at any of the drug doses tested 1–10 mg/kg).

Interestingly we did observe increased immobility during the 1 h EEG recording period after IP CNO injections of 5 and 10 mg/kg in our G_i-DREADD mice compared to vehicle or 1 mg/kg treated mice and CNO treated non-DREADD WT controls. In animal models of absence epilepsy, SWDs are accompanied by behavioural arrest/freezing during the seizure episode (Noebels et al., 1990). In our study, we witnessed behavioural arrest/immobility during seizure activity and also between bursts of seizures. In contrast, non-DREADD WT controls injected with the same doses of CNO showed no significant increased immobility compared to before CNO or vehicle treatment. Hence we conclude that increased immobility after 5 and 10 mg/kg IP CNO injection into G_i-DREADD mice is not an off-target/sedative effect of clozapine conversion but may be linked to increased anxiety (Tovote et al., 2015; Babaev et al., 2018) as a result of DREADD-mediated silencing of PV+ interneurons, as PV knock-out mice also display decreased locomotion (Farré-Castany et al., 2007; Wöhr et al., 2015). Likewise, higher drug doses of CNO administered focally directly into the brain of G_i-DREADD mice resulted in less distance travelled in the open-field, these animals spent more time stationary. However, again there were no significant effects observed in non-DREADD WT controls.

The differential effects of acute and chronic silencing of specific PV+ interneurons within CTC network microcircuits and the functional implications on network oscillations will require further investigation. Focal inhibition of RTN PV+ interneurons would be expected to not only reduce feed-forward inhibition to the TC relay neurons but also intra RTN inhibition. Previous studies, have suggested that the RTN is critical to SWD generation, but different studies have produced seemingly conflicting functional consequences of altered inhibition within RTN. For example, lesioning rostral RTN eliminates SWDs; whereas blocking GABA_A receptors in RTN increases SWDs (Vergnes and Marescaux, 1992; Feeney et al., 1977; Meeren et al., 2009; Zhou et al., 2015). Altering inhibition within one feed-forward inhibitory circuit could also induce compensatory changes in another CTC component via changes in phasic or tonic inhibition or both. The functional impact of altering intra-RTN inhibition and RTN-mediated feed-forward inhibition of TC relay neurons *in vivo* will need to be determined chronically, using multi-electrode array techniques.

5. Conclusions

Our data demonstrate for the first time that selectively silencing PV+ interneurons in feed-forward inhibitory microcircuits in the CTC network *in vivo*, by acute focal injection of CNO into the SS cortex or thalamus of PV-Cre-dependent G_i-DREADD mice, can induce absence-like seizures and bursts of pathological oscillations with characteristic SWD-like morphology on EEG. This suggests that one underlying mechanism for the generation of absence seizures in some rodent models of absence epilepsy (e.g. stargazer and Gria4^{-/-}) and potentially some human patients, is disinhibition within feed-forward CTC microcircuits. Hence, these inhibitory interneurons could be a target for future improved treatment strategies for some cases of childhood absence epilepsy. Furthermore, dysfunctional PV+ GABAergic interneurons in other brain regions could be important in comorbid brain disorders such as anxiety, autism and schizophrenia.

Supplementary data to this article can be found online at <https://doi.org/10.1016/j.nbd.2019.104610>.

Author contributions

BL was responsible for conception, hypothesis development and design of the research, also secured the funding. SP conducted the experiments and data analyses. Interpretation of the results were conducted jointly. BL wrote the paper. All authors contributed to draft versions of the manuscript and approved the final version.

Acknowledgements

The authors thank Professor Greg Anderson (University of Otago) for sharing male G₇-DREADD mice. We also thank the staff of the Otago Centre for Confocal Microscopy (OCCM) for technical support. This work was supported by grants from the University of Otago and Deans Bequest Fund awarded to B.L. We also acknowledge the University of Otago Doctoral Scholarship awarded to S.P.

References

- Adotevi, N.K., Leitch, B., 2016. Alterations in AMPA receptor subunit expression in cortical inhibitory interneurons in the epileptic stargazer mutant mouse. *Neuroscience* 339, 124–138.
- Adotevi, N.K., Leitch, B., 2017. Synaptic changes in AMPA receptor subunit expression in cortical parvalbumin interneurons in the Stargazer model of absence epilepsy. *Front. Mol. Neurosci.* 10, 434.
- Adotevi, N.K., Leitch, B., 2019. Cortical expression of AMPA receptors during postnatal development in a genetic model of absence epilepsy. *Int. J. Dev. Neurosci.* 73, 19–25.
- Agulhon, C., Boyt, K.M., Xie, A.X., Friocourt, F., Roth, B.L., McCarthy, K.D., 2013. Modulation of the autonomic nervous system and behaviour by acute glial cell Gq protein-coupled receptor activation in vivo. *J. Physiol.* 591, 5599–5609.
- Alexander, G.M., Rogan, S.C., Abbas, A.I., Armbruster, B.N., Pei, Y., Allen, J.A., Nonneman, R.J., Hartmann, J., Moy, S.S., Nicoletis, M.A., McNamara, J.O., Roth, B.L., 2009. Remote control of neuronal activity in transgenic mice expressing evolved G protein-coupled receptors. *Neuron* 63 (1), 27–39.
- Arain, F.M., Boyd, K.L., Gallagher, M.J., 2012. Decreased viability and absence-like epilepsy in mice lacking or deficient in the GABA_A receptor $\alpha 1$ subunit. *Epilepsia* 53 (8), e161–e165.
- Arain, F., Zhou, C., Ding, L., Zaidi, C., Gallagher, M.J., 2015. The developmental evolution of the seizure phenotype and cortical inhibition in mouse models of juvenile myoclonic epilepsy. *Neurobiol. Dis.* 82, 164–175.
- Armbruster, B.N., Li, X., Pausch, M.H., Herlitze, S., Roth, B.L., 2007. Evolving the lock to fit the key to create a family of G protein-coupled receptors potentially activated by an inert ligand. *Proc. Natl. Acad. Sci.* 104, 5163–5168.
- Armstrong, C., Soltesz, I., 2012. Basket cell dichotomy in microcircuit function. *J. Physiol.* 590 (4), 683–694.
- Avoli, M., 2012. A brief history on the oscillating roles of thalamus and cortex in absence seizures. *Epilepsia* 53, 779–789.
- Babaev, O., Chatain, C.P., Krueger-Burg, D., 2018. Inhibition in the amygdala anxiety circuitry. *Exp. Mol. Med.* 50 (4), 18.
- Bailey, K.R., Crawley, J.N., 2009. Anxiety-related behaviors in mice. In: *Methods of Behavior Analysis in Neuroscience, 2nd edition*. CRC Press/Taylor & Francis.
- Barad, Z., Shevtsova, O., Arbutnot, G.W., Leitch, B., 2012. Selective loss of AMPA receptors at corticothalamic synapses in the epileptic stargazer mouse. *Neuroscience* 217, 19–31.
- Beenhakker, M.P., Huguenard, J.R., 2009. Neurons that fire together also conspire together: is normal sleep circuitry hijacked to generate epilepsy? *Neuron* 62, 612–632.
- Calin, A., Stancu, M., Zagrean, A.M., Jefferys, J.G.R., Ilie, A.S., Akerman, C.J., 2018. Chemogenetic recruitment of specific interneurons suppresses seizure activity. *Front. Cell. Neurosci.* 12, 293.
- Cammarota, M., Losi, G., Chiavegato, A., Zonta, M., Carmignoto, G., 2013. Fast spiking interneuron control of seizure propagation in a cortical slice model of focal epilepsy. *J. Physiol.* 591 (4), 807–822.
- Celio, M.R., 1986. Parvalbumin in most gamma-aminobutyric acid-containing neurons of the rat cerebral cortex. *Science* 231 (4741), 995–997.
- Chung, W.K., Shin, M., Jaramillo, T.C., Leibel, R.L., LeDuc, C.A., Fischer, S.G., ... Chetkovich, D.M., 2009. Absence epilepsy in apathetic, a spontaneous mutant mouse lacking the h channel subunit, HCN2. *Neurobiol. Dis.* 33 (3), 499–508.
- Cope, D.W., Di Giovanni, G., Fyson, S.J., Orbán, G., Errington, A.C., Lőrincz, M.L., ... Crunelli, V., 2009. Enhanced tonic GABA A inhibition in typical absence epilepsy. *Nat. Med.* 15 (12), 1392.
- Crunelli, V., Nathalie, L., 2002. Childhood absence epilepsy: genes, channels, neurons and networks. *Nat. Rev. Neurosci.* 3 (5), 371–382.
- Crunelli, V., Leresche, N., Cope, D.W., 2012. GABA-A receptor function in typical absence seizures. In: *Jasper's Basic Mechanisms of the Epilepsies* [Internet], 4th edition. National Center for Biotechnology Information (US).
- del Río, M.R., DeFelipe, J., 1994. A study of SMI 32-stained pyramidal cells, parvalbumin-immunoreactive chandelier cells, and presumptive thalamocortical axons in the human temporal neocortex. *J. Comp. Neurol.* 342 (3), 389–408.
- Ding, J., Delpire, E., 2014. Deletion of KCC3 in parvalbumin neurons leads to locomotor deficit in a conditional mouse model of peripheral neuropathy associated with agenesis of the corpus callosum. *Behav. Brain Res.* 274, 128–136.
- Dodell-Feder, D., Tully, L.M., Hooker, C.I., 2015. Social impairment in schizophrenia: new approaches for treating a persistent problem. *Curr. Opin. Psychiatry* 28, 236.
- Dong, S., Rogan, S.C., Roth, B.L., 2010. Directed molecular evolution of DREADDs: a generic approach to creating next-generation RASLS. *Nat. Protoc.* 5 (3), 561–573.
- Drexel, M., Romanov, R.A., Wood, J., Weger, S., Heilbronn, R., Wulff, P., et al., 2017. Selective silencing of hippocampal parvalbumin interneurons induces development of recurrent spontaneous limbic seizures in mice. *J. Neurosci.* 37, 8166–8179.
- Ennaceur, A., 2014. Tests of unconditioned anxiety—pitfalls and disappointments. *Physiol. Behav.* 135, 55–71.
- Evans, D.W., Lazar, S.M., Boomer, K.B., Mitchel, A.D., Michael, A.M., Moore, G.J., 2015. Social cognition and brain morphology: implications for developmental brain dysfunction. *Brain Imaging Behav.* 9, 264–274.
- Falkner, A.L., Grosenick, L., Davidson, T.J., Deisseroth, K., Lin, D., 2016. Hypothalamic control of male aggression-seeking behavior. *Nat. Neurosci.* 19, 596–604.
- Farré-Castany, M.A., Schwaller, B., Gregory, P., Barski, J., Mariethoz, C., Eriksson, J.L., ... Albrecht, U., 2007. Differences in locomotor behavior revealed in mice deficient for the calcium-binding proteins parvalbumin, calbindin D-28k or both. *Behav. Brain Res.* 178 (2), 250–261.
- Feeney, D.M., Gullotta, F.P., Pittman, J.C., 1977. Slow-wave sleep and epilepsy: rostral thalamus and basal forebrain lesions suppress spindles and seizures. *Exp. Neurol.* 56 (1), 212–226.
- Fernandez, S.P., Muzerelle, A., Scotto-Lomassese, S., Barik, J., Gruart, A., Delgado-García, J.M., et al., 2017. Constitutive and acquired serotonin deficiency alters memory and hippocampal synaptic plasticity. *Neuropsychopharmacology* 42, 512–523.
- Fishell, G., 2007. Perspectives on the developmental origins of cortical interneuron diversity. In: *Novartis Foundation symposium*. 288. John Wiley, Chichester; New York, pp. 21 (1999).
- Fortress, A.M., Hamlett, E.D., Vazey, E.M., Aston-Jones, G., Cass, W.A., Boger, H.A., et al., 2015. Designer receptors enhance memory in a mouse model of down syndrome. *J. Neurosci.* 35, 1343–1353.
- Frankel, W.N., Mahaffey, C.L., McGarr, T.C., Beyer, B.J., Letts, V.A., 2014. Unraveling genetic modifiers in the *gria4* mouse model of absence epilepsy. *PLoS Genet.* 10 (7), e1004454.
- García-Cabrero, A.M., Marinas, A., Guerrero, R., Córdoba, S.R.D., Serratos, J.M., Sánchez, M.P., 2012. Laforin and Malin deletions in mice produce similar neurologic impairments. *J. Neuropathol. Exp. Neurol.* 71 (5), 413–421.
- Gomez, J.L., Bonaventura, J., Lesniak, W., Mathews, W.B., Sysa-Shah, P., Rodriguez, L.A., Ellis, R.J., Richie, C.T., Harvey, B.K., Dannals, R.F., Pomper, M.G., Bonci, A., Michaelides, M., 2017. Chemogenetics revealed: DREADD occupancy and activation via converted clozapine. *Science* 357 (6350), 503–507.
- Guettier, J.M., Gautam, D., Scarselli, M., De Azua, I.R., Li, J.H., Rosemond, E., ... Roth, B.L., 2009. A chemical-genetic approach to study G protein regulation of β cell function in vivo. *Proc. Natl. Acad. Sci.* 106 (45), 19197–19202.
- Heuermann, R.J., Jaramillo, T.C., Ying, S.W., Suter, B.A., Lyman, K.A., Han, Y., ... Chetkovich, D.M., 2016. Reduction of thalamic and cortical Ih by deletion of TRIP8b produces a mouse model of human absence epilepsy. *Neurobiol. Dis.* 85, 81–92.
- Holland, F.H., Ganguly, P., Potter, D.N., Chartoff, E.H., Brenhouse, H.C., 2014. Early life stress disrupts social behavior and prefrontal cortex parvalbumin interneurons at an earlier time-point in females than in males. *Neurosci. Lett.* 566, 131–136.
- Hu, H., Gan, J., Jonas, P., 2014. Fast-spiking, parvalbumin+ GABAergic interneurons: from cellular design to microcircuit function. *Science* 345 (6196), 1255263.
- Ilg, A.K., Enkel, T., Bartsch, D., Böhner, F., 2018. Behavioral effects of acute systemic low-dose clozapine in wild-type rats: implications for the use of DREADDs in behavioral neuroscience. *Front. Behav. Neurosci.* 12.
- Inda, M.C., DeFelipe, J., Muñoz, A., 2009. Morphology and distribution of chandelier cell axon terminals in the mouse cerebral cortex and claustroramygdaloid complex. *Cereb. Cortex* 19 (1), 41–54.
- Jarre, G., Guillemain, I., Deransart, C., Depaulis, A., 2017. Genetic models of absence epilepsy in rats and mice. In: *Models of Seizures and Epilepsy*. Academic Press, pp. 455–471.
- Jendryka, M., Palchadhuri, M., Ursu, D., van der Veen, B., Liss, B., Kätzler, D., ... Pekcec, A., 2019. Pharmacokinetic and pharmacodynamic actions of clozapine-N-oxide, clozapine, and compound 21 in DREADD-based chemogenetics in mice. *Sci. Rep.* 9 (1), 4522.
- Jiang, X., Lachance, M., Rossignol, E., 2016. Involvement of cortical fast-spiking parvalbumin-positive basket cells in epilepsy. In: *Progress in Brain Research*. 226. Elsevier, pp. 81–126.
- Kaplan, E.S., Cooke, S.F., Komorowski, R.W., Chubykin, A.A., Thomazeau, A., Khibnik, L.A., et al., 2016. Contrasting roles for parvalbumin-expressing inhibitory neurons in two forms of adult visual cortical plasticity. *Elife* 5, e11450.
- Kelsom, C., Lu, W., 2013. Development and specification of GABAergic cortical interneurons. *Cell Biosci.* 3 (1), 19.
- Kim, T.Y., Maki, T., Zhou, Y., Sakai, K., Mizuno, Y., Ishikawa, A., ... Takahashi, E., 2015. Absence-like seizures and their pharmacological profile in tottering-6j mice. *Biochem. Biophys. Res. Commun.* 463 (1), 148–153.
- Krook-Magnuson, E., Armstrong, C., Oijala, M., Soltesz, I., 2013. On-demand optogenetic control of spontaneous seizures in temporal lobe epilepsy. *Nat. Commun.* 4, 1376.
- Letts, V.A., 2005. Stargazer—a mouse to seize!. *Epilepsy Currents* 5 (5), 161–165.
- Lewis, D.A., Curley, A.A., Glausier, J.R., Volk, D.W., 2012. Cortical parvalbumin interneurons and cognitive dysfunction in schizophrenia. *Trends Neurosci.* 35 (1), 57–67.
- Liu, J., Zhang, M.-Q., Wu, X., Lazarus, M., Cherasse, Y., Yuan, M.-Y., et al., 2017.

- Activation of parvalbumin neurons in the rostro-dorsal sector of the thalamic reticular nucleus promotes sensitivity to pain in mice. *Neuroscience* 366, 113–123.
- Lopez, A.J., Kramar, E., Matheos, D.P., White, A.O., Kwapis, J., Vogel-Giernia, A., et al., 2016. Promoter-specific effects of DREADD modulation on hippocampal synaptic plasticity and memory formation. *J. Neurosci.* 36, 3588–3599.
- Lucas, E.K., Jegarl, A., Clem, R.L., 2014. Mice lacking TrkB in parvalbumin-positive cells exhibit sexually dimorphic behavioral phenotypes. *Behav. Brain Res.* 274, 219–225.
- MacLaren, D.A., Browne, R.W., Shaw, J.K., Radhakrishnan, S.K., Khare, P., España, R.A., Clark, S.D., 2016. Clozapine N-oxide administration produces behavioral effects in Long–Evans rats: implications for designing DREADD experiments. *eneuro* 3 (5).
- Maheshwari, A., Marks, R.L., Yu, K.M., Noebels, J.L., 2016. Shift in interictal relative gamma power as a novel biomarker for drug response in two mouse models of absence epilepsy. *Epilepsia* 57 (1), 79–88.
- Mahler, S.V., Aston-Jones, G., 2018. CNO Evil? Considerations for the use of DREADDs in behavioral neuroscience. *Neuropsychopharmacology* 43 (5), 934–936.
- Manvich, D.F., Webster, K.A., Poster, S.L., Farrell, M.S., Ritchie, J.C., Porter, J.H., Weinschenker, D., 2018. The DREADD agonist clozapine N-oxide (CNO) is reverse-metabolized to clozapine and produces clozapine-like interoceptive stimulus effects in rats and mice. *Sci. Rep.* 8 (1), 3840.
- Marín, O., 2012. Interneuron dysfunction in psychiatric disorders. *Nat. Rev. Neurosci.* 13, 107–120.
- McCormick, D.A., Diego, C., 2001. On the cellular and network bases of epileptic seizures. *Annu. Rev. Physiol.* 63 (1), 815–846.
- Meeren, H.K., Pijn, J.P., Van Luijckelaar, E.L., Coenen, A.M., Lopes da Silva, F.H., 2002. Cortical focus drives widespread corticothalamic networks during spontaneous absence seizures in rats. *J. Neurosci.* 22 (4), 1480–1495.
- Meeren, H.K., Veening, J.G., Mödersheim, T.A., Coenen, A.M., Van Luijckelaar, G., 2009. Thalamic lesions in a genetic rat model of absence epilepsy: dissociation between spike-wave discharges and sleep spindles. *Exp. Neurol.* 217 (1), 25–37.
- Menuez, K., Nicoll, R.A., 2008. Loss of inhibitory neuron AMPA receptors contributes to ataxia and epilepsy in stargazer mice. *J. Neurosci.* 28 (42), 10599–10603.
- Meyer, A.H., Katona, I., Blatow, M., Rozov, A., Monyer, H., 2002. In vivo labeling of parvalbumin-positive interneurons and analysis of electrical coupling in identified neurons. *J. Neurosci.* 22 (16), 7055–7064.
- Meyer, J., Maheshwari, A., Noebels, J., Smirnakis, S., 2018. Asynchronous suppression of visual cortex during absence seizures in stargazer mice. *Nat. Commun.* 9 (1), 1938.
- Milenkovic, I., Vasiljevic, M., Maurer, D., Höger, H., Klausberger, T., Sieghart, W., 2013. The parvalbumin-positive interneurons in the mouse dentate gyrus express GABA A receptor subunits alpha1, beta2, and delta along their extrasynaptic cell membrane. *Neuroscience* 254, 80–96.
- Ng, L.H.L., Huang, Y., Han, L., Chang, R.C.C., Chan, Y.S., Lai, C.S.W., 2018. Ketamine and selective activation of parvalbumin interneurons inhibit stress-induced dendritic spine elimination. *Transl. Psychiatry* 8 (1), 272.
- Nguyen, R., Morrissey, M.D., Mahadevan, V., Cajanding, J.D., Woodin, M.A., Yeomans, J.S., et al., 2014. Parvalbumin and GAD65 interneuron inhibition in the ventral hippocampus induces distinct behavioral deficits relevant to schizophrenia. *J. Neurosci.* 34, 14948–14960.
- Noebels, J.L., Qiao, X., Bronson, R.T., Spencer, C., Davisson, M.T., 1990. Stargazer: a new neurological mutant on chromosome 15 in the mouse with prolonged cortical seizures. *Epilepsy Res.* 7 (2), 129–135.
- Panayiotopoulos, C.P., 2001. Treatment of typical absence seizures and related epileptic syndromes. *Paediatric Drugs* 3 (5), 379–403.
- Paz, J.T., Huguenard, J.R., 2015. Microcircuits and their interactions in epilepsy: is the focus out of focus? *Nat. Neurosci.* 18 (3), 351.
- Paz, J.T., Bryant, A.S., Peng, K., Fenno, L., Yizhar, O., Frankel, W.N., ... Huguenard, J.R., 2011. A new mode of corticothalamic transmission revealed in the Gria4^{-/-} model of absence epilepsy. *Nat. Neurosci.* 14 (9), 1167–1173.
- Paz, J.T., Davidson, T.J., Frechette, E.S., Delord, B., Parada, I., Peng, K., ... Huguenard, J.R., 2013. Closed-loop optogenetic control of thalamus as a tool for interrupting seizures after cortical injury. *Nat. Neurosci.* 16 (1), 64–70.
- Pelkey, K.A., Chittajallu, R., Craig, M.T., Tricoire, L., Wester, J.C., McBain, C.J., 2017. Hippocampal GABAergic inhibitory interneurons. *Physiol. Rev.* 97 (4), 1619–1747.
- Perova, Z., Delevich, K., Li, B., 2015. Depression of excitatory synapses onto parvalbumin interneurons in the medial prefrontal cortex in susceptibility to stress. *J. Neurosci.* 35 (7), 3201–3206.
- Petitjean, H., Pawlowski, S.A., Fraine, S.L., Sharif, B., Hamad, D., Fatima, T., ... Braz, J.M., 2015. Dorsal horn parvalbumin neurons are gate-keepers of touch-evoked pain after nerve injury. *Cell Rep.* 13 (6), 1246–1257.
- Pina, M.M., Young, E.A., Ryabinin, A.E., Cunningham, C.L., 2015. The bed nucleus of the stria terminalis regulates ethanol-seeking behavior in mice. *Neuropharmacology* 99, 627–638.
- Polack, P.O., Guillemain, I., Hu, E., Deransart, C., Depaulis, A., Charpier, S., 2007. Deep layer somatosensory cortical neurons initiate spike-and-wave discharges in a genetic model of absence seizures. *J. Neurosci.* 27 (24), 6590–6599.
- Raper, J., Morrison, R.D., Daniels, J.S., Howell, L., Bachevalier, J., Wichmann, T., Galvan, A., 2017. Metabolism and distribution of clozapine-N-oxide: implications for non-human primate chemogenetics. *ACS Chem. Neurosci.* 8 (7), 1570–1576.
- Rogan, S.C., Roth, B.L., 2011. Remote control of neuronal signaling. *Pharmacol. Rev.* 63, 291–315.
- Roth, B.L., 2016. DREADDs for neuroscientists. *Neuron* 89 (4), 683–694.
- Schevon, C.A., Weiss, S.A., McKhann Jr., G., Goodman, R.R., Yuste, R., Emerson, R.G., Trevelyan, A.J., 2012. Evidence of an inhibitory restraint of seizure activity in humans. *Nat. Commun.* 3, 1060.
- Sciolino, N.R., Plummer, N.W., Chen, Y.W., Alexander, G.M., Robertson, S.D., Dudek, S.M., ... Jensen, P., 2016. Recombinase-dependent mouse lines for chemogenetic activation of genetically defined cell types. *Cell Rep.* 15 (11), 2563–2573.
- Seibenhener, M.L., Michael, C.W., 2015. Use of the Open Field Maze to measure locomotor and anxiety-like behavior in mice. *J. Visualized Exp.* JoVE 96, e52434.
- Sessolo, M., Marcon, I., Bovetti, S., Losi, G., Cammarota, M., Ratto, G.M., ... Carmignoto, G., 2015. Parvalbumin-positive inhibitory interneurons oppose propagation but favor generation of focal epileptiform activity. *J. Neurosci.* 35 (26), 9544–9557.
- Shiri, Z., Manseau, F., Lévesque, M., Williams, S., Avoli, M., 2015. Interneuron activity leads to initiation of low-voltage fast-onset seizures. *Ann. Neurol.* 77 (3), 541–546.
- Sohal, V.S., Zhang, F., Yizhar, O., Deisseroth, K., 2009. Parvalbumin neurons and gamma rhythms enhance cortical circuit performance. *Nature* 459 (7247), 698–702.
- Tamamaki, N., Yanagawa, Y., Tomioka, R., Miyazaki, J.I., Obata, K., Kaneko, T., 2003. Green fluorescent protein expression and colocalization with calretinin, parvalbumin, and somatostatin in the GAD67-GFP knock-in mouse. *J. Comp. Neurol.* 467 (1), 60–79.
- Tanahira, C., Higo, S., Watanabe, K., Tomioka, R., Ebihara, S., Kaneko, T., Tamamaki, N., 2009. Parvalbumin neurons in the forebrain as revealed by parvalbumin-Cre transgenic mice. *Neurosci. Res.* 63 (3), 213–223.
- Tovote, P., Fadok, J.P., Lüthi, A., 2015. Neuronal circuits for fear and anxiety. *Nat. Rev. Neurosci.* 16 (6), 317–331.
- Trevelyan, A.J., Sussillo, D., Yuste, R., 2007. Feedforward inhibition contributes to the control of epileptiform propagation speed. *J. Neurosci.* 27 (13), 3383–3387.
- Vergnes, M., Marescaux, C., 1992. Cortical and thalamic lesions in rats with genetic absence epilepsy. In: *Generalized Non-Convulsive Epilepsy: Focus on GABA-B Receptors*. Springer, Vienna, pp. 71–83.
- Vreugdenhil, M., Jefferys, J.G., Celio, M.R., Schwaller, B., 2003. Parvalbumin-deficiency facilitates repetitive IPSCs and gamma oscillations in the hippocampus. *J. Neurophysiol.* 89 (3), 1414–1422.
- Warren, R.A., Agmon, A., Jones, E.G., 1994. Oscillatory synaptic interactions between ventroposterior and reticular neurons in mouse thalamus in vitro. *J. Neurophysiol.* 72, 1993–2003.
- Williams, S.R., Stuart, G.J., 2000. Site independence of EPSP time course is mediated by dendritic/h in neocortical pyramidal neurons. *J. Neurophysiol.* 83, 3177–3182.
- Wöhr, M., Orduz, D., Gregory, P., Moreno, H., Khan, U., Vörckel, K.J., ... Schwaller, B., 2015. Lack of parvalbumin in mice leads to behavioral deficits relevant to all human autism core symptoms and related neural morphofunctional abnormalities. *Transl. Psychiatry* 5 (3), e525.
- Xia, F., Richards, B.A., Tran, M.M., Josselyn, S.A., Takehara-Nishiuchi, K., Frankland, P.W., 2017. Parvalbumin-positive interneurons mediate neocortical-hippocampal interactions that are necessary for memory consolidation. *Elife* 6, e27868.
- Xu, X., Roby, K.D., Callaway, E.M., 2010. Immunohistochemical characterization of inhibitory mouse cortical neurons: three chemically distinct classes of inhibitory cells. *J. Comp. Neurol.* 518 (3), 389–404.
- Yamazaki, M., Le Pichon, C.E., Jackson, A.C., Cerpas, M., Sakimura, K., Searce-Lavie, K., Nicoll, R.A., 2015. Relative contribution of TARPs γ -2 and γ -7 to cerebellar excitatory synaptic transmission and motor behavior. *Proc. Natl. Acad. Sci.* 112 (4), E371–E379.
- Yekhlief, L., Breschi, G.L., Lagostena, L., Russo, G., Taverna, S., 2015. Selective activation of parvalbumin- or somatostatin-expressing interneurons triggers epileptic seizure like activity in mouse medial entorhinal cortex. *J. Neurophysiol.* 113 (5), 1616–1630.
- Yi, F., Ball, J., Stoll, K.E., Satpute, V.C., Mitchell, S.M., Pauli, J.L., ... Gerber, D.J., 2014. Direct excitation of parvalbumin-positive interneurons by M1 muscarinic acetylcholine receptors: roles in cellular excitability, inhibitory transmission and cognition. *J. Physiol.* 592 (16), 3463–3494.
- Zhou, C., Ding, L., Deel, M.E., Ferrick, E.A., Emeson, R.B., Gallagher, M.J., 2015. Altered intrathalamic GABA neurotransmission in a mouse model of a human genetic absence epilepsy syndrome. *Neurobiol. Dis.* 73, 407–417.
- Zhu, H., Pleil, K.E., Urban, D.J., Moy, S.S., Kash, T.L., Roth, B.L., 2014. Chemogenetic inactivation of ventral hippocampal glutamatergic neurons disrupts consolidation of contextual fear memory. *Neuropsychopharmacology* 39 (8), 1880–1892.
- Zhu, H., Aryal, D.K., Olsen, R.H.J., Urban, D.J., Swearingen, A., Forbes, S., et al., 2016. Cre-dependent DREADD (Designer Receptors Exclusively Activated by Designer Drugs) mice. *Genesis* 54, 439–446.
- Zou, D., Chen, L., Deng, D., Jiang, D., Dong, F., McSweeney, C., et al., 2016. DREADD in parvalbumin interneurons of the dentate gyrus modulates anxiety, social interaction and memory extinction. *Curr. Mol. Med.* 16, 91–102.